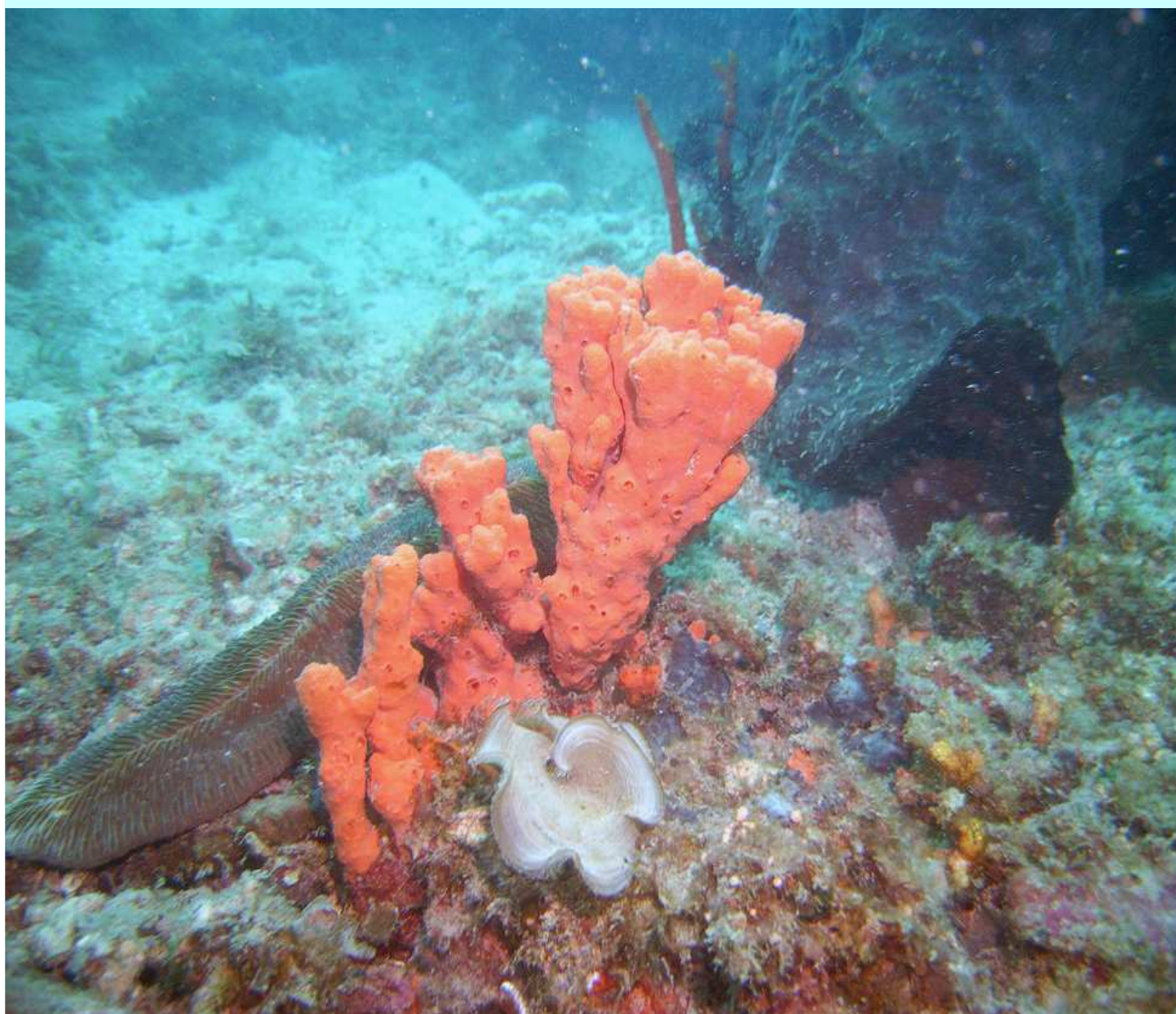Dissertation

Isolation and Structure Elucidation of Bioactive Secondary Metabolites from Indonesian Marine Sponges

Triana Hertiani

Isolation and Structure Elucidation of Bioactive Secondary Metabolites from Indonesian Marine Sponges

(Isolierung und Strukturaufklärung bioaktiver Sekundärstoffe aus Indonesischen marinen Schwämmen)

Inaugural-Dissertation
zur

Erlangung des Doktorgrades
Der Mathematisch-Naturwissenschaftlichen Fakultät der
Heinrich-Heine-Universität Düsseldorf

vorgelegt von

Triana Hertiani
aus Jakarta, Indonesien

April 2007

Umschlag: Unterwasserbild von *Agelas* n.sp. aus Peniki East Island aufgenommen durch Dr. Nicole J. de Voogd, verwendet mit freundlicher Genehmigung der Urheberin

Erklärung

Hiermit erkläre ich ehrenwörtlichen, daß ich die vorliegende dissertation, "Isolierung und Strukturaufklärung bioaktiver Sekundärstoffe aus Indonesischen marinen Schwämme" selbständig angefertigt und keine anderen als die angegebenen Quellen und Hilfsmittel benutzt habe. Ich habe diese Dissertation in gleicher oder ähnlicher Form in Keinem anderen Prüfungsverfaren vorgelegt. Außerdem erkläre ich, daß ich bisher noch keine weiteren akademischen Grade erworben oder zu erworben versucht habe.

Düsseldorf, den 17.04.2007

Triana Hertiani

Acknowledgements

For Agus and Abyan Hadna, with heart full of love and thanks

Zusammenfassung

Marine Organismen, besonders Schwämme bieten eine Vielzahl von Naturstoffen mit interessanten biologischen Wirkungen. Untersuchungen auf dem Gebiet der marinen Sekundärstoffe haben längerfristig zum Ziel, natürliche Leitstrukturen zu finden, die als potentielle Ideengeber für die Entwicklung von Medikamenten dienen können.

Die vorliegende Arbeit befaßt sich mit der Isolierung und Strukturaufklärung von Inhaltstoffen aus indonesischen marinen Schwämmen und der Charakterisierung möglicher biologischer Wirkungen der gefundenen Verbindungen. Schwammproben wurden an mehreren Stellen in Indonesien gesammelt. Eine Kombination chemischer und biologischer Methoden wurde zur Erforschung der potentiellen Arzneistoffe verwendet. Extrakte wurden auf antibakterielle, antifungale und zytotoxische Aktivität sowie in Proteinkinase-Tests untersucht, daneben kamen verschiedene chromatographische und spektroskopische Methoden zur Anwendung, um die chemisch interessantesten Substanzen zu isolieren.

Der erste Abschnitt der Forschungsarbeit bestand aus der Isolierung und Identifizierung der Sekundärstoffe aus den Proben, wobei die Strukturen der einzelnen Verbindungen durch Massen- (EI, FAB, ESI) und Kernresonanz-Spektroskopie (^{1}H-NMR, ^{13}C-NMR, DEPT, COSY, HMBC, HMQC) aufgeklärt wurden. Durch unterschiedliche chromatographische Trennmethoden (hauptsächlich Säulenchromatographie mit verschiedenen stationären Phasen) wurden insgesamt 35 Naturstoffe isoliert, von denen 14 Verbindungen neue Derivate darstellen. Im zweiten Teil der Arbeit wurden die isolierten Sekundärstoffe in den bereits

beschriebenen Bioassays auf eine mögliche biologische Aktivität getestet.

Im Folgenden aufgeführt sind die Verbindungen, die isoliert und in ihrer Struktur aufgeklärt und deren biologische Wirkungen weiter charakterisiert worden sind.

1. Schwämme der Gattung Agelas

Die Bearbeitung bisher nicht identifizierter Schwammarten der Gattung Agelas ergab insgesamt 16 bromierte Pyrrol-Derivate, wobei es sich bei elf Substanzen um neue Verbindungen handelt. Verschiedene Strukturen bromierter Pyrrole mit neuen funktionellen Gruppen wurden entdeckt, darunter Agelanin A (**2**), Agelanin B (**3**), und Agelanesine (**4** bis **7**). Die erhebliche zytotoxische Wirkung gegen murine Lymphoma-Zellen (L5178Y) wurde bei allen Agelanesinen nachgewiesen ($IC_{50} < 10$ µg/mL).

2. *Agelas nakamurai*

Aus dem Schwamm *Agelas nakamurai* wurden insgesamt zehn Verbindungen isoliert, davon ein neues monobromiertes Pyrrol-Derivat, Longamide C (**20**) und 2 neue Diterpene (-)-Agelasine-D (**18**) und (-)-Ageloxime-D (**17**). (-)-Ageloxime-D inhibierte wirksam die Biofilm-Bildung, zeigte aber keine Wachstumshemmung des Testorganismus *S. epidermidis*. Im Gegensatz dazu ist (-)-Agelasine-D antibiotisch wirksam, zeigte aber im Biofilm-Assay keine inhibitorische Aktivität. Sowohl (-)-Agelasine-D als auch (-)-Ageloxime-D erwiesen sich als toxisch gegenüber den Cyprislarven von *Balanus improvisus* Darwin, wobei die Wirkung von (-)-Ageloxime-D um das 10-fache stärker war als die des (-)-Agelasine-D.

2. *Pseudoceratina purpurea*

Die Bearbeitung des Extraktes des Schwammes *Pseudoceratina purpurea*

ergab fünf bromierte Tyrosin-Derivate. Die Antifouling-Substanz, Aplysamine-2 (**27**) sowie die Biokonversionsprodukte des Isofistularins-3, (**+**)-Aeroplysinin-1 (**28**) und das Bisoxazolidinon-Derivat (**29**), sowie aus dem Lösungsmittel resultierende Artefakte, Dienone-dimethoxyketal (**30**) und Dienone-methoxy-ethoxyketal (**31**) wurden identifiziert.

3. Schwämme der Gattung Axynissa

Die Suche nach bioaktiven Verbindungen als Proteinkinase-Hemmstoffe führten zur Isolierung zweier Bisabolen-Phenol-Derivate, (**+**)-Curcuphenol (**33**) und (**+**)-Curcudiol (**34**) aus den aktiven Fraktionen nicht weiter identifizierter Schwämme der Gattung Axynissa aus den Gewässern um Ambon, Maluku.

4. *Mycale phyllophilla*

Die Untersuchung des Schwamm-Extrakts aus *Mycale phyllophyla* ergab die Anwesenheit von 5-Pentadecyl-1*H*-pyrrole-2-carbaldehyd (**32a**) und (6'*E*)-5-(6'pentadecenyl)-1*H*-pyrrole-2-carbaldehyd (**32b**) in einer zytotoxisch aktiven Fraktion.

5. *Rhabdastrella rowi*

Das Chinolin-4-ol (**35**) aus dem Extrakt des marinen Schwammes *Rhabdastrella rowi* in einer sehr geringen Menge erhalten. Bis jetzt ist diese Verbindung nur synthetisch erhalten und als Naturstoff noch nicht beschrieben worden.

Table of Contents

List of Tables

List of Figures

Abbreviations

$[\alpha]_D$	:	Specific rotation at the sodium D-line
br	:	broad signal
COSY	:	Correlation spectroscopy
d	:	doublet
dd	:	doublet of doublet
ddd	:	Doublet of doublet of doublet
DEPT	:	Distortionless Enhancement by Polarization Transfer
DMSO-d_6	:	Deuterated dimethylsulfoxide
DNA	:	Deoxyribonucleic acid
dt	:	doublet of triplet
EC_{50}	:	Effective Dose, 50%, the plasma concentration required for obtaining 50% of a maximum effect in vivo
EI-MS	:	Electron Ionization Mass Spectrometry
ESI-MS	:	Electrospray Ionization Mass Spectrometry
EtOAc	:	Ethyl acetate
EtOH	:	Ethanol
eV	:	Electron volt
HMBC	:	Heteronuclear Multiple Bond Correlation Experiment
HMQC	:	Heteronuclear Multiple Quantum Coherence
HPLC	:	High Performance Liquid Chromatography
HRESIMS	:	High Resolution Electrospray Ionization Mass Spectrometry
Hz	:	Hertz
IC_{50}	:	Half maximal inhibitory concentration of a drug that is required for 50% inhibition in vitro
LC/MS	:	Liquid Chromatography/ Mass Spectrometry
LC_{50}	:	Lethal Dose, 50% (median lethal dose)
m	:	multiplet
MeOD	:	Deuterated methanol
MS	:	Mass spectrometry
m/z	:	mass per charge
n-BuOH	:	Normal butanol
NMR	:	Nuclear magnetic resonance
n.sp.	:	New species
ppm	:	parts per million
q	:	quartet
ROESY	:	Rotational Frame Nuclear Overhauser Effect Spectroscopy
RP-18	:	Reversed Phase C-18
RT	:	Retention time
s	:	singlet
SCUBA	:	Self Contained Underwater Breathing Apparatus
TFA	:	Trifluoroacetic acid
TLC	:	Thin Layer Chromatography
t	:	triplet
UV	:	Ultra violet
VLC	:	Vacuum liquid chromatography

I. Introduction

I.1.   Significance of study

Since ancient times, nature has been an important source of medicines. This fact is illustrated by the large number of natural products currently used in medical practice, which were earlier identified through folklore knowledge of the medicinal properties of plants, animal extracts, and minerals (Amador *et al.*, 2003). A recent analysis of natural products as sources of new drugs over the period 1981 – 2002 by Newman and collaborators (2003) indicates that even though 67% of the 877 small molecule new chemical entities (NCEs) are formally synthetic, but 16.4% correspond to synthetic molecules containing pharmacophores derived directly from natural products, whereas 12% can be categorized as natural product mimics (Cragg *et al.*, 2006; Newman *et al.*, 2003). Therefore, actually over 60% of the NCEs can be related to natural products in one way or another (Cragg *et al.*, 2006).

Microorganisms are also defined as a prolific source of novel bioactive compounds from nature. They have yielded some of the very important pharmaceutical products such as the antibiotics penicillin and aminoglycosides, as well as the anticancer drugs anthracyclins and bleomycin. Marine compounds on the other hand are under-represented in current pharmacopoeias, but it is noteworthy to mention that the aquatic environment will become invaluable source of novel compounds in the future (Amador *et al.*, 2003).

The ocean which covers almost 75% of the Earth's surface provides a huge biodiversity with potential as immeasurable source of natural products (Whitehead, 1999). But due to the lack of an analogous ethno-medical history, together with the

relative technical difficulties in collecting marine organisms, the development of marine-derived natural products as therapeutic agents is still in its infancy. Nevertheless, significant efforts to isolate and identify new marine-derived natural products have been made over the last few decades by collaboration of both pharmaceutical companies and academic institutions, accompanied by funding supports from government agencies (Amador *et al.*, 2003). Systemic investigations directed towards the collection and characterizations of marine natural products, as well as the evaluation of their biological activity have been established (Christian *et al.*, 1997; Amador *et al.*, 2003). These efforts result in a large number of novel marine-derived compounds reported in the literature over the past decade (Mayer and Gustafson, 2003; Amador *et al.*, 2003). Currently, some of these agents have entered preclinical and also clinical trials which can be expected that the number will increase in the future (Amador *et al.*, 2003).

According to Proksch and co-workers (2002), the majority of marine natural products currently in clinical trial or under clinical evaluation are produced by invertebrates. The soft bodied, sessile or slow-moving marine invertebrates that usually lack of morphological defense structure like spines or a protective shell reflect the ecological importance of the chemical constituents to the respective invertebrates (Proksch *et al.*, 2002).

Many of these natural products also act as regulators of specific biological functions. Some of them have pharmacological activity due to their specific interactions with receptors and enzymes. They need to be highly potent on a molecular basis and retain a relatively low solubility since they become immediately diluted by large volumes of seawater (McConnell *et al.*, 1994). It has been repeatedly shown that the accumulation of toxic or distasteful natural product is an effective

strategy to fight off potential predators (e.g. fishes) or to force back neighbours competing for space (Proksch *et al.*, 2002; Proksch and Ebel, 1998; Proksch, 1999; McClintock and Baker, 2001). These secondary metabolites, which are produced as a result of evolutionary pressures to reserve or enhance an organisms ecological success (Proksch, 1999), have evolved into structurally diverse and usually stereo-chemically complex compounds with specific biological activity (Edrada *et al.*, 2000) many of which belong to novel chemical groups not found in terrestrial sources (Carte, 1993).

Sponges in particular, have been reported as the prime source of marine bioactive metabolites (Blunt *et al.*, 2005). Pharmaceutical interest in sponges was aroused in the early 1950s by the discovery of the unusual nucleosides spongothymidine and spongouridine in the marine sponge *Cryptotethia crypta* (Bergmann and Feeney, 1950, 1951). These nucleosides were the basis for the synthesis of Ara-C, the first marine-derived anticancer agent, and the antiviral drug Ara-A (Prokch *et al.*, 2002).

Up to now more than 17,000 marine products have been described (MarinLit, 2006) of which sponges are responsible for more than 5300 different products (Faulkner 2000, 2001, 2002). The chemical diversity of sponge products is remarkable, in addition to the unusual nucleosides, bioactive terpenes, sterols, cyclic peptides, alkaloids, fatty acids, peroxides, and amino acid derivatives (which are frequently halogenated) (Sipkema *et al.*, 2005).

The area of the Pacific Ocean comprising the Indonesian Archipelago, the Philippines, The Malaysian Peninsula, and New Guinea are considered to have the highest marine biodiversity in the world (Sheppard and Wells, 1988; Roberts *et al.*, 2002). As the central and richest part of a larger Indo West Pacific region, Indonesia

alone has been reported to possess almost 830 sponge fauna species (obvious synonym not counted) (Van Soest, 1989) which exist in a high rate of dissimilarity among different area (Amir, 1992; Calcinai *et al.*, 2005). Increased feeding pressure from fishes and possibly from predatory invertebrates such as mollusk, not to mention higher microbial infection in tropical areas might be the reason for more interesting and more diverse secondary metabolites found in sponges that live in this region (Proksch *et al.*, 2002). Therefore, they might provide a huge source of potential new drugs from the sea or compounds to serve as lead structure for drug development. As new and more complicated diseases are encountered worldwide, the need for new chemotherapeutic agent is increased. On the other hand, Indonesian marine sponges as sources of bioactive natural products are still not yet well investigated. This fact could be observed as only few literature reports on bioactive marine metabolites from this tropical region have been published (Blunt *et al.*, 2006). Therefore studies on bioactive substances from marine sponges collected from this area are highly required.

I.2.   Literature background

I.2.1.   Natural products of marine origin

The oceans, which cover almost 75% of the Earth's surface, contain a variety of species, many of which have no terrestrial counterparts. Thus represents an attractive source of novel bioactive natural products which prior to 1980, had been largely unexploited. Fortunately, technological advances over recent years have aided marine natural products chemists and also have fueled a rapidly growing interest in the hidden secrets of the oceans (Whitehead, 1999).

Bioactive marine natural products can be defined as biologically active products including primary and secondary metabolites derived from marine sources

(Gudbjarnason, 1999). Primary metabolites are essential to growth and life in all living systems, and are formed by a limited number of metabolic reactions. They serve as building blocks for synthesis of macromolecules, proteins, nucleic acids, carbohydrates and lipids. Secondary metabolites, on the other site are not essential to the life of the producing organisms. They are formed from primary metabolites, and many of them enhance the survival fitness of the organism. Some secondary metabolites may also serve as chemical weapons used against bacteria, fungi, insects, and large animals (Gudbjarnason, 1999).

Even though most of the "natural products" of interest to the pharmaceutical industry are secondary metabolites, the interest in products of primary metabolites such as various marine lipids, enzymes and complex heteropolysaccharides is increased (Gudbjarnason, 1999). In fact, the division between primary and secondary metabolites of sponges is a little hazy (Faulkner, 1984), as could be seen in an unusual carboxylic acid of phospholipids found in marine sponges *Higginsia tethyoides* (Ayanoglu *et al.*, 1983; Faulkner, 1984), and amides of 2-methylene-β-alanine from *Spongia cf. zimocca* (Yunker and Scheuer, 1978; Faulkner, 1984).

Database provided by MarinLit (2002) shows that the source of new marine natural products is dominated by sponges (37%) followed by coelenterates (21%). Interestingly most of metabolites investigated in the preclinical and clinical trials are derived from sponges as well (Blunt *et al.*, 2005) which somehow define their role as a potential source of new drug candidate.

Presumed biogenetic origin of the new substances from marine source has systematically assigned by Blunt and co-workers (2004) showing the domination of the terpenoid biogenesis pathway. This fact is not surprising regarding the chemistry

of the two largest groups examined; sponges and coelenterates are dominated by terpenoids as well (Blunt *et al.*, 2004). Several studies show that these metabolites play an important role in antipredation, space competition, and control of epibiont overgrowth of the host organisms (Thakur and Müller, 2004).

In the early years of marine natural products research, there was less emphasis put on biological testing. But recently, focus on biological properties of these compounds is increased. Comparison of biological testing carried out on marine metabolites up to 2004 (Marinlit, 2004) describes the domination of anticancer activity (41%), followed by studies covering bioassay on mechanism of actions, structure activity relationship, etc. (21%) and antibiotics, including antifungal, antituberculosis and antimalarial (20%) (Blunt *et al.*, 2006). This is somehow correlated to the fact that cancer is the major public health burden in the United States and in other developed countries. Currently, it has been reported that one of every four deaths in the United States is due to cancer (Jemal *et al.*, 2004). A great unmet medical need in chemotherapeutic agents to overcome the development of multi-drug resistance has also lead the progress towards marine anticancer drugs. Increasing clinical importance of drug resistant bacterial pathogens such as in tuberculosis and MRSA (multiple resistant *S. aureus*) diseases has lead to the urgency for antibacterial research (Shu, 1998). Other progressing categories are in drugs for pain and asthmatic conditions where the interest is centered on *Conus* toxin and analogues of sponge sterols respectively (Newman and Cragg, 2004).

I.2.2. Sources, collection, screening and supply of marine bioactive metabolites

The process of discovering marine pharmaceuticals starts with the collection of marine organisms. This is often the most important step in the entire research

program because the quality of the collections influences all future research (Faulkner, 2000). The progress in scuba-diving techniques and deep-water collection instruments has been crucial, which has allowed the improvement of sample collection of previously inaccessible marine organisms (Amador *et al.*, 2003).

In order to avoid adverse impact to the collection site, a combination of high biological diversity and density should be of consideration in finding the collection site. The collected samples must be accurately sorted, and similar organisms should rather be splitted than lumped together. Careful documentation is also very important for future re-collection. A sub-sample should be put aside for taxonomic studies, while the bulk sample must be rapidly frozen or stored in solvent to retard bacterial degradation of the specimens (Faulkner, 2000).

Crude extracts must be prepared for biological screening. Assays that require careful interpretation and provide a lot of information per assay are ideal, although they are more difficult to be used during a bioassay-guided fractionation. Considering the fact that some crude extracts may not be well tolerated by some bioassay, one may randomly isolate pure compounds on the basis of interesting chemical structures and screen libraries of pure compounds (Faulkner, 2000).

Despite that marine ecosystem is extremely rich and diverse; one should consider the limitation of resources in developing marine pharmaceuticals. In addition, the natural concentrations of many marine-derived pharmacologically active compounds are often minute and sometimes less than 10^{-6}% of the organism wet weight (Proksch *et al.*, 2003). As an example, close to 1 metric tonne (wet weight) of the tunicate *E. turbinata* is needed to obtain approximately 1 g of the promising anticancer drug ecteinascidin 743 (ET 743) (Mendola, 2000; Proksch *et al.*, 2003). Continued collection from wild source will soon lead to an overexploitation and

possible extinction of the natural producer of many pharmacologically promising marine natural products (Proksch *et al.*, 2003). Identification and development of synthetic or semi synthetic approaches as ultimate sources of supply has been suggested to be the final goal (Amador *et al.*, 2003). But since in many cases chemical synthesis for highly complex structures like ET 743 which features numerous chiral centres is not economically feasible, cultivation of sponges, tunicates and other chemically interesting marine invertebrates in the sea (mariculture) seems to be a promising alternative in the future (Proksch *et al.*, 2003). Another possible alternative is by using bioreactor for cultivation of sponge cell culture. The latter approach, in particular, will only be successful if the growth conditions of sponges in its natural environment can be formulated (Müller *et al.*, 2003)

The expected limitations in the supply of marine macroorganisms, and the fact that there is a tremendous biological reserve of marine microorganisms, make the latter as an attractive source in searching for pharmaceutical compounds (Amador *et al.*, 2003). It is quite widely accepted that many sponge metabolites are produced by symbiotic microorganisms. This hypothesis is supported by the finding that the natural products from some classes of sponge are very similar to those known from terrestrial microorganisms (Whitehead, 1999).

Nowadays, the compounds derived from marine sources are systematically tested for relevant biomedical properties including anti-proliferative effects. A major screening system is carried out by the National Cancer Institute of the USA, which looks for selective activity in a panel of 60 human tumor cell lines (Christian *et al.*, 1997; Amador *et al.*, 2003). Alternative strategies which screen for substances with inhibitory properties towards specific enzymatic reactions employ a more

mechanistic-based approach. Beside its specificity, this type of assay can focus on a number of discrete drug targets. The potentially confounding effects of toxic components at the same time are avoided which allows the bioassay screening of crude extracts (Bevan *et al.*, 1995; Amador *et al.*, 2003). By adaptation to high-throughput method, it offers the potential to readily screen hundreds or thousands of extracts in parallel against numerous therapeutic targets. Furthermore, as the results, the study of marine anticancer compounds is yielding not only the discovery and development of new drugs, but also the identification of new molecular targets for therapeutic intervention (Amador *et al.*, 2003).

I.2.3. Sponge as source of bioactive natural products

I.2.3.1. Sponges (Porifera)

Phylum Porifera (sponges) are metazoans that are united by the unique possession of choanocytes chambers, a system of afferent and efferent canals with external pores, lacking a tissue grade of construction but having a highly mobile cell population capable of totipotency, and possessing siliceous or calcitic spicules in many (but not all) species (Hooper *et al.*, 2002). They are aquatic animals that occur in all oceans as well as in fresh water and have a wide distribution from tropical to temperate to arctic regions. They also grow at all depths and in brackish and fresh water, as thin encrusting coatings on rocks and wood, or as long thin branching fingers attached to the bottom, or in the typical rounded form (Pearse *et al.*, 1987). Sponges lack conventional nerves and muscle, which means movement is only at the pace of the individual crawling cell (Leys *et al.*, 2005).

The outer space of a sponge is covered with inhalant pores where the ambient water is drawn into the sponge. These pores represent why sponges have been called "Porifera" (pore bearing). Sponges pump water through their unique body

plan of canals and chambers to phagocytose food particles (Pearse *et al.*, 1987). The amoebocytes and choanocytes are the work force of the sponge, which create the body. The choanocytes are composed of a flagellum and a collar (collar cells). The collar cells serve as lining of the canals, force water through the sponge which brings oxygen and nutrients while removing carbon dioxide and waste (Pechenik, 2000); as well as very likely to also release gametes (Simpson, 1984). The amoebocytes secrete spicules which stack up together to form the sponge skeleton. It had been thought that the "ground" space between the two cell layers which surround the sponges, the external pinacoderm and the internal choanoderm (endopinacoderm), the mesophyl, comprises mostly functional independent cells (Pechenik, 2000). However, the remarkable discoveries of cell surface-bound receptors existence and their extra- (binding sites for ligands) as well as intracellular segments (association with signal transduction molecules) in the last few year demonstrated that the sponge molecules allow the establishment of a distinct body plan (Kaandorp and Kübler 2001).

Sponges reproduce either sexually or asexually. In sexual reproduction, eggs and sperm unite to make a free-swimming larva that settles on a surface. Asexually, small, internal buds called gemules are produced which then become new sponges. Sponges can also reconstitute themselves if their cells are separated into a suspension (Pechenik, 2000).

There are an estimated 15,000 sponge species living today, but only about half of them have been described and named. Their ecology and survival is often of reliant upon the ability to produce unique bioactive compounds (Leys *et al.*, 2005). Three classes of sponges have been defined. Each class is characterized by a unique body plan features. Demosponges are cellular and most are supported by a

siliceous skeleton of two and four-rayed spicules. Hexactinellid or glass sponges on the other hand have a six-rayed glass skeleton and are syncytial rather than cellular. The third class, calcareous sponges are characterized by a calcium carbonate skeleton and cellular organization. This group comprises less than 5% of living sponges, and is the only group of which the three grades of sponge body design-asconoid, syconoid and leuconoid-are apparent (Leys *et al*., 2005).

I.2.3.2. Role of metabolites in host organism

In order to evaluate the biomedical potential of any plant or animal, both the chemical ecology of the organisms as well as its evolutionary history must be considered (Faulkner, 2000). It is probable that chemical defense mechanisms evolved with the most primitive microorganisms have been replaced in many more advanced organisms by physical defense and/or the ability to run or swim away and hide. Considering that sessile, soft bodied marine invertebrates are lack of obvious physical defenses, they may rely on bioactive metabolites as a form of defense. Furthermore, based on assumption that secondary metabolites evolved from primary metabolites in a random manner, any newly produced secondary metabolite that offered an evolutionary advantage to the producing organisms would contribute to the survival of the new strain. Therefore organism with a very long evolutionary history such as sponge has ample opportunity to perfect their chemical defenses (Faulkner, 2000). Huge number of different secondary metabolites discovered in marine sponges, as well as complexity of the compounds and their biosynthetic pathways (and corresponding kilo bases of DNA for the programming of their synthesis) can be regarded as an indication of their importance for survival (Proksch, 1994).

Nevertheless, in tropical regions some sponges are chemically defended while others are not (Paul *et al.*, 2006). A research performed on the Carribbean reef sponges by Walters and Pawlik (2005) discovered that after an artificially wound, the sponges which were not chemically defended healed at significantly faster rates than the chemically defended species. In addition, morphology was also important since tubular shaped individuals healed faster than vasiform shaped individuals of *Niphates digitalis*. The authors proposed that Caribbean reef sponges have adapted to overcome fish predation either by investing in the production of chemical defenses or by rapid wound-healing response after injury (Paul *et al.*, 2006).

Substance against biofouling is one example of the secondary metabolites benefit to the host organisms. To safeguard their water-pumping capacity, sponges as filter feeder cannot tolerate biofilm formation or settlement of barnacles or bryozoans on their surface (Proksch, 1994). Another interesting example is the sponges capability to create a relatively toxic bare zone surrounding them (Thompson, 1985) to conquest the densely populated rocks or corals and to compete with faster growing organisms. This poison on the other way around can selectively be used without self destruction (Sipkema *et al.*, 2005).

It has been found that sponge-associated bacteria might be the actual producers of a number of compounds isolated from sponges. *Ocillatoria spongeliae*, a cyanobacterial symbiont that can constitute up to 40% of *Dysidea herbacea*, is proven to be the real producer of antimicrobial polybrominated biphenyl ethers which might keep the sponge free of other bacteria (Faulkner *et al.*, 1994). The growth of these such microorganisms as symbionts is possibly under control of the sponge host to serve as source of food or supplies other metabolic products (Müller *et al.*, 1981).

A collaboration involving sponges and their symbiotic microorganisms (bacteria and fungi) to produce an array of bioactive compounds against foreign attackers was proposed by Müller and co-workers (2004) to be driven by environmental biotic constraints which provide four form of protection. (i) *Single protection*, where bioactive molecules are produced either by the host (sponge) against attacking microorganisms or eukaryotes, e.g. acetylenic compounds (Richelle-Maurer *et al.*, 2003), or by symbiotic bacteria or fungi which act as antibiotics, e.g. cribrostatin (Pettit *et al.*, 2000) and as cytostatic agents, e.g. sorbicillactone A (Bringmann *et al.*, 2003). Functionally, these compounds act (most probably) only as defense molecules (Müller *et al.*, 2004). (ii) *Dual form of protection*, where the secondary metabolites are directed against the non-self organisms and also positively modulate the host metabolism. The first proven example is that of okadaic acid (Wiens *et al.*, 2003). (iii) *Immune protection*, where the sponges produce proteinaceous bioactive molecules that arrest the growth of bacteria, e.g. perforin (Thakur *et al.*, 2003) and tachylectin (Schröder *et al.*, 2003), or destroy eukaryotic cells, e.g., agglutinins (Mangel *et al.*, 1992). (iv) *Indirect protection*, where the sponges facultatively comprise surface bacteria that produce antifouling secondary metabolites (Thakur *et al.*, 2003), e.g. tribromophenol (Clare *et al.*, 1999; Müller *et al.*, 2004).

I.2.3.3. Current status in sponge derived bioactive natural products

As already mentioned earlier, compounds from marine sources that have entered into preclinical and clinical trials are dominated by sponge metabolites such as girolline (from *Pseudoaxinyssa cantharella*), bengamide derivative (*Jaspis* sp.) and peloruside A (*Mycale hentsheli*) (Table I.1, Newman and Cragg, 2004).

Table I.1 Status of Marine-Derived Natural Products in Clinical and Preclinical Trials (according to Newman and Cragg, 2004; Simmons *et al.*, 2005)

Name	Source	Status (disease)	Comment
didemnin B	*Trididemnum solidum* (tunicate)	Phase II (cancer)	a cyclic depsipeptide; dropped middle 90s
dolastatin 10	*Dolabella auricularia* (marine microbe derived; cyanophyte)	Phase I/II (cancer)	a linear peptide, many derivatives made synthetically; no positive effects in Phase II trials; no further trials known
girolline	*Pseudoaxinyssa cantharella* (sponge)	Phase I (cancer)	a 2-aminoimidazole derivative; discontinued due to hypertension
bengamide derivative	*Jaspis digonoxea* (sponge-derived)	Phase I (cancer)	ε-lactam peptide derivative, licensed to Novartis, Met-AP1 inhibitor, withdrawn 2002
Cryptophycins (also arenastatin A)	*Nostoc* sp. (blue green algae) and *Dysidea arenaria* (sponge)	Phase I (cancer)	16-membered macrolides, from a terrestrial cyanophyte, but also from a sponge as arenastatin A; synthetic derivative licensed to Lilly by Univ. Hawaii, but withdrawn 2002
bryostatin 1	*Bugula neritina* (bryozoa)	Phase II (cancer)	a macrocylic lactone; now in combination therapy trials; licensed to GPC Biotech by Arizona State Univ.; maybe produced by bacterial symbiont
TZT-1027	synthetic dolastatin	Phase II (cancer)	a linear peptide; also known as auristatin PE and soblidotin
cematodin	synthetic derivative of dolastatin 15	Phase I/II (cancer)	a linear peptide; some positive effects on melanoma pts in Phase II; dichotomy on fate
ILX 651, synthadotin	synthetic derivative of dolastatin 15	Phase I/II (cancer	a linear peptide; in phase II for melanoma, breast, NSCLC
ecteinascidin 743	*Ecteinascidia turbinate* (ascidian)	Phase II/III (cancer) in 2003	a tetrahydroisoquinoline alkaloid, licensed to Ortho Biotech (J&J); produced by partial synthesis from microbial metabolite
aplidine	*Aplidium albicans* (tunicate)	Phase II (cancer)	dehydrodidemnin B, made by total synthesis
E7389	*Lissodendoryx* sp. (sponge)	Phase I (cancer)	Elsai's synthetic halicondrin B derivative
discodermolide	*Discodermia dissolute* (sponge)	Phase I (cancer)	a polyhydroxylated lactone, licensed to Novartis by Harbor Branch Oceanographic Institution
kahalalide F	*Eylsia rufescens* (mollusc)/ *Bryopsis* sp. (green macroalga)	Phase II (cancer)	a depsipeptide, licensed to PharmaMar by Univ. Hawaii; revision of structure
ES-285 (spisulosine)	*Spisula polynyma* (marine clam)	Phase I (cancer)	an alkyl amino alcohol, *Rho*-GTP inhibitor
HTI-286 (hemiasterlin derivative)	*Cymbastella* sp. (sponge)	Phase II (cancer)	a linear peptide; synthetic derivative made by Univ. British Columbia; licensed to Wyeth
KRN-7000	*Agelas mauritianus* (sponge)	Phase I (cancer)	an agelashin derivative (α-galacosyl-ceramide)
squalamine	*Squalus acanthias* (dogfish shark)	Phase II (cancer)	an amino steroid; antiangiogenic activity
E-941 (Neovastat)	shark	Phase II/III (cancer)	defined mixture of < 500JDa from cartilage; antiangiogenic activity as well
NVP-LAQ824	synthetic	Phase I (cancer)	an indolic cinnamyl hydroxamate; derived from psammaplin, trichostatin, and trapoxin structures
laulimalide	*Cacospongia mycofijiensis* (sponge)	preclinical (cancer)	a macrolide; synthesized by variety of investigators
curacin A	*Lyngbya majuscule* (cyanobacterium)	preclinical (cancer)	a thiazole lipid; synthesized, more soluble combi-chem derivatives being evaluated

Table I.1 continued

Name	Source	Status (disease)	Comment
eleutherobin	*Eleutherobia* sp. (octacoral)	preclinical (cancer)	a diterpene glycoside; synthesized and derivatives made by combichem; can be produced by aquaculture
sarcodictyin	*Sarcodictyon roseum* (corals)	preclinical (cancer) (derivatives)	a diterpene; combi-chem synthesis performed around structure
peloruside A	*Mycale hentscheli* (sponge)	preclinical (cancer)	a 16 membered macrolide ring compound
salicylihalimides A	*Haliclona* sp. (sponge)	preclinical (cancer)	a polyketide; first marine Vo-ATPase-inhibitor; similar materials from microbes, synthesized
thiocoraline	*Micromonospora marina* (actinomycete)	preclinical (cancer)	a thiodepsipeptide; DNA polymerase α inhibitor
ascididemin	(tunicates)	preclinical (cancer)	an aromatic alkaloid, reductive DNA-cleaving agents
variolins	*Kirkpatrickia variolosa* (sponge)	preclinical (cancer)	a heterocyclic alkaloid; Cdk inhibitors
dictyodendrins	*Dictyodendrilla verongiformis* (sponge)	preclinical (cancer)	a pyrrolocarbazole derivative; telomerase inhibitors
GTS-21 (a.k.a. DMBX)	Synthetic	Phase I (Alzheimer's)	modification of a worm toxin; licensed to Taiho by Univ. Florida
manoalide	*Luffariaella variabilis* (sponge)	Phase II (antipsoriatic)	a sesterpenoid, discontinued due to formulation problems
IPL-576, 092 (a.k.a HMR-4011A)	*Petrosia contignata* (sponge)	Phase II (antiasthmatic)	a polyhydroxylated sterol; derivative of contignasterol; licensed to Aventis
IPL-512, 602	derivative of 576092	Phase II (antiasthmatic)	with Aventis
IPL-550, 260	derivative of 576092	Phase I (antiasthmatic)	with Aventis
ziconotide (a.k.a. Prialt)	*Conus magnus* (snails)	Phase III (neuropathic pain)	a 25 aminoacid peptide, licensed by Elan to Warner Lambert
CGX-1160	*Conus geographus* (snails)	Phase I (pain)	contulakin G
CGX-1007	*Conus geographus* (snails)	Phase I (pain & epilepsy)	conantokin G, a 16-amino acid *O*-linked glycopeptide; discontinued
AMM336	*Conus catus* (snails)	preclinical (pain)	ω-conotoxin CVID
χ-conotoxin	*Conus* sp. (snails)	preclinical (pain)	conotoxin MR1A/B
CGX-1063	Thr10-contulakin G	preclinical (pain)	modified toxin
ACV1	*Conus victoriae* (snails)	preclinical (pain)	α-conotoxin Vc1.1

Marine sponges as the most primitive of all multi cellular animals are probably the most commonly exploited marine organisms which could be seen in the domination of marine metabolites which are reported to be derived from sponges. Most of these metabolites are novel, structurally diverse compounds, many of which have no clear biogenetic origin (Blunt *et al.*, 2005). Sponges, particularly those without spicules, frequently produce large quantities of secondary metabolites that are thought to deter potential predators and to inhibit the growth of fouling organisms.

Because many sponges contain symbiotic microorganisms, there is always some uncertainty concerning the true origin of sponge metabolites. However, the majority of metabolites are now believed to be produced by the sponges, possibly in specialized spherulous cells (Faulkner, 1984).

Even though a number of sponge products have entered preclinical and clinical trials, up to now only Ara-A and Ara-C (derivatives of the sponge unusual nucleosides discovered by Bergman and Feeney) have advanced to the pharmaceutical market as antiviral and antileukemic agents, respectively (McConnell *et al.*, 1994; Sipkema *et al.*, 2005). It could be explained by the fact that bioactivity alone is not enough to determine which compound can enter drug development by the pharmaceutical industry. Factors such as establishment of a cost-effective source for large-scale supply, and "drugability" in a human model system are more likely to be considered. Compounds which are expensive to produce or scarcely available will only can enter drug development if they really have unique pharmacological profiles including new mechanisms of action against a particular drug target or disease. This fact is illustrated by those sponge-derived compounds which have advanced to human clinical testing. They were all found to be amenable to cost-effective production, thus solving the supply question early-on in the development continuum (Sipkema *et al.*, 2005).

I.2.3.3.1. Halogen containing metabolites

Marine sponges are a rich source of highly halogenated compounds. Their function in sponges is presumably to resist feeding by fish and fouling by barnacles, bacteria, and fungi (Gribble, 2004). Despite the relative concentrations of chloride, bromide and iodide ions in sea water (559 mM, 0.86 mM and 0.45 µM respectively);

there exists a marked predominance of bromine containing metabolites (Faulkner, 1995). Although chloride is more abundant than bromide in the oceans, marine organisms utilize (oxidize) more bromide than chloride for incorporation into organic compounds. This may reflect the wealth of bromoperoxidase (BPO) relative to chloroperoxidase (CPO) in marine life, and the fact that chlorine cannot be oxidized to active chlorine by BPO (Gribble, 1996b, 1998). Bromide ions have then greater ease to be oxidized and give bromonium species which react readily as electrophils with unsaturated species (Whitehead, 1999).

Halogen containing heteroatomatic natural products is particularly common class of sponge derived secondary metabolites. Perhaps due to their enormous reactivity towards electrophilic halogenation reactions, pyrroles, indoles, phenols, and tyrosines are commonly found to be halogenated in sponges (Gribble, 2004).

In particular, brominated pyrroles have been isolated on several occasions as major constituents of marine sponges. Many of the simpler members of this class of compounds are structurally related as they comprise two heterocyclic rings linked by a linear chain (Whitehead, 1999). Over the last thirty years, numerous similar alkaloids with various structures and interesting biological activities have been isolated essentially (but not exclusively) from various species of Agelasidae, Hymeniacidonidae and Axinellidae (Williams and Faulkner, 1996).

As an example is tauroacidins A and B, two novel taurine-residue-containing bromopyrrole alkaloids which were isolated from an Okinawan sponge *Hymeniacidon* sp. (Fig.I.1) (Kobayashi *et al.*, 1997). Both alkaloids were reported to show inhibitory activity against EGF receptor kinase and *c-erb B*-2 kinase (IC_{50}, 20μg ml^{-1} each) (Kobayashi *et al.*, 1997).
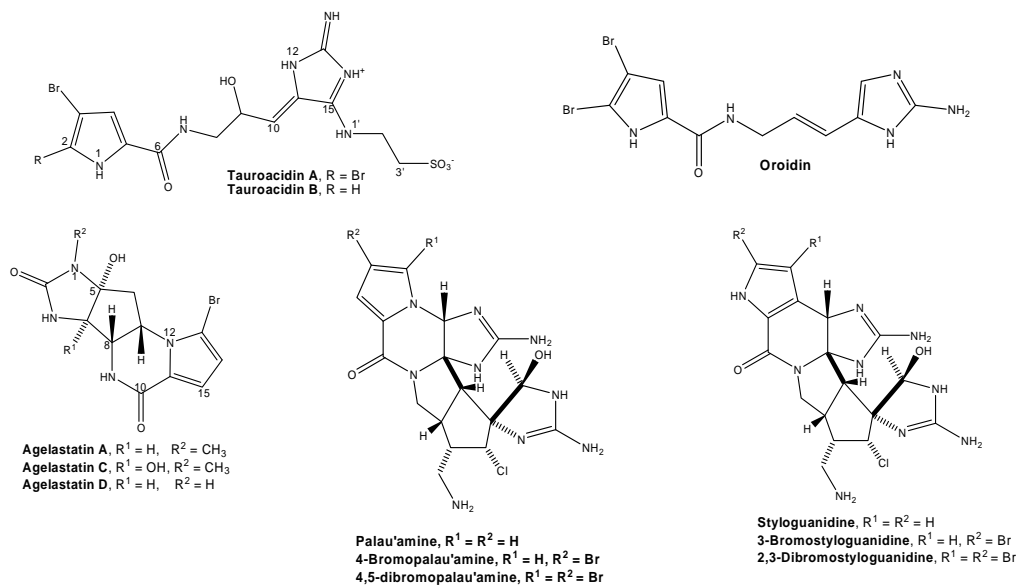
Fig.I.1. Some halogen containing pyrroles from sponges

Another example of bromopyrrole alkaloids is the agelastatins. These compounds have a unique fused tetracyclic skeleton which may formally be derived from an open chain pyrroloaminopropylimidazole precursor similar in structure to oroidin (Whitehead, 1999). In 1998, Molinski and collaborators reported the isolation of the known agelastatin A together with two new alkaloids, agelastatins C and D from a West Australian sponge *Cymbastela* sp. (Axinellidae). Agelastatin A was highly toxic to brine shrimp with LC_{50} of 1.7 ppm (5.0 μM) whereas agelastatin C was much less toxic with LC_{50} of ~ 220 ppm. Insecticidal activity of agelastatin A was reported to be comparable to a commercial preparation of the biopesticide *Bacillus thuringiensis* (Hong *et al.*, 1998; Whitehead, 1999).

The palau'amines as another series of complex, halogen containing alkaloids belonging to oroidin family exhibit six contiguous rings and an unbroken chain of eight chiral centers (Whitehead, 1999). Palau'amine and its 4-bromo and 4,5-dibromo derivatives were isolated in 1998 by Scheuer and co-workers together

with three previously reported ring A regioisomers (styloguanidines), from the sponge *Stylotella aurantium* collected near Wonder Channel and Rock Islands, Republic of Belau. Palau'amine itself was reported to display a remarkable range of biological activities with an $IC_{50} < 18$ ngml^{-1} in the mixed lymphocyte reaction and IC_{50}'s of 0.1 and 0.2 μgml^{-1} against P-3888 and A-549 cel lines, respectively (Whitehead, 1999). The preclinical studies of this compound are currently in progress for anti-fungal, anti-tumor and immunosuppressive agent (Kinnel *et al.*, 1998; Whitehead, 1999).

Other important halogen containing secondary metabolites from sponges are the brominated compounds biogenetically related to tyrosine (Fig.I.2). Although this group of compounds is more likely to be found in Verongid sponges (Hamman and Scheuer, 1993; Tabudravu and Jaspars, 2002), nevertheless, König and Wright (1993) have reported the isolation of bromotyrosine-derived alkaloids (agelorins A and B, and 11-epifistularin-3) from *Agelas oroides*.

Psammaplin A, a symmetrical bromotyrosine disulfide possessing oxime moieties isolated from Verongid sponges, was found to have potent cytotoxicity to P 388 cells (IC_{50} of 0.3 μgml^{-1}) and to co-occur with its dimeric metabolite, bisaprasin (Arabshahi and Schmitz, 1987; Quiñoà and Crews, 1987; Rodriquez *et al.*, 1987). The fact that the psammaplins have been isolated from a diversity of sponge "sources" and that brominated aromatic amino acid derivatives are common in marine bacteria suggest that these metabolites may actually be derived from biosynthetic pathway of microorganisms living in association with sponges (Simmons *et al.*, 2005).

Both psammaplin A and bisaprasin were reported to be dual inhibitors of the DNA methyl transferase and histone deacetylase (Pina *et al.*, 2003). This is an

interesting finding considering the potential relationship between DNA methyl transferase and histone deacetylase as epigenetic modifiers of tumor suppressor gene activity (Pina *et al.*, 2003). Furthermore, psammaplin A has also been reported to inhibit topoisomerase II (Kim *et al.*, 1999) and aminopeptidase N with in vitro angiogenesis suppression (Shim *et al.*, 2004). However, due to the physiological instability of the psammaplin class, direct clinical development has thus far precluded. Nevertheless, its analogue substance, NP-LAQ824 (Remiszewski, 2003), has recently entered phase I clinical trials in patients with solid tumors or leukemia (Simmons *et al.*, 2005).
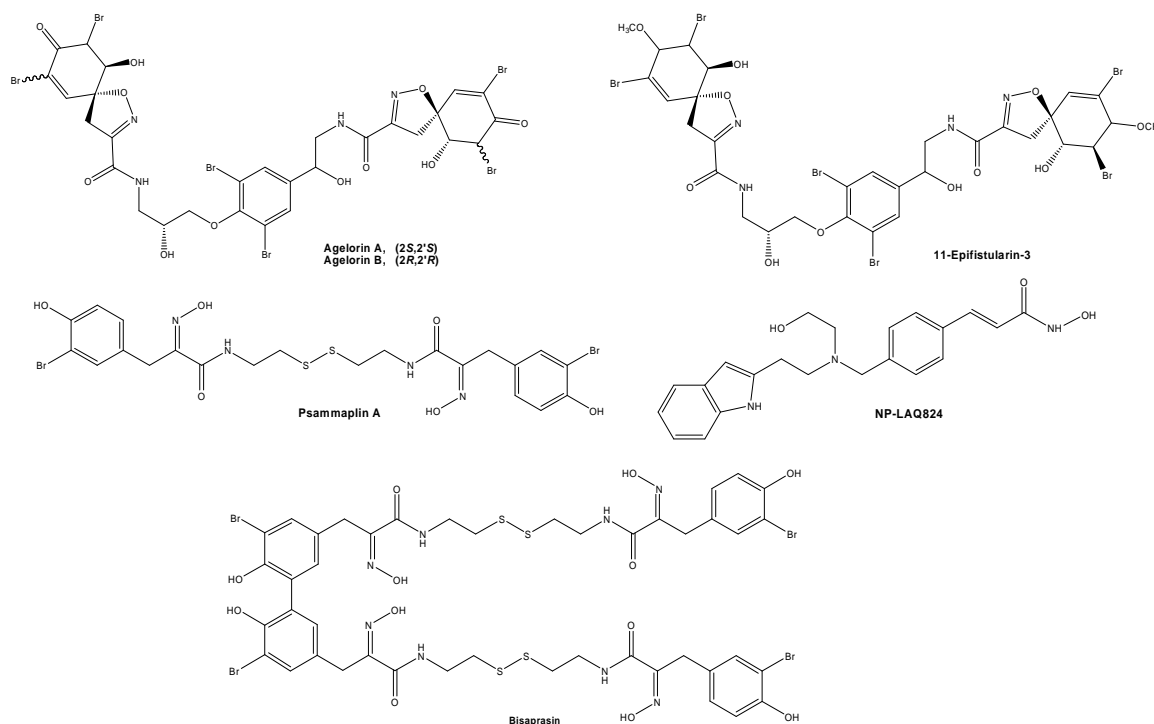
Fig.I.2. Some bromotyrosine derived sponge metabolites

I.2.3.3.2. Terpenoids

Based on data provided by MarinLit (2002), metabolites biogenetically derived from terpenes are observed to dominate in the reported marine products as well as in sponge metabolites. Sesterterpenes is found to be the major terpenoids

sponge metabolites followed by diterpenes, triterpenes (steroids) and meroterpenes, respectively (Blunt *et al.*, 2004). Many marine terpenoids feature uncommon functionality and/ or carbon skeletons which are unique, and as such their detection, isolation and structure elucidation present exciting and rewarding challenges (Capon, 2001). Several studies show that sponges are rich in terpenoids and steroids which function in anti-predation, space competition and control of epibiont overgrowth (Thakur and Müller, 2004).

Keyzers and Davies-Coleman (2005) in their review on antiinflamatory derived compounds from marine sponge have mentioned the domination of isoprenoid derived metabolites, especially sesterterpenes as major reported bioactive substances. Manoalide, a sesterterpene originally isolated from *Luffariella variabilis* is a sponge-derived antiinflamatory agent (de Silva and Scheuer, 1980), which was found to irreversibly inhibit the release of arachidonic acid from membrane phospholipids by the enzyme phospholipase A_2 (PLA_2) (Glaser and Jacobs, 1986, 1987). The pharmacophore of manoalide was reported to contain two masked aldehyde groups (hemiacetals) that reacted with lysine residues on the interfacial binding site of PLA_2, which further prevented the enzyme from binding to membranes rather than blocking the active sited of PLA_2 (Glaser *et al.*, 1989; Ortiz *et al.*, 1993; Potts *et al.*, 1992a, 1992b; Faulkner, 2000). Manoalide was patented by the University of California and licensed to Allergan Pharmaceuticals, who took it through to Phase I clinical trials for the treatment of psoriasis. Allergan and several other companies have used manoalide as the starting point for medicinal chemistry programs, but so far, no drug that is obviously based on manoalide has reached the market (Faulkner, 2000) due to formulation problems (Newman and Cragg, 2004). However, manoalide is used as a standard drug for PLA_2 inhibition and is

commercially available (Faulkner, 2000). During the development program, lack of sponge material was never a problem but the presence of both manoalide and luffariellin, which are difficult to separate, in some specimens of *L. variabilis* might have presented a problem if manoalide had proved to be a successful drug (Kernan *et al.*, 1987; Faulkner, 2000).

IPL-576092, a derivative of contignasterol was introduced into clinical trials as an antiasthma agent by Inflazyme in conjunction with Aventis Pharma under the code number HMR-4011A (Newman and Cragg, 2004). Contignasterol itself was reported to be isolated from marine sponge *Petrosia contignata* (Thiele) by Burgoyne *et al.* (1992), with the absolute configuration being reported later by Yang and Andersen (2002). This compound and its chemically modified derivatives were observed to inhibit the release of histamine from rat mast cells (Takei *et al.*, 1994) and also from the lung tissue of guinea pigs (Bramley *et al.*, 1995). Inflazyme has reported that IPL-576092 successfully completed a Phase II "Allergen Challenge" trial in April 2002 as a novel oral therapy for asthma and that it is now in clinical trials for inflammatory diseases of the skin and eye (Newman and Cragg, 2004).

Other interesting examples of terpene metabolites are sesquiterpenes and diterpenes containing isocyano, thiocyano, and formamide functionalities found in marine sponges of families Axinellidae and Dictyonellidae (Fusetani, 2004). These metabolites exert a wide range of biological activities, e.g., antifungal, cytotoxic, ichtyotoxic, and antimalarial (Chang, 2000) as well as antifouling activity (Fusetani *et al.*, 1996; Okino *et al.*, 1995, 1996a, 1996b; Hirota *et al.*, 1996; Nogata *et al.*, 2003). Among these terpenoids, particulary important as antifouling agents are kalihinene X (Fusetani *et al.*, 1996); kalihipyran B (Okino *et al.*, 1995), 15-formamidokalihinene (Okino *et al.*, 1995), and 10β-formamidokalihinol A (Hirota *et al.*, 1996). All showed

inhibition of the larval settlement and metamorphosis at concentrations less than 0.1 μg mL^{-1}, while their toxicity towards the barnacle cyprids was very low with LD$_{50}$ >100 μg mL^{-1} (Fusetani, 2004).
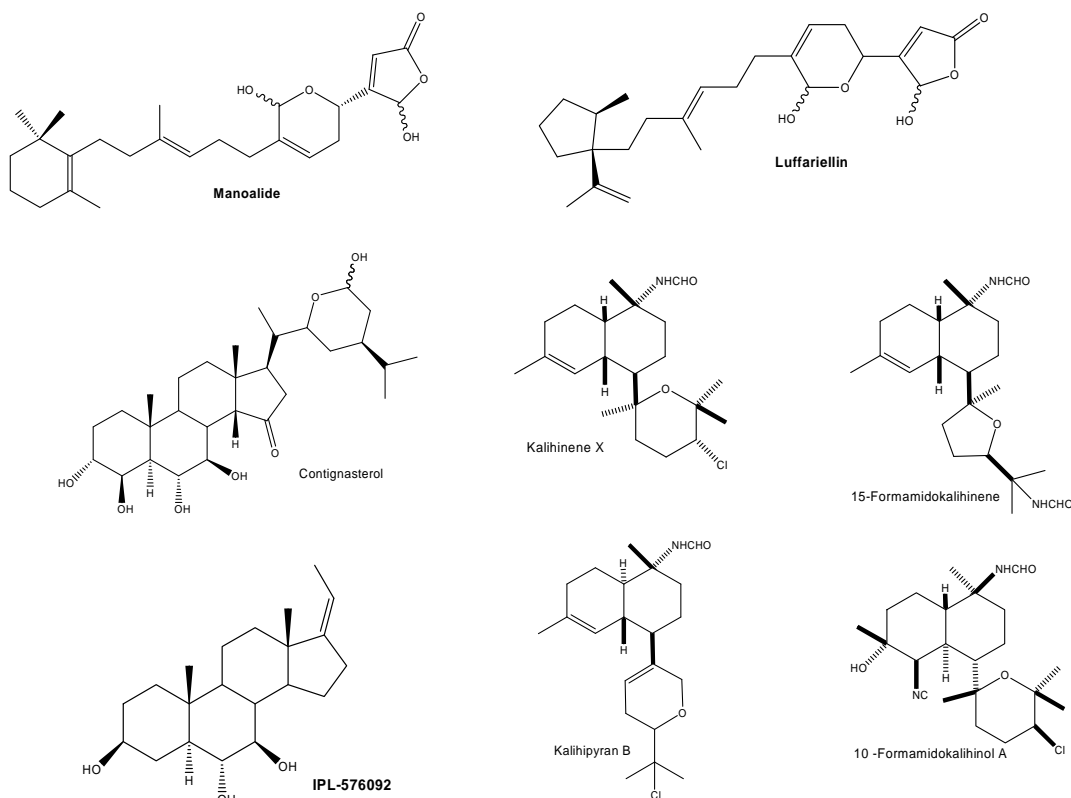
Fig.I.3. Some terpenoid derivatives from marine sponge

I.3.   Statement of the objectives

Screening for potential drug candidates has been developed in recent years by using a number of high throughput and cost-effective assays. The compounds may be derived from new synthetic approaches such as combinatorial chemistry, or from natural sources (Bevan *et al.*, 1995). At first, the combinatorial chemistry approach was assumed to be the only promising route to identify lead structures for therapeutic use. However, presently, bioprospecting of natural products from marine sessile such as sponges appears superior to the chemical approach. It means that

the economical value of these natural products as potential lead structures is increased far higher than those compounds gained from chemical synthesis (Müller *et al.*, 2004). Marine-derived natural products with their unique structural features and pronounced biological activities may serve as lead structures for potential new drugs. Sponges as sessile invertebrates which mostly lack morphological defense structures have so far identified to be the major source of marine derived compounds including some of the most interesting drug candidates (Proksch *et al.*, 2003).

Even though sponges can be found in all seas, they reach the highest biodiversity in the tropical region. The Indonesian archipelago, in particular with its close to 18,000 different islands and its teeming coral reefs, is known to be a hot spot of sponge biodiversity (Proksch *et al.*, 2003). Considering that the sponges in tropical areas have more pressure from predation (Carpenter, 1986; Proksch *et al.*, 2002) as well as microbiological infection (Proskch *et al.*, 2002), Indonesian sponges can be expected to provide interesting and diverse new secondary metabolites.

This study is focused on the isolation and structure elucidation of bioactive natural products derived from Indonesian marine sponges. The sponge specimens were collected from four different places in Indonesia i.e., off-coast Menjangan island (northern part of Bali) and off coast Watudodol, Bali strait in October 2003; off coast Ujung Pandang, Celebes in 1996, and off-coast Peniki island, an island belonging to Seribu Islands, northern part of Java in October 2005. Bioassay conducted in this study covered antimicrobials i.e antibacterial and antifungal; cytotoxicity against L5178Y mouse lymphoma cells; protein kinase inhibition; antifouling and biofilm inhibition using *S. epidermidis*. Chemical structures of the isolated compounds were elucidated on the basis of extensive spectroscopic analysis involving one and two dimensional NMR spectroscopy as well as mass spectrometry.

24

II. Materials and Methods

II.1. Collection sites

Fig.II.1. Site of collection map (map was reproduced from *www.undp.or.id*)
1: Menjangan Island, Bali; 2: Watudodol, Bali Strait; 3: Peniki East Island, Seribu Islands;
4: Ambon, Maluku

II.2. Biological materials

Sponge specimens were collected by SCUBA diving in four different collection sites in Indonesia (Fig.II.1) and directly preserved in ethanol. The voucher specimens (sponge 2 – 6) were identified by Dr. Rob. W.M. Van Soest (Zoological Museum, Amsterdam, The Netherlands); and sponge 1 (see Section II.2.1) was identified by Dr. Nicole de Voogd (Institute for Biodiversity and Ecosystem Dynamics, University of Amsterdam, The Netherlands).

II.2.1. *Agelas* n.sp. (sponge 1)

The red-orange sponge (Fig.II.2) was collected from Peniki East Island, Indonesia on October 2005 by Dr. Nicole J. de Voogd. The taxonomical identification

of this undescribed *Agelas* species is still under investigation at the National Museum of Natural History, Leiden, The Netherlands. The sponge classification falls as follows: phylum Porifera; class Demospongiae; order Agelasida; family Agelasidae; genus *Agelas*; species *Agelas* n.sp. (de Voogd & Parra, in prep.)

II.2.2. *Agelas nakamurai* (sponge 2)

The second *Agelas* specimen investigated in this study (Fig.II.2) was a bright orange sponge collected by Susilo Hadi (Dept. of Zoology, Faculty of Biology, GMU, Indonesia) at a depth of 12 m off coast of Menjangan Island (North of Bali Island), Indonesia on October 2003. A voucher specimen has been deposited in the Zoological Museum Amsterdam under reg. no. ZMAPOR18297. Like sponge 1 (II.2.1), this Demospongiae sponge belongs to the family Agelasidae; genus *Agelas*, species: *Agelas nakamurai* (Van Soest, 2002).

Agelas species are usually large, bright-coloured and conspicuous inhabitants of shallow-water reefs and other clean-water environment (Van Soest, 2002). The sponge genus *Agelas* has been widely known to possess pyrrole 2-carboxylic acid derivatives which are usually brominated. In some species, the occurrence of unique terpenoids derivatives i.e. sesquiterpenoid derivatives of hypotaurocyamines and or adenine derivatives of diterpenes has been reported (Braekman *et al.*, 1992).

II.2.3. *Pseudoceratina purpurea* (sponge 3)

The sponge was collected on October 2003 by SCUBA diving in Watudodol, Banyuwangi, by Juswono (Dept. of Zoology, Faculty of Biology, GMU, Indonesia) at a depth of 10–30 m (Fig.II.2). A voucher specimen is deposited in the Zoological Museum Amsterdam under reg. no. ZMAPOR17800.

This sponge belongs to the taxonomic class of Demospongiae; order Verongida; family Pseudoceratinidae; genus *Pseudoceratina* (Bergquist and Cook, 2002); species *Pseudoceratina purpurea* (Carter). It showed sticky surface, elastic and irregular in shape, a firm consistency, brown colour with dark blue and yellow spots. According to Bergquist and Cook (2002), Pseudoceratinidae sponges exhibit fibre skeleton, which is sparse, dendritic and with no investing bark. The fibres are extremely irregular, knotted in places, expanding and contracting along their length and below the surface fanning out in brushes. Pigmentation is uniform throughout the sponge, the surface is conulose and the texture rubbery, flexible in ramose forms, tending to incompressible in massive species. Sponge order Verongida is well-known due to their tyrosine biogenetically related compounds. It is believed that these constituents may be produced by associated bacteria (Simmons *et al.*, 2005)

II.2.4. *Axynissa sp.* **(sponge 4)**

This yellowish brown sponge was collected in Ambon with SCUBA diving by Frank Bohnenstengel at a depth of 20 ft, in October 1996 (Fig.II.2). A voucher specimen is deposited in the Zoological Museum in Amsterdam under reg. no. ZMAPOR19077. It belongs to the class Demospongiae; order Halichondrida; family Halichondriidae; genus *Axinyssa* (Erpenbeck and Van Soest, 2002).

According to Erpenbeck and Van Soest (2002), the sponge genus *Axynissa* is massive, lobate or tubular sponges with conulose surface. Ectosomal region lacks a distinct surface skeleton, largely organic, tough, with sparsely scattered spicules and protruding spicule bundles. Choanosomal skeleton is disorganized with spicules strewn in confusion and/or composed of vaquely ascending, widely spaced vertical tracts of large oxeas or strongyloxeas, forming loose bundles. Choanosome is with poor or moderate spongin development, but heavy intespicular collagen; spicule

27

density relatively low. Spicules are oxeas, strongyloxeas or stylote modifications, usually of only one size class (Erpenbeck and Van Soest, 2002).
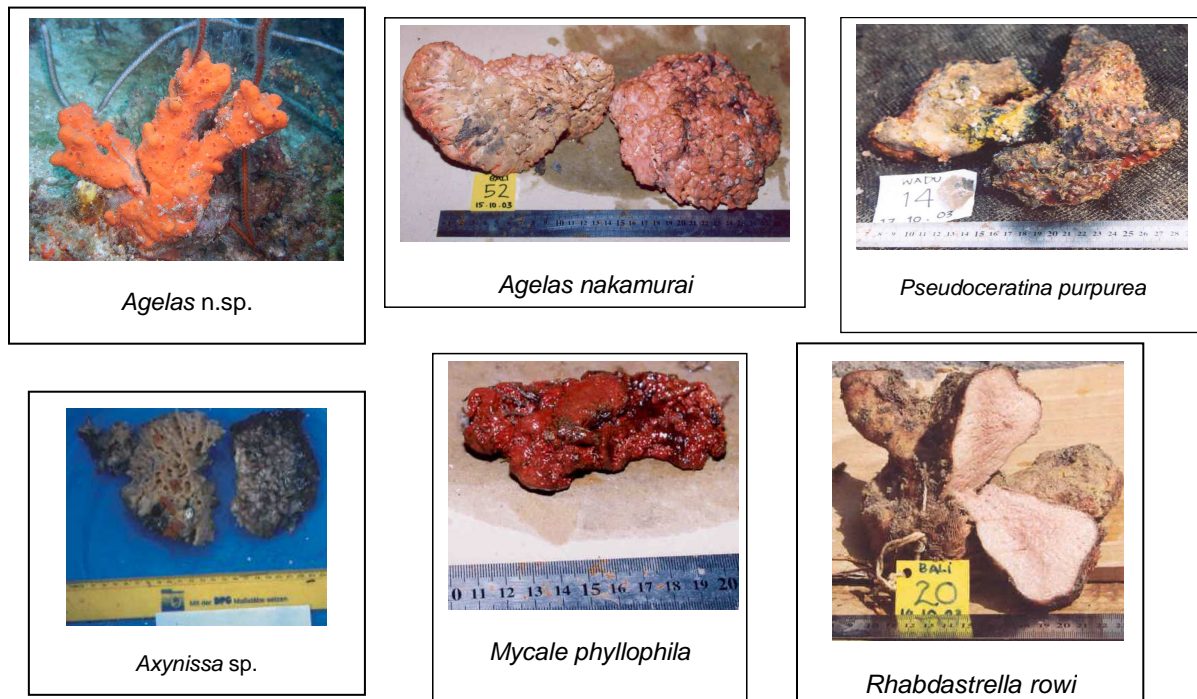
Fig.II.2. Sponge specimen pictures
(*Agelas* n.sp. picture was taken by Dr. Nicole J. de Voogd; *A. nakamurai*, *P. purpurea*, *M. phyllophyla* and *R. rowi* pictures were taken by Juswono; *Axynissa* sp. picture was taken by Frank Bohnenstengel)

II.2.5. *Mycale phyllophila* (Hentschel) (sponge 5)

This red brownish with firm consistency sponge (Fig. II.2) was collected in October 2003 by Susilo Hadi (Dept. of Zoology, Faculty of Biology, GMU, Indonesia), near Menjangan Island (North of Bali Island) from the depth of 10 – 30 m. A voucher specimen is deposited in the Zoological Museum in Amsterdam under reg. no. ZMAPOR18344. This sponge belongs to the class Demospongiae; order Poecilosclerida; family Mycalidae; genus Mycale (Van Soest and Hajdu, 2002); species *Mycale phyllophila* (Hentschel).

II.2.6. *Rhabdastrella rowi* (Dendy) (sponge 6)

This brownish sponge (Fig.II.2) was collected from the depth of 12 m near Menjangan Island (North of Bali Island), Indonesia in October 2003 by Juswono

(Dept. of Zoology, Faculty of Biology, GMU, Indonesia). A voucher specimen was deposited in the Zoological Museum in Amsterdam, under reg. no. ZMAPOR1829. Its taxonomic classification is as follows, phylum Porifera; class Demospongiae; order Astrophorida; family Ancorinidae; genus *Rhabdastrella* (Uriz, 2002); species *Rhabdasterella rowi* (Dendy).

II.3. Isolation methods

II.3.1. General laboratory chemicals

The chemicals used in the detection and isolation methods were anisaldehyde (4-methoxybenzaldehyde), hydrochloric acid and concentrated sulphuric acid (all provided by Merck, Darmstadt, Germany); ammonium hydroxide, glacial acetic acid, (Fluka, Seelze, Germany); dimethylsulfoxide, trifluoroacetic acid 99%, extra pure (Acros$^{®}$ organic, Geel, Belgium).

II.3.2. Solvents

Solvents used for separation techniques were acetone; acetonitrile; dichloromethane; ethyl acetate; *n*-hexane; methanol. These solvents were purchased from the Institute of Chemistry HHU Düsseldorf. They were distilled before using and special grade were used for spectroscopic measurements. Others solvent used were *n*-butanol and acetone (Fluka, Seelze, Germany), ethanol (Merck, Darmstadt, Germany)

II.3.3. General equipments

Balance : Sartorius RC210P; Sartorius BL1500

Centrifuge : Biofuge

Fraction collector : Retriever II

Freeze dryer : LYOVAC GT2; Pump TRIVAC D10E

Hotplate	: Camag
Syringe	: Hamilton 25, 100, 250, and 500 μL
Mill	: Molinex 354
Magnetic strirer	: Variomag Multipoint HP
Mixer	: Braun
pH meter	: electrode Inolab; Behrotest pH 10 set
Rotary evaporator	: Büchi Rotavap RE111; Büchi Rotavap R-200, Vacuubrand MG 2C
Drying Ovens	: Heraeus T5050
Sonicator	: Bandelin sonorex RK 102
UV lamp	: Camag (254 and 366)
Vacuum Exicator	: Savant SpeedVac SPD 111V
Nitrogen pump	: Pump Savant VLP80
Pulsatic pump	: Duramat

II.4.   General isolation procedure

II.4.1.   Extraction and Solvent partitioning

Sponge specimens were dried at room temperature and by lyophilization (if necessary) after decantation of ethanol in which the sponge specimen was preserved. These sponge samples were then ground and exhaustively extracted with methanol followed by dichloromethane. Crude extracts were obtained by evaporating the supernatants under reduced pressure.

Solvent partitioning of the crude extracts was commonly initiated with *n*-hexane and aqueous methanol (90:10 v/v) at a ratio of 1:1. While the hexane phase was obtained by evaporation of the organic solvent, the aqueous phase was

concentrated under reduced pressure and partitioned further between water and ethyl acetate at equal volumes. The ethyl acetate fraction was obtained and again concentrated while the water phase was then partitioned with *n*-butanol to obtain the butanol fraction.

Crude extracts and fractions were then chemically investigated and analyzed by using thin layer chromatography (TLC), analytical HLPC and LC/MS to determine further isolation work.

II.4.2. Chromatographic methods

II.4.2.1. Thin layer chromatography

Thin layer chromatography (TLC) method was utilized to detect mixtures of compounds in samples, or to check the purity level of compounds during separation work. TLC was conducted for each fraction prior to further chemical work, in order to choose the appropriate solvent systems to be used as mobile phase for column chromatography, to get an overview of the identity and the qualitative purity of the fraction and the isolated compounds.

TLC was performed on precoated TLC plates (AluO), silica gel 60 F_{254} (layer thickness 0.2 mm, Merck, Darmstadt, Germany) for semi polar to non polar substances and with precoated TLC RP18 F_{254} plates (layer thickness 0.25 mm, Merck, Darmstadt, Germany) for more polar substances. Common mobile phase used for non polar substances was *n*-hexane:ethyl acetate (90:10; 80:20; 70:30, v/v); for semi polar substances was CH_2Cl_2:MeOH (95:5; 90:10; and 80:20, v/v) and *n*-butanol:acetic-acid:H_2O (4:1.5 v/v, upper phase) for semi polar to polar compounds. TLC on RP18 F_{254} was performed by using the different solvent ratios of MeOH:H_2O (90:10; 80:20; 70:30; 60:40 and 30:70, v/v).

Spots on the TLC describing the separation of compounds were detected under UV absorbance at 254 and 366 nm, followed by spraying the TLC plates with anisaldehyde-H_2SO_4 reagent and subsequent heating at 110° C or by spraying with Dragendroff reagent (for alkaloids).

The spray reagent anisaldehyde/H_2SO_4 was prepared as described below:

For 100 mL reagent, 10 mL glacial acetic acid was added to 85 mL methanol followed by 5 mL concentrated H_2SO_4 (added slowly) and 0.5 mL anisaldehyde. The reagent was stored in an amber coloured bottle and kept refrigerated until used.

The spray reagent Dragendorff was made as described below:

Solution A is made by dissolving 0.5 g bismuth nitrate ($Bi(NO_3)_3$ $5H_2O$) in 20 mL of 20% acetic acid. Solution B is 5 mL solution of 40% KI in water. Before usage, 20 mL solution A is mixed with 5 mL solution B and 70 mL water. The reagent was then stored in an amber coloured bottle and kept refrigerated until used.

II.4.2.2. Vacuum liquid chromatography

Vacuum liquid chromatography (VLC) was used as an initial separation procedure of large amounts of samples. The apparatus consists of a 500 cm sintered glass funnel with an inner diameter of 6 cm. Silica gel 60 (40 – 63 μm mesh size, Merck, Darmstadt, Germany) was packed to a hard cake at a height of 10 – 20 cm under applied vacuum. The sample used was mixed with small amount of silica gel using volatile solvents and applied onto the top of column, followed by paper disk and sea sand (approx. 2 cm in height). The elution scheme was started with the most lipophilic solvent e.g. 100% *n*-hexane and followed gradually by increasing amount of more polar solvent (e.g. ethyl-acetate) until 100% ethyl-acetate was reached. The elution was then followed by step gradient elution of dichloromethane and methanol

(starting from 100% dichloromethane to 100% methanol) to give successive fractions. The flow of solvent was induced in a closed system using vacuum to yield fractions collected in round bottom flasks.

II.4.2.3. Column chromatography

Fractions derived from liquid-liquid partitioning or VLC were subjected to repeated column chromatography using appropriate stationary and mobile phase (solvent systems) previously determined by TLC. The following separation systems used in this study were as follows.

A. Normal phase chromatography, using silica gel 60 (40 – 63 µm mesh size, Merck, Darmstadt, Germany) in conjunction with a non-polar mobile phase such as *n*-hexane, dichlormethane, etc. Thus hydrophobic compounds elute more quickly than hydrophilic compounds.

B. Size exclusion chromatography, using Sephadex LH20, (25 – 100 µm mesh size, Merck, Darmstadt, Germany). This method is involving separations based on molecular size of compounds being analysed. The stationary phase consists of porous beads. The larger compounds will be excluded from the interior of the bead and thus will elute first. The smaller compounds will be allowed to enter the beads and elute according to their ability to exit from the small sized pores they were internalised through. Sephadex LH-20 is the preferred stationary phase since it swells adequately in organic solvents (e.g. methanol). The useful fractionation range is approximately between molecular weight of 100 – 4000. Thus compounds of molecular weight of approx 4000 are usually not retained by Sephadex LH20 (Salituro and Dufresne, 1998).

II.4.2.4. Low pressure liquid chromatography

Low pressure liquid chromatography was performed on prepacked LOBAR® columns. In order to increase effieciency on the separation, low pressure (40 – 60 mbar) was applied to run the mobile phase through the columns. The following separation systems used were as follows.

A) Stationary phase: RP-18, 40-63 μm (LOBAR®, size A and B); solvent system: step gradient mixture of methanol-water

B) Stationary phase: silica gel 60, 40-63 μm (LOBAR®, size A and B); solvent system: step gradient mixture of dichloromethane-methanol

II.4.2.5. High performance liquid chromatography

A modern high performance liquid chromatography system (HPLC) consists of the reservoir of mobile phases, the pump, solvent mixer, auto-sampler, auto-injector, the separation column, and the detector. The main difference between HPLC and other modes of column chromatography is that the size of stationary phase particles is comparatively low (3-10 μm) and are tightly packed to give a very uniform column bed structure. HPLC utilizes high pressure pumps to run the solvent through the bed thus increase the efficiency of the separation (Stead, 1998).

Chemicals used in this study for HPLC were nanopure water (distilled and heavy metals free water) obtained by passing distilled water through nano- and ion exchange filter cells (Barnsted, France); methanol Chromanorm® for HPLC (VWR, Leuven, Berlgium); phosphoric acid Normapur® (85% p.a, Merck, Darmstadt, Germany); acetonitrile for HPLC (Acros® organic, Geel, Belgium); formic acid 98 – 100% p.a. (Riedel-de Haën®, Sigma-Aldrich, Seelze, Germany).

II.4.2.6. Analytical HPLC

The analytical HPLC technique was performed to identify the distribution of peaks either from crude extracts or fractions, as well as to evaluate the purity and identity of isolated compounds. Compounds were applied onto the column by auto sampler machine which injected a plug of sample dissolved in appropriate solvent. Different components in the sample mixture passed through the column at different rates depend on their partitioning behaviour between the mobile liquid phase and the stationary phase, resulted the difference in their retention time.

Equiments used in this study were as follows.

Program   : Chromeleon version 6.3

Pump   : Dionex P580A LPG

Detector   : Dionex, Photodiode Arrray Detector UVD 340S

Autosampler   : ASI-100T

Column Thermostat: STH 585

Column   : Knauer, 5.0 mmID; packing material 5 μm

Eurospher-100 C-18

As standard analytical program, column was initially equilibrated isocratically with 10:9 [methanol: acidic-nanopure water (adjusted to pH 2 with phosphoric acid)] in 5 minutes then the solvent was gradually changed to 100% methanol in 30 minutes which was continued to 40 minutes with 100% methanol. Injection volume was 20 μL. Compounds having chromophores are detected by UV-Vis diode array detector at 240 nm, 254 nm, 280 nm and 365 nm. The result could be automatically compared with internal spectral library data.

II.4.2.7. Liquid chromatography/mass spectroscopy

Liquid chromatography/mass spectroscopy is a separation technique which can be used to a very wide range of organic compounds, including non-volatile and thermally fragile molecules. This method is useful prior to the fractionation of target compounds, to detect the presence of new compounds and compounds which do not have chromophores. In LC-MS, the liquid chromatography is combined with mass spectrometers to provide useful information regarding the molecular weight, identity, quantity, as well as the purity of samples. The sensitivity and selectivity are increased considering that even though two compounds may have similar UV spectra or retention time or even similar mass spectra; it is unlikely for two different compounds to have all these similarities (Ardrey, 2003).

LC/MS equipment used in this study was the Finnigan LCQ-DECA (mass spectrometer); Agilent 1100 series for HPLC system (pump, detector and autosampler): column Knauer, 125 mm L, 2 mm ID, prepacked with Eurospher-100 C18 (5 μm) and with integrated pre-column. As standard analytical program, column was initially equilibrated isocratically with 10:9 [acetonitrile: acidic-nanopure water (containing1% formic acid)] in 5 minutes then the solvent was gradually changed to acetonitrile 100% in 30 minutes which was continued to 10 minutes with 100% acetonitrile. HPLC was run on a Eurospher C-18 reversed phase column.

II.4.2.8. Semi-preparative HPLC

Natural products are commonly available only as minor components or mixtures of closely related structures in the extract. In such cases, a separation technique which offers sensitivity and resolving power such as HPLC will be required. The semi-preparative HPLC was utilized for the purification or isolation of pure

compounds from fractions previously obtained from other methods of column chromatography. The solvent system, either gradient or isocratic and the program used were determined primarily based on the previous analytical HPLC data. These included the retention time of the target compounds and the complexity of the mixture. The sample dissolve in appropriate solvent was injected into the system, in a maximum concentration of 2 mg/mL. The solvent system was pumped through the column at a flow rate of 5 mL/min. The eluted peaks, which were detected by the online UV detector and recorded on chromato-integrator, were separately collected in glass test tubes.

Equipment used in this study for semi-preparative HPLC (LaChrom Merck Hitachi) were as follows,

Pump   : LaChrom L-7100

Detector   : UV detector LaChrom L-7400

Printer   : Kipp & Zonen Flatbed Recorder type BD 11E

Column   : Knauer, 8.0 mmID; packing material 10 μm

        Eurospher-100 C-18

II.5. Isolation of secondary metabolites from *Agelas* n.sp. (Fig.II.3a)

Lyophilized sponge tissue (198 g) was ground and extracted exhaustively with acetone followed by methanol. After removing solvent under reduced pressure, the resulting methanol extract was partitioned between *n*-hexane and 90% MeOH-water to yield the hexane fraction. The residue was partitioned further between ethyl acetate and H_2O to obtain the ethyl acetate fraction (4.3 g). The water phase was partitioned against *n*-BuOH to yield the butanol (3.5 g) and the water fractions.

The ethyl acetate fraction was subjected to silica gel G60 vacuum liquid chromatography (VLC) by using mobile phase with increasing polarity from 100% *n*-hexane to 100 % ethyl acetate followed by 100% dichloromethane to 100% MeOH. This method yielded 21 fractions including fraction 12 which was later identified as **midpacamide** (**13**, 2.0 g). Other VLC fractions were separated further as follows. Fraction 10 (700 mg) was purified by using a silica gel column G60 (DCM-MeOH, 95:5) to obtain the new **4-(4,5-dibromo-1-methyl-1*H*-pyrrole-2-carboxamido) butanoic acid** (**1,** 190 mg). Fraction 14 was chromatographed over a LoBar® silica G60 column (DCM-MeOH, 95:5) to yield sub-fraction 14.5. This sub-fraction was then purified by using Sephadex column LH20 (MeOH) to yield the new **agelanin A** (**2**, 8 mg). **Agelanin B** (**3**, 25 mg) was obtained through purification of fraction 17 (1.0 g) with LoBar® silica G60 (DCM-MeOH, 98:2) followed by Sephadex LH 20 with MeOH as eluent. Fraction 16 (2.6 g) was separated with a LoBar® Silica G60 column (DCM-MeOH, 95:5) to afford the known **methyl-4,5-dibromo-1-methyl-1*H*-pyrrole-2-carboxylate** (**16,** 21 mg) and sub-fraction 16.8 which was purified further over a LoBar® RP-18 column (MeOH-H_2O, 3:7) to afford 6 compounds as follows, the known **dibromophakellin HCl** (**11a,** 17 mg), new **dibromohydroxyphakellin HCl** (**12,** 47 mg), and, the new bromopyrrole congeners having bromotyrosine moiety, **agelanesin A** (**4**, 20 mg) and **agelanesin C** (**6**, 6 mg), and iodotyrosine moiety, **agelanesin B** (**5**, 24 mg) and **agelanesin D** (**7**, 7 mg).

Agelongine (**14**), the new **mauritamide B (8)**, **mauritamide C** (**9**), and **2-(4,5-dibromo-1-methyl-1*H*-pyrrole-2-carboxamido)ethanesulfonic acid** (**10)** were yielded from butanol fraction (3.5 g) (Fig.II.3c). Sephadex LH 20 was used to purify the butanol fraction resulting to 12 fractions. Fraction 11 is identified as **10** (6 mg),

while fraction 1 (2 g) was chromatographed further by using LoBar® RP-18 (MeOH-H$_2$O, 4:6) obtaining the known **agelongine** (**14,** 20 mg), **mauritamide B** (**8**, 88 mg) and **mauritamide C** (**9**, 33 mg).

Acetone extract (6.7 g) was chromatographed over a Sephadex LH20 column (MeOH) to yield compound **15** (**4,5-dibromo-1-methyl-1*H*-pyrrole-2-carboxylic acid**, 100 mg) and fraction 16. Purification of fraction 16 in LoBar® RP18 (MeOH:H$_2$O, 8:2) yielded compound **11b** (**dibromophakelin base**, 3 mg) (Fig.II.3d).
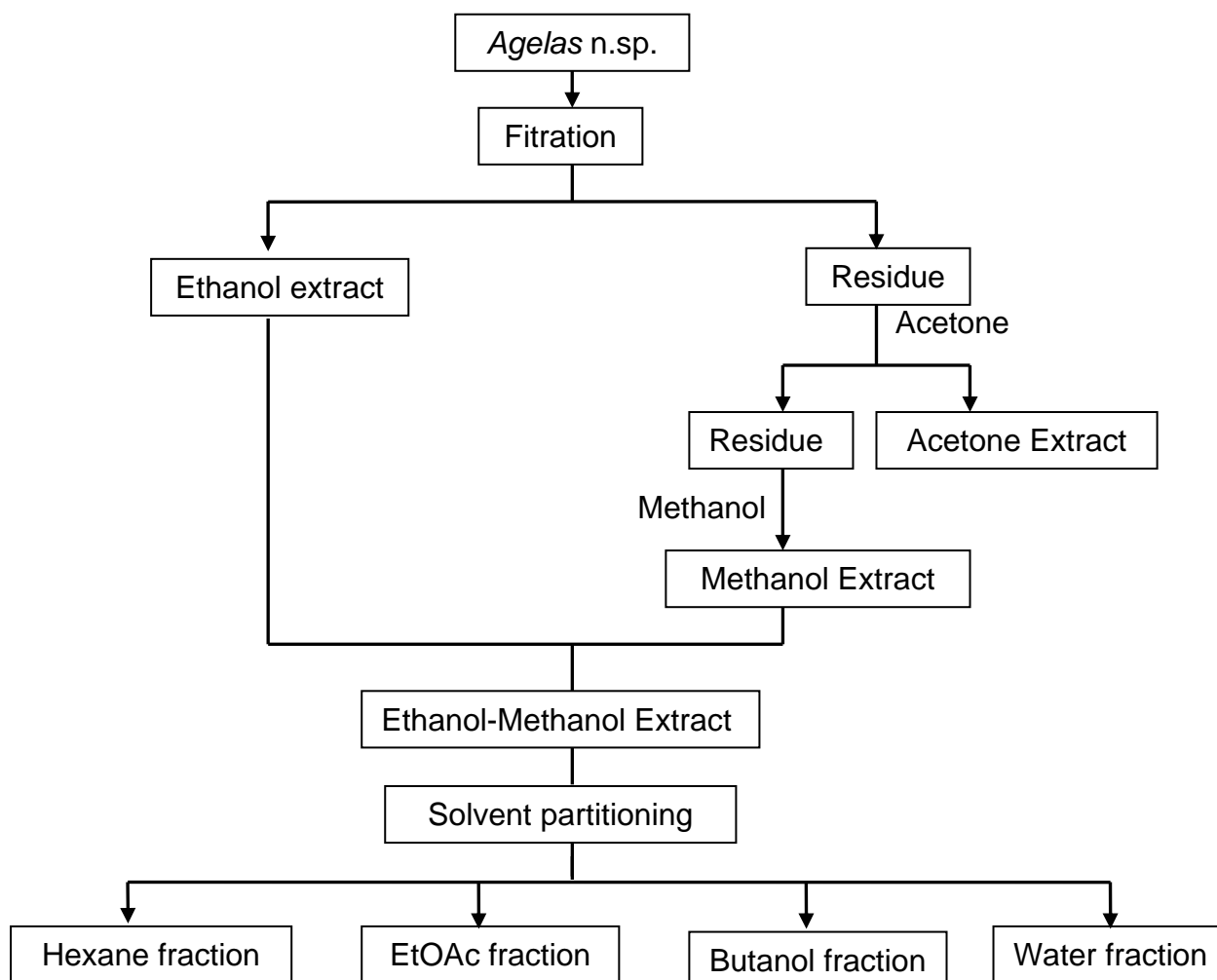
Fig.II.3a. Fractionation scheme of *Agelas* n.sp.

```
                          ┌─────────────────────┐
                          │   Agelas n.sp.      │
                          │   EtOAc fraction    │
                          └─────────────────────┘
                                    │
                                 ┌─────┐
                                 │ VLC │
                                 └─────┘
```

Fraction 10	Fraction 12	Fraction 14	Fraction 16	Fraction 17

Silica G60 (DCM:MeOH 95:5)

LoBar Silica G60 (DCM:MeOH, 95:5)

Sephadex LH20 (MeOH)

Midpacamide (**13**, 2.0 g)

LoBar Silica (DCM:MeOH, 95:5)

Agelanin B (**3**, 25 mg)

4-(4,5-Dibromo-1-methyl-1*H*-pyrrole-2-carboxamido) butanoic acid (**1**,190 mg)

Sub-fraction 14.5

Sephadex LH20 (MeOH)

Methyl-4,5-dibromo-1-methyl-1*H*-pyrrole-2-carboxylate (**16**, 21 mg)

Sub-fraction 16.8

Agelanin A (**2**, 8 mg)

LoBar RP18 (MeOH:H_2O, 3:7)

Dibromo-hydroxyphakellin HCl (**12**, 47 mg)

Dibromo-phakellin HCl (**11a**, 17 mg)

Agelanesin A (**4**, 20 mg)

Agelanesin B (**5**, 24 mg)

Agelanesin C (**6**,6 mg)

Agelanesin D (**7**, 7 mg)

Fig.II.3b. Isolation scheme of *Agelas* n.sp. metabolites (EtOAc fraction)
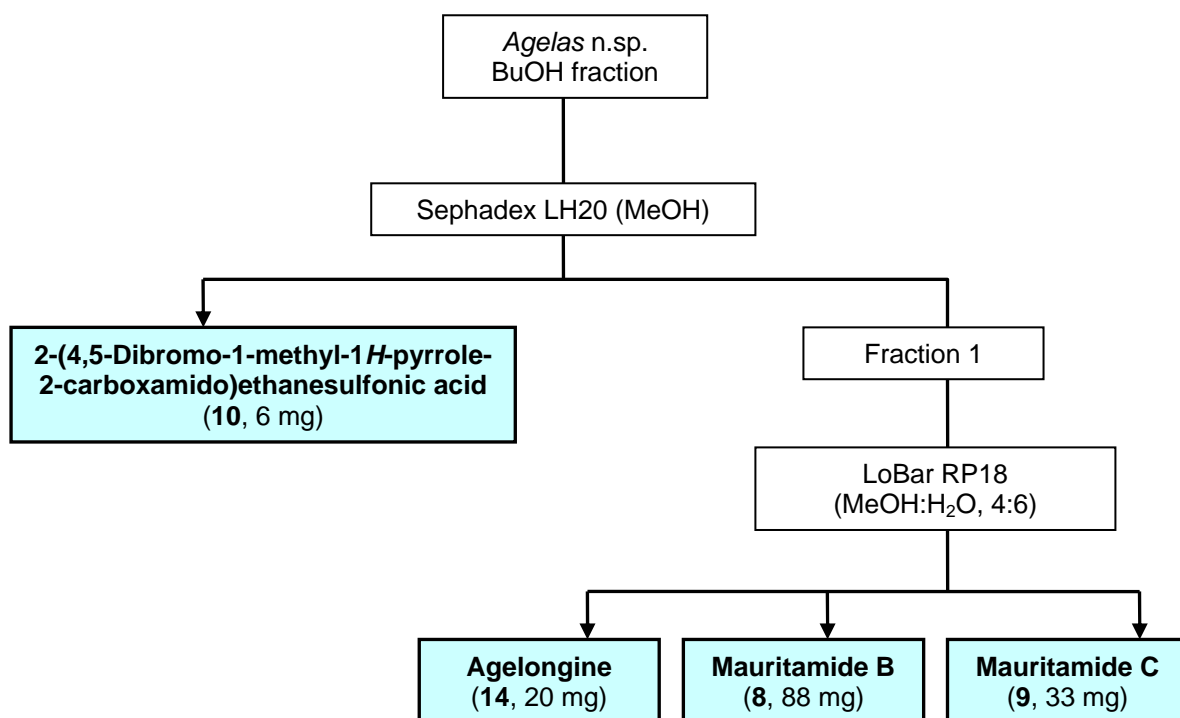
Fig.II.3c. Isolation scheme of *Agelas* n.sp. metabolites (butanol fraction)
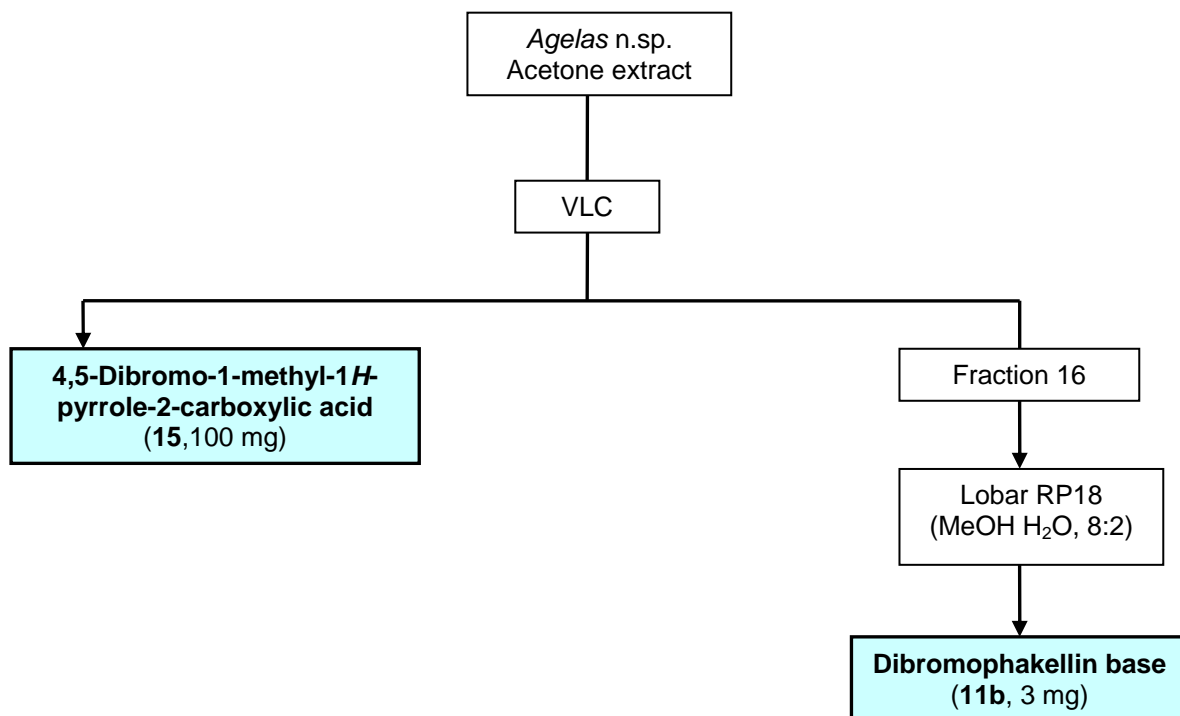
Fig.II.3d. Isolation scheme of *Agelas* n.sp. metabolites (acetone extract)

II.6.   Isolation of secondary metabolites from *Agelas nakamurai* (Fig.II.4)

Sponge tissue was separated from the supernatant (ethanol) and dried at room temperature. Dried sponge tissue (250.7 g) was ground and extracted exhaustively with methanol. After removing solvent under reduced pressure, the resulting extract was combined with the ethanol extract to yield total weight of 37.9 g. Total crude extract was solvent partitioned between *n*-hexane and 90% MeOH-water to obtain the hexane fraction (516 mg). The aqueous methanolic residue was partitioned further between ethyl acetate and H_2O to obtain the ethyl acetate fraction (3.8 g). The resulting water phase was partitioned against *n*-BuOH to afford the butanol extract (12.6 g).

The ethyl acetate fraction (3 g) was subjected to a silica gel G60 vacuum liquid chromatography (VLC) by using eluent with increasing polarity from 100% *n*-hexane to 100 % ethyl acetate followed by 100% dichloromethane to 100% MeOH, resulting to 21 fractions. Fraction 3 was chromatographed over a Sephadex LH20 column by using MeOH as eluent resulting to 12 sub-fractions. Subfraction 3.4 was subjected to semi preparative HPLC RP18 using gradient composition of methanol-water as mobile phase to obtain 2 new compounds, **ageloxime D** (**17**, 110 mg) and **longamide C** (**20**, 1.13 mg). The program used for each injection as follows, 0' – 3': MeOH 80%; 3' – 5': 80% - 100% MeOH; 5' – 13': MeOH 100%; 13' – 15': MeOH 80%. Sub-fraction 3.5 (132 mg) was later identified to be a mixture of compounds **23** (**4-bromo-1*H*-pyrrole-2-carboxylic acid**) and **25** (**9-methyl adenine**) at a ratio of 1:1. Fraction 4 was subjected to a Sephadex LH20 column by using MeOH as eluent to obtain sub-fraction 4.3. This fraction was then purified using a silica gel G60 column by using dichloromethane and methanol solvent mixture in ratio of 95:5, yielding **(-)-agelasine D** (**18**, 1.95 g) and **(+)-agelasidine C** (**19**, 67 mg). Fraction 6

was purified over a Sephadex LH20 column by using methanol to obtain **hymenidin** (**22**, 41 mg), and sub-fraction 6.8 (1 mg) which is a mixture of **adenosine** (**24)** and **4-bromo-1*H*-pyrrole-2-carboxamide** (**26**) at a ratio of 1:1. Compound **21** (**mukanadin C**, 11.8 mg) was obtained by chromatography of the of ethyl acetate fraction (800 mg) over a silica gel G60 column using dichloromethane and methanol (95:5) as eluent.
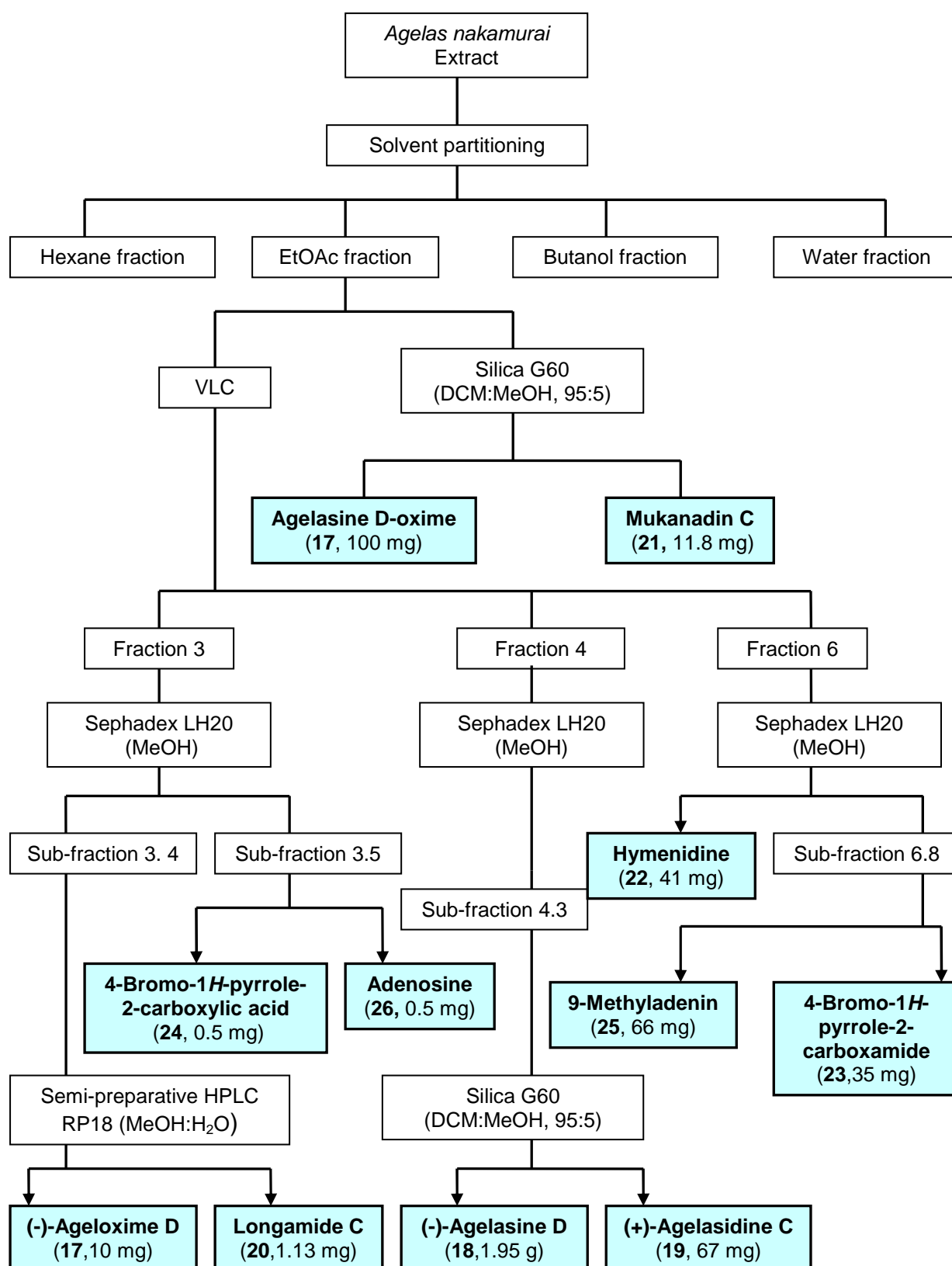
Fig.II.4. Isolation scheme of *Agelas nakamurai* metabolites

II.7. Isolation of secondary metabolites from *Pseudoceratina purpurea* (Fig.II.5)

Sponge tissue was separated from the supernatant (ethanol) and dried at room temperature. Dried sponge tissue was ground and extracted exhaustively with methanol. After removing the solvent under reduced pressure, the resulting methanol extract was combined with the ethanol extract to obtain a total weight of 26 g. This total crude extract was partitioned between *n*-hexane and 90% MeOH-water to obtain the hexane fraction (516 mg). The residue was partitioned further between ethyl acetate and H_2O to obtain the ethyl acetate fraction (2.6 g), and finally the water phase was partitioned against *n*-BuOH to yield the butanol fraction (1.2 g).

The ethyl acetate fraction was subjected to Sephadex LH20 column with MeOH as eluent, to yield **aplysamine-2** (**27**, 11 mg) and 9 fractions. Fraction 3 was chromatographed over a Sephadex LH20 column (MeOH) to obtain **aeroplysinin-1** (**28,** 79 mg). Fraction 4 was subjected to a Sephadex LH20 column (MeOH) to obtain **5-[3,5-dibromo-4-[(2-oxo-5-oxazolidinyl)methoxy]phenyl]-2-oxazolidinone** (**29**, 26.0 mg).

The butanol fraction was chromatographed over a Sephadex LH20 column by using MeOH as eluent resulted to 28 fractions. Fraction 4 was then purified by using semi-preparative HPLC RP18 in gradient composition of methanol and water to obtain **dienone dimethoxyketal** (**30**, 70 mg) and **dienone methoxy-ethoxy ketal** (**31**, 2 mg). The HPLC solvent system program was run as follows, 0 – 5': 10% MeOH; 5' – 20': 10% to 100% MeOH; 20' – 23': 100% MeOH; 23' – 25': 10% MeOH.
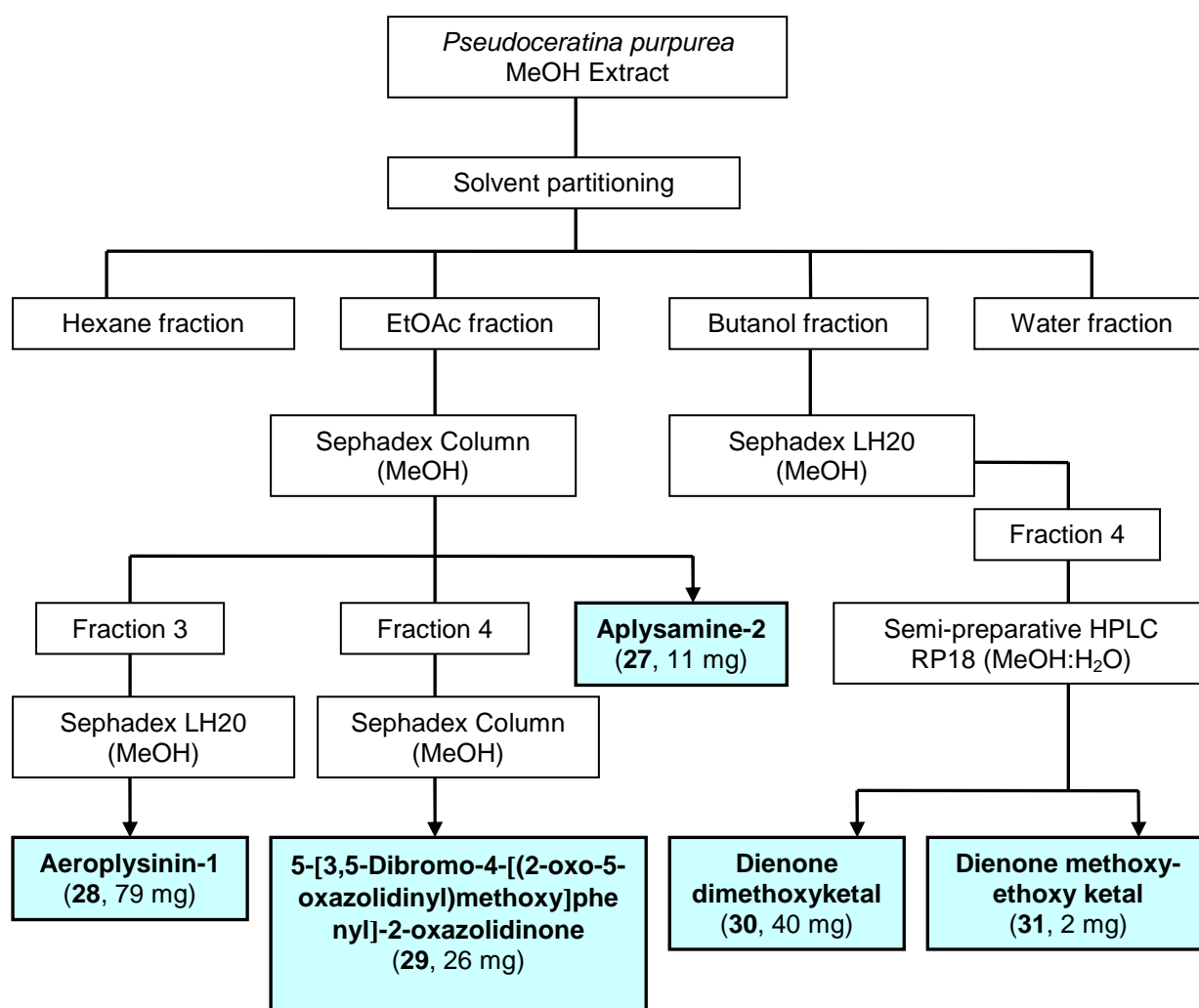
Fig.II.5. Isolation scheme of *Pseudoceratina purpurea* metabolites

II.8.   Isolation of secondary metabolites from *Mycale phylophylla* (Fig.II.6)

Sponge tissue was separated from the supernatant (ethanol) and dried at room temperature. Dried sponge tissue (10.9 g) was ground and extracted exhaustively with methanol. After removing the solvent under reduced pressure, the resulting methanol extract was combined with the ethanol extract to obtain a total weight of 1.9 g. This crude extract was partitioned between ethyl acetate and water to obtain the ethyl acetate fraction (0.7 g).

The ethyl acetate fraction was subjected to silica gel G60 vacuum liquid chromatography (VLC) by using mobile phase with increasing polarity from 100% *n*-hexane to 100 % ethyl acetate followed by 100% dichloromethane to 100% MeOH, resulted 16 fractions. Fraction 3 (28 mg, 0.25% of sponge dried weight) was later identified as a mixture of **32a** and **32b** at a ratio of 2:1.

```
          ┌─────────────────────┐
          │  Mycale phylophylla │
          │      Extract        │
          └─────────┬───────────┘
          ┌─────────┴───────────┐
          │ Solvent partitioning│
          └─────────┬───────────┘
        ┌───────────┴──────────────┐
┌───────────────┐          ┌────────────────┐
│ EtOAc fraction│          │  Water fraction│
└───────┬───────┘          └────────────────┘
    ┌───┴───┐
    │  VLC  │
    └───┬───┘
┌───────────────────────┐
│  Fraction 3 (23 mg)   │
│(hexane:ethylacetate,9:1)│
└───────────┬───────────┘
    ┌───────┴───────────┐
┌──────────────┐  ┌──────────────┐
│5-pentadecyl- │  │(E)-5-(pentadec│
│1H-pyrrole-2- │  │-6-enyl)-1H-   │
│carbalaldehyde│  │pyrrole-2-     │
│   (32a)      │  │carbalaldehyde │
│              │  │    (32b)      │
└──────────────┘  └──────────────┘
```
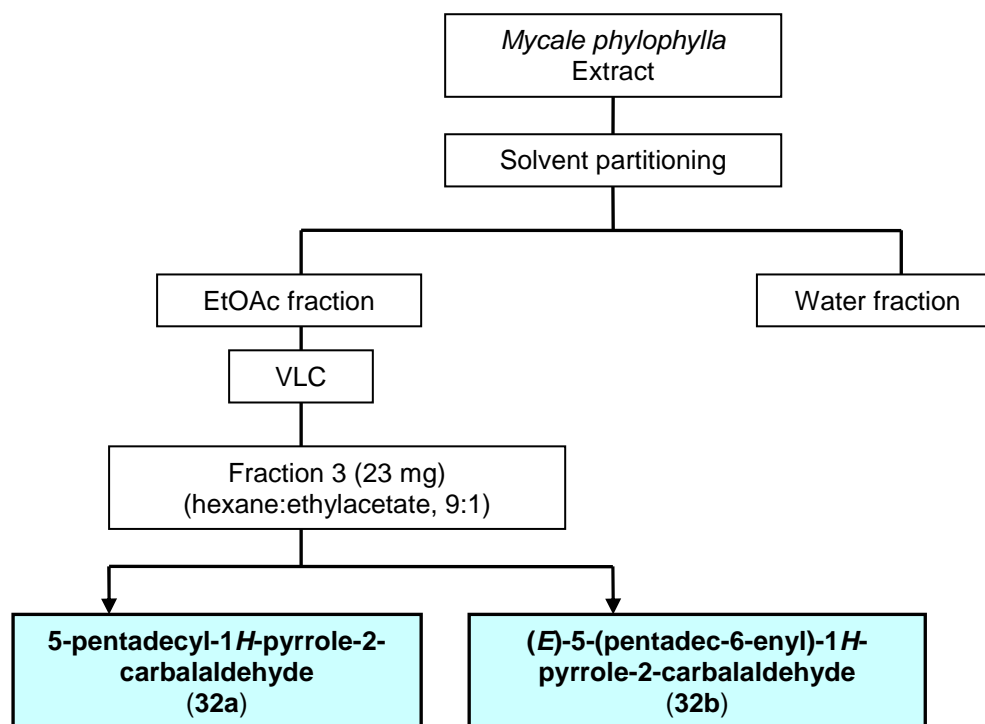
Fig.II.6. Isolation scheme of *Mycale phylophylla* metabolites

II.9. Isolation of secondary metabolites from *Axynissa* sp. (Fig.II.7)

Dried sponge tissue was ground and extracted exhaustively with methanol. After removing the solvent under reduced pressure, the methanol extract was combined with the ethanol extract to obtain total weight of 2 g. The crude extract was subjected to silica gel G60 vacuum liquid chromatography (VLC) by using mobile phase with increasing polarity from 100% *n*-hexane to 100 % ethyl acetate followed by 100% dichloromethane to 100% MeOH, resulting to 10 fractions. Fraction 2

(hexane:ethyl-acetate, 3:1) was later identified as **(+)-curcuphenol** (**33**, 19 mg) and fraction 3 (hexane:ethyl-acetate, 1:1) as **(+)-curcudiol** (**34**, 24 mg).
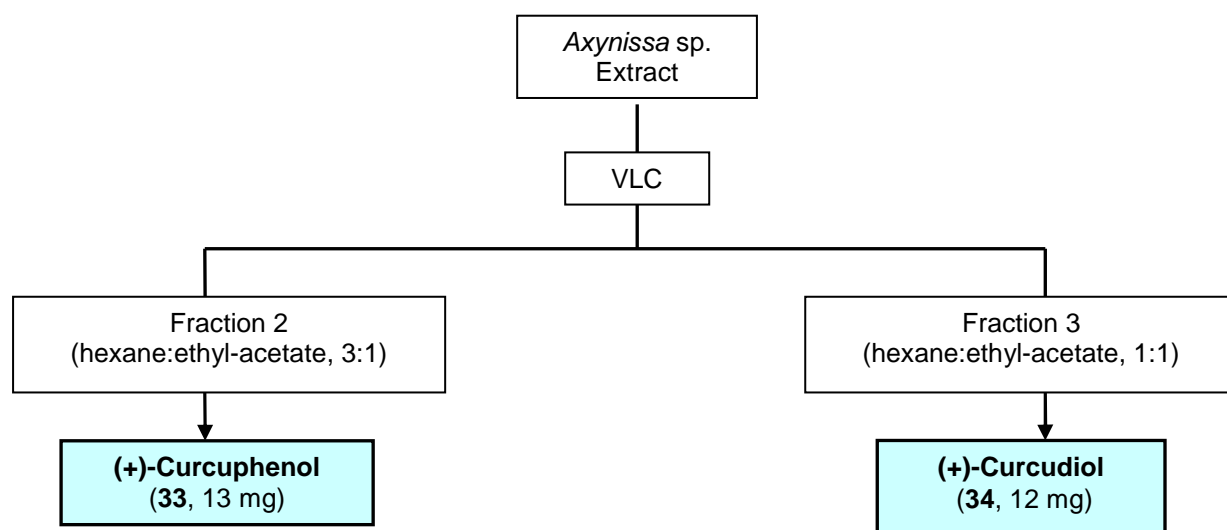
Fig.II.7. Isolation scheme of *Axynissa* sp. metabolites

II.10.   Isolation of secondary metabolites from *Rhabdastrella rowi* (Fig.II.7)

Sponge tissue was separated from the supernatant (ethanol) and dried at room temperature. Dried sponge tissue (184 g) was ground and extracted exhaustively with methanol. After removing the solvent under reduced pressure, the methanol extract was combined with the ethanol extract to yield total weight of 44 g. The extract was partitioned between *n*-hexane and 90% MeOH-water to yield the hexane fraction (0.7 g). The residue was partitioned between ethyl acetate and H_2O to obtain ethyl acetate fraction (1.4 g), and finally the water phase was partitioned against *n*-BuOH to obtain the butanol (2.3 g) and water fractions (18 g). Observation of the fractions chemical profiles in analytical HPLC showed that only ethyl acetate fraction which was promising to be further investigated.

The ethyl acetate fraction was chromatographed over a silica gel G60 vacuum liquid chromatography (VLC) by using eluents with increasing polarity from

100% *n*-hexane to 100 % ethyl acetate followed by 100% dichloromethane to 100% MeOH which gave 17 fractions. Fraction 6 was chromatographed over a Sephadex LH20 column by using MeOH as an eluent which resulted to 24 sub-fractions. Sub-fraction 6.10 was subjected to semi preparative HPLC RP18 by gradient elution of methanol-water as mobile phase to obtain compound **35** (1 mg). The program used for the solvent system was as follows, 0' – 8': MeOH 10%; 8' – 15': 10% - 50% MeOH; 15' – 20': 50 - 100% MeOH; 20' – 23': 100% MeOH; 23' – 25': 10% MeOH.
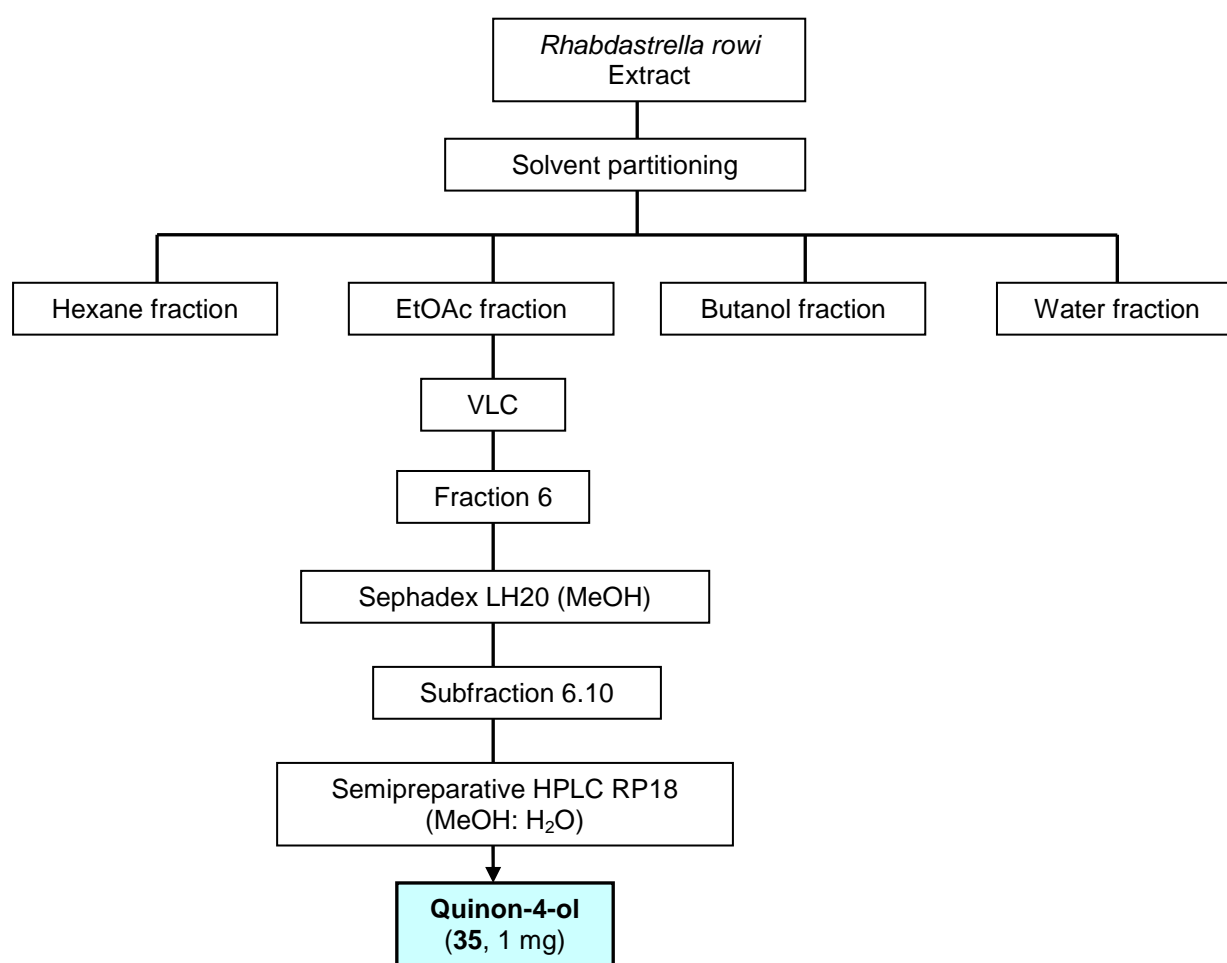
Fig.II.8. Isolation scheme of *Rhabdastrella rowi* metabolite

II.11.   Structure elucidation of the isolated compounds

II.11.1. Mass spectrometry (MS)

Low resolution MS were measured by EI, and FAB-MS on a Finnigan MAT 8430 mass spectrometer. Measurements were done by Dr. Tommes (Institute of Inorganic and Structure Chemistry, HHU, Düsseldorf, Germany)**.**

EIMS (Electron ionization mass spectrometry), is an analysis which involves vaporising a compound in an evacuated chamber and then bombarding it with highly energetic electrons that have been accelerated through a potential difference of 50 – 70 volts (V) across the volume of the ion source. The high energy electron stream not only ionises an organic molecule (requiring about 5 – 15 eV) but also causes extensive fragmentation (Smith, 2005). The fragmentation is very useful because it provides structural information for interpreting unknown spectra (Van Bramer, 1998).

FAB (fast atom bombardment) uses high energy atoms to sputter and ionize the sample in a single step. In this technique, a beam of rare gas neutrals is focused on the liquid or solid sample. The impact of this high energy beam causes the analyte molecules to sputter into the gas phase and ionize in a single step. This technique is suitable for compounds with molecular weight up to a few thousand Dalton. Since no heating is required, FAB is useful for studying thermally labile compounds that decompose in conventional inlets (Van Bramer, 1998). It uses a beam of neutral gas (Ar or Xe atoms) (Smith, 2005).

ESIMS (electro spray ionisation mass spectrometry) is a method which has allowed LC/MS to become routine analytical tools (Smith, 2005). Basically ESI works by converting the HPLC effluent, already containing the sample in ionic form, into an aerosol. The resulting spray is subjected to a chamber at atmospheric

pressure in the presence of high voltage and heated drying gas. As the solvent of the charged droplets evaporates, electrostatic repulsions between the increasingly concentrated charges cause the droplets to break part resulting the analyte ions finally desorbed into the vapour phase, passed into the sampling capillary, then into the mass analyzer (Smith, 2005).

For the most part, the nature of the ions analyzed by ESI will be determined during the chromatographic run. At low pH, protonated molecules (sometimes protonated several times) will predominate. The fragmentation is minimal since little additional energy is imparted to these ions, allows ESI as an additional tool to determine molecular mass of compounds that do not produce an $M^{+\bullet}$ by EIMS (Smith, 2005).

Structure information of the analyte can be obtained by coupling ESI with MS/MS. MS/MS or also known as tandem mass spectrometry refers to instruments in which two independent stages of *m/z* analyses are used (Smith, 2005). According to de Hoffman (1996), this method helps to elucidate fragmentation pathways for the molecule being studied or when used in conjunction with ionization techniques like ESI that produce little fragmentation, to determine the structure of the analyte (Smith, 2005). Data ESIMS in this study was obtained from the LC/MS measurement (see II.4.2.7).

High resolution mass spectrometry is a method of analyses capable of determining the "exact mass" of an ion. This is very useful in structure elucidation procedure considering the fact that each element has a slightly different mass defect. The "mass defect" is the difference between the mass of the isotope and the nominal mass (which is equivalent to the number of protons and neutrons). High resolution

mass spectrometry can distinguish compounds with the same nominal mass but different exact mass caused by different elemental composition (Van Bramer, 1998). In this study, data high resolution mass spectrometry was obtained from mass spectrometer Micromass Q-Tof 2. Measurement was done by Dr. Manfred Nimtz and Dr. Victor Wray (Helmholtz Insitute for Infection Research, Braunschweig, Germany).

II.11.2. Nuclear magnetic resonance spectroscopy

^{1}H and ^{13}C NMR spectra were recorded at $300°$K on Bruker DPX 300, ARX 400, 500 or AVANCE DMX 600 NMR spectrometers, by Dr. W. Peters (Institute of Inorganic and Macromolecular Chemistry, HHU, Düsseldorf, Germany) and Dr. Victor Wray (Helmholtz Institute for Infection Research, Braunschweig, Germany). All 1D and 2D spectra were obtained using the standard Bruker software. The samples were dissolved in appropriate deuterated solvents i.e chloroform-d_1 (Merck, Darmstadt, Germany); dichloromethane-d_2; DMSO-d_6; methanol-d_4 (Eurisotop, France). Solvent signals (i.e. δ_H 3.3 and δ_C 49.0 for CD_3OD) were considered as internal reference signal for calibration. The observed chemical shift values (δ) were given in ppm, and the coupling constant (J) in Hz.

II.11.3. The optical activity

Optical rotation was determined on a Perkin-Elmer 241 MC polarimeter by measuring the angle of rotation at a wavelength of 589 nm of a Na/Hg vapour lamp. Samples were measured in a 0.5 ml cuvette with 0.1 dm length and unless stated different was run at room temperature ($25°$ C). Solvent used in this method were spectroscopy grade as follows: chloroform and methanol (Sigma-Aldrich, Steinheim, Germany); water and ethanol (Fluka, Seelze, Germany). The specific optical rotation was calculated using the expression:

$$[\alpha]_\lambda^{\mathrm{T}} = \frac{100 \times \alpha}{l \times c}$$

Where $[\alpha]_\lambda^{\mathrm{T}}$: specific rotation at a given temperature and wavelength;

α: the measured angle of rotation in degrees;

T: temperature in degrees Centigrade;

λ: wavelength (for historical reasons the sodium D-line, 589 nm);

l: the length in dm of the polarimeter tube;

c: the concentration of the substance expressed as g/100 ml of solution

(Screier *et al.*, 1995)

II.12. Bioassay

II.12.1. Cytotoxicity assay

Cytotoxicity assays were carried out by Prof. Dr. W.E.G. Müller and co-workers (Institute of Advanced Molecular Biology Univ. Mainz, Germany). The cytotoxicity against L5178Y mouse lymphoma cells was determined using the microculture tetrazolium (MTT) assay and compared to that of untreated controls (Carmichael *et al.*, 1987). Stock solutions of test samples were prepared in EtOH 96% (v/v). Exponentially growing cells were harvested, counted, and diluted appropriately. 50 μL cell suspension containing 3750 cells was pipetted into 96-well microtiter plates. Subsequently, 50 μL of the test samples solution containing the appropriate concentration were added to each well. The concentration range was 3 – 10 μg/mL. The small amount of EtOH present in the wells did not affect the experiments. The test plates were incubated at 37° C with 5% CO_2 for 72 h. A solution of 3-(4,5-dimethylthiazol-2-yl)-2,5-diphenyltetrazolium bromide (MTT) was prepared at 5 mg/mL in phosphatase-buffered saline (PBS: 1,5 mM KH_2PO4 6.5 mM

Na$_2$HPO$_4$, 137 mM NaCl, 2.7 mM KCl; pH 7,4), and from this solution, 20 µL was pipetted into each well. The yellow MTT penetrates the healthy living cells, and in the presence of mitochondrial dehydrogenases, MTT is transformed to its blue formazan complex. After an incubation period of 3 h 45 min at 37° C in a humidified incubator with 5% CO$_2$, the medium was centrifuged (15 min, 20°C, 210 g) with 200 µL of DMSO, and the cells were lysed to liberate to formed formazan product. After thorough mixing, the absorbance was measured at 520 nm using a scanning microtiter-well-spectrometer. The color intensity is correlated with the number of healthy living cells. The ED$_{50}$ was estimated by logit regression (Sachs, 1984).

Cell survival was calculated using the formula:

$$\text{Survival (\%)} = \frac{100 \times (Abs_{tc} - Abs_{cm})}{(Abs_{utc} - Abs_{cm})}$$

Where Abs_{tc}: Absorbance of treated cells;

Abs_{cm}: Absorbance of culture medium;

Abs_{utc}: Absobance of untreated cells.

All experiments were carried out in triplicate and repeated three times. As controls, media with 0.1% EGMME/DMSO were included in the experiments.

II.12.2. Protein kinase inhibition screening assay

Samples were sent to ProQinase GmbH, Freiburg, Germany, for screening on protein kinase inhibition. The samples were subjected to protein kinase screening assays to provide further information on their mechanism of action particularly in the alteration of cell cycle pathways in a tumour cell. As cancer cells proliferate, multiple alterations are developed which also include DNA repair genes, thus enhancing their mutability and plasticity (Rao, 1996). Considering that protein kinases are much

involved in the cell cycle pathways, they can be a potential cancer therapeutic target (Fabbro *et al.*, 2002).

The inhibitory profile of the samples tested was determined using 24 protein kinases. The samples were tested at two concentrations (1×10^{-06} g/mL and 1×10^{-05} g/mL) in singlicate (n = 1).

Stock solutions were dissolved in DMSO (1×10^{-03} g/mL) in column 3 – 12 of one 96-well micronic box. Columns 1 and 2 were filled with micronic tubes containing 100% DMSO. The box is in the following referred to as "master box", transferred to -20°C for later use. Prior to testing, 10 μL of each tube of the micronic box were transferred into a 96 well microtiter plate and diluted with 90 μL 100% DMSO, resulting in a "dilution plate" with 1×10^{-4} g/mL/100% DMSO stock solutions. From each well of the dilution plate, 7 x 5 μL was aliquoted into 7 identical "copy plates". The copy plates were transferred to -20°C for later use.

Assays were performed by using a separate copy plate for each set of 4 kinases. Upon thawing of the stock solutions, 45 μL H_2O were added to each well of the copy plate. To minimize precipitation, H_2O was added to each well only a few minutes before the transfer of the compound solutions into the assay plates. The plate was shaken thoroughly, resulting in a "compound dilution plate" with a concentration of 1×10^{-05} g/mL in 10% DMSO. This plate was used for the transfer of 5 μL compound solution into the assay plates. The final volume of the assay was 50 μL. All compounds were tested at a final assay concentration of 1×10^{-06} g/mL in 1% DMSO in singlicate.

All protein kinases were expressed in Sf9 insect cells as human recombinant GST-fusion proteins of His-tagged proteins by means of the baculovirus expression

system. Kinases were purified by affinity chromatography using either GSH-agarose (Sigma) or Ni-NTH-agarose (Qiagen). The purity of each kinase was checked by SDS-PAGE/silver staining and the identity of each kianse was verified by western blot analyses with kinase specific antibodies or by mass spectroscopy.

A proprietary protein kinase assay (^{33}PanQinase$^{®}$ Activity Assay) was used for measuring the kinase activity of the 24 protein kinases. All kinase assays were performed in 96-well FlashPlatesTM from Perkin Elmer/NEN (Boston,MA, USA) in a 50 µL reaction volume. The reaction cocktail was pipetted in 4 steps in the following order: 20 µL of assay buffer; 5 µL of ATP solution (in H_2O); 5 µL of test compound (in 10% DMSO); 10 µL of substrate/10µL of enzyme solution (premixed).

The protein kinases used for determination of inhibitory profiles as well as the amounts of enzyme and substrate used per well as described in Table II.1

The assay contained 60mM HEPES-NaOH, pH 7.5, 3 mM $MgCl_2$, 3 mM MnCl2, 3 µM Na-orthovanadate, 1.2 mM DTT, 50 µg/mL PEG_{20000}, 1 µM [γ-^{33}P]-ATP (approx. 5 x 10^{05} cpm per well).The reaction cocktails were incubated at 30° C for 80 minutes. The reaction was stopped with 50 µL of 2% (v/v) H_3PO_4. Plates were aspired and washed two times with 200 µL of 0.9% (w/v) NaCl. Incorporation of ^{33}Pi was determined with a microplate scintillation counter (Microbeta Trilux, Wallac).

All assays were performed with a BeckmanCoulter/Sagian robotic system.

The residual activity (in %) for each well of a particular plate was calculated by using the following formula:

Res. Activity (%) = 100 X [(cpm of compound-low control) / (high control-low control]

Low control reflects the unspecific binding of radioactivity to the plate in the absence of a protein kinase but in the presence of the substrate, while high control

reflects full activity in the absence of any inhibitor. The difference between high and

low control was taken as 100% activity.

Table II.1. Protein kinases, enzymes and substrate used per well for determination inhibitory profiles

No.	Kinase	Kinase ng/50μL	Substrate	Substrate ng/50μL
1.	AKT1	100	GSK3(14-27)	1000
2.	ARK5	100	Autophosphorylation	-
3.	Aurora-A	50	tetra(LRRWSLG)	500
4.	Aurora-B	200	Tetra(LRRWSLG)	250
5.	B-RAF-VE	20	MEK1-KM (Lot 011)	250
6.	CDK2/CycA	100	Histone H1	125
7.	CDK4/CycD1	50	Rb-CTF (SP009)	500
8.	CK2-alpha1	200	p53-CTM 11.6.99	250
9.	EGF-R	25	Poly(Glu, Tyr)$_{4:1}$	125
10.	EPHB4	10	Poly(Glu, Tyr)$_{4:1}$	125
11.	ERBB2	200	Poly(Glu, Tyr)$_{4:1}$	125
12.	FAK	200	Poly(Glu, Tyr)$_{4:1}$	125
13.	IGF1-R	25	Poly(Glu, Tyr)$_{4:1}$	125
14.	SRC	10	Poly(Glu, Tyr)$_{4:1}$	125
15.	VEGF-R2	50	Poly(Glu, Tyr)$_{4:1}$	125
16.	VEGF-R3	100	Poly(Glu, Tyr)$_{4:1}$	125
17.	COT	400	Autophosphorylation	-
18.	PLK1	50	Casein	250
19.	SAK	200	Autophosphorylation	-
20.	TIE2	200	Poly(Ala,Glu,Lys,Tyr)$_{6:2:5.1}$	250
21.	FLT3	100	Poly(Ala,Glu,Lys,Tyr)$_{6:2:5.1}$	125
22.	INS-R	25	Poly(Ala,Glu,Lys,Tyr)$_{6:2:5.1}$	125
23.	MET	10	Poly(Ala,Glu,Lys,Tyr)$_{6:2:5.1}$	125
24.	PDGFR-beta	50	Poly(Ala,Glu,Lys,Tyr)$_{6:2:5.1}$	125
25	PAK4*	25		
26	PDK1*	25		

*only tested on aeroplysinin-1, hymenidin, (+)-curcuphenol, and (+)-curcudiol.

II.12.3. Antimicrobial activity

Microorganisms used

The crude extracts and selected pure compounds were tested for activity

against the following standard strains: gram positive *Bacillus subtilis*; gram negative

bacteria *Escherichia coli*; the yeast *Saccharomyces cerevisiae* and two

pytopathogenic fungal strains *Cladosporium herbarum* and *C. curcumerinum*.

Culture preparation

The agar diffusion assay was performed according to the Kirby-Bauer Test (DIN 58940) (Bauer *et al.*, 1996). Prior to testing, a few colonies (3 to 10) of the organisms to be tested were sub cultured in 4 ml of tryptose-soy broth (Sigma, FRG) and incubated for 2 to 5 h to produce a bacterial suspension of moderate cloudiness. The suspension was diluted with sterile saline solution to reach the density which is visually equivalent to that of $BaSO_4$ standards. The standards were prepared by adding 0.5 ml of 1% $BaCl_2$ to 99.5 mL of 1% H_2SO_4 (0.36 N). The prepared bacterial broth is inoculated onto Müller-Hinton-Agar plates (Difco, USA) and dispersed by means of sterile beads.

Agar diffusion assay

For screening, aliquots of the test solution were applied to sterile filter-paper discs (5 mm diameter, Oxid Ltd.) using a final disc loading concentration of 500 μg for the crude extract and 50 and 100 μg for pure compounds. The impregnated discs were placed on agar plates previously seeded with the selected test organisms, along with the discs containing solvent blanks. The plates were incubated at 37° C for 24 hour and anti-microbial activity was recorded as the clear zones of inhibition surrounding the discs. The diameter was measured in mm.

II.12.4. Biofilm Inhibition Assay

Biofilm inhibition assay was carried out by Dr. Ute Hentschel and co-workers at the Research Centre for Infectious Diseases, Würzburg University, Germany).

Biofilms are formed by the colonization of solid supports (bone, implants and cathethers) by adherent bacteria (Gualtieri *et al.*, 2006). The ability to form biofilm on a plastic surface (e.g., cathethers) affords at least two properties, the adherence of

cells to a surface and accumulation to form multilayered cell clusters (Götz, 2002). The second phase of biofilm formation requires the polysaccharide intercellular adhesion (PIA) located at the cell surface (Mack *et al.*, 1994), in which the cells are embedded and protected against the host's immune defence and antibiotic treatment (Götz, 2002).

Biofilm inhibition was investigated by using an adherent-assay in a polystyrene microtiter culture plate. The culture is diluted with fresh TSB (Tryptone Soya Broth) in a ratio of 1: 99 (20 µL of culture + 1980 µL of medium). Every 200µL of this suspension was pipetted into each of the well of a 96-hole tissue culture plate where every strain was added 8-fold. *S. epidermidis* RP62A (wild type) serves as a positive control while *S. carnosus* TM 300 is used as a negative control. The plates are incubated at 37 ℃ for 18 hours. Then the cultu ral vessels are emptied carefully. Afterwards the plates are washed three times with PBS (Phosphate Buffered Saline) buffer. The adhering bacteria then were fixed by a heating block at approx. 60 ℃ and coloured with crystal-violet for 5 min. The excess colouring material was washed under flowing water. After it dried the density of the biofilm is determined with an ELISA reader at a wavelength of 490 nm. Absorbance values less than 0.120 are evaluated as negative, whereas values between 0.120 and 0.240 was evaluated as weak adherent and results more than 0.240 as strong adherent. The limit value of 0.120 is equivalent to the triple average value of the negative control.

II.12.5. Antifouling activity

Antifouling activity test was done by S. Ortlepp at Tjärnö Marine Biological Laboratory, Sweden. Cyprid larvae of *Balanus improvisus* Darwin were reared in a laboratory culture as described by Berntsson and co-workers (2000).

The experiment for evaluating the effects of the substances on settlement and mortality was run using polystyrene petri dishes (diameter 48 mm) to which 10 ml of the substances dissolved in different concentrations in filtered seawater (0.2 µm) with 0.1 % DMSO were added. Competent cyprids (16 ± 2 individuals) were added to each dish run in four replicates. Dishes containing filtered seawater and dishes containing filtered seawater with 0.1 % DMSO served as controls. Dishes were maintained for 3-4 days at room temperature after they were examined under a stereomicroscope for attached and metamorphosed individuals, and also for dead cyprids. The substances were tested in the concentrations of 0.01, 0.10, 1.00, and 10 µM dissolved in 0.10 % DMSO. A solvent control with 0.10 % DMSO was run parallel to the sample.

III. RESULTS

III.1. Secondary metabolites from *Agelas* n.sp.

Sponges of the genus *Agelas* (Agelasidae) are well known to accumulate bromopyrrole type of compounds (Braekman *et al.*, 1992; Lindel *et al.*, 2000b). These compounds most probably play a role in the sponge's mechanism of defence against fish feeding (Pawlik *et al.*, 1995; Chanas *et al.*, 1996; Assmann *et al.*, 2000).

Cytotoxicity and protein kinase inhibition screening assay on the *Agelas* n.sp. crude extract exhibited no promising activity. But nevertheless, preliminary chemical investigation discovered interesting profiles regarding the presence of several new brominated pyrrole derivatives. Compound peaks observed from the analytical HPLC chromatogram showed UV absorption maxima at around 270 nm which is characteristic for 2-pyrrole carboxamide substituted chromophores (Jaffe and Orchin, 1962). Some UV absorption pattern modifications were observed for several compounds, such as additional band peaks or bathochromic shift of the band peaks. LC/MS experiment discovered that these substances are all brominated. Pseudo molecular ion cluster peaks having two mass unit differences at a ratio of 1:1 for one bromine or 1:2:1 for two bromines or 1:2:2:1 for three bromines were detected. This phenomena are characteristic in bromines bearing compounds, which can be explained by the natural abundance of both ^{79}Br and ^{81}Br isotope at a ratio of 49.5:50.5 (Smith, 2005).

Fourteen compounds were isolated and elucidated. Eleven of them are new brominated pyrrole derivatives.
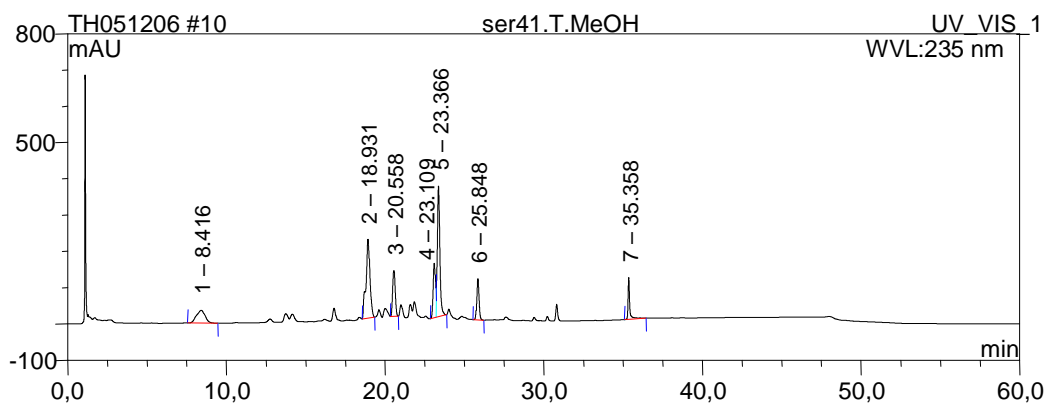
Fig.III.1. Chemical profile of the *Agelas* n.sp. crude extract observed in analytical HPLC
Peak 1: dibromophakellin HCl; 2: agelongine; 3: mauritamide C; 4: mauritamide B; peak 5: midpacamide; 6: agelanin B; 7: 4,5-dibromo-1-methyl-1*H*-pyrrole-2-carboxylic acid

III.1.1. 4-(4,5-dibromo-1-methyl-1*H*-pyrrole-2-carboxamido) butanoic acid (**1,**

new compound
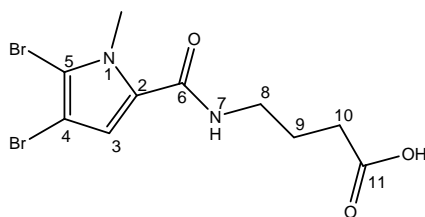
Fig.III.2. Compound **1**
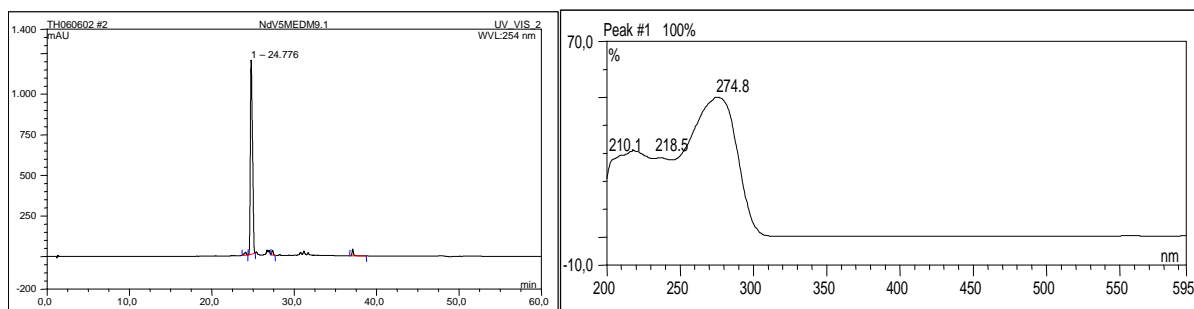
Fig.III.3. Analytical HPLC data of compound **1**
left: HPLC profile in 254 nm, RT: 24.78; right: UV absorption spectrum, λ_{max} = 202.9, 276.9 nm
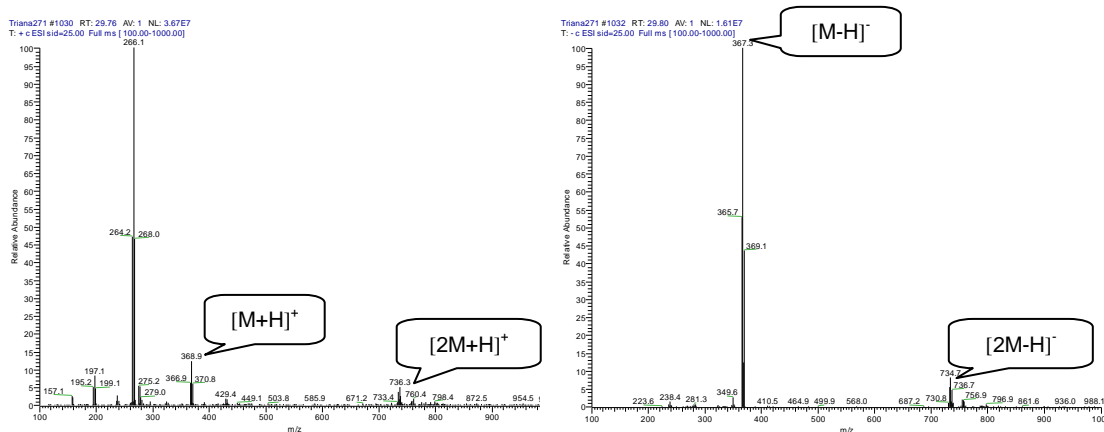
Fig.III.4. ESI-MS data of compound **1**

Compound **1** was isolated as a dark brown oil (190 mg, 0.096% of the sponge dried weight). It was separated from a fraction which showed cytotoxicity to L5178Y mouse lymphoma cells, but unfortunately the pure substance was not active (Table III.36).

This compound is assigned as a new butanoic acid derivative of the 4,5-dibromo-1-methyl-1*H*-pyrrole-2-carboxamide. It exhibits the usual UV absorption pattern for pyrrole 2-carboxamide as shown in Fig.III.3. ESIMS experiment shows pseudo molecular ion cluster peaks at *m/z* 367/369/371 [M+H]$^+$ having a ratio 1:2:1 (Fig.III.4). This finding suggests the presence of a dibrominated compound. The molecular formula of $C_{10}H_{13}Br_2N_2O_3$ was deducted from HRESIMS (*m/z* experimental = 366.9300; *m/z* calculated = 366.9293 [M+H]$^+$) and the ^{13}C NMR analysis.

^1H NMR (DMSO-*d$_6$*) of compound **1** (Fig.III.5) shows a singlet signal in the lower field at δ_H 6.98 assigned as the pyrrole proton (H-3). This signal is correlated to a deshielded methyl group at δ_H 3.85 (s, 1-NCH$_3$) in ^1H-^{13}C HMBC spectrum (Fig.III.8), which reveals the substructure 4,5-dibromo-1-methyl-1*H*-pyrrole-2-carboxamide.
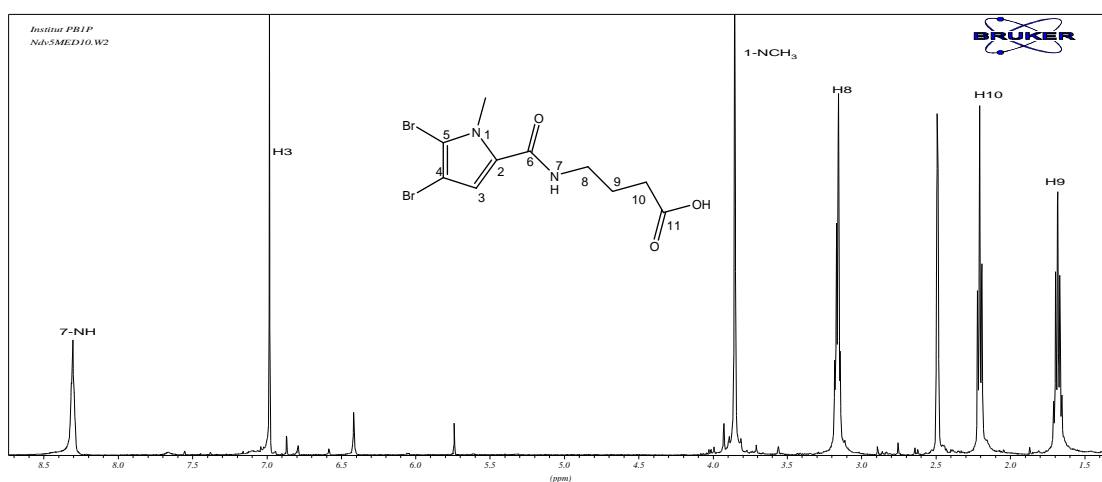
Fig.III.5. ^{1}H NMR spectrum of compound **1 (**DMSO-d_6, 500 MHz)
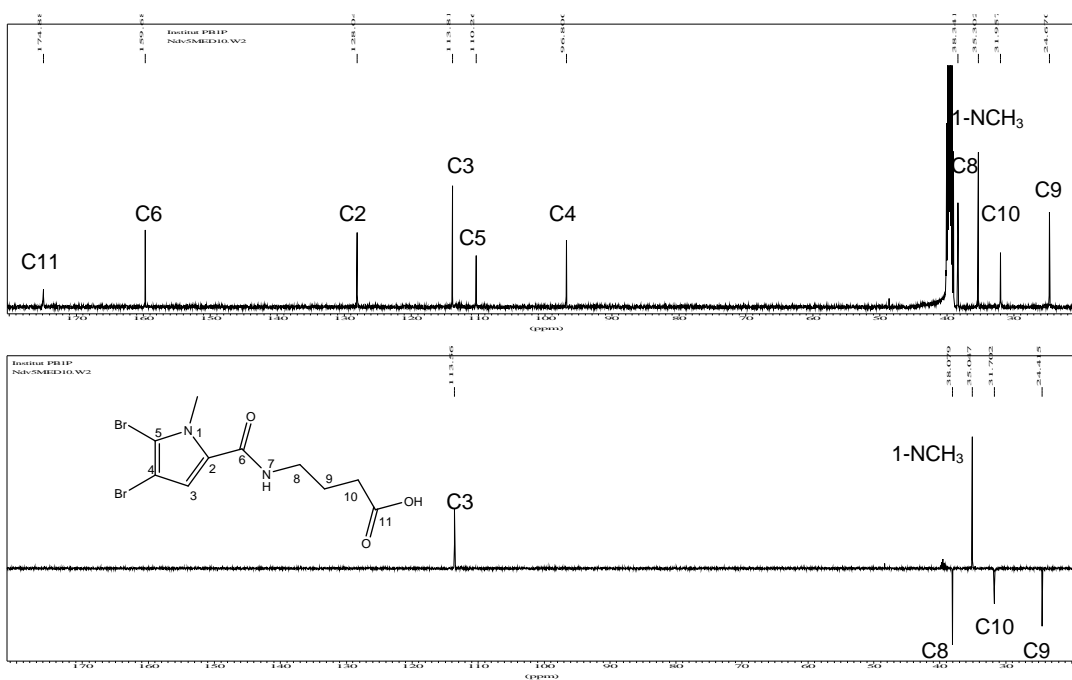
Fig.III.6. ^{13}C NMR (above) and DEPT (below) spectra of compound **1** (DMSO-d_6, 125 MHz)

A second substructure assignment was based on the ^{1}H-^{1}H COSY spectrum (Fig.III.7). It exhibits one isolated spin system correlating a propylene chain to an amide function (δ_H 8.31, t, $J = 5.5$ Hz, 7-NH; δ_H 3.16, dd, $J = 5.5$ Hz, H$_2$-8; δ_H 1.68, t, $J = 5.5$ Hz, H$_2$-9; δ_H 2.21, t, $J = 5.5$ Hz, H$_2$-10). This spin system suggests a presence of a propylene amide substructure.
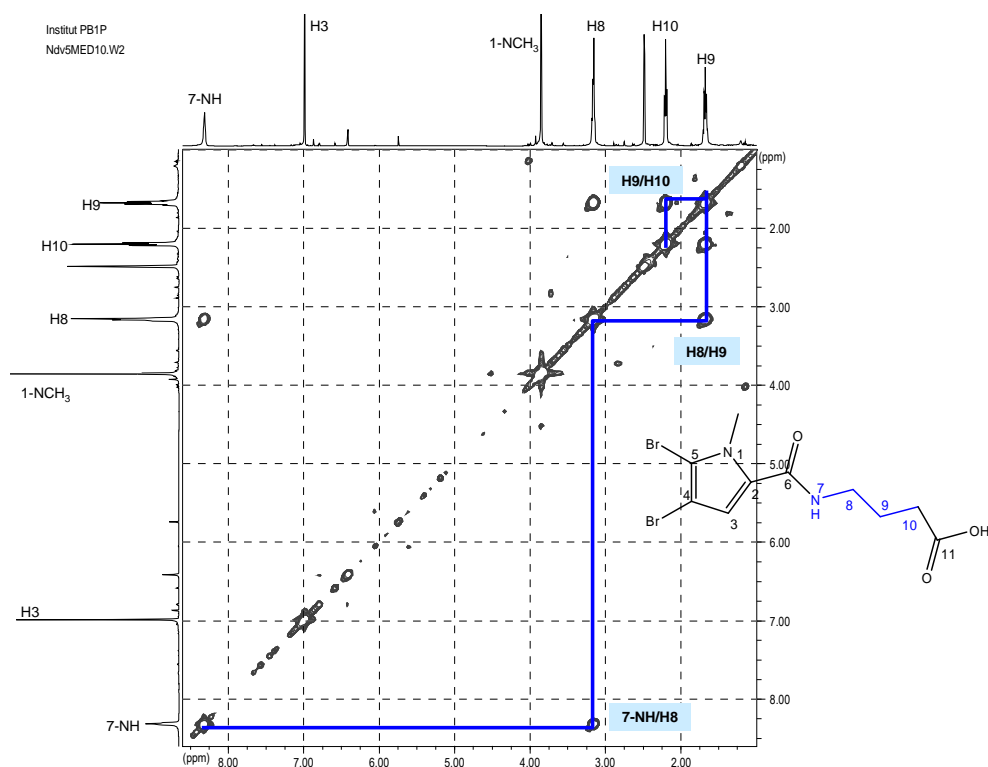
Fig.III.7. ^{1}H–^{1}H COSY correlation observed in compound **1** (DMSO-d_6)

Data obtained from the ^{13}C NMR spectrum (Fig.III.6) shows two deshielded quartenary carbon at δ_C 159.7 and 174.9 which are interpreted as a carboxamide and a carboxylic acid function, respectively. Intense cross peaks observed in ^{1}H - ^{13}C HMBC spectrum correlates the carboxylic acid carbon to H$_2$-9 and the carboxamide carbon to H$_2$-8 ($^3J_{C-H}$). This evidence suggests that the 4,5-dibromo-1-methyl-1*H*-pyrrole-2-carboxamide unit is connected to a carboxylic acid function through the propylene chain. NMR data comparison to a similar compound, 4-(4-bromo-1*H*-pyrrole-2-carboxamido)-butanoic acid isolated from Indonesian marine sponge *Agelas nakamurai* (Murti, 2006), supported the chemical structure proposed for compound **1** (Table III.1). Thus, the structure of compound **1** was elucidated as **4-(4,5-dibromo-1*H*-methyl-1*H*-pyrrole-2-carboxamido) butanoic acid.**
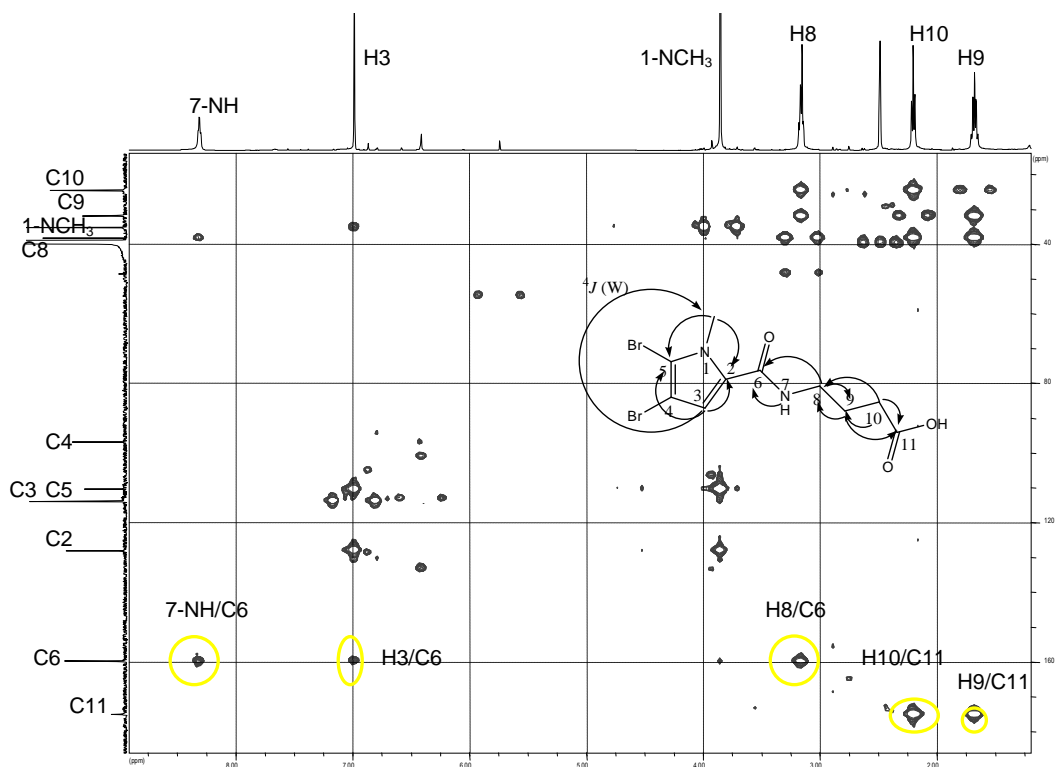
Fig.III.8. ^{1}H-^{13}C HMBC correlations observed in compound **1** (DMSO-*d$_6$*)

Table III.1. NMR data of compound 1 in comparison to 4-(4-bromo-1*H*-pyrrole-2-carboxamido)-butanoic acid

No.	4-(4-Bromo-1*H*-pyrrole-2-carboxamido)-butanoic acid [b]			Compound 1 [a]		
	^{1}H		^{13}C	^{1}H		^{13}C
	δ	Integration, multiplicity, *J* in Hz	δ, DEPT	δ	Integration, multiplicity, *J* in Hz	δ, DEPT
1-NCH$_3$	-	-	-	3.85	-	35.3, CH$_3$
2	-	-	127.1, C	-	-	128.0, C
3	6.75	1H, d, 1.5	112.8, CH	6.98	1H, s	113.8, CH
4	-	-	97.2, C	-	-	96.8, C
5	6.89	1H, d, 1.5	122.6, CH	-	-	110.3, C
6	-	-	162.3, C=O	-	-	159.7, C
7-NH	-	-	-	8.31	1H, t, 4.9	-
8	3.34	2H, t, 6.9	39.2, CH$_2$	3.16	2H, dd, 6.6, 5.0	38.3, CH$_2$
9	1.86	2H, q, 7.12	25.6, CH$_2$	1.68	2H, t, 6.9, 7.2	24.7, CH$_2$
10	2.34	2H, t, 7.4	32.3, CH$_2$	2.20	2H, t, 7.2	31.9, CH$_2$
11	-	-	177.1, C=O	-	-	174.9, C=O

[a] Data were recorded in DMSO-*d$_6$* at 500 MHz (^{1}H) and 125 MHz (^{13}C), multiplicities and coupling constant are given in Hz; [b] Data were recorded in MeOD at 500 MHz (^{1}H) and 125 MHz (^{13}C), multiplicities and coupling constant are given in Hz (Murti, 2006)

III.1.2. Agelanin A (**2,** new compound)
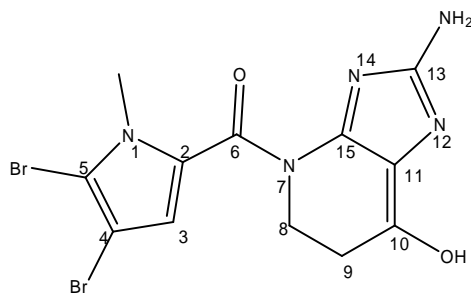
Fig.III.9. Compound **2**
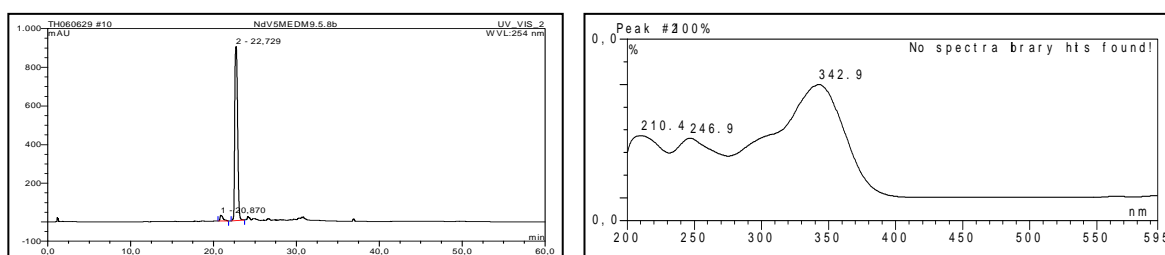
Fig.III.10. Analytical HPLC data of compound **2**
Left: HPLC profile in 254 nm, RT: 22.73; right: UV absorption spectrum, λ_{max} = 210.4, 246.9, 342.9 nm
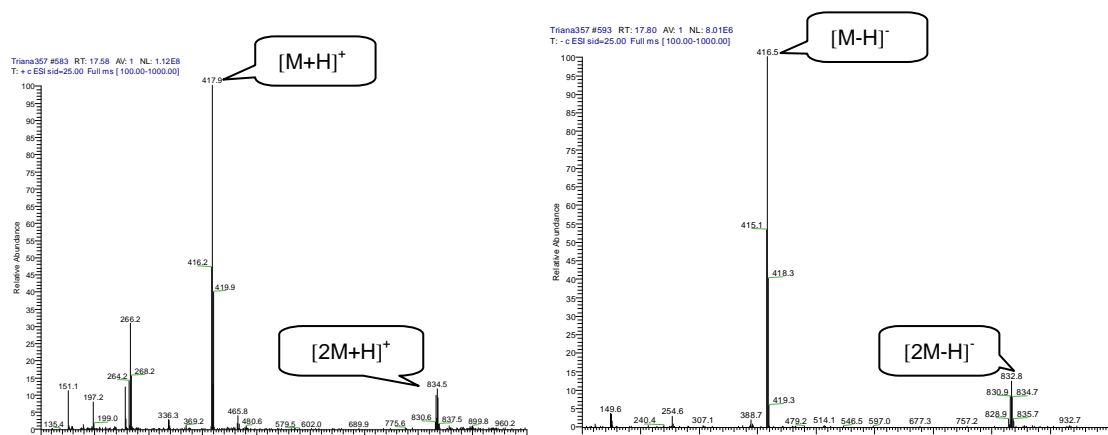
Fig.III.11. ESIMS data of compound **2**

Compound **2** was obtained as a brown amorphous substance (8 mg, 0.004%
of the sponge dried weight). It gives a distinct UV absorption pattern in comparison to
other bromopyrrole carboxamide congeners isolated from this sponge. The major
band peak is shifted about 70 nm to longer wavelength at 342.9 nm (Fig.III.10), which

might be due to an extended conjugated system and or to an additional hydroxyl unit in the molecule. ESIMS experiment with compound **2** results in intensive pseudo molecular ion cluster peaks at *m/z* 416/418/420 [M+H]$^+$ having an intensity ratio of 1:2:1. This finding corresponds to the presence of two bromines in the molecule (Fig.III.10). Molecular formula $C_{12}H_{12}Br_2N_5O_2$ was deducted from HRESIMS (*m/z* experimental = 415.9370; *m/z* calculated = 415.9358 [M+H]$^+$) together with the ^{13}C NMR analyses.

NMR data (Table III.2) exhibit similar signal patterns for 1*N*-methyl-4,5-dibromopyrrole 2-carboxamide substructure as can be found e.g. in compound **1**. Intense cross peaks correlating the signals of NCH_3 protons at δ_H 3.64 and pyrrole proton (H-3) at δ_H 6.62 to the C-5 at δ_C 110.2 and C-2 at δ_C 129.0 in the ^{1}H-^{13}C HMBC spectrum secures the substructure (Fig.III.16).

^{1}H NMR spectrum shows two broad signals in the lower field region. Signal at δ_H 11.15 (1H) is assigned as a hydroxyl group while the signal at δ_H 6.27 (2H) as protons of an imidazolamine moiety. ^{1}H-^{13}C HMBC experiment demonstrates a correlation of the hydroxyl proton to C-15 at δ_C 152.7 and C-11 at δ_C 110.5.
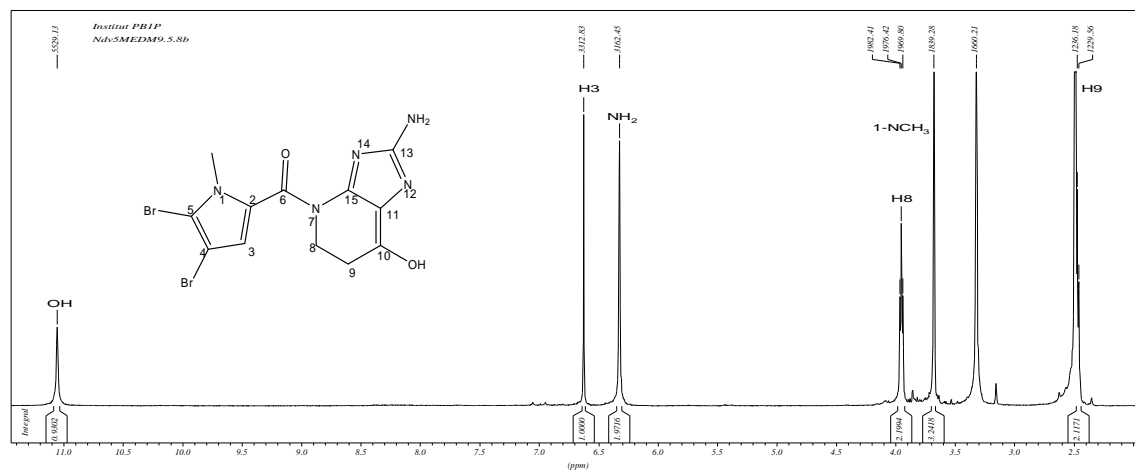
Fig.III.12. ^{1}H NMR data of compound **2 (**DMSO-d_6, 500 MHz)
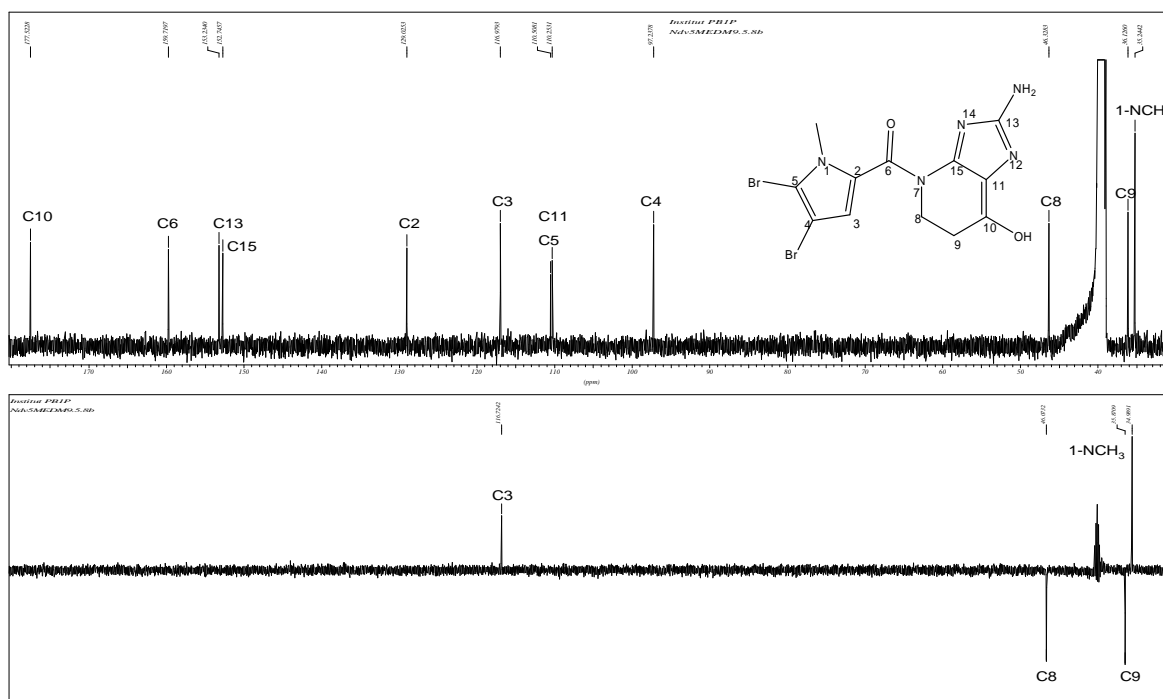
Fig.III.13. ^{13}C-NMR (above) and DEPT (below) spectra of compound **2** (DMSO-d_6, 125 MHz)

^{1}H NMR signal of the ethylidene unit are shifted to the lower field at δ_H 3.97 (2H, dd, J = 6.0, 6.6 Hz, H$_2$-8) and 2.47 (2H, t, J = 6.6 Hz, H$_2$-9). This may be caused by its position between two electronegative substituents. Intense cross peaks ($^3J_{C-H}$) in ^{1}H-^{13}C HMBC correlates H-8 to deshielded quartenary carbon signals at δ_C 159.7

(C-6) and at 177.5 (C-10) (Fig.III.16), while H_2-9 only correlates to C-10. $^1H - ^1H$ COSY experiment detects only one spin system in the molecule which correlates H_2-8 to H_2-9 (Fig.III.14). Hence this recommends that the *N*-amide is saturated. At first this finding leads to a dihydropyridone substructure. The question arouse from the chemical shift of the second carbonyl unit. It should be much more shifted to lower field (~δ_C 195) as could be also observed in cenocladamide (δ_C 194.1), a dihydropyridone alkaloid from *Piper cenocladum* (Dodson *et al.*, 2000). Therefore it is suggestive to replace the dihydropyridone unit with a tetrahydropyridinol function.

The substructure assembly was based on the ^{1}H-^{13}C HMBC data. Thus structure of compound **1** is determined as (2-amino-7-hydroxy-5,6-dihydroimidazo[4,5-*b*]pyridin-4-yl)(4,5-dibromo-1-methyl-1*H*-pyrrole-2-yl) methanone and named **agelanin A**.

Despite its very unique and rare modes of cyclization, a related compound, dibromoagelaspongin HCl was reported before from a Tanzanian sponge, *Agelas* sp. (Fedoreyev *et al.*, 1989).
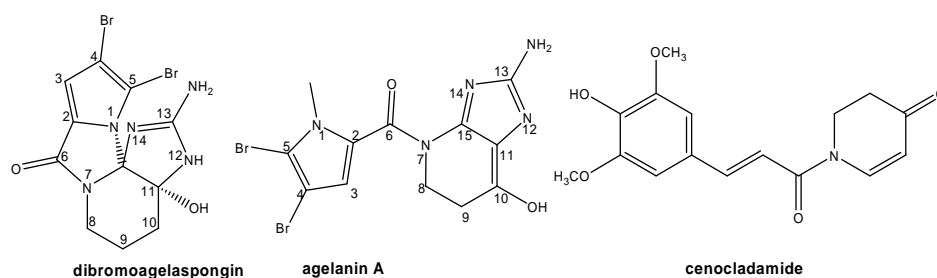
Fig.III.14. Structure of agelanin A and related compounds, cenocladamide (Dodson *et al.*, 2000) and dibromoagelaspongin (Fedoreyev *et al.*, 1989)
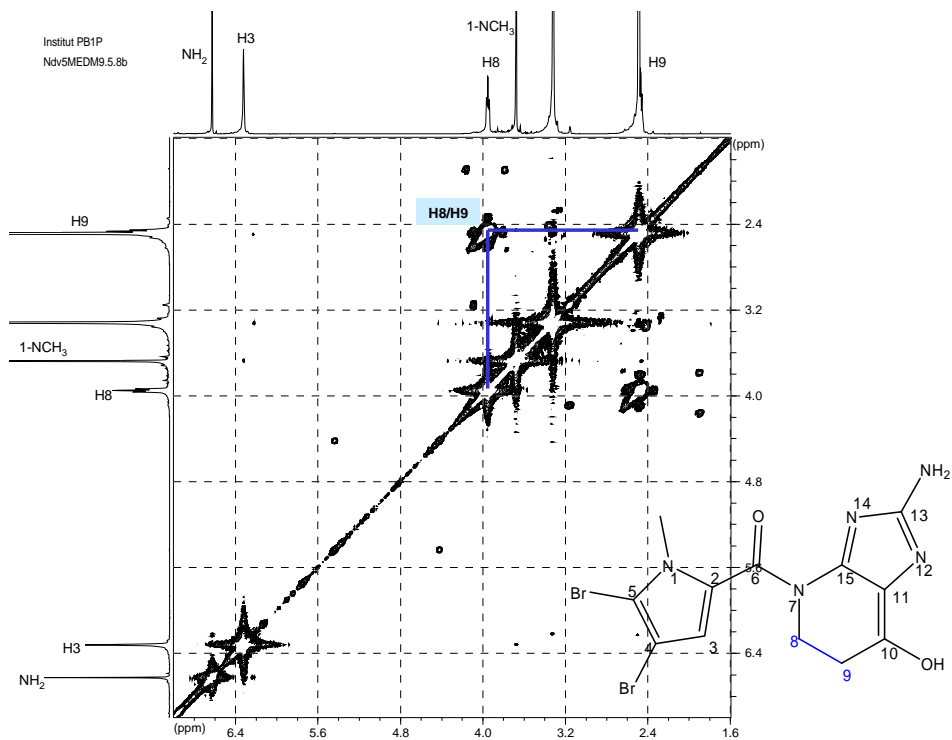
Fig.III.15. ^{1}H-^{1}H COSY spectrum of compound **2** (DMSO-d_6)
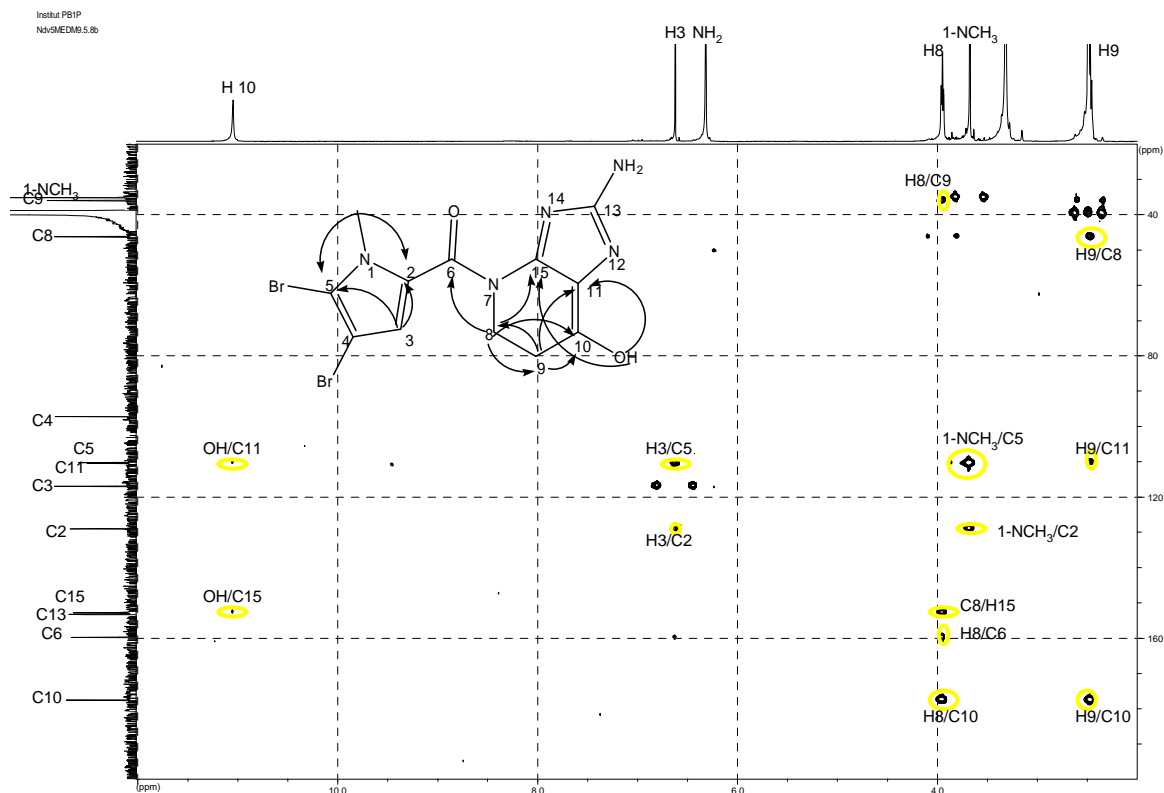
Fig. III.16. ^{1}H-^{13}C HMBC correlations observed in compound **2** (DMSO-d_6)

Table III.2. ^{1}H and ^{13}C-NMR data of compound 2 $^{a)}$

| No. | ^{1}H | | ^{13}C, DEPT |
	δ	Integration, multiplicity, *J* in Hz	
1-NCH$_3$	3.64	3H, s	35.2, CH$_3$
2	-	-	129.0, C
3	6.62	1H, s	117.0, CH
4	-	-	97.2, C
5	-	-	110.2, C
6	-	-	159.7, C=O
8	3.97	2H, dd, 6.0, 6.6	46.3, CH$_2$
9	2.47	2H, t, 6.6	36.1, CH$_2$
10	-	-	177.5, =C-OH
11	-	-	110.5, C
13	-	-	153.2, C
15	-	-	152.7, C
NH	11.15	1H, b s	-
NH$_2$	6.37	2H, b s	-

$^{a)}$ Data were recorded in DMSO-d_6 at 500 MHz (^{1}H) and 125 MHz (^{13}C), multiplicities and coupling constant are given in Hz.

III.1.3.   Agelanin B (**3,** new compound)
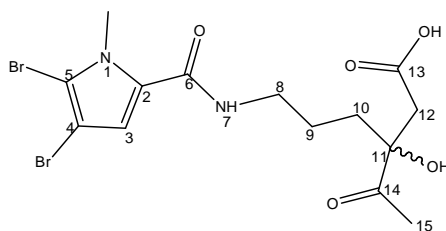
Fig.III.17. Compound **3**

Fig.III.18. Analytical HPLC data of compound **3**
Left: HPLC profile in 254 nm, RT: 25.93; right: UV absorption spectrum, λ_{max} = 208.8 and 275.6 nm
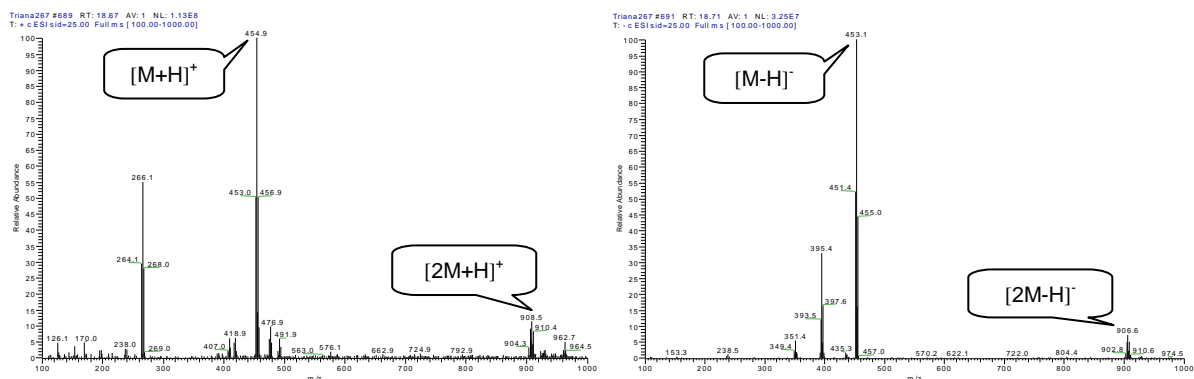
Fig.III.19. ESI-MS data of compound **3**

Compound **3** was obtained as a brown oily substance (25 mg, 0.013% of the sponge dried weight). This optically active compound exhibits a [α_D^{20}] value of -18.7º ± 2.8º (*c* 0.06, CH$_3$OH). Preliminary investigation by using analytical HPLC experiment discovered a typical UV absorption for pyrrole 2-carboxamide (Fig.III.18). ESIMS pseudo molecular ion cluster peaks at *m/z* 453/455/457 [M+H]$^+$ having an intensity ratio of 1:2:1 indicate a dibrominated compound. Molecular formula of C$_{14}$H$_{19}$Br$_2$N$_2$O$_5$ was deducted from HRESIMS (*m/z* experimental = 452.9680; *m/z* calculated = 452.9661 [M+H]$^+$) and ^{13}C NMR analyses.

NMR data (Table III.3) suggests a close relationship to midpacamide (compound **13**). Careful investigation of the ^{13}C and 2D NMR data proves unique structure of this compound where the imidazolidine-dione unit in midpacamide is replaced with a linear chain, 3-hydroxy-4-oxo-pentanoic acid moiety.
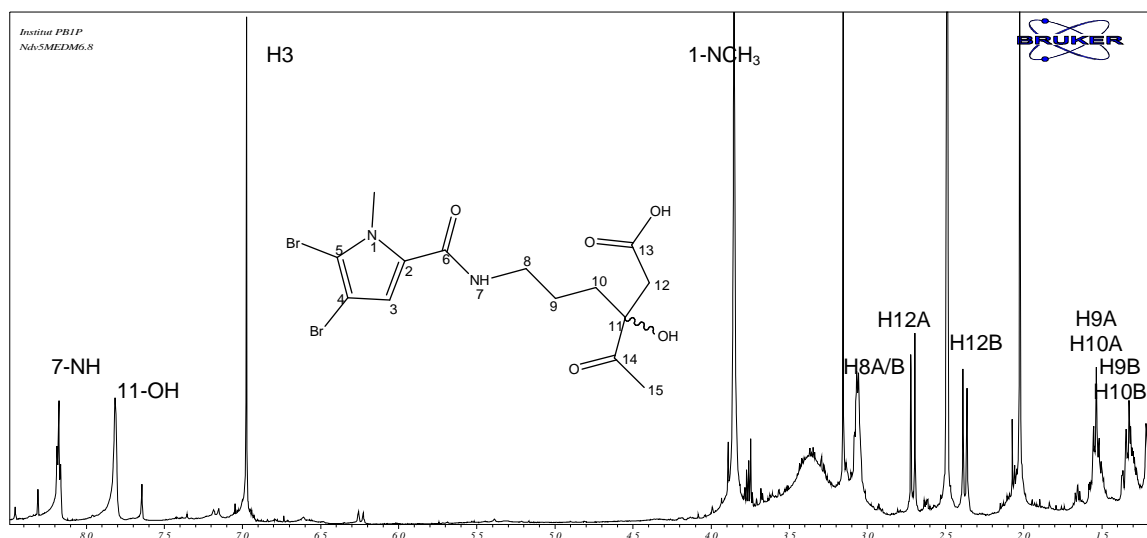
Fig.III.20. ^{1}H NMR spectrum of compound **3** (DMSO-d_6,500 MHz)

4,5-Dibromo-1-methyl-1*H*-pyrrole-2-carboxamide substructure was assigned based on a pyrrole proton at δ_H 6.97 (s) and a 1-NCH$_3$ signal at δ_H 3.85 (s). The ^{1}H - ^{13}C HMBC correlations of these protons to C-5 signal at δ_C 110.1 and C-2 at δ_H 128.2 support the pyrrole substructure (Fig.III.24). Other substructures observed are that of *N*-propylacetamide chain (δ_H 8.17, t, J = 5.7 Hz, 7-NH; δ_H 3.06, dt, J = 7.2, 5.7 Hz, H-8A/B; δ_{H2} 1.53, H-9A and H-10A; δ_{H2} 1.32, m, H-9B and H-10B); two geminal protons of an isolated methylene unit (δ_H 2.71, d, J = 12.9 Hz, H-12A and δ_H 2.37, d, J = 12.9, H-12B); a broad singlet signal derived from an hydroxyl group at δ_H 7.81; and a methyl ketone unit at δ_H 2.02 (s). Coupling constant between the geminal protons (12.9 Hz) indicates that the hydrogens are diastereotopic.
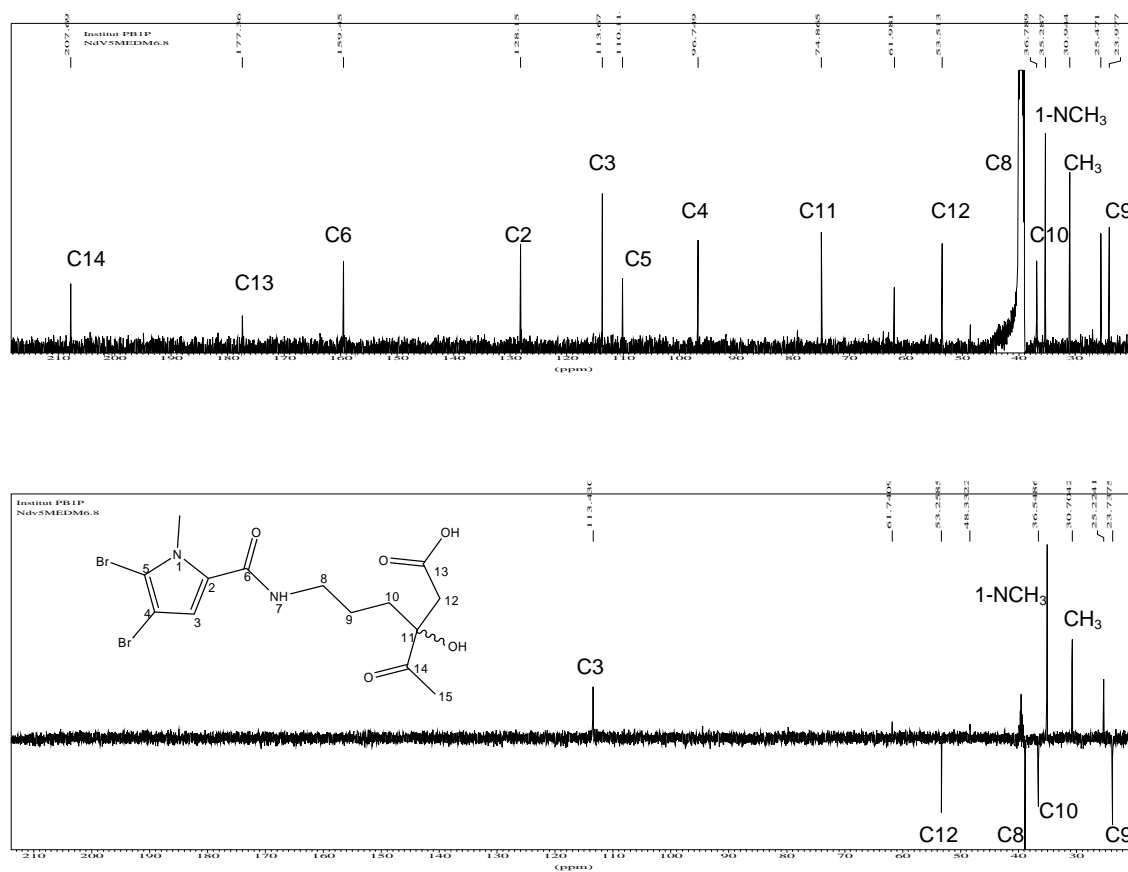
Fig.III.21. ^{13}C-NMR (above) and DEPT (below) spectra of compound **3 (**DMSO-d_6,125 MHz)

^{13}C NMR spectrum (Fig.III.21) supports the 4,5-dibromo-1-methyl-1*H*-pyrrole-2-carboxamide substructure as shown by resonances at δ_C 128.2 (C, C-2); δ_C 113.7 (CH, C-3); δ_C 96.7 (C, C-4); δ_C 110.1 (C, C-5); 159.4 (C=O, C-6); δ_C 35.3 (CH$_3$, 1-NCH$_3$), as well as the propylene chain presence shown at δ_C 38.8, CH$_2$, C-8; δ_C 24.0, CH$_2$, C-9; δ_C 36.8, CH$_2$, C-10). Two additional carbonyl groups are revealed by deshielded quaternary carbons at δ_C 207.7, assigned as a ketone unit and at δ_C 177.4, assigned a carboxylic acid function. The ketone unit is supported by a methyl keto signal at δ_C 30.9, δ_H 2.02 (s). A quartenary carbon at δ_C 74.9 is assigned as a hydroxyl bearing *sp^3* carbon (C-11). Based on ^{1}H-^{13}C HMQC analysis, the resonance

at δ_C 53.5 is a deshielded tertiary carbon assigned as C-12 (Fig.III.23).
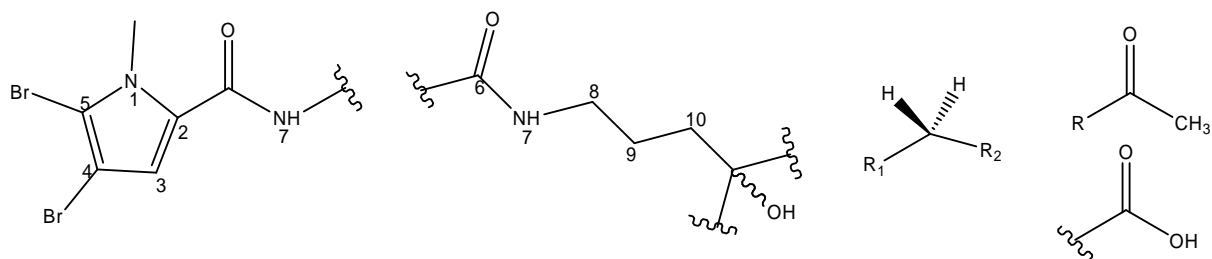
Fig.III.22. Different substructures detected in 1D-NMR experiment of compound **3**

2D NMR experiments provided data to assemble the different substructures. ^{1}H - ^{1}H COSY spectrum (Fig.III.19) exhibited two separate spin systems comprising a propylcarboxamidyl moiety and isolated geminal protons (H_2-12) correlating to each other. Further, the ^{1}H-^{13}C HMBC (Fig.III.24) indicates correlations of these methylene protons to the carbon ketone (C-14) and to the propylene chain (C-10) ($^3J_{C-H}$), whereas $^2J_{C-H}$ correlations were observed to the carboxylic carbon (C-13) and to C-11. These findings support the presence of a 3-hydroxy-4-oxo-pentanoic acid moiety to which the propylcarboxamidyl chain is attached. ^{1}H-^{13}C HMBC experiment also exhibited $^4J_{C-H}$ correlations from H-10B to C-13; H-12B to C-15 and H-15; to C-12 as described in Fig.III.25. Thus the complete structure of compound **3** was concluded as 3-acetyl-6-(4,5-dibromo-1-methyl-1*H*-pyrrole-2-carboxamido)-3-hydroxyhexanoic acid and assigned the trivial name **agelanin B.**
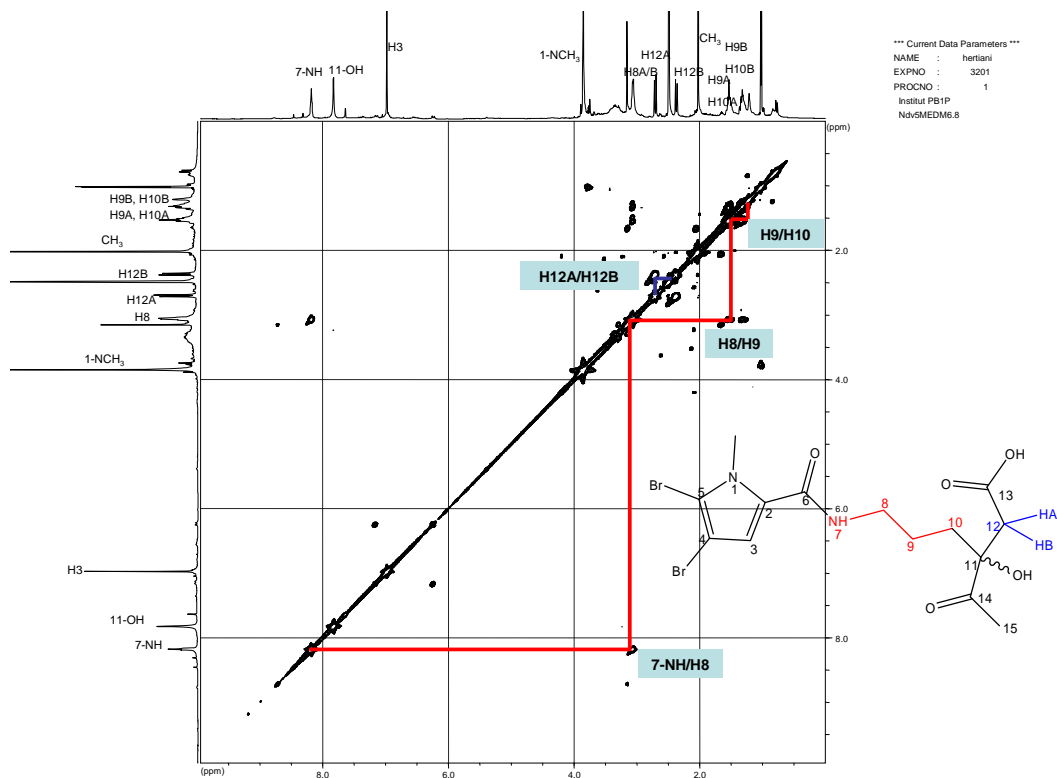
Fig.III.23. ^{1}H–^{1}H COSY spectrum of compound **3** (DMSO-d_6)
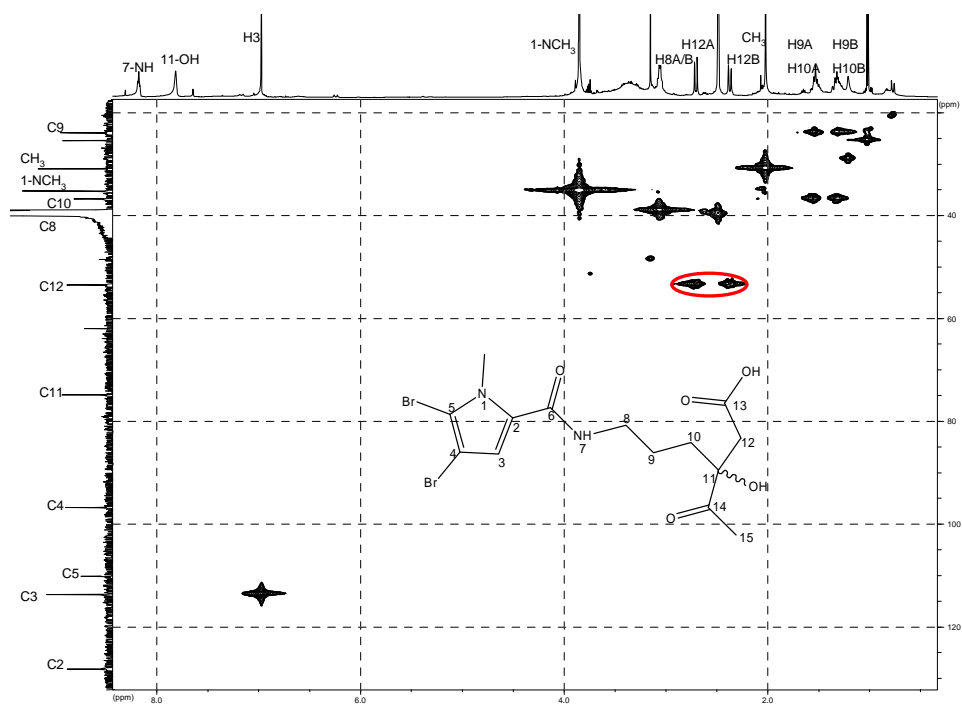
Fig.III.24. ^{1}H–^{13}C HMQC spectrum of compound **3** (DMSO-d_6)
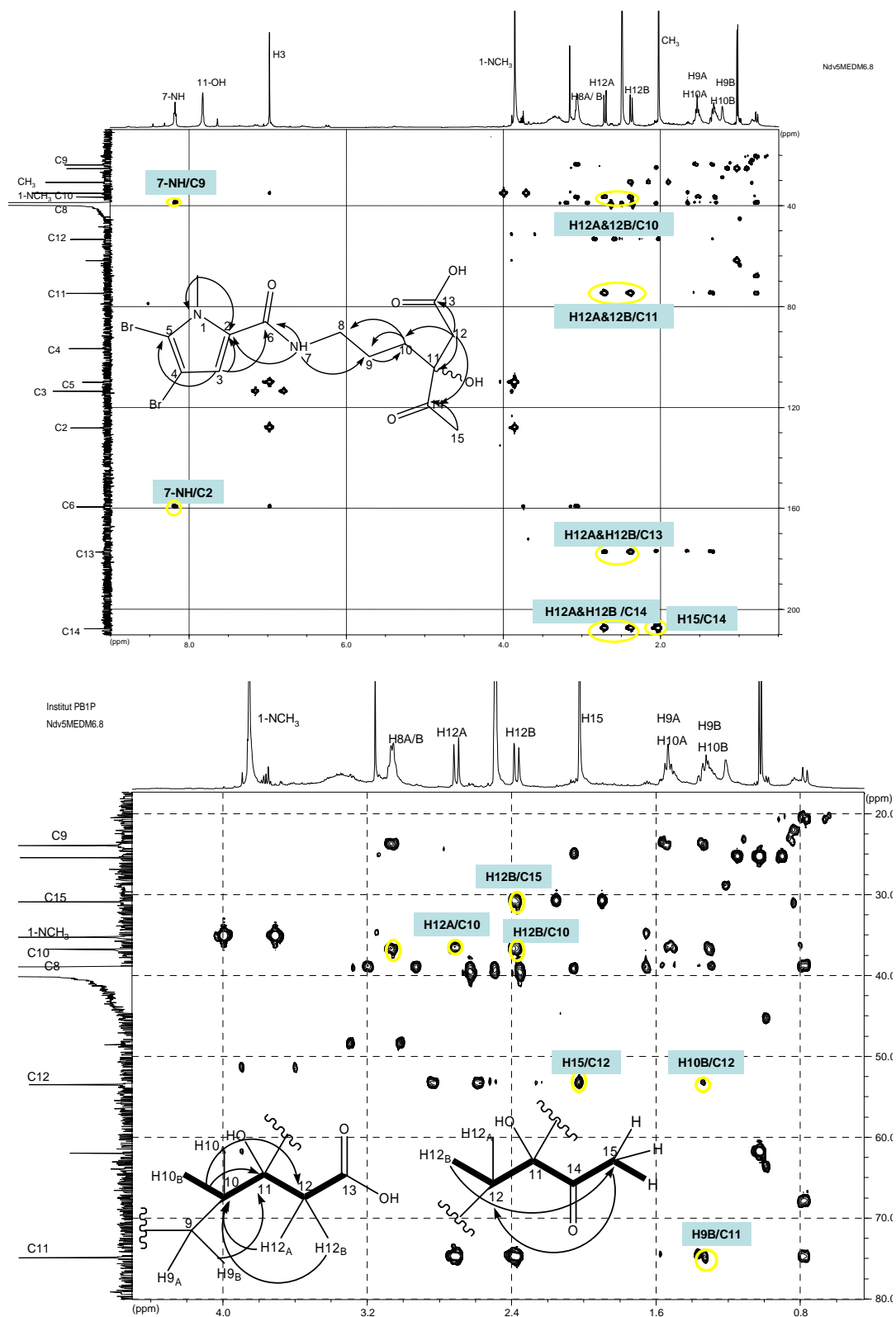
Fig.III.25. ^{1}H-^{13}C HMBC spectrum of compound **3** (DMSO-d_6)

Table III.3. NMR data of compound **3** in comparison to midpacamide (**13**) [b)]

No.	Midpacamide [b,c)]			Compound 3 [a,c)]		
	^{1}H		^{13}C	^{1}H		^{13}C
	δ	Integration, multiplicity, *J* in Hz	δ, DEPT	δ	Integration, multiplicity, *J* in Hz	δ, DEPT
2	-	-	127.3, C	-	-	128.2, C
3	6.66	1H, s	113.8, CH	6.97	1H, s	113.7, CH
4	-	-	97.9, C	-		96.7, C
5	-	-	111.7, C	-		110.1, C
6	-	-	157.9, C=O	-		159.4, C=O
7-NH	6.29	1H, bt, 5.5	-	8.17	1H, t, 5.7	-
8	3.39	2H, dt, 6.0	38.6, CH$_2$	3.06	2H, dt, 7.2, 5.7	38.8, CH$_2$
9	1.75	2H, m	28.7, CH$_2$	1.53 / 1.32	1H, m (A) / 1H, m (B)	24.0, CH$_2$
10	1.94 / 1.65	1H, m (A) / 1H, m (B)	25.0, CH$_2$	1.53 / 1.32	1H, m (A) / 1H, m (B)	36.8, CH$_2$
11	4.10	1H, t, 5.1	56.9, CH	-	-	74.9, C
12	6.73, b s		-	2.71 / 2.37	1H, d, 12.9 (A) / 1H, d, 12.9 (B)	53.5, CH$_2$
13	-	-	160.7, C	-	-	177.4, C=O
15		1H, b s	174.3, C=O	2.02	3H, s	30.9, CH$_3$
14-NCH$_3$	3.00	-	24.6, CH$_3$	-	-	207.7, C=O
1-NCH$_3$	3.95	3H, s	35.7, CH$_3$	3.85,	3H, s	35.3, CH$_3$

[a)] Data were recorded in DMSO-*d$_6$* at 500 MHz (^{1}H) and 125 MHz (^{13}C); [b)] Data were recorded in CDCl$_3$ at 500 MHz (^{1}H) and 125 MHz (^{13}C); [c)] multiplicities and coupling constant are given in Hz

## III.1.4. Agelanesin A (**4,** new compound)
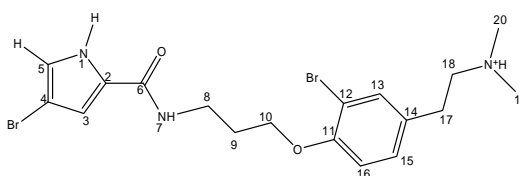
Fig.III.26. Compound **4**
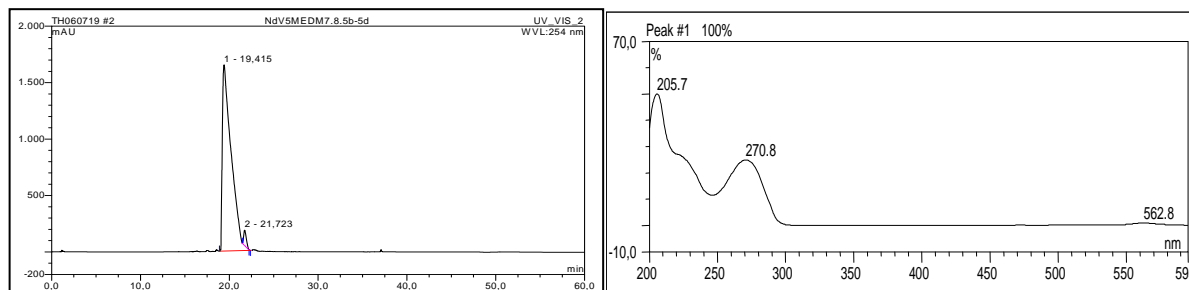
Fig.III.27. Analytical HPLC data of compound **4**
Left: HPLC profile in 254 nm, RT: 19.41; right: UV absorption spectrum, λ_{max} = 205.7 nm and 270.8 nm
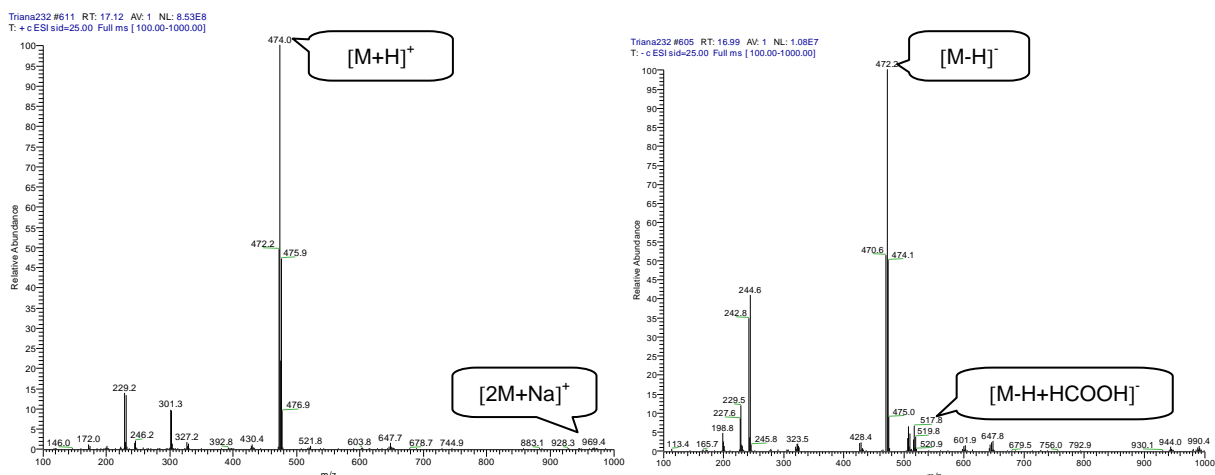
Fig.III.28. ESI-MS data of compound **4**

Compound **4** was obtained as a yellow oily substance in an amount of 20 mg (0.01% of the sponge dried weight). UV absorption pattern observed for compound **4** (Fig.III.27) is slightly different in comparison to the other 2-pyrrole carboxamide congeners isolated from this sponge. It has an additional band peak at 205.7 nm with no changes in the λ_{max} at 270.8 nm suggesting a presence of another chromophore besides the pyrrole carboxamide.

Combined analysis of HRESIMS and ^{13}C-NMR spectra of compound **4** corresponds to the molecular formula of $C_{18}H_{24}Br_2N_3O_2$ (*m/z* experimental = 472.0250; *m/z* calculated = 472.0235 [M+H]$^+$). Intensive pseudo molecular ion clusters peaks are observed in the ESI-MS spectrum at *m/z* 472/474/476 [M+H]$^+$ having an intensity ratio of 1:2:1 which indicates the presence of a dibrominated compound.
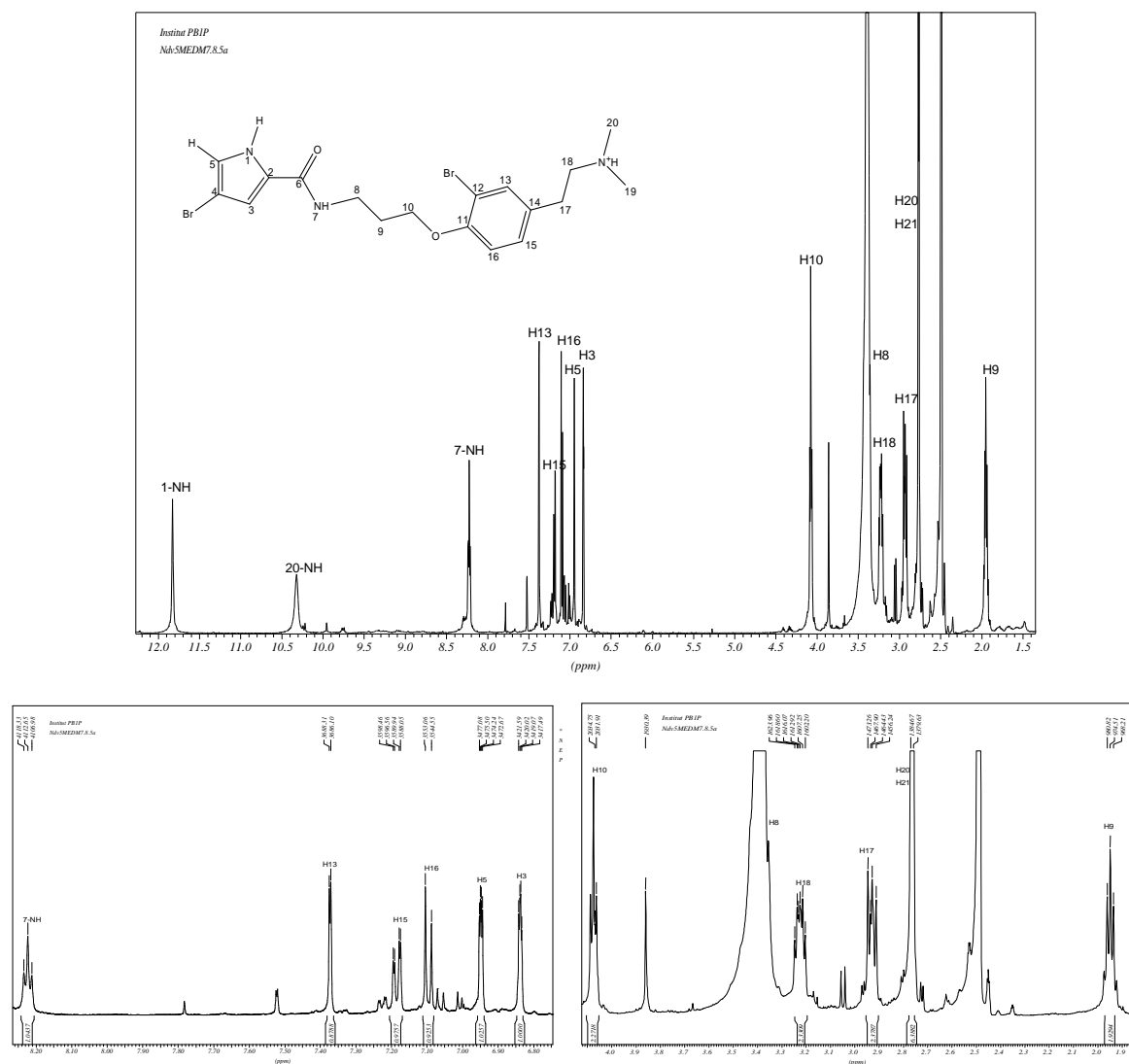
Fig.III.29. ^{1}H-NMR data of compound **4** (DMSO-d_6, 500 MHz)

^{1}H NMR spectrum of compound **4** shows six well-separated signals in the upper field region (Fig.III.29). Five methylene signals are confirmed while the sixth signal at δ_H 2.76 (6H, d, J = 5.0 Hz) is assigned as a signal of a dimethylammonium unit coupled to a broad singlet at δ_H 10.3. The signal at δ_H 4.08 is suggestive of methylene protons adjacent to an oxygen while a methylene unit next to a carboxamide group is exhibited by a resonance at δ_H 3.35. ABX systems were found in the lower field region in addition to the proton signals of the pyrrole ring as

observed at δ_H 6.83 (1H, d, J = 1.9, 0.6 Hz, H-3); 6.94 (1H, d, J = 1.9, 0.6 Hz, H-5); and an NH signal at δ_H 11.82.

Further investigation of the ABX ring system leads to a 1,2,4-trisubstituted benzene ring based on the ^{1}H NMR signals at δ_H 7.42 (1H, d, J = 2.2 Hz, H-13); 7.15 (1H, dd, J = 1.9, 8.5 Hz, H-15); 6.99 (1H, d, J = 8.5 Hz, H-16). ^{13}C NMR signals (Fig.III.30) suggests the presence of a halogenated phenol through a highly shielded quaternary carbon signal at δ_C 110.8 (C-12) and a deshielding effect due to an oxygenated substitution observed for a quaternary carbon signal at around δ_C 152.9 (C-11). The typical chemical shift signal for a bromine-bearing carbon (C-12) found in **4** can be also observed in known bromotyrosine derivatives like purealidin A (Ishibashi *et al.*, 1991) and purpuramine J (Tabudravu and Jaspars, 2002).

Four spin systems are detected in ^{1}H-^{1}H COSY (Fig.III.32). One spin system correlates the two pyrrole protons; one correlates the dimethylammonium unit to an ethylidene chain; another spin system connects the O-CH_2 to the NH-CH_2 through one methylene unit suggesting an oxypropylamide chain; and one spin system indicates the ABX ring. This evidence suggests that compound **4** is a monobrominated pyrrole connected to a trisubstituted tyramine through an oxypropylamide chain.
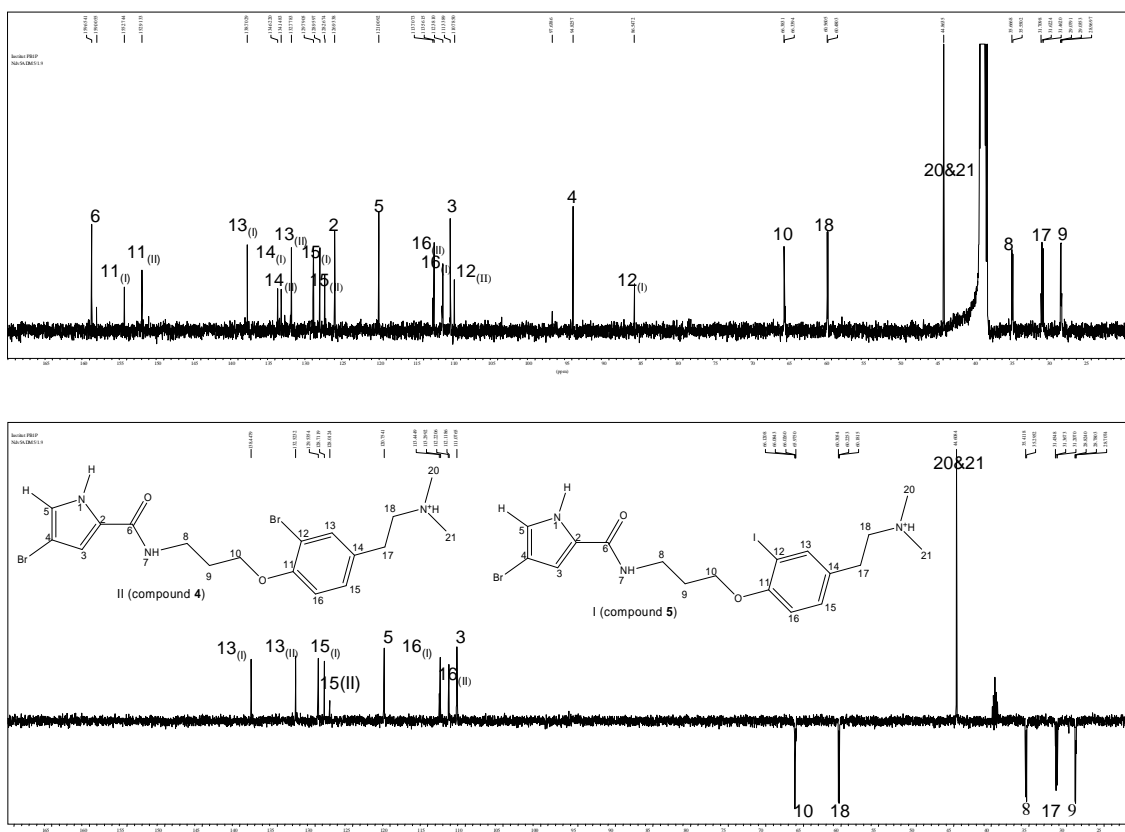
Fig.III.30. ^{13}C-NMR data of compounds **4** and **5** in 1:1 mixture of the base form
Peaks I refer to **5** and II to **4** (DMSO-d_6, 125 MHz)
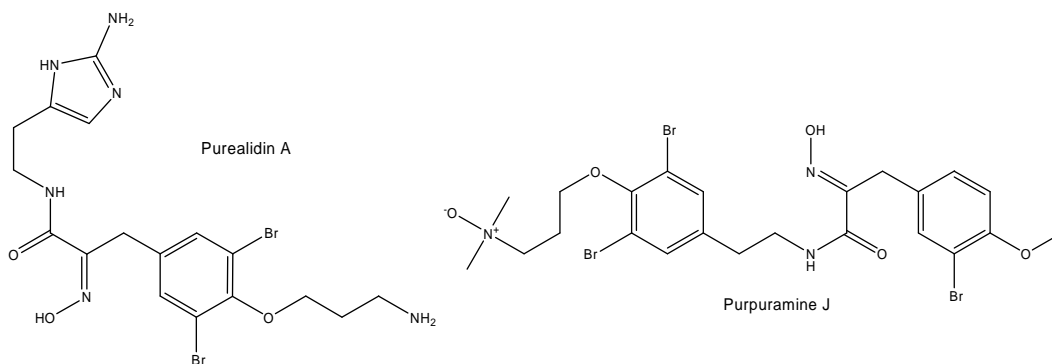
Fig.III.31. Structures of purealidin A (Ishibashi *et al.*, 1991) and purpuramine J (Tabudravu and Jaspars, 2002).
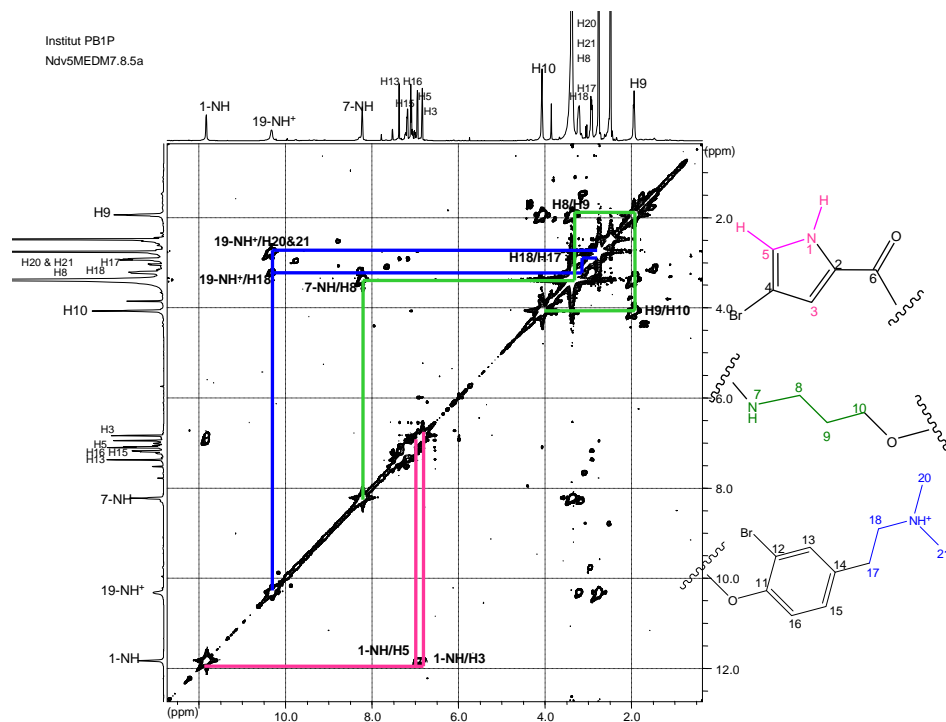
Fig.III.32a. ^{1}H-^{1}H COSY correlations observed in compound **4**
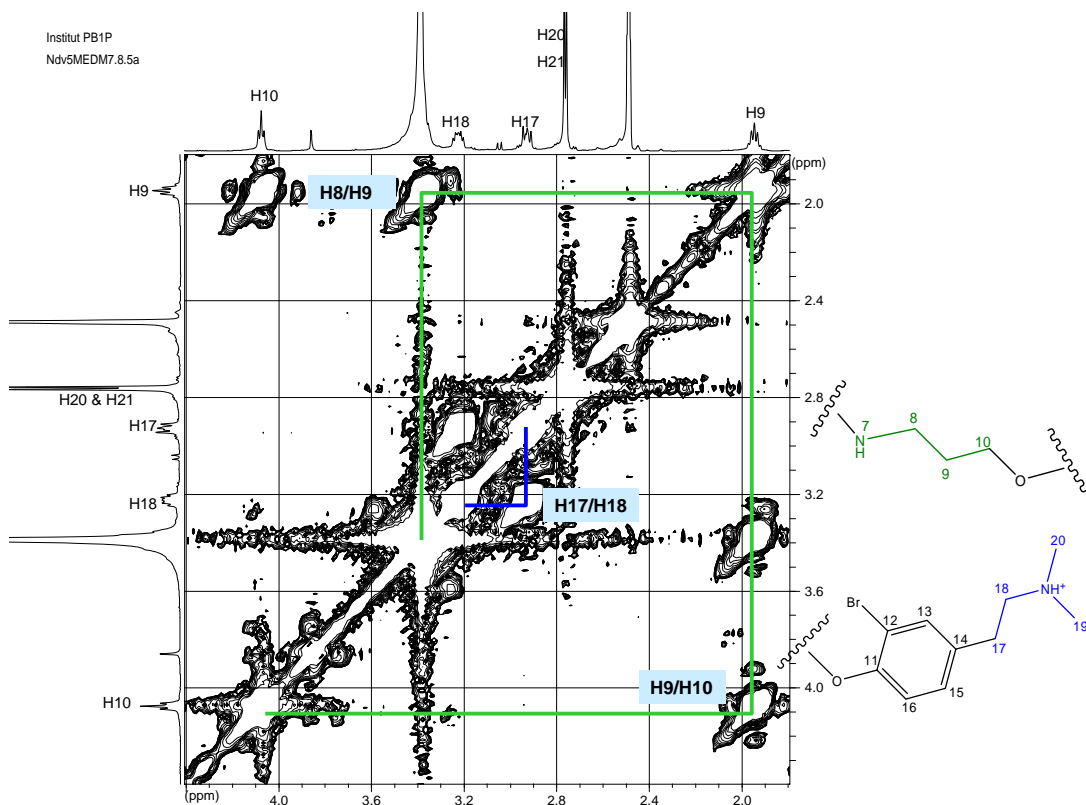
Fig.III.32b. ^{1}H-^{1}H COSY expansion of the correlations in aliphatic region observed in compound **4**
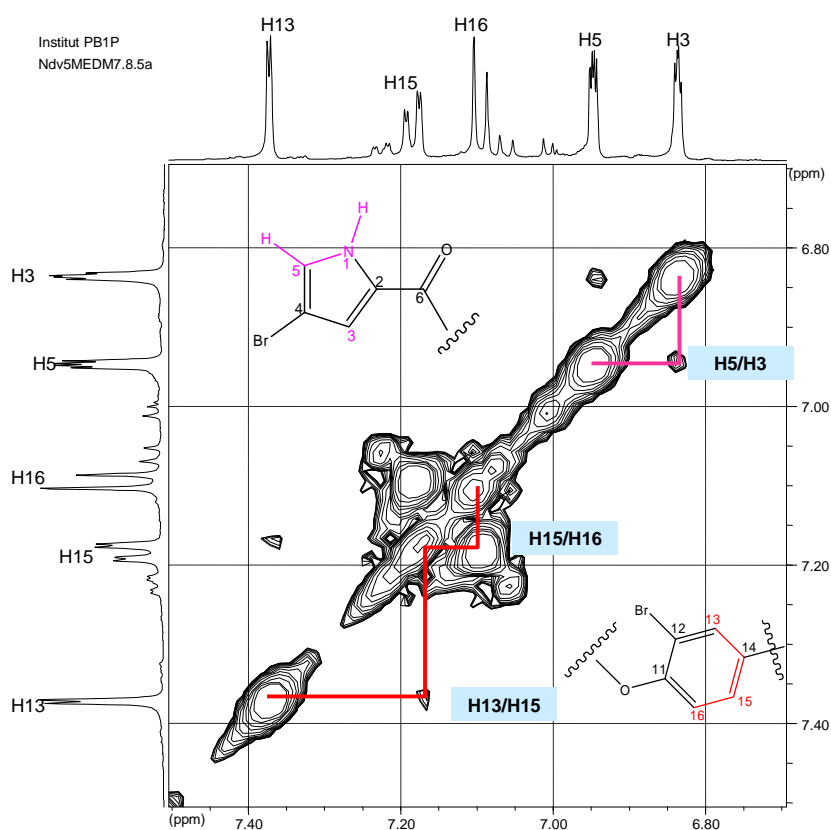
Fig.III.32c. ^{1}H-^{1}H COSY expansion of the correlations in aromatic region observed in compound **4**

^{1}H-^{13}C HMBC as shown in Fig.III.33 confirms the connection of each substructure proposed by the COSY spectrum. Intensive cross peak correlating H-10 to C-11 secures the connection of the oxypropylamide to the benzene ring. Cross peaks correlating the benzene ring protons to the *N,N*-dimethylethanaminium chain carbons as well as from the *N,N*-dimethylethanaminium chain protons to the benzene ring carbons confirm the tyramine unit.

Thus the structure of **4** is concluded as 4-bromo-*N*-(3-(2-bromo-4-2-(dimethylamino)ethyl)phenoxy) propyl)-1*H*-pyrrole-2-carboxamide to which the name **agelanesin A** is assigned (Fig.III.26)
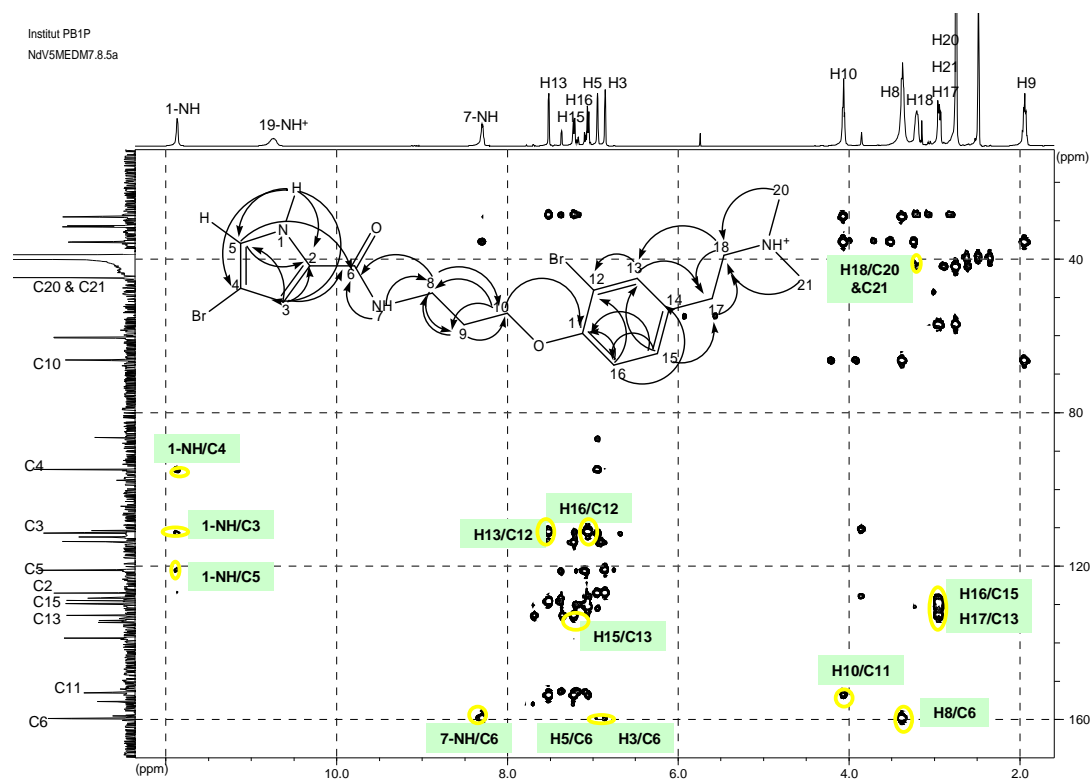
Fig.III.33. ^{1}H - ^{13}C NMR spectrum of compound **4** (DMSO-d_6)

III.1.5. Agelanesin B (**5,** new compound)
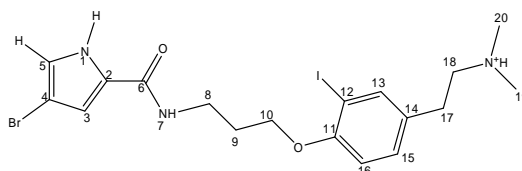

Fig.III.34. Compound **5**

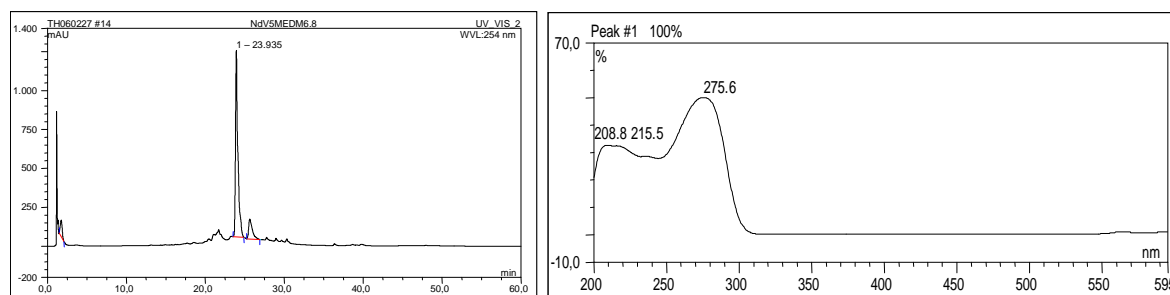
Fig.III.35. Analytical HPLC data of compound **5**

Left: HPLC profile in 254 nm RT: 21.56; right: UV absorption spectrum, λ$_{max}$ = 208.4 nm and 270.9 nm
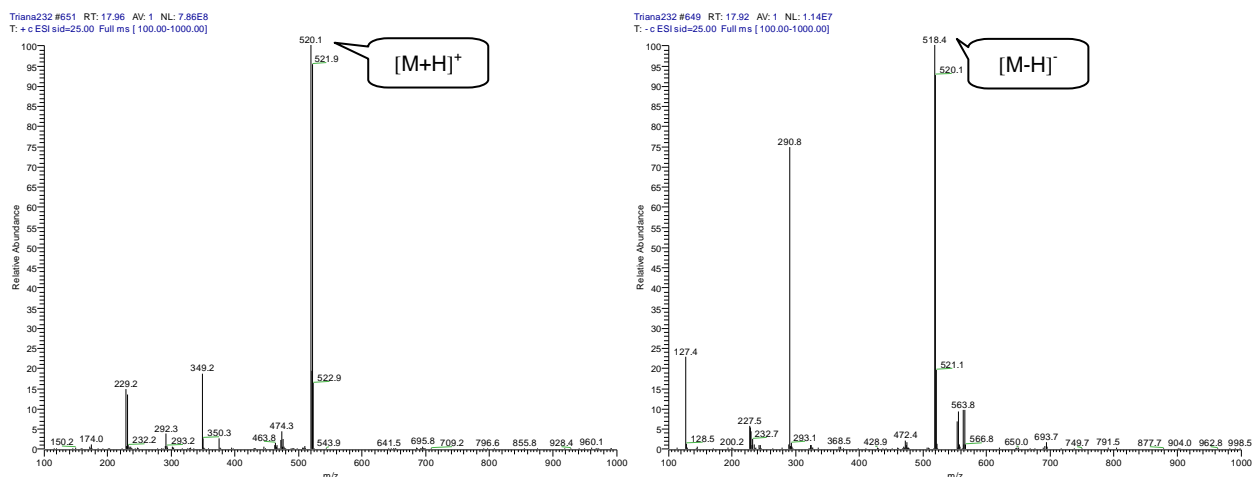
Fig.III.36. ESI-MS data of compound **5**

Compound **5** was obtained as a yellow oily substance in an amount of 24 mg (0.012% of the sponge dried weight). Analytical HPLC profile of compound **5** in comparison to compound **4** reveals a retention time shift from 19.41 min to 21.56 min (Fig.III.35). A slight bathochromic effect in the UV absorption spectrum of peak I is observed from 205.7 nm to 208.4 nm. ESI-MS shows pseudo molecular ion cluster peaks at *m/z* 519/521 [M+H]$^+$ having an intensity ratio of 1:1 indicating the presence of one bromine atom in the molecule. Combined analysis of HRESIMS and ^{13}C-NMR spectra indicates the molecular formula of $C_{18}H_{24}BrIN_3O_2$ (*m/z* experimental = 520.0110; *m/z* calculated = 520.0097 [M+H]$^+$).
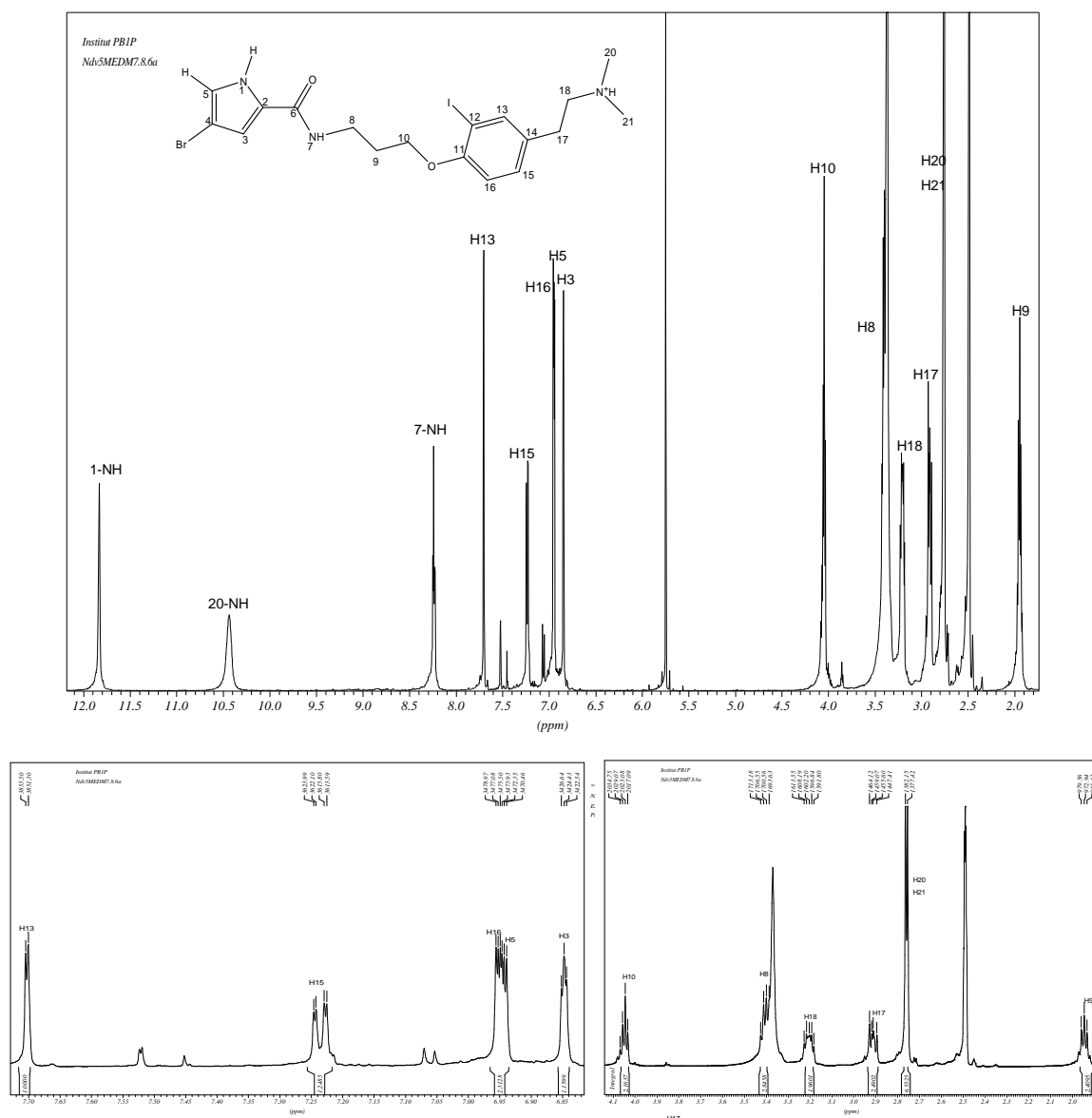
Fig.III.37. ¹H-NMR spectrum of compound **5** (DMSO-*d₆*, 500 MHz)

NMR spectral data of compound **5** (Table III.4) shows close relationship to compound **4**. Compound **5** exhibits 6 proton signals in the higher field region which are almost identical to the one found in compound **4**. It also shows comparable proton signals in the lower field region with some remarkable differences in chemical shifts in the benzene ring signals (Table III.4). The H-13 and H-15 signals are shifted to the lower field at δ_H 7.70 (1H, d, *J* = 1.9 Hz) and at δ_H 7.23 (1H, dd, *J* = 2.2, 8.5

Hz), respectively, while H-16 is shifted more upfield at δ_H 6.88 (1H, d, *J* = 8.5 Hz, H-16) in comparison to the ones in compound **4**. These signals fit a 1,2,4-trisubstituted benzene substructure as found in compound **4** with a different substituent at position 12.

Four spin systems are detected in the ^{1}H - ^{1}H COSY spectrum correlating the pyrrole ring protons; methylenes and the amide of the oxypropylamide chain, the benzene protons and the *N,N*-dimethylethanaminium protons.

^{13}C NMR experiment was done on the base form mixture of compounds **4** and **5** at ratio of 1:1 in DMSO-*d_6*. The signals obtained confirm the proposed structure as well as the similarity to compound **4** (Fig. III.30). Signals of the benzene ring are shifted to the lower field i.e. C-11 (δ_C 155.3) and C-13 (δ_C 138.7), while C-16 (δ_C 112.4) and C-12 (δ_C 86.5) are shifted to the upper field region. Extremely high field quartenary carbon observed for C-12 clearly distinguish the *sp^2* carbon atoms linked to iodine which were also observed in an iodotyrosine compound, dakaramine isolated from sponge *Ptilocaulis spiculifer* (Diop *et al.,* 1996).
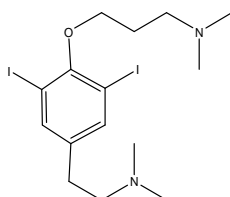
Fig.III.38. Structure of dakaramine (*Diop et al.*,1996)

^{1}H-^{13}C correlations (HMBC) of compound **5** as shown in Fig.III.39 give information needed to assemble the substructures. Hence the structure of compound **5** is determined as 4-bromo-*N*-(3-(4-(2-(dimethyl-amino)ethyl)-2-iodophenoxy) propyl)-1*H*-pyrrole-2-carboxamide (Fig. III.34) and was named **agelanesin B**.
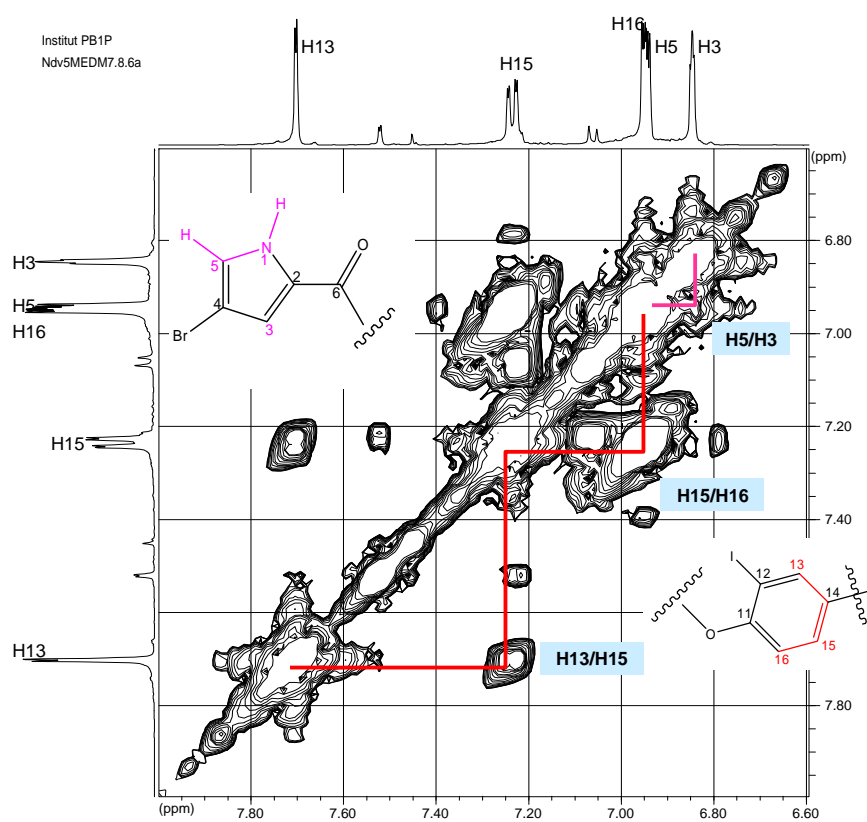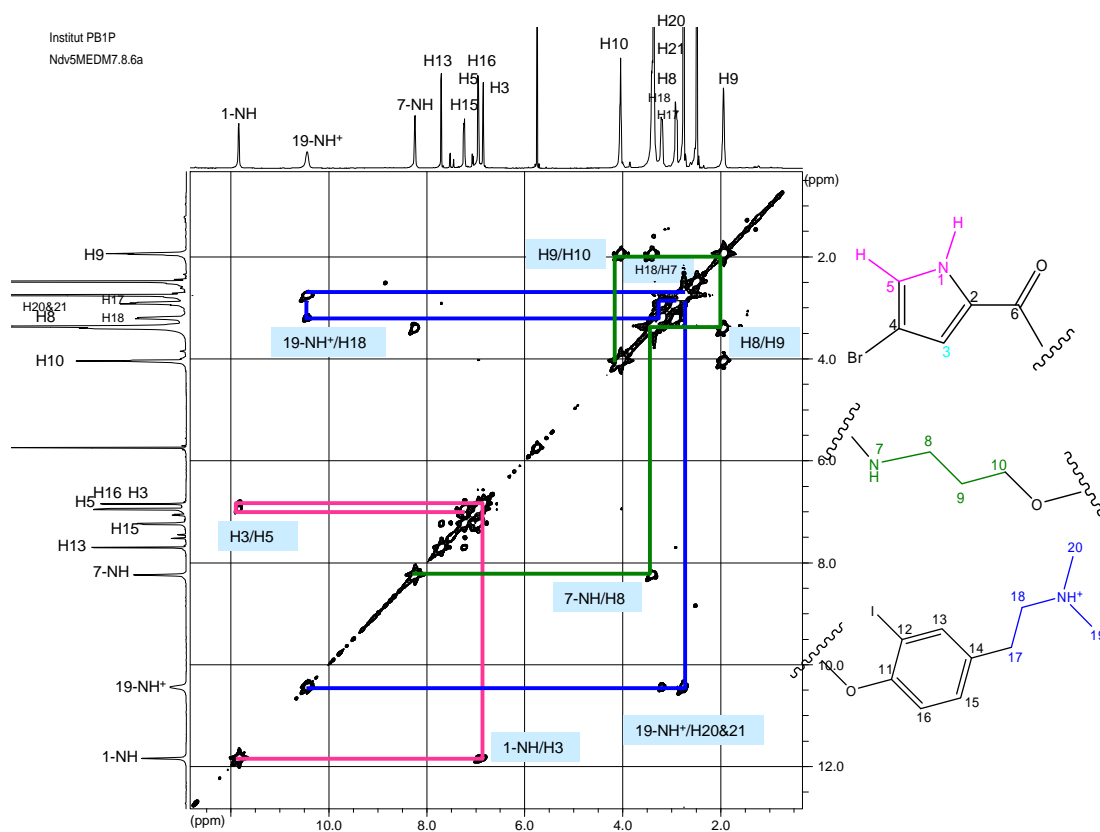
Fig.III.39. ^{1}H-^{1}H COSY spectrum of compound **5** (DMSO-*d6*)
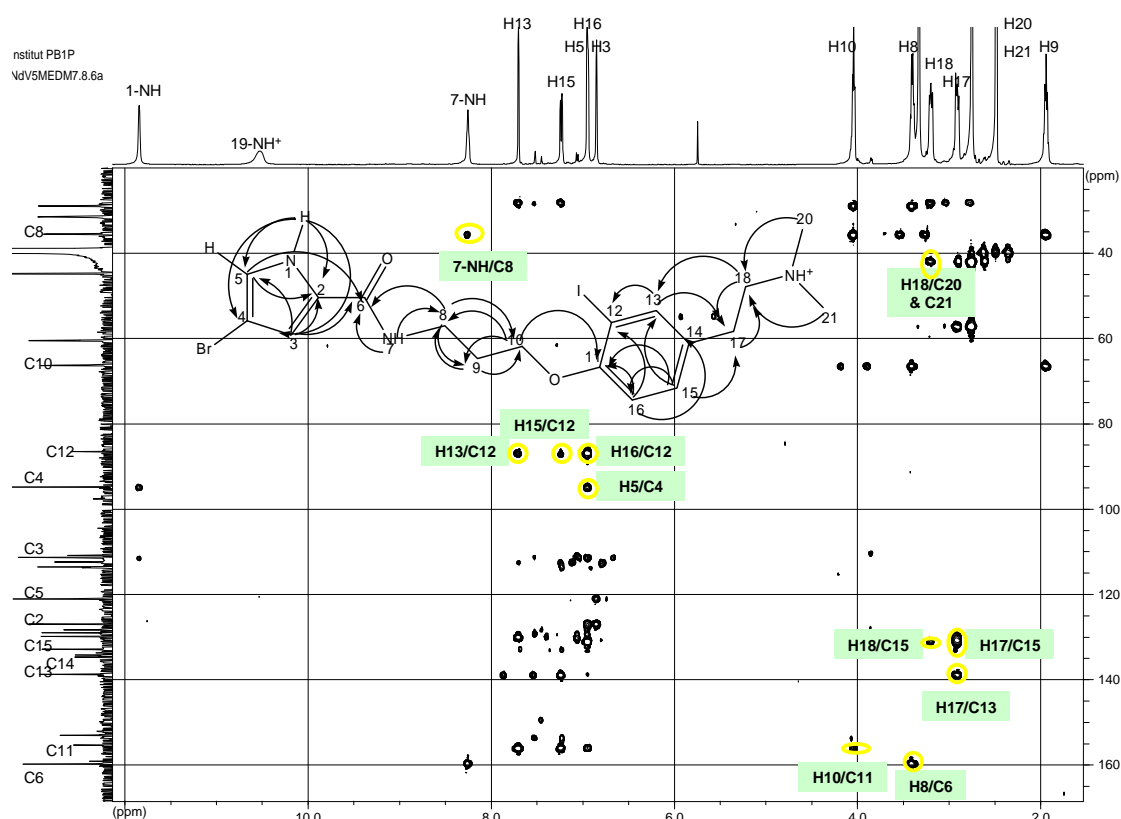
Fig.III.40. ^{1}H-^{13}C HMBC spectrum of compound **5** (DMSO-d_6)

Table III.4. ^{1}H and ^{13}C-NMR data of compound **4** and **5**

No.	Compound 4 [a]			Compound 5 [a]		
	^{1}H		^{13}C	^{1}H		^{13}C
	δ	Multiplicity, *J* in Hz	δ, DEPT	δ	Multiplicity, *J* in Hz	δ, DEPT
1-NH	11.82	b s	-	11.70	b s	-
2	-	-	126.9, C	-	-	126.9, C
3	6.84	dd, 1.9, 0.6	111.3, CH	6.85	dd, 1.9, 0.6	111.3, CH
4	-		94.8, C	-		94.8, C
5	6.95	dd, 1.9, 0.6	121.0, CH	6.94	dd, 1.9, 0.6	121.0, CH
6	-		159.6, C=O	-	-	159.6, C=O
7-NH	8.22	t, 5.5	-	8.23	t, 5.6	-
8	3.40	m	35.4, CH$_2$	3.41	m	35.4, CH$_2$
9	1.95	dt, 6.1, 6.3, 12.6	29.0, CH$_2$	1.95	dt, 6.3, 12.6	29.0, CH$_2$
10	4.07	t, 6.3	66.4, CH$_2$	4.04	t, 6.3	66.4, CH$_2$
11	-	-	152.9, C	-	-	155.3, C
12	-	-	110.8, C	-	-	86.5, C
13	7.37	d, 2.2	132.8, CH	7.70	d, 1.9	138.7, CH
14	-	-	134.1, C	-	-	134.6, C
15	7.18	dd, 1.9, 8.5	129.0, CH	7.23	dd, 2.2, 8.5	129.8, CH
16	7.09	d, 8.5	113.6, CH	6.96	d, 8.5	112.4, CH
17	2.93	dt, 8.5, 5.4	31.4, CH$_2$	2.92	m	31.3, CH$_2$
18	3.23	m	60.6, CH$_2$	3.20	m	60.6, CH$_2$
19-NH$^+$	10.32	d, 1.9	-	10.40	d, 1.9	-
20&21	2.76	d, 5.0	44.9, CH$_3$	2.76,	s	44.9, CH$_3$

[a] Data were recorded in DMSO-d_6 at 500 MHz (^{1}H) and 125 MHz (^{13}C), multiplicities and coupling constant are given in Hz.

III.1.6. **Agelanesin C** (**6**, new compound)
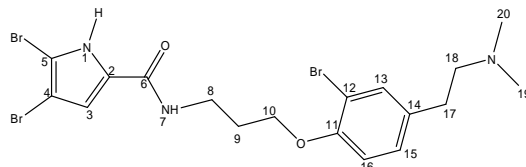
Fig.III.41. Compound **6**
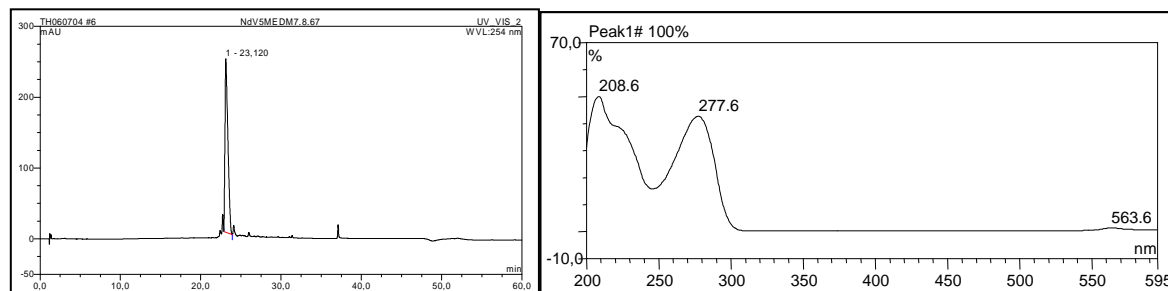
Fig.III.42. Analytical HPLC data of compound **6**

Left: HPLC profile in 254 nm, RT: 23.12; right: UV absorption spectrum, λ_{max} = 208.6 nm and 277.6 nm
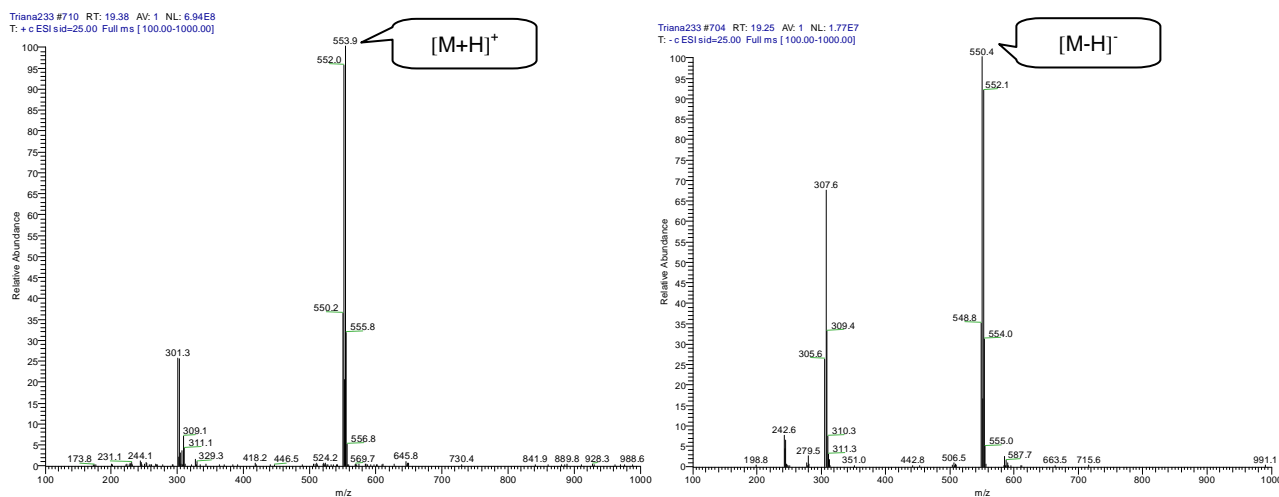
Fig.III.43. ESI-MS data of compound **6**

Compound **6** was obtained as a yellow oily substance in an amount of 6 mg (0.003% of the sponge dried weight). Analytical HPLC investigation also reveals a close structural relationship with compounds **4** and **5**. Its retention time is at 23.12 min and the UV absorption spectrum of both major bands are shifted to 208.6 nm (I) and to 277.6 nm (II) in comparison the its congeners. Higher degree of halogenation in the pyrrole ring may play a role to shift the λ_{max} of bands II from ~ 270 nm to ~ 277

nm. The presence of more bromine atom in the molecule is shown by ESI-MS pseudo molecular ion cluster peaks at *m/z* 550/552/554/556 [M+H]+ having an intensity ratio of 1:2.2:1. Combined analysis of HRESIMS and ^{13}C-NMR spectra of compound **6** fits the molecular formula of $C_{18}H_{23}Br_3N_3O_2$ (*m/z* experimental = 549.9350; *m/z* calculated = 549.9340 [M+H]+).
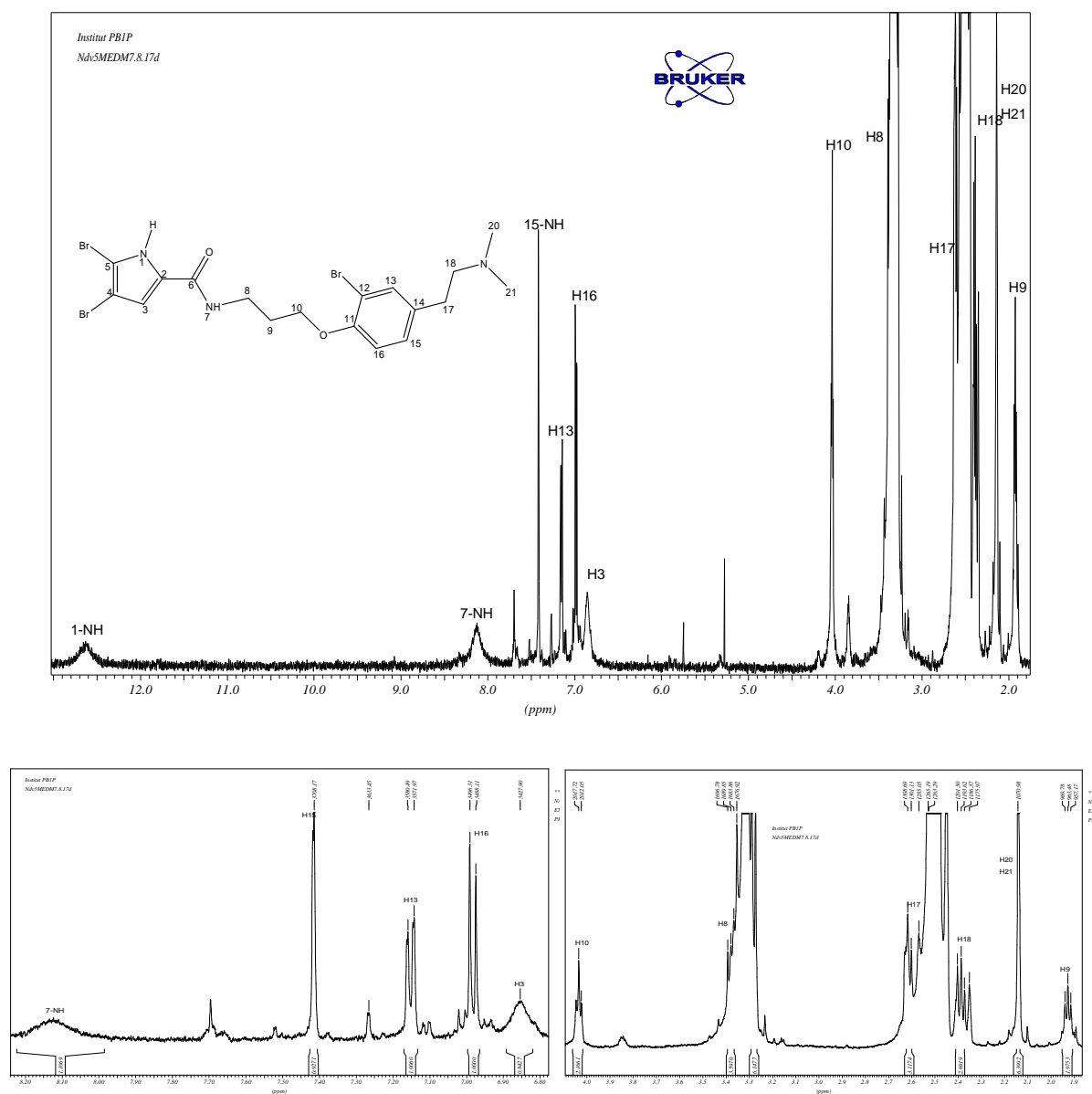
Fig.III.44. ^{1}H-NMR data of compound **6** (DMSO-d_6, 500 MHz)
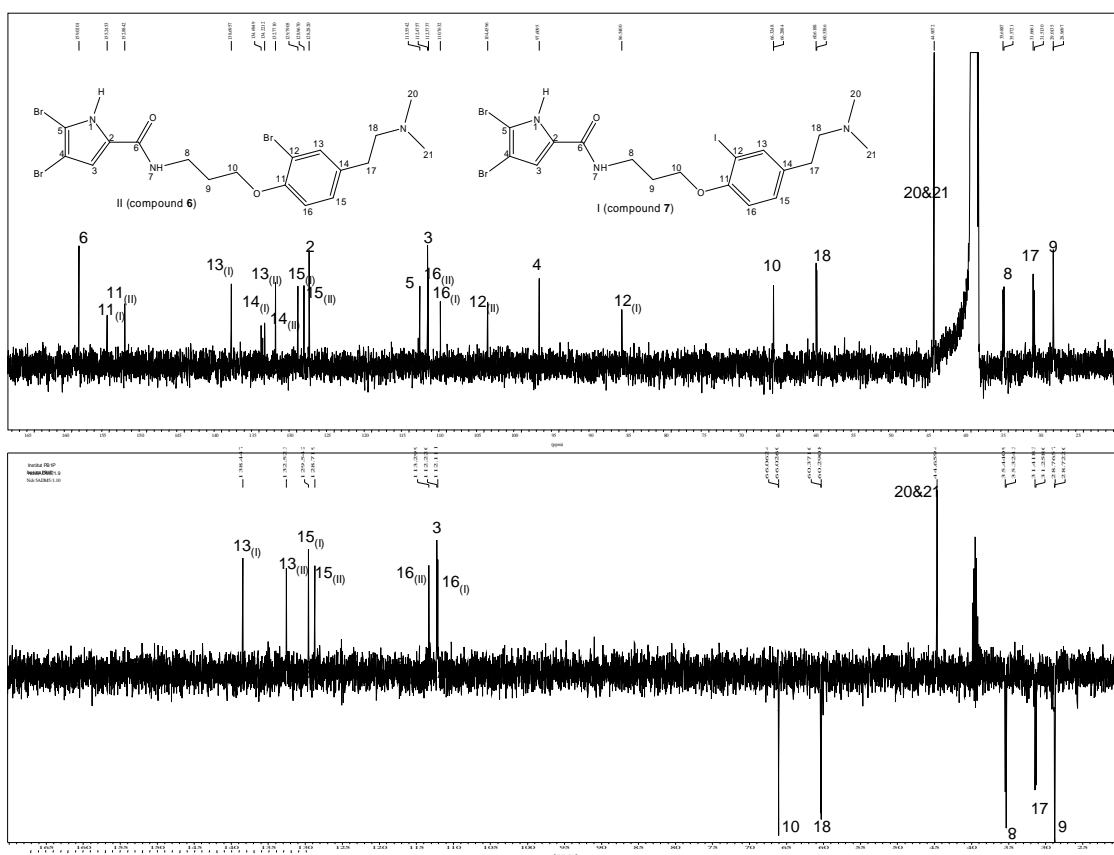
Fig.III.45. ^{13}C-NMR data of compound **6** and **7** in 1:1 mixture (DMSO-d_6,125 MHz)
Peaks I refer to **7** and II to **6**

^{1}H NMR spectrum of compound **6** as also can be observed in compounds **4** and **5**, and shows six well-separated signals at the upper field region (Fig.III.44). But unlike its previous congener, compounds **4** and **5** which were isolated as dimethylammonium salts, compound **6** was obtained in the dimethylamine base form. The absence of proton 19-NH$^+$ and the appearance of the *N*-dimethyl signal as a sharp singlet at δ_H 2.14 support this phenomenon. Supportive evidence is also provided by the presence of ethylidene chain protons in compound **6** at δ_H 2.62 (2H, m, H$_2$-17) and 2.38 (2H, m, H$_2$-18). These signals are shifted to the upper field in comparison to the ethylidene chain in *N,N*-dimethylethanaminium salt.

^{1}H-^{1}H COSY confirms the correlation of the *N,N*-dimethylethaneamine protons (Fig.III.46). The second spin system observed connects one multiplet signal of 7-NH

at δ_H 8.12 to the oxypropylidene chain at δ_H 3.38 (2H, m, H$_2$-8), 1.92 (2H, m, H$_2$-9), and 4.04 (2H, m, H$_2$-10). The pyrrole proton appears as a broad singlet correlated to a broad signal of 1-NH at δ_H 12.55. This finding suggests the presence of a three-substituted pyrrole ring. An ABX ring system is observed as the fourth spin system.

Further investigation of the ABX ring system confirms the presence of 1,2,4-trisubstituted benzene ring based on the ^{1}H NMR signals at δ_H 7.42 (1H, d, J = 1.9 Hz, H-15); 7.15 (1H, dd, J = 2.2, 8.5, H-15); 6.98 (1H, d, J = 8.5 Hz, H-16). ^{13}C NMR data of the benzene ring are reminiscent to those of compound **4**. The C-12 quaternary carbon signal at δ_C 110.8 (Fig.III.45) indicates that the tyramine unit is brominated as is also observed in compound **4**.

^{1}H-^{13}C HMBC spectrum (Fig.III.47) confirms the connectivity of each of the substructures. Hence the chemical structure of compound **6** as a 4,5-dibromo-*N*-3-(2-bromo-4-(2-(dimethylamino)ethyl)phenoxy)propyl)-1*H*-pyrrole-2-carboxamide (Fig.III.41) is determined and is named **agelanesin C**.
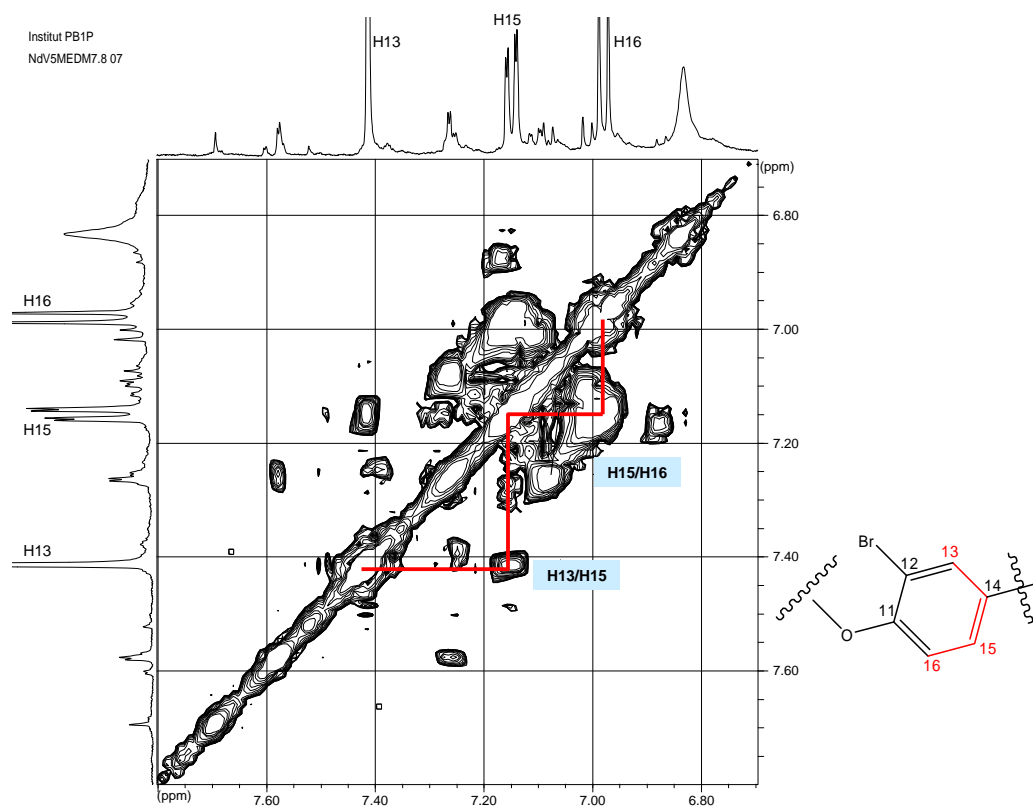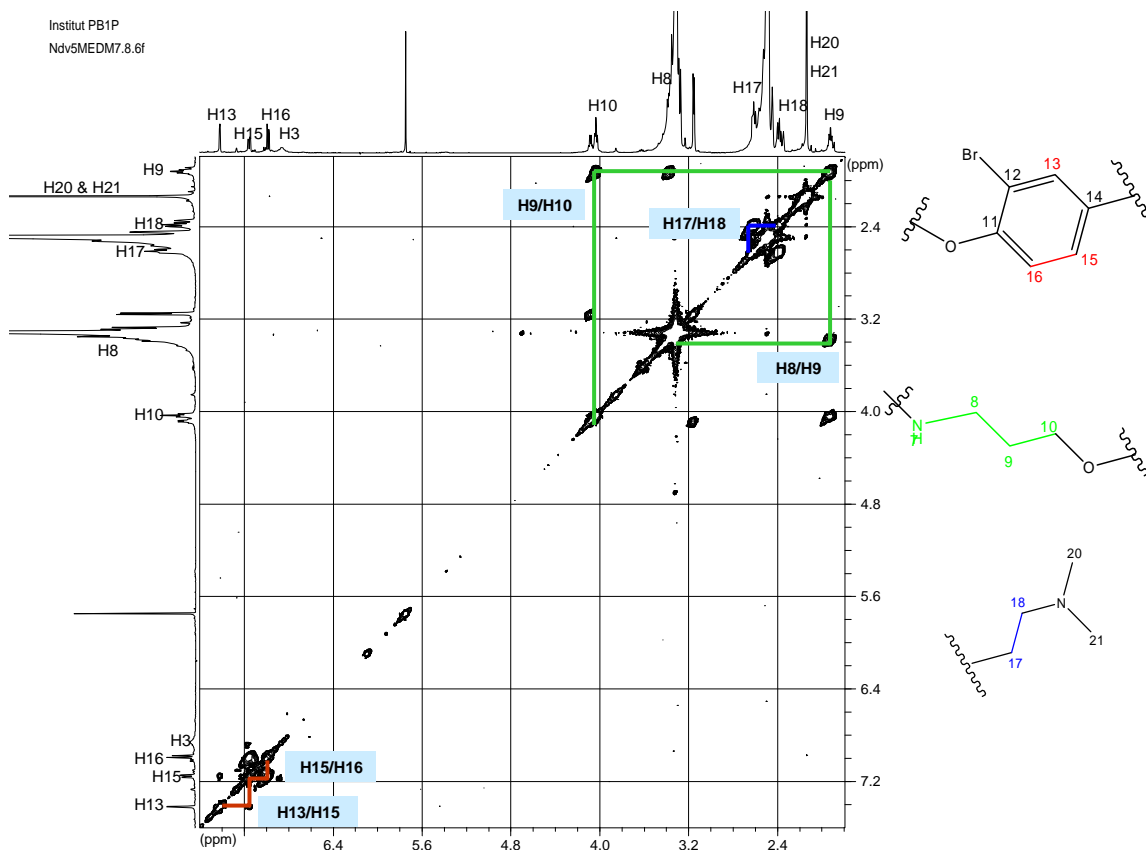
Fig.III.46. ^{1}H-^{1}H COSY spectrum of compound **6** (DMSO-d_6)
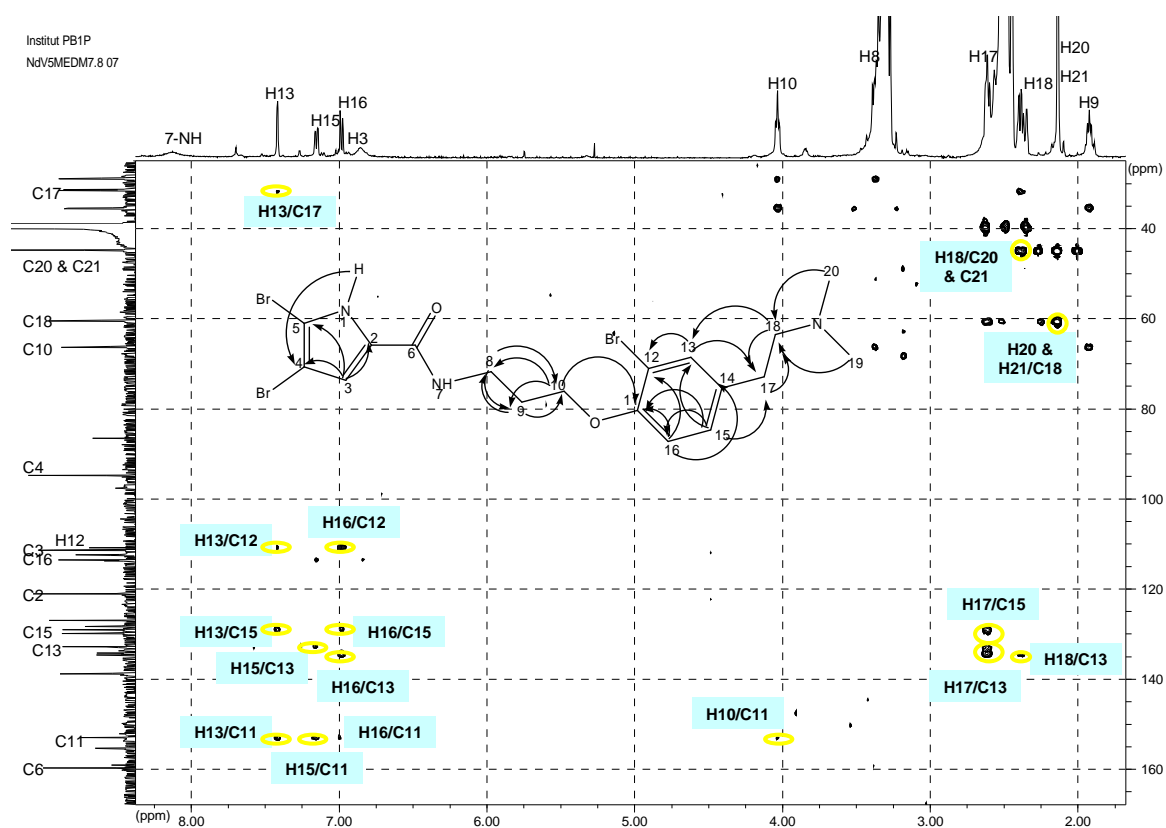
Fig.III.47. ^{1}H-^{13}C HMBC of compound **6**

III.1.7. **Agelanesin D** (**7**, new compound)
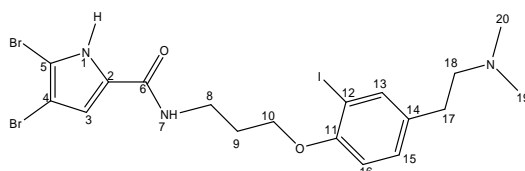
Fig.III.48. Compound **7**
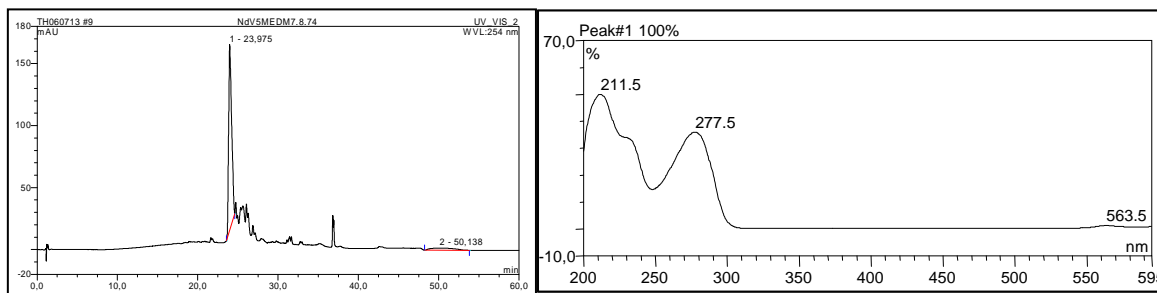
Fig.III.49. Analytical HPLC data of compound **7**
Left: HPLC profile in 254 nm, RT: 23.97; right: UV absorption spectrum, λ_{max} = 211.5 nm and 277.9 nm
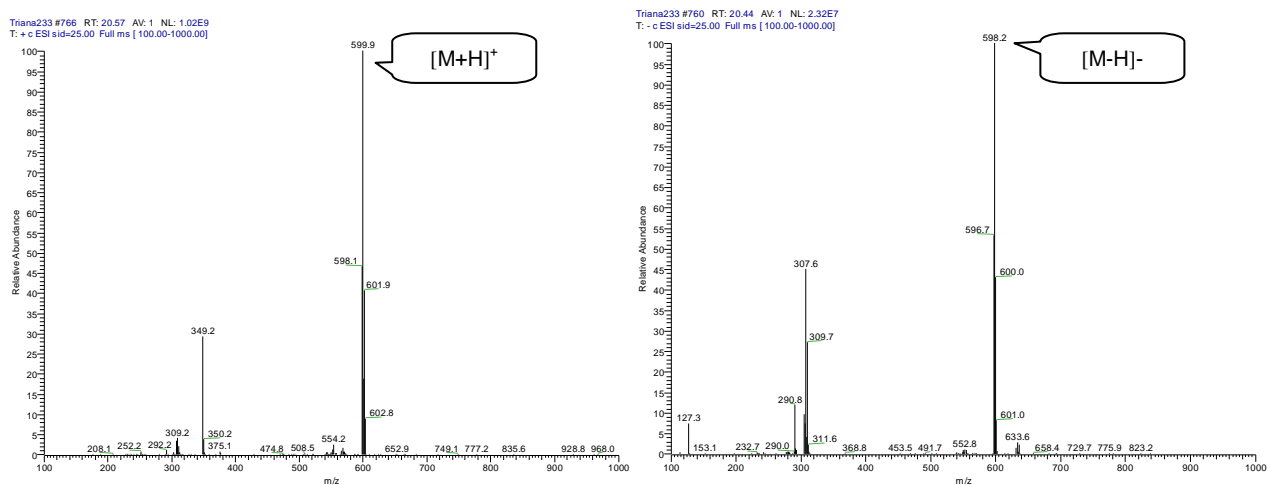
Fig.III.50. ESI-MS data of compound **7**

Compound **7** was obtained as a white powder (7 mg, 0.003% of the sponge dried weight). The UV absorption pattern of a dibrominated pyrrole carboxamide congeners, λ_{max} of band II is observable at 277 nm (Fig.III.49). A slight bathochromic effect of band peak I (211.5 nm) in comparison to compound **6** is observed. The presence of an iodine substituent instead of a bromine seems to play a role to cause this effect. In comparison to other halogenated tyramine congeners isolated from this sponge, compound **7** is more non polar having a retention time of 23.97 min. The occurrence of two bromine atoms is evidenced by its ESI-MS pseudo molecular ion cluster peaks at *m/z* 598/600/602 [M+H]$^+$ having a intensity ratio of 1:2:1 (Fig.III.50). Combined analysis of HRESIMS and ^{13}C-NMR spectra of **7** fits the molecular formula of $C_{18}H_{23}Br_2IN_3O_2$ (*m/z* experimental = 597.9210; *m/z* calculated = 597.9202 [M+H]$^+$).
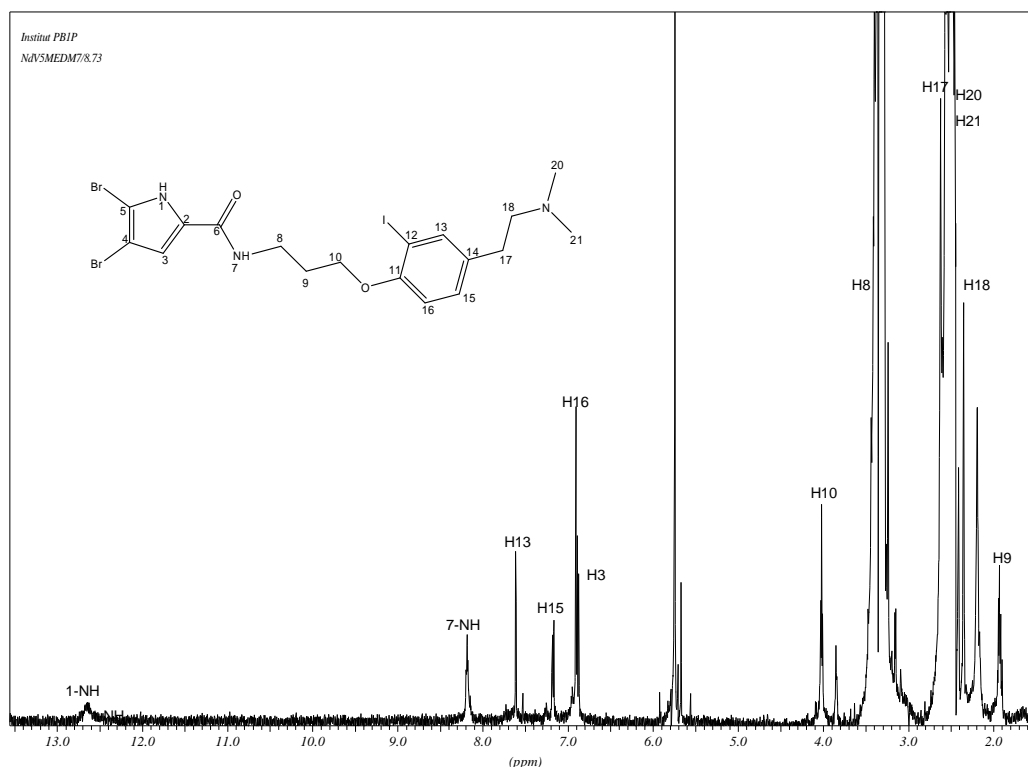
Fig.III.51. ^{1}H-NMR data of compound **7** (DMSO-d_6, 500 MHz)

NMR spectral data of **6** and **7** (Table III.5) support the close structural relationship among these compounds. Because of the insufficient amount of the compound, ^{13}C-NMR and 2D data were obtained from measurement of compounds **6** and **7** as a mixture at a ratio of 1:1.

^{1}H NMR spectrum as also can be observed in compounds **4** to **6**, showing six well-separated signals at the upper field region due to the presence of a *N,N-*dimethylethanamine unit at δ_H 2.62 (2H, m, H$_2$-17), 2.42 (2H, m, H$_2$-18), 2.17 (6H, s, H$_3$-20 and H$_3$-21) and an oxypropylamide at δ_H 3.39 (2H, m, H$_2$-8), δ_H 1.93 (2H, m, H$_2$-9), and δ_H 4.03 (2H, m, H$_2$-10) (Fig.III.51). ^{1}H-^{1}H COSY confirms a similar set of substructures like the presence of pyrrole ring and the ABX ring system. The pyrrole proton at δ_H 6.90 (1H, d, *J* = 0.9 Hz) is coupled to a broad signal of an NH-pyrrole at

δ_H 12.55 and suggests the presence of a three-substituted pyrrole ring.
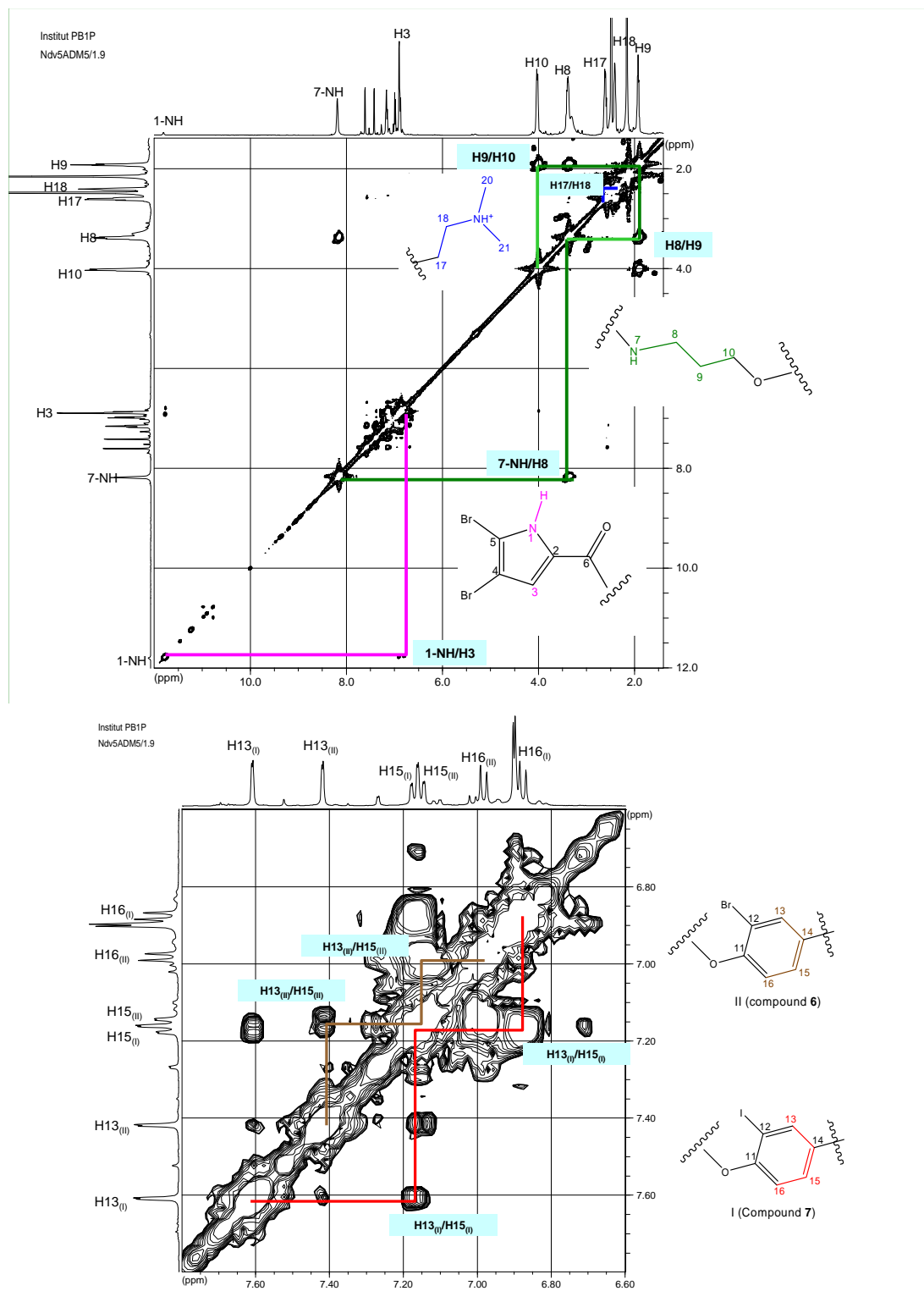
Fig.III.52. ^{1}H - ^{1}H COSY data of compound **6** and **7** in a mixture of 1:1 (DMSO-d_6)
Peaks I refer to **7** and II to **6**
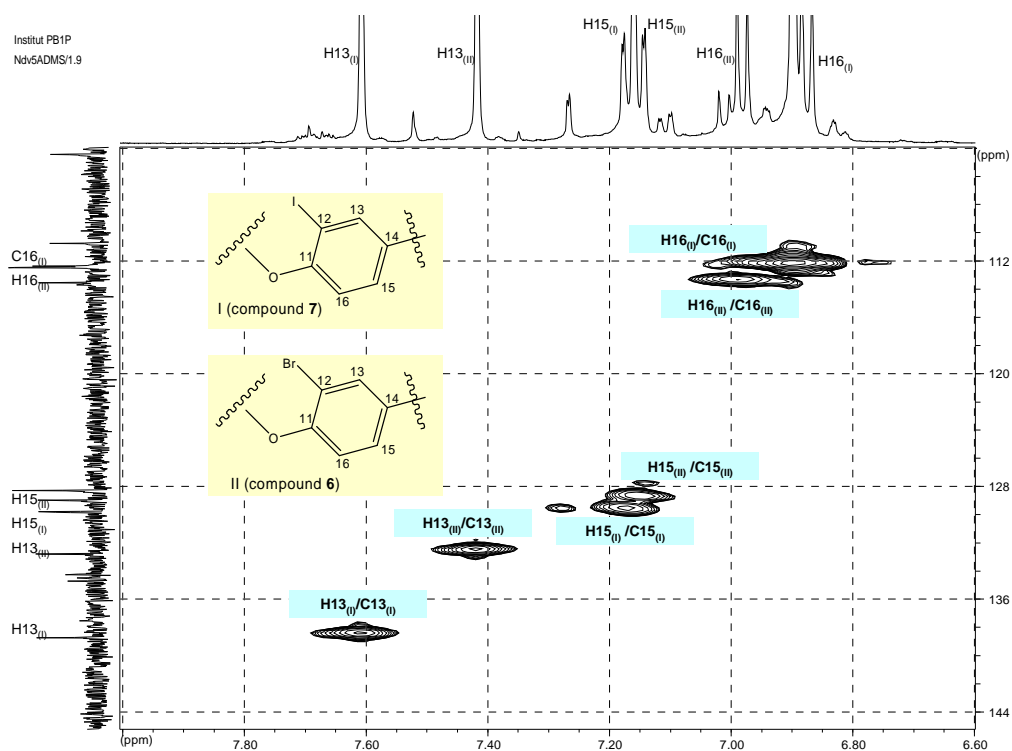
Fig.III.53. ^{1}H-^{13}C HMQC expansion of the benzene ring of **6** and **7** in a 1:1 mixture (DMSO-d_6)
Peaks I refer to **7** and II to **6**
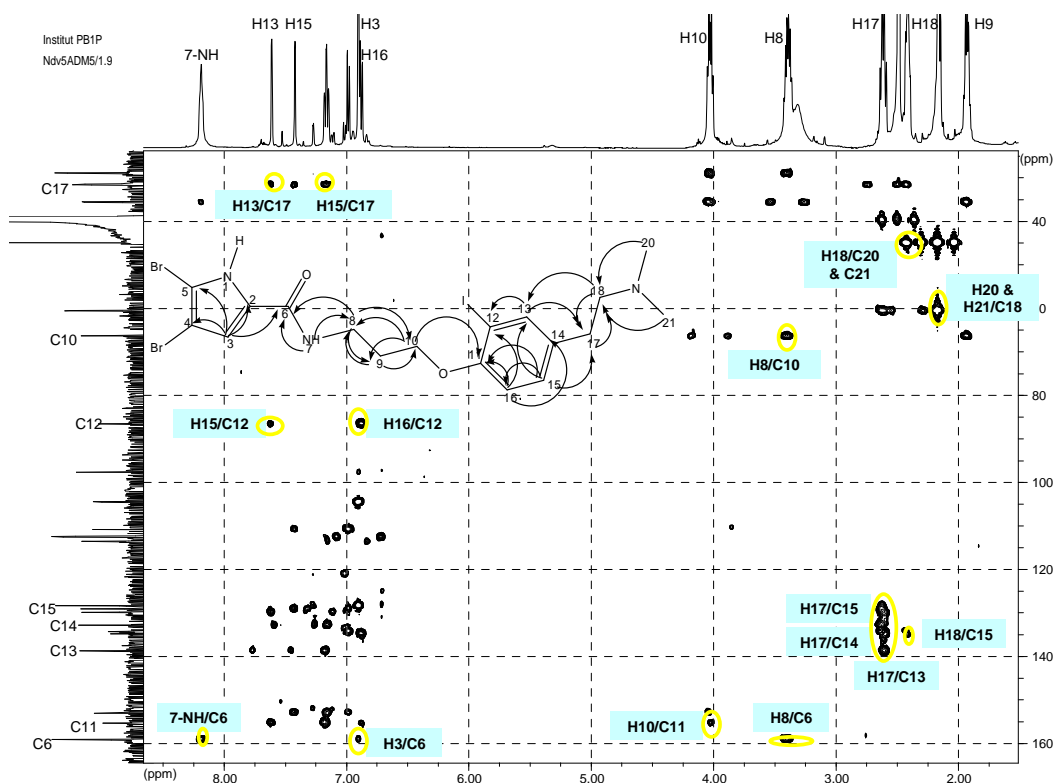
Fig.III.54. ^{1}H-^{13}C HMBC data of compound **7** (DMSO-d_6)

The presence of 1,2,4-trisubstituted benzene ring is shown by ^{1}H NMR signals at δ_H 7.61 (1H, d, *J* = 1.9 Hz, H-15); δ_H 7.17 (1H, dd, *J* = 1.9, 8.5 Hz, H-15); δ_H 6.88 (1H, d, *J* = 8.5 Hz, H-16) (Fig.III.51). Combined analysis of ^{1}H–^{13}C HMQC and HMBC data showed that there were two sets of ^{13}C resonances (I and II) belonging to both compounds **7** and **6**, respectively. C-12 of compound **7** is observed to be shifted extremely high field to δ_C 86.5 in comparison to compound **6** (δ_C 110.8) (Fig.III.45) which is reminiscent to the phenomena found in compounds **4** and **5**. Therefore this is suggestive for the presence of an iodine substitution at C-12.

After careful investigation of the chemical data compound **7** is established as a new 4,5-dibromo-*N*-3-(4-(2-dimethyl-amino)ethyl)-2-iodophenoxy)propyl)-1*H*-pyrrole-2-carboxamide, another member of the new agelanesin group (**agelanesin D**).

Table III.5. ^{1}H and ^{13}C-NMR data of compound **6** and **7** [a)]

No.	Compound 6			Compound 7		
	[1]H		[13]C	[1]H		[13]C
	δ	Multiplicity, *J* in Hz	δ, DEPT	δ	Multiplicity, *J* in Hz	δ, DEPT
1-NH	12.55	b s	-	12.55	b s	-
2	-	-	128.3, C	-	-	128.3, C
3	6.85	d, 0.9	112.5, CH	6.90	d, 0.9	112.5, CH
4	-	-	97.6, C	-	-	97.6, C
5	-	-	104.5, C	-	-	104.5, C
6	-	-	159.0, C	-	-	159.0, C
7-NH	8.12	m		8.19	m	
8	3.38	m	35.7, CH_2	3.39	m	35.7, CH_2
9	1.92	m	29.0, CH_2	1.93	m	29.0, CH_2
10	4.04	m	66.3, CH_2	4.03	m	66.3, CH_2
11	-	-	152.9, C	-	-	155.2, C
12	-	-	110.8, C	-	-	86.5, C
13	7.42	d, 1.9	132.8, CH	7.61	d, 1.9	138.7, CH
14	-		134.2, C	-	-	134.7, C
15	7.15	dd, 2.2, 8.5	129.0, CH	7.17	dd, 1.9, 8.5	129.8, CH
16	6.98	d, 8.5	113.5, CH	6.88	d, 8.5	112.4, CH
17	2.62	m	31.7, CH_2	2.62	m	31.5, CH_2
18	2.38	m	60.6, CH_2	2.42	m	60.6, CH_2
20&21	2.14	s	44.9, CH_3	2.17	s	44.9, CH_3

[a)] Data were recorded in DMSO-d_6 at 500 MHz (^{1}H) and 125 MHz (^{13}C), multiplicities and coupling constant are given in Hz.

### III.1.8. **Mauritamide B** (**8**, new compound)
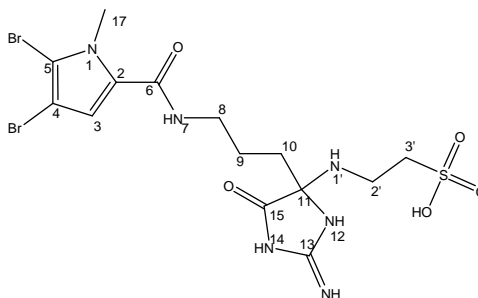
Fig.III.55. Compound **8**
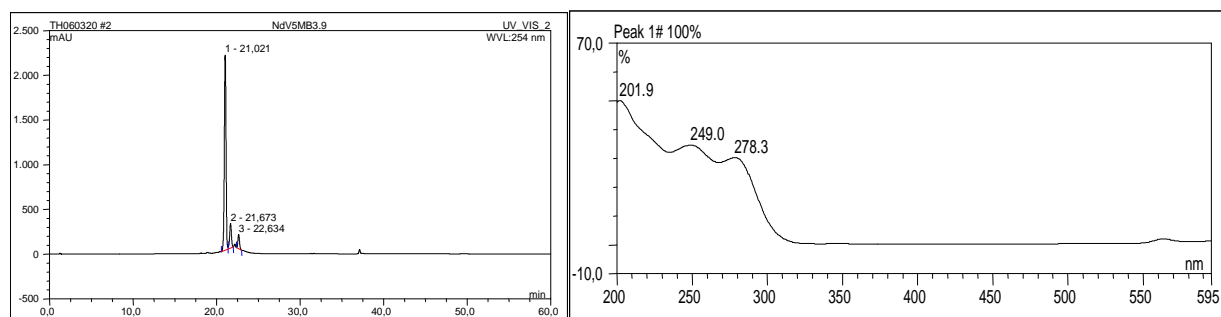
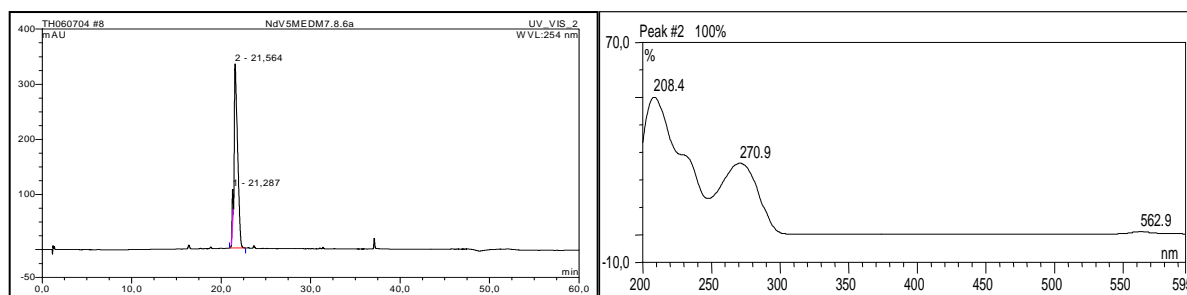

Fig.III.56. Analytical HPLC data of compound **8**

Left: HPLC profile in 254 nm, RT: 21.02; right: UV absorption spectrum, λ_{max} = 201.9; 249.0; 278.3 nm
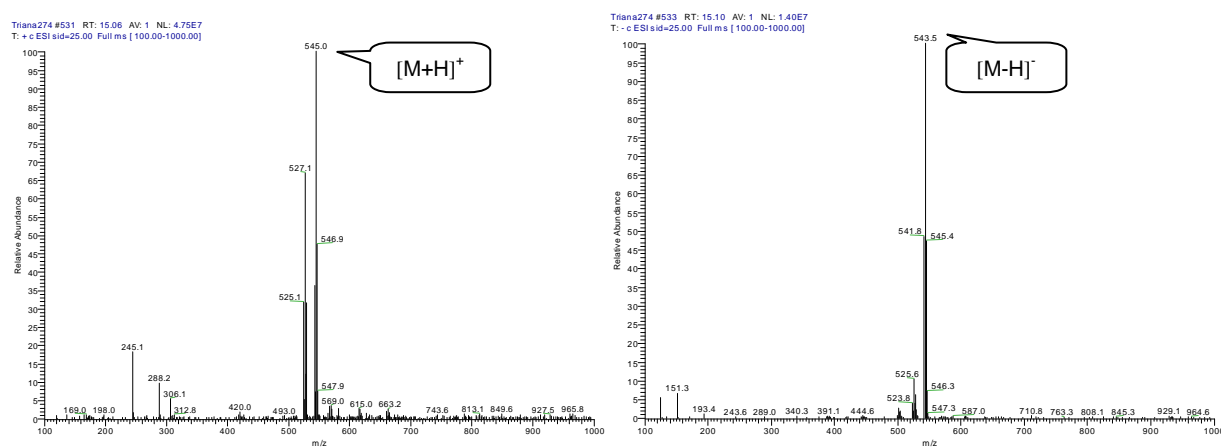
Fig.III.57. ESI-MS data of compound **8**

Compound **8** was isolated as a brown oil at an amount of 88 mg which is 0.04% of the sponge dried weight. This optically active compound exhibits $[\alpha]_D^{20}$ value of -5.5° ± 0.7 (*c* 0.57, CH$_3$OH). It shows a characteristic UV spectrum with a λ_{max} ~270 nm for 2-pyrrole carboxamide, but the absorption band observed at around 250 nm is more intense, suggesting that the compound possesses an additional

chromophore (Fig.III.56). HRESIMS data in combination with the ^{13}C-NMR spectrum analysis fits a molecular formula of $C_{14}H_{21}Br_2N_6O_5S$ (*m/z* experimental = 542.9660, *m/z* calculated = 542.9661 [M+H]$^+$). The presence of two bromine atoms in the molecules is shown by the ESI-MS pseudo molecular ion cluster at *m/z* 543/545/547 [M+H]$^+$ having an intensity ratio of 1.2:1 (Fig.III.57).

NMR spectral data in DMSO-d_6 of **8** exhibit a singlet signal at δ_H 6.99 which is correlated to a *sp^2* carbon at δ_c 113.9 in ^{1}H-^{13}C HMQC experiment. This evidence together with the signal of the deshielded methyl group at δ_H 3.86 (3H, s), δ_c 35.3 indicates the occurrence of a three substituted 1*N*-methyl pyrrole substructure. These phenomena were also observed in several other congeners isolated from this sponge such as in compounds **1** - **3**.

^{1}H-^{1}H COSY experiment data reveal two separate spin systems which are identified as an isolated propylamide chain (-CH$_2$-CH$_2$-CH$_2$-NH-C=O) at δ_H 1.84 (H$_2$-10), 1.27 (H$_2$-9), 3.14 (H$_2$-8), 8.2 (NH-7), and a tauryl chain (-NH-CH$_2$-CH$_2$-SO$_3$-) at δ_H 9.51 (NH-1'), 3.60 (H$_2$-2') and 2.74 (H$_2$-3'). Three broad signals observed in ^{1}H NMR represent the NH groups of an aminoimidazolone group. The ^{1}H-^{13}C HMBC experiment provides the information needed to combine the substructures. Cross peaks which correlate proton signals at δ_H 3.14 (H$_2$-8) and 8.2 (NH-7) to the carboxamide carbon at δ_C 159.7 suggest that the propylene chain is attached to a 4,5-dibromo-1-methyl-1*H*-pyrrole-2-carboxamide substructure through the carboxamide unit. Tauryl chain is connected to the aminoimidazolone group and the propylamide through a quaternary *sp^3* ring carbon at δ_C 91.5 (C-11) as proven by a long range coupling ($^4J_{C-H}$) of H$_2$-2' to a keto carbon of the aminoimidazolone function

at δ_C 179.6 (C-15). The cross peaks of H$_2$-10 couple to C-15 ($^3J_{C-H}$) and to C-11 ($^2J_{C-H}$), while NH-12 couples to C-10 ($^3J_{C-H}$) and C-11 ($^2J_{C-H}$).
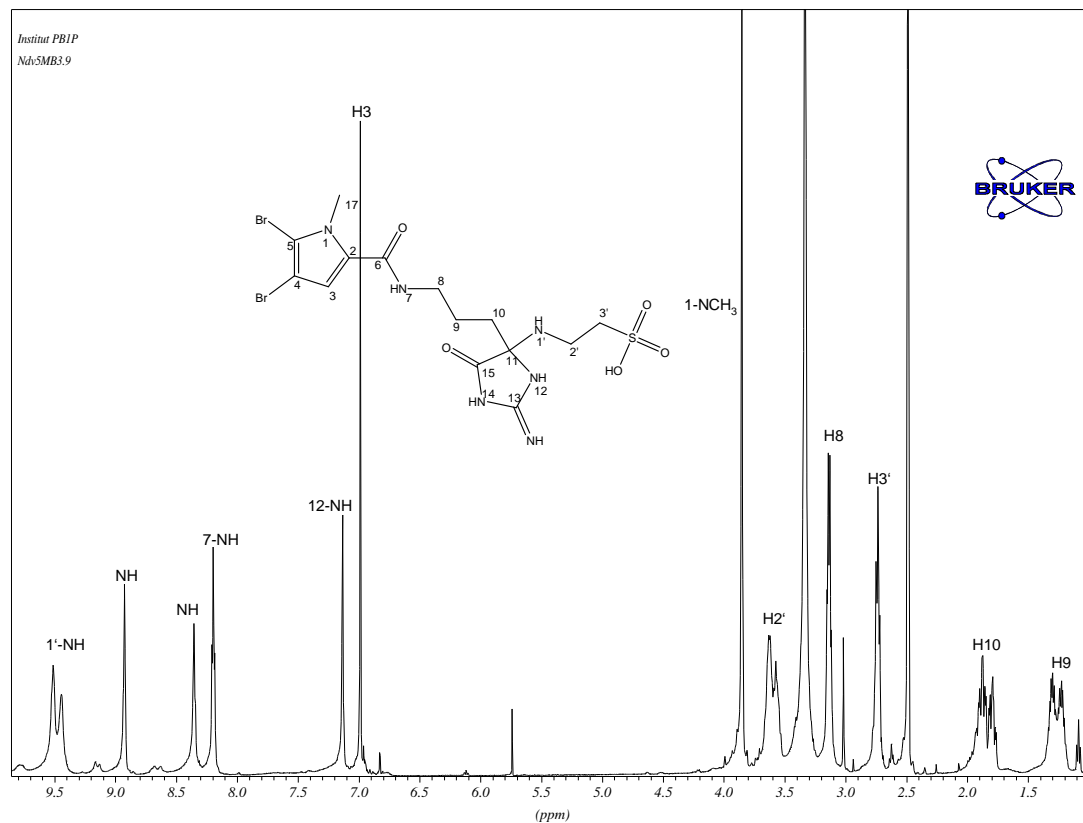
Fig.III.58. ^{1}H NMR data of compound **8** (DMSO-d_6, 500 MHz)

^{1}H NMR and ^{13}C NMR data of **8** are reminiscent of the known mauritamide A (Jiménez and Crews, 1994). The difference of 14 mass units in the molecular weight and the lack of the methyl ester signal suggest that the taurine methyl ester function in **8** is hydrolized.
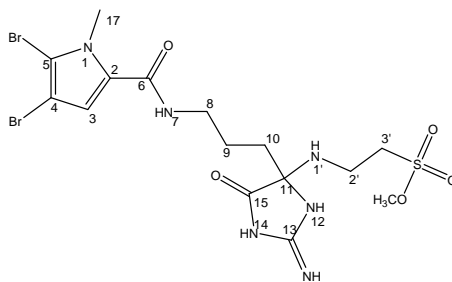
Fig.III.59. Mauritamide A (Jiménez and Crews, 1994)

After careful interpretation of the experimental data, compound **8** is concluded as 2-(4-(3-(4,5-dibromo-1-methyl-1*H*-pyrrole-2-carboxamido)propyl)-2-imino-5-oxo-imidazolidin-4-ylamino)ethanesulfonic acid, which is a a new derivative of mauritamide A and is assigned to the trivial name **mauritamide B**.
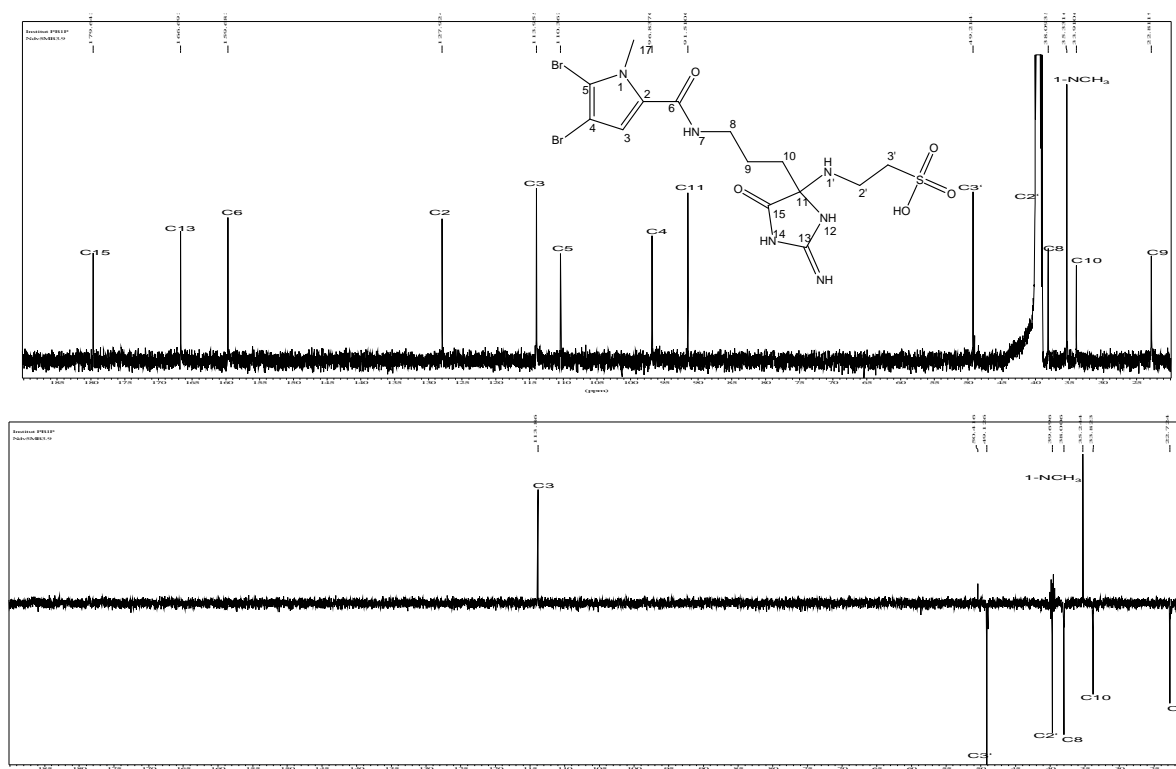
Fig.III.60. ^{13}C NMR and DEPT spectra of compound **8** (DMSO-d_6, 125 MHz)
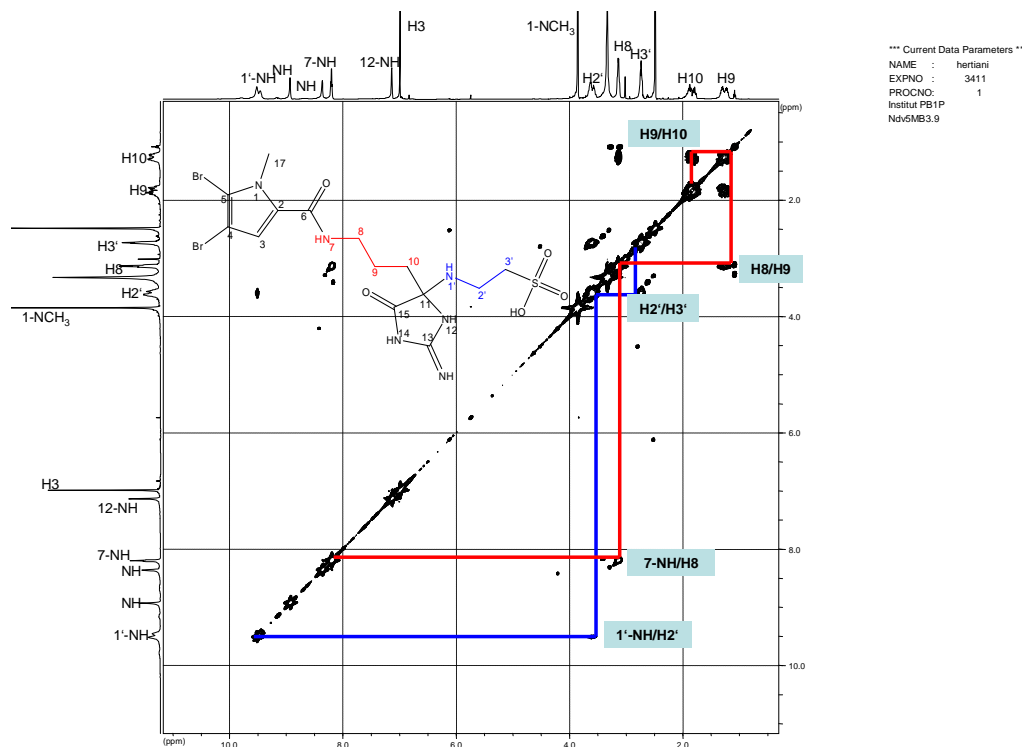
Fig.III.61. ^{1}H-^{1}H COSY spectrum of compound **8** (DMSO-d_6)
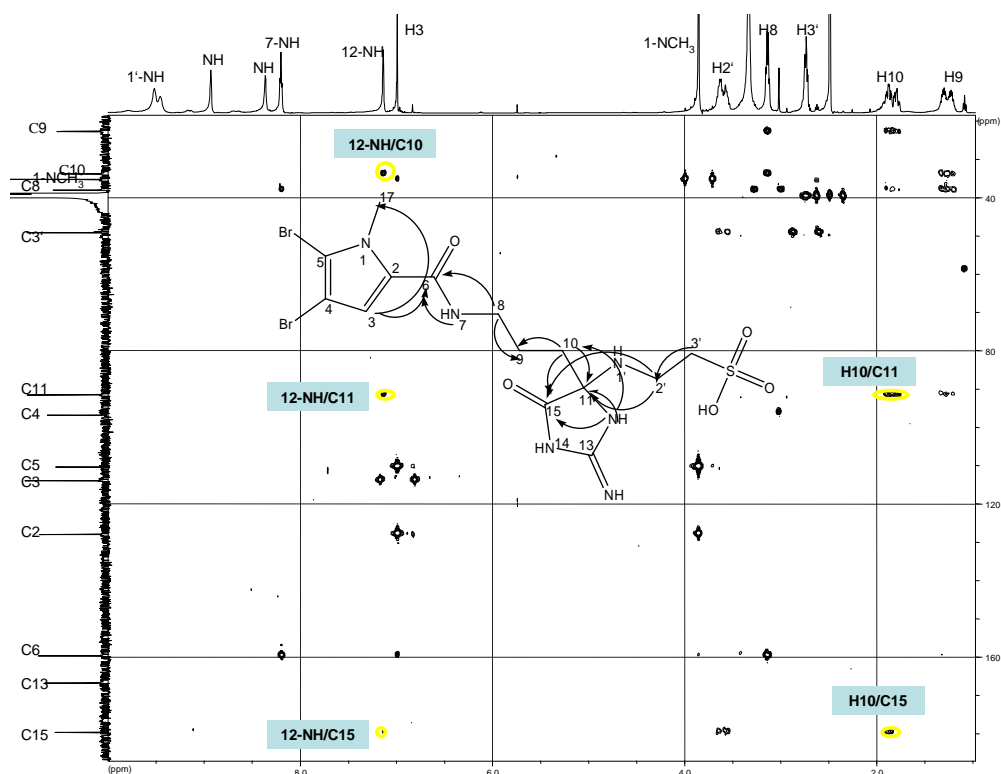
Fig.III.62. ^{1}H-^{13}C HMBC spectrum of compound **8** (DMSO-d_6)

Table III.6. ^{1}H and ^{13}C-NMR data of compound **8** in comparison to mauritamide A

No.	Compound 8 [a)]		Mauritamide A [a) b)]	
	^{1}H-NMR	^{13}C-NMR	^{1}H-NMR	^{13}C-NMR
2	-	127.9, C	-	127.89, s
3	6.99, s	113.9, CH	6.99, s	114.00, d
4	-	96.8, C	-	96.90, s
5	-	110.4, C	-	110.45, s
6	-	159.7, C=O	-	159.71, s
7	8.20, t, 5.4	-	8.20, t	-
8	3.14, m	38.1, CH$_2$	3.12, m	38.05, t
9	1.27, m	22.8, CH$_2$	1.23, m	22.69, t
10	1.84, m	33.9, CH$_2$	1.88, m	33.13, t
11	-	91.5, C	-	96.23, s
13	-	166.7, C=N	-	167.18, s
15	-	179.6, C=O	-	176.73, s
1-NCH$_3$	3.86, s	35.3, CH$_3$	3.85, s	35.40, q
1'	9.51, b s	-	9.8, t	-
2'	3.60, m	39.7, CH$_2$	3.63, m	38.94, t
3'	2.74, t, 7.2	49.2, CH$_2$	2.76, t	49.06, t
O-CH$_3$	-	-	3.02, s	50.55, q
12-NH	7.13, b s [c)]	-	9.36, s	
14-NH	8.93, b s [c)]	-	9.18, s	
C=NH	8.36, b s [c)]	-	8.62, s	

[a)] Data were recorded in DMSO-d_6 at 500 MHz (^{1}H) and 125 MHz (^{13}C), multiplicities and coupling constant are given in Hz; [b)] Jiménez and Crews (1994); [c)] Signals might be interchanged

III.1.9. Mauritamide C (**9**, new compound)
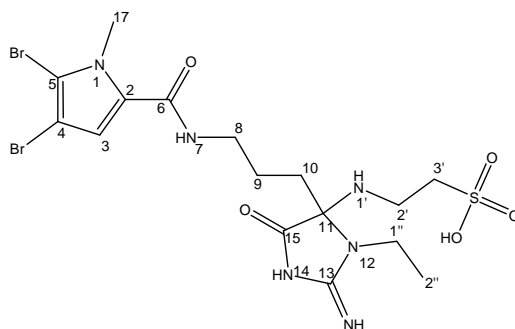

Fig.III.63. Compound **9**
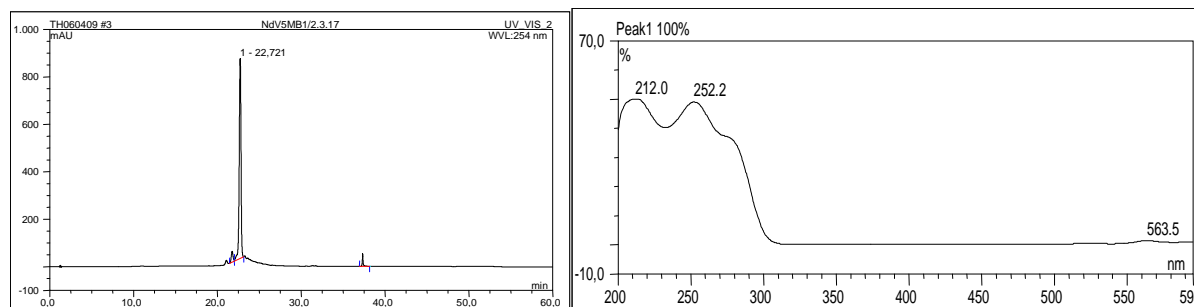
Fig.III.64. Analytical HPLC data of compound **9**
Left: HPLC profile in 254 nm, RT: 22.72; right: UV absorption spectrum, λ_{max} = 212.0 and 252.2 nm

Fig.III.65. ESI-MS data of compound **9**

Compound **9** was obtained as a yellow amorphous substance at an amount of 33 mg which is 0.016% of the sponge dried weight. This optically active compound exhibits $[\alpha]_D^{20}$ value of -5.2° ± 0.5 (*c* 0.59, CH_3OH). Its UV spectrum and NMR data exhibit similarities with mauritamide B (**8**) (see Table III.7). Its retention time is slightly delayed to 22.72 min in comparison to mauritamide B which has RT = 21.01 min. HRESIMS data in combination with the ^{13}C-NMR spectrum analysis fits the molecular formula of $C_{16}H_{25}Br_2N_6O_5S$ (*m/z* experimental = 570.9980, *m/z* calculated = 570.9974 [M+H]$^+$). The presence of two bromine atoms in the molecule is shown by the ESI-MS molecular ion cluster at *m/z* 571/573/575 [M+H]$^+$ having an intensity ratio of 1.2:1 (Fig.III.65).
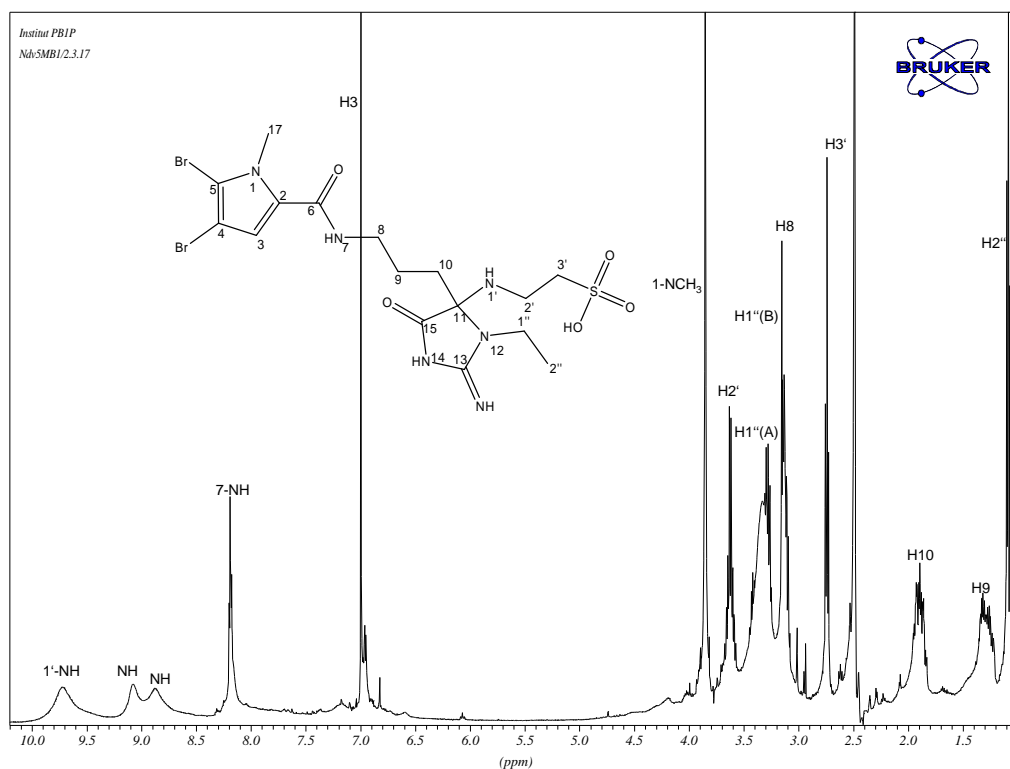
Fig.III.66. ^{1}H NMR data of compound **9** (DMSO-d_6, 500 MHz)

Compound **9** has a molecular weight which 28 mass units larger than that of **8** which might be due to an additional ethyl unit. Signals at the aliphatic region in ^{1}H NMR spectrum at δ_H 3.13 (1H, m, H-1"A), 3.28 (1H, m, H-1"B) and at δ_H 1.09 (2H, t, J = 6.9 Hz, H$_2$-2") as well as in ^{13}C NMR spectrum at δ_C 58.7 (CH$_2$, C-1") and 14.9 (CH$_3$, C-2") indicate the position of the ethyl unit adjacent to an oxygen atom or tertiary amine group. The presence of an ethyl moiety was exhibited by the additional spin system in ^{1}H–^{1}H COSY spectrum (Fig.III.68). Considering the chemical structure of mauritamide A, compound **9** was first proposed to be an ethyl ester derivative of **8**. Since there are no significant changes observed for the taurine unit signals or in the propylamide chain, this additional ethyl chain is suggested to be attached to the aminoimidazolone ring. This proposed structure is supported by the ^{1}H-^{13}C HMBC

data (Fig.III.69) as shown by a cross peak between H-1"A and H1"B and C-11 ($^3J_{C-H}$). Since other part of the molecule fits the mauritamide B data, the structure of **9** was elucidated as 2-(4-(3-(4,5-dibromo-1-methyl-1*H*-pyrrole-2-carboxamido) propyl)-3-ethyl-2-imino-5-oxoimidazolidin-4-yl-amino) ethane-sulfonic acid (Fig.III.63) and was named **mauritamide C**.
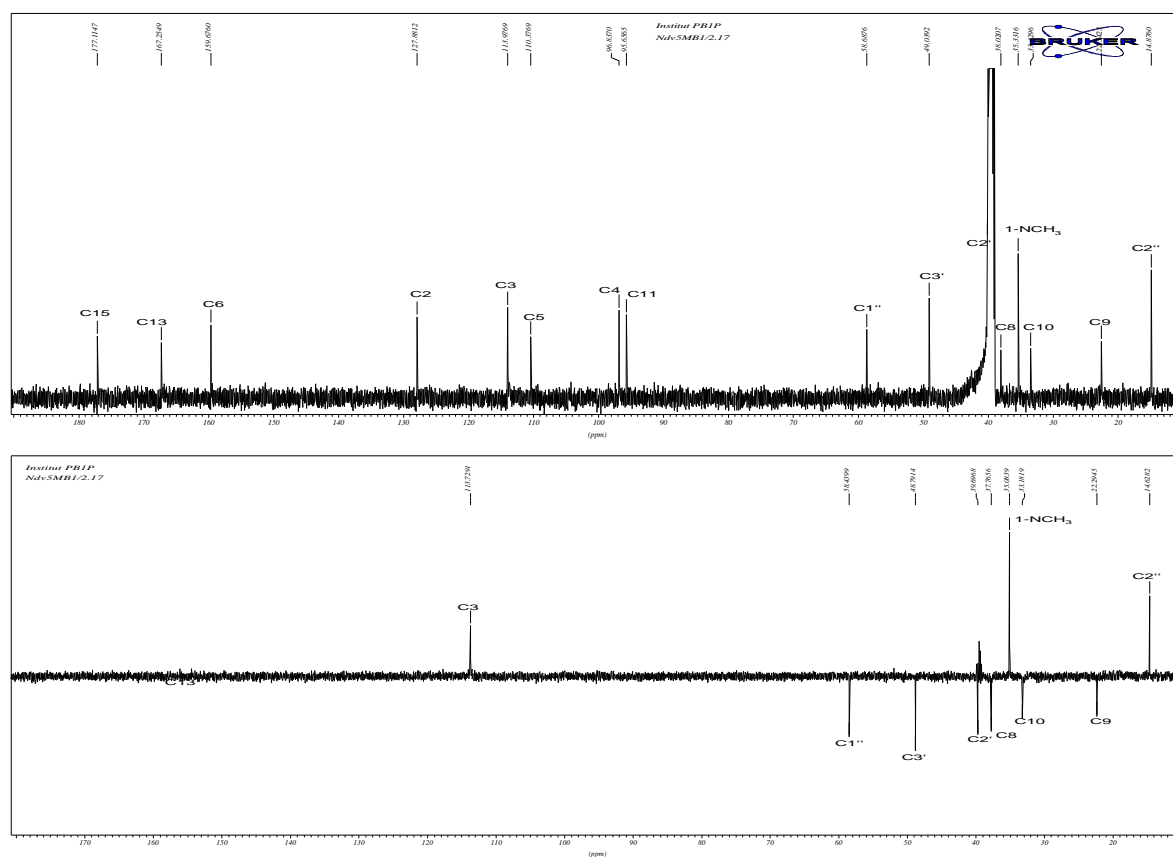
Fig.III.67. ^{13}C NMR and DEPT spectra of compound **9** (DMSO-d_6, 125 MHz)
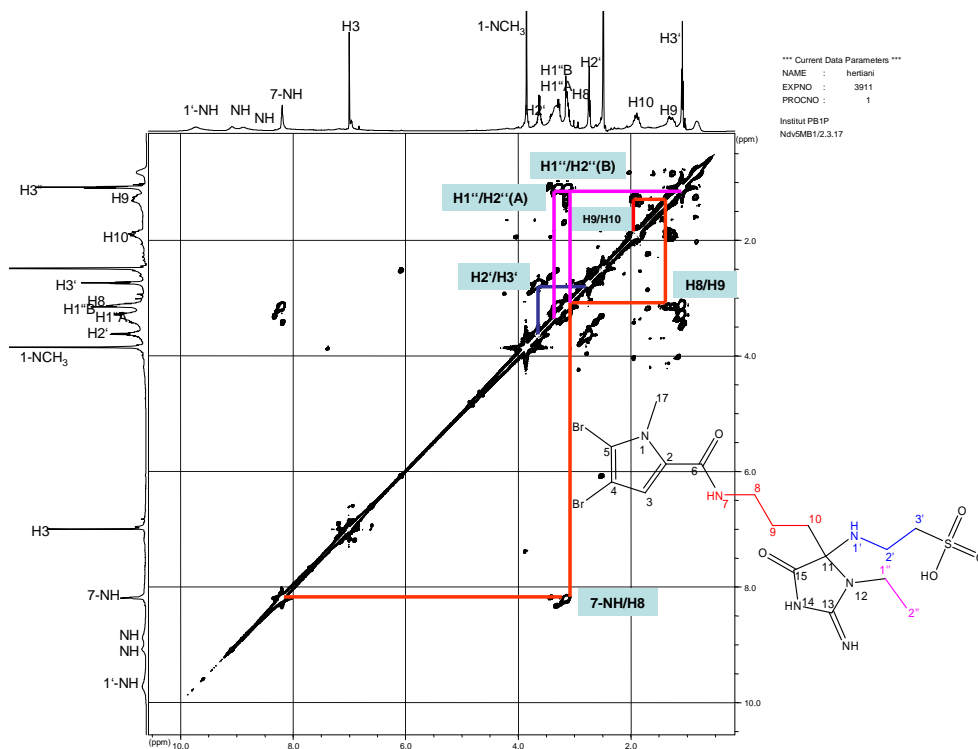
Fig.III.68. ^{1}H-^{1}H COSY spectrum of compound **9** (DMSO-d_6)

Table III.7. ^{1}H and ^{13}C-NMR data of mauritamide C (**9**) in comparison to mauritamide B (**8**)

No.	Mauritamide B [a]		Mauritamide C [a]	
	^{1}H-NMR	^{13}C-NMR	^{1}H-NMR	^{13}C-NMR
2	-	127.9, C	-	127.9, C
3	6.99, s	113.9, CH	7.00, s	114.0, CH
4	-	96.8, C	-	96.8, C
5	-	110.4, C	-	110.4, C
6	-	159.7, C=O	-	159.7, C=O
7	8.20, t, 5.4	-	8.19, t, 5.4	-
8	3.14, m	38.1, CH$_2$	3.14, m	38.0, CH$_2$
9	1.27, m	22.8, CH$_2$	1.30, m	22.5, CH$_2$
10	1.84, m	33.9, CH$_2$	1.90, m	33.4, CH$_2$
11	-	91.5, C	-	95.7, C
13	-	166.7, C=N	-	167.2, C=N
15	-	179.6, C=O	-	177.1, C=O
1-NCH$_3$	3.86, s	35.3, CH$_3$	3.86, s	33.4, CH$_3$
1'	9.51, b s	-	9.73, b s [b]	-
2'	3.60, m	39.7, CH$_2$	3.63, m	39.7, CH$_2$
3'	2.74, t, 7.2	49.2, CH$_2$	2.75, t. 7.2	49.0, CH$_2$
1''A	-	-	3.28, m	58.7, CH$_2$
1''B	-	-	3.11, m	
2''	-	-	1.09, t, 6.9	14.9, CH$_3$
12-NH	7.13, b s [b]	-	-	-
14-NH	8.93, b s [b]	-	9.07, b s [b]	-
C=NH	8.36, b s [b]		8.88, b s [b]	-

[a] Data were recorded in DMSO-d_6 at 500 MHz (^{1}H) and 125 MHz (^{13}C), multiplicities and coupling constant are given in Hz; [b] Signals might be interchanged
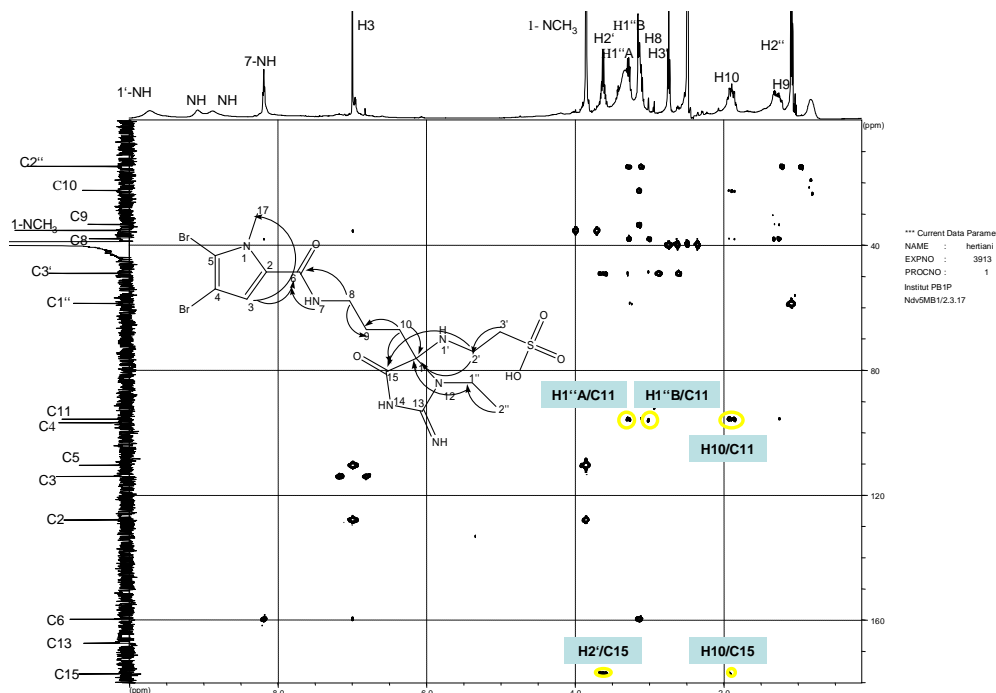
Fig.III.69. ^{1}H - ^{13}C HMBC spectrum of compound **9** (DMSO-d_6)

III.1.10. 2-(4,5-dibromo-1-methyl-1*H*-pyrrole-2-carboxamido)ethanesulfonic acid

(**10**, new compound)
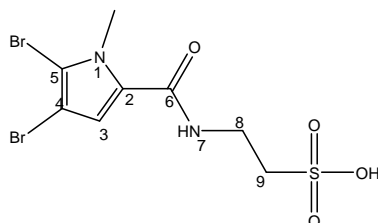
Fig.III.70. Compound **10**
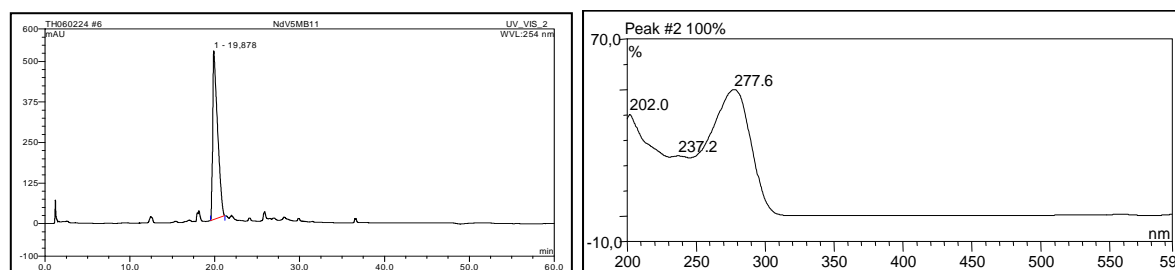
Fig.III.71. Analytical HPLC data of compound **10**
Left: HPLC profile in 254 nm, RT: 19.68; right: UV absorption spectrum, λ_{max} = 202.0; 237.2; 277.6 nm
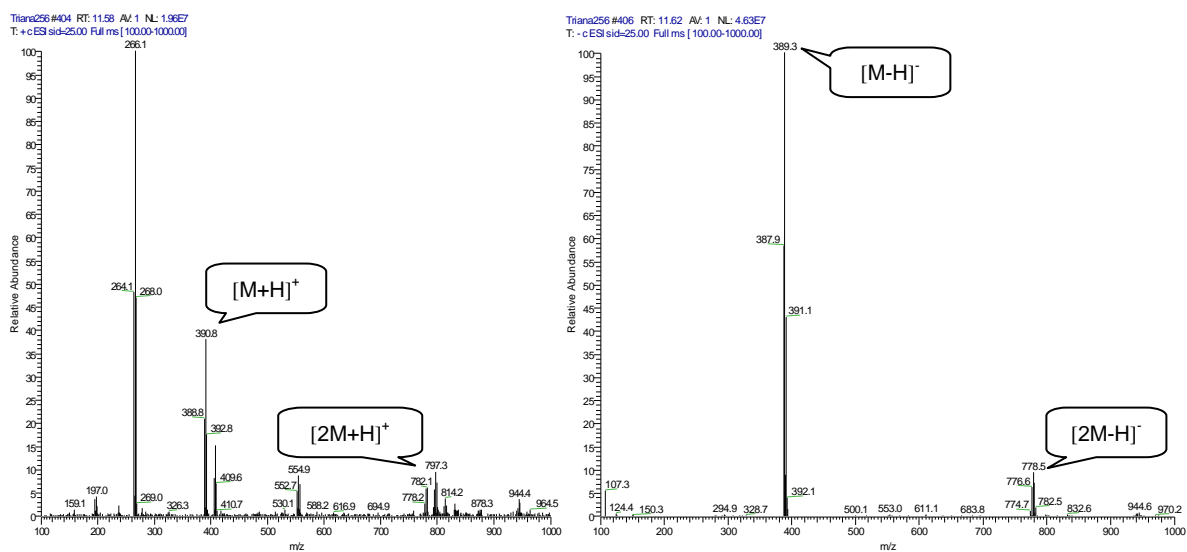
Fig.III.72. ESI-MS data of compound **10**

Compound **10** was obtained as a white amorphous substance at an amount of 6 mg which is 0.003% of the sponge dried weight. It is the third congener bearing a taurine unit that is isolated from this sponge. The typical UV absorption spectral pattern for pyrrrole-2-carboxamide is observed (Fig.III.71). The presence of two bromine atoms is detected in ESI-MS as an intensive pseudo molecular ion cluster at *m/z* 389/391/393 [M+H]$^{+}$ having an intensity ratio of 1:2.1 (Fig.III.72). HRESIMS data and ^{13}C NMR analysis fits to the molecular formula of $C_8H_{11}Br_2N_2O_4S$ (*m/z* experimental = 388.8820, *m/z* calculated = 388.8806 [M+H]$^{+}$).

Table III.8. 1D and 2D NMR data of compound **10** [a]

No.	^{1}H		^{13}C	HBMC [c]	COSY
	δ	Integration, multiplicity, *J* in Hz	δ, DEPT		
2	-	-	128.1, C		
3	6.83	1H, s	113.4, CH		
4	-	-	96.8, C	2,5	
5	-	-	110.3, C		
6	-	-	159.3, C		
7-NH	8.17	2H, t, 5.2	-	6	8,9
8	3.44	2H, dd, 6.2, 13.6	35.7, CH$_2$	6,7,9	7-NH,9
9	2.62	2H, dd, 7.6, 7.0	50.1, CH$_2$		7-NH,8
1-NCH$_3$	3.86	-	35.2, CH$_3$	2,5	

[a] Data were recorded in DMSO-d_6 at 500 MHz (^{1}H) and 125 MHz (^{13}C), multiplicities and coupling constant are given in Hertz; [b] Signals might be interchanged; [c] H→C
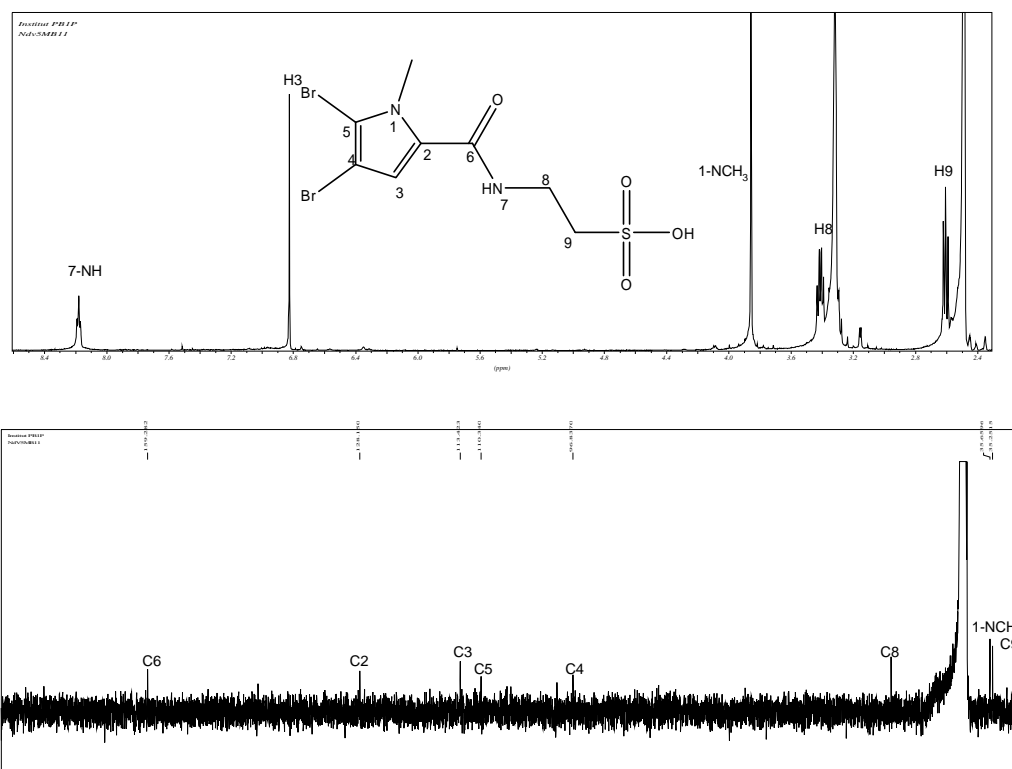
Fig.III.73. ^{1}H (above) and ^{13}C NMR spectra (below) of compound **10** (DMSO-d_6)

Five proton signals in ^{1}H-NMR represent a proton of a tri-substituted pyrrole at δ_H 6.83 (s, H-3), a deshielded methyl signal at δ_H 3.86 (s, 1-NCH$_3$), and protons of the amide and ethylene chain at δ_H 8.18 (t, J = 5.4 Hz, 7-NH), 3.4 (dt, J = 7.2, 5.7 Hz, H$_2$-8) and δ_H 2.6 (t, J = 7.2 Hz, H$_2$-9). ^{1}H–^{1}H COSY spectrum shows only one spin system correlating the protons of the propylamide chain. The ^{13}C-NMR data exhibit only eight carbons for a 4,5-dibromo-1-methyl-1H-pyrrole-2-propylcarboxamide structure. These NMR data together with an excess of 81 mass units for its molecular weight suggest the presence of a sulfonyl group. A close look to the taurine moiety of the previous derivatives, **mauritamide B** (**8**) and **C** (**9**) confirms its presence. The methylene carbon next to the sulfonyl group in previous congeners appears at δ_C 49.2, while in compound **10** it is found at δ_C 49.7 (C-9). ^{1}H–^{13}C HMBC spectrum

confirms the proposed structure. Hence compound **10** is then determined as the new

2-(4,5-dibromo-1-methyl-1H-pyrrole-2-carboxamido)ethanesulfonic acid.

III.1.11. Dibromophakellin HCl and Dibromophakellin base (**11a** and **11b**, known compounds)
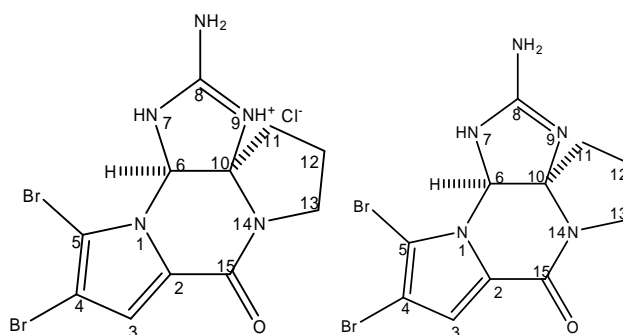
Fig.III.74. Compound **11a** (left) and compound **11b** (right)
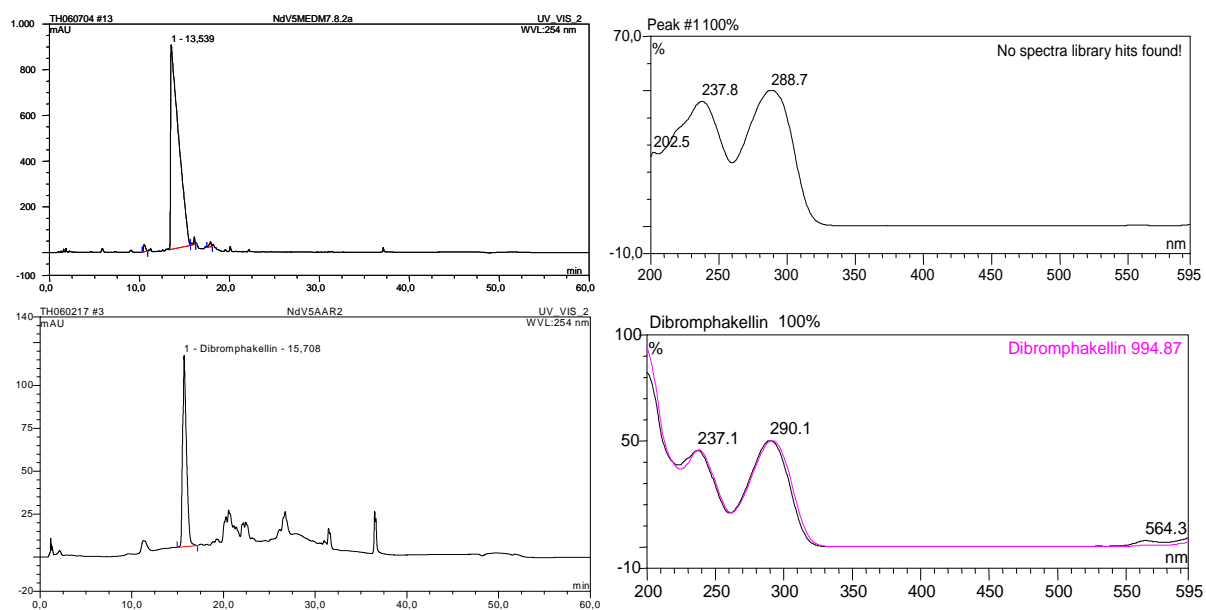
Fig.III.75. Analytical HPLC data of compound **11a** and **11b**
Left: HPLC profile in 254 nm, RT: 13.54 (**11a**); 15.71 (**11b**); right: UV absorption spectrum, λ_{max} = 237.8; 288.7 nm (**11a**); 237.1; 290.1 nm (**11b**)
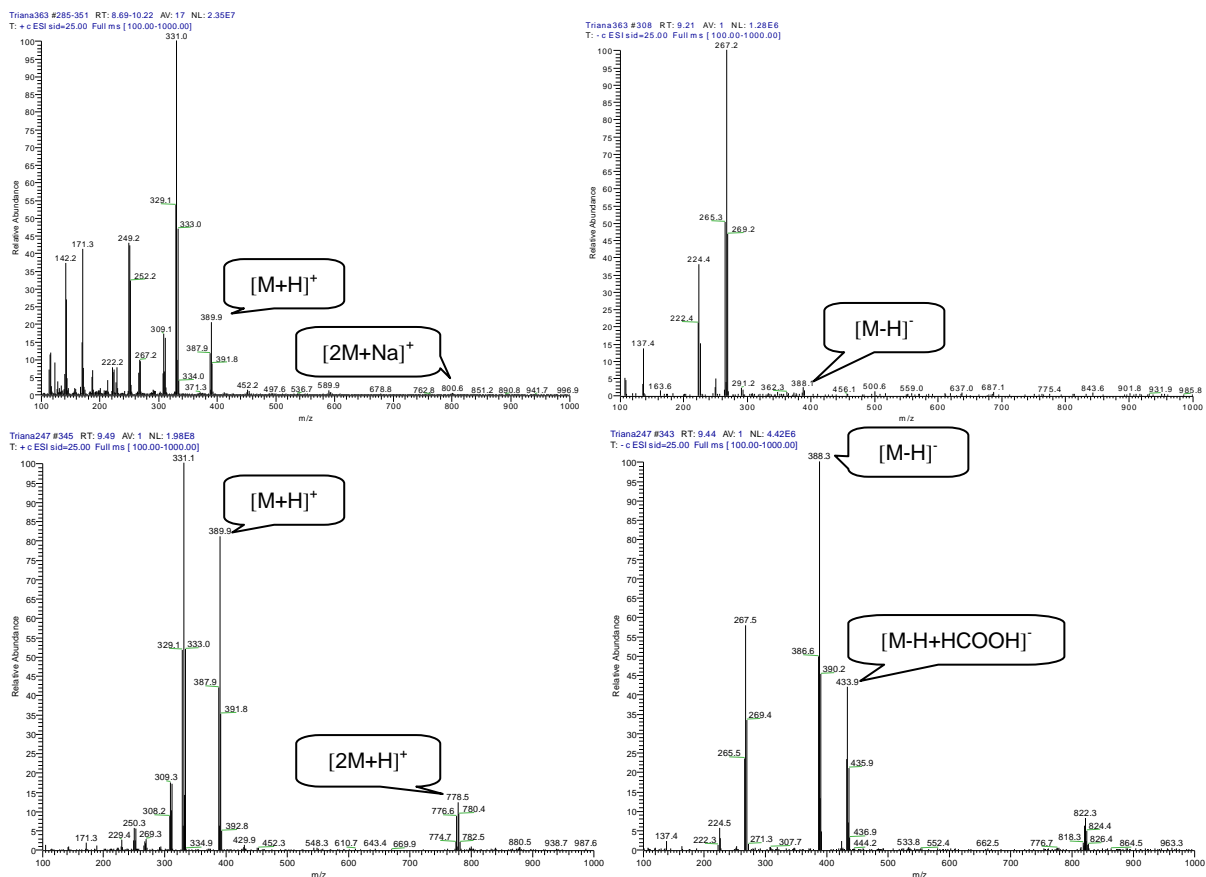
Fig.III.76. ESI-MS data of compound **11a** (above) and **11b** (below)

Compound **11a** and **11b** were obtained as white amorphous substances at amounts of 17 mg (0.008% of the sponge dried weight) and 3 mg (0.0015% of the sponge dried weight), respectively. The UV absorption spectrum of compound **11b** fits the internal spectral library data base for dibromophakellin base. However compound **11a** exhibited a comparable but not so identical UV spectrum to **11b**. Both ESIMS spectra of **11a** and **11b** indicate the presence of a dibrominated moiety which is shown as a cluster of molecular ion peaks at *m/z* 388/390/392 [M+H]$^+$ at an intensity ratio of 1:2:1. This finding is coherent with the molecular formula of dibromophakellin ($C_{11}H_{11}Br_2N_5O$). (-)-Dibromophakellin base and (-)-dibromophakellin HCl were previously reported from the marine sponge *Phakellia*

flabellata (Sharma and Burkholder, 1971; Sharma and Magdoff-Fairchild, 1977), whereas the enantiomer, (+)-dibromophakellin was reported from *Pseudaxynissa cantharella* by De Nanteuil *et al.* (1985).

The ^{1}H NMR spectrum of **11a** reveals the presence of a highly deshielded methine proton (H-6), a –CH$_2$CH$_2$CH$_2$NCO– unit, a proton of a substituted pyrrole ring and three proton signals in the lower field for a guanidinium moiety. Compound **11a** and **11b** show a chemical shift difference for H-11A and H-6 (see Table III.9). H-11A in **11a** is shifted more downfield in comparison to that in **11b** as a result of the guanidine double bond at the endocyclic 8, 9 position. This double bond caused protonation at N-9 (Sharma and Magdoff-Fairchild, 1977).

Beside H-11A, H-6 of **11a** experiences a deshielding effect and it is shifted for about 0.5 ppm in comparison with its base form. The evidence for some positive charge on N-7 of cations is provided by the large downshield shift (0.5 – 0.6 ppm) of H-6. During protonation, the guanidinium double bond had entirely shifted to the 7, 8 positions, then the resonance of H-6 would have been deshielded by 1.5 – 1.8 ppm (1 – 1.3 ppm for the double bond plus 0.5 ppm for the positive charge) (Sharma and Magdoff-Fairchild, 1977). Based on this assumption, a downfield shift of 0.5 ppm in the resonance of H-6 should correspond to about 35% imminium character at the 7, 8 positions of phakellinium cations (Sharma and Magdoff-Fairchild, 1977).
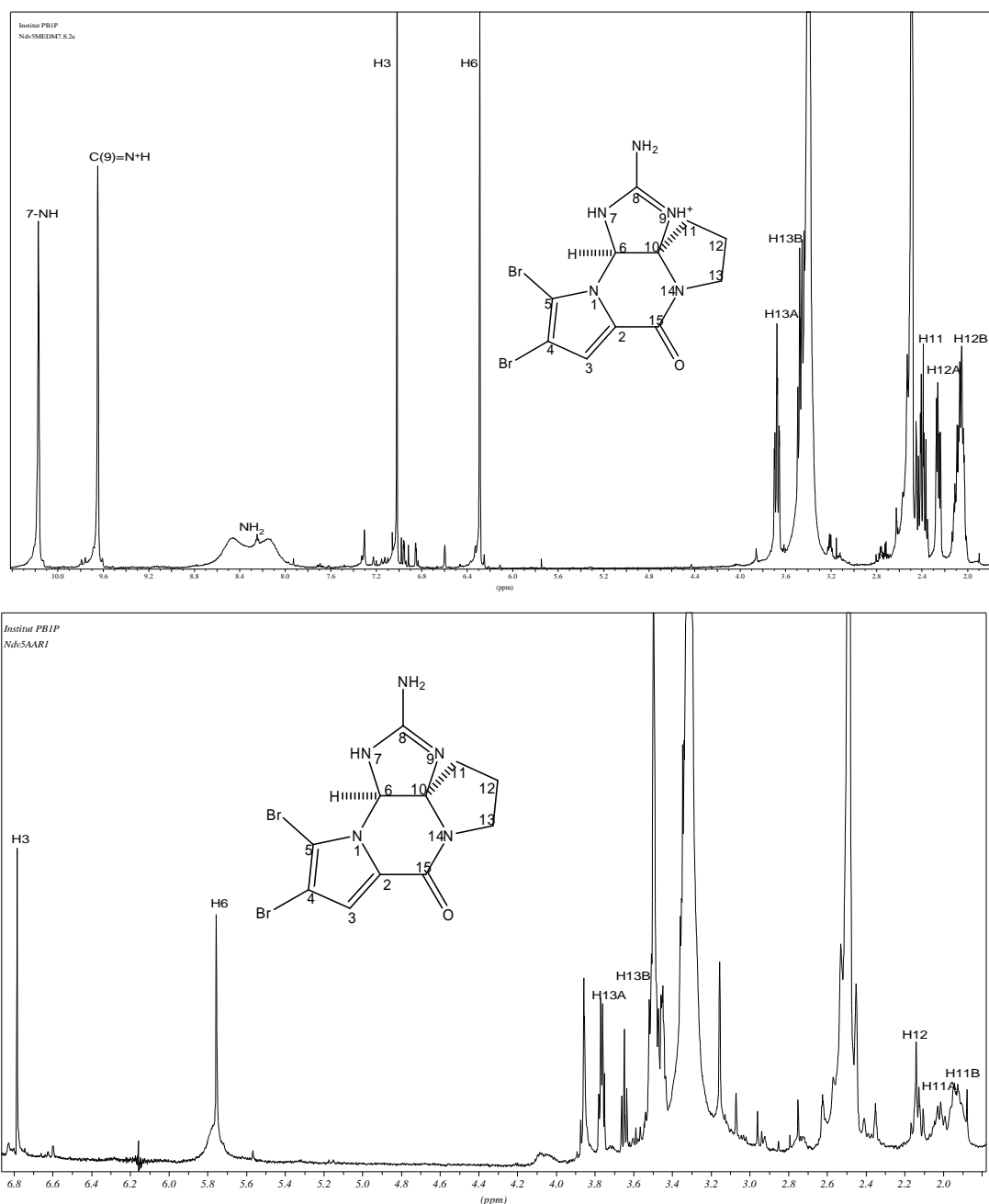
Fig.III.77. ^{1}H NMR spectra of **11a** (above) and **11b** (below) (DMSO-d_6, 500 MHz)

The presence of proton 7-NH, C9=NH$^+$ and NH$_2$ were indicated by signals at

δ_H 10.17, 9.65 and 8.3 respectively. The lowest field signal is assigned to 7-NH

because this resonance is deshielded by the anisotropy of the bromine atom present

at position 5 of the 4,5-dibromophakellinium cation. It is noteworthy that the vicinal

protons of the system 7-NH-C6-H6 do not exhibit spin-spin interactions which are

consistent with the dihedral angle of ~90° between 7-NH, C-6, and H-6 bonds. If the protonation of phakellin has taken place at N-7, then the dihedral angle between C-6, H-6, and 7-NH' (the second proton of N-7) would be about 10°. In this case, the resonances of H-6 and 7-NH should appear as doublets (Sharma and Magdoff-Fairchild, 1977).
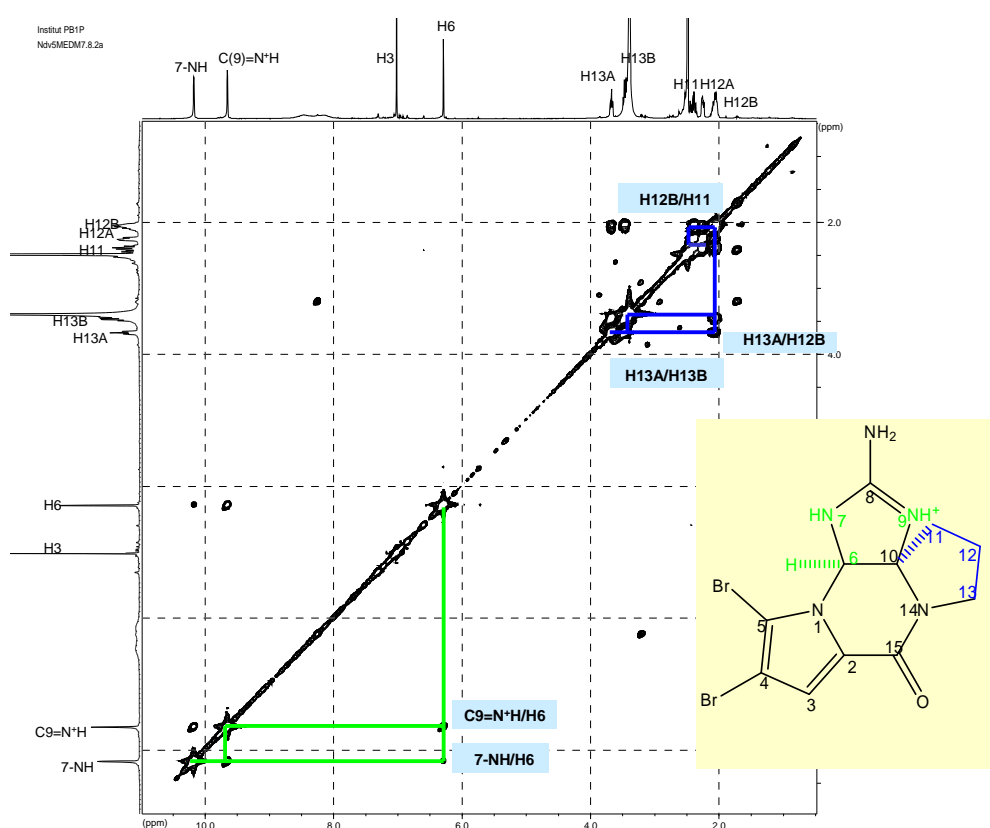
Fig.III.78. ^{1}H–^{1}H COSY spectrum of compound **11a** (DMSO-d_6)

The ^{13}C NMR of **11a** is consistent with the general structure proposed for phakellins (Table III.9). The chemical shift of C-6 confirmed that this carbon atom is directly linked to two electron-withdrawing groups, the guanidine moiety and the pyrrole nitrogen (Sharma and Magdoff-Fairchild, 1977).

Careful interpretation of the spectroscopy data with comparison to the literature suggests that compound **11a** is **(+)-dibromophakellin HCl** and compound

11b is the free base form, **(+)-dibromophakellin**. The two optically active compounds exhibit $[\alpha]_D^{25}$ value of +91.7º ± 1.9º (*c* 0.31, MeOH) for compound **11a** and $[\alpha]_D^{25}$ value of +20 5º ± 6.3º (*c* 0.09, MeOH) for compound **11b**. The absolute configuration of (+)-dibromophakellin as illustrated in Fig.III.80 as reported by De Nanteuil *et al*. (1985) using X-ray crystallography.
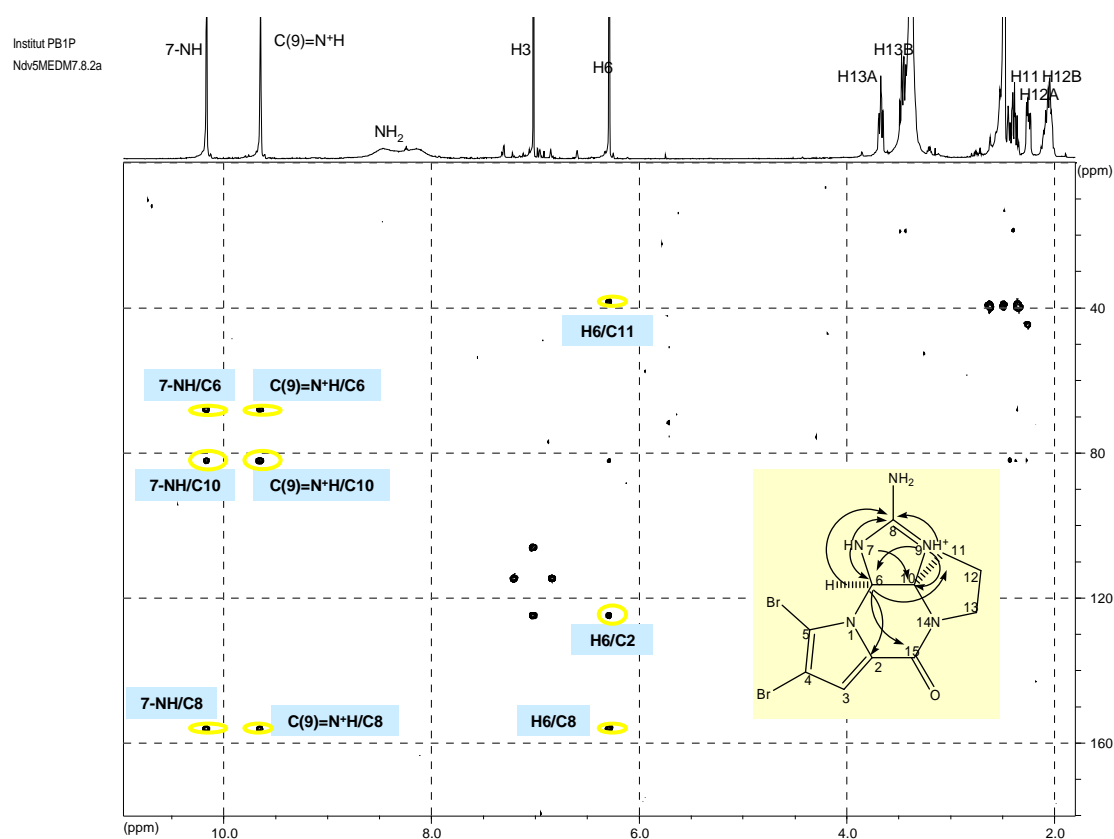
Fig.III.79. ^{1}H–^{13}C HMBC spectrum of compound **11a** (DMSO-d_6)
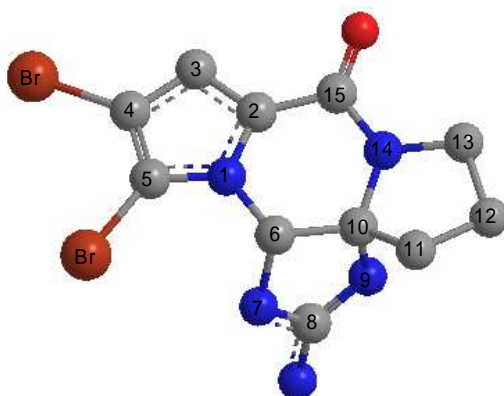
Fig.III.80. Absolute configuration of (+)-dibromophakellin described by De Nanteuil *et al.* (1985)

III.1.12. **Dibromohydroxyphakellin HCl** (**12**, new compound)
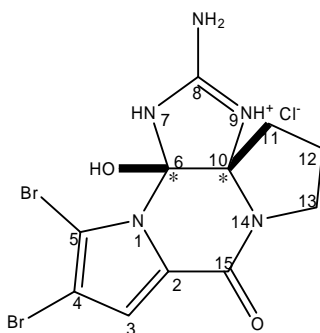
Fig.III.81. Compound **12***
* Relative stereochemistry is shown

Fig.III.82. Analytical HPLC data of compound **12**
Left: HPLC profile in 254 nm, RT: 4.76; right: UV absorption spectrum, λ_{max} = 241.3; 292.6 nm
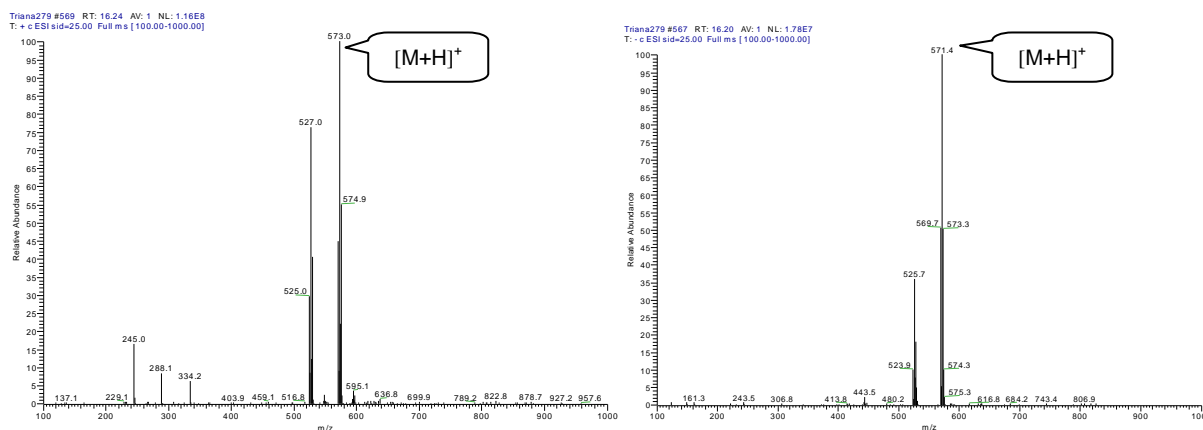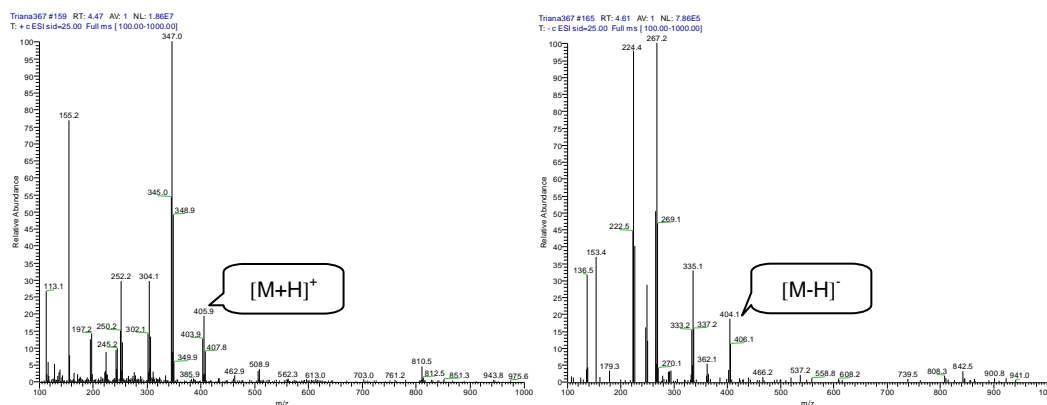
Fig.III.83. ESI-MS data of compound **12**

Compound **12** was obtained as a clear crystal at an amount of 47 mg which is 0.093% of the sponge dried weight. This substance appears quite early with a retention time of 4.76 min (10% MeOH) in analytical HPLC chromatogram. Its UV spectrum shows a λ_{max} at 241.3 and 292.6 nm at almost the same intensities (Fig.III.82). ESI-MS pseudo molecular ion cluster at *m/z* 404/406/408 [M+H]$^+$ having an intensity ratio of 1:2:1 indicates the presence of two bromines in the molecule (Fig.III.83). Molecular formula of $C_{11}H_{12}Br_2N_5O_2$ was deducted from HRESIMS data (*m/z* experimental = 403.9360, *m/z* calculated = 403.9352 [M+H]$^+$) and ^{13}C-NMR analyses. It exhibits $[\alpha]_D^{25}$ value of -6.6º $\pm$ 0.7º (*c* 0.23, MeOH).

^{1}H NMR data suggest that the compound is a phakellin derivative. The presence of two bromines in the molecule leads to a dibrominated phakellin congener. An excess of 16 mass units in comparison to dibromphakellin (compound **11a** and **11b**) indicates an additional hydroxyl function in the molecule. Comparison of the ^{1}H NMR data to those of the known dibromophakellin, helps in the assignment of each of the proton signals. It is implied that the guanidine double bond is placed at the endocyclic 8, 9 positions, and 9-NH is protonated. The resonance in the resulting cation is then inhibited. This kind of structure results in a deshielding effect of

pyrrolidine proton (H-11) in comparison to its congener dibromophakellin base (δ_H 3.50, compound **11b**) (Sharma and Magdoff-Fairchild, 1977).

A *sp²* proton at δ_H 6.90 (s) is assigned as the pyrrole ring proton and a broad signal at δ_H 7.19 is first suspected as H-6. Based on the signals of dibromophakellin HCl (**11a**), the presence of 7-NH, C9=NH⁺ and NH₂ is indicated by signals at δ_H 9.82, δ_H 9.80 and δ_H 8.77, respectively. The lowest field signal is assigned to 7-NH because the resonance is deshielded by anisotropy effect of the bromine atom present at position 5 of the 4,5-dibromophakellinium cation (Sharma and Magdoff-Fairchild, 1977).
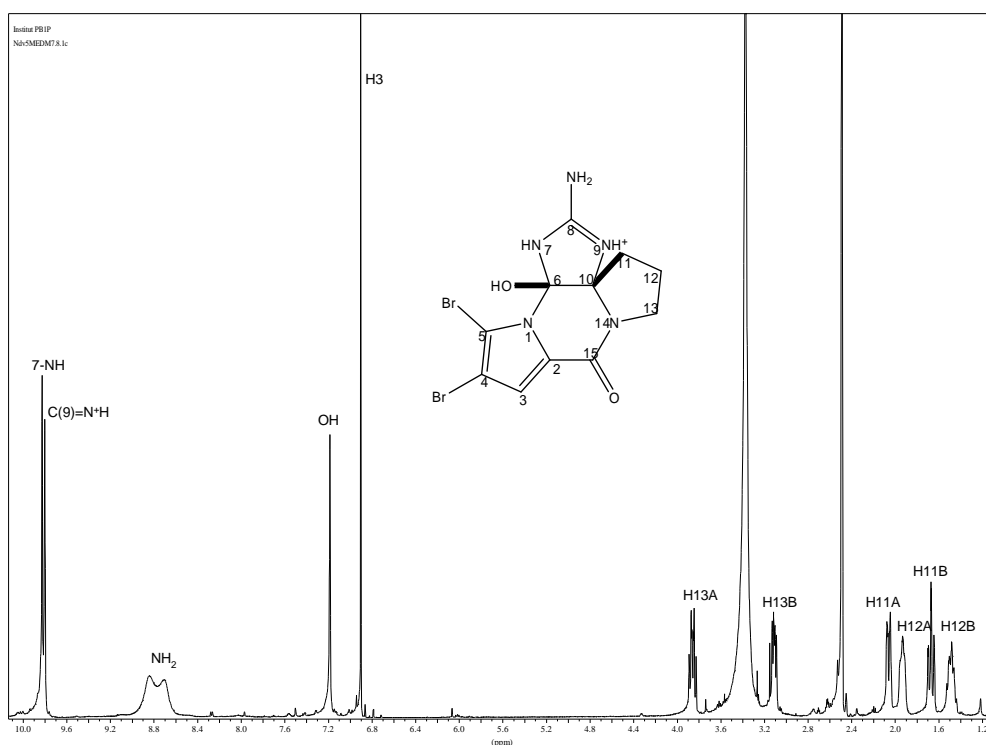
Fig.III.84. ¹H NMR of **12*** (DMSO-*d₆*, 500 MHz)
*Relative stereochemistry is shown

¹³C-NMR data (Table III.9) exposed an unusual chemical shift of C-6 at δ_C 89.5 in comparison to **11a** at δ_C 68.1. It is doubtful to expect that an OH substitution

at N-7 can shift C-6 to the lower field in about 21 ppm. However, the DEPT experiment shows C-6 as a quartenary carbon. This information explains the chemical shift of C-6 as well as the position of the hydroxyl group. C-6 was directly linked to not only two but three electron-withdrawing groups, the guanidine moiety, pyrrole nitrogen and the hydroxyl group. Therefore the proton at δ_H 7.19 is assigned as the OH group and the signal at δ_H 9.82 as 7-NH. This proposed structure was confirmed by ^{1}H-^{13}C HMBC spectrum as shown in Fig.III.87 which exhibits correlation of the hydroxyl proton to C-6 and C-10.
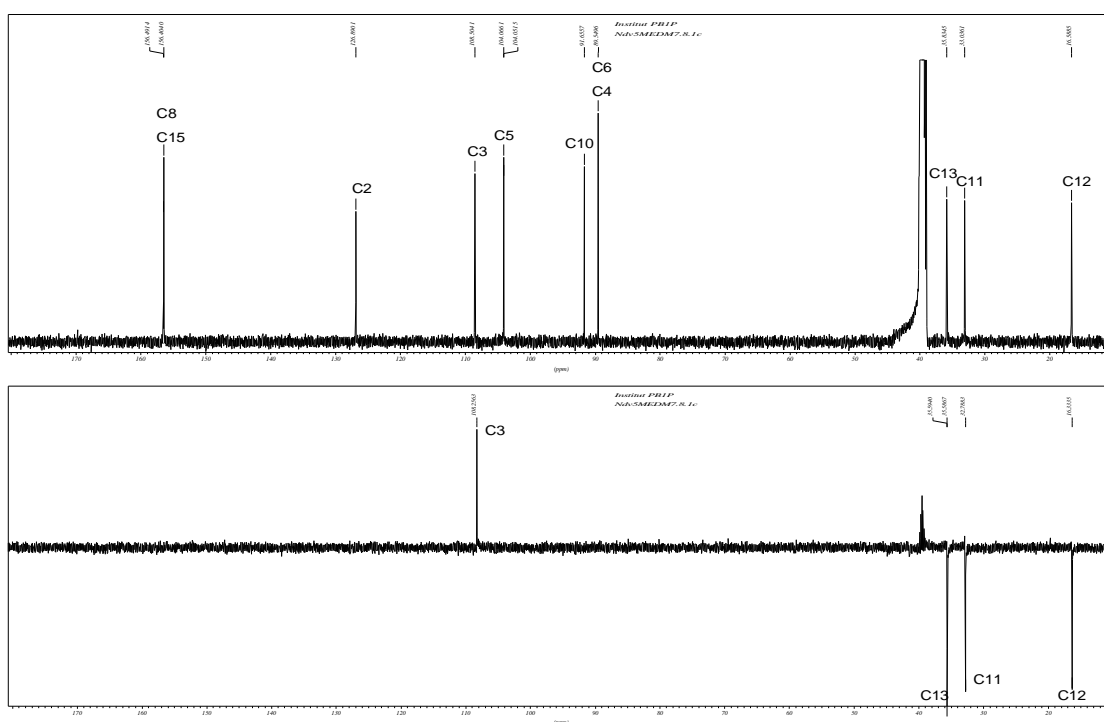
Fig.III.85.^{13}C NMR and DEPT spectra of **12** (DMSO-d_6, 125 MHz)
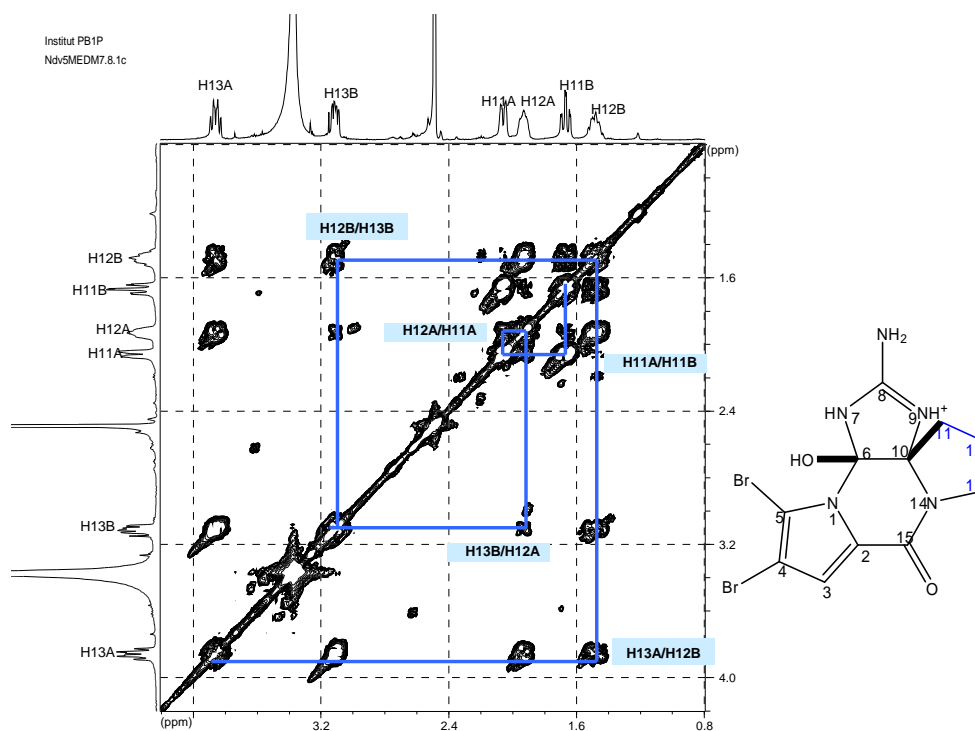
Fig.III.86. ^{1}H–^{1}H COSY data of **12*** (DMSO-d_6)
*Relative stereochemistry is shown
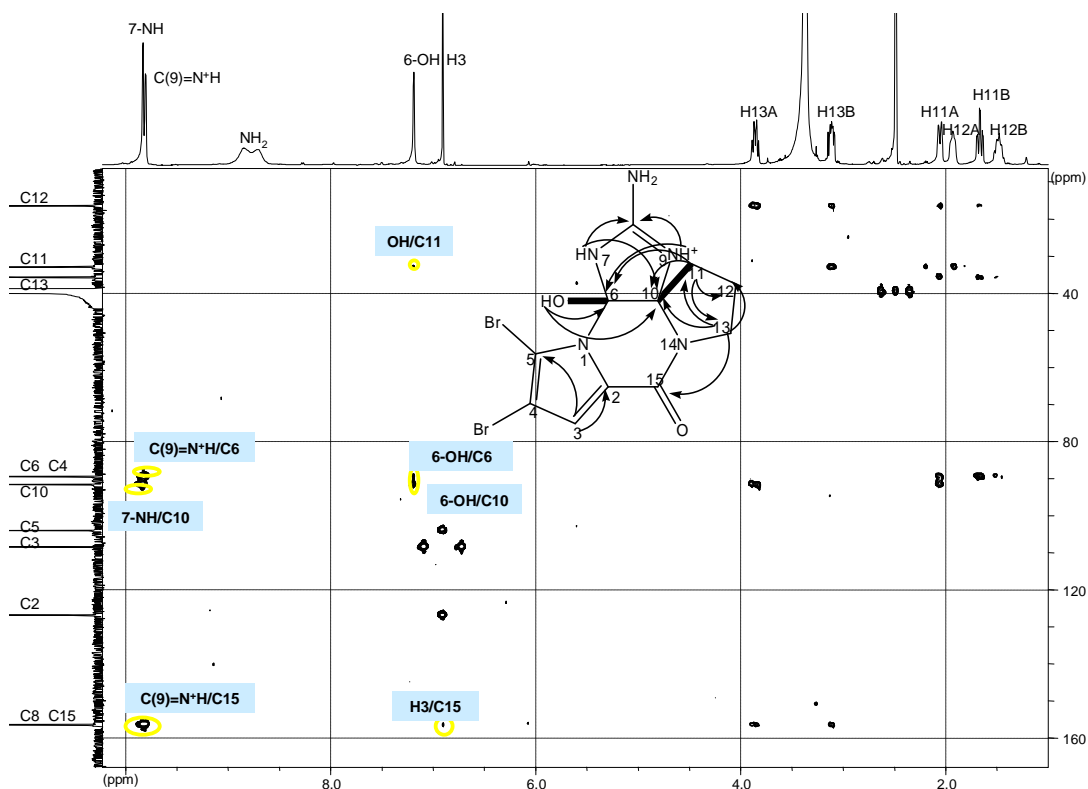
Fig.III.87. ^{1}H–^{13}C HMBC spectrum of **12*** (DMSO-d_6)
*Relative stereochemistry is shown

Table III.9. NMR data of compound **12** in comparison to dibromophakellin HCl (**11a**) and dibromophakellin base (**11b**)

No.	Compound 12 [a]		Compound 11a [a]		Compound 11b [a]
	1H-NMR (δ, multiplicity, *J* in Hz)	**13C-NMR** (δ, DEPT)	**1H-NMR** (δ, multiplicity, *J* in Hz)	**13C-NMR** [b] (δ, DEPT)	**1H-NMR** (δ, multiplicity, *J* in Hz)
2	-	126.9, C	-	125.1	-
3	6.90, s	108.5, CH	7.02, s	108.4	6.79, s
4	-	89.5, C	-	n.d	-
5	-	104.1, C	-	106.3	-
6-OH	7.19, b s (OH)	89.5, C=O	6.29, d, 1.3 (H6)	68.1	5.75, s
8	-	156.5, C=O	-	156.2	-
10	-	91.6, C	-	82.3	-
11A 11B	2.06, ddd, 2.8, 14.1, 11.3 1.67, dt, 2.8, 13.6	33.0, CH$_2$	2.40, m	38.6	2.02, m 1.93, m
12A 12B	1.93, m 1.49, m	16.6, CH$_2$	2.26, m 2.05, m	19.1	2.14, m
13A 13B	3.86, ddd, 3.1, 9.8, 12.9 3.11, ddd, 5.7, 1.9, 7.9	35.8, CH$_2$	3.68, dt, 2.5, 8.8 3.46, ddd, 1.9, 8.8, 8.5	44.8	3.77, dd, 5.0, 10.1 3.50, m
15	-	156.4, C	-	n.d	-
7-NH	9.82, s	-	10.17, s	-	3.78 – 3.75, m
C(9)=N$^+$H	9.80, s	-	9.65, s	-	
NH$_2$	8.77, b d	-	8.35, b d	-	

[a] Data were recorded in DMSO-d_6 at 500 MHz (1H) and 125 MHz (13C) multiplicities and coupling constant are given in Hz; [b] Data were abstracted from 1H -13C HMBC; n.d: not detected
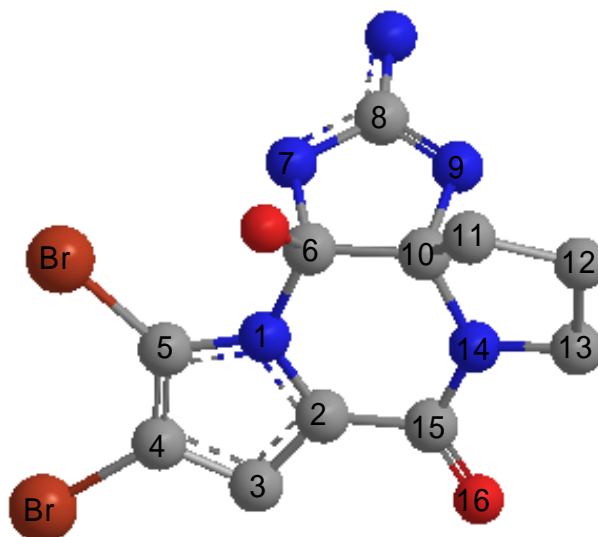
Fig.III.88. Compound **12** relative configuration based on 1H–1H ROESY
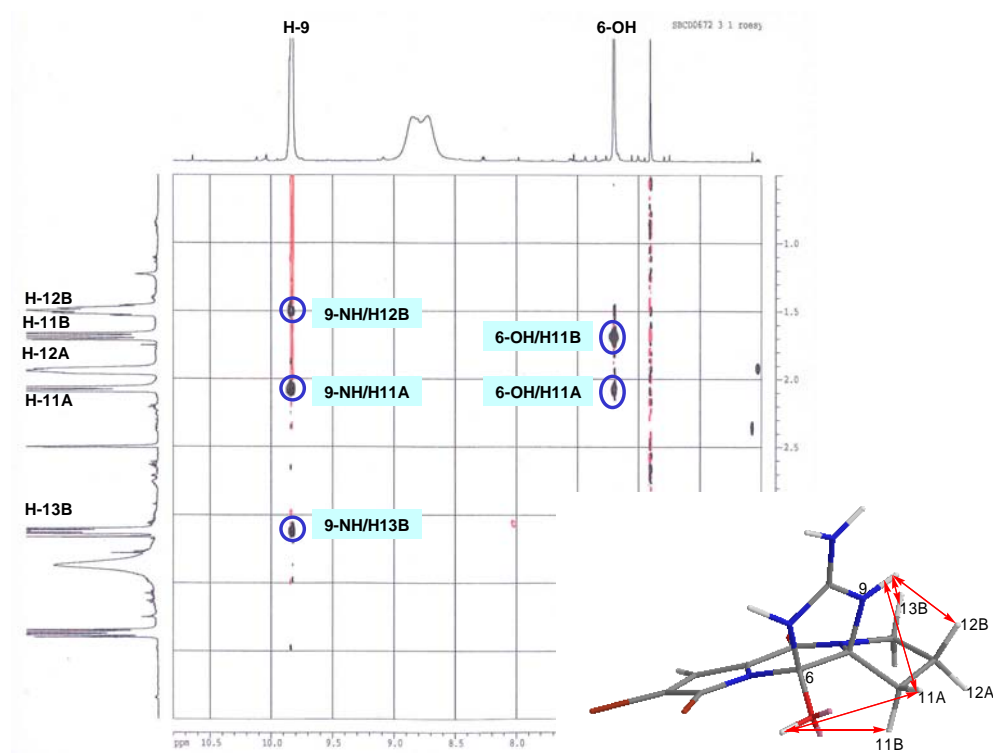
Fig.III.89a. ^{1}H–^{1}H ROESY of compound **12** detected in DMSO-d_6
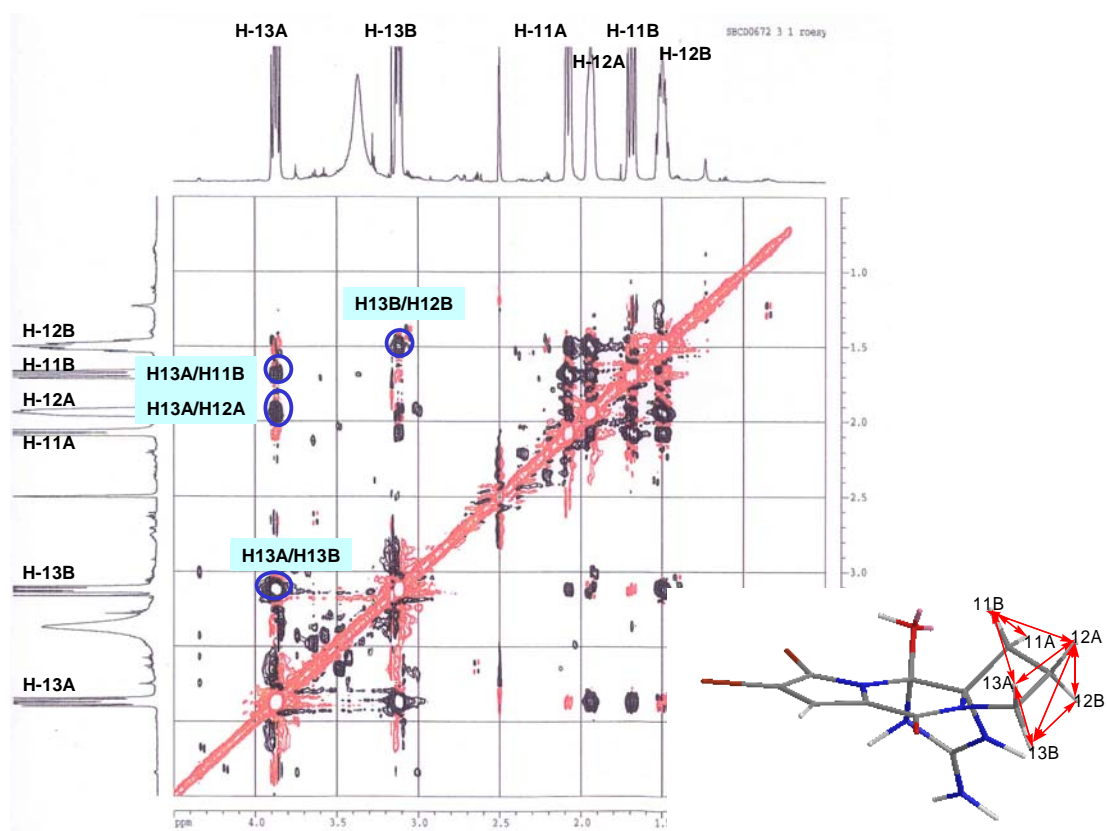
Fig.III.89b. ^{1}H–^{1}H ROESY of compound **12** detected in DMSO-d_6

Relative stereochemistry is assigned through a ROESY experiment. The ROESY spectrum showed NOE cross peaks between the hydroxyl proton and H-11A/B while on the other hand only H-11A gave an NOE with 9-NH. This evidence leads to the configuration of **12** in Fig.III.88. This relative stereochemistry is also comparable to that of dibromophakellin HCl (**11a**). Considering that compound **12** has $[\alpha]_D^{25}$ value of -6.6º ± 0.7º (*c* 0.23, MeOH) while compound **11a** has $[\alpha]_D^{25}$ value of +91.7º ± 1.9º (*c* 0.31, MeOH), implies that compound **12** is the (-)-enantiomer of **11a**. After careful interpretation of the spectral data available, compound **11** is determined as a (-)-**dibromohydroxyphakellin HCl**, a new member of phakellin group of compound.

### III.1.13. Midpacamide (**13**, known compound)
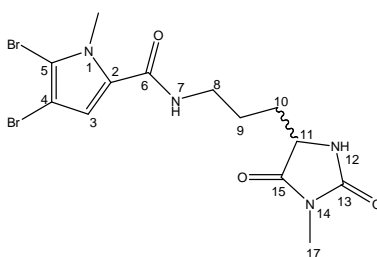
Fig.III.90. Compound **13**
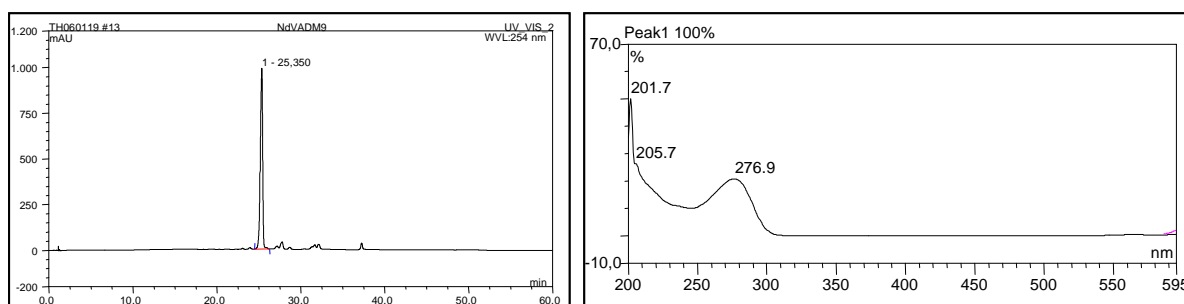
Fig.III.91. Analytical HPLC data of compound **13**
Left: HPLC profile in 254 nm, RT: 25.35; right: UV absorption spectrum, λ_{max} = 201.7; 205.7; 276.9 nm
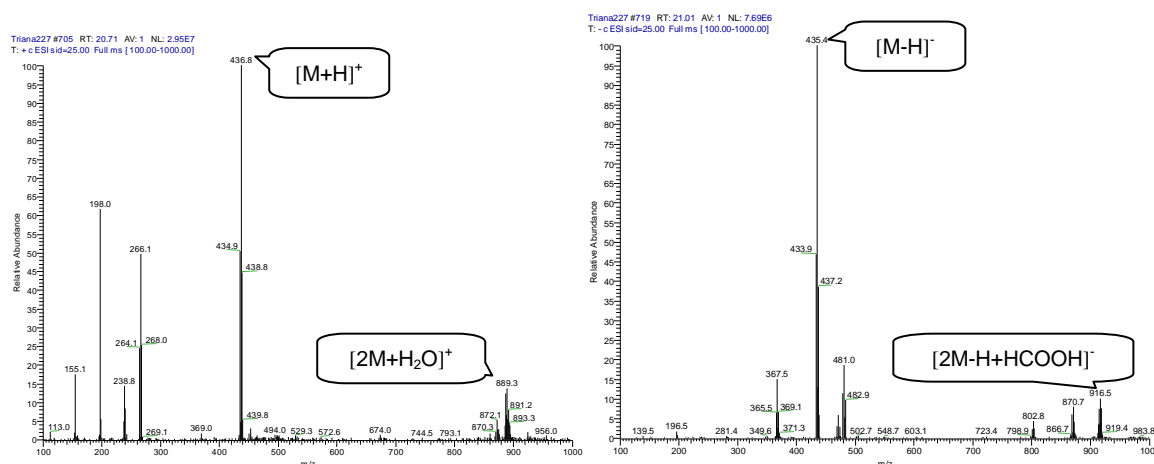
Fig.III.92. ESI-MS spectrum of compound **13**

In this study, compound **13** or the known congener midpacamide (C$_{13}$H$_{16}$Br$_2$N$_4$O$_3$) was isolated as the major compound of the *Agelas* nsp. (2.0 g, 1.01% of the sponge dried weight). This 4,5-dibromo-1-methyl-*N*-(3-(4-methyl-2,5-dioxoimidazolidin-4-yl)propyl)-1*H*-pyrrole-2-carboxamide was obtained as a white greenish powder and exhibited $[\alpha]_D^{20}$ value of +3.0º ± 1.2º (*c* 0.4, CHCl$_3$). This compound was reported for the first time by Chevolot and collaborators (1977) to be isolated from an unidentified marine sponge, and was later reported to be found in *Agelas mauritiana* by Fathi-Afshar and Allen (1988).

Compound **13** showed UV absorbances at λ_{max} 201.7 nm and 276.9 nm (Fig.III.91). ESIMS of the molecule exhibited pseudo-molecular ion peaks at *m/z* 435/437/439 [M+H]$^+$ having an intensity ratio of 1:2:1 suggesting the presence of a dibrominated compound (Fig.III.92). This finding is compatible to the molecular formula of C$_{13}$H$_{16}$Br$_2$N$_4$O$_3$ of midpacamide.

Fig.III.93. ^{1}H NMR spectrum of compound **13** (CDCl$_3$, 500 MHz)

Fig.III.94. ^{13}C NMR (above) and DEPT (below) spectra of compound **13** (CDCl$_3$, 125 MHz)
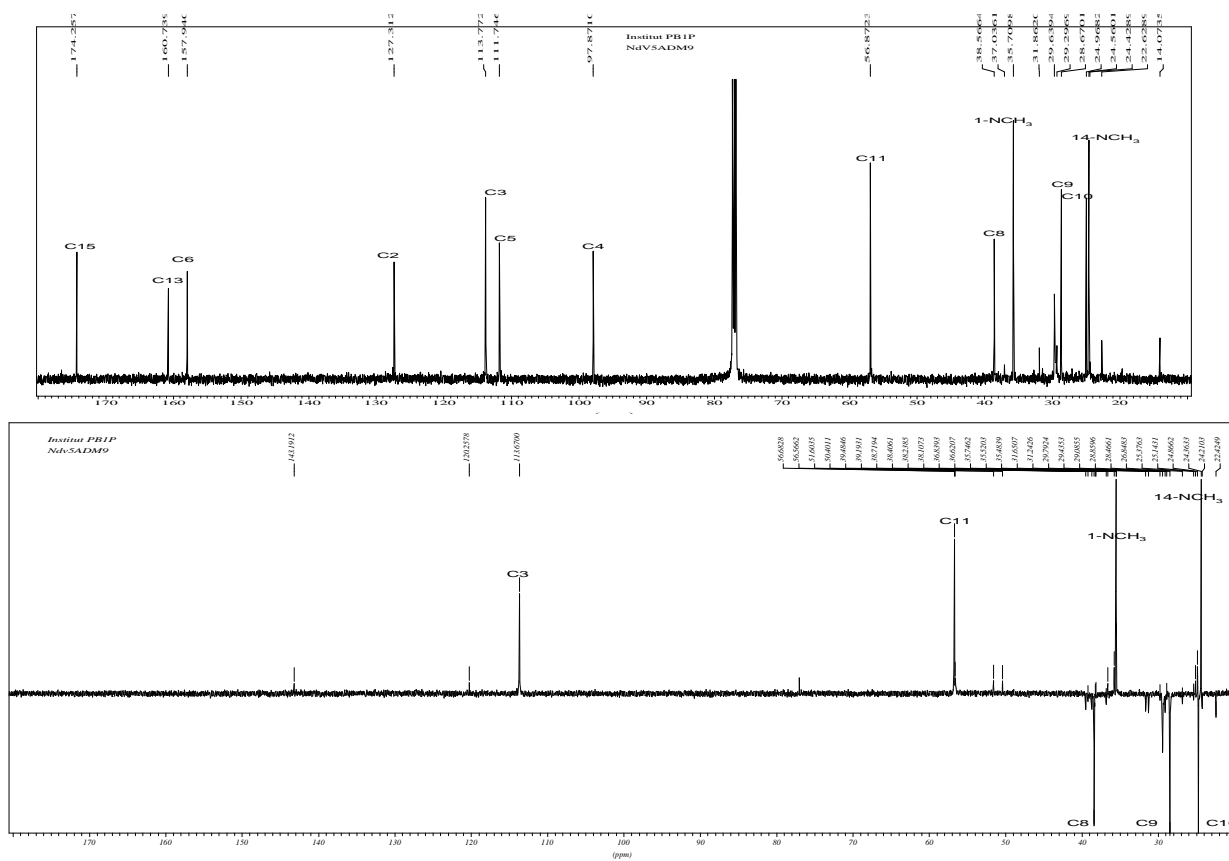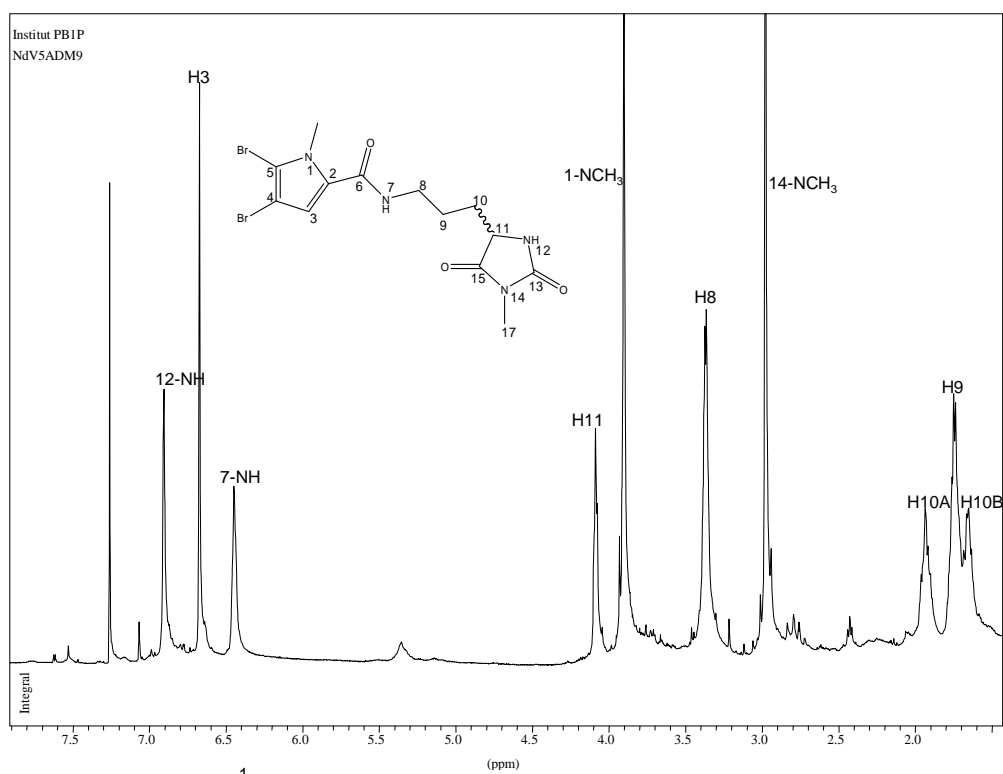
NMR data of compound **13** shows one sp^2 signal at δ_H 6.66 as a sharp singlet and a NCH$_3$ signal at δ_H 3.92 (s). This finding together with the UV absorption maximum at around 270 nm fit the 4,5-dibromo-1-methyl-1*H*-pyrrole-2-carboxamide structure. This substructure, as also observed in previously mentioned congeners is confirmed through an HMBC experiment (Fig.III.96).

Four sp^3 signals in its ^{1}H-NMR spectrum at δ_H 3.39 (2H, dt, $J = 6.0$ Hz, H$_2$-8); 1.75 (2H, m, H$_2$-9); 1.94 (1H, m, H-10A) and1.65 (1H, m, H-10B) prove the presence of a propylene chain. This chain is confirmed in its ^{1}H-^{1}H COSY spectrum as one spin system commencing from 7-NH at δ_H 6.29 (bt, $J = 5.5$) to proton 8→9→10A and 10B→11 (δ_H 4.10, t, $J = 5.1$ Hz)→12-NH (δ_H 6.73, b s).

^{13}C NMR data in the aliphatic region show characteristic resonances due to three sp^3 methylenes at δ_C 38.6 (C-8); 28.7 (C-9); 25.0 (C-10) and one sp^3 methine at δ_C 56.9 (C-11). Three sp^2 quartenary carbons at δ_C157.9; δ_C 160.7 and δ_C 174.3 are assigned to carbonyl functions of the carboxamide and the imidazolidinedione. The presence of a deshielded methyl group at δ_H 3.00, δ_C 24.6, suggests that the imidazolidinedione moiety is methylated at N-14 or N-12. Data abstracted from the ^{1}H–^{1}H COSY spectrum showing the correlation of C-11 to 12-NH indicate that the methyl group must be connected to N-14. Hence the structure of compound **13** is determined as **midpacamide.**

Fig.III.95. ^{1}H–^{1}H COSY spectrum of compound **13** (CDCl$_3$)

Fig.III.96. ^{1}H–^{13}C HMBC spectrum of compound **13** (CDCl$_3$)
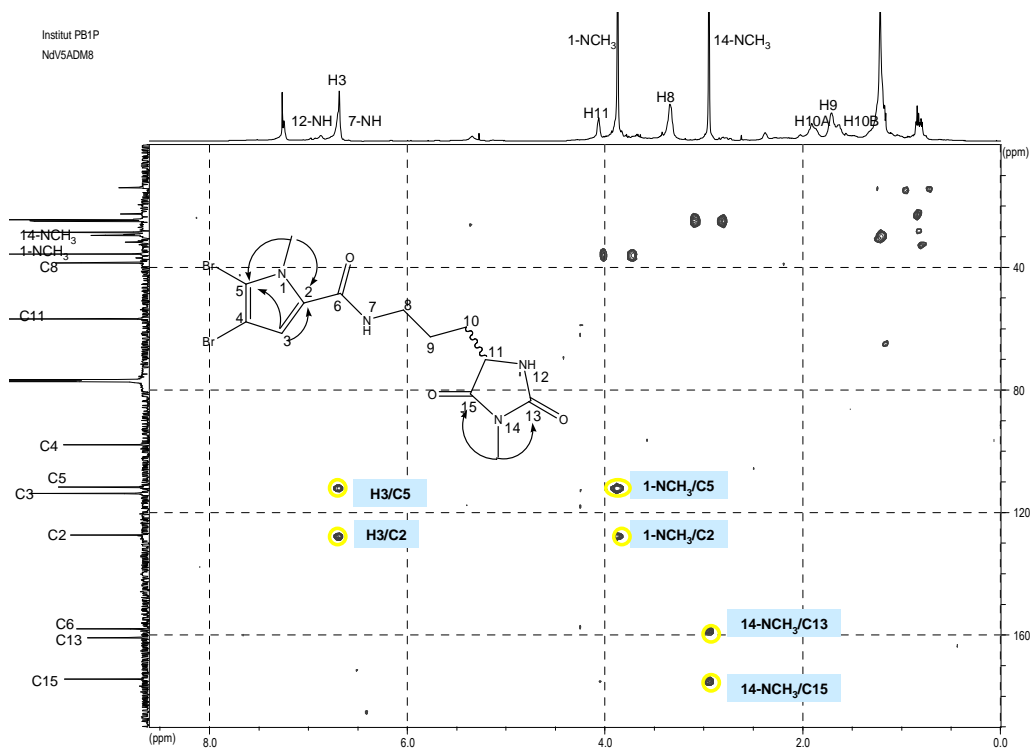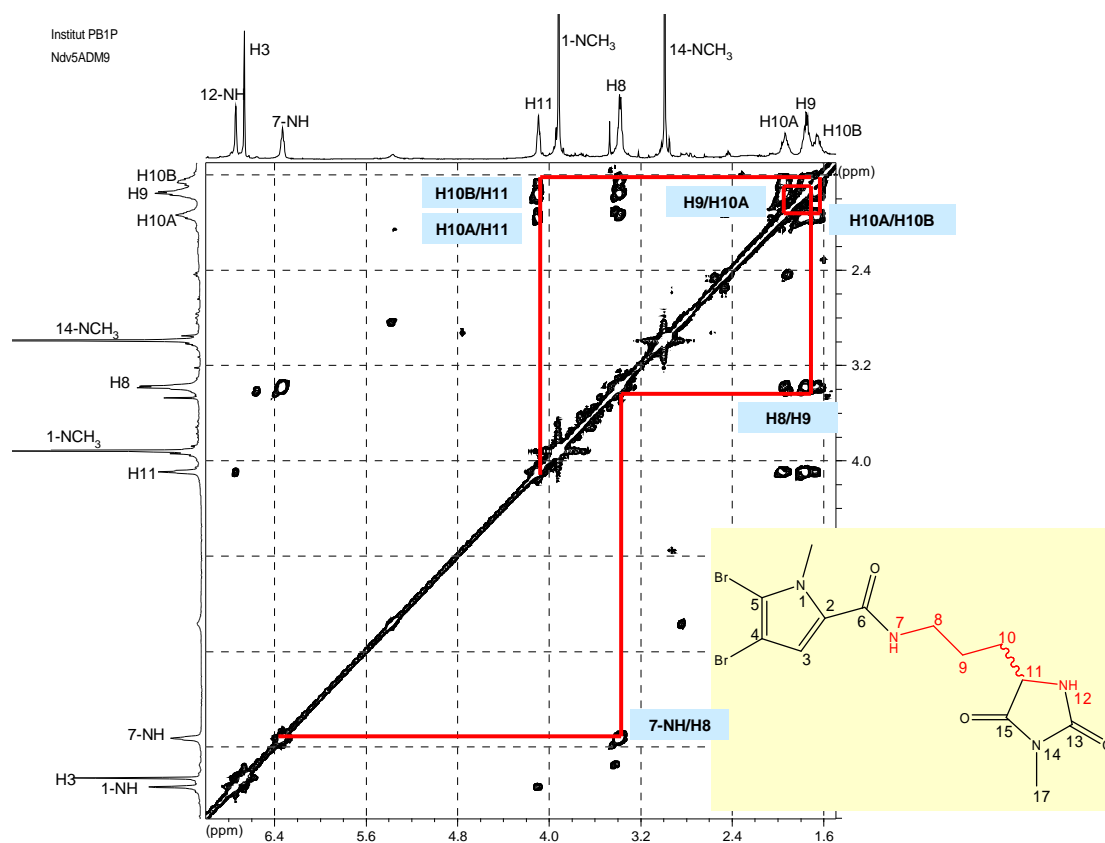
Table III.10. NMR data of compound **13** in comparison to midpacamide

No.	Compound 13 [a)]			Midpacamide [c)]		
	^{1}H		^{13}C	^{1}H		^{13}C
	δ	Integration, multiplicity, *J* in Hz	δ, DEPT	δ	Integration, multiplicity, *J* in Hz	δ, DEPT
2	-	-	127.3, C	-	-	127.4, C
3	6.66	1H, s	113.8, CH	6.6	1H, s	113.7, CH
4	-	-	97.9, C	-	-	98, C
5	-	-	111.7, C	-	-	111.9, C
6	-	-	157.9, C=O	-	-	157.6, C=O
7-NH	6.29	1H, bt, 5.5	-	6.2 [b)]	1H, bt, 5.5	-
8	3.39	2H, dt, 6.0	38.6, CH$_2$	3.42	2H, m	38.8, CH$_2$
9	1.75	2H, m	28.7, CH$_2$	1.6 – 2.02,	4H, m	28.7, CH$_2$
10	1.94 1.65	1H, m (A) 1H, m (B)	25.0, CH$_2$			25.1, CH$_2$
11	4.10	1H, t, 5.1	56.9, CH	4.12	1H, m	56.7, CH
12-NH	6.73	1H, b s	-	6.52 [b)]	1H, s	-
13	-	-	160.7, C=O	-	-	160.7, C=O
15	-	-	174.3, C=O	-	-	174.1, C=O
1-NCH$_3$	3.92	3H, s	35.7, CH$_3$	3.95, s	3H, s	35.8, CH$_3$
14-NCH$_3$	3.00	3H, s	24.6, C	3.02, s	3H, s	24.6, CH$_3$

[a)] Data were recorded in CDCl$_3$ at 500 MHz (^{1}H) and 125 MHz (^{13}C), multiplicities and coupling constant are given in Hertz; [b)] exchangeable signal; [c)] Fathi-Afshar and Allen (1988)

III.1.14. Agelongine (**14**, known compound)
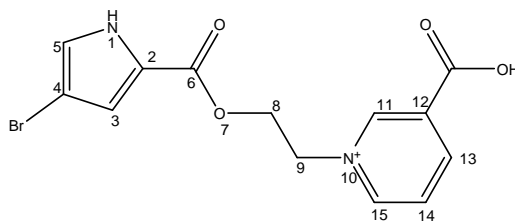
Fig.III.97. Compound **14**
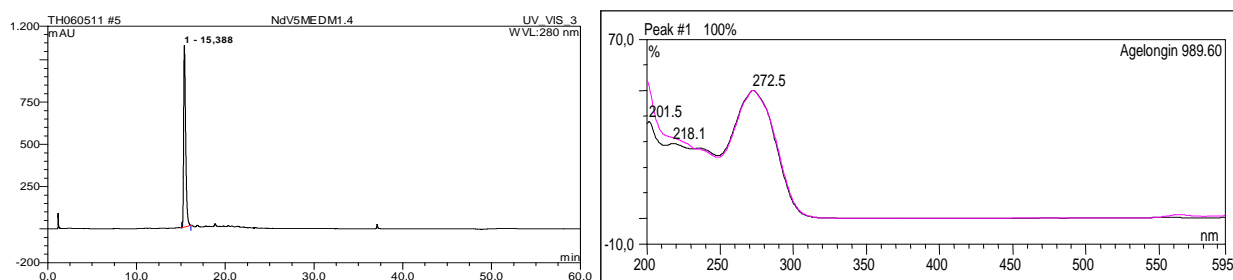
Fig.III.98. HPLC analytic result of compound **14**

Left: HPLC profile in 254 nm, RT: 15.39; right: UV absorption spectrum, λ_{max} = 201.5; 218.1; 272.5 nm
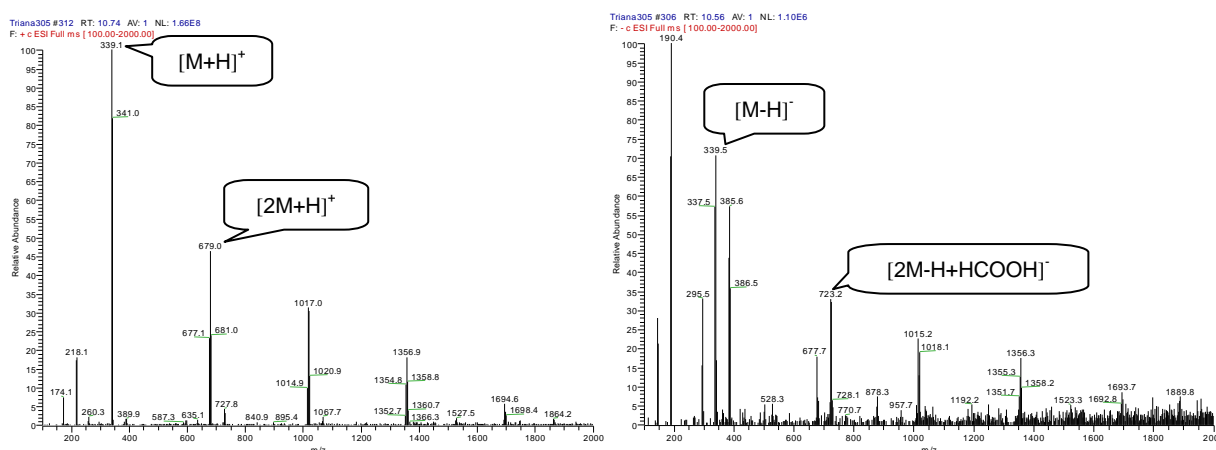
Fig.III.99. ESI-MS data of compound **14**

Agelongine was first reported by Cafieri and collaborators (1995) as an anti-serotonergic agent isolated from *Agelas longissima*. This compound is quite unique in comparison to other brominated pyrrole of *Agelas* sponges while it has a pyridinium ring instead of a imidazole nucleus while an ester linkage replaces the amidic bond.

UV absorption spectrum of **14** exhibits usual bands for brominated pyrrole-2-carboxamide (Fig.III.98). ESIMS spectrum shows intense pseudo molecular ion peaks at *m/z* 338 and 340 having an intensity ratio of 1:1 which indicates the presence of a mono-brominated compound. It fits the molecular formula for agelongine, $C_{13}H_{13}BrN_3O_3^+$. This optically inactive compound was obtained as a white amorphous substance at an amount of 20 mg which is 0.01% of the sponge dried weight.
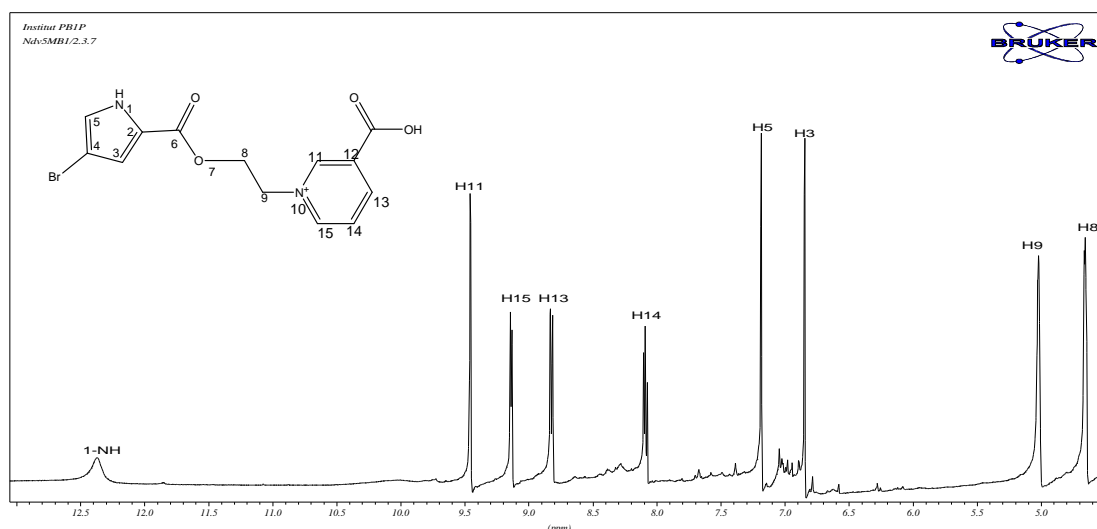
Fig.III.100. ¹H-NMR data of compound **14** (DMSO-d_6, 500 MHz)

¹H NMR spectrum of compound **14** exhibits eight well separated signals. Six of which were in the sp^2 region, while the triplets resulting from two mutually coupled methylenes are found at δ_H 4.80 and 5.10. This deshielding effect is probably a result of two heteroatoms flanked to them. The extremely low field chemical shifts of signals (δ_H 8.14, dd; 8.99, dt; 9.05, dt; 9.42, s) in its ¹H NMR spectrum are assigned to the β-substituted pyridium ring. A 3,5-disubtituted pyrrole is suggested by ¹H signals at δ_H 6.89 (s) and 7.05 (s), as well as ¹³C NMR resonances at δ_C 125.6, CH; 98.2, C; 118.5, CH; and 123.0, C. The presence of an aromatic ester function and of a carboxylate group was shown by the quaternary carbon signals at δ_C 161.0 and 167.0. The ¹³C spectrum exhibited six tertiary carbons in the sp^2 region for the aromatic rings signals of aromatic rings and three quaternary carbons (Table III.11).
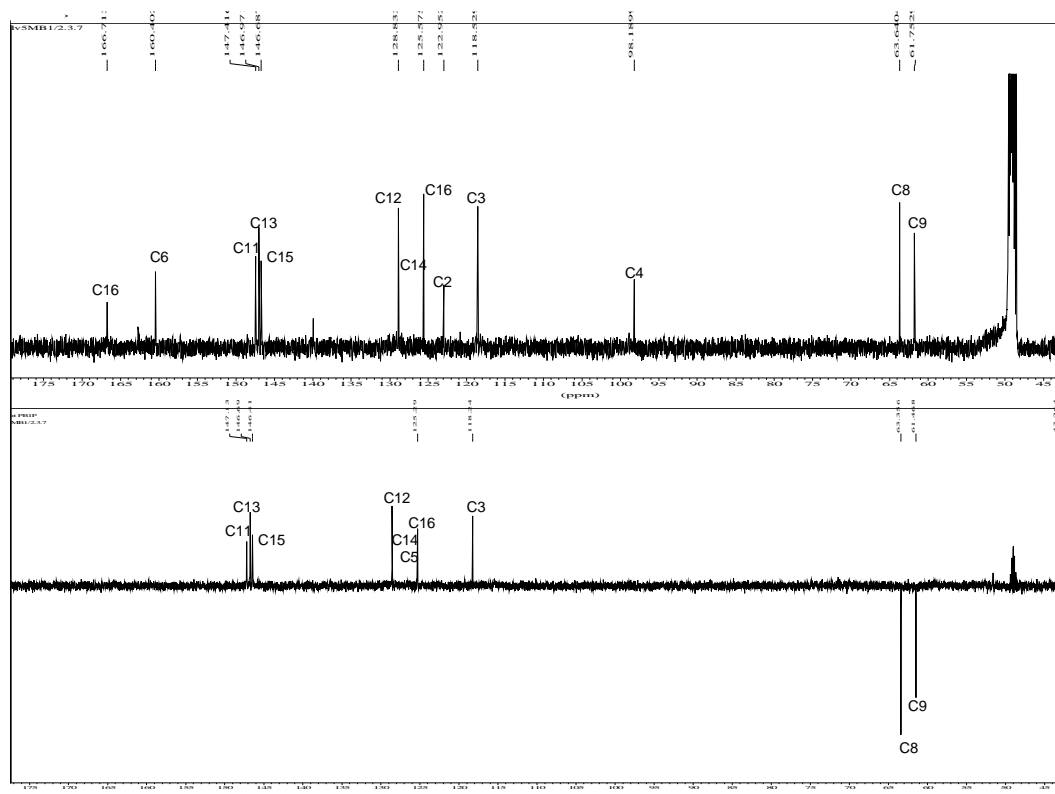
Fig.III.101. ^{13}C-NMR (above) and DEPT (below) spectra of compound **14** (MeOD, 125 MHz)

The 2D COSY spectrum shows the presence of three distinct spin systems, belonging to two nitrogen-containing heteroatomatic rings and to the above mentioned ethylene unit. The 2D HMBC spectrum confirms the connectivities among the substructures. Cross peaks correlating H-5 and H-8 to a carbonyl function at δ_C 160.4 (C=O) and from the pyridinium ring proton to another carbonyl function at δ_C 166.7 (C=O) confirm the assignment of those carbonyls as C-6 and C-16, respectively. Assignment of H-8 at δ_H 4.76 and H-9 at δ_H 5.06 are also secured by the cross peaks from H-8 to C-6 and H-11 to C-9 as well as H-9 to C-15. Thus the structure of compound **14** is determined as **agelongine**.
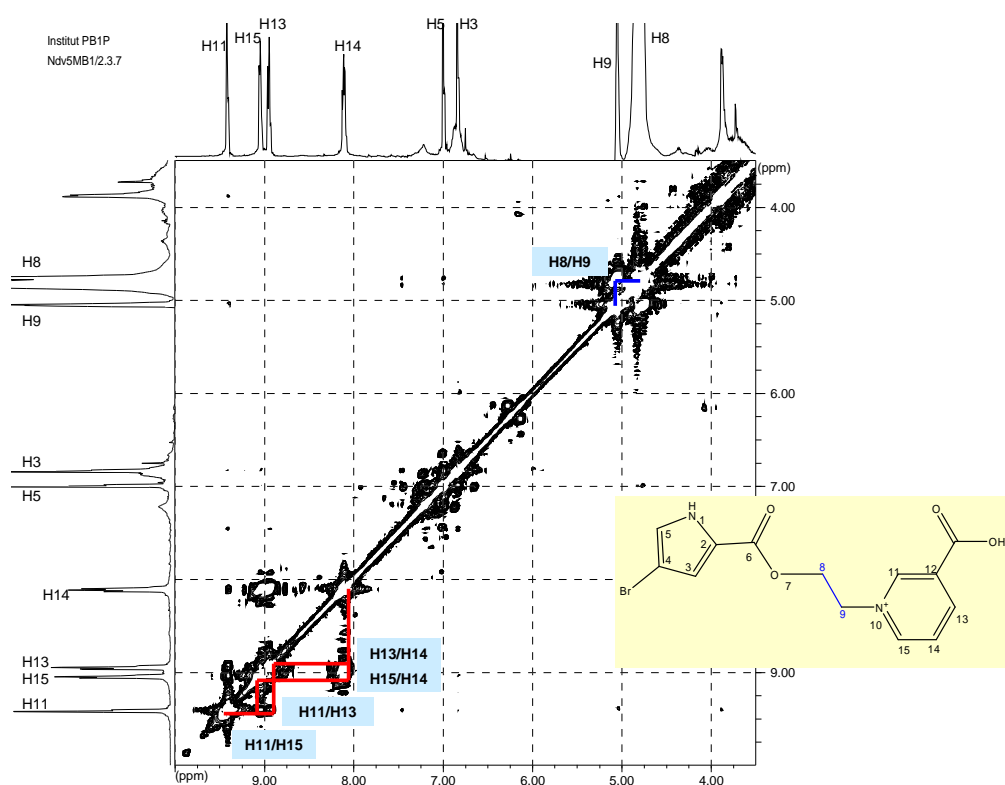
Fig.III.102. ^{1}H–^{1}H COSY spectrum of compound **14** (MeOD)
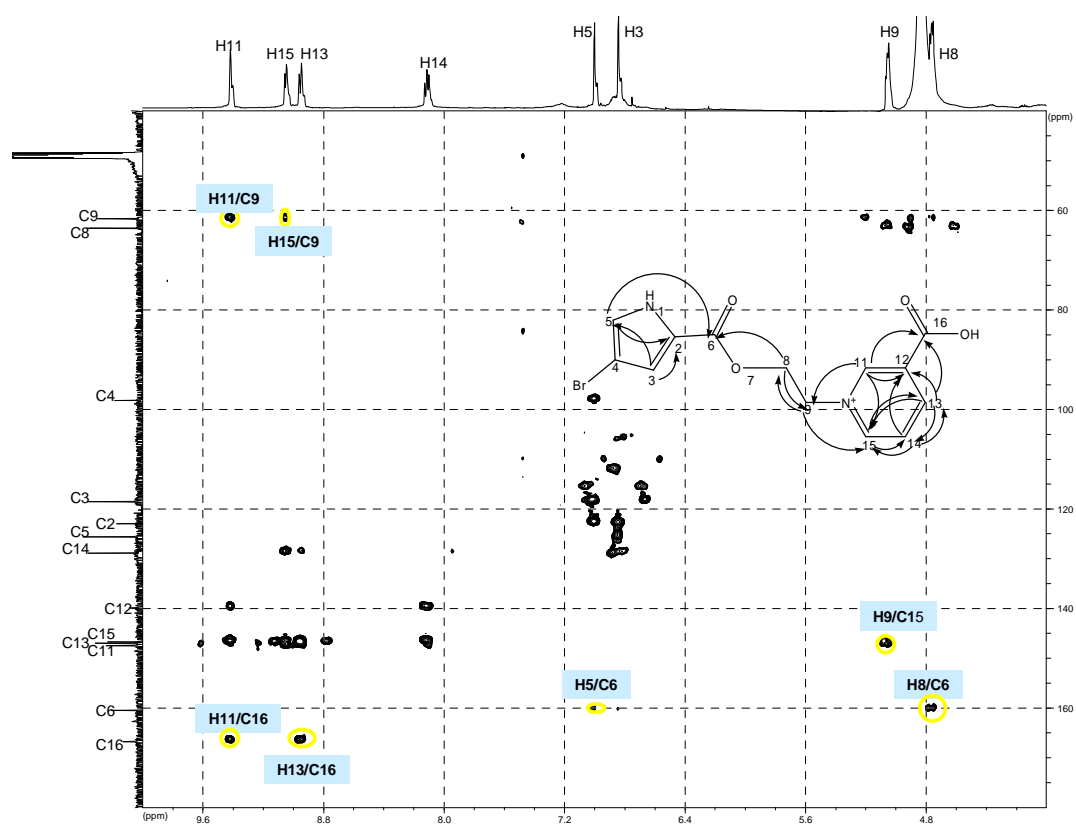
Fig.III.103. ^{1}H–^{13}C HMBC spectrum of compound **14** (MeOD)

Agelongine was reported to have antagonistic activity on serotonergic receptors (Cafieri *et al.*, 1995). This activity was also found in some *Agelas* bromopyrroles possessing a linear chain in their structure (Nakamura *et al.*, 1984a; Kobayashi *et al.*, 1986).

Table.III.11. NMR data of compound **14** in comparison to agelongine

No.	Agelongine [a) b)]		Compound 14 [a)]	
	^{1}H-NMR (δ, multiplicity, *J* in Hz)	^{13}C-NMR (δ, DEPT)	^{1}H-NMR (δ, multiplicity, *J* in Hz)	^{13}C-NMR (δ, DEPT)
2.	-	123.0, C		122.9, C
3.	6.89, d, 1.5	118.5, CH	6.84, s	118.5, CH
4.	-	98.2, C		98.2, C
5.	7.05, d, 1.5	125.6, CH	7.01, s	125.6, CH
6.		161,0, C		160.4, C
8.	4.80, t, 5.5	63.6, CH2	4.76, t, 4.7	63.6, CH2
9.	5.07, t, 5.5	61,7, CH2	5.06, t, 4.7	61.7, CH2
11.	9.42, s	147.4, CH	9.44, s	147.7, CH
12.		140.2, C		139.9, C
13.	8.99, dt, 7.7, 1.5	147.0, CH	8.95, d, 7.9	147.0, CH
14.	8.14, dd, 7.7, 6.2	128.8, CH	8.12, dd, 7.6, 6.3	128.8, CH
15.	9.05, dt, 6.2, 1.5	146.6, CH	9.07, d, 6.0	146.7, CH
16.		167.0, C		166.7, C

[a)] Data were recorded in MeOD at 500 MHz (^{1}H) and 125 MHz (^{13}C) multiplicities and coupling constant are given in Hz; [b)] Cafieri *et al.* (1995)

III.1.15. 4,5-dibromo-1-methyl-1*H*-pyrrole-2-carboxylic acid (**15**, known compound)
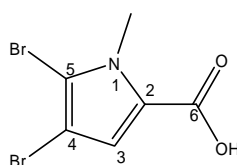
Fig.III.104. Compound **15**
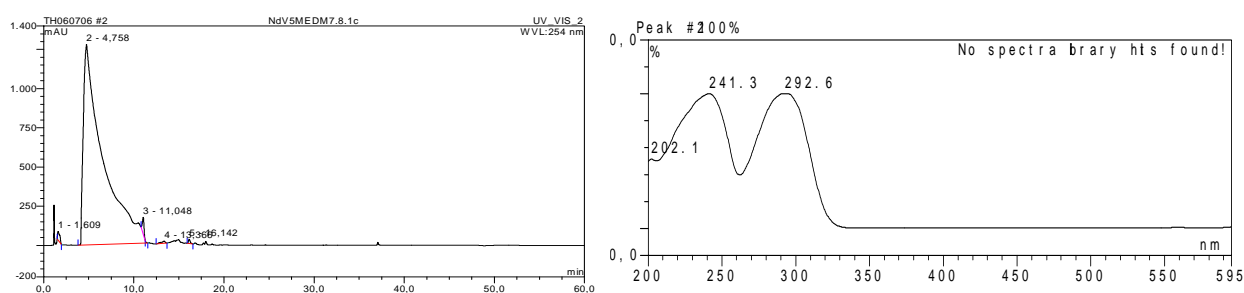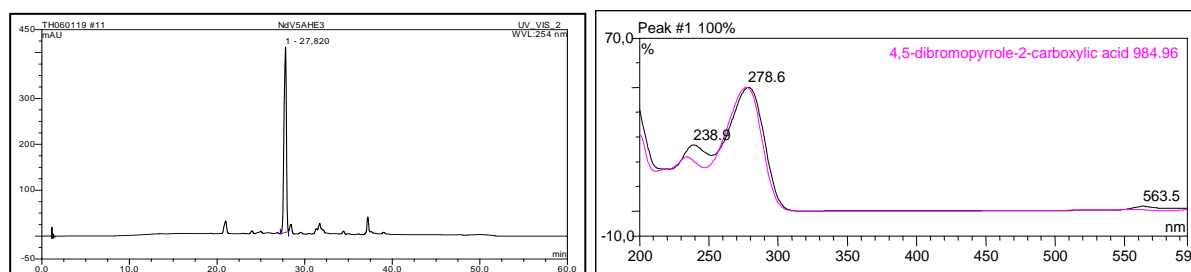

Fig.III.105. Analytical HPLC data of compound **15**
Left: HPLC profile in 254 nm, RT: 27.82; right: UV absorption spectrum, λ_{max} = 238.9; 278.6 nm.
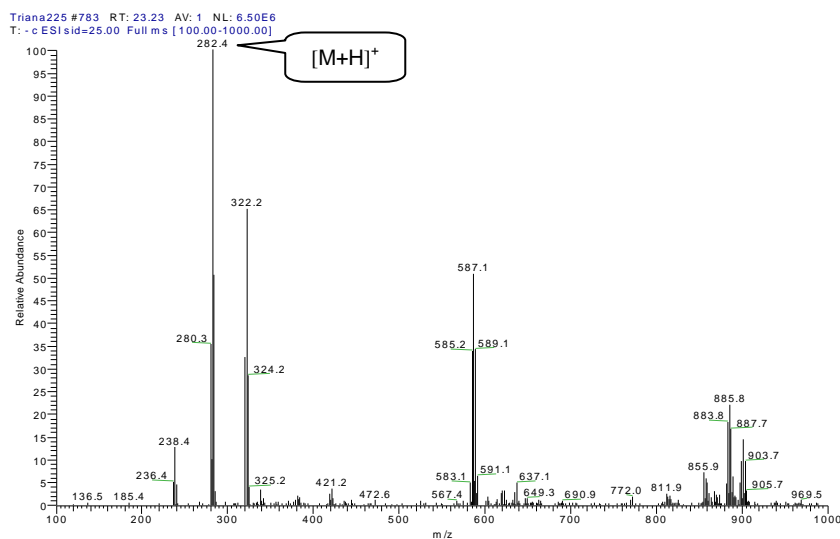
Fig.III.106. ESIMS result of **15**

Compound **15** was isolated as a white amorphous substance at an amount of 100 mg which is 0.05% of the sponge dried weight. It exhibits a UV absorption spectrum which matched with the internal spectral library data base for 4,5-dibromopyrrolecarboxylic acid (Fig.III.105). ESIMS experiment implies two bromines in the molecule as shown by a cluster of pseudo molecular ion peaks at *m/z* 280/282/284 [M-H]⁻ having an intensity ratio of 1:2:1 (Fig.III.106). It fits the molecular formula for 4,5-dibromo-1-methyl-1*H*-pyrrole-2-carboxylic acid, $C_6H_5Br_2NO_2$. NMR data (Table III.12) supports the proposed structure. After careful interpretation of its chemical and spectral data, compound **15** is determined as the known natural product **4,5-dibromo-1-methyl-1*H*-pyrrole-2-carboxylic acid.**

III.1.16. Methyl-4,5-dibromo-1-methyl-1*H*-pyrrole-2-carboxylate (**16,** known compound)
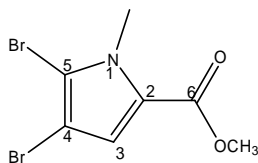
Fig.III.107. Compound **16**
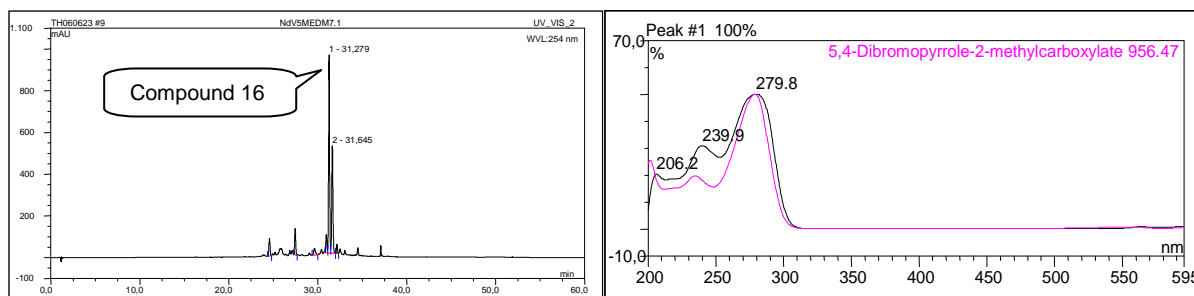
Fig.III.108. Analytical HPLC data of compound **16**
Left: HPLC profile in 254 nm, RT: 27.82; 31.28; right: UV absorption spectrum, λ_{max} = 206.2; 239.9; 279.8 nm.
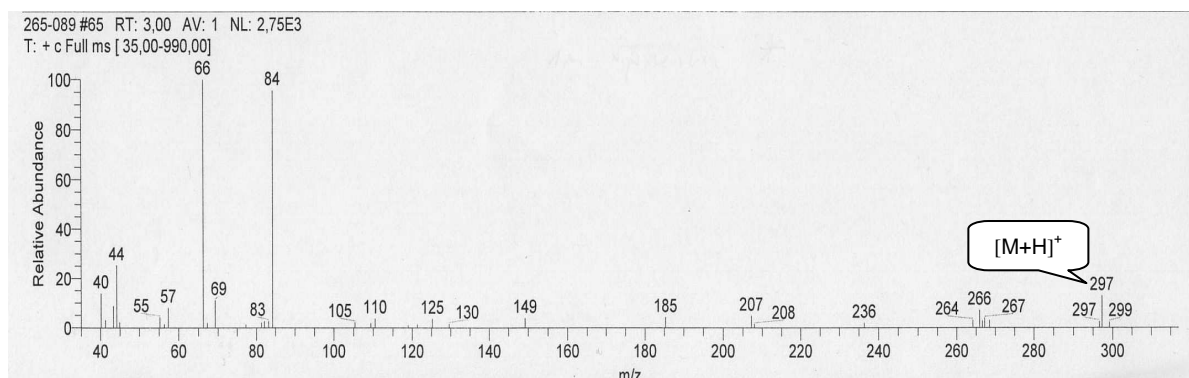
Fig.III.109. EI-MS result of **16**

Compound **16** was obtained as a white amorphous substance at an amount of 21 mg (0.01% of the sponge dried weight). Chemical investigation using analytical HPLC indicates the presence of a methyl-4,5-dibromo-1-methyl-1*H*-pyrrole-2-carboxylate (Fig.III.108). EIMS experiment suggests a dibrominated compound as shown by pseudo molecular ion peaks at *m/z* 295/297/299 g/mol having an intensity ratio of 1:2:1 (Fig.III.109). NMR data of **16** correspond to **methyl-4,5-dibromo-1-**

methyl-1*H*-pyrrole-2-carboxylate described by Fathi Afshar and Allen (1988) (Table

III.12).

Table III.12. ^{1}H-NMR data of compound **15** and **16** [a)]

No.	compound 15		compound 16	
	δ	Integration, multiplicity, *J* in Hz	δ	Integration, multiplicity, *J* in Hz
3	7.13	1H, s	7.13	1H, s
1-NCH$_3$	3.96	3H, s	3.82	3H, s
OCH$_3$	-	3H, s	3.98	3H, s

[a)] Data were recorded in CDCl$_3$ at 500 MHz (^{1}H), multiplicities and coupling constant are given in Hertz

III.2.   Secondary metabolites from *Agelas nakamurai*

Beside the brominated pyrrole family of compounds, *Agelas* sponges are

also known to possess bioactive substances derived from diterpene alkaloids which

include agelasines, agelasimines and agelasidines. These diterpenes seem to be

unique to *Agelas* sponges but unlike the brominated pyrroles which are widespread

in the genus *Agelas*, these diterpenoids were only reported in some species

(Braekman *et al*., 1992).

The sponge *Agelas nakamurai* analyzed in this study was collected near Bali

Island, Indonesia in October 2003. Preliminary chemical investigation of the ethyl-

acetate fraction in analytical HPLC exhibits three major peaks which were identified

as 4-bromopyrrole carboxamide, hymenidine and agelasine D, respectively

(Fig.III.110). The bromopyrrole 2-carboxamide derivatives isolated from this sponge

are all monobrominated. This property is observed in ESI-MS spectrum as

pseudomolecular ion cluster peaks having difference of two mass units at an intensity

ratio of 1:1.

From the investigated sponge, three new compounds have been isolated

From the investigated sponge, three new compounds have been isolated which includes a brominated pyrrole derivative, longamide C (**20**) and two 9'-methyl adeninium diterpene derivatives, (-)-ageloxime D (**17**) and (-)agelasine D (**18**), together with seven known compounds i.e. (+)-agelasidine C, hymenidin, 4-bromopyrrole carboxylic acid, 4-bromopyrrole carboxamide, mukanadin C, adenosine, and 9-methyladenine.
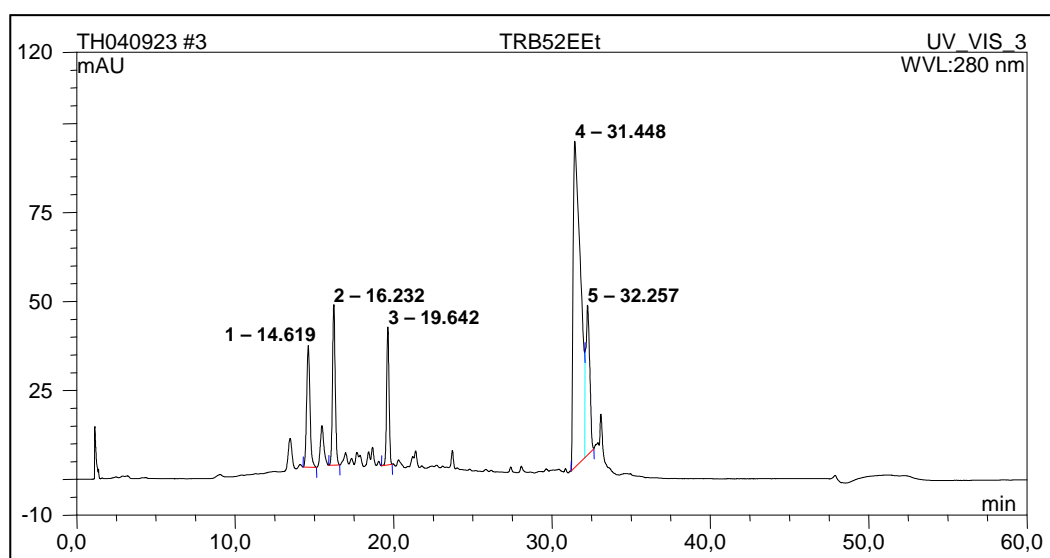
Fig.III.110. Chemical profile of *Agelas nakamurai* EtOAc fraction in analytical HPLC at 280 nm
Peak 1: 4-bromopyrrole carboxamide; 2: hymenidin; 3: 4-bromopyrrole carboxylic acid;
4: agelasine-D; 5: ageloxime-D

III.2.1. Diterpenoids from *Agelas nakamurai*

III.2.1.1. (-)-Ageloxime D (**17**, new compound)
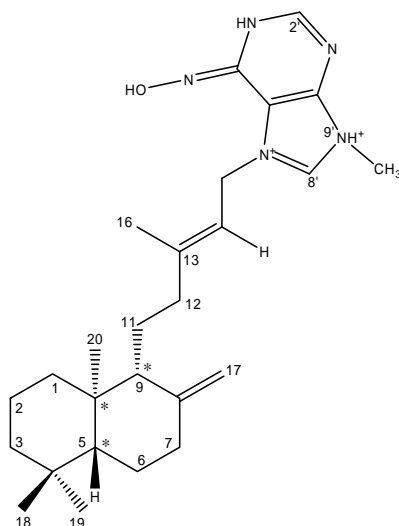
Fig.III.111. Compound **17***
*Relative stereochemistry is shown
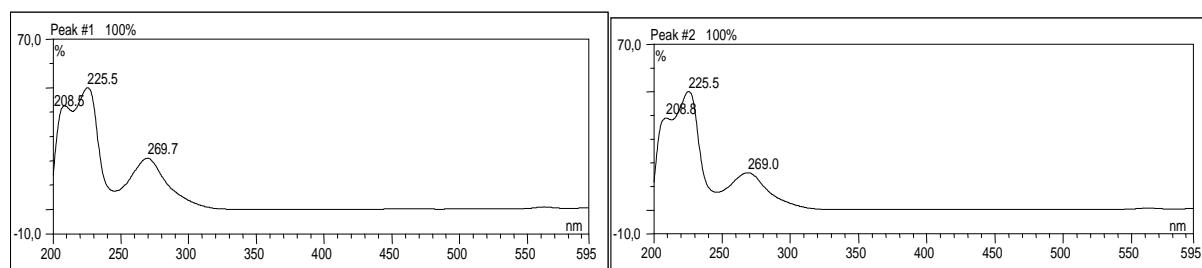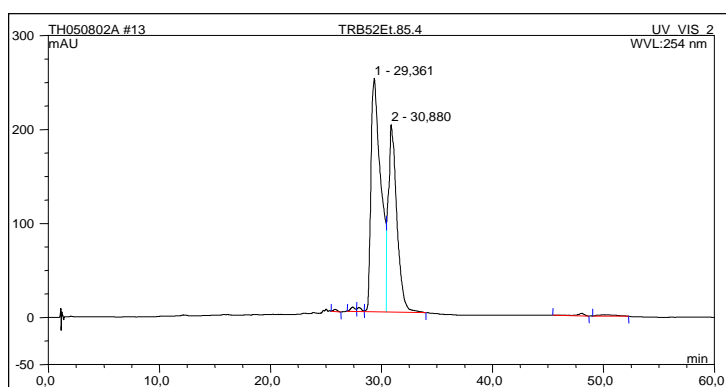
Fig.III.112. Analytical HPLC data of compound **17**
Left: HPLC profile in 235 nm, RT: 29.36 (peak 1) and 30.88 (peak 2); right: UV absorption spectrum,
λ_{max} = 208.5; 225.5; 269.7.5 nm (peak 1); 208.8; 225.5; 269.0 nm (peak 2)
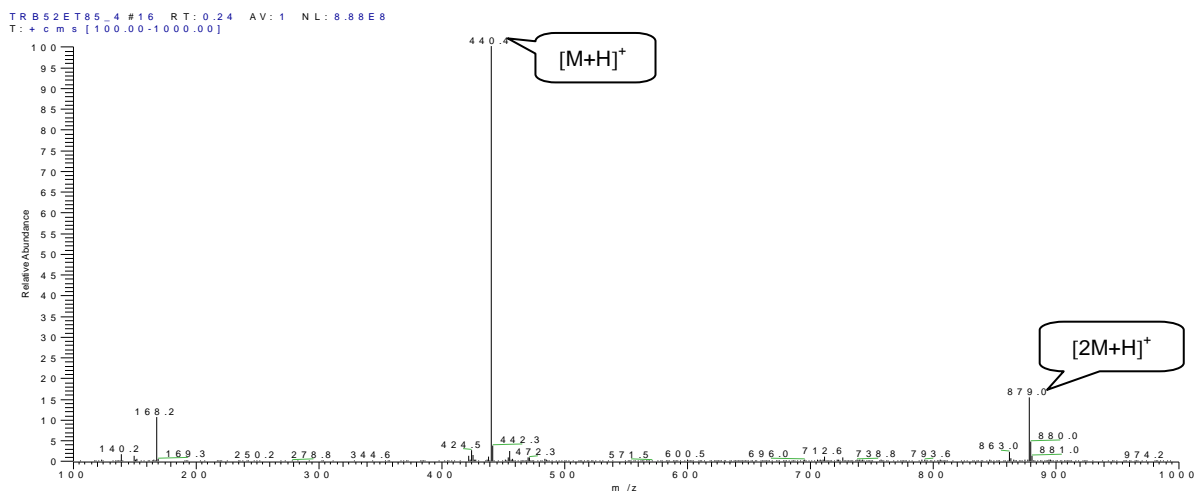
Fig.III.113. ESI-MS result of compound **17**

Compound **17** was obtained as yellow-brownish oily substance in an amount of 110 mg (0.069% of the sponge dried weight). The presence of agelasine D in the crude extract and the similarity of the UV absorption pattern suggest that compound **17** is related to agelasine. Compound **17** shows a split peak in analytical HPLC spectrum (Fig.III.112), most probably caused by tautomerism as explained in Fig.III.117. The ESI-MS exhibits intense molecular ion peaks at *m/z* 440 [M+H]$^+$ (Fig.III.113). The difference of 18 mass units in comparison to agelasine D suggests the presence of an additional hydroxyl group. It corresponds to the molecular formula of $C_{26}H_{42}N_5O$ (*m/z* experimental = 440.3390; *m/z* calculated = 440.3389 [M+H]$^+$) deducted from HRESIMS data. It gave an optical rotation value of $[\alpha]_D^{25}$ = -6.3° $\pm$ 0.6 (*c* 0.5, MeOH).
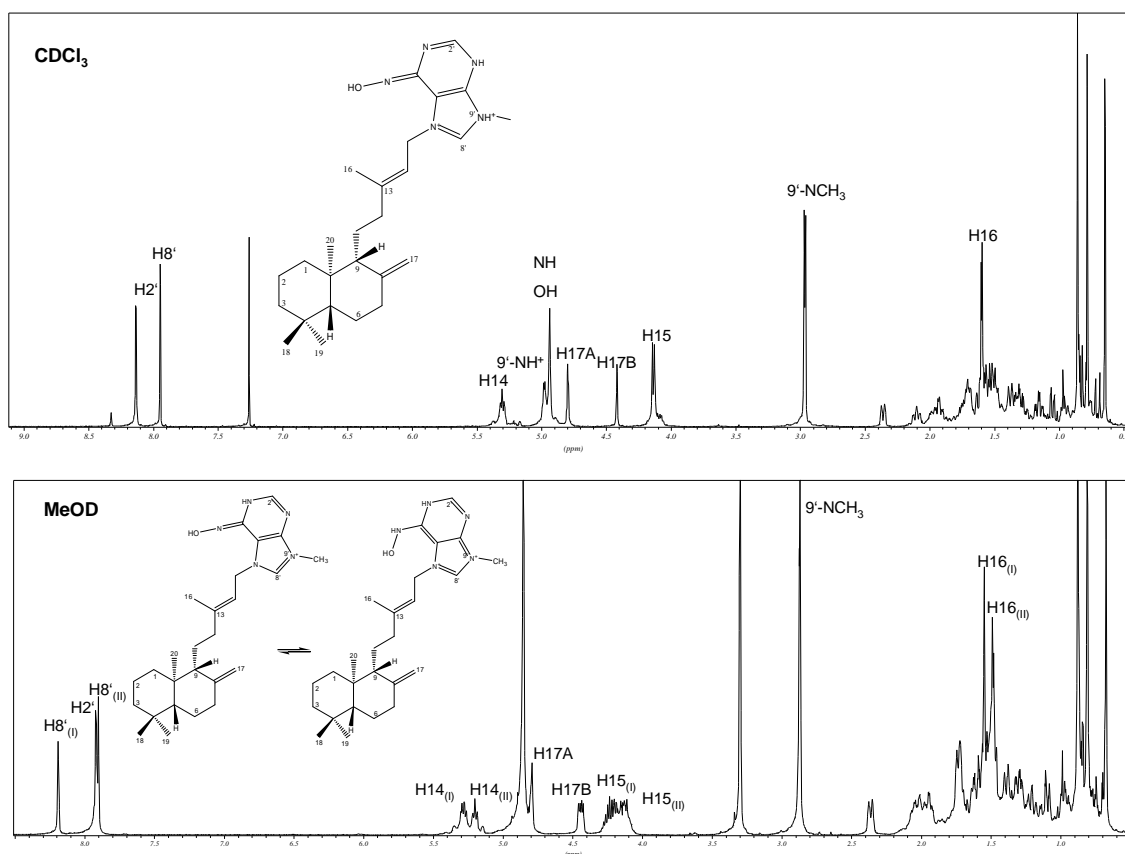
Fig.III.114. ^{1}H NMR spectrum of compound **17** in CDCl$_3$ (above) and in MeOD (below)

Interestingly, the NMR spectra of this compound experience two sets of signal replication depending on the solvent used. MeOD will cause the replication while in CDCl$_3$, probably caused by the acidic environment, the replication disappears. Protons which experience the replication are as follows, H-15 at δ_H 4.12 [2H, d, J = 6.6, H$_2$-15$_{(I)}$] and δ_H 4.22 [2H, d, J = 6.6, H$_2$-15$_{(II)}$]; H-14 at δ_H 5.20 [1H, d, J = 6.6, H-14$_{(I)}$] and δ_H 5.28 [1H, d, J = H-14$_{(II)}$], H-16 at δ_H 1.54 [3H, s, H$_3$-16$_{(I)}$] and δ_H 1.48 [1H, d, H-16$_{(II)}$], H-8' at δ_H 7.90 [1H, d, H-8'$_{(I)}$] and δ_H 8.20 [1H, d, H-8'$_{(II)}$]. This phenomenon is also observed for H-17B as well as for all carbons of the adeninium unit carbons, C-14 and C-15.

146
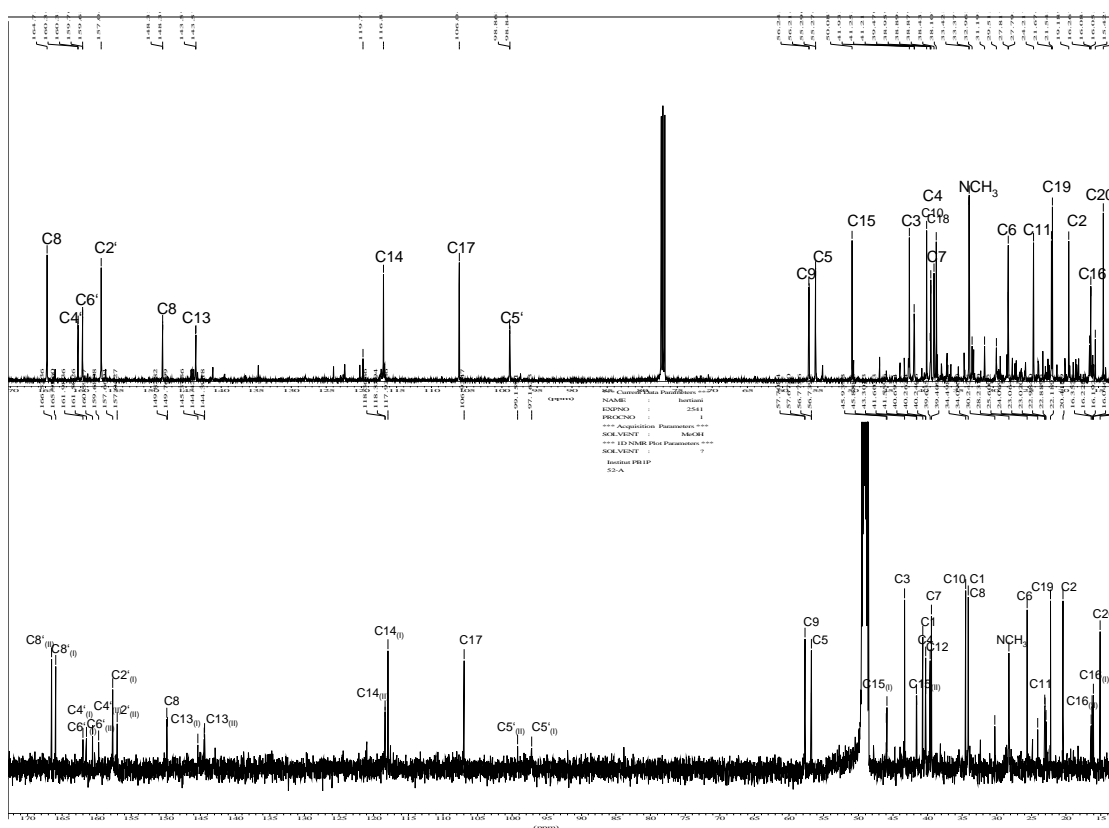
Fig.III.115. ^{13}C NMR spectra of compound **17** in CDCl$_3$ (above) and in MeOD (below)

Proton and carbon signals in the region are comparable to those of agelasine D (Nakamura *et al.*, 1984b) as described in Table III.13. The difference is observed for the protons on 9'-methyl adeninium moiety, H-14 and H-15. Signal of H-8' is shifted far upper field to δ_H 7.86 (CDCl$_3$, 500 MHz) in comparison to δ_H 10.94 in agelasine D (CDCl$_3$, 400 MHz, Nakamura *et al.*, 1984b); whereas the H-2' signal at δ_H 8.50 in agelasine D (CDCl$_3$, 400 MHz, Nakamura *et al.*, 1984b), is shifted to δ_H 8.05 in compound **17** (CDCl$_3$, 500 MHz). Proton NCH$_3$ is shifted to the upper field at δ_H 2.90 and appears as a doublet having *J* = 4.7 Hz. On the other hand, ^{13}C NMR interpretation discovers that C-8' is shifted more down field to δ_C 165.9 and 166.5 (MeOD, 125 MHz) in compound **17**, while in agelasine D it appears at δ_C 142.6 (MeOD, 22.5 MHz, Nakamura *et al.*, 1984b). Signals for H-15 and H-14 are shifted

to the upper field in comparison to agelasine D, i.e. δ_H 5.25 and δ_H 4.19, respectively. The signal for C-16 exhibits an upfield vinyl methyl group at δ_C 16.0 suggesting an *E* configuration of the olefinic bond at C-14 as also found in the (+)-agelasine D.

^{1}H-^{1}H COSY spectrum in CDCl$_3$ reveals one continuous spin system correlating the H-8' to the diterpene unit as well as a spin system correlating the signal of the NCH$_3$ proton (δ_H 2.90, 3H, d, *J* = 4.7 Hz) to an NH signal at δ_H 4.99 (d, *J* = 4.7 Hz). At first this evidence suggests a methylation of the C-6'-amine. But ^{1}H – ^{13}C HMBC spectrum reveals a correlation between the proton NCH$_3$ to C-8', which is somehow too far if the methyl group is sitting on the C6'-amine. Therefore it is suggestive that this methyl group is still attached to N-9' like in agelasine D. But unlike in agelasine D, the double bond in the adeninium part of compound **17** is positioned at 7' and 8' while N-9' is protonated. The resonance in the resulting cations is inhibited. It explains the appearance of proton NCH$_3$ as a doublet and its shift to the upper field region.

These finding are not sufficient to explain the placement of the hydroxyl group in this compound. 1D and 2D NMR secure the presence of a diterpene part as in agelasine D, but reveal the differences in the 9'-methyl adeninium part. Therefore this suggests the position of this hydroxyl group in the adeninium unit. The signal of the hydroxyl group appears at δ_H 4.95 overlapping with the NH signal of the pyrimidine ring. Correlation of this signal to carbon 2', 4', 5' and 9'-NH$^+$CH$_3$ is observed in the ^{1}H-^{13}C HMBC spectrum and is plausibly due to the NH group. Therefore these can not be used to predict the hydroxyl position. Comparison of the NMR data to the known agelasine D showed that C-8' and C-6' are the most affected signals. C-8' is shifted from δ_C 142.6 in agelasine D (CD$_3$OD, 22.5 MHz, Nakamura *et*

al., 1984b) to the lower field at δ_C 165.9/166.5, while C-6' is shifted from δ_C 153.9 in agelasine D (CD$_3$OD, 22.5 MHz, Nakamura *et al.*, 1984b) to δ_C 161.5/160.6 in compound **17** (CD$_3$OD, 125 MHz).

In order to predict the position of the hydroxyl group, it is important to investigate the tautomerism found in this compound. Actually, the tautomerism phenomenon has been already well-described in purine related compounds such as adenine, hypoxanthine and theirs derivatives. Dreyfus *et al.* (1975) explained that formal structures of the purine molecule as well as theoretical considerations show the existence of several tautomeric forms arising either (a) from prototropy involving an extranuclear atom (e.g. keto-enol and amine-imine tautomerism), or (b) prototropy involving only ring atoms (e.g., the N(1)H, N(3)H, N(7)H, and N(9)H tautomers of purine) (Dreyfus *et al.*, 1975). Chenon and collaborators (1975) reported that the N(9)H tautomer of adenine is the most stable form in comparison to N(7)H, and that the amine form of adenine is more stable than the imine tautomer (Fig.III.116).
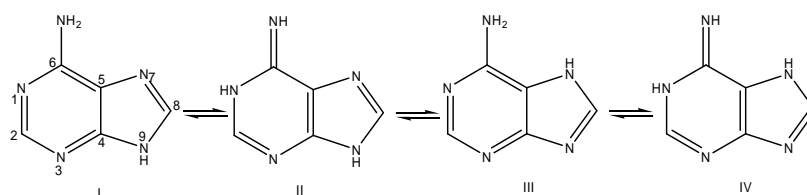
Fig.III.116. Tautomerism found in adenine (Pullman *et al.*, 1969)

Unlike in adenine, hypoxanthine exhibits two type of tautomerism, prototropic (imidazole moiety), and lactam-lactim (pyrimidine portion). Wolfenden (1969) described that the keto [C(6)=O] and enol [C(6)-OH] forms of inosine in aqueous solution were equally favoured. This finding recommend that in compound **17**, the amine group on C-6' is replaced with an oxime group, which may lead to a tautomerism as illustrated in Fig.III.117. Both tautomers will be present at almost

equal ratio which causes duplication of resonances in its NMR spectra and UV

peaks.
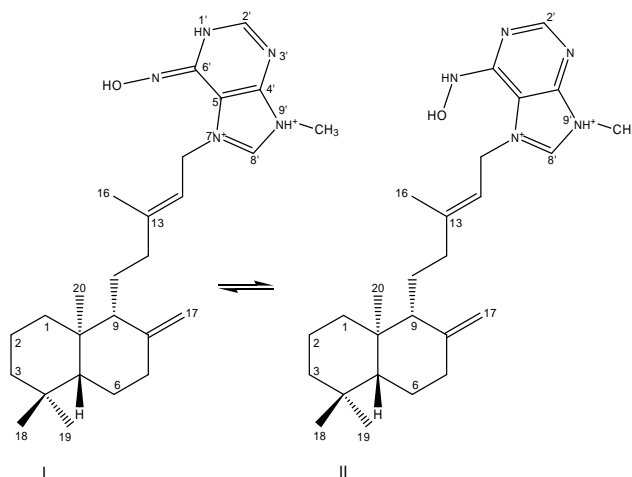
Fig.III.117. Proposed tautomerism in compound **17***

*Relative stereochemistry is shown

A possible related compound was previously reported from *Agelas*

mauritana by Nakatsu *et al.* (1984). This research group once detected a presence of

an unstable base in the crude extract which may be related to the agelasines. This

compound exhibits almost similar proton NMR pattern to compound **17** in the

adeninium moiety. Unlike agelasines which has C-8' protons at >10 ppm and C-2' at

around 8.50 ppm, this major metabolite of *Agelas mauritiana* displays more upfield

signal, at δ_H 8.01 and δ_H 8.31 (Nakatsu *et al.*, 1984). However, unlike **17** this

compound was unstable; therefore it can not be obtained pure. Another difference

observed is that the chemical shift of C-15 in compound **17** is shifted more upfield in

comparison to agelasine-D, while Nakatsu *et al.* (1984) reported that in their case,

the C-15 proton was shifted more downfield.

From the [1]H–[1]H ROESY spectrum of compound **17**, NOE correlations were

observed for H_3-20 to H-11A, H-9, H_2-6 and H_3-19, as well as for H-5 to H_3-18, H_2-6,

H-9; H-7A to H-7B, and H-11A (Fig.III.122) suggesting the relative configuration of

compound **17** as a seen in Fig.III.111. That means **17** has an identical relative stereochemistry with the known (+)-agelasine D (Nakamura and collaborators (1984b) (Fig.III.130). However, the optical rotation found was $[\alpha]_D^{25}$ = -6.3° ± 0.6 (*c* 0.5, MeOH) which is the opposite of that of the known (+)-agelasine D, $[\alpha]_D^{25}$ = +10.4 (*c* 1.1, MeOH). Hence the complete structure of **17** was determined and named as   **(-)-ageloxime-D**.

Table III.14. NMR data of compound **17** in comparison to (+)-agelasine-D

No.	(+)-Agelasine D [a), b)]			Compound 17 [a)]		
	^{1}H-NMR		^{13}C-NMR	^{1}H-NMR		^{13}C-NMR
	δ	Integration, multiplicity, *J* in Hz	δ, DEPT	δ	Integration, multiplicity, *J* in Hz	δ, DEPT
1	0.6 – 2.4	16H, m	39.4, CH$_2$	0.84	2H, m	40.7, CH$_2$
2			20.3, CH$_2$	1.10	2H, m	20.4, CH$_2$
3A			43.2, CH$_2$	1.34	1H, br d, 12.9	43.3, CH$_2$
3B				1.10	1H, dd, 4.1, 12.6	
5			57.4, CH	1.00	1H, dd, 12.0, 1.6	56.8, CH
6			25.5, CH$_2$	1.25	2H, m	25.6, CH$_2$
7A			39.4, CH$_2$	2.31	1H, br d, 12.6	39.4, CH$_2$
7B				1.87	1H, dt, 4.7, 12.9	
9			56.8, CH$_2$	1.52	1H, m	58.3, CH
11A			40.2, CH$_2$	1.65	1H, m	41.6, CH$_2$
11B				1.45	1H, m	
12A			22.5, CH$_2$	2.04	1H, m	25.6, CH$_2$
12B				1.92	1H, m	
4	-	-	40.6, C	-	-	40.2, C
8	-	-	149.0, C	-	-	149.8, C
10	-	-	34.4, C	-	-	34.5, C
13			149.5, C		-	145.4/144.4, C
14	5.41	1H, br t, 6.5	115.9, CH	5.30	2H, t, 6.6	117.9/118.4, CH
15	5.72	2H, br d, 6.5	48.8, CH$_2$	4.12	1H, d, 6.6	45.9/41.6, CH$_2$
16	1.86	3H, br s	17.1, CH$_3$	1.53	3H, d, 2.84	16.0/16.2, CH$_3$
17A	4.81	1H, br s	106.9, CH$_2$	4.78	1H, s	107.0, CH$_2$
17B	4.43	1H, br s		4.38	1H, s	
18	0.87	3H, s	34.0, CH$_3$	0.81	3H, s	34.1, CH$_3$
19	0.79	3H, s	22.1, CH$_3$	0.73	3H, s	20.4, CH$_3$
20	0.65	3H, s	15.0, CH$_3$	0.59	3H, s	15.1, CH$_3$
2'	8.50	1H, s	156.9, CH	8.05	1H, s	157.7/157.3, CH
4'	-	-	150.7, C	-	-	162.0/160.6, C
5'	-	-	111.0 C	-	-	97.2/99.2, C
6'-NH$_2$	6.76	2H, br s [c)]	153.9, C	4.95	2H, br s [c)]	161.5/160.6, C
8'	10.94	1H, s	142.6, CH	7.95	1H, s	165.9/166.5, CH
9'-N$^+$H	-	-	-	4.99	1H, d, 4.7	-
9'-CH$_3$	4.10	3H, br s	32.0, CH$_3$	2.90	3H, d, 4.7	28.2, CH$_3$

[a)] Data were recorded in CDCl$_3$ for ^{1}H and CD$_3$OD for ^{13}C, multiplicities and coupling constant are given in Hz; [b)] Nakamura *et al.* (1984b); [c)] exchangeable signal
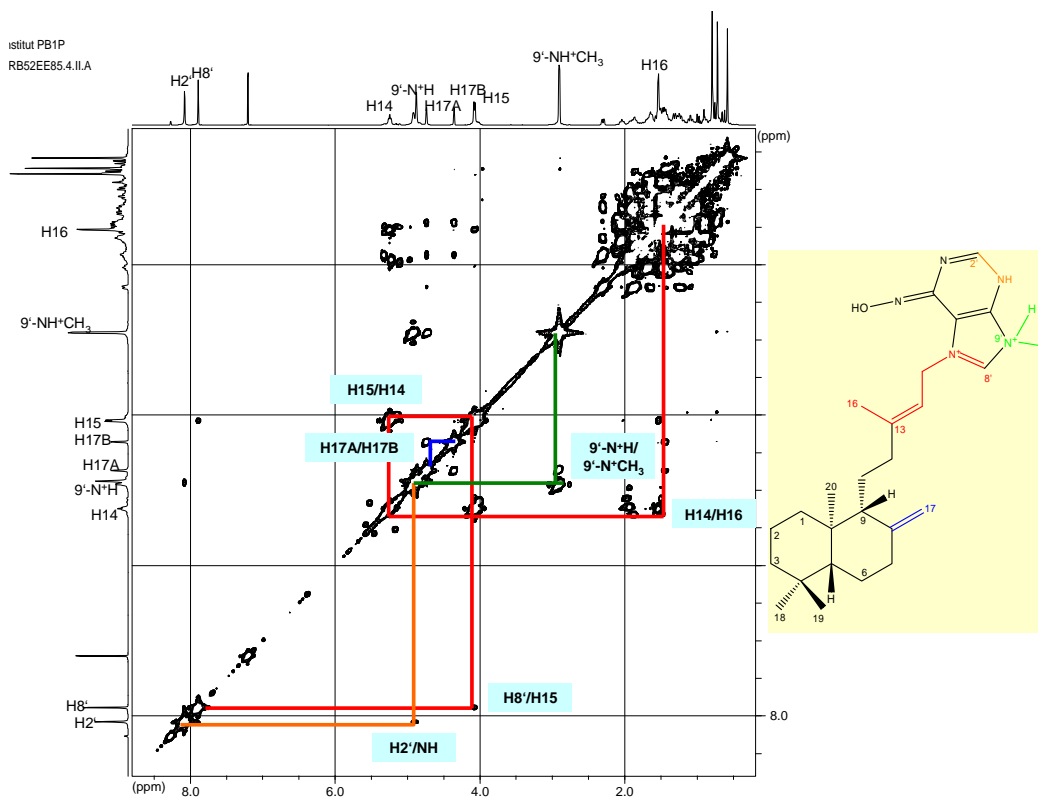
Fig.III.118a. ^{1}H–^{1}H COSY spectrum of compound **17*** (in CDCl$_3$)
*Relative stereochemistry is shown
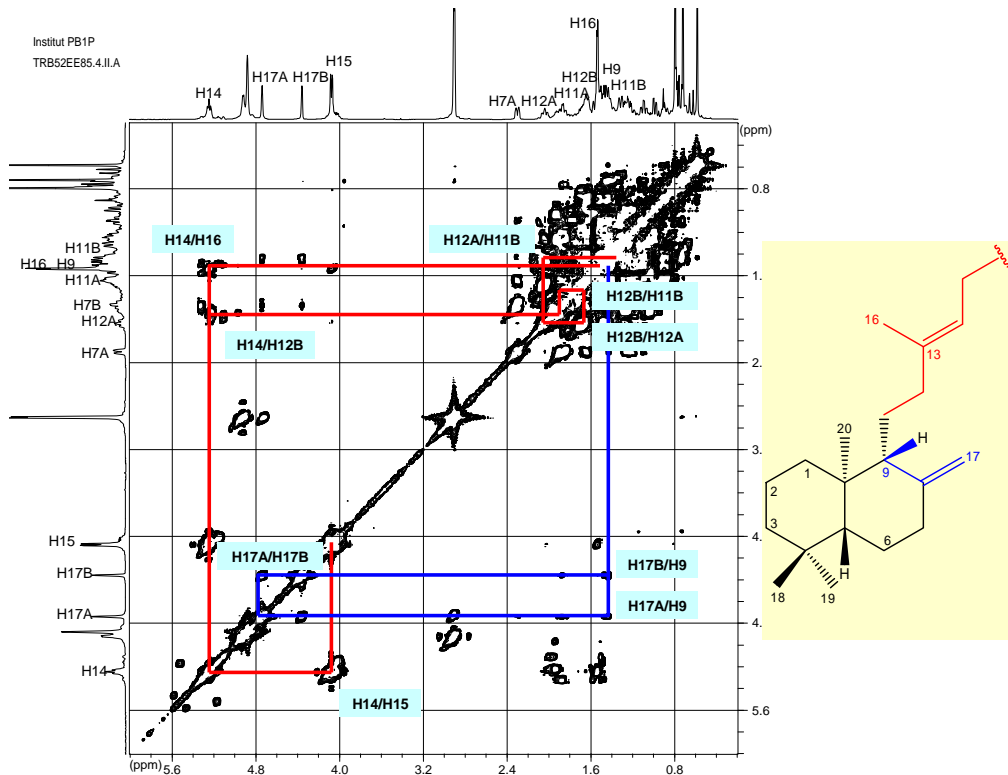
Fig.III.118b. ^{1}H–^{1}H COSY spectrum expansion of the diterpene part of compound **17*** (in CDCl$_3$)
*Relative stereochemistry is shown

152
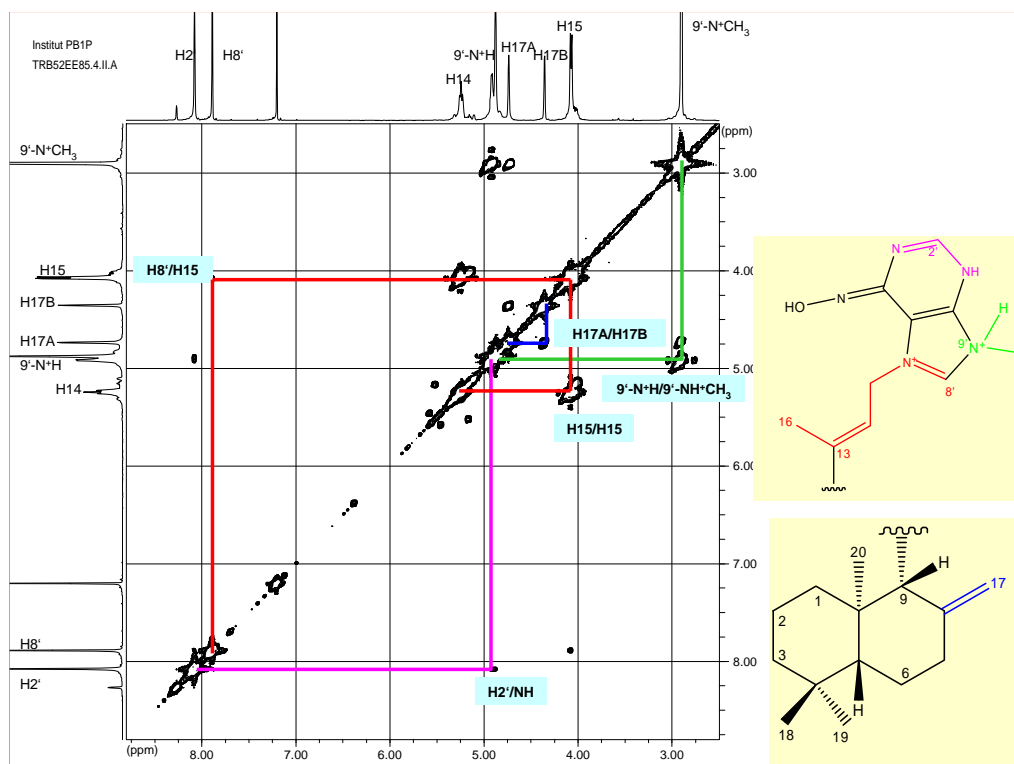
Fig.III.118c. ^{1}H–^{1}H COSY spectrum expansion of the adeninium and the exomethylene unit of
compound **17*** (in CDCl$_3$)
*Relative stereochemistry is shown
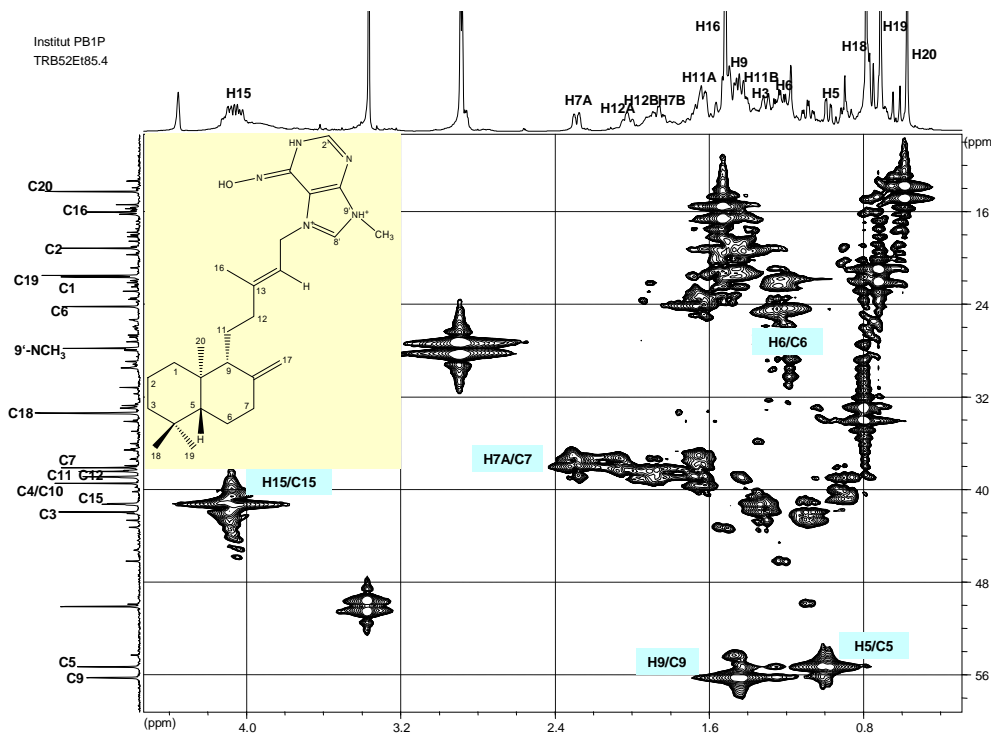
Fig.III.119. ^{1}H–^{13}C HMQC spectrum of compound **17*** (MeOD)
*Relative stereochemistry is shown
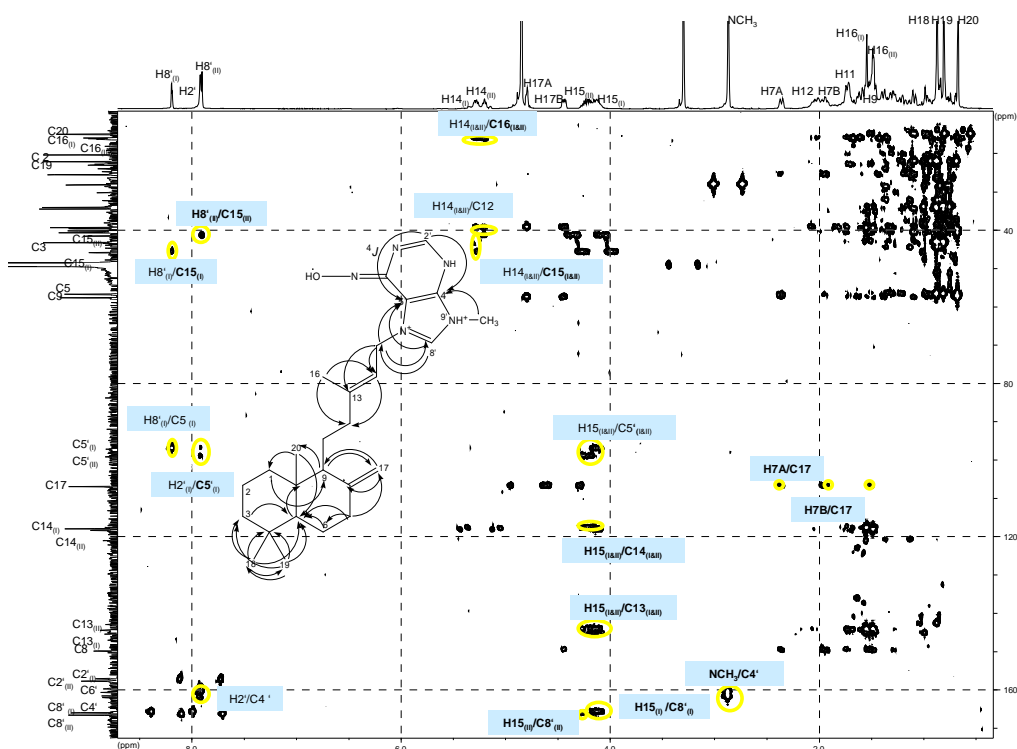
Fig.III.120. ^{1}H–^{13}C NMR spectrum of compound **17** (MeOD)
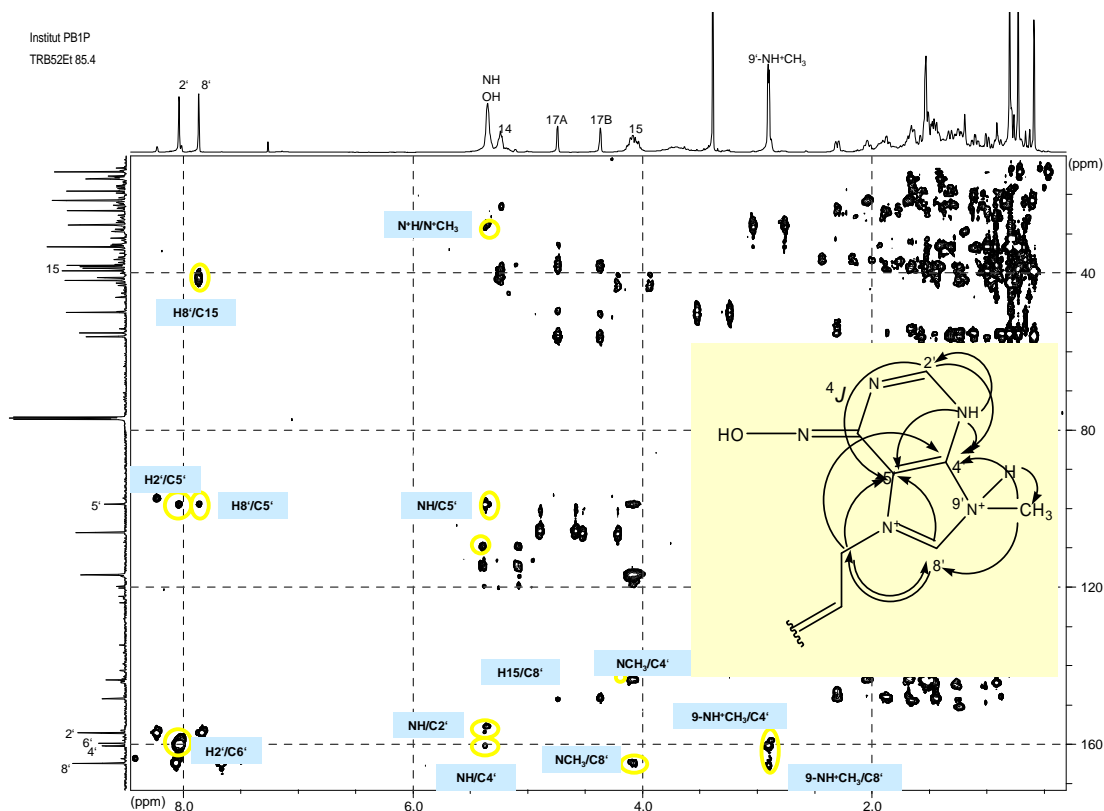
Fig.III.121. ^{1}H–^{13}C NMR spectrum of compound **17** (CDCl$_3$)
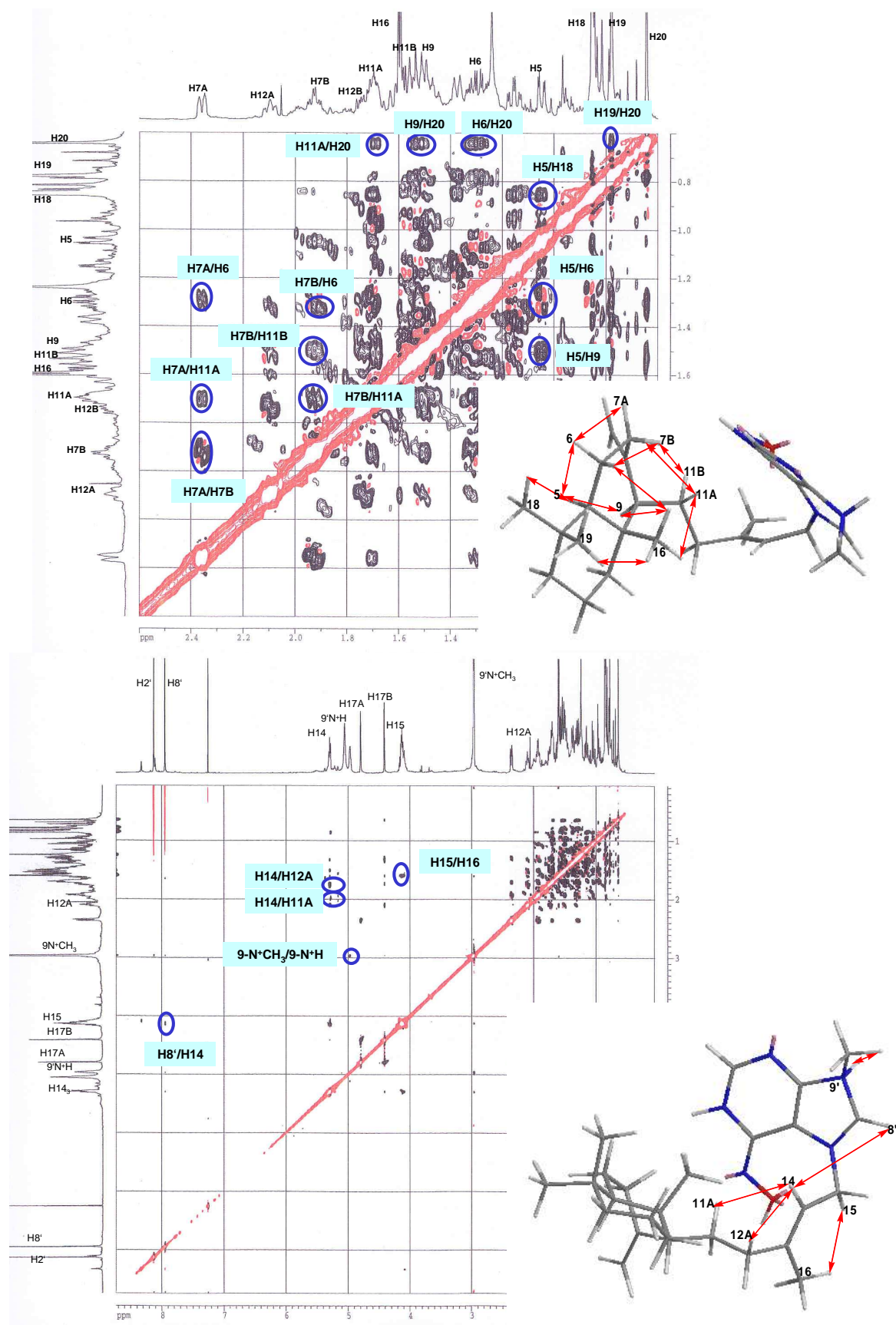
Fig.III.122. ^{1}H–^{1}H ROESY spectrum of compound **17** (in CDCl$_3$)

III.2.1.2. (-)-Agelasine D (**18**, new compound)
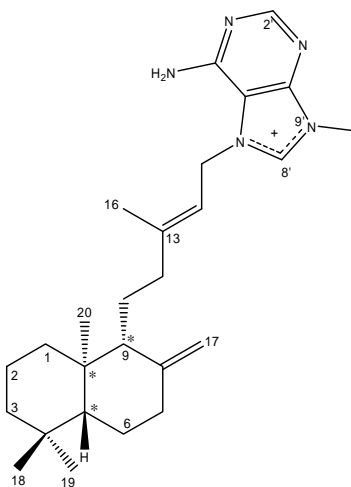
Fig.III.123. Compound **18***
*Relative stereochemistry is shown
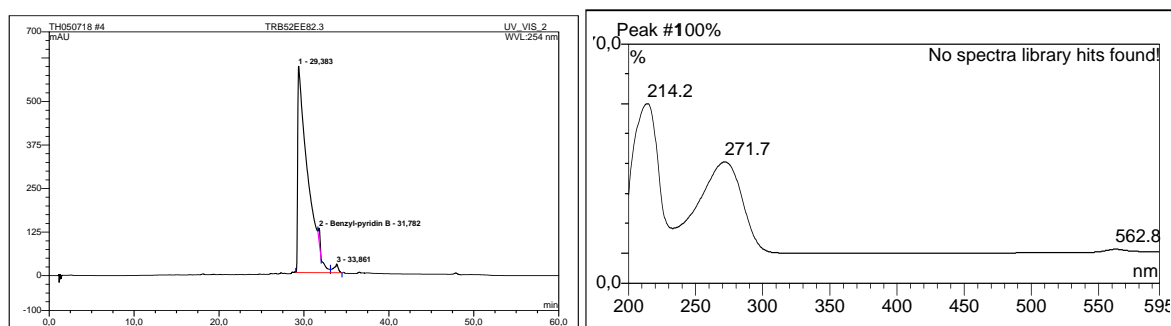
Fig.III.124. Analytical HPLC data of compound **18**
Left: HPLC profile in 254 nm, RT: 29.38; right: UV spectrum, λ_{max} = 214.2; 271.7 nm
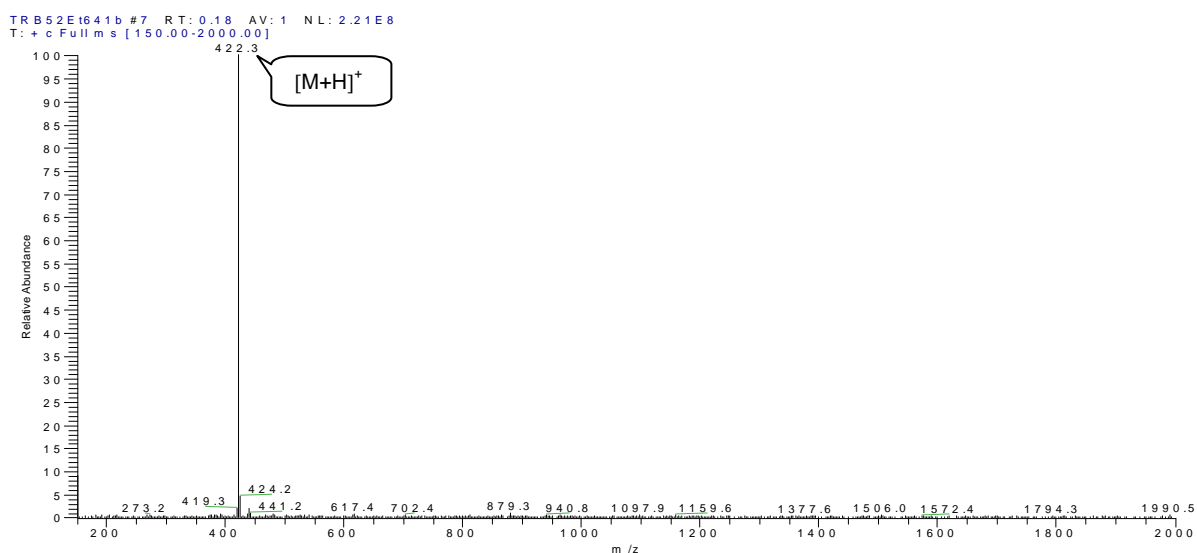
Fig.III.125. ESI-MS spectrum of compound **18**

Agelasine is a diterpenoid bearing a quartenary 9'-methyladenine in its molecule. To date there are at least 10 agelasine congeners reported in the literature from *Agelas* sponges.

Compound **18** is the major compound from this investigated sponge *Agelas nakamurai*. It was obtained as a white amorphous substance in an amount of 1.95 g (0.78% of the sponge dried weight). This optically active compound exhibits $[\alpha]_D^{25}$ value of -19.8 ° ± 0.4 (*c* 0.5, MeOH), while Nakamura and collaborators (1984b) declare $[\alpha]_D^{25}$ value of (+) agelasine D as +10.4 (*c* 1.1, MeOH). Molecular formula of $C_{26}H_{41}N_5$ fits with molecular weight deducted from ESI-MS molecular ion peak at *m/z* 422 [M+H][+]. UV absorption pattern exhibits λ_{max} of 214.2 and 271.7 nm. The ^{13}C and ^{1}H NMR data is identical to that of agelasine-D.
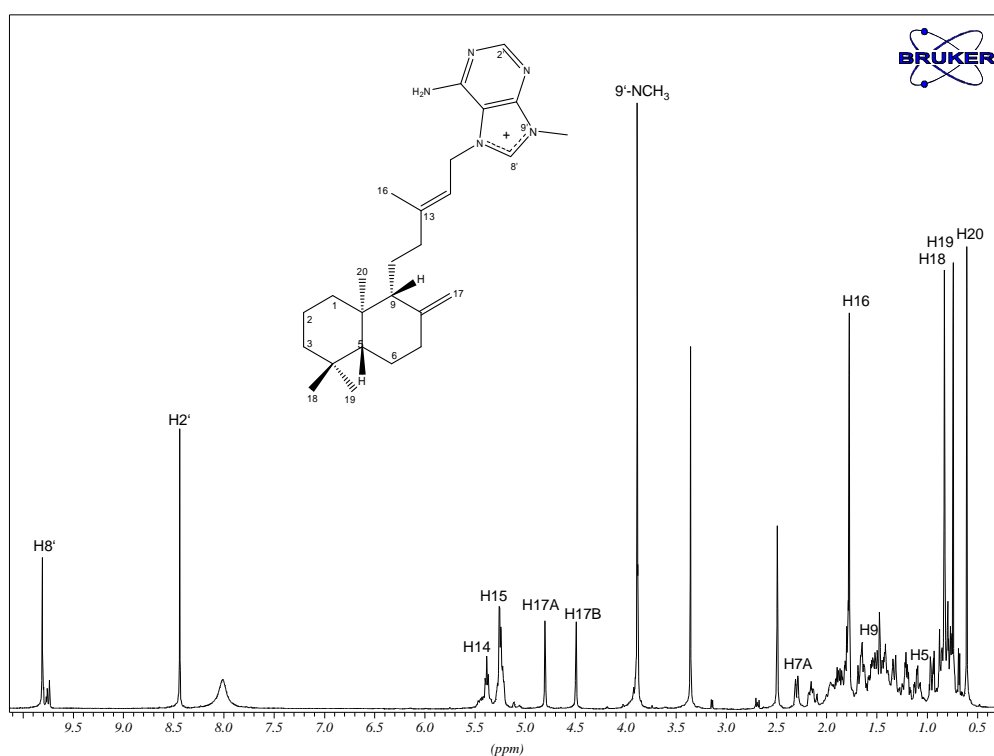
Fig.III.126. ^{1}H NMR of compound **18*** (CDCl$_3$, 500 MHz)
*Relative stereochemistry is shown
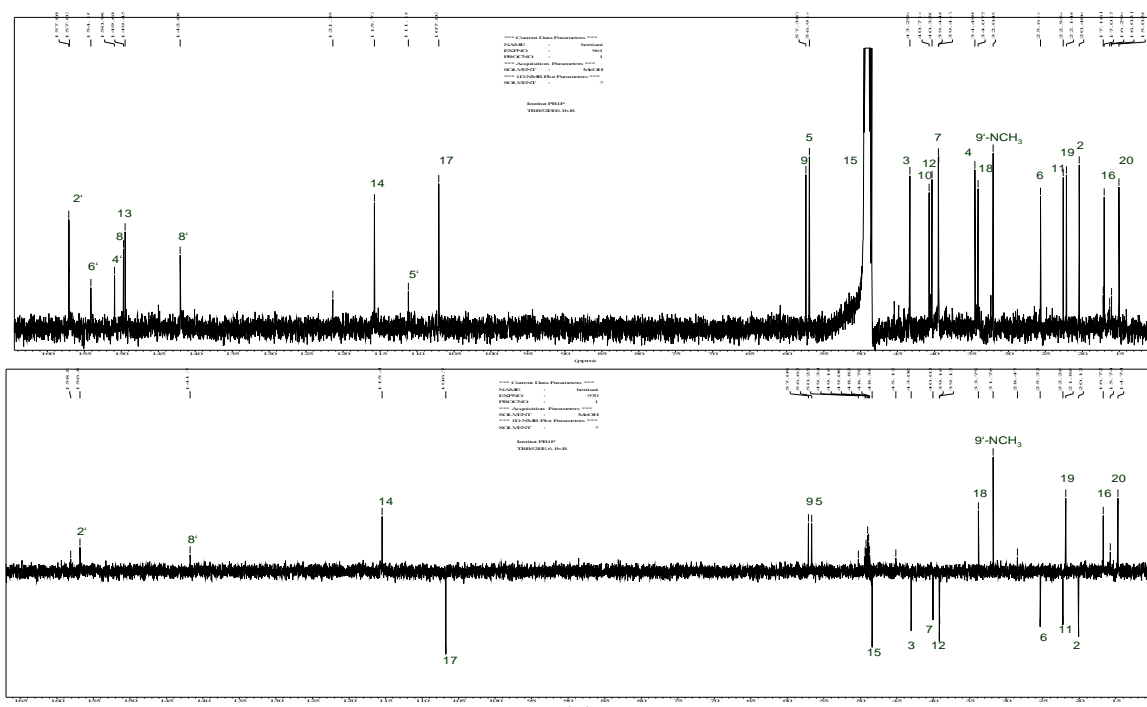
Fig.III.127. ^{13}C NMR and DEPT spectra of compound **18** (MeOH, 125 MHz)

^{1}H NMR spectrum of compound **18** indicates the presence of a 9'-methyladenine moiety shown by signals of NCH$_3$ at δ_H 3.88 (3H, s) and of NH$_2$ at δ_H 7.98 (2H, s), and of two aromatic protons at δ_H 8.45 (1H, s) referring to H-2' and at δ_H 9.68 referring to H-8'. This is also supported by the ^{13}C NMR spectral data (Table III.14). The molecular formula suggests that the remaining portion except for the adenine moiety consisted of a diterpene with four degrees of unsaturation. ^{13}C NMR spectrum shows resonances due to four olefinic carbons of the diterpene part at δ_C 148.0 (C, C-8), 145.7 (C, C-13), 115.5 (CH, C-14) and 106.4 (CH$_2$) as well as the resonances of four methyl signals at δ_C 16.7 (C-16), 33.2 (C-18), 21.5 (C-19), and 14.3 (C-20). Whereas ^{1}H NMR spectrum shows three olefinic protons due to an exomethylene function as exhibited by signal at δ_H 4.81 and 4.50 (1H each, s) and a methine proton at δ_H 5.40 (1H, t, *J* = 7.2 Hz). These findings suggest a presence of a labdane-related carbon skeleton.

Fig.III.128. ^{1}H-^{1}H COSY spectrum of compound **18*** (DMSO-d_6)
*Relative stereochemistry is shown
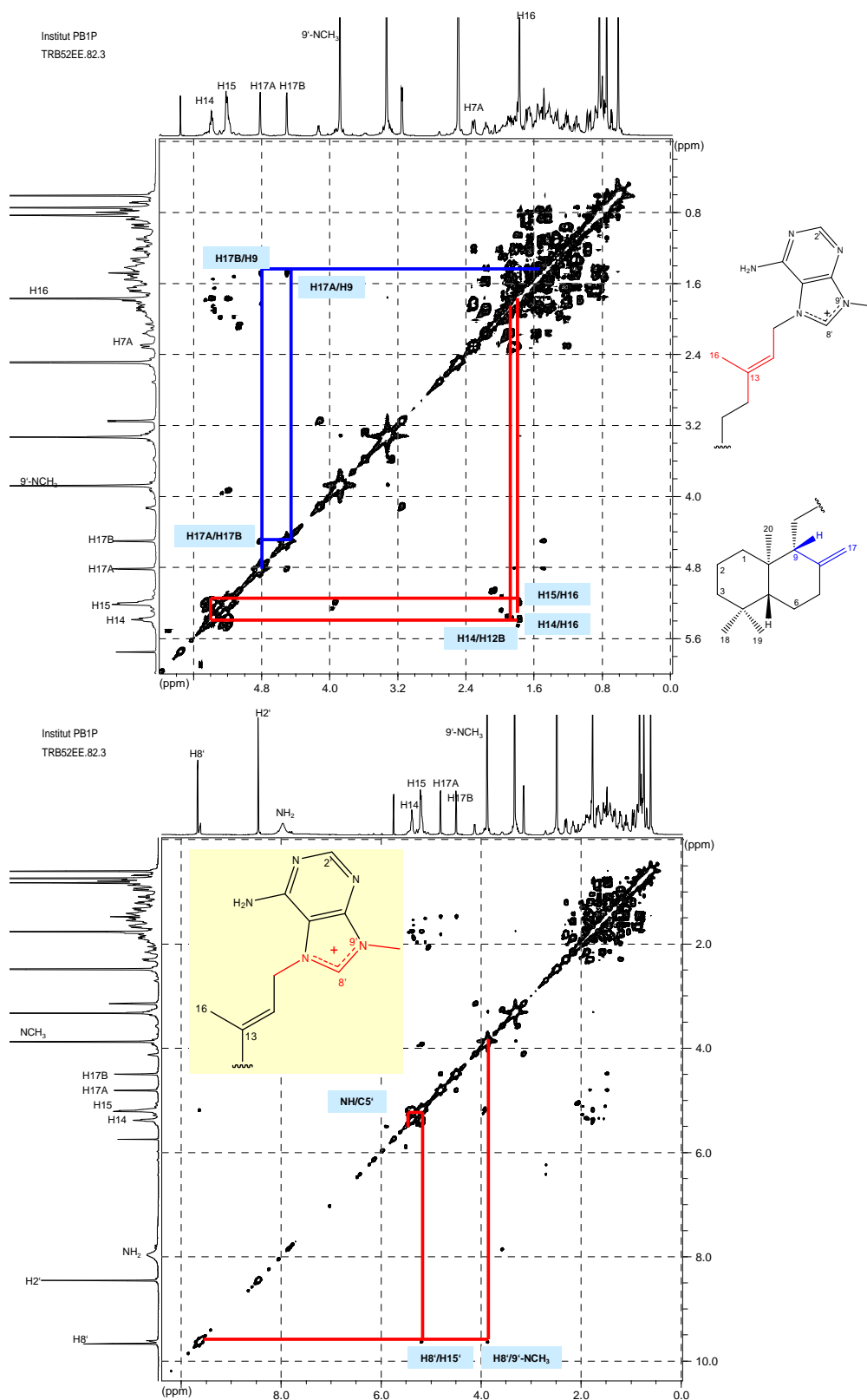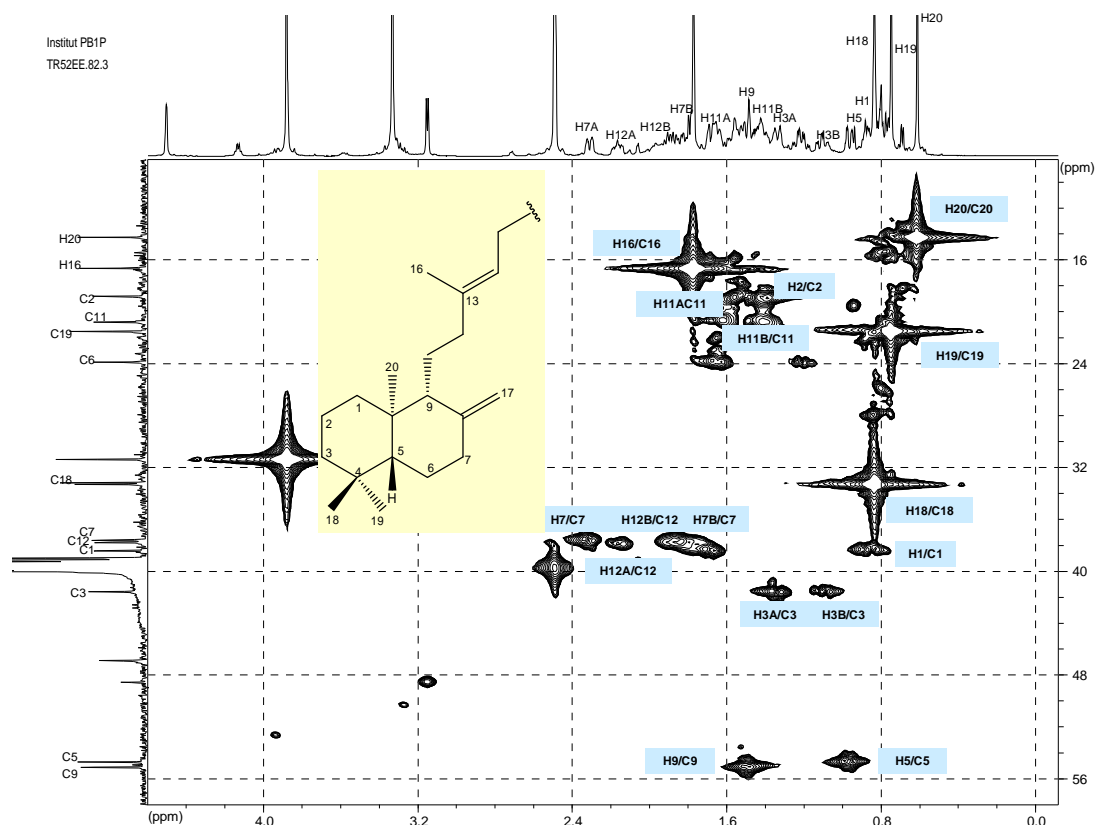
Fig.III.129. ^{1}H–^{13}C HMQC spectrum of the diterpene part of compound **18*** (DMSO-d_6)
*Relative stereochemistry is shown

^{1}H–^{1}H COSY shows allylic couplings connecting 9'-NCH$_3$ to H-8' which in turn is coupled to H$_2$-15 and then to H-14; H-14 to H$_3$-16 and to H$_2$-12, and further to H$_2$-11 and H-9; as well as connects H$_2$-17 to H-9 and H$_2$-7. This finding together with the C-15 signal at δ_C 48.6 (C-15) and H$_2$-15 proton signal at δ_H 5.20 (2H, d, *J* = 7.2 Hz) which is comparable to those of (+)-agelasine D in the literature (Table III.14). This finding confirms that the 9'-methyladenine moiety is attached to the diterpene part at position N-7'. ^{1}H–^{13}C HMBC spectrum exhibits cross peaks correlating H-8' to C-15 and from the 9'-NCH$_3$ protons to C-8', and C-4' as well as from H-2' to C-6' and C-4' which secures the attachment of the diterpene part to the adenine moiety at position 7' and the methyl substitution at 9'. ^{1}H–^{13}C HMBC spectrum also reveals the position of the geminal methyl H$_3$-18 and H$_3$-19 at C-4 by showing cross peaks

correlating them to the same carbons i.e., C-5 and C-3 and to each other. The third methyl group (C-20) is correlated to C-5, C-9 and C-1 suggesting its position at C-10 (Fig.III.131).

The ^{1}H -^{1}H ROESY spectrum of **18** shows a similar relative stereochemistry as found in compound **17** (Fig.III.130). Since the optical rotation of the isolated agelasine D has a negative value of $[\alpha]_D^{25} = -19.8$ ° $\pm$ 0.4 (*c* 0.5, MeOH), it is suggested that **18** is the enantiomer of (+)-agelasine D reported by Nakamura *et al.* (1984b) considering that they both differ only in the $[\alpha]_D^{25}$ value. Thus, the structure of compound **18** is determined as **(-)-agelasine D**.
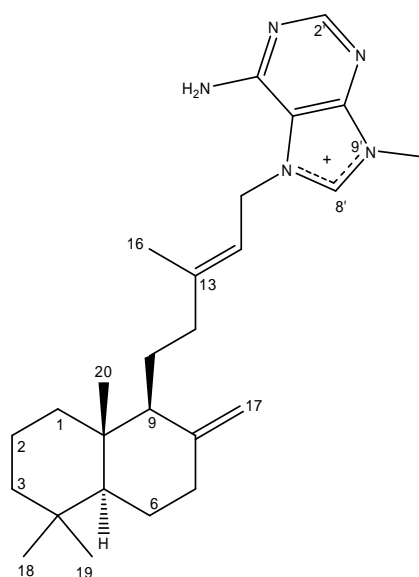
Fig.III.130. Absolute configuration of (+)-agelasine D according to Nakamura *et al.* (1984b)

161
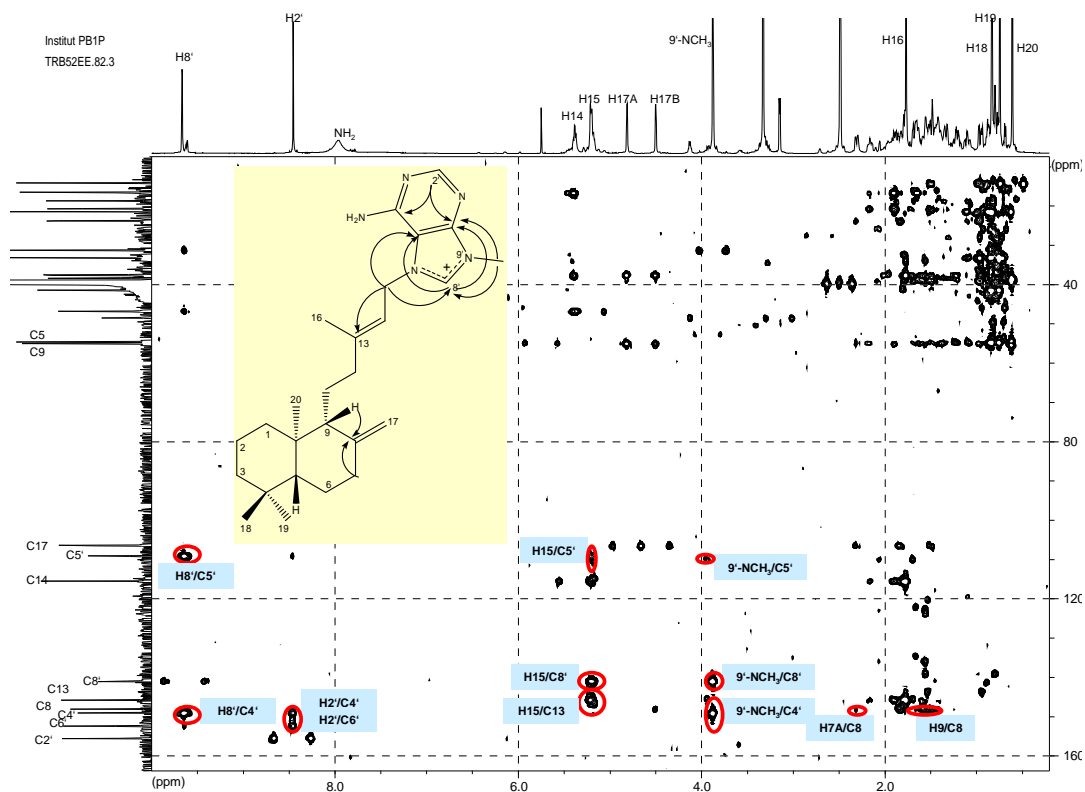
Fig.III.131a. ^{1}H–^{13}C HMBC spectrum of compound **18** (DMSO-d_6)
*Relative stereochemistry is shown
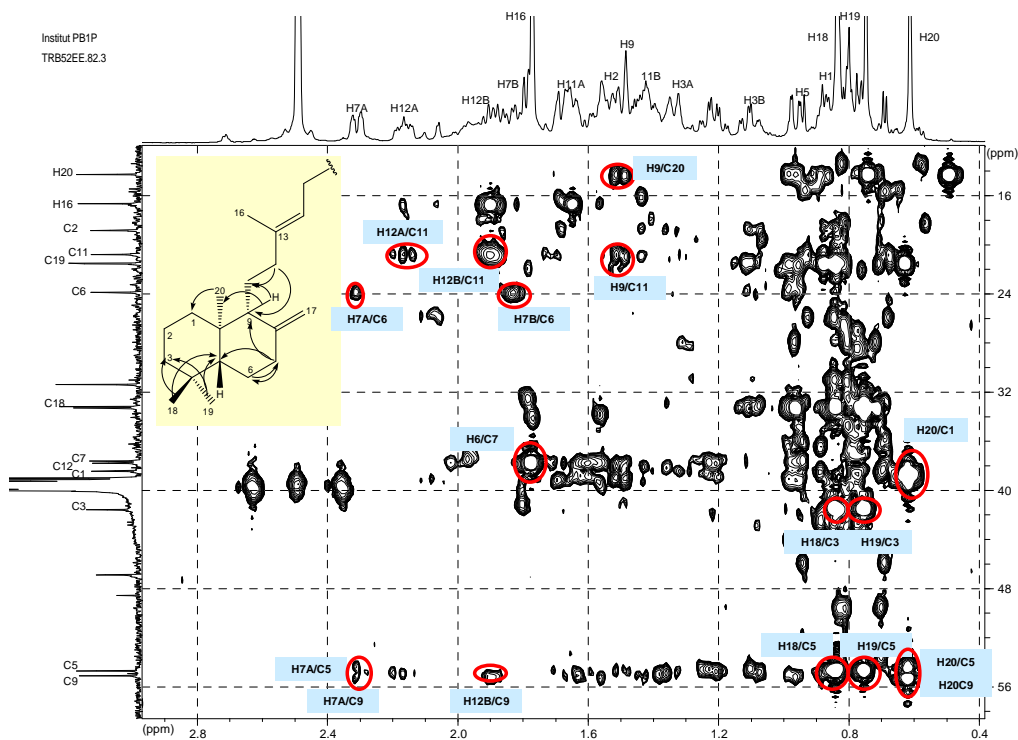
Fig.III.131b. ^{1}H–^{13}C HMBC spectrum of compound **18** (DMSO-d_6)
*Relative stereochemistry is shown
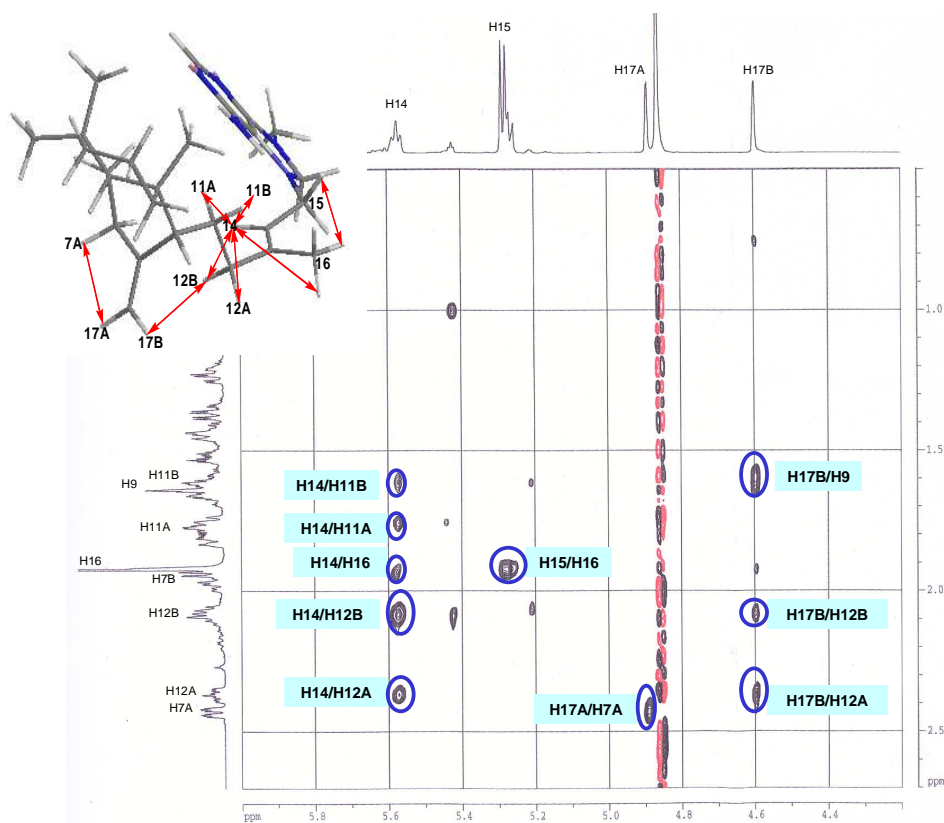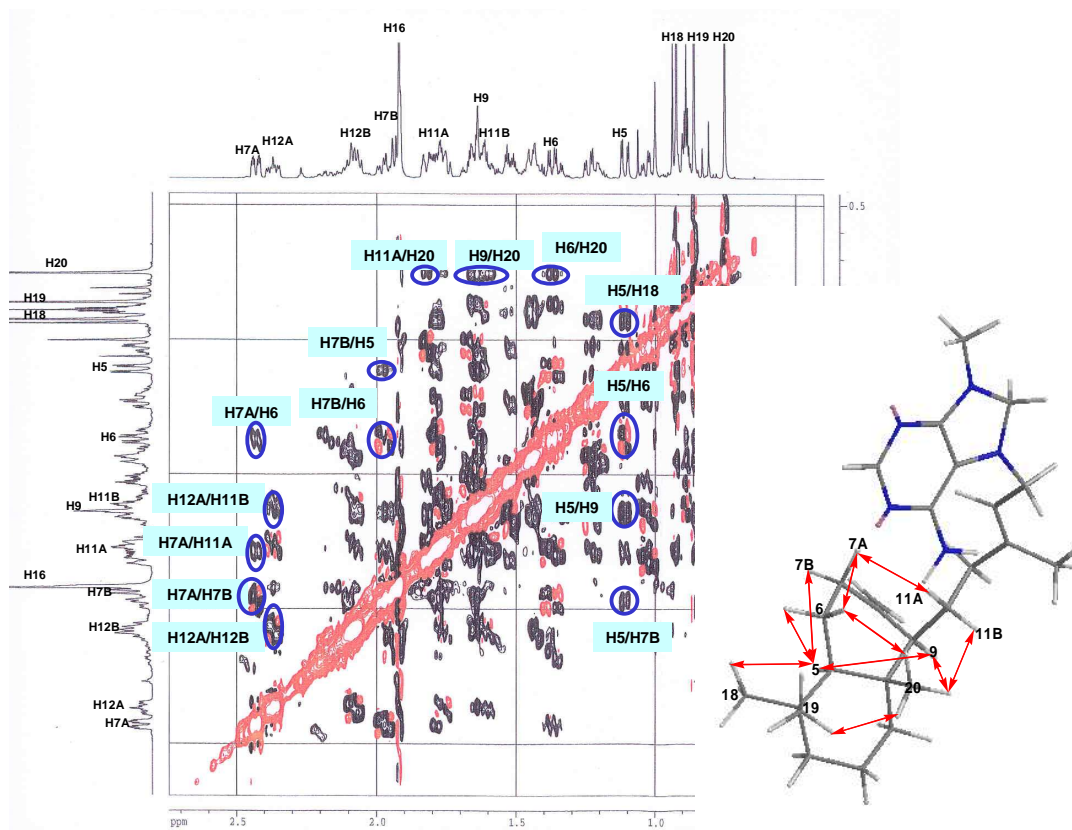
Fig.III.132. ^{1}H–^{1}H ROESY spectrum of compound **18** (MeOD)

Table III.14. NMR data of compound **18** in comparison to (+)-agelasine-D

No.	(+)-Agelasine D [b)]			Compound 18 [a)]		
	^{1}H-NMR		^{13}C-NMR	^{1}H-NMR		^{13}C-NMR
	δ	Integration, multiplicity, *J* in Hz	δ, DEPT	δ	Integration, multiplicity, *J* in Hz	δ, DEPT
1	0.6 – 2.4	16H, m	39.4, CH$_2$	0.87	2H, m	38.4, CH$_2$
2			20.3, CH$_2$	1.42	2H, m	18.8, CH$_2$
3A			43.2, CH$_2$	1.34	1H, br d, 12.9	41.6, CH$_2$
3B				1.22	1H, dd, 4.1, 12.6	
5			57.4, CH	0.96	1H, m	54.7, CH
6			25.5, CH$_2$	1.68	2H, m	23.9, CH$_2$
7A			39.4, CH$_2$	2.31	1H, dq, 2.5, 12.6	37.6, CH$_2$
7B				1.84	1H, dd, 5.0, 12.9	
9			56.8, CH$_2$	1.49	1H, br d, 11.3	55.1, CH
11A			40.2, CH$_2$	1.66	1H, m	37.8, CH$_2$
11B				1.10	1H, m	
12A			22.5, CH$_2$	2.16	1H, m	20.8, CH$_2$
12B				1.90	1H, m	
4	-	-	40.6, C		-	39.3, C
8	-	-	149.0, C		-	148.0, C
10	-	-	34.4, C		-	33.3, C
13			149.5, C		-	145.7, C
14	5.41	1H, br t, 6.5	115.9, CH	5.40	1H, t, 7.2	115.5, CH
15	5.72	2H, br d, 6.5	48.8, CH$_2$	5.20	2H, d, 7.2	48.6, CH$_2$
16	1.86	3H, br s	17.1, CH$_3$	1.77	3H, s	16.7, CH$_3$
17A	4.81	1H, br s	106.9, CH$_2$	4.81	1H, s	106.4, CH$_2$
17B	4.43	1H, br s		4.50	1H, s	
18	0.87	3H, s	34.0, CH$_3$	0.83	4H, s	33.18, CH$_3$
19	0.79	3H, s	22.1, CH$_3$	0.75	3H, s	21.53, CH$_3$
20	0.65	3H, s	15.0, CH$_3$	0.60	3H, s	14.29, CH$_3$
2'	8.50	1H, s	156.9, CH	8.45	1H, s	155.5, CH
4'	-	-	150.7, C		-	149.0, C
5'	-	-	111.0 C		-	109.1, C
6'-NH$_2$	6.76	2H, br s [c)]	153.9, C	7.98	2H, b s [c)]	152.3, C
8'	10.94	1H, s	142.6, CH	9.68	1H, s	141.0, CH
N9'-CH$_3$	4.10	3H, br s	32.0, CH$_3$	3.88	3H, s	31.4, CH$_3$

[a)] Data were recorded in DMSO-d_6 at 500 MHz (^{1}H) and 125 (^{13}C) multiplicities and coupling constant are given in Hz; [b)] Data were recorded in CDCl$_3$ for ^{1}H (400 MHz) and CD$_3$OD for ^{13}C (22.5 MHz), multiplicities and coupling constant are given in Hz (Nakamura et *al*., 1984b); [c)] exchangeable signal

III.2.1.3. **(+)-Agelasidine C** (**19**, known compound)
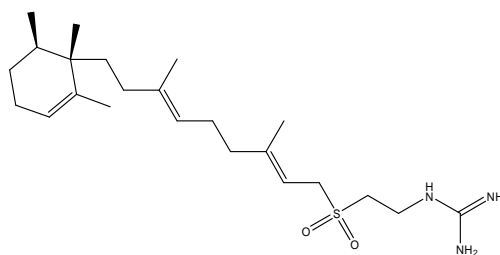
Fig.III.133. Compound **19**
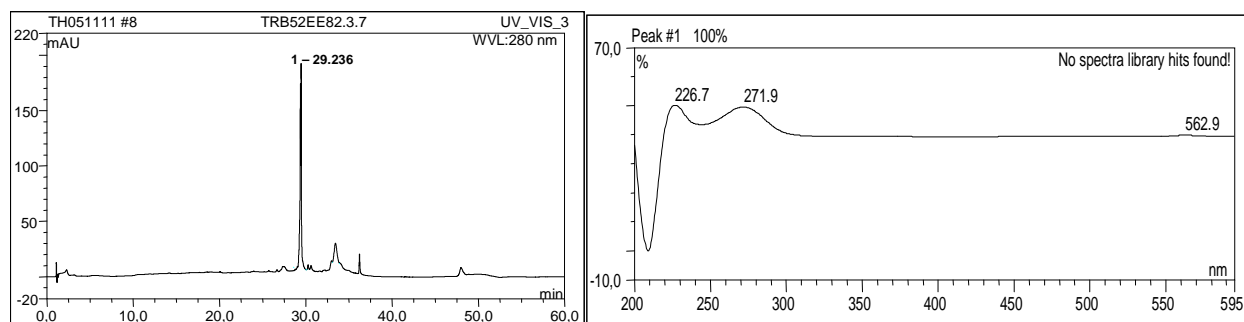
Fig.III.134. Analytical HPLC data of compound **19**
Left: HPLC profile in 280 nm, RT: 29.24; UV spectrum, λ_{max} = 226.7; 271.9 nm
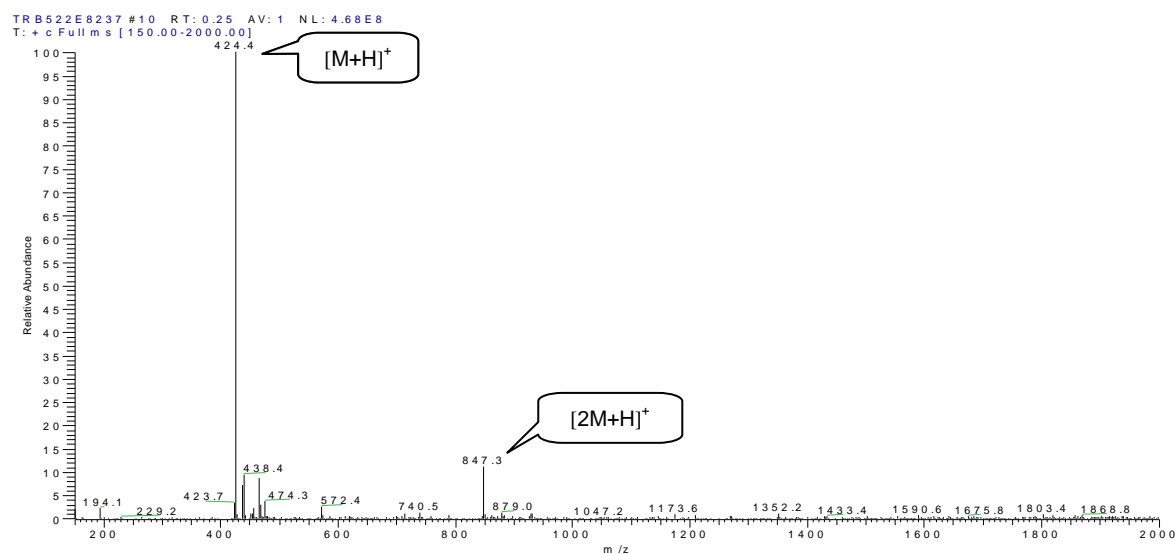
Fig.III.135. ESI-MS spectrum of compound **19**

Compound **19** was obtained as a brown oily substance (67 mg, 0.029% of the sponge dried weight). It shows ESI-MS ion peak at *m/z* 424 [M+H]$^+$ which is consistent with the molecular formula $C_{23}H_{41}N_2O_3S$ of agelasidine C. (+)-Agelasidine C is a diterpene derivative of hypotaurocyamine, which was first reported to be isolated from *Agelas nakamurai* by Nakamura and collaborators (1985a). It was reported to have $[\alpha]_D^{25}$ value of +8.5º ± 0.2º (*c* 2.0, CH$_3$OH), while in this study compound **19** exhibits $[\alpha]_D^{25}$ value of +4.7º ± 0.2º (*c* 2.0, CH$_3$OH). The (-) antipode of agelasidine C has been reported from a marine sponge *Agelas clathrodes* (Morales and Rodriguez, 1992)
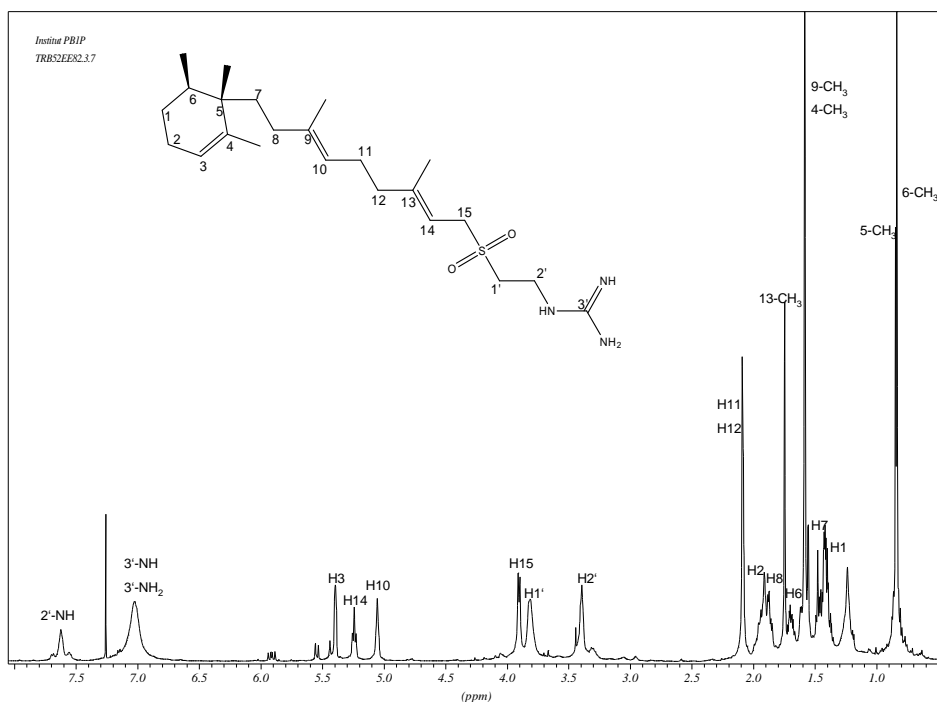
Fig.III.136. ^{1}H-NMR spectrum of compound **19** (CDCl$_3$, 500 MHz)
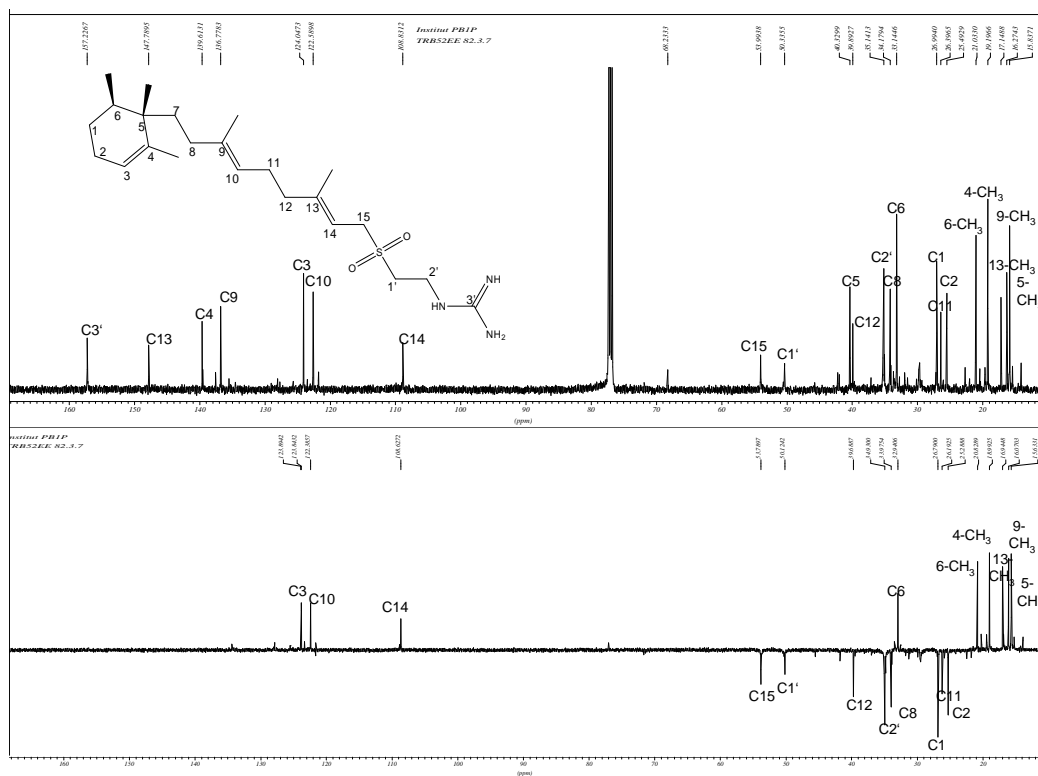
Fig.III.137. ^{13}C-NMR spectrum of compound **19** (CDCl$_3$, 125 MHz)

Comparison of NMR spectra between (+)-agelasidine C and compound **19** as shown in Table III.14 confirms their being identical. ^{1}H NMR spectrum shows

signals at δ_H 0.86 (s, 3H), 0.87 (d, 3H, J = 7 Hz), 1.61 (br s, 3H), 5.40 (br s, 1H) of 1-alkyl-1,2,6-trimethyl-2-cyclohexene ring system. An isolated spin system at δ_H 3.91 (2H, d, J = 7.6 Hz) and δ_H 5.25 (1H, t, J = 7.6 Hz), due to the allyl grouping connected to a sulphur unit is observed. Another isolated spin system was also observed which coupled signals at δ_H 3.81 (2H) and 3.39 (2H) to NH signal at δ_H 7.63 and in turn correlates to the signals of the NH and NH_2 at δ_H 7.03. This suggests the presence of an ethylene guanidine moiety which is confirmed with a presence of a quaternary carbon at δ_C 157.2 in ^{13}C NMR signal. The ethylene guanidine moiety is suggested to be attached to a sulfonyl group by the deshielded ethylene signal observed at δ_C 35.2 and δ_C 50.3. High-field olefinic methyl signals at δ_C 16.3 and 17.1 indicates that this compound contained two trans-(CH_3)-C=CH units, on C-9 to C-15. ^{1}H–^{13}C HMBC spectrum confirm the connection of each substructures Fig.III.139. Hence compound **19** is determined as **(+)-agelasidine C**.
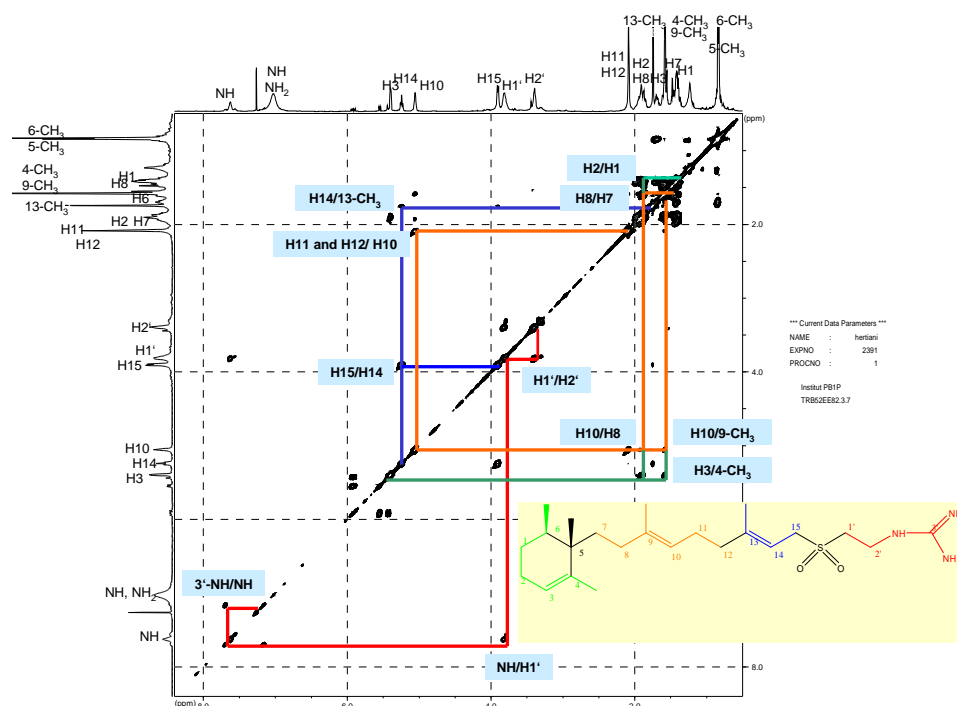
Fig.III.138. ^{1}H–^{1}H COSY spectrum of compound **19** (CDCl$_3$)
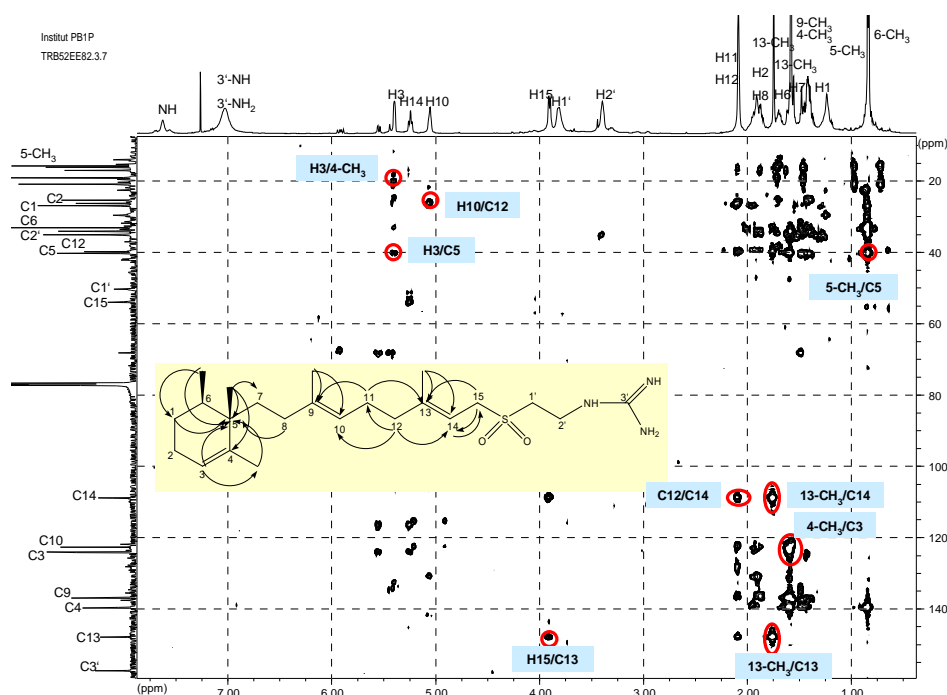
Fig.III.139. ^{1}H–^{13}C HMBC spectrum of compound **19** (CDCl$_3$)

Table III.15 NMR data of compound **19** in comparison to (+)-agelasidine C

No	(+)-Agelasidine C [a), b)]			Compound 19 [a)]		
	^{1}H-NMR		^{13}C-NMR	^{1}H-NMR		^{13}C-NMR
	δ	Integration, multiplicity, *J* in Hz	δ, DEPT	δ	Integration, multiplicity, *J* in Hz	δ, DEPT
6-CH$_3$	0.86	3H, s	21.4, CH$_3$	0.83	3H, s	21.0, CH$_3$
5-CH$_3$	0.87	3H, d, 7.0	16.2, CH$_3$	0.86	3H, d, 5.7	15.8, CH$_3$
9-CH$_3$	1.61	3H, br s	16.3, CH$_3$	1.59	3H, br s	16.3, CH$_3$
4-CH$_3$	1.61	3H, br s	19.4, CH$_3$	1.59	3H, br s	19.2, CH$_3$
13-CH$_3$	1.78	3H, br s	17.0, CH$_3$	1.71	3H, br s	17.1, CH$_3$
1	1.20 – 2.40	13H, m	26.4, CH$_2$	1.41	2H, m	27.0, CH$_2$
2			28.0, CH$_2$	1.93	2H, m	25.5, CH$_2$
6			34.4, CH	1.69	1H, m	33.1, CH
7			35.3, CH$_2$	1.47	2H, m	35.1, CH$_2$
8			36.4, CH$_2$	1.88	2H, m	34.2, CH$_2$
11			27.2, CH$_2$	2.09	2H, br s	26.4, CH$_2$
12			40.8, CH$_2$	2.09	2H, br s	39.9, CH$_2$
3	5.40	1H, br s	124, CH	3.39	1H, br s	124.0, CH
4	-	-	140.5, C	-	-	139.6, C
5	-	-	41.4, C	-	-	40.3, C
9	-	-	137.6, C	-	-	136.8, C
10	5.10	1H, br s	124.0, CH	5.07	1H, br s	124.0, CH
13	-	-	148.0, C	-	-	147.8, C
14	5.30	1H, t, 8.0	110.6, CH	5.25	1H, t, 7.6	108.8, CH
15	3.91	2H, d, 8.0	54.5, CH$_2$	3.91	2H, d, 7.6	54.0, CH$_2$
1'	3.75	2H, t, 6.0	51.4, CH$_2$	3.81	2H, b s	35.2, CH$_2$
2'	3.34	2H, t, 6.0	36.0, CH$_2$	3.39	2H, b s	50.3, CH$_2$
3'-NH$_2$, 3'-NH			158.5, C=NH	7.03	3H, br s	157.2, C=NH
-NH-			-	7.63	1H, br s	-

[a)] Data were recorded in CDCl$_3$, at 500 MHz (^{1}H) and 125 (^{13}C) multiplicities and coupling constant are given in Hz; [b)] Nakamura *et al.*, 1985a

III.2.1. Brominated pyrrole from *Agelas nakamurai*

III.2.1.1. Longamide C (*N*-methyl debromolongamide B methyl ester, **20**, new compound)
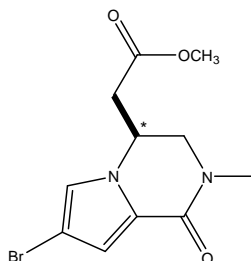
Fig.III.140. Compound **20*****
Relative stereochemistry is shown

Fig.III.141. Analytical HPLC data of compound **20**
Left: HPLC profile in 240 nm, RT: 21.35; right: UV spectrum, λ_{max} = 202.1, 234.8, 281.1 nm
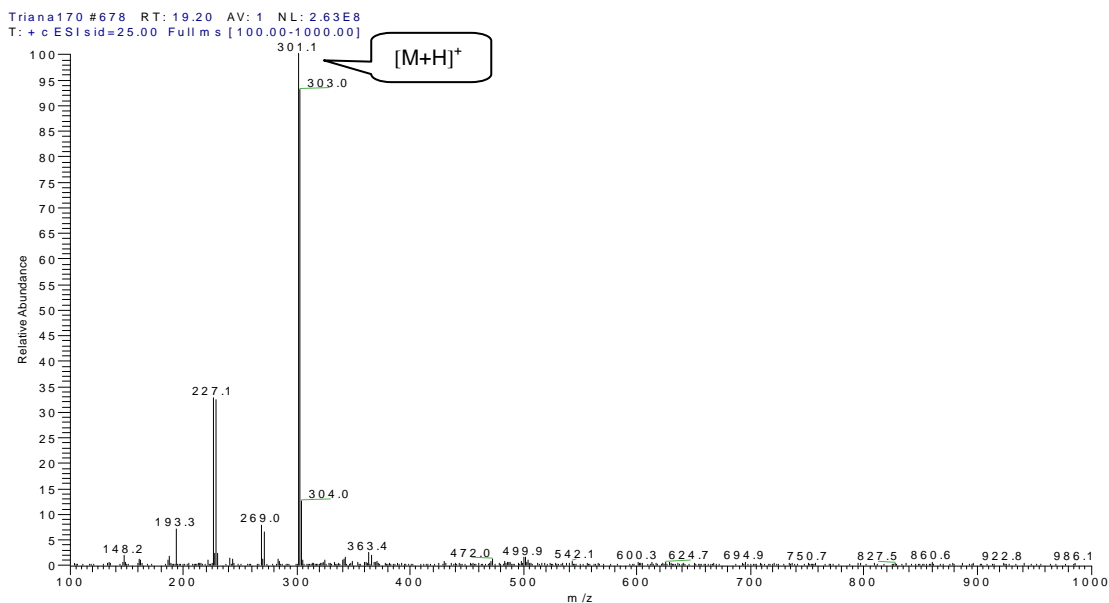
Fig.III.142. ESI-MS result of compound **20**

Compound **20** was obtained as a colourless solid at amount of 1.13 mg

(0.0004% of the sponge dried weight). The UV spectrum of compound **20** is comparable to that of mukanadin C (**21**) which is also isolated from the same sponge, suggesting a similar chromophoric moiety. ESIMS pseudo-molecular ion peaks at *m/z* 301/303 [M+H]$^+$ in an intensity ratio of 1:1 indicate the presence of two bromine atoms. Molecular formula of $C_{11}H_{14}BrN_2O_3$ was deduced from HREIMS which is in accordance to six degrees of unsaturation (*m/z* experimental = 301.0180, *m/z* calculated = 301.0188 [M+H]$^+$). This finding led to the closely related substance from *Homoaxinella* sp., (±)-longamide B methyl ester (Umeyama *et al.*, 1998).

(*S)*-(+)-Longamide methyl ester   (*R)*-(-)-Longamide methyl ester
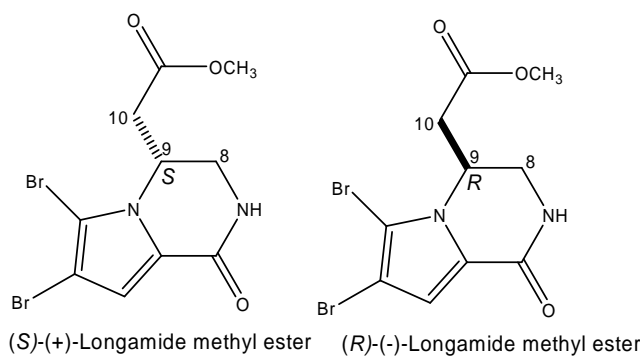
Fig.III.143. Longamide B methyl ester (Umeyama *et al.*, 1998)

Umeyama and collaborators (1998) reported that longamide B methyl ester (Fig.III.143) was obtained as a racemate of mixture 9*S* and 9*R* enantiomers, whereas (*S*)-(-)-longamide B methyl ester was produced synthetically by Patel and collaborators (2005). This dibrominated pyrrole derivative has a molecular weight of 364/366/368 g/mol with an intensity ratio of 1:2:1. A molecular weight difference of 64 mass units with that of compound **20** was observed. Considering the isotopic pattern of compound **20,** this is an evidence that the isolated compound has one bromine less, while an additional excess of 15 mass units plausibly refers to a methyl group substituent.

The ^{1}H NMR spectrum of compound **20** in CDCl$_3$ reveals two *sp^2* proton signals at δ_H 6.89 (1H, s, H-3) and 6.79 (1H, s, H-5) suggesting the bromination at position 4. Absence of the NH pyrrole signal in CDCl$_3$ indicates that the *N*-pyrrole is plausibly substituted. This finding together with the presence of a methine signal at δ_H 4.64 (1H, m) which is coupled to a deshielded methylene signal at δ_H 3.95 (1H, dd, *J* = 4.2, 12.9 Hz, H-8A) and 3.42 (1H, dd, *J* = 3.2, 12.9 Hz, H-8B) and to another methylene at δ_H 2.80 (2H, *J* = 3.2, 7.3 Hz, H$_2$-10) as exhibited in the ^{1}H–^{1}H COSY spectrum suggests the presence of a pyrrolopyrazinone ring. ^{1}H–^{13}C HMBC experiment was not performed on this compound because of the very small yield (1.13 mg).

Comparison of the ^{1}H NMR data in CDCl$_3$ with the known synthetic product, (*S*)-(-) longamide B methyl ester (Patel *et al.*, 2005) as shown in Table III.16 exhibits similarities. The major difference observed besides the degree of substitution of the pyrrole ring is the absence of an amide proton signal. The presence of an N-methyl signal at δ_H 3.10 (3H, s) suggests that the amide function is methylated.
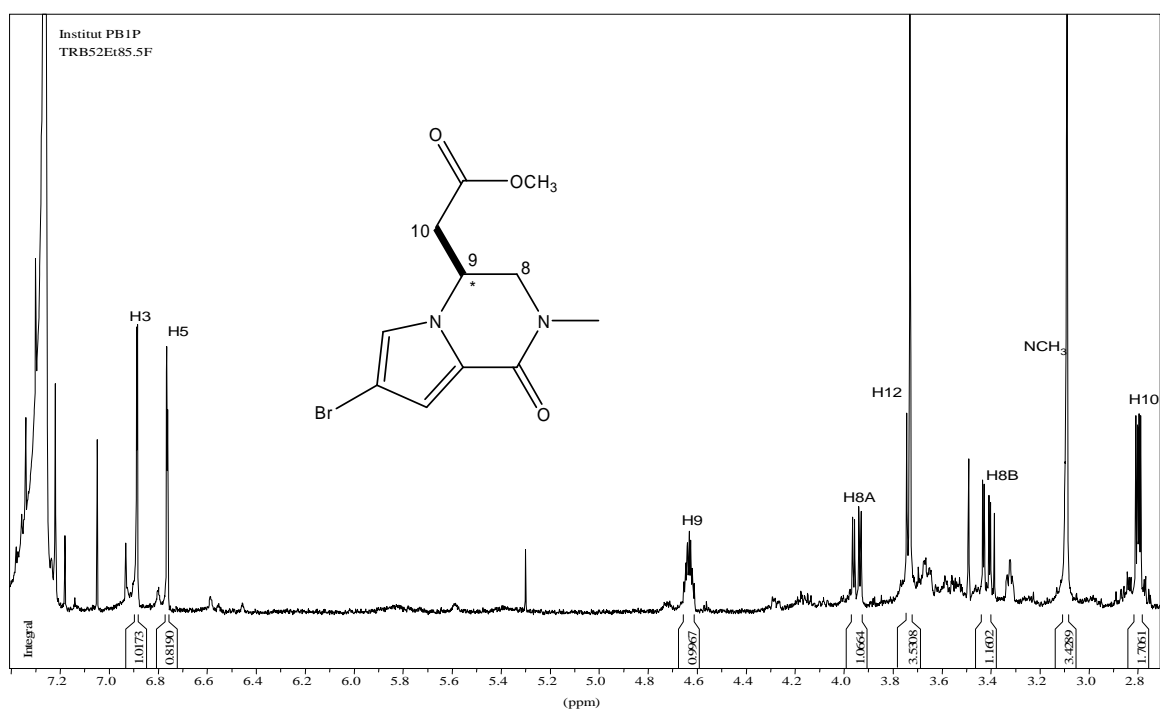
Fig.III.144. ^{1}H NMR spectrum of compound **20*** (CDCl$_3$, 500 MHz)
*Relative stereochemistry is shown
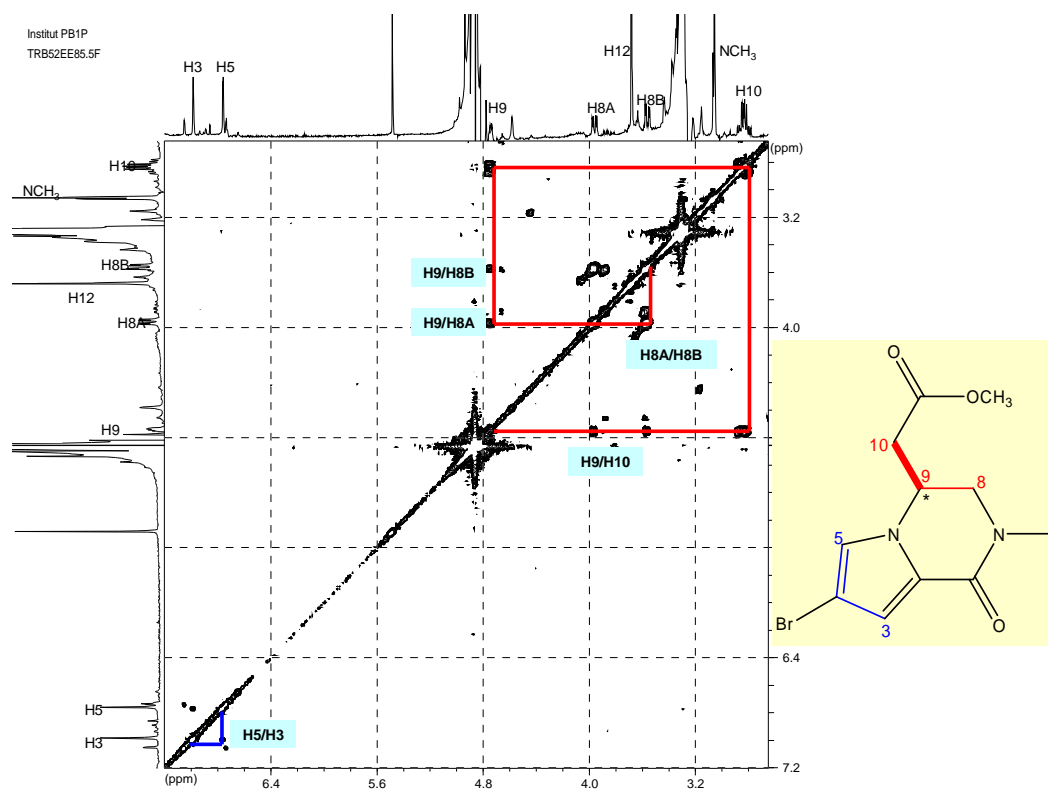
Fig.III.145. ^{1}H–^{1}H COSY spectrum of compound **20*** (MeOD)
*Relative stereochemistry is shown

Based on the coupling pattern of NH (d, J = 5.0 Hz) , H-8 (dd, J = 13.0, 3.5 Hz, and dd, J = 13.0, 5.0 Hz) and H-9 (ddd, J = 10.5, 3.5, 3.5 Hz) observed in longamide B methyl ester, Umeyama and collaborators (1998) determined an equatorial orientation of the proton at the C-9 position, whereas the bulky substitution at the C-9 position is considered to be axial-like because of the influence of bromine at the C-5 position. The absolute stereochemistry at the sole asymmetric carbon at C-9 of the separated (-)-longamide methyl ester and its antipode was determined based on their CD spectra. (+)-Longamide B methyl ester was established as S on the basis of its negative Cotton effects at 226 nm ($\Delta\in$ -2.64), whereas the absolute stereochemistry at C-9 of (-)-longamide B methyl ester was established as R on the basis of positive Cotton effects at 226 nm ($\Delta\in$ +1.96) (Umeyama *et al.*, 1998). The relative stereochemistry as well as the conformational behaviour of compound **20** is assigned through a ROESY experiment. NOE correlations are exhibited between H-9 to H_2-10, H-8A and H-8B; H-9 and H_2-10 to H-5; and of H-8A and H-8B to the *N*-methyl, as well as from H-8B to H_2-10 (Fig.III.147a and Fig.III.147b). These results indicate a half chair conformation of the six-membered ring where the bulky substitution at C-9 is quasiaxial oriented and H-9 is quasiequatorial. In this conformation, the *N*-methyl will only be seen through space by H-8A and H-8B, and not by H-9 neither nor by H_2-10. The coupling patterns observed for H-9 (m); H-8A (dd, J = 4.2, 12.9 Hz); H-8B (dd, J = 3.2, 12.9 Hz) and H_2-10 (dd, J = 7.3, 3.2 Hz) support the proposed conformation. If H-9 is oriented axially, the coupling constant between H-9 and H-8A will be found at around 9 − 12 Hz which is not the case for longamide C ($^3J_{H8A/H9}$ = 4.2 Hz). Hence, the relative stereochemistry of longamide C (**20**) is determined as illustrated in Fig.III.146. Unfortunately, an optical rotation

experiment was not performed on this compound due to its loss during transport from

Braunschweig to Düsseldorf.
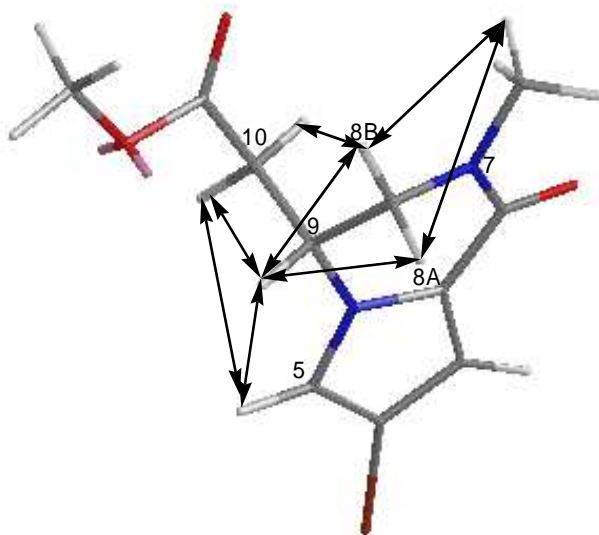
Fig.III.146. Plausible conformation of longamide C (**20**) based on the ROESY and ^{1}H coupling pattern data

A detailed analysis of the NMR data reveals that compound **20** is a 5-debromo-N(7)-methyl analogue of the known compound (*S*)-(-)-longamide B methyl ester. Thus the structure of compound **20** is determined as a methyl 2-(7-bromo-2-methyl-1-oxo-1,2,3,4-tetrahydropyrrolo[1,2-α]pyrazin-4-yl)acetate and is named **longamide C**.

Fig.III.147a. ^{1}H–^{1}H ROESY spectrum of compound **20*** (CDCl$_3$)
*Relative stereochemistry is shown

Fig.III.147b. ^{1}H–^{1}H ROESY spectrum of compound **20*** (CDCl$_3$)
*Relative stereochemistry is shown
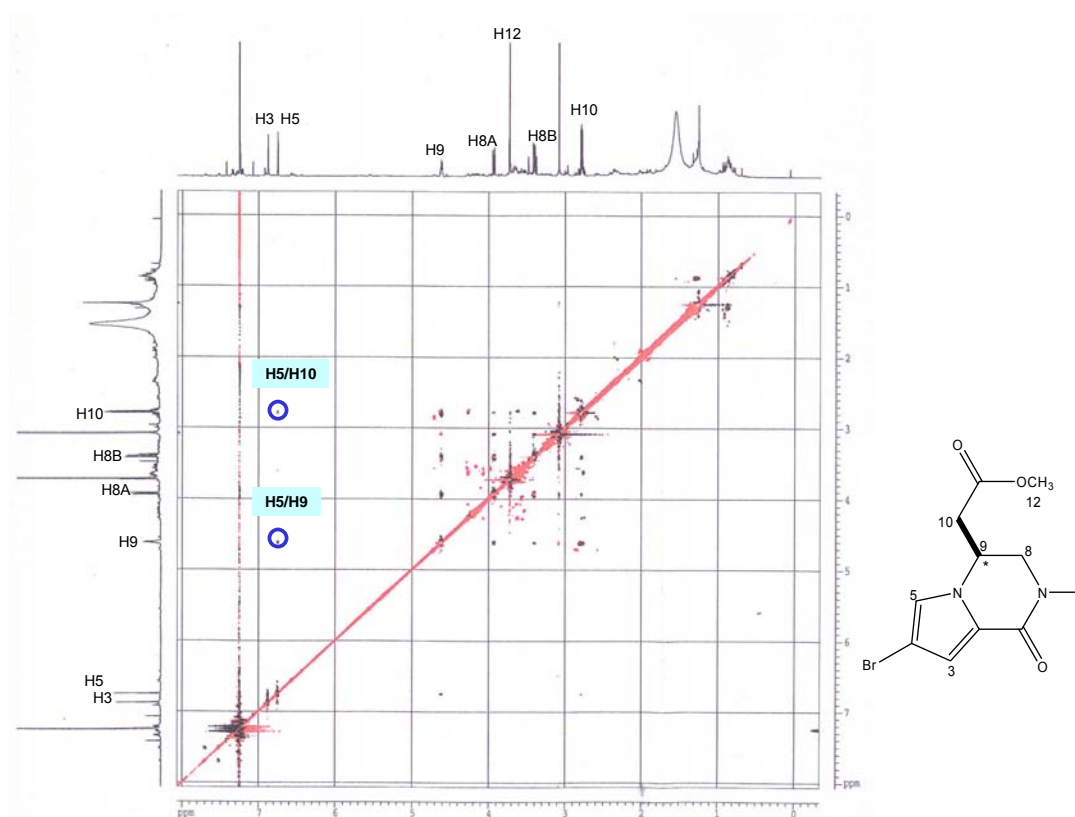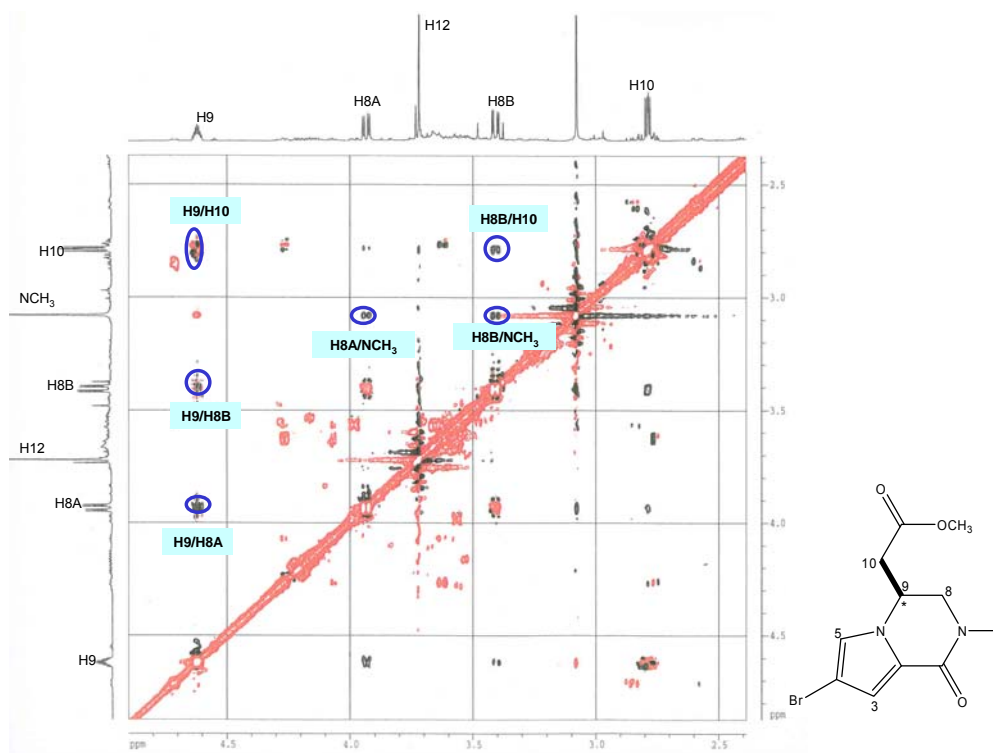
Table III.16. NMR data of compound in comparison to (*S*)-(-) longamide B methyl ester

	(*S*)-(-) Longamide B methyl ester [a) b)]			Compound 20 [a) c)]	
	1H-NMR		13C-NMR	1H-NMR	
No.	δ	Integration, multiplicity, *J* in Hz	δ	δ	Integration, multiplicity, *J* in Hz
2	-	-	125.1, C		-
3	-	-	116.7, C	6.89	1H, s
4	6.93	1H, s	101.7, CH		-
5	-	-	107.0, C	6.79	1H, s
6	-	-	159.9, C=O	-	-
NH	6.26	1H, b s	-	-	-
NCH$_3$	-	-	-	3.10	3H, s
8A	3.86	1H, ddd, 13.3, 4.0, 1.4		3.95	1H, dd, 4.2, 12.9
8B	3.61	1H, ddd, 13.4, 5.3, 1.3	43.5, CH$_2$	3.42	1H, dd, 3.2, 12.9
9	4.68	1H, m	50.7, CH	4.64	1H, m
10A	2.95	1H, dd, 16.7, 10.8		2.80	2H, dd, 7.3, 3.2
10B	2.54	1H, ddd, 16.8, 3.1, 1.5	35.6, CH$_2$	-	-
11	-	-	170.5, C=O	-	-
OCH$_3$	3.67	3H, s	52.6, CH$_3$	3.72	3H, s

[a)] Data were recorded in CDCl$_3$, at 500 MHz, multiplicities and coupling constant are given in Hz; [b)] Data were recorded in CDCl$_3$, 1H NMR at 300 MHz, 13C NMR at 75 MHz, multiplicities and coupling constant are given in Hz (Patel *et al.*, 2005); [c)] HMBC experiment was not performed on **20** due to very small yield

III.2.1.2. Mukanadin C (**21**, known compound)
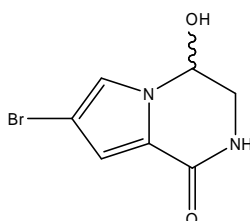
Fig.III.148. Compound **21**
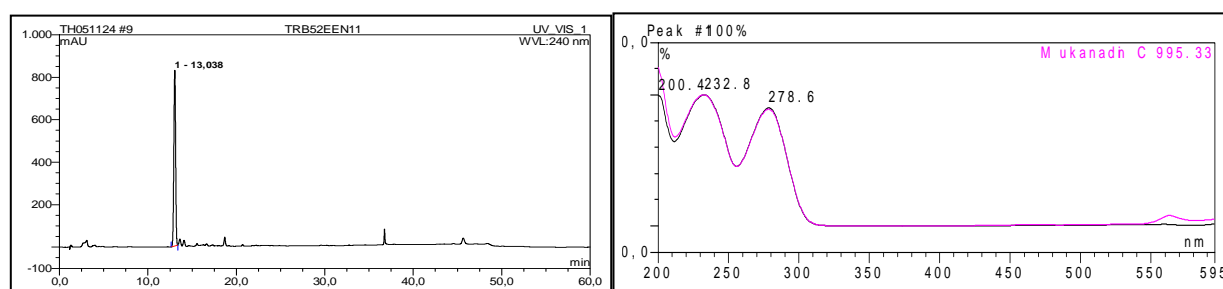
Fig.III.149. Analytical HPLC data of compound **21**
Left: HPLC profile in 240 nm, RT: 13.04; right: UV absorption spectrum, λ$_{max}$ = 202.4; 232.8; 278.6 nm
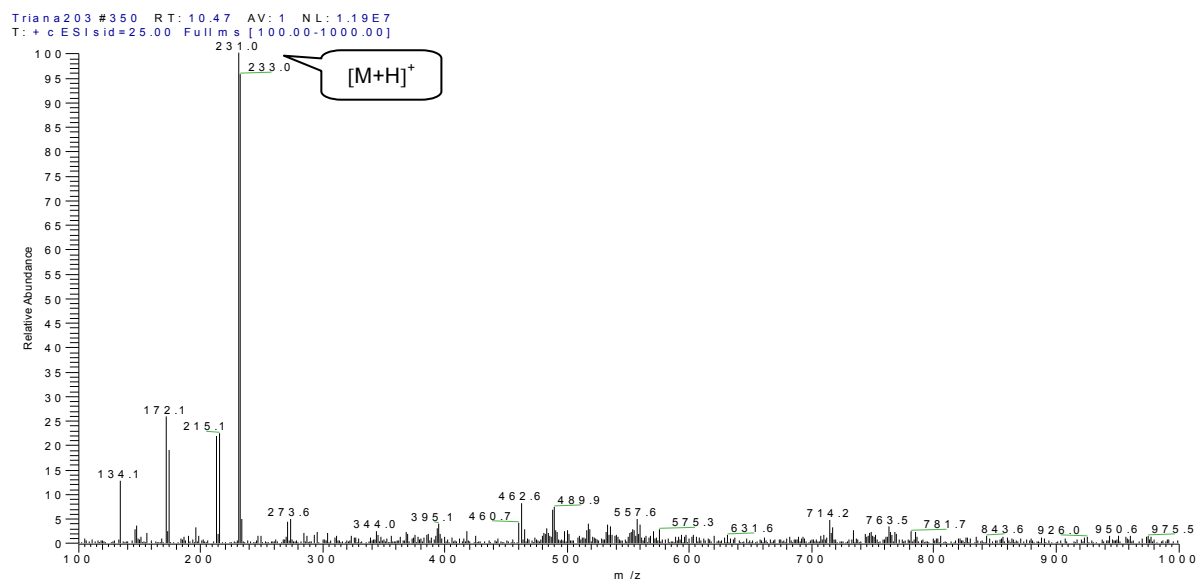
Fig.III.150. ESI-MS spectrum of compound **21**

Compound **21** was obtained as a white amorphous substance at an amount of 12 mg (0.005% of the sponge dried weight). This optically active compound occurs as a racemic mixture which is shown by $[\alpha]_D^{25}$ value of +0.0º ± 0.2º (*c* 2.0, CH$_3$OH). ESIMS result shows molecular ion cluster peaks at *m/z* 231 and 233 [M+H]$^+$ having an intensity ratio of 1:1, implying a mono-brominated compound (Fig.III.50). UV absorption pattern and the retention time in analytical HPLC correspond to the internal HPLC library data base for mukanadin C (Fig.III.149). Mukanadin C was first reported by Uemoto group (1999) from *Agelas nakamurai*. This compound has been reported to exhibit moderate antimicrobial activity (Cafieri *et al.*, 1995).
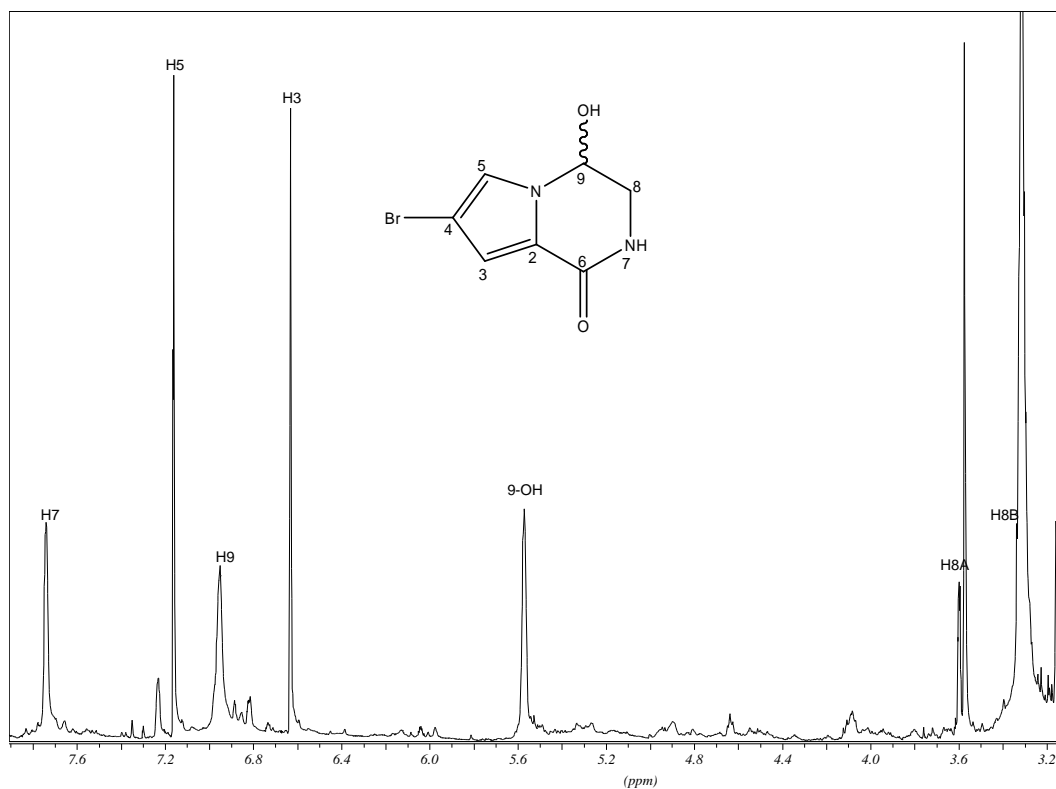
Fig.III.151. ^{1}H-NMR spectrum of compound **21** (MeOD, 500 MHz)

NMR data of compound **21** are comparable to the known compound mukanadin C as shown in Table III.17. Its ^{1}H-^{1}H COSY spectrum reveals a spin system coupling the pyrrole ring protons at δ_H 6.63 (s, H-2) and δ_H 7.16 (s, H-4), while a second spin system is observed between the deshielded sp^3 methine signal at δ_H 6.95 (s, H-9) and a geminal hydroxyl group at δ_H 5.57 (br s) which is in turn coupled to a methylene signal at δ_H 3.62 (1H, dd, J = 10.4, 1.6, 3.1 Hz, H-8A) and at δ_H 3.3 (H-8B) under the water signal of DMSO-d_6, and finally ended to an exchangeable proton at δ_H 7.75 (br s, 7-NH). After careful interpretation and comparison of the physical and spectral data to those in the literature, compound **21** is determined as the known derivate **mukanadin C**.
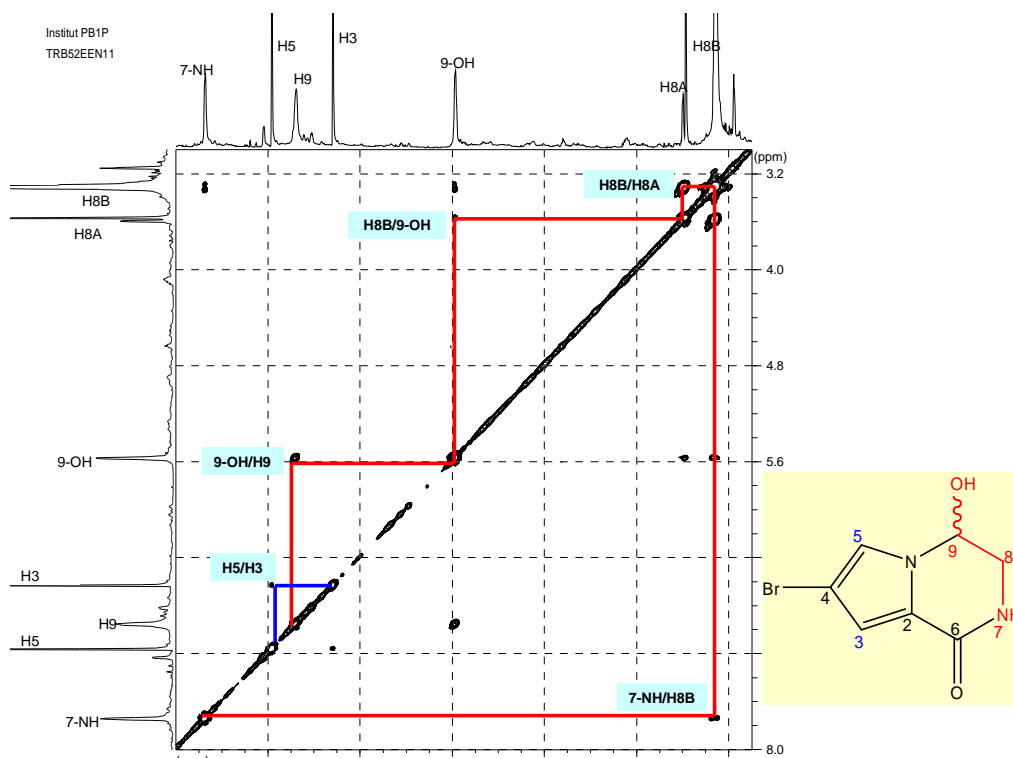
Fig.III.152. ^{1}H–^{1}H COSY spectrum of compound **21** (DMSO-d_6)

Table III.17. ^{1}H-NMR data of compound **21** in comparison to mukanadin C

No H.	Mukanadin C [a,b]		Compound 21 [a]	
	δ	H, multiplicity, *J* in Hz	δ	H, multiplicity, *J* in Hz
3	6.63	1H, d, 1.9	6.63	1H, s
5	7.16	1H, d, 1.9	7.15	1H, s
NH	7.73	1H, br s	7.75	1H, br s
8A	3.59	1H, ddd, 13.2, 3.3, 1.7	3.62	1H, dd, 10.4, 3.1, 1.6
8B	3.30	under HDO signal	3.30	Under HDO signal
9	6.75	1H, d, 5.7	6.95	1H, br s
OH	5.57	1H, br d, 3.8	5.57	1H, br s

[a] Data were recorded in DMSO-d_6, at 500 MHz, multiplicities and coupling constant are given in Hz; [b] Jadulco (2003)

III.2.1.3. Hymenidin (**22**, known compound)
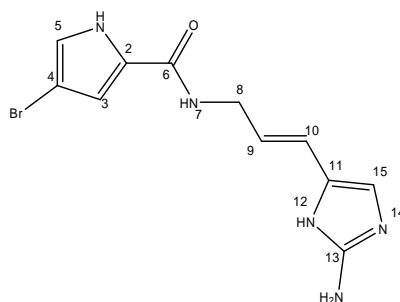
Fig.III.153. Compound **22**
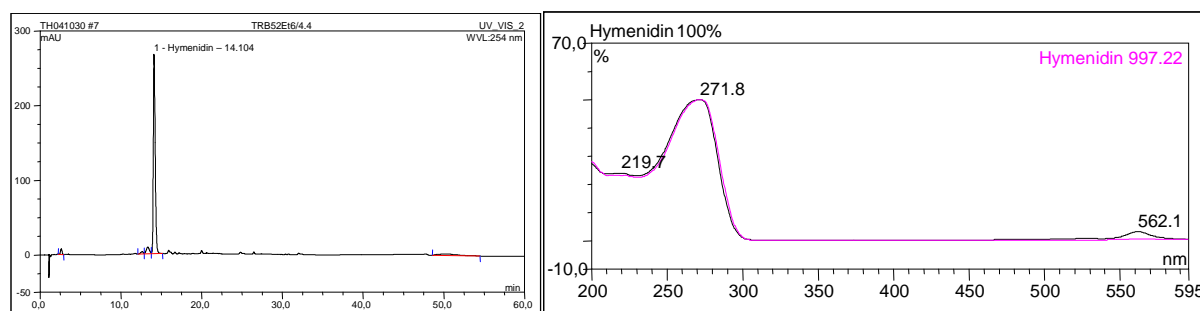
Fig.III.154. Analytic HPLC data of compound **22**
Left: HPLC profile in 254 nm, RT: 14.10; right: UV absorption spectrum, λ_{max} = 219.7; 271.8 nm
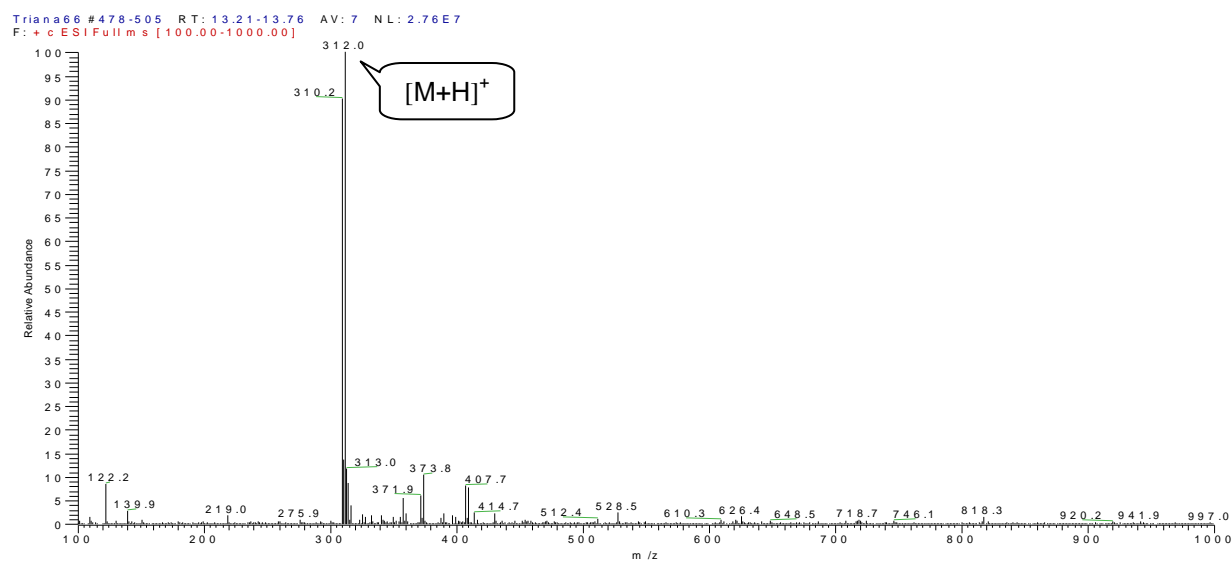
Fig.III.155. ESI-MS data of compound **22**

Compound **22** was obtained as a yellow amorphous substance at an amount of 41 mg (0.016 % of the sponge dried weight). Chemical investigation using analytical HPLC corresponds to the internal spectral library data base for hymenidin, which is supported by its ESIMS data. UV absorption pattern (Fig.III.154) is typical to that of pyrrole 2-carboxamide at ~ 270 nm (Jaffe and Orchin, 1962). ESIMS isotopic cluster at *m/z* 309/311 having an intensity ratio of 1:1 [M+H]$^+$ indicates a mono-brominated compound. This finding together with its NMR spectra data corresponds to the molecular formula $C_{11}H_{12}BrN_5O$ of hymenidin.

^{1}H NMR spectrum in MeOD confirms the signals for hymenidin (Table III.16). Signals in the aromatic region at δ_H 6.80 (d, *J* = 1.6 Hz, H-3) and δ_H 6.92 (d, *J* = 1.6

Hz, H-5) correspond to the pyrrole ring protons, while the signal at δ_H 6.74 is assigned as the proton of the amino imidazole ring. Olefinic proton signals are observed at δ_H 6.10 (dt, J = 16.1, 5.5 Hz, H-9) and 6.29 (d, J = 16.1 Hz, H-10). Coupling constant values of 16.1 Hz between H-9 and H-10 indicate a *trans*-olefinic function (Kobayashi *et al.*, 1986). These findings and comparison with the literature data determines compound **22** as **hymenidin**.

Hymenidin was previously isolated from the sponges *Hymeniacidon* sp. (Kobayashi *et al.*, 1986) and from *Stylissa carteri* (Baker, 2004).
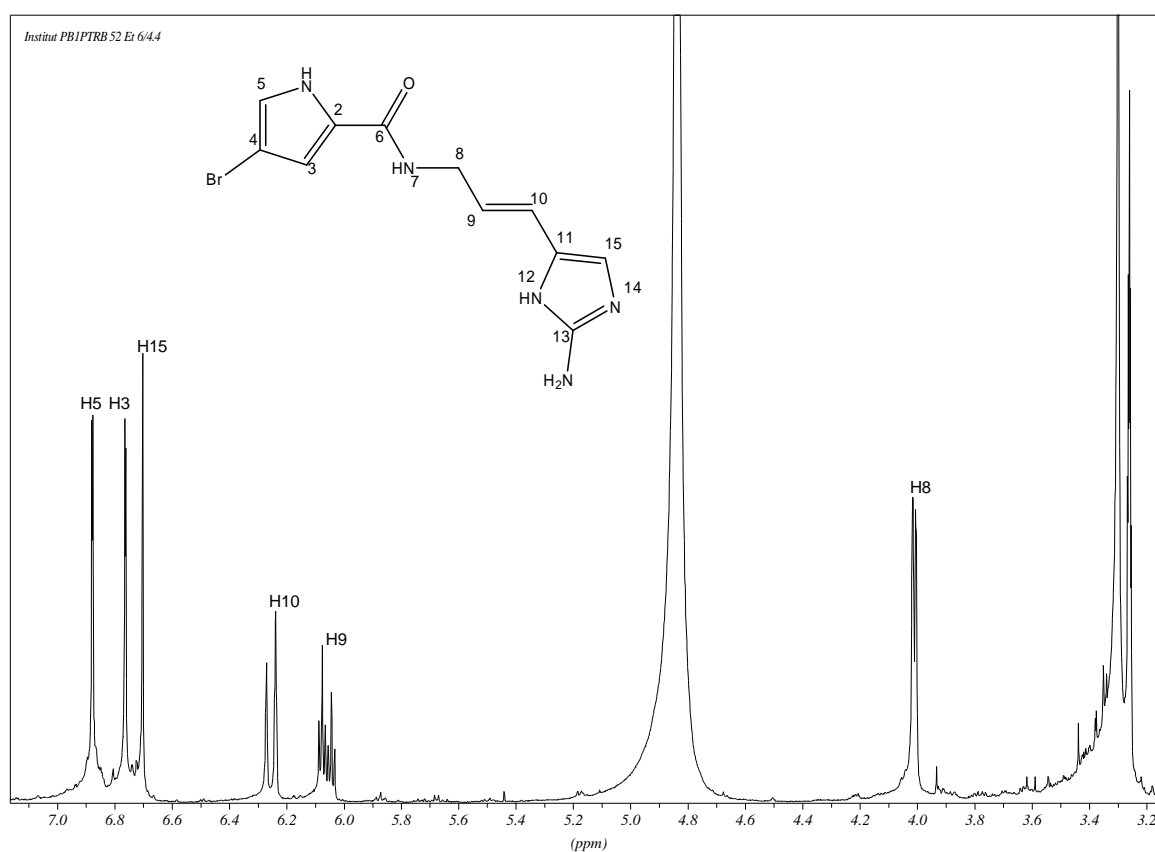
Fig.III.156. ^{1}H-NMR spectrum of compound **22** (MeOD, 500 MHz)

Table III.18. ^{1}H-NMR data of compound **22** in comparison to hymenidin

Atom No.	Compound 22 [a]		Hymenidin [a] [b]	
	δ	Integration, Multiplicity (*J* in Hz)	δ	Integration, Multiplicity (*J* in Hz)
3	6.80	1H, d, 1.6	6.71	1H, d, 1.6
5	6.92	1H, d, 1.6	6.85	1H, d, 1.6
8	4.05	2H, dd, 1.3, 5.4	3.96	2H, dd, 5.4, 5.4
9	6.10	1H, dt, 16.1, 5.5	6.15	1H, dt, 16.1, 5.4
10	6.29	1H, d, 16.1	6.25	1H, d, 16.1
15	6.74	1H, s	6.70	1H, s

[a] Data were recorded in MeOD at 500 MHz, multiplicities and coupling constant are given in Hz; [b] Baker (2004)

III.2.1.4. 4-bromo-1*H*-pyrrole-2-carboxylic acid (**23**, known compound)
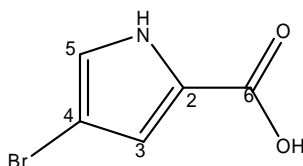
Fig.III.157. Compound **23**
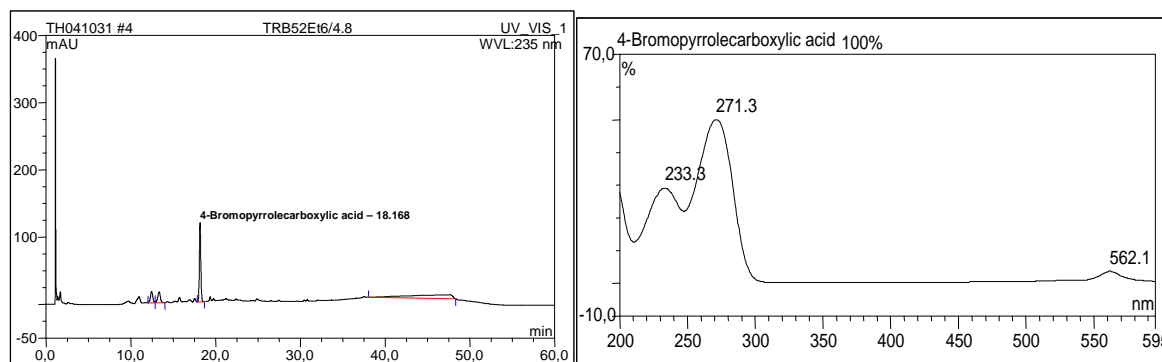
Fig.III.158. HPLC analytic result of compound **23**
Left: HPLC profile in 235 nm, RT: 18.17; right: UV absorption spectrum, λ_{max} = 233.3; 271.3 nm
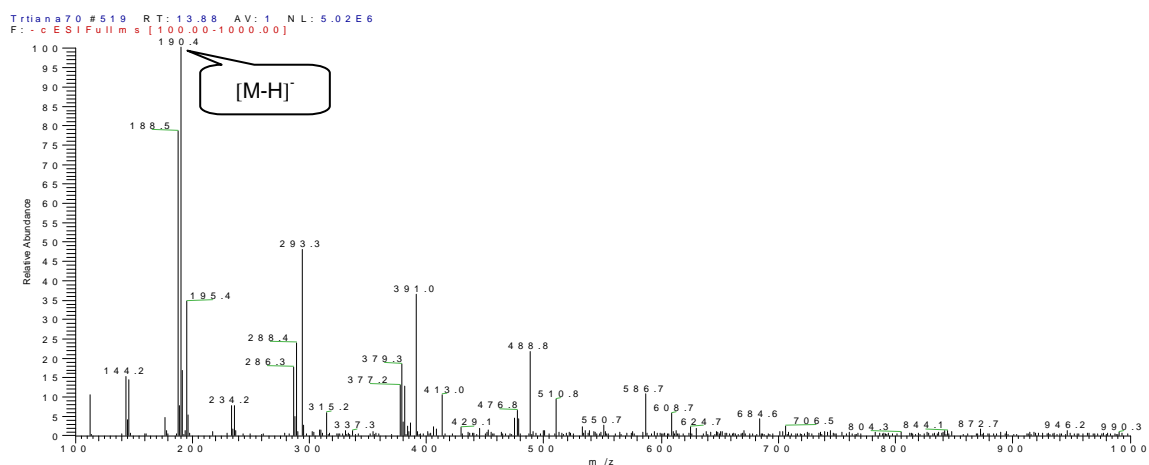
Fig.III.159. ESI-MS data of compound **23**

Compound **23** in this study was obtained as a dark brown amorphous substance at an amount of 66 mg (0.024% of the sponge dried weight). Its analytical HPLC spectrum matched the internal spectral library data base for 4-bromopyrrole carboxylic acid, in agreement with its ESIMS data. UV absorption pattern is again supportive for the presence of 2-carboxylic acid pyrrole. ESIMS pseudo molecular ion cluster at *m/z* 188/190 [M-H]$^-$ having an equal intensity is compatible to the molecular formula $C_5H_4BrNO_2$ of 4-bromopyrrole carboxylic acid. Furthermore, NMR data of compound **23** confirm the proposed structure as described in Table III.19.

^{1}H NMR experiment in MeOD detects two proton signals of the pyrrole ring δ_H 6.92 (1H, d, *J* = 1.6 Hz, H-5) and at δ_H 6.80 (1H, d, *J* = 1.6 Hz, H-3). The coupling constant between the two protons is suggestive for *meta* coupling. Therefore bromine substitution should be at position 4, as is also supported by the up-field chemical shift of C-4 at δ_C 97.4. Hence, compound **23** is identified as the known derivative **4-bromo-1*H*-pyrrole-2-carboxylic acid.**

Table III.19. ^{1}H-NMR data of compound **23** in comparison to 4-bromo-1*H*-pyrrole-2-carboxylic acid

Atom No.	Compound 23 [a]			4-bromo-1*H*-pyrrole-2-carboxylic acid [c]	
	^{1}H-NMR		^{13}C-NMR [b]		
	δ	Integration, Multiplicity (*J* in Hz)		δ	Integration, Multiplicity (*J* in Hz)
1-NH	n.d.	n.d.	-	12.10	1H, s
2	-	-	125.0	-	-
3	6.92	1H, d, 1.6	123.8	7.10	1H, d, 1.6
4	-	-	97.4	-	-
5	6.80	1H, d, 1.6	117.2	6.74	1H, d, 1.6
6	-	-	n.d.	-	-
6-OH	n.d.	n.d.	-	12.56	1H, b s

[a] Data were recorded in MeOD at 500 MHz, multiplicities and coupling constant are given in Hz; [b] data are abstracted from HMBC spectrum; [c] Data were recorded in DMSO-d_6 at 500 MHz, multiplicities and coupling constant are given in Hz (Murti, 2006); n.d.: not detected
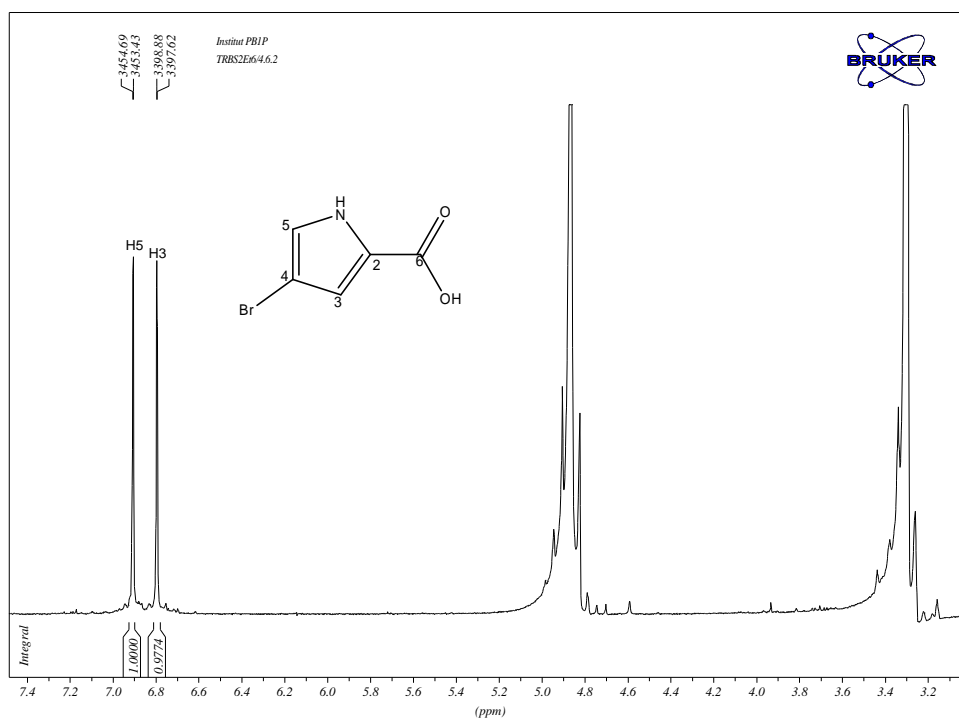
Fig.III.160. ^{1}H-NMR spectrum of compound **23** (MeOD, 500 MHz)

III.2.1.5. 4-Bromo-1*H*-pyrrole-2-carboxamide (**24**, known compound)
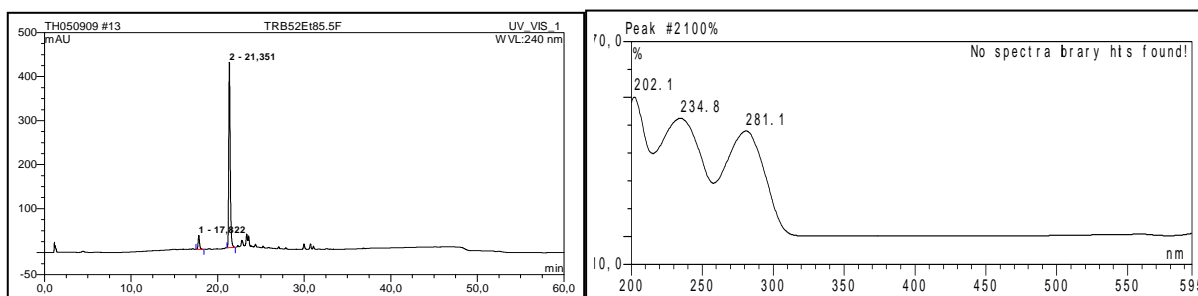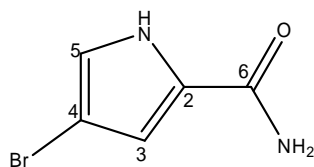

Fig.III.161. Compound **24**
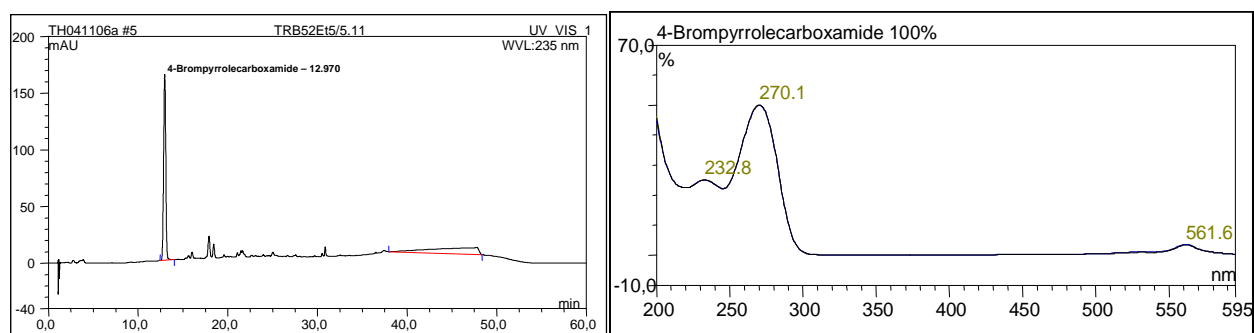
Fig.III.162. Analytic HPLC data of compound **24**
Left: HPLC profile in 240 nm, RT: 12.97; right: UV absorption spectrum, λ_{max} = 232.8; 270.1 nm

184
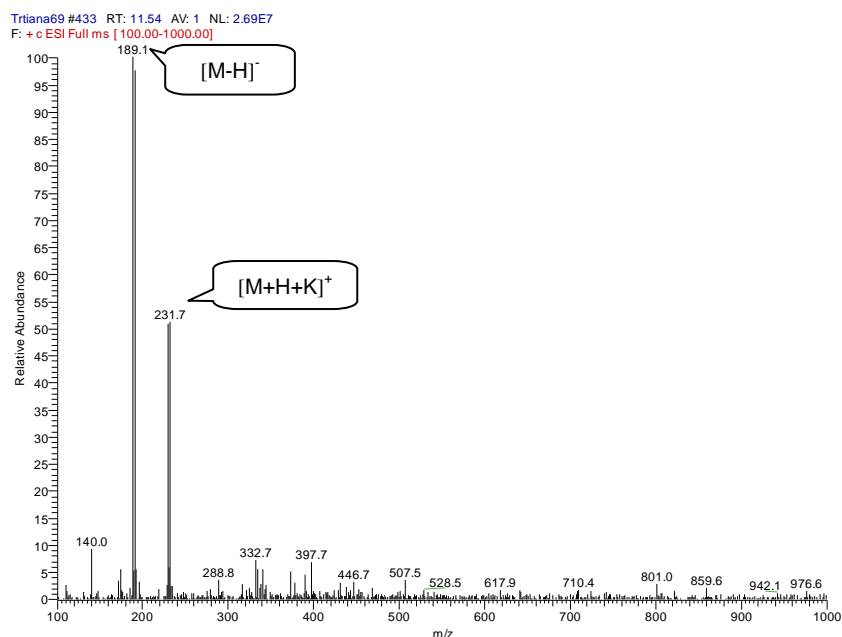
Fig.III.163. ESI-MS data of compound **24**

Compound **24** was obtained as a brown amorphous substance at an amount of 35 mg (0.014% of the sponge dried weight). Its UV absorption spectrum matched the internal spectra library for 4-bromopyrrole carboxamide (Fig.III.162). Pseudo molecular ion cluster at *m/z* 189/191 [M+H]$^+$ having an equal intensity is compatible to the molecular formula $C_5H_5BrN_2O$ of 4-bromopyrrole carboxamide. ^{1}H NMR data of compound **24** in DMSO-d_6 confirm the proposed structure as illustrated in Fig.III.164. The position of the bromine atom is confirmed by the pyrrole proton signals at δ_H 6.95 (dd, *J* = 1.6, 2.8 Hz, H-5) and at δ_H 6.83 (dd, 1.6, 2.5 Hz, H-3) (Mancini *et al.*, 1997; Pretsch, 2000; Hassan, 2004). The coupling constant of 1.6 Hz reveals the *meta* orientation of H-5 to H-3. Thus structure of compound **24** is determined as **4-bromo-1*H*-pyrrole-2-carboxamide.**

4-Bromo-1*H*-pyrrole-2-carboxamide was previously isolated from the marine sponges *Acanthella carteri* (Mancini *et al.*, 1997), *Axinella damicornis* (Hassan *et al.*, 2004) and *Agelas nakamurai* (Murti, 2006). It exhibits antimicrobial activity against

gram-positif bacteria and fungi (Iwagawa *et al.*, 1998), and cytotoxic activity against

NSCLC-N6 (human non-small-cell-lung carcinoma (IC_{50} = 4.8 µg/ml) (Hassan, 2004)
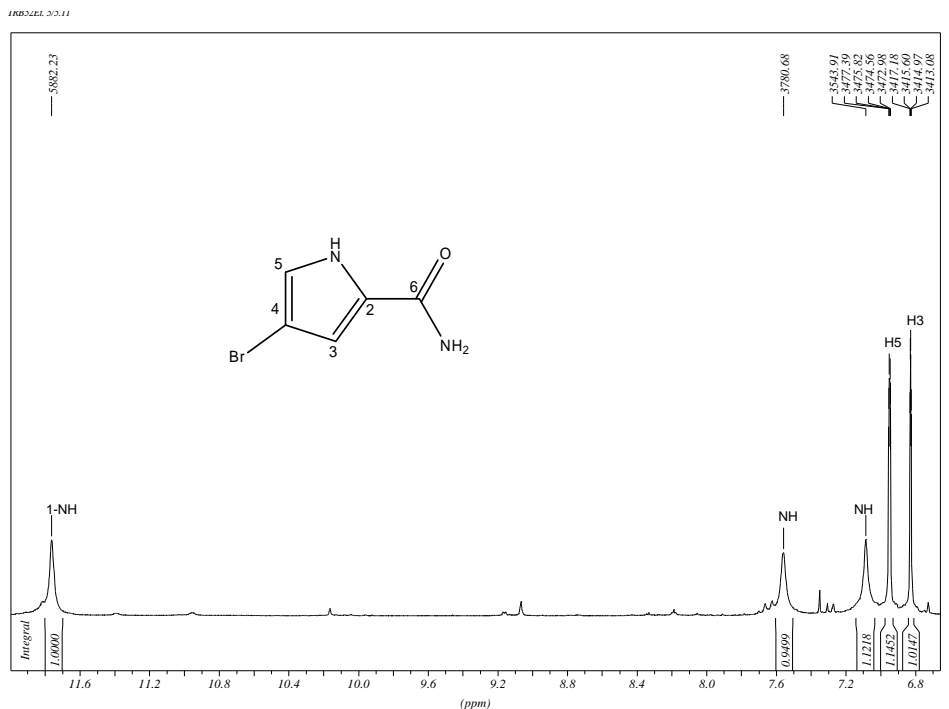
Fig.III.164. ^{1}H-NMR spectrum of compound **24** (DMSO-d_6, 500 MHz)

Table III.20. ^{1}H-NMR data of compound **24** in comparison with 4-bromo-1*H*-pyrrole-2-carboxamide

Atom No.	Compound 24 [a]		4-bromo-1*H*-pyrrole-2-carboxamide [a,b]	
	δ	Integration, Multiplicity (*J* in Hz)	δ	Integration, Multiplicity (*J* in Hz)
1-NH	11.76	1H, b s	11.80	1H, b s
NH$_2$	7.56	1H, b s	7.50	1H, b s
	7.09	1H, b s	7.10	1H, b s
5	6.95	1H, dd. 1.6, 2.8	6.97	1H, dd 1.7, 2.9
3	6.83	1H, dd, 1.6, 2.5	6.85	1H, dd 1.7, 2.9

[a] Data were recorded in DMSO-d_6 at 500 MHz, multiplicities and coupling constant are given in Hz; [b] Hassan (2004)

III.2.2. Other compounds isolated from *Agelas nakamurai*

III.2.2.1. 9-Methyladenine (**25**, known compound)
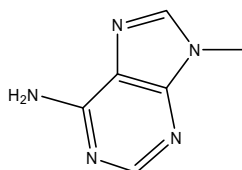
Fig.III.165. Compound **25**
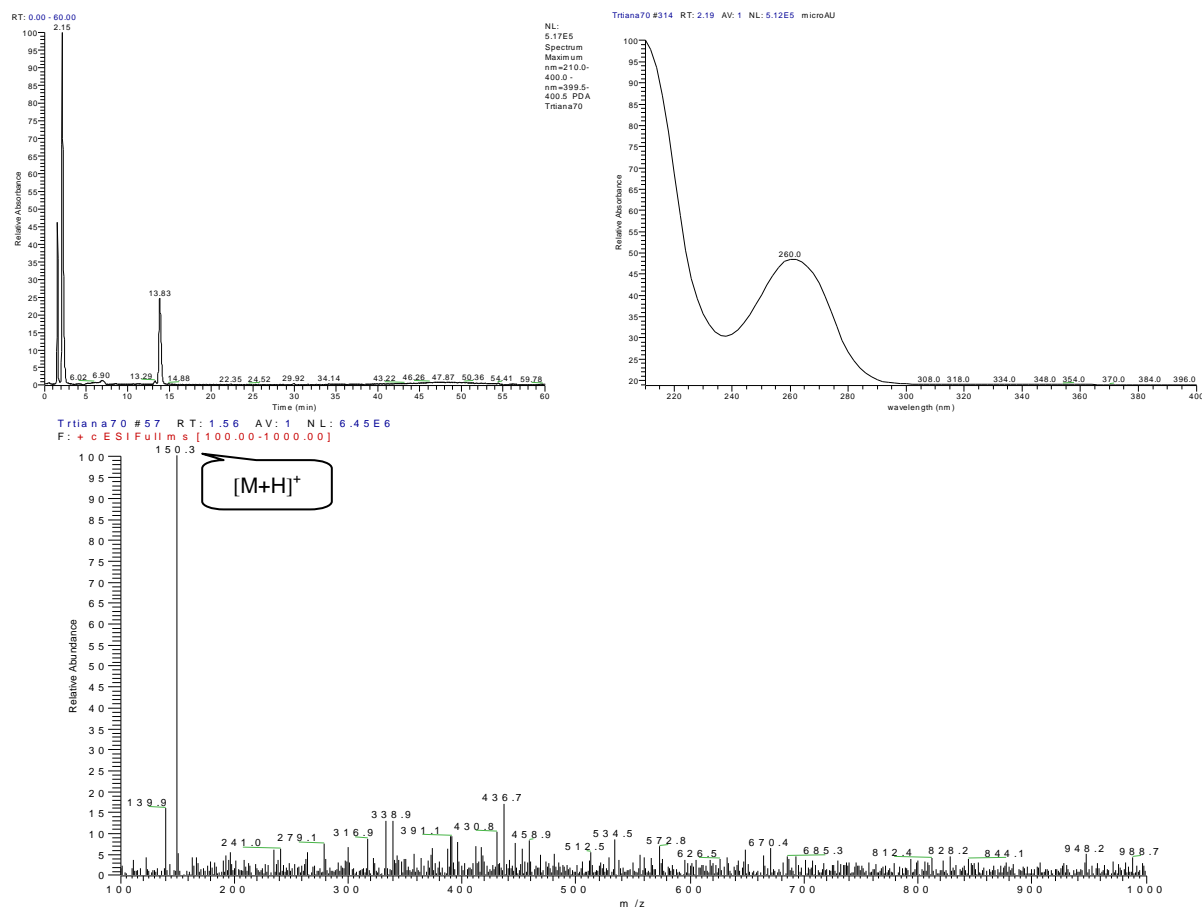
Fig.III.166. LCMS data of compound **25**
Above-left: RT: 2.15; right: UV absorption spectrum, λ_{max} = 260 nm; below: ESI-MS data

Compound **25** was isolated together with compound **23**, and the mixture was obtained as a brown oil at an amount of 66 mg (0.026% of the sponge dried weight). It elutes very early in HPLC chromatogram at RT = 2.15 min and show the ESIMS pseudo molecular ion peak at *m/z* 150 [M+H$^+$] which fits the molecular formula $C_{10}H_{13}N_5O_4$ of methyladenine.
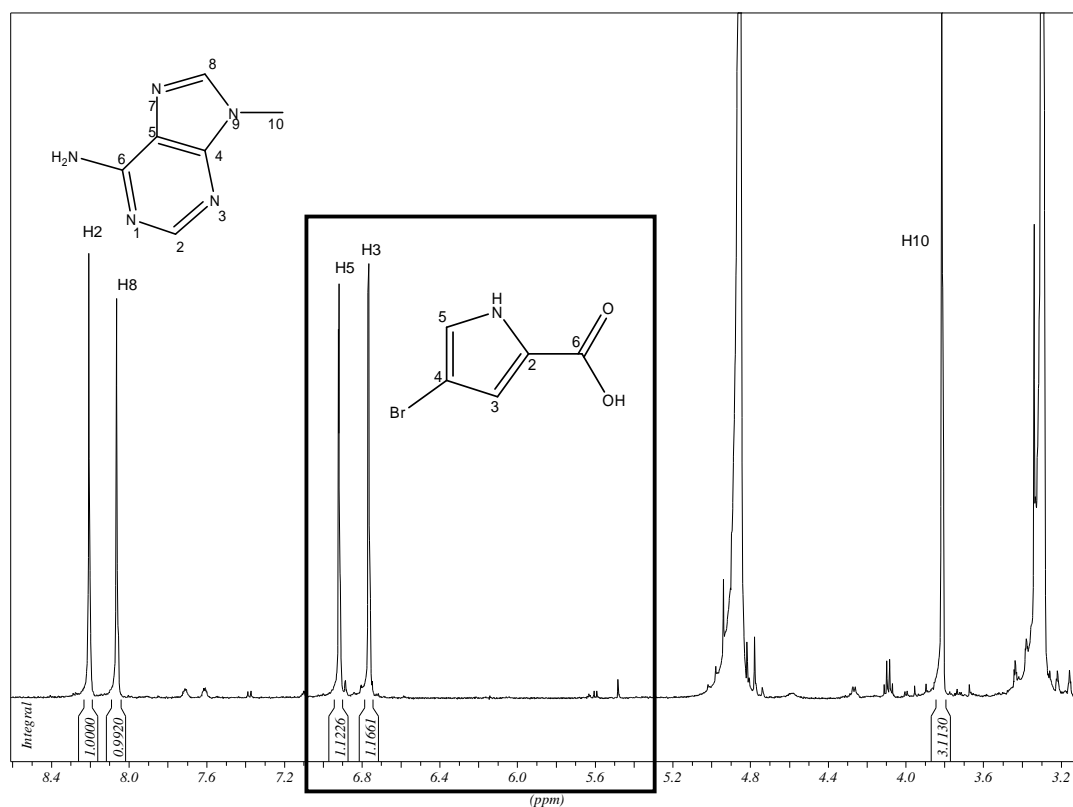
Fig.III.167. ^{1}H-NMR spectrum of compound **25** in a 1:1 mixture with compound **23** (MeOD, 500 MHz)

^{1}H NMR spectrum confirms the structure for methyl-adenine as evidenced by the detection of two deshielded sp^2 signals at δ_H 8.05 (1H, s) and δ_H 8.21 (1H, s) implying the adenine protons, and one NCH$_3$ signal at δ_H 3.81 (s) suggesting that the imidazole ring is methylated. According to Chenon and collaborators (1975), the 9-NH tautomer of adenine is the most stable form in comparison to the 7-NH. Therefore 9-methyladenine is more preferred than 7-methyladenine. ^{1}H–^{13}C HMBC spectrum supports this argument (Fig.III.168), as intensive cross peaks correlate the NCH$_3$ to C-4 (J^3_{C-H}) and C-8. ^{1}H-NMR data in comparison to adenosine (compound **26**) confirm the structure (Table III.21). Hence compound **25** is identified as **9-methyladenine**.
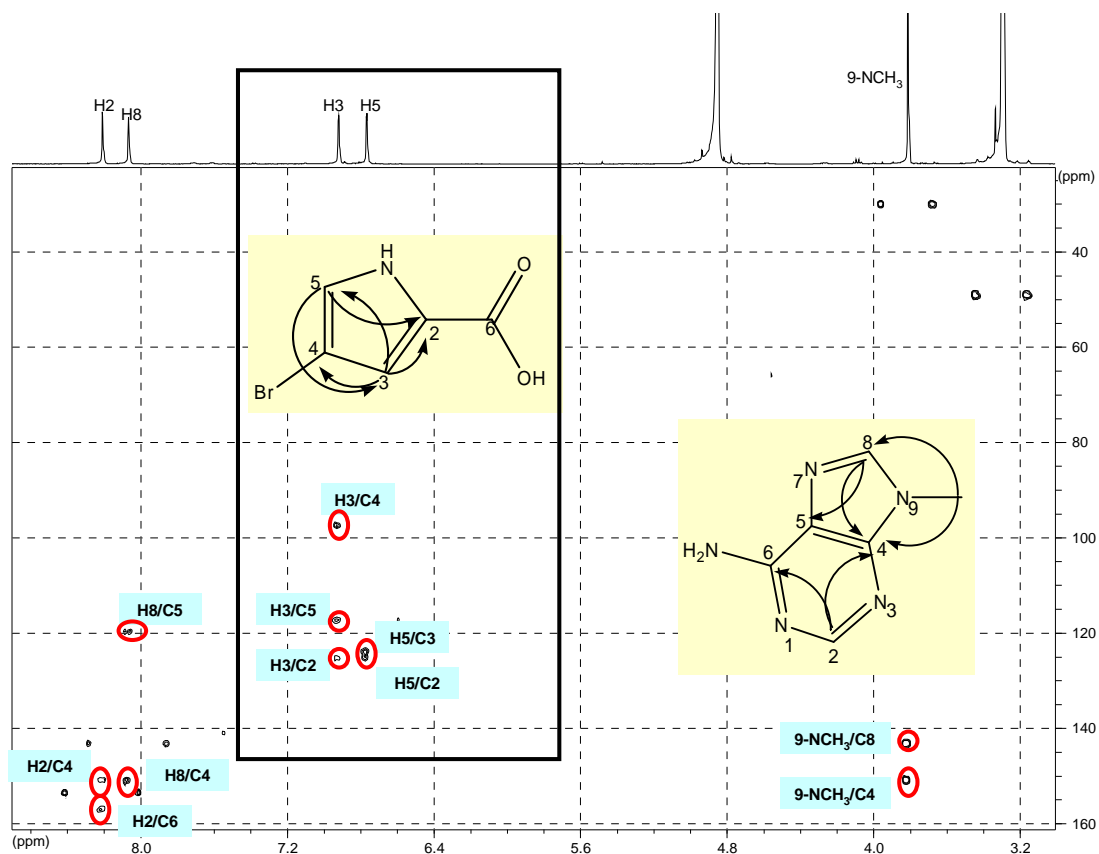
Fig.III.168. ^{1}H – ^{13}C HMBC spectrum of compound **25** in a 1.1 mixture with compound **23** (MeOD)

III.2.2.2. Adenosine (**26**, known compound)
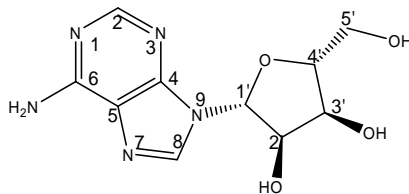
Fig.III.169. Compound **26**
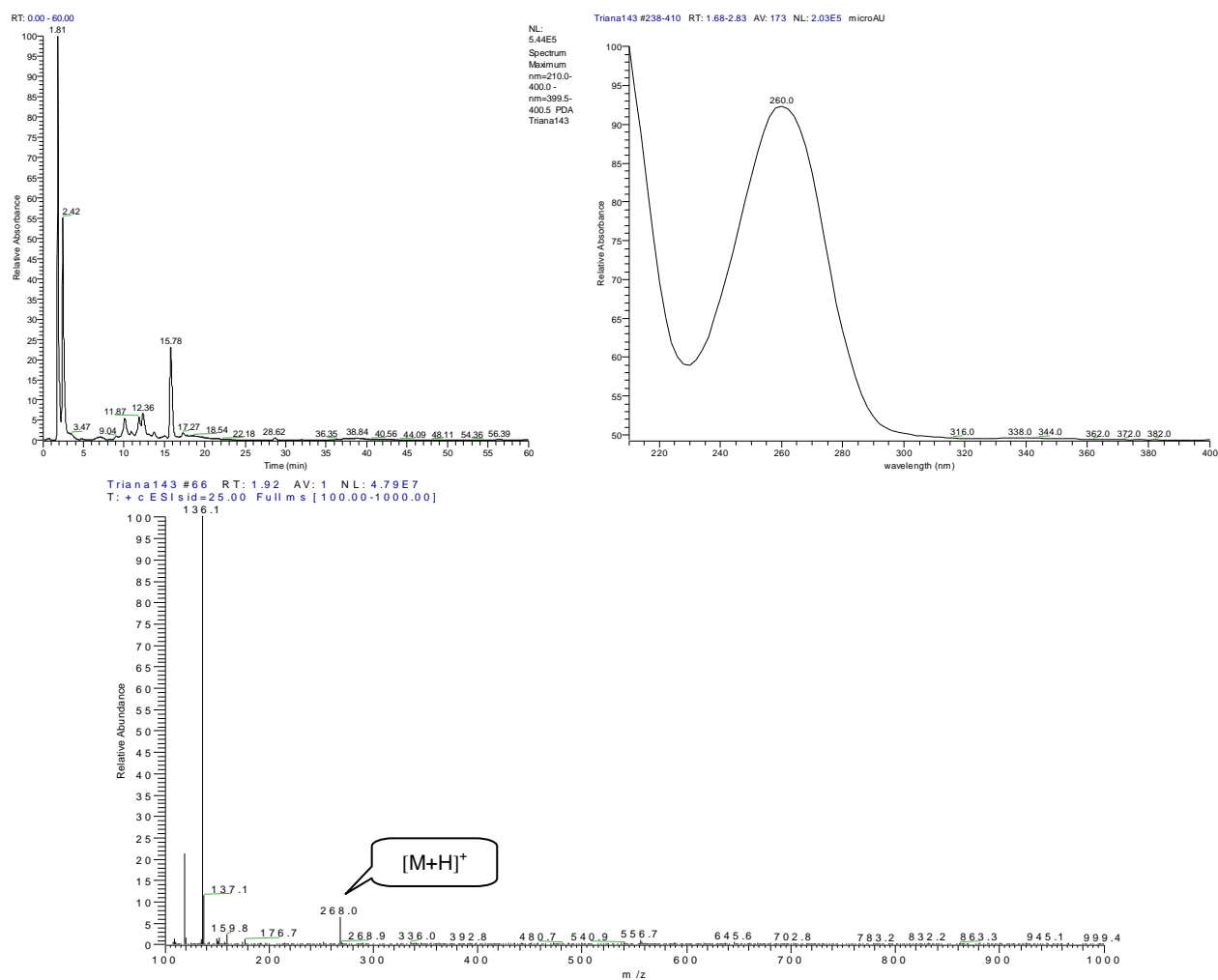
Fig.III.170. LCMS data of compound **26**
Above-left: RT: 1.81 and 2.42; right: UV absorption spectrum, λ_{max} = 260 nm
Below: ESIMS data of compound **26**

Compound **26** was isolated in a mixture with compound **23** in amount of 1 mg (0.0004% of the sponge dried weight). It shows a molecular ion peak at *m/z* 268 [M+H]$^+$ which together with ^{1}H NMR spectrum suggests the molecular formula $C_{10}H_{13}N_5O_4$ of adenosine.

The ^{1}H NMR spectrum shows two signals in the aromatic region at δ_H 8.2 (1H, s) and δ_H 8.30 (1H, s) which belong to the two protons in the purine nucleus implying an adenine moiety. Anomeric proton signal at δ_H 5.95 (d, *J* = 6.3 Hz), is indicative for the presence of a sugar function. This finding is supported by the

occurrence of the sugar proton signals at δ_H 4.32 (H-4'), 4.16 (H-3'), 3.88 (H-5'A), 3.62 (H-5'B), and 4.72 (H-2'). ^{1}H–^{1}H COSY spectrum reveals a spin system which correlates the protons of a ribose sugar and supports the proposed chemical structure (Fig.III.172).

After careful interpretation of NMR data in comparison to the literature (Baker, 2004), compound **26** is concluded to be **adenosine**.

Adenosine is a purine derivative that is widely distributed in nature. It is one of the principal nucleosides of nucleic acids. Purine and pyrimidines nucleotides are also major energy carriers, subunits of nucleic acids and precursors for the synthesis of nucleotide cofactors such as NAD.
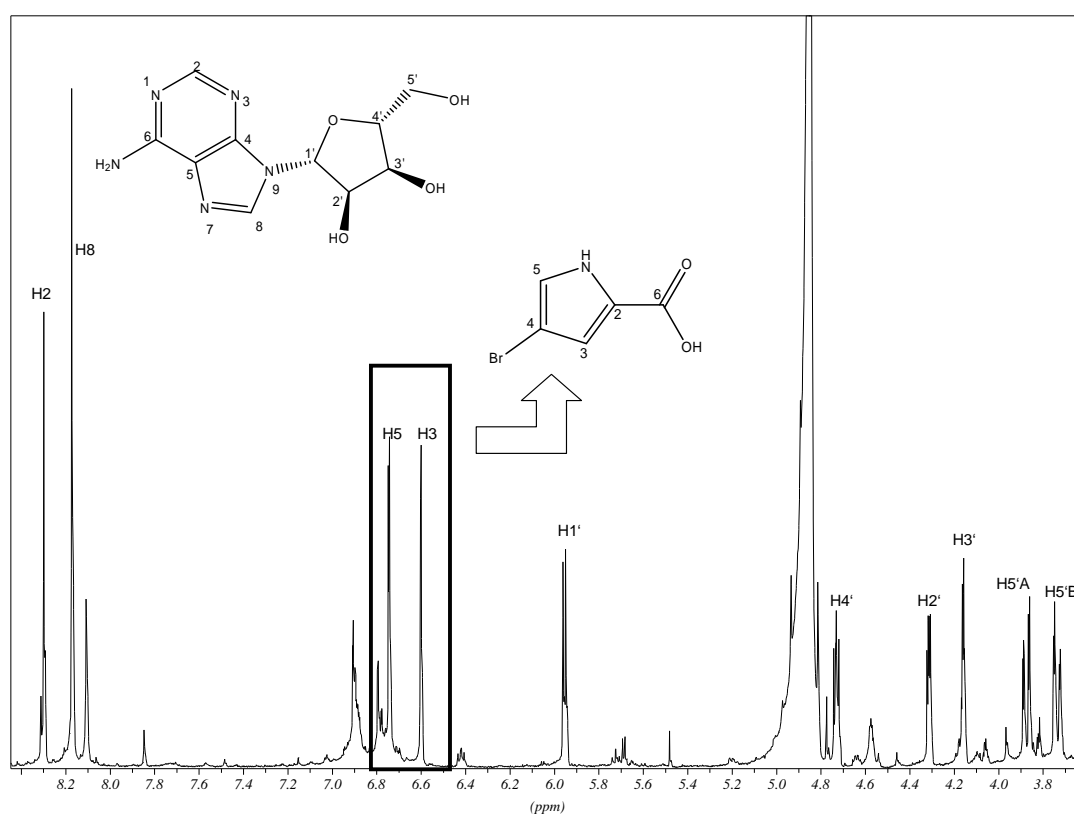
Fig.III.171. ^{1}H-NMR spectrum of compound **26** in 1.1 mixture with compound **23** (MeOD, 500 MHz)
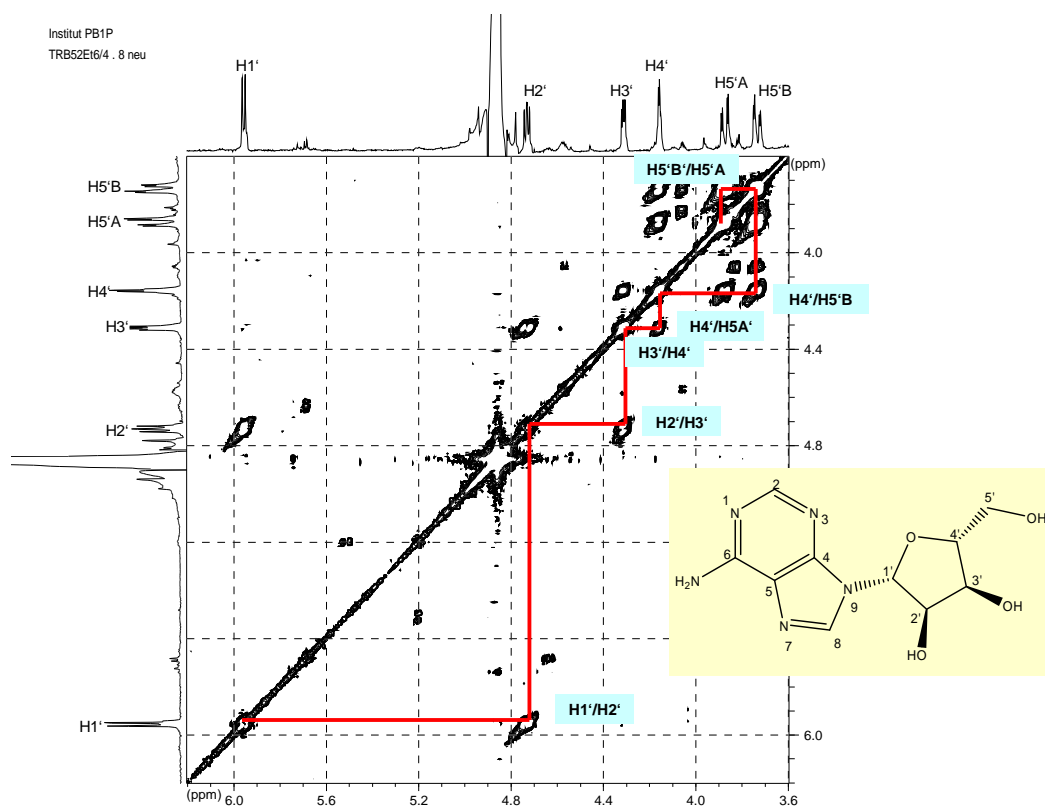
Fig.III.172. ^{1}H – ^{1}H COSY spectrum of compound **26** (MeOD)

Table III.21. NMR data of Compound **25** and **26** in comparison to adenosine

Atom No.	Compound 25 [a]			Compound 26 [a]			Adenosine [c]		
	^{1}H-NMR		^{13}C-NMR [b]	^{1}H-NMR		^{13}C-NMR [b]	^{1}H-NMR		^{13}C-NMR [b]
	δ	Integration, Multiplicity (*J* in Hz)	δ	δ	Integration, Multiplicity (*J* in Hz)	δ	δ	Integration, Multiplicity (*J* in Hz)	δ
2	8.21	1H, s	153.4	8.29	1H, s	136.6	8.30	1H, s	n.d.
4	-	-	150.8	-		165.4			
6	-	-	156.9	-		173.1			
5	-	-	119.6	-		141.7			
8	8.07	1H, s	143.1	8.16	1H, s	157.6	8.20	1H, s	n.d.
9-NCH$_3$	3.81	3H, s	29.9	-	-	-	-	-	-
1'	-	-	-	5.95	1H, d, 6.3	91.0	5.95	1H, d, 6.3	91.2
2'	-	-	-	4.72	1H, dd, 5.1, 6.3	72.4	4.72	1H, t, 6.3, 5.4	72.6
3'	-	-	-	4.32	1H, dd, 2.8, 5.1	75.2	4.32	1H, dd, 2.5, 5.1	74.0
4'	-	-	-	4.16	1H, dd, 2.5, 5.1	87.9	4.26	1H, dd, 2.8, 5.1	87.5
5'A	-	-	-	3.88	1H, dd, 2.5, 12.6	63.2	3.90	1H, dd, 12.6, 2.8	61.6
5'B	-	-	-	3.62	1H, dd, 2.8, 12.6		3.75	1H, dd, 12.6, 2.8	

[a] Data were recorded in MeOD at 500 MHz, multiplicities and coupling constant are given in Hz; [b] data are abstracted from HMBC spectrum; [c] Data were recorded in DMSO-*d$_6$* at 500 MHz, multiplicities and coupling constant are given in Hz (Baker, 2004); n.d.: not detected

III.3.   Secondary metabolites from *Pseudoceratina purpurea*

Sponges of the order Verongida are known to produce a wide range of bromotyrosine compounds with interesting biological activities. The unusually large number of biosynthetically related compounds has been linked to the potentially large number of chemical variations that are possible within the aromatic ring and/or side chains of the tyrosine moiety (Tabudravu and Jaspars, 2002). The aromatic ring can be either maintained, reduced, or oxidized (Capon and MacLeod, 1987) or mono- or dibrominated (Minale *et al.*, 1976; Yagi *et al.*, 1993). Usually it is based on 3,5-dibromo-tyrosine or less frequently 3-bromo-, 3-chloro-, 3,5-dichloro-, or 3-bromo-5-chloro-tyrosine (Kazlauskas *et al.*, 1981; D'Ambrosio, *et al.*, 1984). The bromotyrosine moiety can also undergo rearrangement to a spirooxepinisoxaline system, presumably via a common oxide intermediate as in the cases of the psammaplins (Roll *et al.*, 1985; Ichiba and Scheuer, 1993; Copp and Ireland, 1992). Other metabolites entail two or more tyrosine units through either amide bonding, as in aerothionin and homoaerothionin which also incorporate biogenic amines (Moody *et al.*, 1972), or ether bonds as in bastadins (Kazlauskas, *et al.*, 1981) or both bond types exemplified by fistularin-3 (Gopichand and Schmitz, 1979). In many cases, a single tyrosine unit is involved, as with dienone (dibromoverongiaquinol) (D'Ambrosio, *et al.*, 1982 and 1984), and aeroplysinin-1 (Fattorusso *et al.*, 1972).

Preliminary study on crude extracts of *Pseudoceratina purpurea* collected from Watudodol, Indonesia shows that it contains several bromotyrosine compounds (Fig.III.173).
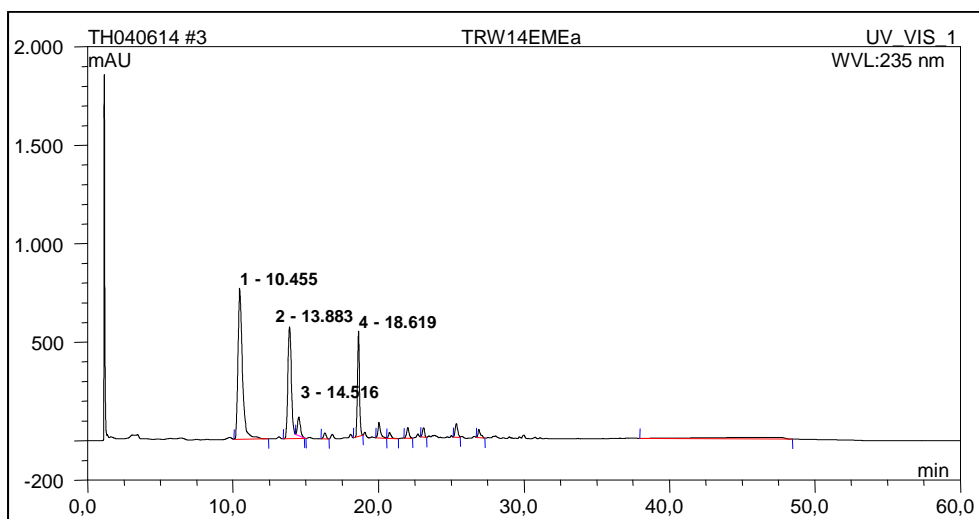
Fig.III.173. Chemical profile of *Pseudoceratina purpurea* ethyl acetate fraction detected by analytical HPLC at 235 nm (MeOH)
Peak 1: dienone dimethoxy ketal; peak 2: aeroplysinin-1; peak 3: dienone methoxy-ethoxy ketal; peak 4: bisoxazolidinone derivative

III.3.1. Aplysamine-2 (**27**, known compound)
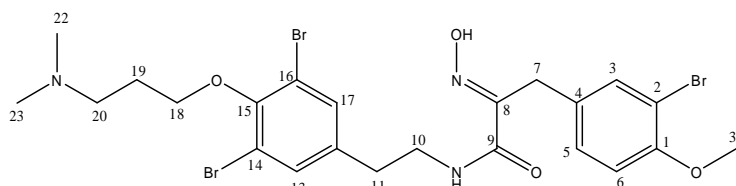
Fig.III.174. Compound **27**
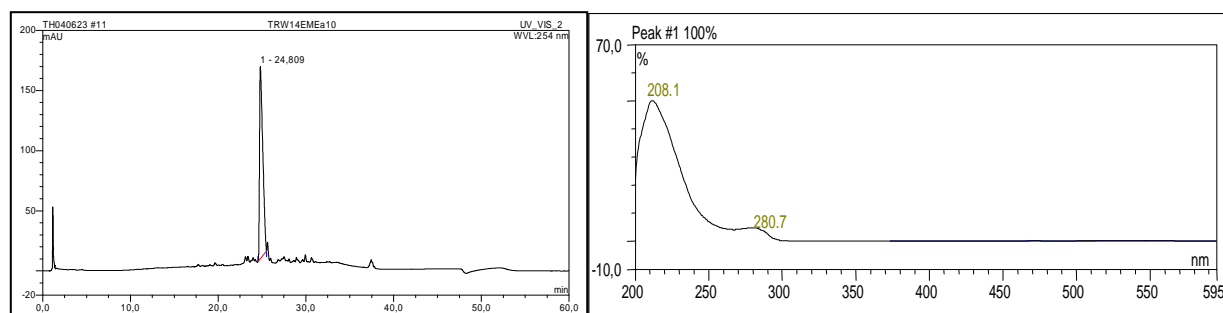
Fig.III.175. Analytical HPLC data of compound **27**
Left: HPLC profile in 254 nm, RT: 24.81; right: UV absorption spectrum, λ_{max} = 208.1; 280.7 nm
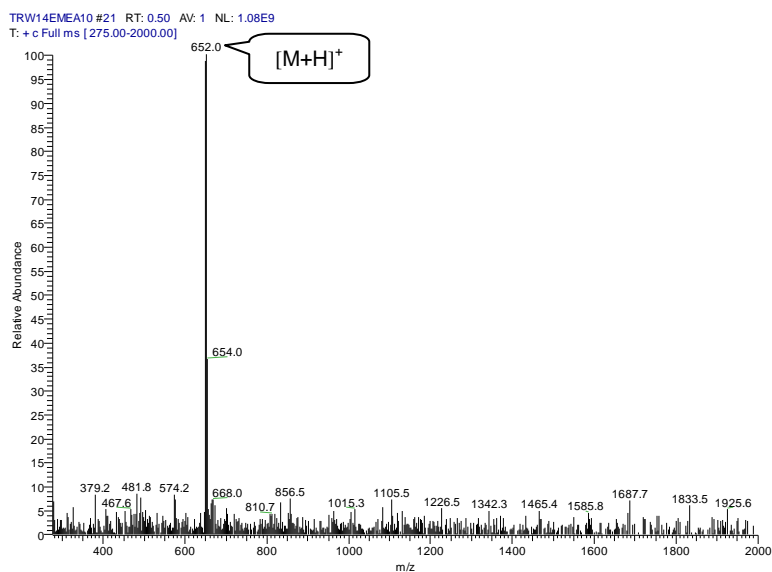
Fig.III.176. ESI-MS data of compound **27**

Compound **27** was obtained as a brown amorphous substance at an amount of 11.0 mg (0.042% of crude extract). ESIMS data reveals molecular weight of 647/649/651/653 g/mol in an intensity ratio of 1:2:2:1, and indicates possession of three bromines in the molecule. It corresponds to the molecular formula $C_{23}H_{28}Br_3N_3O_4$ for aplysamine-2. Aplysamine-2 was previously reported from the Australian marine sponge *Aplysina* sp. (Xynas and Capon, 1989), *Psammaplysilla purpurea* (Venkateswarlu *et al.*, 1999), *Pseudoceratina verrucosa* (Benharref *et al.*, 1996) and from *Pseudoceratina purpurea* (Kijjoa *et al.*, 2005).

^{1}H NMR spectrum reveals five protons in the low-field region showing 2 separated aromatic systems, three protons for an ABX ring system (ring A) and a symmetrical substituted aromatic unit (ring B). ^{1}H–^{1}H COSY spectrum (Fig.III.179) exhibits three separated spin systems and correlates the protons of ring A to an isolated deshielded methylene at δ_H 3.79 (2H, s, H_2-7). The second spin system correlates ring B protons to a methylene function at δ_H 2.76 (2H, d, *J* = 7.1 Hz, H_2-11) which in turn correlates further to another deshielded methylene at δ_H 3.45 (2H, d, *J* =

7.1 Hz, H_2-10). The third spin system is assigned as an oxypropylamine moiety based on the correlation of three methylene units at δ_H 3.96 (2H, dd, J = 6.0, 1.9 Hz, H_2-18), δ_H 2.03 (2H, dd, J = 6.0, 1.9 Hz, H_2-19), and δ_H 2.67 (2H, t, J = 6.0 Hz, H_2-20). The occurrence of two identical methyl groups at δ_H 2.29 (6H, s) recommends a tertiary amine group bearing two methyl groups.
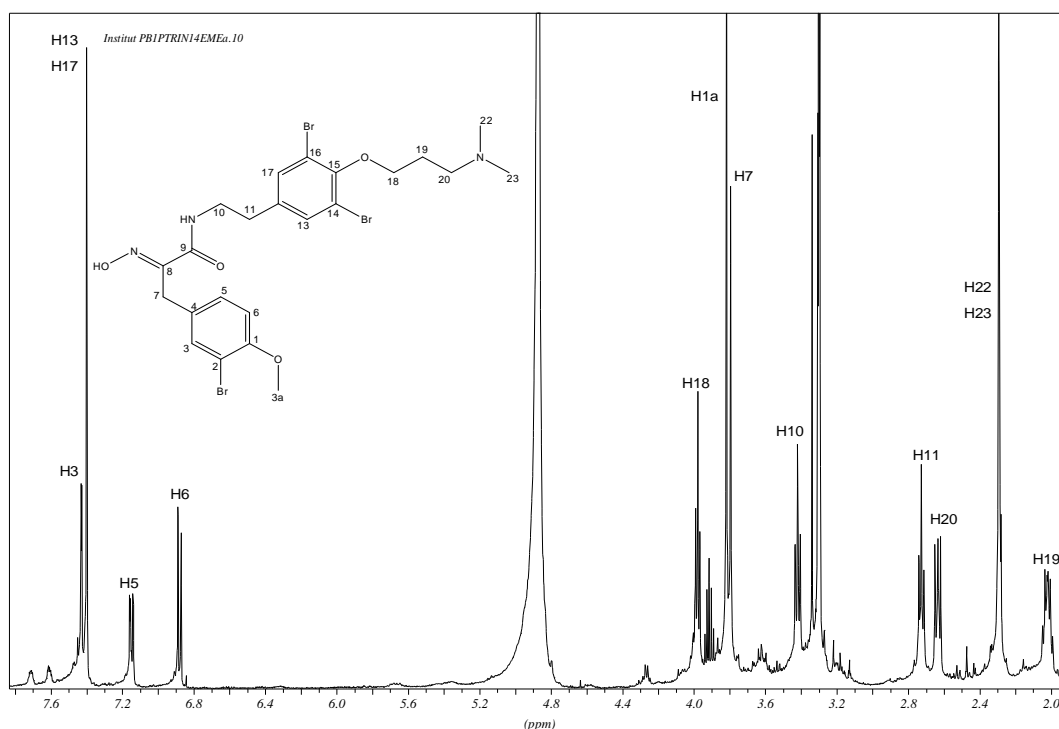
Fig.III.177. ^{1}H-NMR spectrum of compound **27** (MeOD, 500 MHz)

^{1}H–^{13}C HMBC spectrum supports these data and enables the assemblage of the substructures (Fig.III.180). Cross peak correlates a quaternary carbon at δ_C 155.9 (C-3) to a methoxy function at δ_H 3.81 (s, H-3A), H-5 at δ_H 7.15 (1H, dd, J = 8.5, 2.2 Hz), and H-4 at δ_H 6.88 (1H, d, J = 8.5 Hz) suggests that ring A is methoxylated. Another cross peaks correlates H-4 to a quaternary carbon at δ_C 112.1 (C-2) which indicates a bromine substitution. Therefore ring A is assigned as a 2-bromo-1-methoxybenzene which is further substituted by a methylene function (H-7) at

position 4. This methylene correlates to two deshielded quaternary carbons at δ_C 152.8 (C-8) and 165.8 (C-9). C-8 is assigned as an imino function (C=N) while C-9 as a carboxamide. HMBC cross peak correlating C-9 to H-10 and deshielded effect experiences by the H-10 at δ_H 3.45 (C-9) suggests a direct connection of the ethylidene chain (C-10—C-11) to the carboxamide function (C-9—NH). On the other side, C-9 is linked to C-7 through C-8. An oxime function is assigned at C-8. Furthermore, upfield chemical shift of C-7 at δ_C 28.7 implies an *E* configuration about the oxime functionality (Xynas and Capon, 1989).
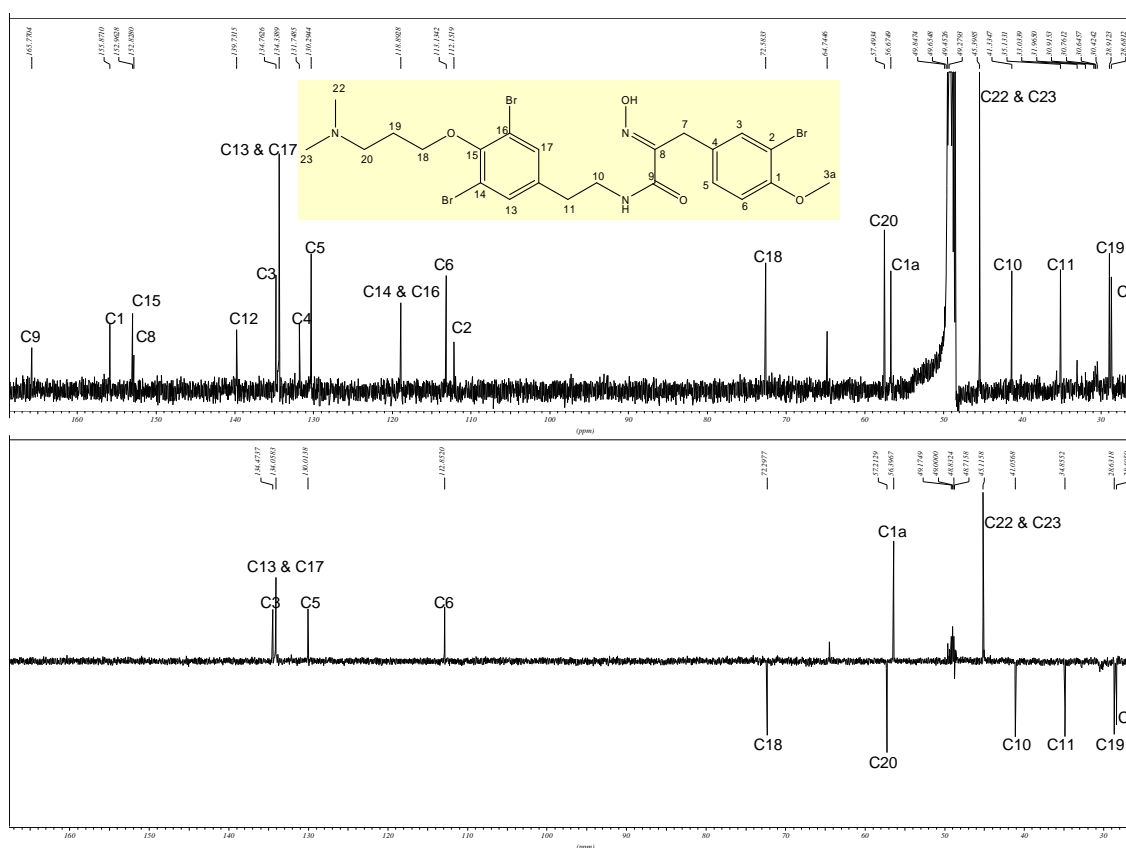
Fig.III.178. ^{13}C-NMR (above) and DEPT (below) spectra of compound **27** (MeOD, 125 MHz)

An allylic coupling of H-17 and H-13 to H-11 in ^{1}H–^{1}H COSY spectrum reveals that the ethylidene chain (C-10—C-11) is directly attached to the second ring (ring B). This finding is supported by ^{1}H–^{13}C HMBC spectrum showing cross peaks of

H-10 to a quaternary carbon of ring B (C-12) at δ_C 139.7, and of H-11 to tertiary

carbons at δ_C 134.3 (C-13 and C-17) as well as from H-13 and H-17 to carbon C-11.

Cross peaks of H-13 and H-17 to the brominated quaternary carbon at δ_C 118.9 are

likewise observed. Symmetrical signals found and the multiplicity of H-13 and H-17

recommend that ring B bears two bromines in *meta* position to each other. In *ortho*

position to the bromine substituents, C-17 and C-13 are unsubstituted while the

carbon in *meta* position (C-12) is linked to the ethyleneamide moiety. HMBC cross

peak correlates H-18 of the oxypropyldimethylamine to C-15 (δ_C 153.0, C) suggesting

that this moiety is linked to ring B in *ortho* position to the carbons bearing bromines.

Fig.III.179. ^{1}H-^{1}H COSY spectrum of compound **27** (MeOD)
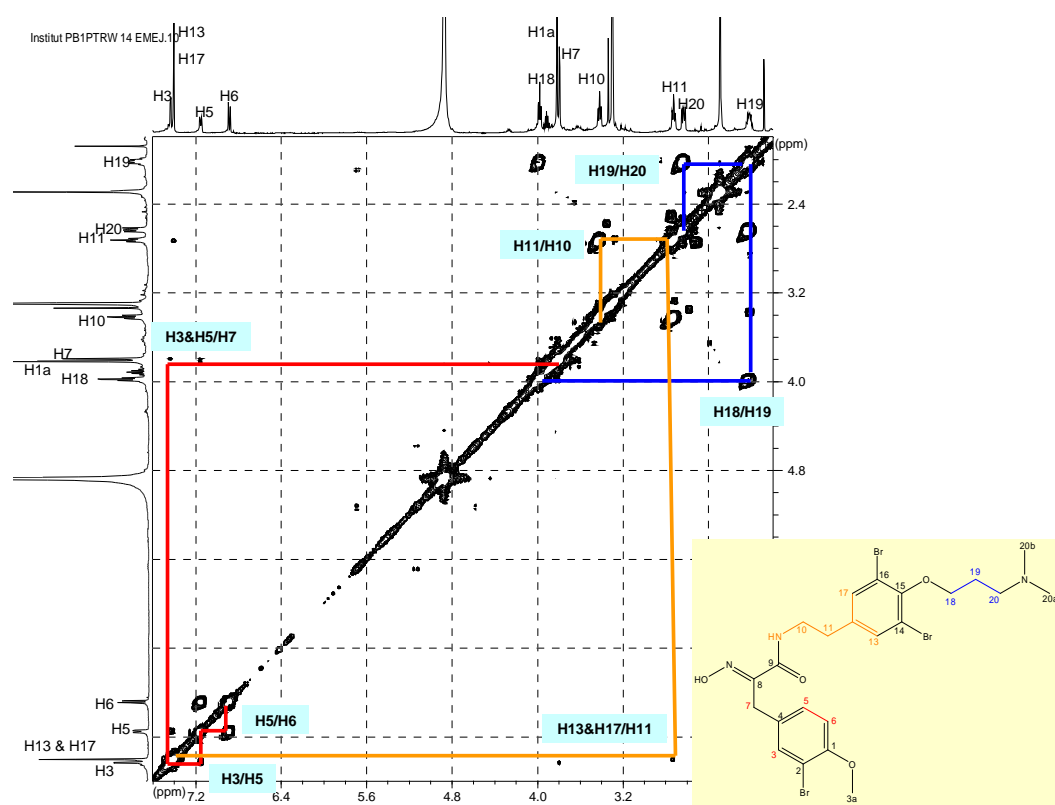
After careful investigation of the physical and spectral data in comparison to

the literature, compound **27** is distinguished as the known congener **aplysamine-2**, a

member of bromotyrosine derived secondary metabolite.
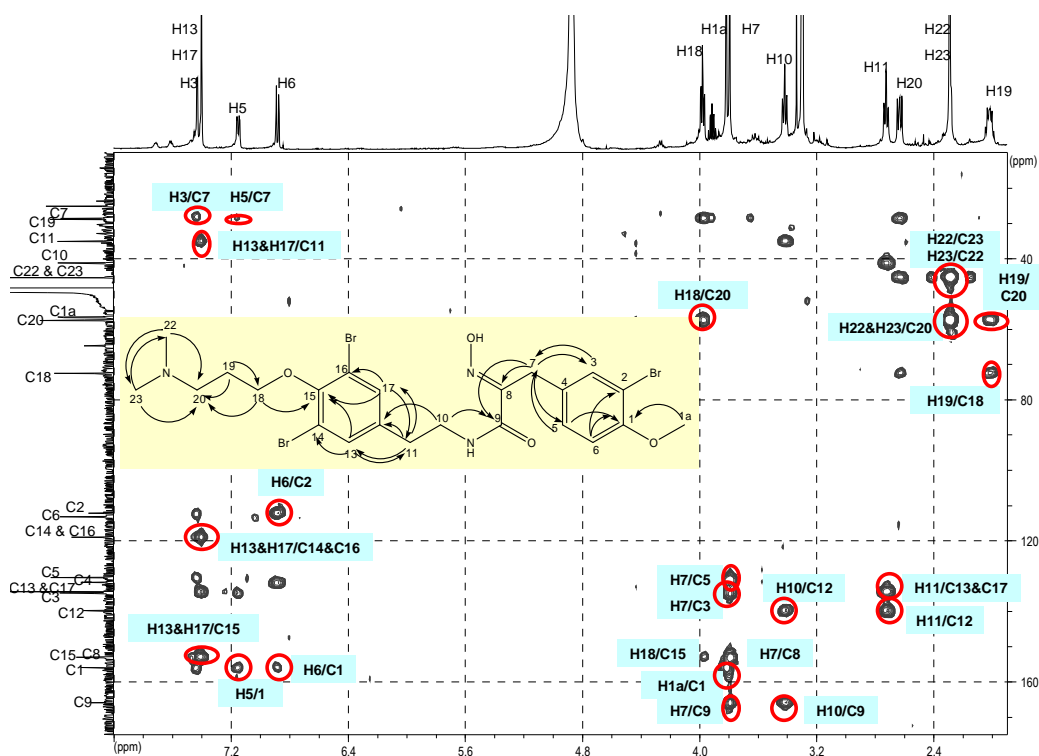
Fig.III.180. ^{1}H - ^{13}C HMBC spectrum of compound **27** (MeOD)

Table III.22. NMR data of compound **27** in comparison to aplysamine-2

Atom No.	Compound 27 [a]			Aplysamine-2 [a] [b]		
	^{1}H		^{13}C	^{1}H		^{13}C(δ)
	δ	multiplicity, J in Hz	δ, DEPT	δ	multiplicity, J in Hz	
1	-	-	155.9, C	-	-	155.8, C
2	-	-	112.1, C	-	-	130.3, C
3	7.43	1H, d, 2.2	134.7, CH	7.43	1H, d, 2.2	134.7, CH
1a (OMe)	3.81	3H, s	56.7, CH$_3$	3.81	3H, s	56.7, CH$_3$
4	-	-	131.7, C	-	-	113.1, C
5	7.15	1H, dd, 8.5, 2.2	130.0, CH	7.17	1H, dd, 2.2, 8.5	131.7, CH
6	6.88	1H,d, 8.5	113.1, CH	6.88	1H, d, 8.5	112.1, CH
7	3.79	2H, s	28.7, CH$_2$	3.79	2H, s	28.7, CH$_2$
8	-	-	152.8, C=N	-	-	152.9, C
9	-	-	165.8, C=O	-	-	165.8, C
10	3.45	2H, t, 7.1	41.3, CH$_2$	3.41	2H, t, 7.0	41.3, CH$_2$
11	2.76	2H, t, 7.1	35.1, CH$_2$	2.73	2H, t, 7.0	35.2, CH$_2$
12	-	-	139.7, C	-	-	140.3, C
13/17	7.40	2H, s	134.3, CH	7.42	2H, s	134.4, CH
14	-	-	118.9, C	-	-	118.7, C
15	-	-	153.0, C	-	-	152.1, C
16	-	-	118.9, C	-	-	118.7, C
18	3.96	2H, dd, 6.0,1.9	72.6, CH$_2$	4.05	2H, t, 5.5	71.7, CH$_2$
19	2.03	2H, dt, 6.0,1.9	28.9, CH$_2$	2.25	2H, tt, 5.5, 7.6	26.4, CH$_2$
20	2.67	2H, t, 6.0	57.5, CH$_2$	3.46	2H,t, 7.6	56.9, CH$_2$
22 & 23	2.29	6H, s	45.4, CH$_3$	2.93	6H, s	43.7, CH$_3$

[a] Data were recorded in MeOD at 500 MHz, multiplicities and coupling constant are given in Hz;
[b] Xynas and Capon (1989)

III.3.2. **(+)-Aeroplysinin-1** (**28**, known compound)
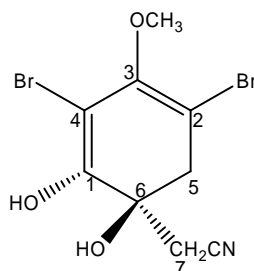
Fig.III.181. Compound **28**
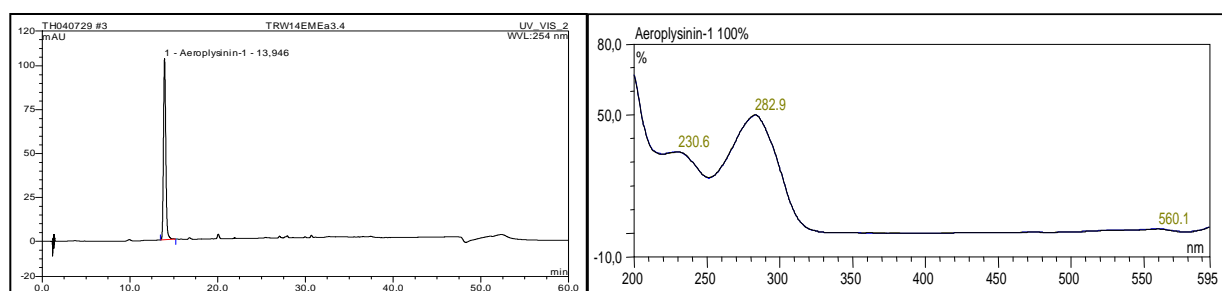
Fig.III.182. Analytical HPLC data of compound **28**

Left: HPLC profile in 254 nm RT: 13.95; right: UV absorption spectrum, λ_{max} = 230.6; 282.9 nm
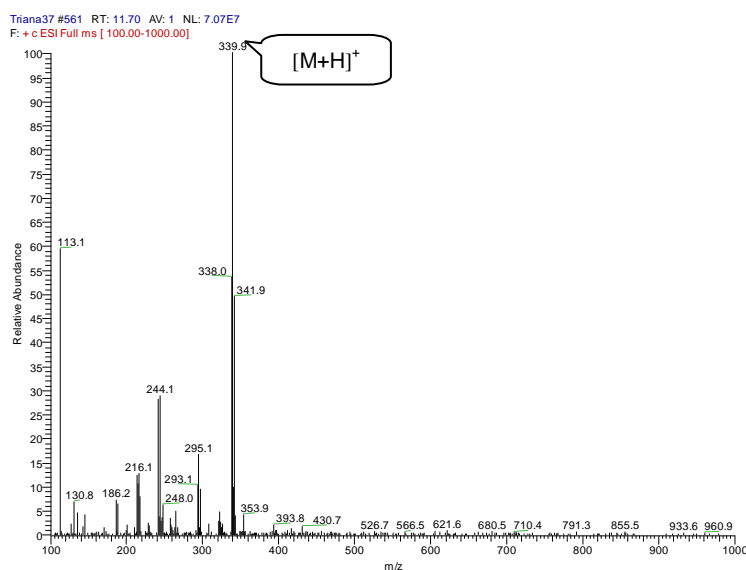
Fig.III.183. ESI-MS data of compound **28**

Compound **28** was obtained as a brown oily substance in an amount of 79 mg (0.30 % of sponge crude extract). Its analytical HPLC spectrum matched the internal spectral library data base for aeroplysinin-1. This finding is supported by the ESIMS isotopic ion cluster of a dibrominated compound at *m/z* 338/340/342 [M+H]$^+$ having an intensity ratio of 1:2:1. This corresponds to the molecular formula

$C_9H_9Br_2NO_3$ of aeroplysinin-1.

^{1}H NMR spectrum (Table III.23) supports the proposed structure. It exhibits a methylene group at δ_H 2.77 (2H, d, *J* = 7.2 Hz, H-7), a methoxy group at δ_H 3.74 (s, 3H), a *sp^2* proton signal at δ_H 6.29 (1H, d, *J* = 1.0 Hz, H-5) and a methine unit next to an electronegative atom at δ_H 4.06 (1H, d, *J* = 1.3 Hz, H-1). Hence this supports the structure of compound **28** as **aeroplysinin-1**.
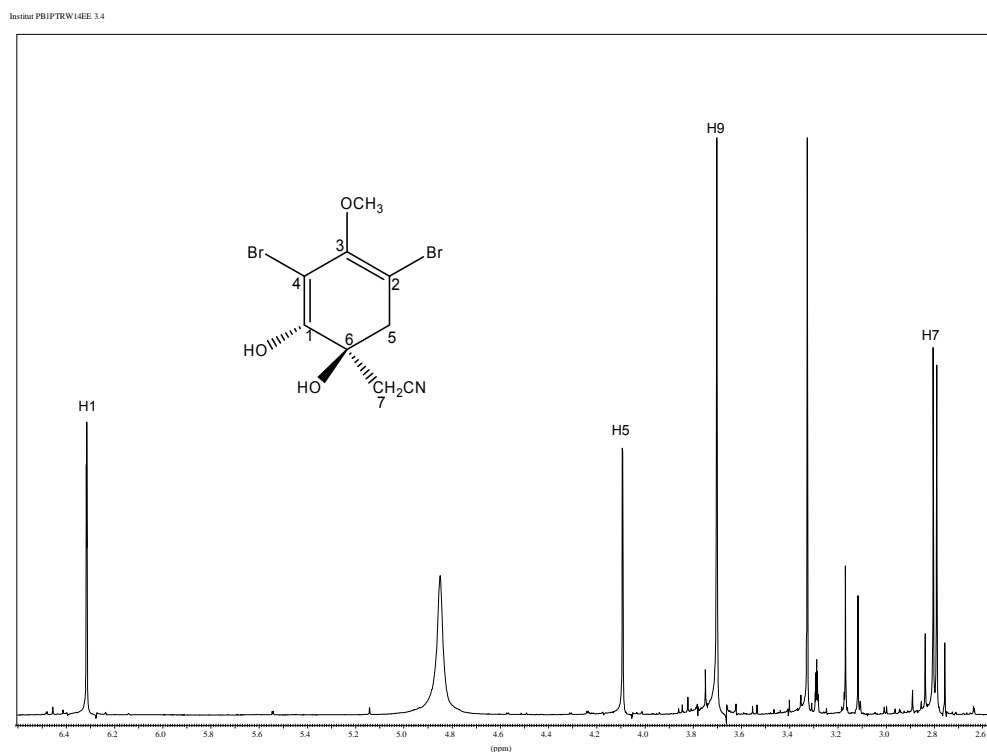
Fig.III.184. ^{1}H NMR spectrum of compound **28** (MeOD, 500 MHz)

Aeroplysinin-1 is optically active due to a chiral center on C-1. Therefore two possible stereoisomers exist. $[\alpha]_D^{20}$ value +110.91° ± 0.46° (*c* 0.5, CH$_3$OH) of compound **28** is compatible to the reported optical rotation of (+)-aeroplysinin-1 ($[\alpha]_D^{20}$ = +186° (*c* 0.5, CH$_3$OH) (Fattorusso *et al.*, 1970). The absolute configuration of the dextrorotatory enantiomer was provided by the determination of the CD curve (Fulmor *et al.*, 1970).

Table.III.23. ^{1}H NMR data of compound **28** in comparison to (+)-aeroplysinin-1

| Atom No | Compound 28 [a] | | | (+)-Aeroplysinin-1 [b] | |
| | ^{1}H | | ^{13}C [c] | ^{1}H | |
	δ	Integration, multiplicity, *J* in Hz	δ	δ	Integration
1	4.06	1H, d, 1.3	78.7	4.10	1H
2	-	-	114.2	-	-
3	-	-	148.7	-	-
4	-	-	121.4	-	-
5	6.29	1H, d, 1.0	133.1	6.34	1H
6	-	-	74.5	-	-
7	2.77	2H, d, 7.2	26.9	2.74	2H
8	-	-	118.2	-	-
9	3.73	3H, s	n.d.	3.70	3H
1-OH	n.d.		-	4.16	1H
6-OH	n.d.		-	2.28	1H

[a] Data were recorded in MeOD at 500 MHz, multiplicities and coupling constant are given in Hz; [b] Data were recorded in CD_3CN, (Fattorusso *et al.*, 1970); data are abstracted from HMBC spectrum; n.d.: not detected

(+)-Aeroplysinin-1 was first isolated from marine sponge *Aplysina aerophoba* (*Verongia aerophoba*) (Fattorusso *et al.*, 1970), and later it is also reported from other marine sponges e.g., *Psammaplysilla purpurea* (Chang and Weinheimer, 1977), *Aiolochroia crassa*, *Verongula rigida*, and *Aplysina archeri* (Makarieva *et al.*, 1981). The enantiomorphic form, (-)-aeroplysinin-1 was reported from the marine sponges, *Ianthella ardis* (Cosulich and Lovell, 1971; Fulmor *et al.*, 1970) and *Verongula gigantea* (Makarieva *et al.*, 1981). The racemic form is also described from *Verongula gigantean,* and *Aiolochroia crassa* (Makarieva *et al.*, 1981). Both enantiomers are reported to be active against gram positive and gram negative bacteria (Fulmor *et al.*, 1970). Antiangiogenic activity was also reported for aeroplysinin-1 (Rodríquez-Nieto *et al.*, 2002) as well as cytotoxicity activity against Ehrlich ascites tumor and HeLa tumor cell lines (Koulman *et al.*, 1996).

III.3.3. 5-(3,5-dibromo-4-((2-oxooxazolidin-5yl)methoxy)phenyl)oxazolidin-2-

one (**29**, known compound)
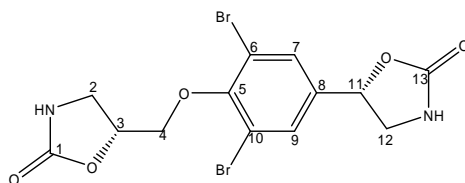
Fig.III.185. Compound **29**
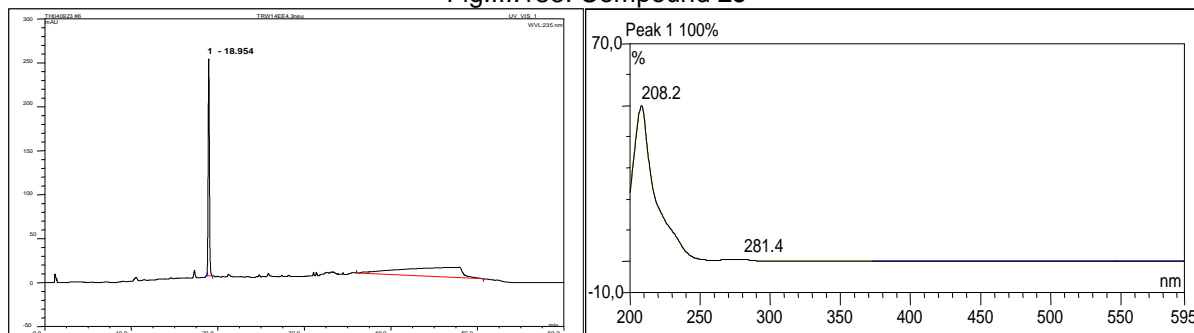
Fig.III.186. Analytical HPLC data of compound **29**
Left: HPLC profile in 235 nm RT: 18.95; right: UV absorption spectrum, λ_{max} = 208.2; 281.4 nm
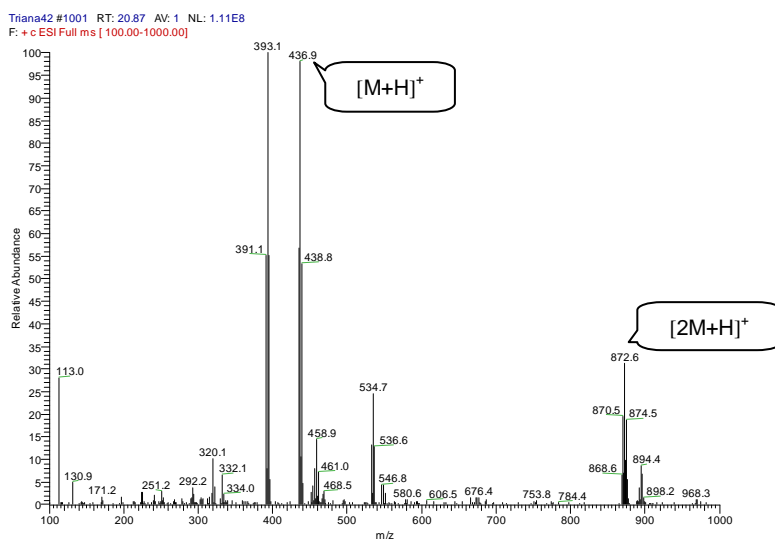
Fig.III.187. ESI-MS data of compound **29**

Compound **29** was obtained as a white amorphous substance in an amount of 26 mg (0.10% of crude extract). It shows similar UV absorption pattern with aplysamine-2 (compound **27**) suggesting the presence of a similar chromophore. ESIMS isotopic pseudo molecular ion peaks at *m/z* 435/437/439 [M+H]$^{+}$ at an intensity ratio of 1:2:1 suggests the presence of two bromines in the molecule. These

findings recommend a bromotyrosine-related compound. Furthermore, the molecular weight is compatible with molecular formula $C_{13}H_{12}Br_2N_2O_5$ of a 5-(3,5-dibromo-4-((2-oxooxazolidin-5yl)methoxy)phenyl)oxazolidin-2-one.
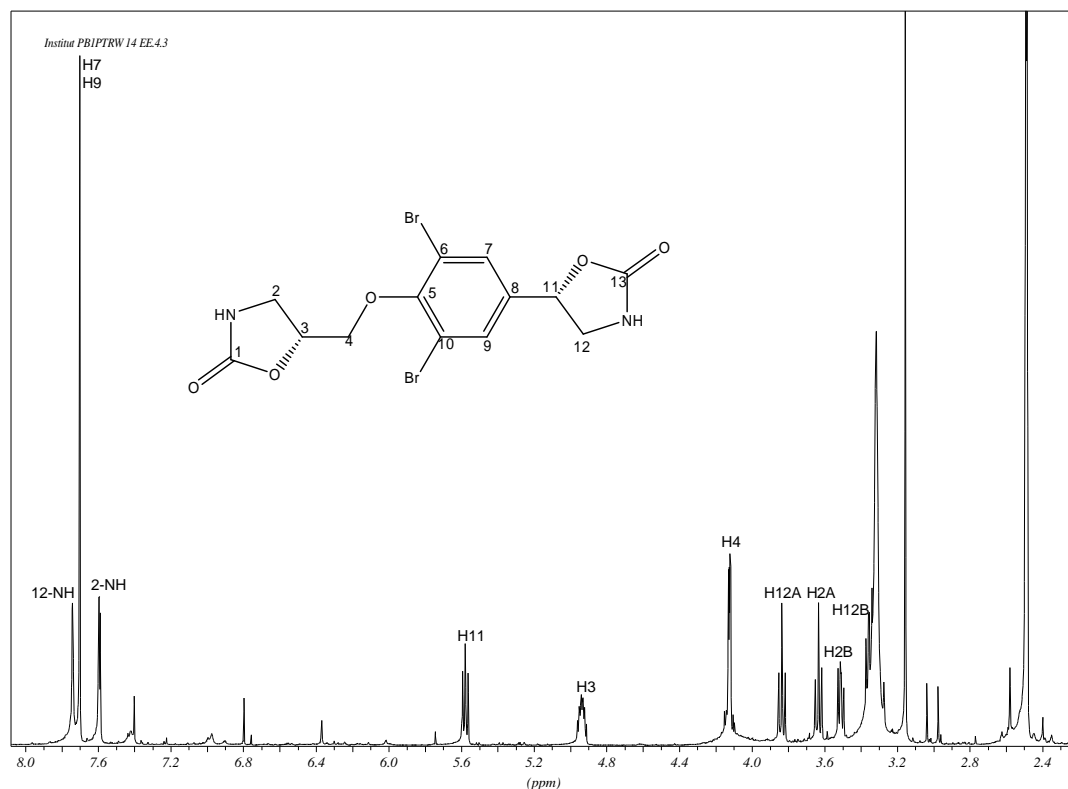
Fig.III.188. ^{1}H-NMR of compound **29** (DMSO-d_6, 500 MHz)

^{1}H NMR supports the proposed structure. A symmetrical tetra-substituted aromatic ring is shown by a singlet proton at δ_H 7.73 integrating for two protons. Furthermore, two oxazolidinone rings are shown by two NH signals at δ_H 7.74 (1H, b s, 12-NH) and δ_H 7.60 (1H, b s, 2-NH); two separated methylene protons coupled to two methine unit at δ_H 5.58 (1H, t, J = 7.9 Hz, H-11) and at δ_H 4.93 (2H, m, H$_2$-3), respectively. These two oxazolidinone ring experience a different environment. The first oxazolidinone ring is directly attached to the aromatic ring, while the second one is connected to the aromatic ring through an oxymethylene unit (H-4). These

assignments are supported by the ^{1}H-^{13}C HMBC spectrum. It reveals a J^3 correlation of the oxazolidinone ring methine proton (H-11) to the aromatic carbons. Furthermore cross peaks of a deshielded methylene proton signal at δ_H 4.13 (2H, m, H$_2$-4) to the carbon of the second oxazolidinone methylene (δ_C 41.1, C-2) as well as to the carbon of the aromatic ring at δ_C 153.1 (C-5) are observed. J^3 correlation of the aromatic protons (H-7 and H-9) to the methine carbon at δ_C 47.0 suggests that the bromines are located at positions 6 and 10. Upfield chemical shifts of carbon 6 and 10 at δ_C 117.5 in comparison to C-7 and C-9 at δ_C 130.4 support this finding.

Careful interpretation of the spectral data in comparison to the literature (Norte *et al.*, 1988; Makarieva *et al.*, 1981; Borders *et al.*, 1974; and Fouad, 2004) established compound **29** as the known derivative **5-(3,5-dibromo-4-((2-oxooxazolidin-5yl)methoxy)phenyl)oxazolidin-2-one**. Concerning the two chiral carbon atoms in compound **29** (C-3 and C-11), four stereoisomers are possible, i.e, (*R*, *R*), (*R*, *S*), (*S*, *R*), (*S*, *S*). Three of them were already reported to be isolated from the nature, while the (*S*, *S*) form has not yet been encountered (Kossuga *et al.*, 2004; Norte *et al.*, 1988; Makarieva *et al.*, 1981; Borders *et al.*, 1974). Analysis of coupling constants of compound **29** in DMSO-d_6 can not clearly differentiate its possible relative configuration, since *J* values for hydrogen couplings in both carbamoyl side chains are ca. 8 Hz. However, a tentative assignment of configuration can be made by comparison of specific rotations as follows. The absolute configuration of the levorotatory (*R,R*) isomer $[\alpha]_D$ -33°, *c* 1.1, MeOH was established unambiguously by single-crystal X-ray diffraction (Norte *et al.*, 1988). Another levorotatory enantiomer showing a $[\alpha]_D$ value of -9.2° (*c* 0.35, MeOH) and

was determined to have a relative configuration (R^*,S^*) (Kossuga *et al.*, 2004). Rogers *et al.* (2005) reported later its absolute configuration as 11R, 6S (note different numbering scheme) by using microscale hydrolysis followed by derivatization with Marfey's reagent. Since compound **29** exhibits magnitude of rotation value of $[\alpha]_D^{20}$ -6.6º ± 0.6º (*c* 0.28, CH$_3$OH), therefore its relative configuration was suggested to be (R^*,S^*).
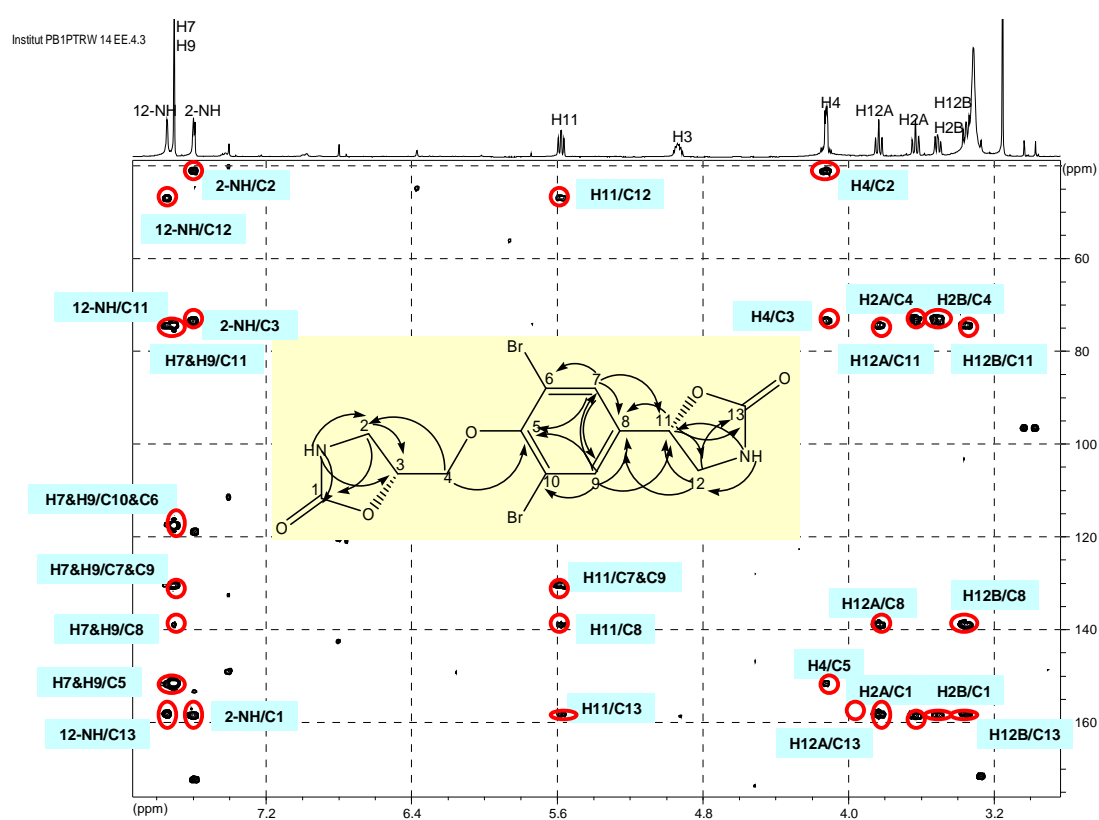
Fig.III.189. ^{1}H–^{13}C HMBC spectrum of compound **29** (DMSO-*d$_6$*)

Table.III.24. NMR data of compound **29** in comparison to 5-(3,5-dibromo-4-((2-oxooxazolidin-5yl)methoxy)phenyl)oxazolidin-2-one

Atom No	Compound 29 [a]		[13]C [c]	5-(3,5-Dibromo-4-((2-oxooxazolidin-5yl)methoxy)phenyl)oxazolidin-2-one [a] [b]		[13]C
	[1]H			[1]H		
	δ	Integration, multiplicity, *J* in Hz	δ	δ	Integration, multiplicity, *J* in Hz	δ, DEPT
1	-	-	158.3	-	-	158.2, C=O
2-NH	7.60	1H, s	-	7.60	1H, s	-
2A	3.63	1H, t, 9.0	41.1	3.65	1H, t, 8.8	41.3, CH$_2$
2B	3.51	1H, dd, 6.9, 9.1		3.53	1H, t, 8.2	
3	4.93	1H, m	73.4	4.95	1H, m	73.6, CH
4	4.13	2H, t, 2.4	73.3	4.14	2H, m	73.1, CH$_2$
5	-	-	153.1	-	-	151.7, C
6 & 10	-	-	117.5	-	-	117.7, C
7 & 9	7.73	2H, s	130.4	7.73	2H, s	130.5, CH
8	-	-	138.9	-	-	139.0, C
11	5.58	1H, t, 7.9	74.3	5.58	1H, t, 8.5	74.4, CH
12-NH	7.74	1H, s	-	7.78	1H, s	-
12A	3.84	1H, t, 9.0	47.0	3.84	1H, t, 8.5	47.0, CH$_2$
12B	3.38	1H, dd, 7.2, 9.1		3.41	1H, dd, 8.5, 6.9	
13	-	-	158.0	-	-	158.5, C=O

[a] Data were recorded in DMSO-d_6 at 500 MHz, multiplicities and coupling constant are given in Hz; [b] Fouad., 2004; [c] data are abstracted from HMBC spectrum

III.3.4. **Dienone dimethoxyketal** (**30**, known compound)
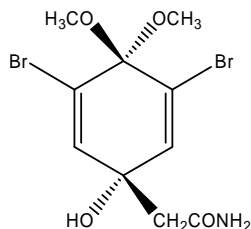
Fig.III.190. Compound **30**
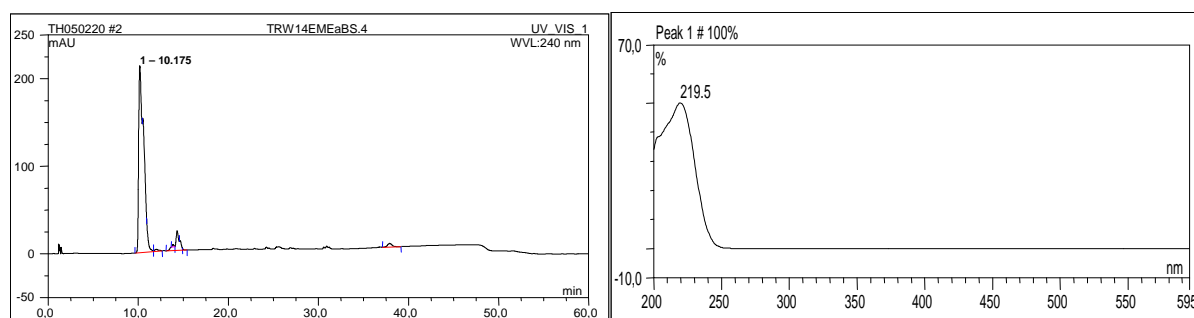
Fig.III.191. Analytical HPLC data of compound **30**
Left: HPLC profile in 240 nm RT: 10.18; right: UV absorption spectrum, λ_{max} = 219.5
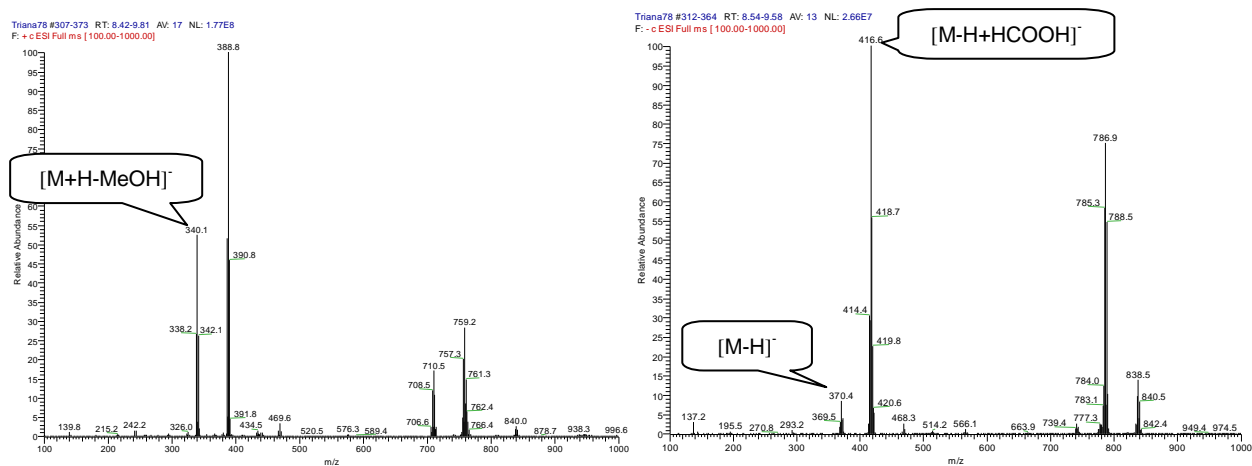
Fig.III.192. ESI-MS data of compound **30**

Compound **30** was isolated as a white amorphous substance with a yield of 40 mg (0.15% of crude extract). It shows $[\alpha]_D^{20}$ value of -4.0º ± 0.6º (*c* 0.65, CH₃OH) and UV maximum absorbance at 219.5 nm. The positive ESIMS spectrum exhibits pseudo molecular ion peaks at *m/z* 338/340/342 [M+H-MeOH]+ having an intensity ratio of 1:2:1 and suggesting the presence of two bromines in the molecule. The molecular weight is compatible with the molecular formula $C_{10}H_{13}Br_2NO_4$ of 2-(3.5-dibromo-1-hydroxy-4,4-dimethoxycyclohexa-2,5-dienyl)acetamide or dienone dimethoxyketal.

Table.III.25. NMR data of compound **30** in comparison to dienone dimethoxyketal

Atom No	Compound 28 [a]			Dienone dimethoxyketal [b]	
	¹H		¹³C [d]	¹H	
	δ	Integration, multiplicity, *J* in Hz	δ	δ	Integration, multiplicity, *J* in Hz
1	-	-	71.6	-	-
2 & 6	6.84	2H, s	143.8	6.79	1H, s
3 & 5	-	-	122.4	-	-
4			98.3	-	-
7	2.53	2H, s	47.4	2.40	2H, s
8	-	-	173.3	-	-
9	3.12	3H, s [c]	n.d.	2.98	3H, s [c]
10	3.18	3H, s [c]	n.d.	3.04	3H, s [c]

[a] Data were recorded in MeOD at 500 MHz; [b] data were recorded in DMSO-*d₆* at 500 MHz (Fouad, 2004); [c] values may be interchanged; [d] data are abstracted from HMBC spectrum; multiplicities and coupling constant are given in Hz n.d.: not detected

^{1}H NMR spectrum confirms the proposed structure. A singlet signal at δ_H 6.81 is assigned as H-2 and H-6, while the singlet signal at δ_H 2.53 is assigned as the protons of a methylene having deshielded effect from the carboxamide function next to it. Two singlet signals at δ_H 3.12 and 3.18 are the signals of the methoxy units at position 4. These methoxy groups appear in different chemical shift because they are chemically but not magnetically equivalent (Fouad, 2004). Hence the structure of compound **30** is established as **dienone dimethoxyketal**.
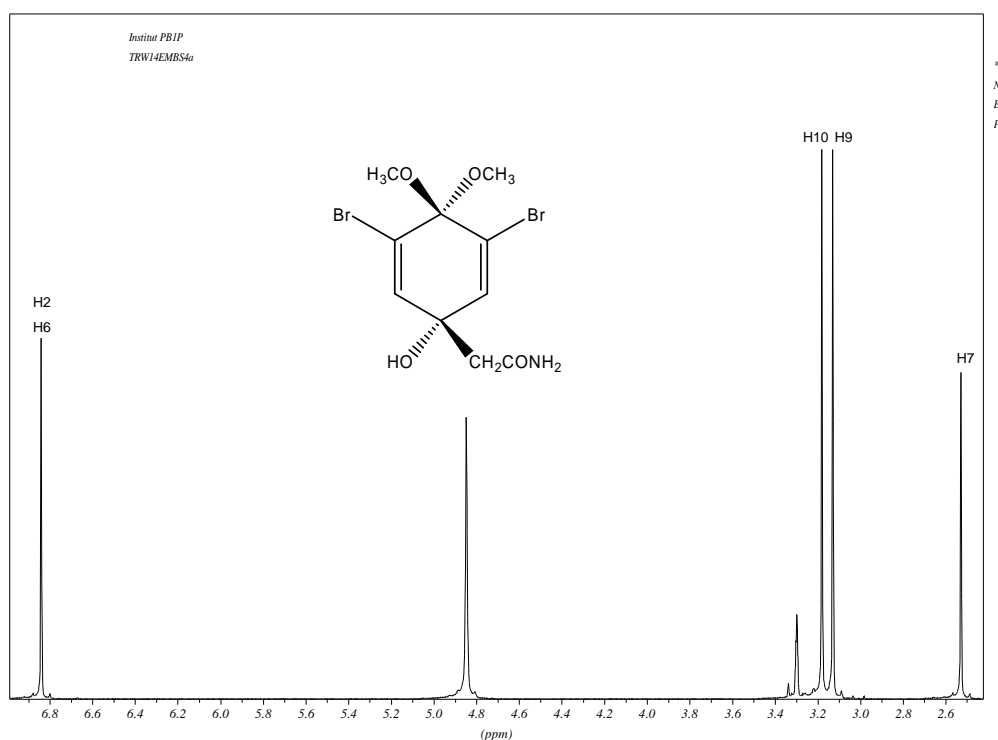
Fig.III.193. ^{1}H NMR spectrum of compound **30** (MeOD 500 MHz)

III.3.5. Dienone methoxy-ethoxyketal (**31**, known compound)
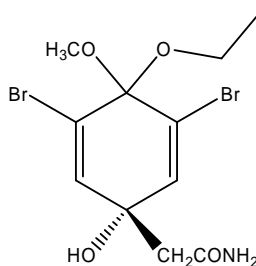
Fig.III.194. Compound **31**
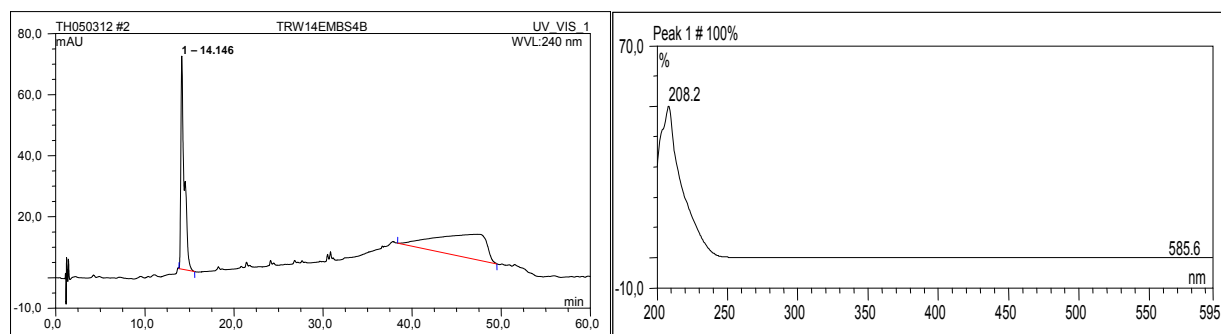
Fig.III.195. Analytical HPLC data of compound **31**
Left: HPLC profile in 240 nm RT: 14.15; right: UV absorption spectrum, λ_{max} = 208.2
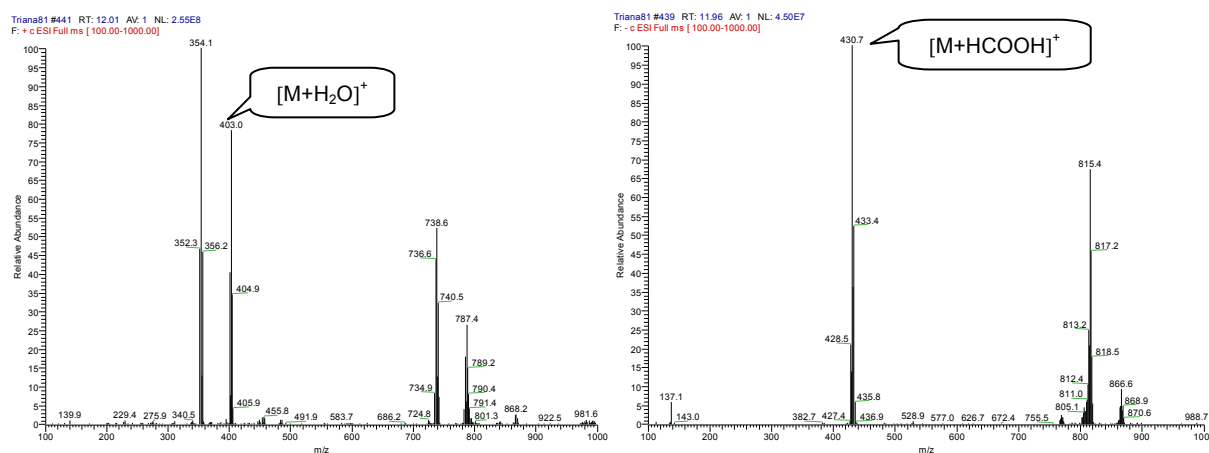
Fig.III.196. ESI-MS data of compound **31**

Compound **31** was obtained as a white amorphous substance with a yield of 2 mg (0.007% of crude extract). It shows $[\alpha]_D^{20}$ value of +1.2º $\pm$ 0.4º (*c* 0.39, CH$_3$OH) and UV maximum absorbance at 208.2 nm. ESIMS pseudo molecular ion peaks at *m/z* 429/431/433 [M-H+HCOOH]⁻ having an intensity ratio of 1:2:1 suggests the presence of two bromines in the molecule. It is compatible with the molecular formula C$_{11}$H$_{15}$Br$_2$NO$_4$ of 2-(3,5-dibromo-4-ethoxy-1-hydroxy-4-methoxycyclohexa-2,5-dienyl)acetamide or dienone methoxy-ethoxyketal.
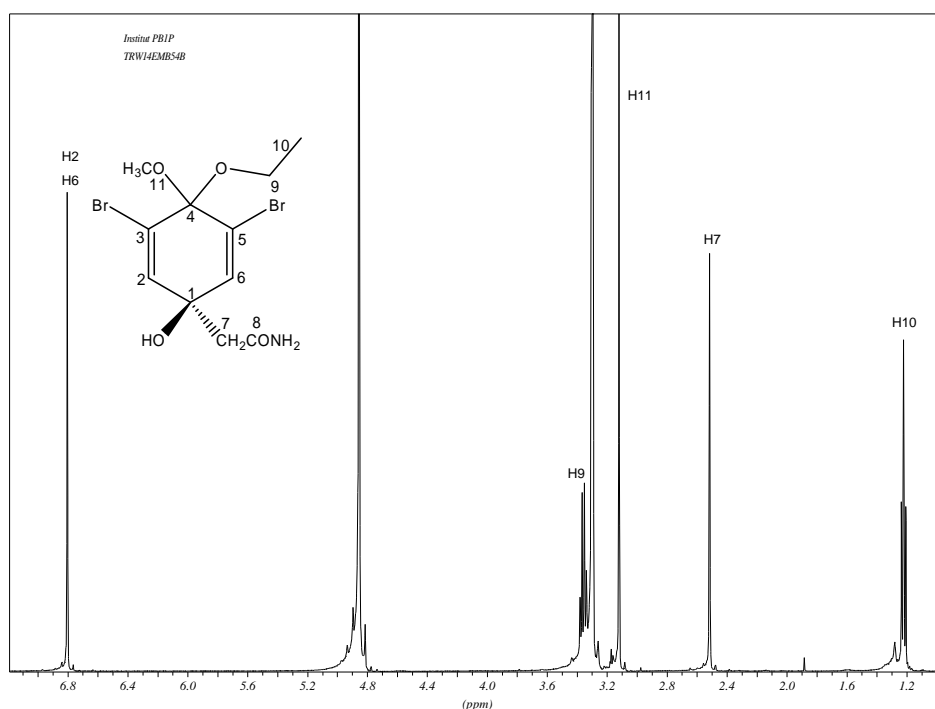
Fig.III.197. ^{1}H NMR spectrum of compound **31** (MeOD, 500 MHz)

^{1}H NMR spectrum confirms the proposed structure. The presence of symmetrical aromatic protons at δ_H 6.80 (H-2 and H-6) as well as the characteristic methylene at δ_H 2.52 which are also found in compound **30** implies a closely related structure. Major similarity found in ^{13}C-NMR data supports this finding. The difference found is the absence of the second methoxy group in position 4 which is in turn replaced with a signal of a deshielded methylene unit at δ_H 3.35 (2H, q, J = 6.9 Hz, H$_2$-9) coupled to a methyl group at δ_H 1.22 (3H, t, J = 6.9 Hz, H$_3$-10). Therefore it is suggestive for a presence of an ethoxy group to replace the second methoxy group. Thus the structure of compound **31** is determined as the known derivate **dienone methoxy-ethoxy ketal**.

Table.III.26. NMR data of compound **31** in comparison to dienone methoxy-ethoxyketal

Atom No	Compound 28 [a]			Dienone methoxy-ethoxyketal [a] [b]		
	[1]H		[13]C [c]	[1]H		[13]C
	δ	Integration, multiplicity, *J* in Hz	δ	δ	Integration, multiplicity, *J* in Hz	δ, DEPT
1	-	-	71.6	-	-	71.8, C
2 & 6	6.80	2H, s	143.3	6.69	2H, d, 1.5	143.0, CH
3 & 5	-	-	122.5	-	-	123.5, C
4	-	-	97.7	-	-	97.7, C
7	2.52	2H, s	47.4	2.52	2H, s	47.4, CH$_2$
8	-	-	173.3	-	-	173.8, C=O
9	3.35	3H, q, 6.9	60.8	3.36	2H, q, 6.9	60.7, CH$_2$
10	1.22	3H, t, 6.9	15.0	1.22	3H, t, 6.9	15.2, CH$_3$
11	3.13	3H, s	n.d.	3.13	3H, s	51.5, CH$_3$

[a] Data were recorded in MeOD at 500 MHz, multiplicities and coupling constant are given in Hz; [b] Fouad (2005), [c] data are abstracted from HMBC spectrum; n.d.: not detected

III.4. Secondary metabolites from *Mycale phylophyla*

Sponges of the genus *Mycale* have been reported to be a rich source of a very chemically diverse group of bioactive natural compounds. The mycalamides (triisooxazole-containing macrolides (Perry *et al.*, 1990); mycalolides (Fusetani *et al.*, 1989); diterpenoid rotalins (Corriero *et al.*, 1989); mycalisines (Kato *et al.*, 1985); polybrominated C-15 acetogenins (Giordano *et al.*, 1990), brominated isocoumarins (Fusetani *et al.*, 1991); and norterpene cyclic peroxides (Capon and Mcleod, 1987) are examples of the different compounds isolated from this genus (Venkatesham *et al.*, 2000).

Until now there has been no report on secondary metabolites from *Mycale phyllophilla*. Analytical HPLC profile (Fig.III.198) shows that the crude extract (1 g) contains two major peaks. These peaks have delayed retention time and are eluted by 100% MeOH showing that both are relatively non polar substances. The first peak has been isolated and identified as a fatty acid derivative (not elucidated further) and the second peak is identified later as a mixture of 5-alkyl 2-pyrrole carbaldehyde derivatives (compound **32a** and **32b**).
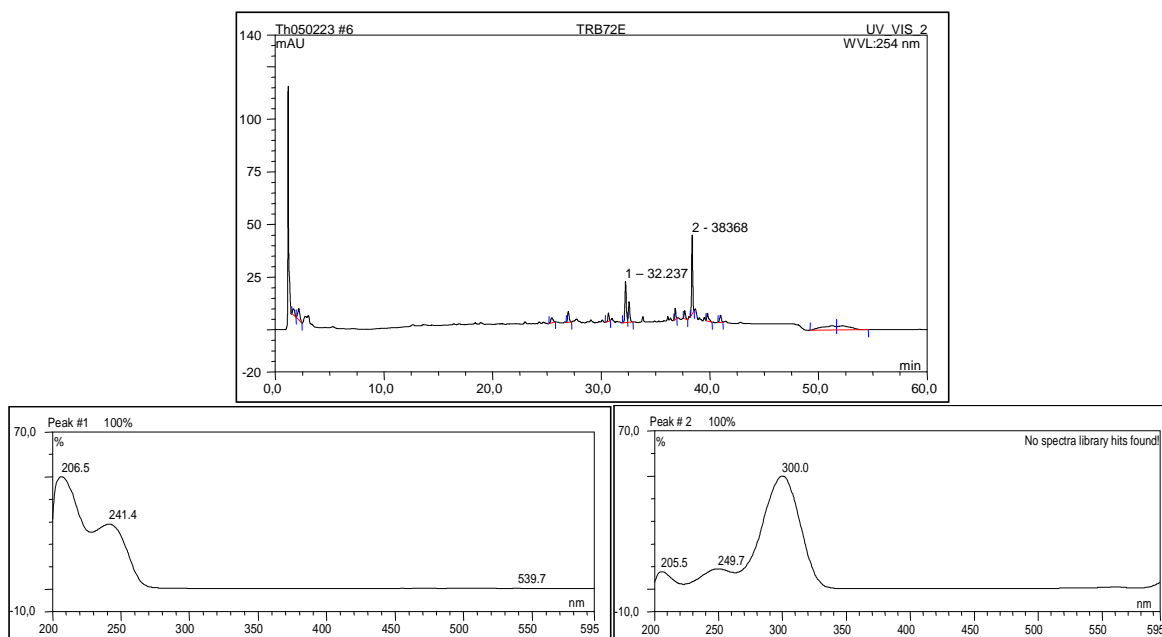
Fig.III.198. Analytical HPLC profile of *Mycale phylophilla* crude extract (above) and the UV absorption patterns of the major substances (below)

III.4.1. **5-Pentadecyl-1*H*-pyrrole-2-carbaldehyde and (6'*E*)-5-(6'Pentadecenyl)-**

1*H*-pyrrole-2-carbaldehyde (**32a** and **32b**, known compounds)
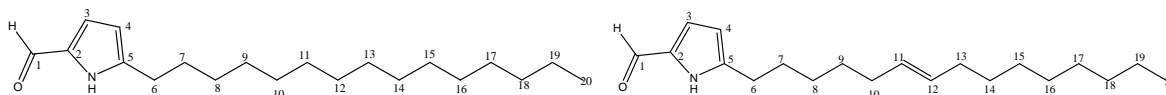
Fig.III.199. Compound **32a** (left) and compound **32b** (right)

Fig.III.200. Analytical HPLC data of compound **32 a** and **32b**
Left: HPLC profile in 235 nm RT: 36.67; right: UV absorption spectrum, λ_{max} = 205.8, 249.6 and 300.4
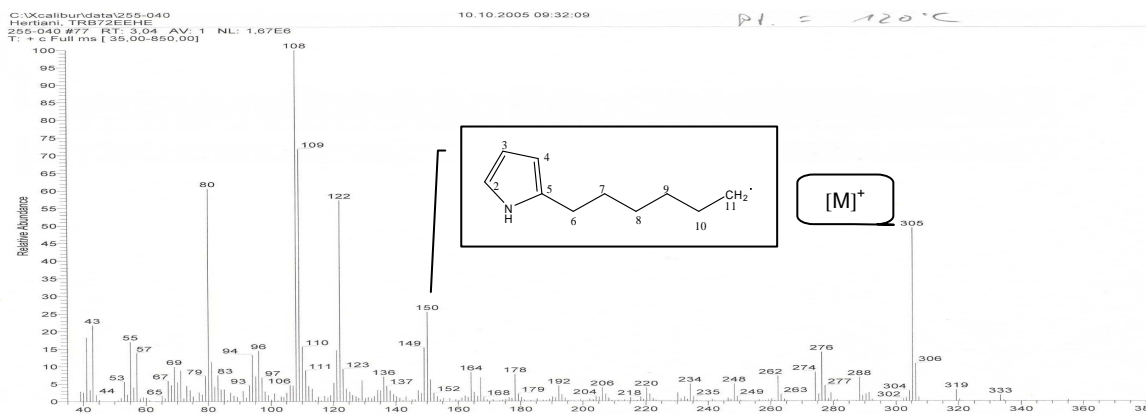
Fig.III.201. EI-MS data of compound **32a** and **32b**

These groups of compounds have previously been isolated from *Mycale tenuispiculata* (Dendy) collected from Arabian Sea (Perry *et al*., 2000) and *Laxosuberites* sp. from the shores of Canton Island (Stierle and Faulkner, 1980). In this study, the mixture of some 5-alkyl 2-pyrrole carbaldehydes were isolated together with a (6'*E*)-5-(6'pentadecenyl)-1*H*-pyrrole-2-carbaldehyde from *Mycale phylophilla* collected from Menjangan Island, Bali Indonesia.

Compound **32a** and **32b** were isolated together as a 2:1 mixture. The optically inactive brown amorphous fraction was obtained at a yield of 28 mg (0.026% sponge dry weight). Its UV spectrum shows λ_{max} at 300.4 nm, which is a typical spectrum for pyrrole 2-carboxaldehyde (Stierle and Faulkner, 1980). EI-MS experiment reveals molecular ion peaks at *m/z* 305, 319 and 333, suggesting the presence of at least three 5-alkyl-2-pyrrole carbaldehydes which differ in the length of the alkyl chain.
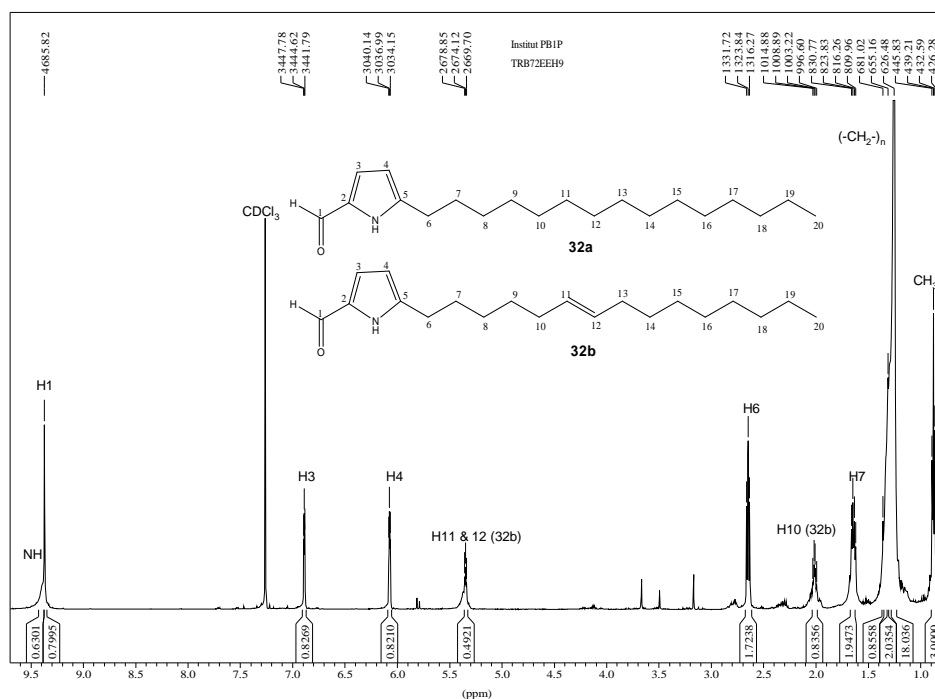
Fig.III.202. ^{1}H-NMR spectrum of compound **32a** and **32b** as a 2:1 mixture (CDCl$_3$, 500 MHz)

^{1}H NMR spectrum exhibits an aldehyde proton signal at δ_H 9.38 (1H, s); protons of the pyrrole ring at δ_H 6.87 (1H, dd, J = 3.2, 2.8 Hz) and at δ_H 6.05 (1H, dd, J = 3.2, 2.8 Hz) which coupled to the NH signal at δ_H 9.41; a deshielded methylene unit signal at δ_H 2.62 (2H, t, J = 7.0 Hz), and a signal for a primary methyl group at δ_H 0.86 (3H, t, J = 6.6 Hz). A coupling constant of 3.2 Hz is typical for $J_{3,4}$ in pyrroles (Jones and Bean, 1977). These findings imply the presence of a 5-alkyl-2-pyrrole-carboxaldehyde derivative. ^{13}C-NMR confirms the aldehyde function by a low field sp^2 signal at δ_c 178.1, while the pyrrole ring carbons are shown by signals at δ_c 143.2 (C); δ_c 131.8 (C); δ_c 122.5 (CH) and 109.2 (CH). The remaining ^{13}C NMR signals are assigned to the *n*-alkyl side chains (Stierle and Faulkner, 1980).
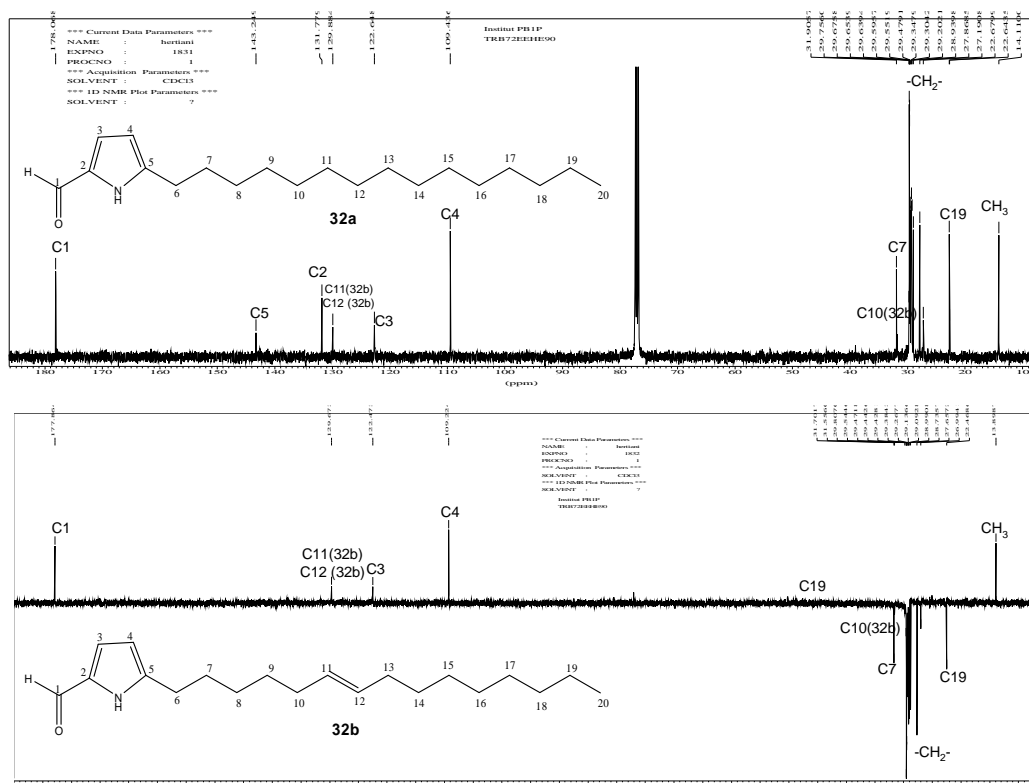
Fig.III.203. ^{13}C - NMR (above) and DEPT (below) spectra of compound **32a** and **32b** as a 2:1 mixture (CDCl$_3$, 125 MHz)

Beside the 5-alkyl 2-pyrrole carboxaldehyde signals, NMR data also imply the presence of a (6'*E*)-5-(6'penta decenyl)-1*H*-pyrrole-2-carbaldehyde derivative. Two olefinic proton signals appear at δ$_H$ 5.30 (1H, t, *J* = 7.5 Hz) as well as the signal of an adjacent methylene unit at δ$_H$ 2.0 (1H, m). These evidences together with the ^{13}C NMR signals at δ$_c$ 129.9 (CH) and δ$_C$ 31.9 (CH$_2$) confirm its structure. The olefinic bond position in the long chain is determined from its mass spectrum. A fragment ion at *m/z* 150 and *m/z* 204 resulted from an allylic cleavage of the side chain indicating that the olefinic bond is separated from the pyrrole ring by five methylene group (Stierle and Faulkner, 1980). The geometry of the double bond was assigned as *E* by the ^{13}C NMR spectral values for allylic methylenes at δ$_C$ 31.9 (CH$_2$) and 31.6 (CH$_2$) (Stierle and Faulkner, 1980).
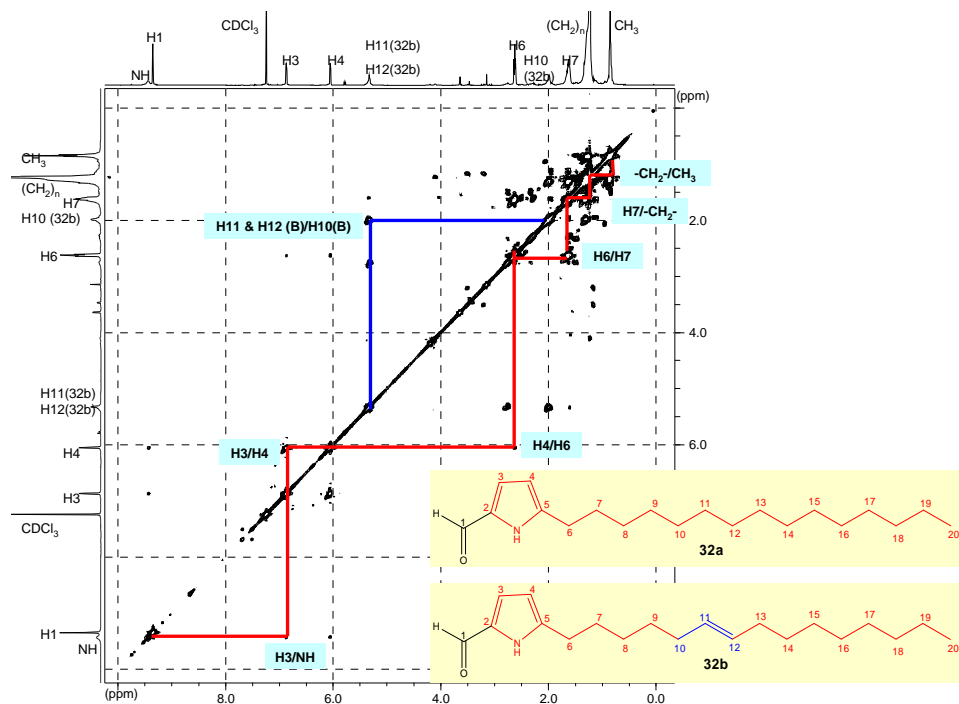
Fig.III.204. ^{1}H-^{1}H COSY spectrum of compound **32a** and **32b** as a 2:1 mixture (CDCl$_3$)

^{1}H–^{1}H COSY spectrum exhibits two different spin systems. The first spin system correlates the alkylene side chain to the pyrrole protons, while the second one correlates the olefinic protons to the rest of the alkylene side chain and the pryrrole ring. HMBC data also secure this argument as cross peaks correlate the olefinic protons to the methylene unit adjacent to it and then to the rest of the alkylene chain observed (Fig.III.205).
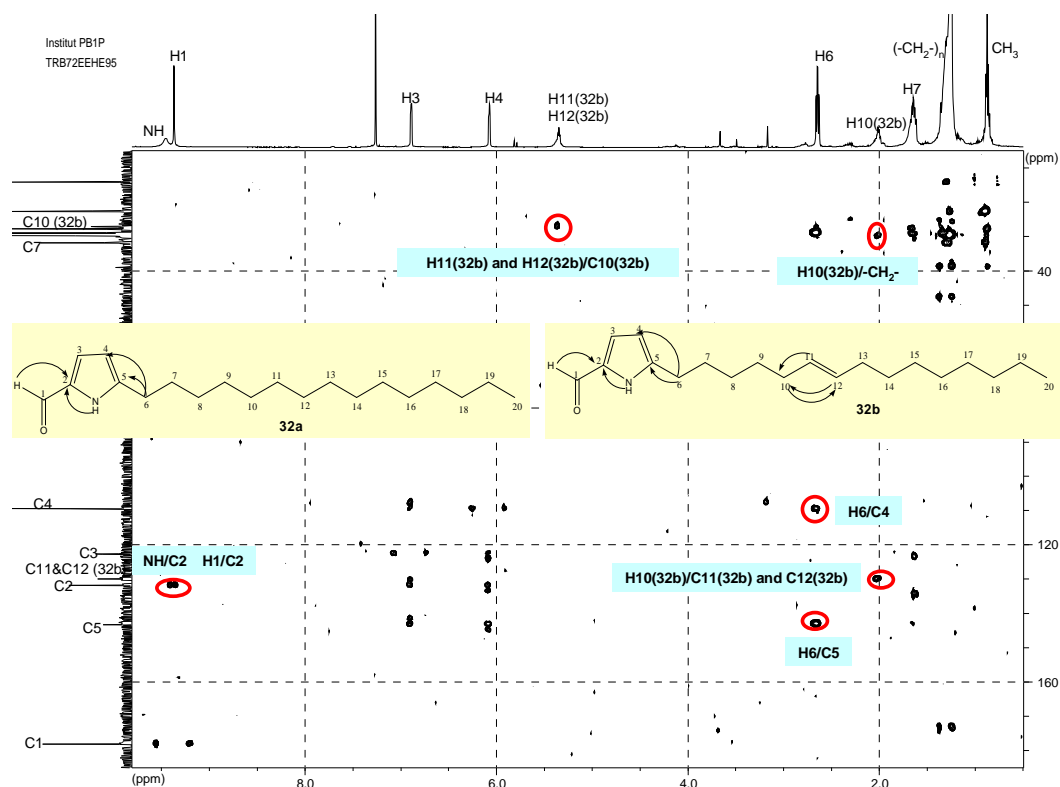
Fig.III.205. ^{1}H–^{13}C HMBC spectrum of compound **32a** and **32b** as a 2:1 mixture (CDCl$_3$)

Table III.27. NMR data of compound **32a** and **32b** in comparison to (6'E)-5-(6'penta decenyl) pyrrole-2-carboxaldehyde

Atom No.	Compound 32a and 32b [a]			(6'E)-5-(6'Penta decenyl) pyrrole-2-carboxaldehyde [b]		
	^{1}H		^{13}C	^{1}H		^{13}C
	δ	Integration, multiplicity, *J* in Hz	δ, DEPT	δ	Integration, multiplicity, *J* in Hz	δ, DEPT
NH	9.41	1H, bs	-	10.15	1H, bs	-
HC=O	9.38	1H, s	178.1, d	9.32	1H, s	178.1, d
3	6.87	1H, dd, 3.2, 2.8	122.6, d	6.82	1H, m	122.7, d
4	6.05	1H, dd, 3.2, 2.8	109.4, d	6.01	1H, m	109.4, d
11 & 12	5.30	1H, t, 4.5	129.9, d	5.34	2H, m	130.0, d
6	2.62	2H, t, 7.8	22.6, t	2.68	2H, t, 7.0	29.6, t
10	1.99	1H, m	31.8, t	2.00	2H, m	31.9, t
7	1.62	2H, m	31.9, t	1.66	2H, m	31.7, t
(-CH$_2$-)$_n$	1.40 – 1.25	27H, br s	29.6, t 29.3, t 29.2, t 28.9, t 27.9, t 27.2, t 22.7, t	1.20	18H, brs	29.5, t 29.3, t 29.2, t 28.9, t 27.9, t 27.2, t 22.7, t
20	0.86	3H, t, 6.6	14.1, q	0.88	3H, t, 6.5	14.1, q
5	-	-	143.2, s	-	-	143.2, s
2	-	-	131.8, s	-	-	131.8, s

[a] Data were recorded in CDCl$_3$, at 500 MHz, multiplicities and coupling constant are given in Hz; [b] Venkatesham *et al.* (2000)

After careful interpretation of the physical and spectral data, in comparison to the literature, this fraction is concluded to be a mixture of several **5-alkyl 2-pyrrole carboxaldehyde derivates** which are different in the side chain length (**32a**) and the (6'*E*)-5-(6'penta decenyl)-1*H*-pyrrole-2-carbaldehyde (**32b**).

5-Alkyl 2-pyrrole carboxaldehyde derivates was first reported from *Laxosuberites* sp. (Stierle and Faulkner, 1980) and later on it was reported to be isolated together with compound **32b** from *Mycale tenuispiculata* (Venkatesham *et al.*, 2000).

III.5. Secondary metabolites from *Axynissa* sp.

Sponges of the genus *Axynissa* have previously been reported to yield a variety of sesquiterpene isothiocyanates, formamides (Marcus *et al.*, 1989), a sesquiterpene isonitrile (Compagnone and Faulkner, 1995) and nitrogenous bisabolenes (Li *et al.*, 1999). These metabolites are thought to inhibit feeding by omnivorous browsers, but they do not deter nudibranches that are specific predators on the sponge (Marcus *et al.*, 1989).
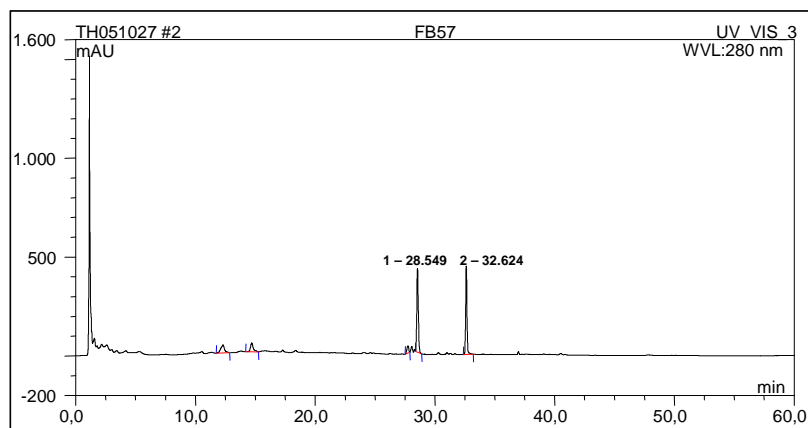
Fig.III.206. Chemical profile of *Axynissa* sp. crude extract detected by analytical HPLC at 280 nm
Peak 1: (+)-curcudiol; peak 2: (+)-curcuphenol

Axynissa sp. in this study was collected from Ambon, Indonesia in 1996.

Chemical profile by analytical HPLC exhibits two major peaks which are later identified as bisabolene type sesuiterpenoids. This group of compounds constitute a class of broadly active natural products biosynthesized by a diverse range of organisms from both terrestrial and marine habitats. It is of particular interest to note that two unique classes of bisabolene type metabolites are recognized based on their C-9 absolute stereochemistry (Cichewicz *et al.*, 2005). All known sponge-derived bisabolenes possess a 9*S* configuration while the remaining marine and terrestrial metabolites exhibit a 9*R* configuration (Harrison and Crews, 1997). From this sponge, two protein kinase inhibitors, (+)-curcuphenol and (+)-curcudiol have been isolated.

III.5.1. **(+)-Curcuphenol** (**33**, known compound)
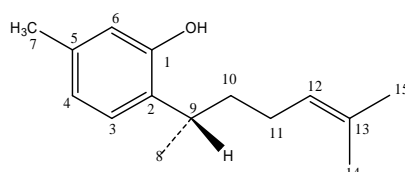
Fig.III.207. Compound **33**
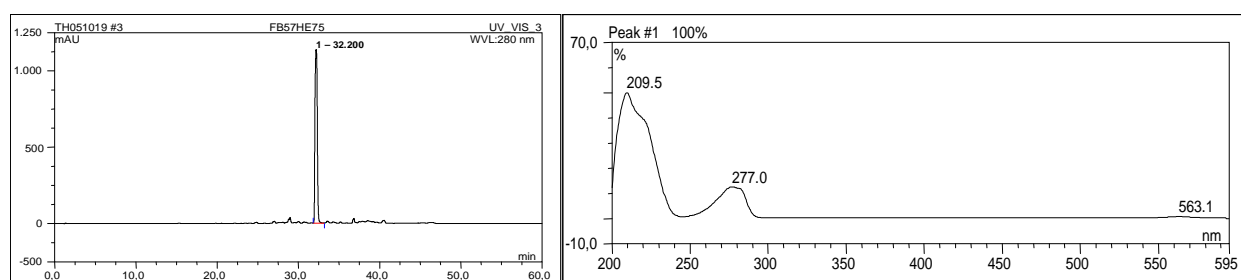
Fig.III.208. Analytical HPLC data of compound **33**
Left: HPLC profile in 235 nm RT: 32.20; right: UV absorption spectrum, λ_{max} = 209.5 and 277.0 nm
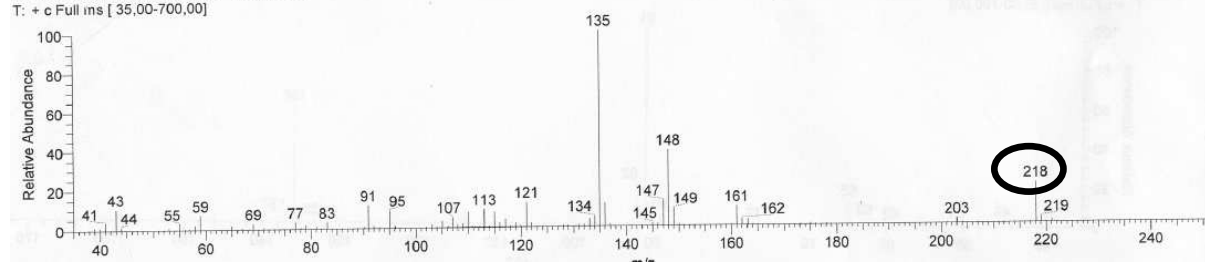
Fig.III.209. EI-MS spectrum of compound **33**

Compound **33** was isolated as a yellow brownish oily substance at an amount of 19 mg (0.95% of the sponge crude extract). This relatively non polar compound appears at a RT of 32.20 min which shows a classical UV absorption spectrum for a phenol functionality with a λ_{max} at 209.5 and 277.0 nm. EIMS reveals the molecular weight of 218 g/mol which is compatible to the molecular formula $C_{15}H_{22}O$ of 5-methyl-2-(6-methylhept-5-en-2-yl)phenol or curcuphenol, a bisabolane type sesquiterpene phenol.
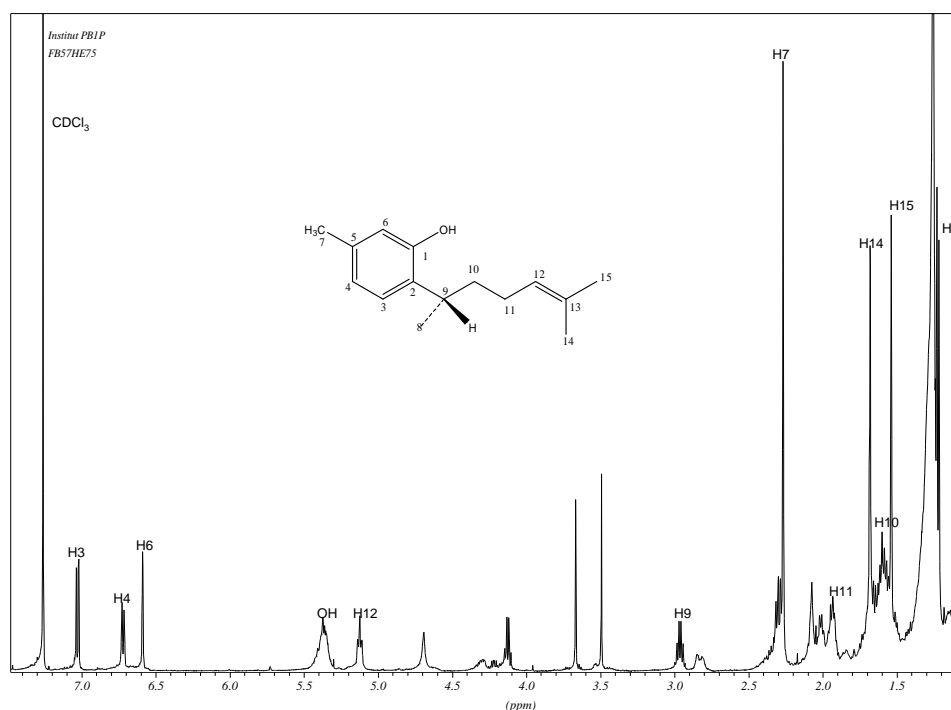
Fig.III.210. ^{1}H-NMR spectrum of compound **33** (CDCl$_3$, 500 MHz)

^{1}H-NMR spectrum in CDCl$_3$ suggests the presence of a terminal isopropylidene group as exhibited by a vinyl proton signal at δ_H 5.13 (1H, t, *J* = 7.1 Hz, H-12) and two vinyl methyl singlets at δ_H 1.68 (3H, s, H$_3$-14) and δ_H 1.54 (3H, s, H$_3$-15). It also reveals the presence of an aromatic methyl group at δ_H 2.28 (3H, s, H$_3$-7) and a benzyl substituted secondary methyl group as a doublet signal at δ_H 1.22 (3H, d, *J* = 6.9 Hz, H$_3$-8) which coupled to a methine multiplet at δ_H 2.96 (1H, m, H-9).

The occurrence of signals arising from a 1,2,4-trisubstituted aromatic ring is observed at δ_H 7.03 (1H, d, *J* = 7.9 Hz, H-3), 6.73 (1H, d, *J* = 7.6 Hz, H-4) and 6.58 (1H, s, H-6). The overall spectrum indicates a phenolic derivative of α-curcumene (McEnroe and Fenical, 1978). Curcumenes itself constitute an important class of monocyclic aromatic sesquiterpenoids that are widely distributed in nature (Joseph-Nathan *et al.*, 1988).
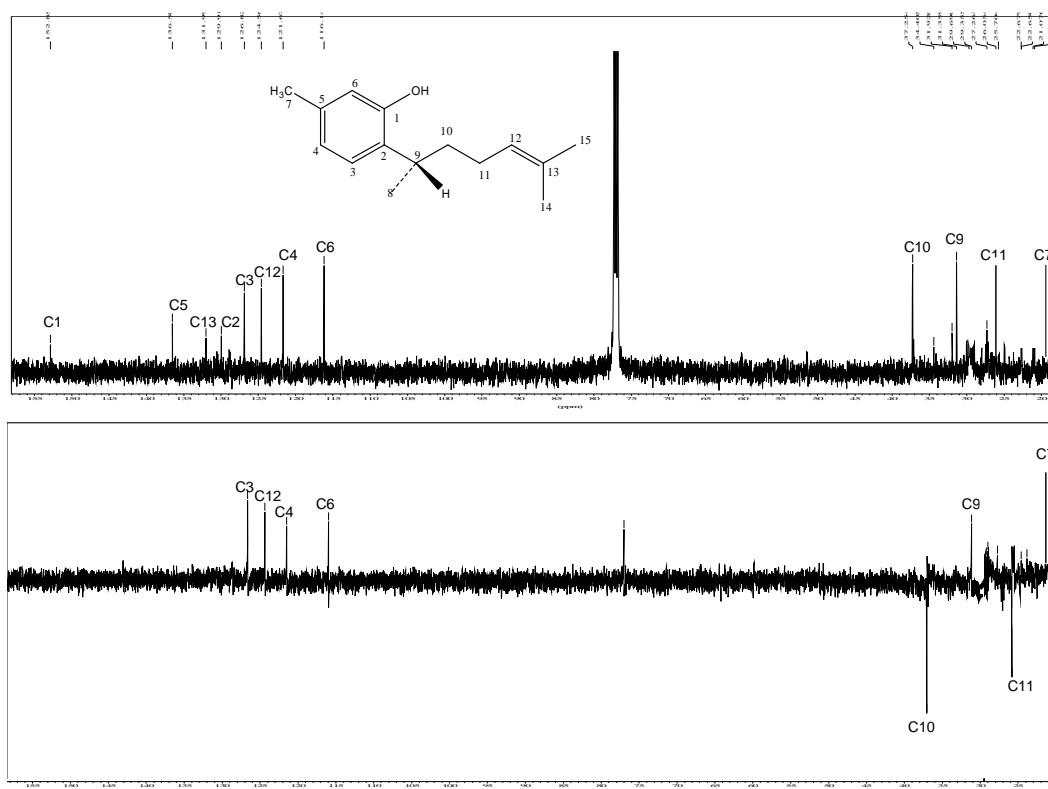
Fig.III.211. ^{13}C-NMR (above) and DEPT (below) spectra of compound **33** (CDCl$_3$, 500 MHz)

^{13}C-NMR and DEPT experiments support the proposed structure (Fig.III.211). Four carbon *sp*^{2} signals derived from the aromatic carbons at δ_C 126.8 (C-3), 121.7 (C-4), and 116.1 (C-6), as well as from the vinylic carbon at δ_C 124.6 (C-12) are observed. Four carbon *sp* signals appear at δ_C 152.8 (C-1), 129.9 (C-2), 136.5 (C-5), and 132.0 (C-13). These findings supports the presence of the 1,2,4 trisubstituted aromatic ring and the dimethylisopropylidene terminal side chain. The

presence of four methyl units is confirmed by signals at δ_C 25.7 (C-14), 17.7 (C-15), 21.1 (C-7) and at 20.9 (C-8). Two methylene signals of the isoprenoid side chain are assigned to δ_C 37.2 (C-10) and 26.0 (C-11), as well as a methine carbon at δ_C 31.3 (C-9).

^{1}H–^{1}H COSY spectrum shows two spin systems (Fig.III.212). One spin system represents the aromatic protons as well as the aromatic methyl group correlation, while the second spin system is derived from the isoprenoid C-8 side chain. ^{1}H–^{13}C HMBC experiment confirms these substructures. Cross peaks correlate the aromatic methyl protons to C-4, C-5 and C-6 implying its substitution at C-5. Cross peaks of H-9 to C-3 as well as H-8 to C-2 confirm the connection of the isoprenoid side chain to the aromatic ring. These findings confirm compound **33** as **curcuphenol**.
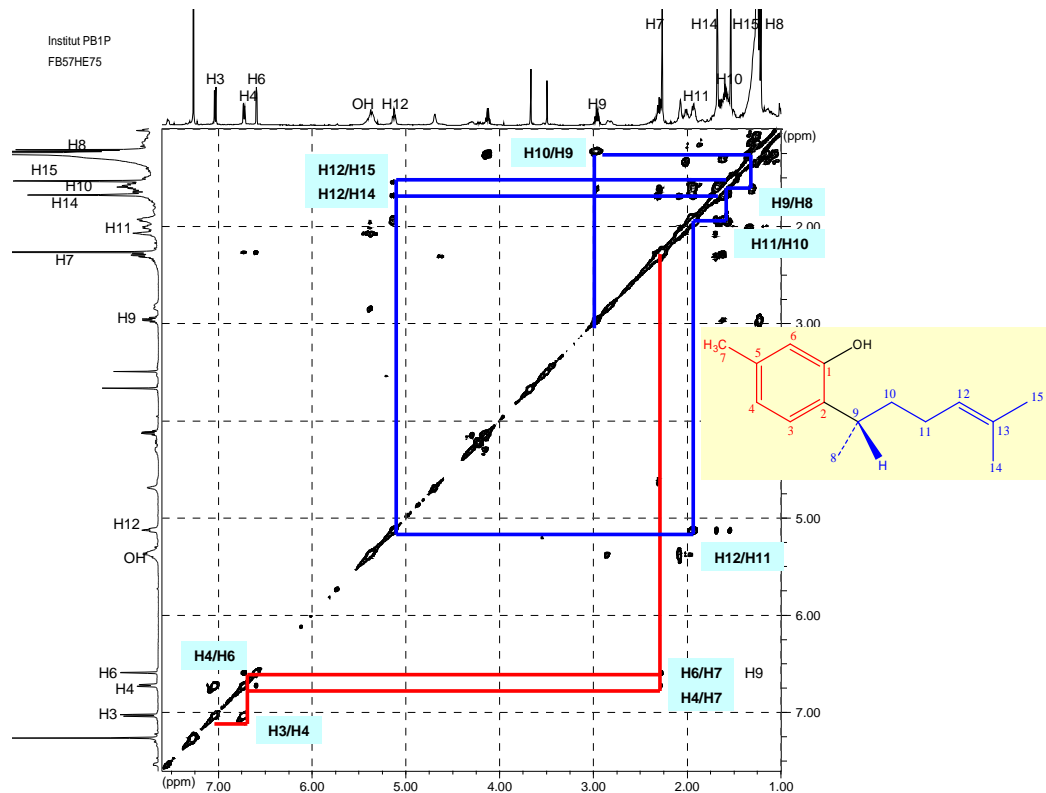
Fig.III.212. ^{1}H–^{1}H COSY spectrum of compound **33** (CDCl$_3$)
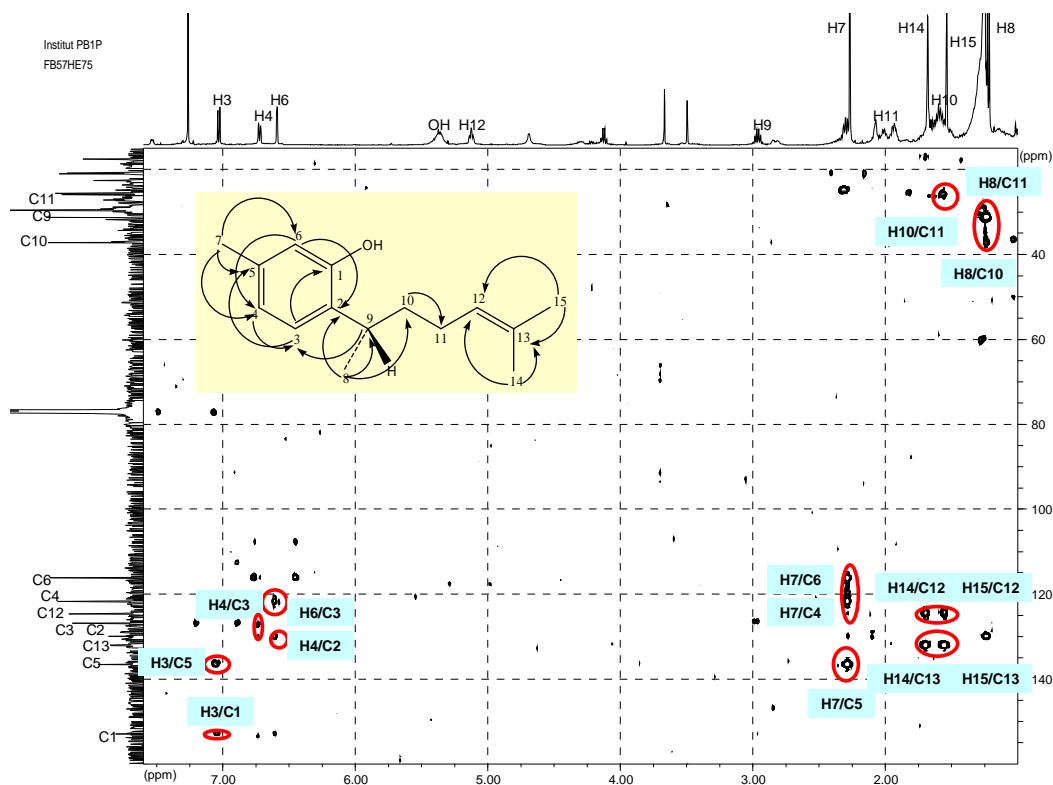
Fig.III.213. ^{1}H–^{13}C HMBC spectrum of compound **33** (CDCl$_3$)

Table III.28. NMR data of compound **33** in comparison to (-)-curcuphenol and (+)-curcuphenol

No	(-)-Curcuphenol [c)]			Compound 33 [a)]			(+)-Curcuphenol [a) b)]		
	^{1}H-NMR		^{13}C-NMR, DEPT	^{1}H-NMR		^{13}C-NMR, DEPT	^{1}H-NMR		^{13}C-NMR DEPT
	δ	Integration, multiplicity, J in Hz		δ	Integration, multiplicity, J in Hz		δ	Integration, multiplicity, J in Hz	
1	-	-	152.95, C	-	-	152.8, C	-	-	152.8, C
2	-	-	130.15, C	-	-	129.9, C	-	-	130.1, C
3	6.87	1H, d, 7.8	126.89, CH	7.03	1H, d, 7.9	126.8, CH	7.18	1H, d, 7.8	126.8, CH
4	6.53	1H, d, 7.8	121.71, CH	6.73	1H, d, 7.6	121.7, CH	6.85	1H, br d, 7.8	121.7, CH
5	-	-	136.45, C	-	-	136.5, C	-	-	136.4, C
6	6.35	1H, s	116.25, CH	6.58	1H, s	116.1, CH	6.68	1H, d, 0.8	116.2, CH
7	2.12	3H, s	21.09, CH$_3$	2.28	3H, s	21.1, CH$_3$	2.38	3H, s	20.7, CH$_3$
OH	5.29	1H, b	-	5.38	2H, m	-			
8	1.17	3H, d, 7.0	20.88, CH$_3$	1.22	3H, d, 6.9	20.9, CH$_3$	1.36	3H, s	21.0, CH$_3$
9	2.91	1H, m	31.53, CH	2.96	1H, sextet	31.3, CH	3.15	1H, m, 7.0	31.3, CH
10	1.40 – 1.70	2H, m	37.34, CH$_2$	1.62	2H, m	37.2, CH$_3$	1.75	2H, m	37.2, CH$_2$
11	1.82	2H, m	26.16, CH$_2$	1.93	2H, m	26.0, CH$_2$	2.09	2H, m, 7.0	26.0, CH$_2$
12	5.03	1H, dd, 7.7	124.71, CH	5.13	1H, t, 7.1	124.6, CH	5.28	1H, m	124.6, CH
13	-	-	131.83, C	-	-	132.0, C	-	-	131.8, C
14	1.64	3H, s	17.66, CH$_3$	1.68	3H, s	25.7, CH$_3$	1.79	3H, s	25.6, CH$_3$
15	1.48	3H, s	25.70, CH$_3$	1.54	3H, s	17.7, CH$_3$	1.68	3H, s	17.5, CH$_3$

[a)] Data were recorded in CDCl$_3$, at 500 MHz for ^{1}H-NMR and 125 MHz for ^{13}C-NMR;
[b)] Tasdemir *et al.*, 2003; [c)] data were recorded in CCl$_4$ for ^{1}H-NMR and in CDCl$_3$ for ^{13}C-NMR (McEnroe and Fenical,1978)

The chiral center at C-9 of curcuphenol can give rise to two possible stereoisomers. Both isomers occur in nature but according to Harrison and Crews

(1997), all known sponge-derived bisabolenes possess a 9S configuration while other marine (e.g. gorgonian coral) and terrestrial metabolites exhibit a 9R configuration. Optical rotation measurement of compound **33** exhibits $[\alpha]_D^{25}$ value of +8.9º ± 0.5º (*c* 0.52, CHCl$_3$), suggesting (+)-curcuphenol isomer. This compound was previously isolated from marine sponge genus *Didiscus* (Wright *et al.*, 1987; Tasdemir *et al.*, 2003) and from *Axynissa aculeata* (Murti, 2006). The antipode, (-)-curcuphenol was isolated from a gorgonian coral *Pseudopterogorgia rigida* (McEnroe and Fenical, 1978).

III.5.2. (+)-Curcudiol (**34**, known compound)
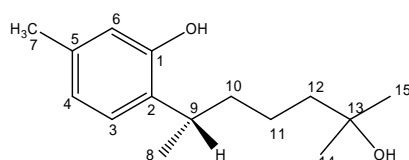
Fig.III.214. Compound **34**
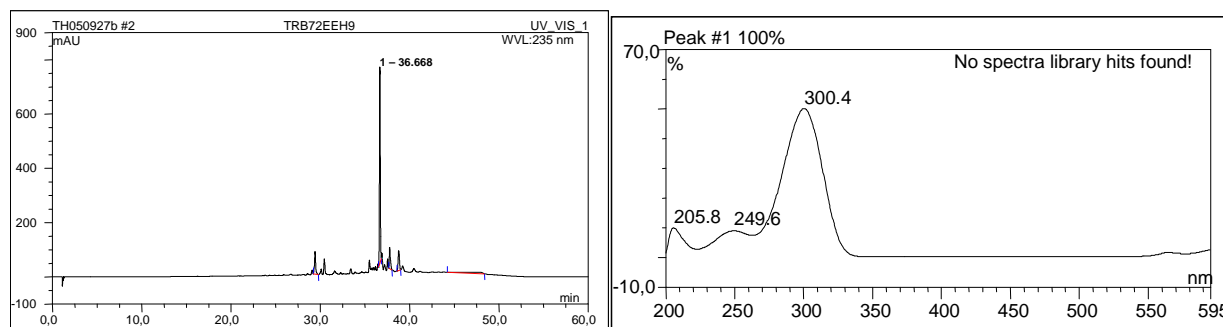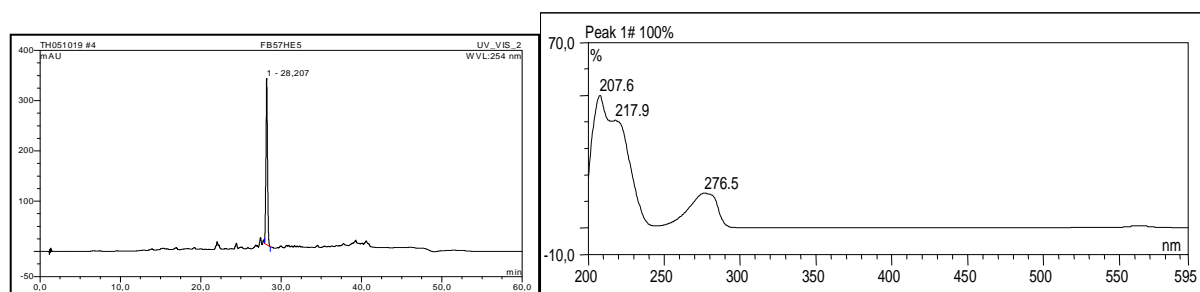

Fig.III.215. Analytical HPLC data of compound **34**
Left: HPLC profile in 235 nm RT: 28.21; right: UV absorption spectrum, λ_{max} = 207.6; 217.9; 276.5 nm
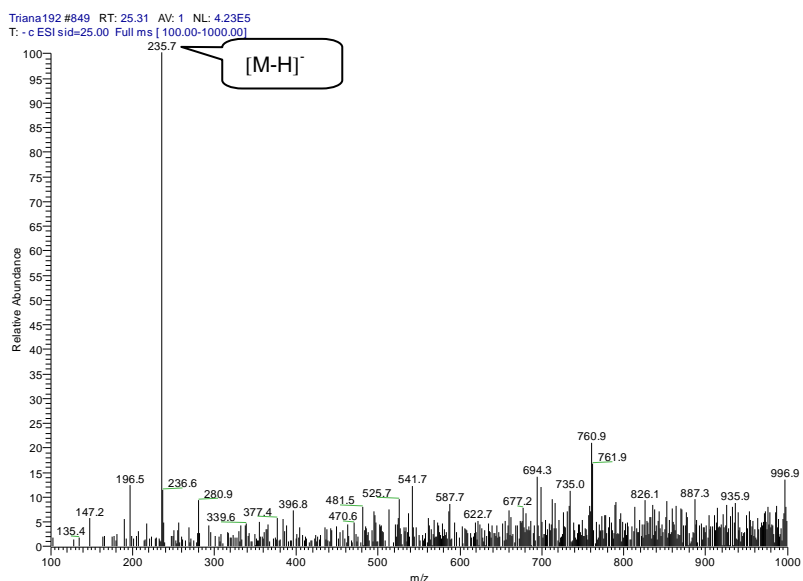
Fig.III.216. ESI-MS spectrum of compound **34**

Compound **34** was isolated as a yellow oil at an amount of 24 mg (1.2% of sponge crude extract). It has a UV spectrum similar to compound **33,** suggesting the presence of a similar chromophore. ESIMS reveals the molecular weight of 236 g/mol which is compatible to the molecular formula $C_{15}H_{24}O_2$ of 2-(6-hydroxy-6-methylheptan-2-yl)-5-methylphenol or the known congener curcudiol, which is another member of the bisabolane type sesquiterpene phenols.
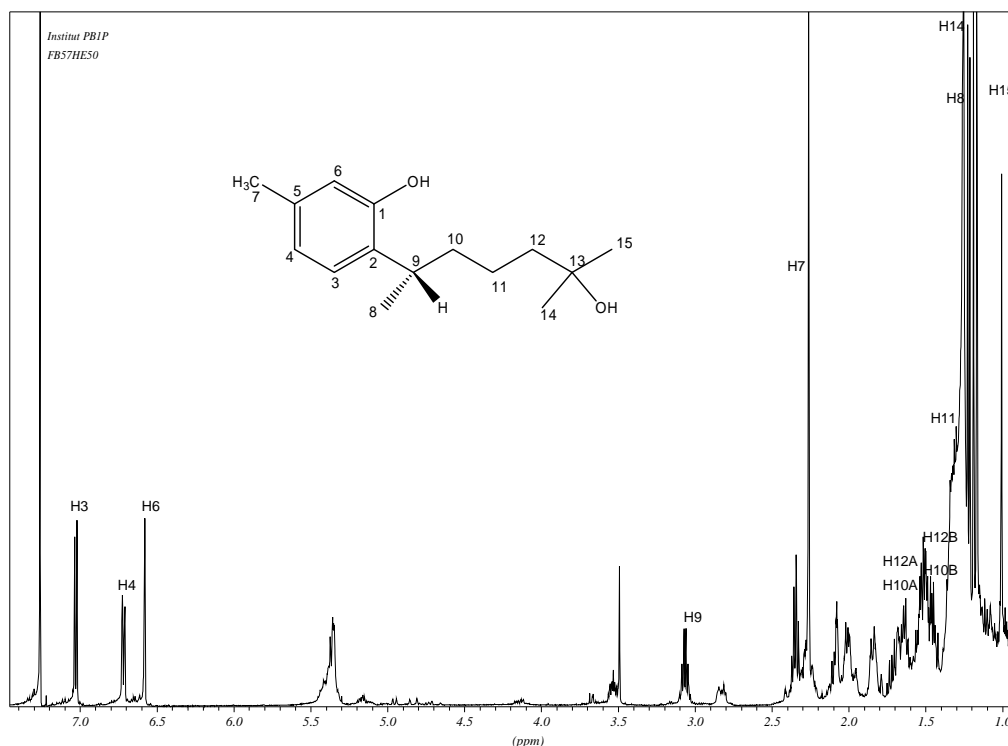
Fig.III.217. ^{1}H-NMR spectrum of compound **34** (CDCl$_3$, 500 MHz)

^{1}H and ^{13}C-NMR spectra of compounds **33** and **34** are almost identical in the aromatic region. Its ^{1}H-NMR spectrum reveals the characteristic signals for a 1,2,4-trisubsituted aromatic ring which is in accordance to its ^{13}C-NMR data. The primary difference found is the resonances observed for the C-12—C-13 olefin of (+)-curcuphenol (**33**) are replaced by the resonances of a quaternary carbon bearing oxygen at δ_C 71.4 (C-13) and of a methylene group at δ_C 43.7 (C-12) of compound **34**. As a result, two geminal methyl functions are shifted upfield in comparison to those of compound **33**. Based on these findings, compound **34** is identified as the known congener curcudiol, a hydrogenation product of curcuphenol. Like its congener, (+)-curcuphenol, compound **34** also exhibits 9*S* configuration with an optical rotation $[\alpha]_D^{25}$ = +3.4º ± 0.5º (*c* 0.41, CHCl$_3$). Hence it is determined as **(+)-curcudiol**.
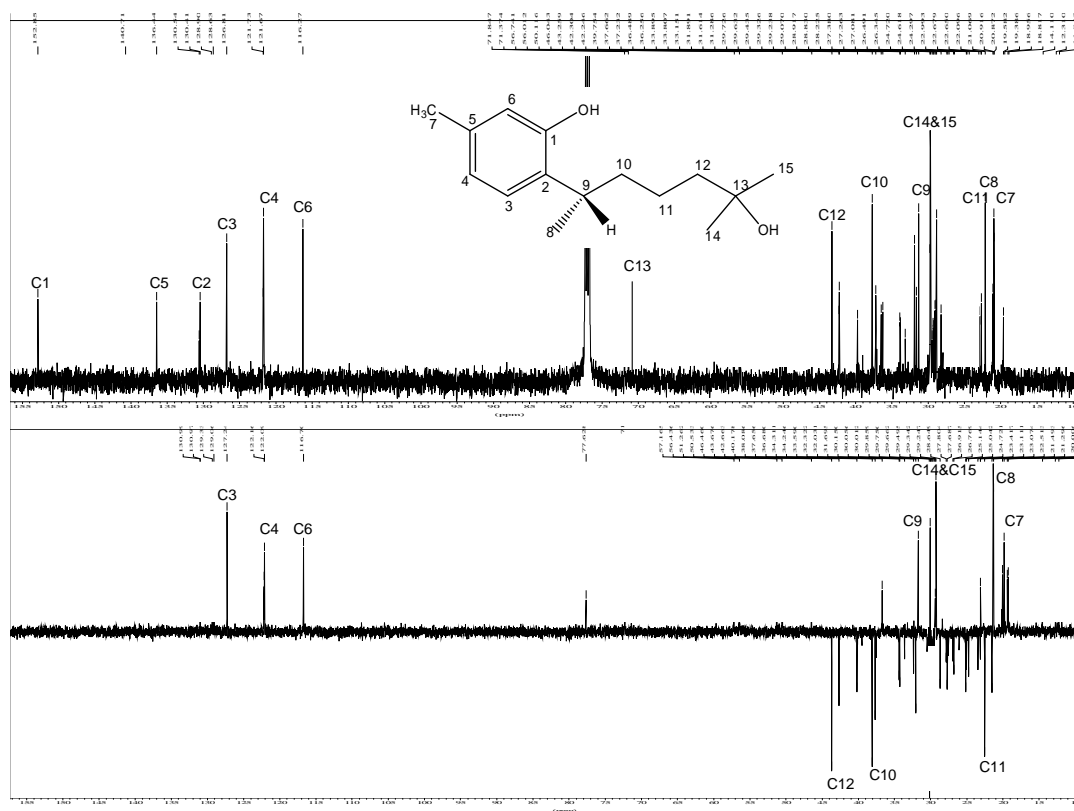
Fig.III.218. ^13C-NMR (above) and DEPT (below) spectra of compound **35** (CDCl₃, 500 MHz)

(+)-Curcudiol has been reported to have weak activity against *Candida albicans* (MIC of 250 µg/mL) (Wright *et al.*, 1987). It shows no activity against L5178Y cell line (mouse lymphoma cells, 10 µg/mL).
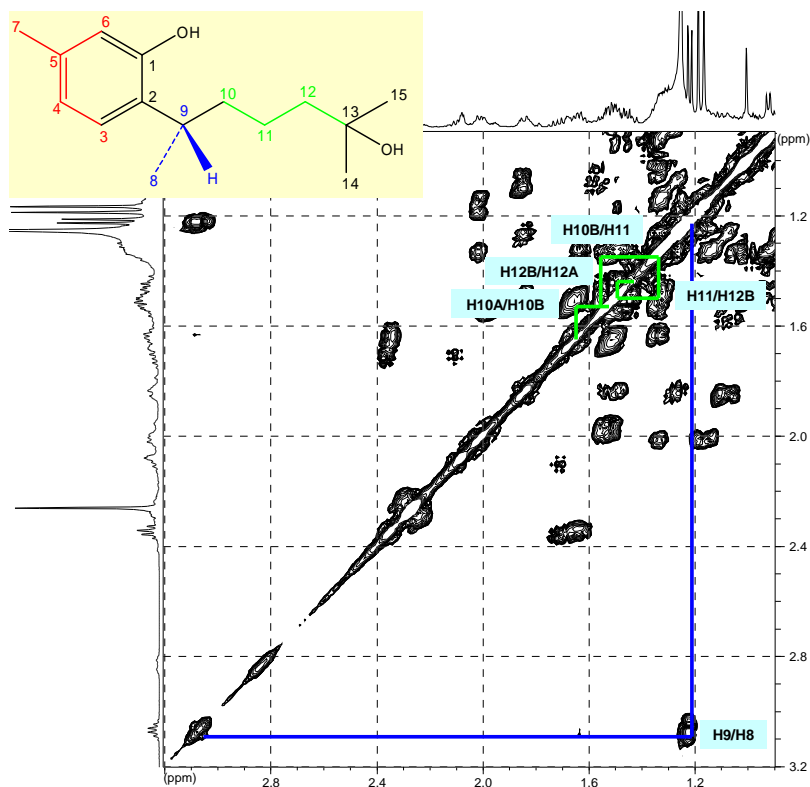
Fig.III.219. ^{1}H–^{1}H COSY spectrum of the C8 isoprenoid side chain of compound **34** (CDCl$_3$)
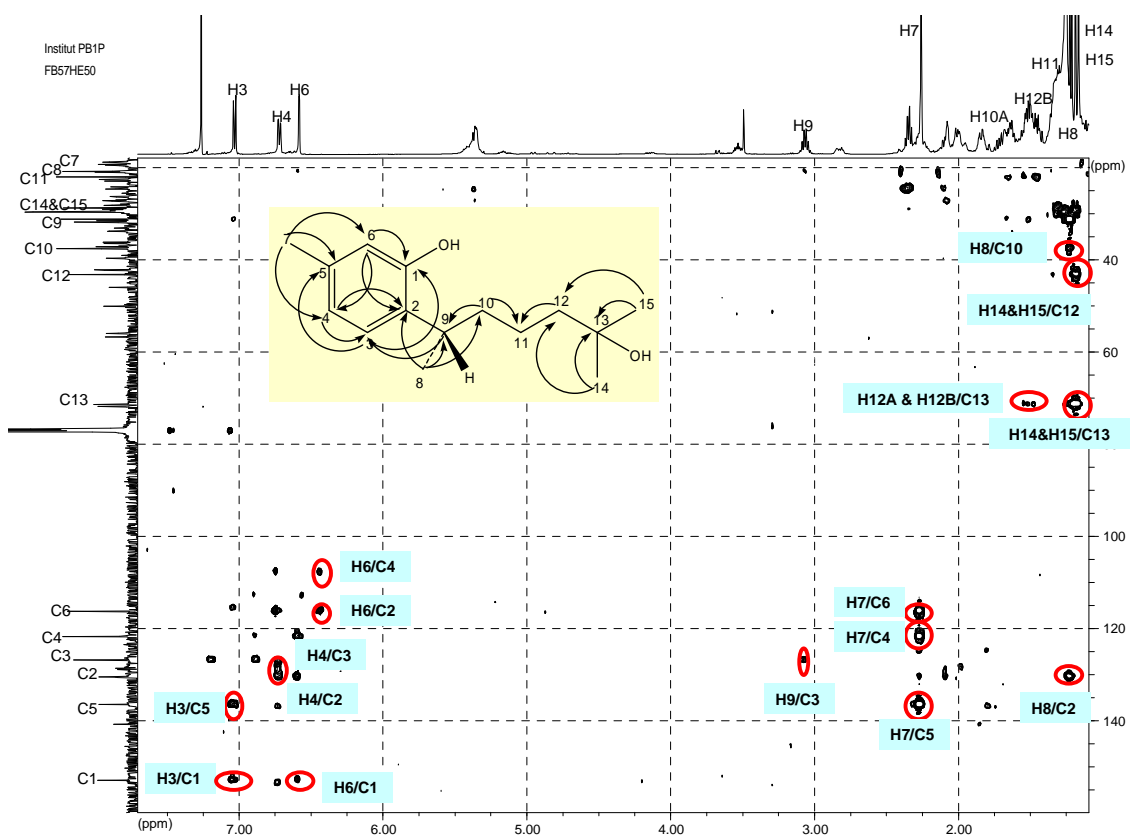
Fig.III.220. ^{1}H–^{13}C HMBC spectrum of compound **34** (CDCl$_3$)

229

Table III.29. NMR data of compound **34** in comparison to (+)-curcudiol

No	Compound 34 [a]			(+)-Curcudiol [b]		
	1H-NMR		13C-NMR	1H-NMR		13C-NMR
	δ	H, multiplicity, *J* in Hz	δ, DEPT	δ	H, multiplicity, *J* in Hz	δ, DEPT
1	-	-	152.8, C	-	-	153.10, C
2	-	-	128.6, C	-	-	130.61, C
3	7.03	1H,d, 7.6	126.8, CH	7.02	1H, d, 7.5	126.72, CH
4	6.73	1H, d, 7.6	121.7, CH	6.70	1H, d, 7.5	121.39, CH
5	-	-	136.4, C	-	-	136.25, C
6	6.58	1H, s	116.3, CH	6.56	1H, s	116.28, CH
7	2.28	3H, s	21.3, CH$_3$	2.09	3H, s	20.84. CH$_3$
OH	5.35	1H, s	-	5.28	1H, s [c]	-
OH	3.68	1H, s	-	3.45	1H, b s [c]	-
8	1.22	3H, d, 6.9	21.5, CH$_3$	1.09	3H, d, 7.2	20.99, CH$_3$
9	3.06	1H, q, 7.1	31.1, CH	2.99	1H, m	31.10, CH
10a	1.64	1H, m	38.1, CH$_2$	1.52	1H, m	37.69, CH$_2$
10b	1.52	1H, m		1.38	1H, m	
11	1.32	2H, m	22.5, CH$_2$	1.21	2H, m	22.03, CH$_2$
12a	1.54	1H, m	43.7, CH$_2$	1.44	1H, m	43.28, CH$_2$
12b	1.49	1H, m		1.31	1H, m	
13	-	-	71.4, C	-	-	71.53, C
14	1.19	3H, s	29.4, CH$_3$	1.07	3H, s	29.48, CH$_3$
15	1.16	3H, s	28.6, CH$_3$	1.04	3H, s	28.68, CH$_3$

[a] Data were recorded in CDCl$_3$, at 500 MHz, multiplicities and coupling constant are given in Hz; [b] Data were recorded in CDCl$_3$ (Wright *et al.*, 1987); [c] exchangeable data

III.6.   **Secondary metabolites from** *Rhabdastrella rowi*

Marine sponges of genus *Rhabdastrella* are commonly distributed in Asian tropical oceans, such as the shallow coral reefs in southern mainland China, New Caledonia, the Philippines (Lv *et al.*, 2004; Rao *et al.*, 1997; Tasdemir *et al.*, 2002; Rao *et al.*, 1998; Bourguet-Kondracki *et al.*, 2000). Only the species *R. globostelata* has been examined chemically, and a series of isomalabaricane-type nortriterpenoids and triterpenoids were isolated (Lv *et al.*, 2004; Rao *et al.*, 1997; Tasdemir *et al.*, 2002; Rao *et al.*, 1998; Bourguet-Kondracki *et al.*, 2000; Fouad *et al.*, 2006). Chemical constituents of *Rhabdastrella rowi* have not yet been reported so far. In this study, *Rhabdastrella rowi* yielded only fatty acids and no isomalabaricane

type compounds which was evident from its analytical HPLC chromatogram. Only compound **35** can be isolated and later identified as **quinolin-4-ol**.

III.6.1. Quinolin-4-ol (**35**, new as natural product)
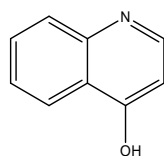
Fig.III.221. Compound **35**
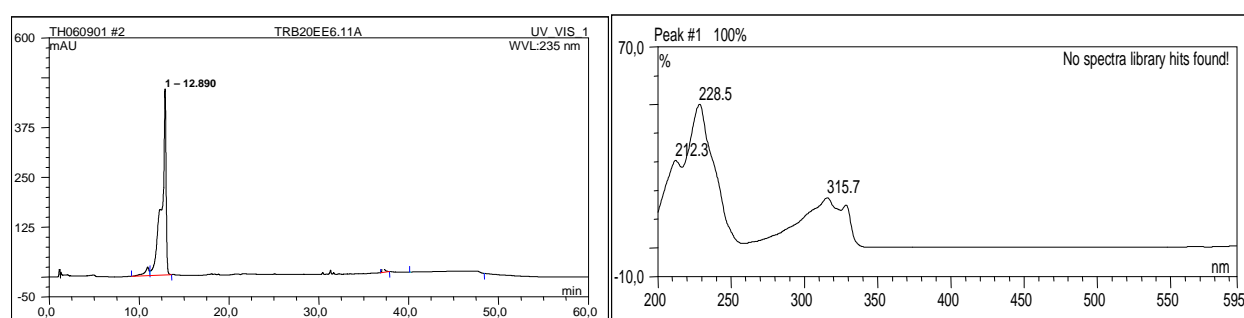
Fig.III.222. Analytical HPLC data of compound **35**
Left: HPLC profile in 235 nm RT: 12.89; right: UV absorption spectrum, λ_{max} = 212.3; 228.5, 315.7 nm
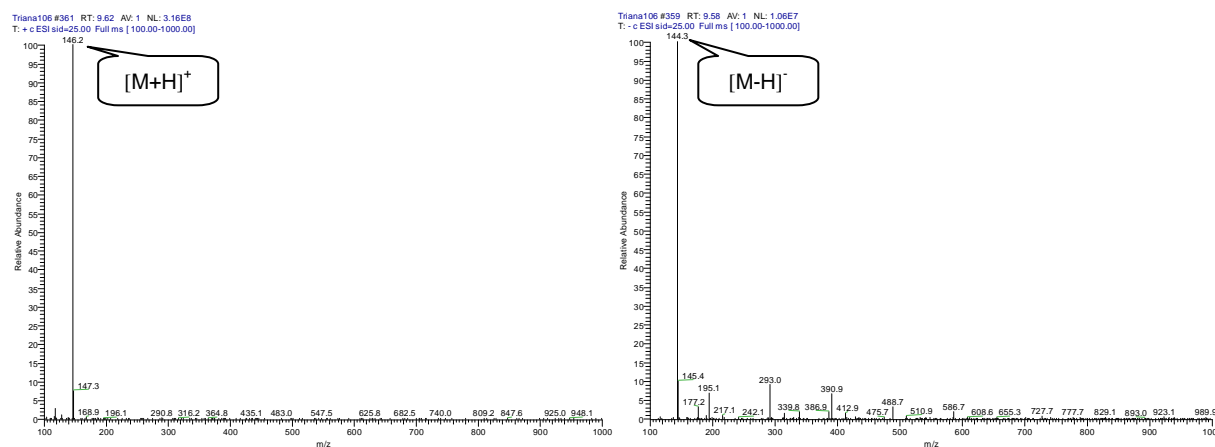
Fig.III.223. ESI-MS spectrum of compound **35**

Compound **35** was isolated as a white amorphous substance with a yield of 2 mg (0.0005% of the sponge dried weight). It gave UV absorption maxima at λ_{max} 212.3, 228.5 and 315.7 nm. ESI-MS reveals the molecular weight of 145 g/mol which is compatible to the molecular formula C_9H_7O for quinolin-4-ol.
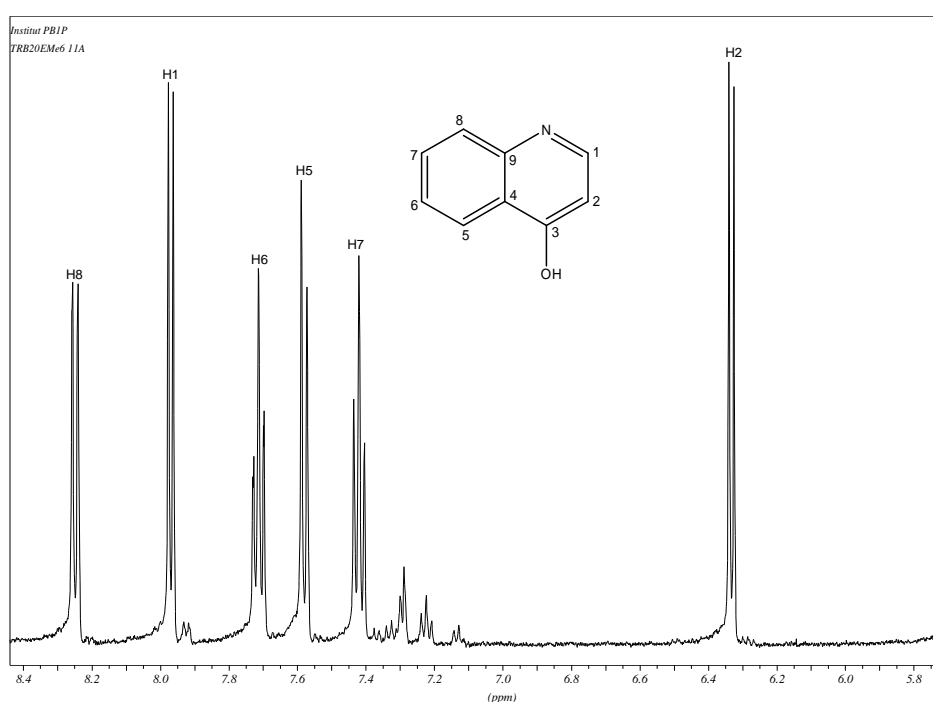
Fig.III.224. ¹H-NMR spectrum of compound **35** (MeOD, 500 MHz)

¹H-NMR spectrum in MeOD shows six proton resonances. ¹H–¹H COSY experiment reveals two spin systems suggesting the presence of two separated aromatic rings. One spin system correlates the protons at δ_H 7.98 (1H, d, *J* = 7.2 Hz, H-1) to the proton at δ_H 6.33 (1H, d, *J* = 7.2 Hz, H-2). The second spin system is a typical ABCD system and, suggests a 5,6-disubstituted benzene ring. Deshielded effect is exhibited by H-8 (δ_H 8.25, 1H, d, *J* = 8.2 Hz) and H-1 which implies the presence of a quinoline unit, while upfield chemical shift of H-2 can be explained by a hydroxyl substitution in *ortho* position. Thus compound **35** is determined as **quinolin-4-ol.**
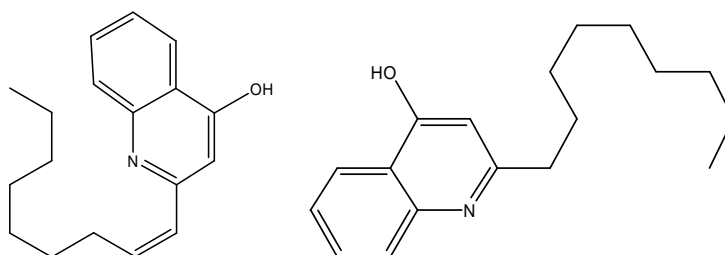
Fig.III.225. 4-hydroxy-2-(1-nonenyl)quinoline (left) and 4-hydroxy-2-nonylquinolin (right) (Debitus *et al.*, 1998)
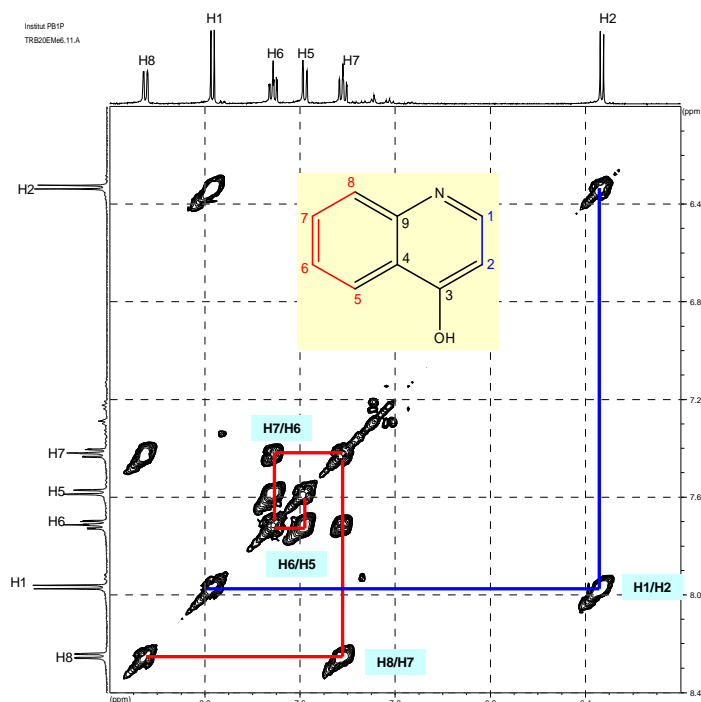
Fig.III.226. ^{1}H – ^{1}H COSY spectrum of compound **35** (MeOD)

Quinolin-4-ol itself has not yet been reported from nature. But its derivatives 4-hydroxy-2-(1-nonenyl)quinoline and 4-hydroxy-2-nonylquinolin (Fig.III.225), were reported to be produced by a bacterium isolated from the marine sponge *Suberea creba* (Debitus *et al.*, 1998).

Table III.30. NMR data of compound **35**

No	δ	Integration, multiplicity, *J* in Hz
		^{1}H-NMR
1	7.98	1H, d, 7.2
2	6.33	1H, d, 7.2
5	7.59	1H, d, 8.2
6	7.73	1H, dd, 8.2, 7.3
7	7.42	1H, dd, 7.6, 7.9
8	8.25	1H, d, 8.2

a) Data were recorded in MeOD, at 500 MHz, multiplicities and coupling constant are given in Hz

III.7. Biological Assay of Isolated Compounds

Selected crude extracts and isolated compounds from this study were tested in several biological assays, including cytotoxicity assay against mouse lymphoma cells L5178Y, anti-fouling assay, protein kinase inhibition, antibacterial, antifungal, and biofilm inhibition.

III.7.1. Cytotoxicity assay

Marine natural products have been prominently featured in the area of cancer research. Biological testing done on marine secondary metabolites is dominated by various tests for anticancer activity (Blunt *et al.*, 2006). In order to screen for promising anticancer agents from natural products, in vitro cytotoxicity assays have been done against mouse lymphoma cells L5178Y, in this study.

Several compounds have shown promising results as the IC_{50} value are less than 10 μg/ml including the new compounds from *Agelas* sponges, agelanesin A (4.5 μg/ml), agelanesin B (4.8 μg/ml), agelanesin C (9.2 μg/ml), agelanesin D (7.8 μg/ml), (-)-ageloxime D (5.5 μg/ml) and (-)-agelasine D (1.7 μg/ml), as well as the known compounds from *Pseudoceratina purpurea*, aplysamine-2 (1.7 μg/ml) and aeroplysinin-1 (0.57 μg/ml) and 5-alkylpyrrole 2-carboxaldehyde derivatives from *Mycale phyllophyla* (1.8 μg/ml) (Table III.26).

Table III.31. List of cytotoxicity assay results

Compound No.	Name of compounds or extracts (10µg/ml)	Sponge source	Growth of L5178Y in % [a]	IC$_{50}$ µg/ml
	Agelas nsp. crude extract	*Agelas* n.sp.	100.8	n.t.
1.	4-(4,5-dibromo-1-methyl-1*H*-pyrrole-2-carboxamido)-butanoic acid	*Agelas* n.sp.	107.5	n.t.
2.	Agelanin A	*Agelas* n.sp.	98.9	n.t.
3.	Agelanin B	*Agelas* n.sp.	92.8	n.t.
4.	**Agelanesin A**	*Agelas* n.sp.	**-0.5**	**4.5**
5.	**Agelanesin B**	*Agelas* n.sp.	**2.3**	**4.8**
6.	**Agelanesin C**	*Agelas* n.sp.	**0.8**	**9.2**
7.	**Agelanesin D**	*Agelas* n.sp.	**-2.3**	**7.8**
8.	Mauritamide B	*Agelas* n.sp.	92.5	n.t.
9.	Mauritamide C	*Agelas* n.sp.	98.6	n.t.
10.	*N*-methyl-4,5-dibromopyrrole taurocarboxamide	*Agelas* n.sp.	117.6	n.t.
11a.	Dibromphakellin HCl	*Agelas* n.sp.	108.8	n.t
11b.	Dibromphakellin	*Agelas* n.sp..	83.0	n.t.
12.	Dibromo-hydroxyphakellin HCl	*Agelas* n.sp.	112.8	n.t.
13.	Midpacamide	*Agelas* n.sp.	46.7	n.t.
14.	Agelongine	*Agelas* n.sp.	99.1	n.t
15.	Methyl-4,5-dibromocarboxylic acid	*Agelas* n.sp.	87.8	n.t
16.	Methyl-4,5-dibromocarboxylic acid methyl ester	*Agelas* n.sp.	83.4	n.t
	Agelas nakamurai crude extract	*Agelas nakamurai*	114.3	n.t.
17.	**Ageloxime-D**	***Agelas nakamurai***	**4.2**	**5.5**
18.	**Agelasine D**	***Agelas nakamurai***	**1.9**	**1.7**
19.	Agelasidine C	*Agelas nakamurai*	37.4	n.t.
21.	Mukanadin-C	*Agelas nakamurai*	78.5	> 10
	Pseudoceratina purpurea crude extract	*Pseudoceratina purpurea*	97.2	n.t
27.	**Aplysamine-2**	***Pseudoceratina purpurea***	**1.0**	**1.7**
28.	**Aeroplysinin-1**	***Pseudoceratina purpurea***	**-0.1**	**0.57**
29.	Bisoxazolidinone derivative	*Pseudoceratina purpurea*	89.6	n.t
30.	Dienone dimethoxyketal	*Pseudoceratina purpurea*	96.5	n.t.
31.	Dienone methoxyethoxyketal	*Pseudoceratina purpurea*	87.4	n.t.
	Mycale phylophilla crude extract	*Mycale phylophilla*	101.2	n.t.
32.	**5-alkyl 2-pyrrole carbaldehyde derivatives**	***Mycale phylophilla***	**8.3**	**1.8**
33.	(+)-Curcuphenol	*Axynissa* sp.	96.2	n.t.
34.	(+)-Curcudiol	*Axynissa* sp.	93.4	n.t.
	Rhabdastrella rowi	*Rhabdastrella rowi*	100.3	n.t
35.	Quinolin-4-ol	*Rhabdastrella rowi*	91.6	n.t

[a] 10 µg/ml sample concentration; n.t.: not tested; negative control = 100%

III.7.2. Anti-fouling

Biofouling organisms such as blue mussels, barnacles, and macroalgae cause serious problems to ship's hulls, cooling systems of power plants, and aquaculture materials (Holmes, 1970; Houghton, 1978). Long-term use of chemical antifoulants such as tributyltin has led to its accumulation and current replacements in coastal sediments (Konstantinou and Albanis, 2004) and to mortality and change of sex of non target organisms (Katranitsas *et al.*, 2003). Therefore, it is necessary to discover or develop antifouling substances with reduced or no toxicity. It is well-known that many marine invertebrates such as sponges and corals remain remarkably free from settlement by fouling organisms. It has been suggested that they have biologically active compounds that prevent other marine organisms from settling and attaching to their bodies (Hattori *et al.*, 1998). In fact, several compounds with such activity have been found among marine invertebrates (Fusetani, 2004).

Sponge-derived antifouling molecules have been found to inhibit the settlement of barnacle larvae (Okino *et al.*, 1995; Tsukamoto *et al.*, 1996a, 1996b, 1996c), inhibit fouling by macroalgae (Hattori *et al.*, 1998; Kubanek *et al.*, 2002), or repell the blue mussel *Mytilus edulis galloprovincialis* (Sera *et al.*, 1999). Brominated pyrroles such as pseudoceratidine (Tsukamoto *et al.*, 1996b), oroidin, and mauritiamine (Tsukamoto *et al.*, 1996c) and bromotyrosine-derived compounds such as ceratinamide A and B, psammaplin A (Tsukamoto *et al.*, 1996a) and moroka'iamine (Schoenfeld *et al.*, 2002) are some examples of sponge derived secondary metabolites having promising activity as anti fouling agents.

Antifouling assay has been done on several selected isolated compounds towards the barnacle *Balanus improvisus* Darwin. The bromotyrosine derived

compound, aplysamine-2 from *Pseudoceratina purpurea* and the adenine-derived diterpenes from *Agelas nakamurai*, (-)-ageloxime-D and (-)-agelasine D and the show 100% inhibition in 4.39 μg/mL, 42.2 μg/mL and 6.47 μg/mL (Ortlepp, 2007), respectively. Both diterpenoids are toxic against the cyprids while aplysamine-2 shows no toxicity in the active concentration (Ortlepp, 2007).
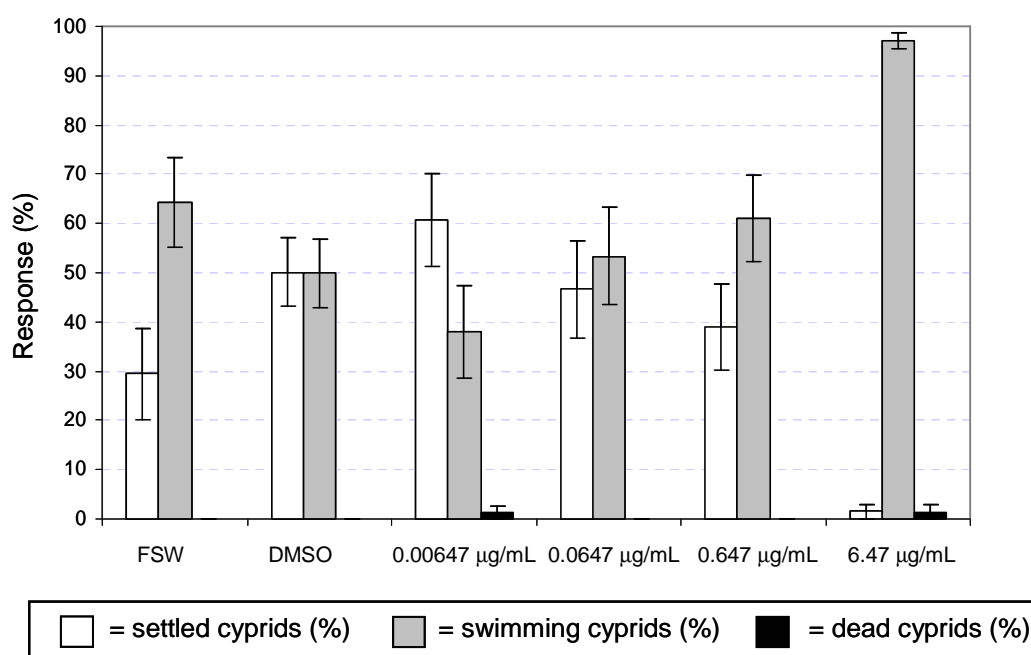
Fig.III.227. Result of antifouling assay of aplysamine-2 (Ortlepp, 2007)
(Data are presented as means percentages ± SE (n=4); FSE: filtered sea water)
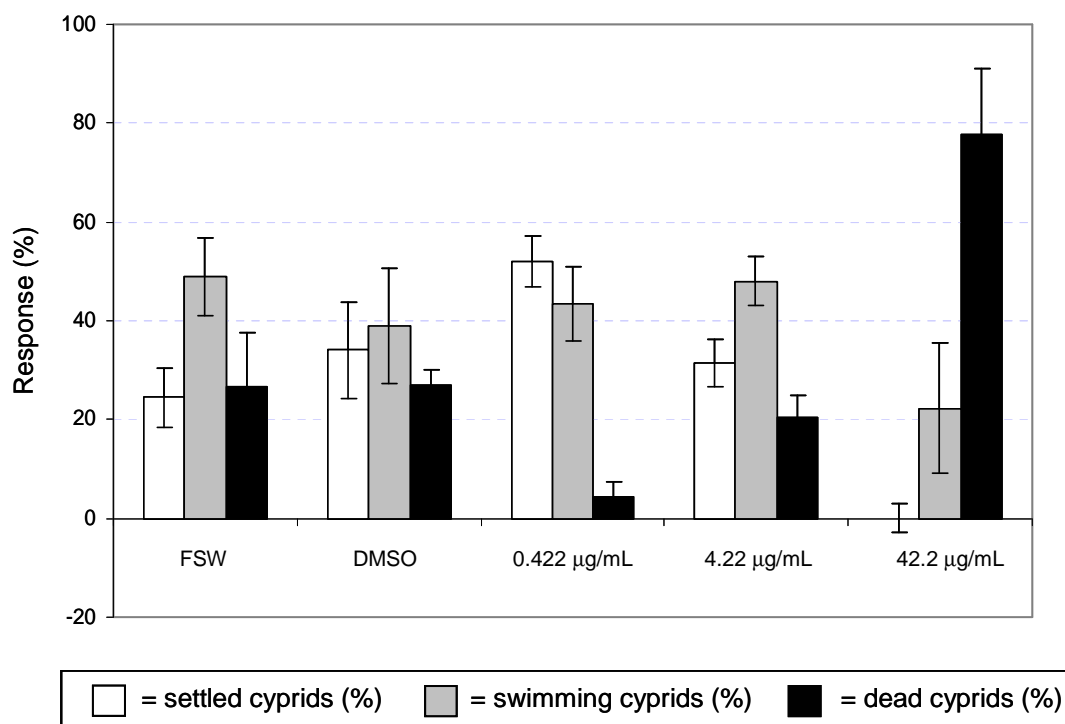
Fig.III.228. Result of antifouling assay of (-)-agelasine D
(Data are presented as means percentages ± SE (n=4); FSE: filtered sea water)
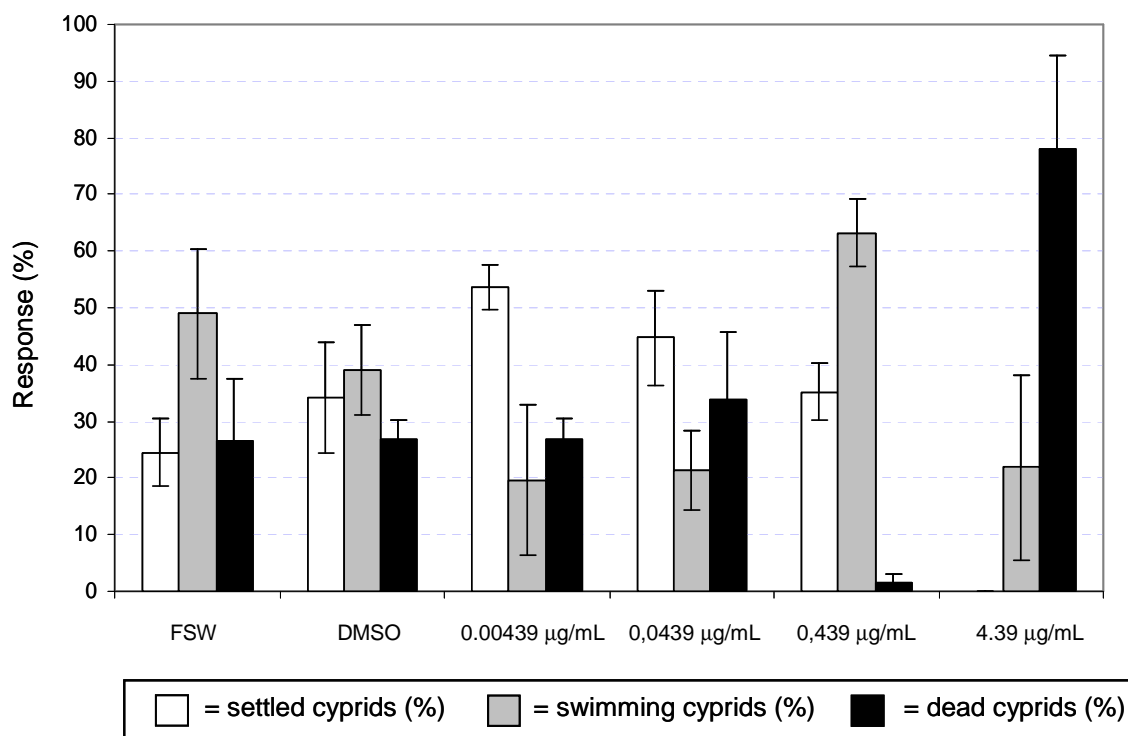
Fig.III.229. Result of antifouling assay of (-)-ageloxime D
(Data are presented as means percentages ± SE (n=4); FSE: filtered sea water)

III.7.2. Protein kinase inhibition test

A number of diseases, including cancer, diabetes, and inflammation, are linked to perturbation of protein kinase–mediated cell signaling pathways. The human genome encodes some 518 protein kinases (Manning *et al.*, 2002), that share a catalytic domain conserved in sequence and structure but which are notably different in how their catalysis is regulated. The ATP-binding pocket is between the two lobes of the kinase fold. This site, together with less conserved surrounding pockets, has been the focus of inhibitor design that has exploited differences in kinase structure and pliability in order to achieve selectivity. Drugs are in clinical trials that target all stages of signal transduction: from the receptor tyrosine kinases that initiate intracellular signaling, through second-messenger generators and kinases involved in signaling cascades, to the kinases that regulate the cell cycle that governs cellular fate (Cohen, 2002; Fabbro *et al.,* 2002; Levitzki, 2003; and Pratt *et al.*, 2004).

Protein kinases play a critical role in cell signalling pathways by catalyzing the transfer of the γ-phosphoryl group from ATP to the hydroxyl groups of protein side chains (Hunter, 2000). The protein kinase superfamily is one of the largest as ~2% of eukaryotic genes encode them. Because of their importance in contributing to a variety of pathophysiologic states, including cancer, inflammatory conditions, autoimmune disorders, and cardiac diseases, intense efforts have been made to develop specific protein kinase inhibitors as biological tools and as therapeutic agents (Showalter and Kraker, 1997).

In this study selected compounds and crude extract were screened for protein kinase inhibition activity using 24 protein kinases. All protein kinases were expressed in Sf9 insect cells as human recombinant GST-fusion proteins of His-

tagged proteins by means of the baculovirus expression system. Only (+)-curcuphenol and (+)-curcudiol which are isolated from *Axynissa* sp. exhibit protein kinase inhibition with IC_{50} value 7.8 μg/ml (SRC) and 9.2 μg/ml (FAK), respectively.

Table.III.32. List of protein kinase inhibition activity results

Compound No.	Name of compounds or extracts	Sponge source	Protein Kinase Inhibition	IC50
	Agelas nsp. crude extract	*Agelas* n.sp.	n.i	n.t.
1.	4-(4,5-dibromo-1-methyl-1*H*-pyrrole-2-carboxamido)-butanoic acid	*Agelas* n.sp.	n.i	n.t.
2.	Agelanin A	*Agelas* n.sp.	n.i	n.t.
3.	Agelanin B	*Agelas* n.sp.	n.i	n.t.
4.	Agelanesin A	*Agelas* n.sp.	n.i	n.t.
5.	Agelanesin B	*Agelas* n.sp.	n.i	n.t.
6.	Agelanesin C	*Agelas* n.sp.	n.i	n.t.
7.	Agelanesin D	*Agelas* n.sp.	n.i	n.t.
8.	Mauritamide B	*Agelas* n.sp.	n.i	n.t.
9.	Mauritamide C	*Agelas* n.sp.	n.i	n.t.
10.	*N*-methyl-4,5-dibromopyrrole taurocarboxamide	*Agelas* n.sp.	n.i	n.t.
11.	Dibromphakellin	*Agelas* n.sp.	n.i	n.t
12.	Dibromo-hydroxyphakellin HCl	*Agelas* n.sp.	n.i	n.t.
13.	Midpacamide	*Agelas* n.sp.	n.i	n.t.
14.	Agelongine	*Agelas* n.sp.	n.i	n.t
15.	Methyl-4,5-dibromocarboxylic acid	*Agelas* n.sp.	n.i	n.t
	Agelas nakamurai crude extract	*Agelas nakamurai*	n.i	n.t.
17.	Ageloxime-D	*Agelas nakamurai*	n.i	n.t
18.	Agelasine D	*Agelas nakamurai*	n.i	n.t
19.	Agelasidine C	*Agelas nakamurai*	n.i	n.t.
22.	Hymenidin	*Agelas nakmurai*	n.i	n.t
	Pseudoceratina purpurea crude extract	*Pseudoceratina purpurea*	n.i	n.t
27.	Aplysamine-2	*Pseudoceratina purpurea*	n.i	n.t
28.	Aeroplysinin-1	*Pseudoceratina purpurea*	n.i	n.t
	Mycale phylophilla crude extract	*Mycale phylophilla*	n.i	n.t.
32.	*5-alkyl 2-pyrrole carbaldehyde derivatives*	*Mycale phylophilla*	n.i	n.t
	Axynissa sp. crude extract	*Axynissa sp.*	n.i	n.t
33.	(+)-Curcuphenol	*Axynissa* sp.	Active (SRC)	SRC: 7.8μg/ml
34.	(+)-Curcudiol	*Axynissa* sp.	Active (FAK)	FAK: 9.2μg/ml

n.t.: not tested; n.i.: no inhibition

III.7.3. Anti-microbial

Anti-microbial activity is reported to be the third most often used biological assay carried out on marine metabolites (Blunt *et al.*, 2006). Increasing clinical importance of drug resistant bacterial pathogens such as in tuberculosis and MRSA (multiple resistant *S. aureus*) diseases has lead to the urgency for more research in this field (Shu, 1998).

Screenings for antifungal and antibacterial against Gram positive bacteria of the selected isolated compounds and crude extracts have been pursued in this study. Only the (-)-agelasine-D and (+)-agelasidine-C from *Agelas nakamurai* show low to moderate activity against *C. herbarum* and *C. curcumerinum*, and only (+)- agelasine D exhibits low activity against *S. cereviseae*. Midpacamide and (-)-agelasine D show low activity against *Bacillus subtillis*.

III.7.3.1. Screening for anti fungal activity

Table.III.33. List of screening antifungal activity results

Comp. No.	Name of compounds or extracts	Sponge source	Growth of *S. cereviseae*		Growth of *C. herbarum*		Growth of *C. cucumerinum*	
			10µl (mm)	20µl (mm)	10µl (mm)	20µl (mm)	10µl (mm)	20µl (mm)
	Nystatin	positive control	14	-	8	-	34	-
	Agelas nsp. crude extract	*Agelas* n.sp.	n.i	2	-	-	-	-
3.	Agelanin B	*Agelas* n.sp.	n.i	n.i	n.i	n.i	n.i	n.i
8.	Mauritamide B	*Agelas* n.sp.	n.i	n.i	n.i	n.i	n.i	n.i
9.	Mauritamide C	*Agelas* n.sp.	n.i	n.i	n.i	n.i	n.i	n.i
10.	*N*-methyl-4,5-dibromopyrrole taurocarboxamide	*Agelas* n.sp.	n.i	n.i	n.i	n.i	n.i	n.i
13.	Midpacamide	*Agelas* n.sp.	n.i	n.i	n.i	n.i	n.i	n.i
14.	Agelongine	*Agelas* n.sp.	n.i	n.i	n.i	n.i	n.i	n.i
15.	Methyl-4,5-dibromocarboxylic acid	*Agelas* n.sp.	n.i	6	n.i	n.i	n.i	n.i
	Agelas nakamurai crude extract	*Agelas nakamurai*	-	-	n.i	n.i	n.i	n.i
17.	Ageloxime-D	*Agelas nakamurai*	n.i	n.i	n.i	n.i	n.i	n.i
18.	**Agelasine D**	***Agelas nakamurai***	**n.i**	**3**	**5**	**6**	**4**	**6**
19.	**Agelasidine C**	***Agelas nakamurai***	**n.i**	**n.i**	**5**	**8**	**4**	**4**
	Pseudoceratina purpurea crude extract	*Pseudoceratina purpurea*	n.i	n.i	n.i	n.i	n.i	n.i
27.	Aplysamine-2	*Pseudoceratina purpurea*	n.i	n.i	n.i	n.i	n.i	n.i
	Mycale phylophilla crude extract	*Mycale phylophilla*	n.i	2	n.i	n.i	n.i	n.i
32.	5-alkyl 2-pyrrole carbaldehyde derivatives	*Mycale phylophilla*	n.i	n.i	n.i	n.i	n.i	n.i

n.i.: no inhibition

III.7.3.2. Screening for anti bacterial activity

Table.III.34. List of screening antibacterial activity results

Compound No.	Name of compounds or extracts	Sponge source	Growth of *B. subtilis* 10µl (mm)	Growth of *B. subtilis* 20µl (mm)
	Penicillin	positive control	11	n.t.
	Gentamycin	positive control	18	n.t.
	Streptomycin	positive control	9	n.t.
3.	Agelanin B	*Agelas* nsp.	n.i.	n.i.
8.	Mauritamide B	*Agelas* nsp.	n.i.	n.i.
9.	Mauritamide C	*Agelas* nsp.	n.i.	n.i.
10.	*N*-methyl-4,5-dibromopyrrole taurocarboxamide	*Agelas* nsp.	n.i.	n.i.
13.	**Midpacamide**	***Agelas* nsp.**	**1**	**3**
14.	Agelongine	*Agelas* nsp.	n.i.	n.i.
15.	Methyl-4,5-dibromocarboxylic acid	*Agelas* nsp.	n.i.	n.i.
	Agelas nakamurai crude extract	*Agelas nakamurai*	n.i.	n.i.
17.	Ageloxime-D	*Agelas nakamurai*	n.i.	n.i.
18.	**Agelasine D**	***Agelas nakamurai***	**1**	**1**
19.	Agelasidine C	*Agelas nakamurai*	n.i.	1
	Pseudoceratina purpurea crude extract	*Pseudoceratina purpurea*	n.i.	n.i.
27.	Aplysamine-2	*Pseudoceratina purpurea*	n.i.	n.i.
	Mycale phylophilla crude extract	*Mycale phylophilla*	n.i.	n.i.
32.	5-alkyl 2-pyrrole carbaldehyde derivatives	*Mycale phylophilla*	n.i.	n.i.

n.i: no inhibition; n.t.: not tested

III.7.4. Biofilm Assay

Biofilms have great significance for public health, because biofilm-associated microorganisms exhibit dramatically decreased susceptibility to antimicrobial agents. This susceptibility may be intrinsic (as a natural outcome of growth in the biofilm) or acquired (due to transfer of extrachromosomal elements to susceptible organisms in the biofilm). The susceptibility of biofilms to antimicrobial agents cannot be determined by means of standard microdilution testing, since these tests rely upon the response of planktonic (suspended) rather than biofilm (surface-associated)

organisms. Instead, susceptibility must be determined directly against biofilm-associated organisms, preferably under conditions that stimulate conditions in vivo (Donlan, 2001)

Biofilm-related infections are very common nocosomial infections (O'Gara and Humpreys, 2001; von Eiff *et al.*, 2002; Costerton *et al.*, 1999; Donlan and Costerton, 2002) and account for significant morbidity and mortality. *Staphylococcus epidermidis* biofilms form at the surface of implants and prostheses and are responsible for the failure of many antibiotic therapies. Up to now, only few antibiotics are relatively active against biofilms (Gualtieri *et al.* 2006).

Biofilms are formed by the colonization of solid supports (bone, implants and cathethers) by adherent bacteria. Several mechanisms have been proposed to explain why only very few molecules are active against biofilms: biofilm-embedded bacteria enter a non-growing (stationary) state, in which they are less succeptibe to growth-dependent antimicrobial killing (Gilbert *et al.*, 1990), physicochemical interaction of certain antibiotics with slime (Gordon *et al.*, 1988) and lower diffusion (Hoyle *et al.*, 1992; Dunne *et al.*, 1993), or changes in the bacterial envelope following adhesion. However, the presence in the biofilms at a high frequency of 'persisters', bacteria that do not grow but do not die in the presence of the antibiotic, might be the cause of these recalcitrant infections (Gualtieri *et al.*, 2006).

In this study several selected isolated compounds have been tested against *Staphylococcus epidermidis* to explore the MIC value, growth inhibition and the biofilm inhibition ability. The new bromopyrrole derivative from *Agelas* nsp., agelanesin B and the new diterpene from *Agelas nakamurai*, (-)-ageloxime D exhibit biofilm-inhibition activity but no growth inhibition of *S. epidermidis* was observed (MIC

value $>$ 20 µg/ml).

Table.III.35. Biofilm assay results

Compound No.	Name of compounds	Sponge source	MIC µg/ml (*S.epidermidis*)	Growth Inhibition	Biofilm Inhibition
1.	4-(4,5-dibromo-1-methyl-1*H*-pyrrole-2-carboxamido)-butanoic acid	*Agelas* n.sp.	>20	n.i.	n.i.
2.	Agelanin A	*Agelas* n.sp.	>20	n.i.	n.i.
3.	Agelanin B	*Agelas* n.sp.	>20	n.i.	n.i.
4.	Agelanesin A	*Agelas* n.sp.	>20	n.i.	n.i.
5.	Agelanesin B	*Agelas* n.sp.	>20	n.i.	n.i.
6.	Agelanesin C	*Agelas* n.sp.	>20	n.i.	n.i.
7.	Agelanesin D	*Agelas* n.sp.	>20	n.i.	n.i.
8.	Mauritamide B	*Agelas* n.sp.	>20	n.i.	n.i.
9.	Mauritamide C	*Agelas* n.sp.	>20	n.i.	n.i.
10.	*N*-methyl-4,5-dibromopyrrole taurocarboxamide	*Agelas* n.sp.	>20	n.i.	n.i.
11.	Dibromophakellin	*Agelas* n.sp.	>20	n.i.	n.i.
12.	Dibromo-hydroxyphakellin HCl	*Agelas* n.sp.	>20	n.i.	n.i.
13.	Midpacamide	*Agelas* n.sp.	>20	n.i.	n.i.
14.	Agelongine	*Agelas* n.sp.	>20	n.i.	n.i.
15.	4,5-Bromopyrrole carboxylic acid	*Agelas* n.sp.	>20	n.i.	n.i.
17.	**(-)-Ageloxime-D**	***Agelas nakamurai***	**>20**	**no**	**yes**
18.	**(-)-Agelasine-D**	*Agelas nakamurai*	**< 0,31**	n.i.	n.i.
19.	**(+)-Agelasidine-C**	*Agelas nakamurai*	**2,5**	n.i.	n.i.
21.	Mukanadin-C	*Agelas nakamurai*	>20	n.i.	n.i.
27.	Aplysamine-2	*Pseudoceratina purpurea*	20	n.i.	n.i.
	Agelasine I*	*Agelas nakamurai* [#]	>20	n.i.	n.i.

n.i.: no inhibition; *: isolated by Murti (2006); [#] collected from Menjangan Island on September 1997 (Murti, 2006)

IV. DISCUSSION

As the central and richest part of the larger Indo West Pacific region, Indonesia has been reported to possess high marine biodiversity including sponges (Van Soest, 1989). Increased feeding pressure from fishes and possibly from predatory invertebrates not to mention higher microbial infection in tropical areas might be the reason for more interesting and more diverse secondary metabolites found in sponges that live in this region in comparison to other ecosystem of the world (Proksch *et al.*, 2002). As new and more complicated diseases are encountered worldwide, the need for new chemotherapeutic agent is increased. Therefore study on the Indonesian sponges is necessary due to them being a potential source of new drugs from the sea or compounds that serve as lead structures for further drug development.

Marine sponges investigated in this study come from several collection sites in Indonesia. Different types of secondary metabolites including some new derivatives are isolated and elucidated. Most of the compounds have no terrestrial counterpart except for the sesquiterpene alcohol obtained from *Axynissa* sp. The isolated compounds can be categorized into two major classifications which include alkaloids and terpenoids. It is interesting to find out that such classification can not be applied strictly here, since diterpenoids such as agelasidine C also contain an amino acid derived moiety, like other alkaloids. Noteworthy, most of the isolated halogenated alkaloids yielded are brominated while only two of them are iodinated. But no chlorinated alkaloid is isolated in this study.

IV.1.   Halogenated alkaloids from marine sponges

High halogen concentration in sea water has a consequence of its contribution in the biosynthesis of some marine metabolites. Catalyzed by haloperoxidases, halogenide anions from sea-water are oxidized (Hoffmann and Lindel, 2003) and then incorporated into organic compounds by specific halogenases (Van Pee, 2001). Enormous reactivity towards electrophilic halogenation reactions is probably the cause why heteroatom containing secondary metabolites such as pyrroles, indoles, phenols, and tyrosines are commonly found to be halogenated in sponges. Their function in sponges is presumably to resist feeding by fish and fouling by barnacles, bacteria, and fungi (Gribble, 2004).

Interestingly, despite the relative higher concentrations of chloride in comparison to bromide and iodide ions in sea water (559 mM, 0.86 mM and 0.45 μM respectively), there exists a marked predominance of bromine containing metabolites (Faulkner, 1995). Greater ease of the bromide ions to be oxidized and give bromonium species which react readily as electrophile with unsaturated species makes marine organisms utilize (oxidize) more bromide than chloride for incorporation into organic compounds (Whitehead, 1999).

The presence of bromine and chlorine in a molecule can be easily distinguished from the molecular ion peak shown by their mass spectra. The molecular ions of chlorine and bromine-containing compounds will show multiple peaks due to the fact that each halogen exists as two isotopes. While ^{79}Br and ^{81}Br exist in relatively equal abundance, the natural chlorine isotopes consist of 75.77% of ^{35}Cl and of 24.23% ^{37}Cl (Smith, 2005). Thus the molecular ion of a chlorine-containing compound will have two peaks, separated by two mass units, in an

intensity ratio of ≈3:1, while in a bromine-containing compounds these two peaks occur in approximately equal intensities. Therefore the presence of one bromine in a molecule e.g. in mukanadin C (**21**) will be represented by two molecular ion peaks having a difference of two mass units in an equal height. In the meantime, the presence of two bromines as in midpacamide (**13**) will appear as three molecular ion peaks having a difference of two mass units in an intensity ratio of 1:2:1. Furthermore in a compound bearing three bromines such as aplysamine-2 (**27**), the molecular ion will appear as multiple peaks having two mass unit differences in a ratio of 1:2:2:1.

The presence of fluorine and iodine, by contrast, is monoisotopic, having masses of 19 and 127 amu respectively (Smith, 2005). Thus neither fluorine nor iodine substitution will cause the above phenomenon as can be observed in agelanesin B (**4**) and agelanesin D (**7**).

The identification of distinct molecular ion pattern of brominated compounds in mass spectrometry using LC/MS is very important. This method can easily distinguish the presence of new brominated metabolites from sponge crude extracts. In LC/MS, after separation with HPLC is achieved, the separated peaks are detected with the UV detector and mass spectrometer. As several compounds can share the same UV pattern, the possibility of them to have the same molecular weight is less. This possibility is even more decreased for brominated compounds, since it is very rare to find different compounds having the same molecular weight with the same degree of bromination.

IV.1.1. Brominated pyrroles from marine sponges genus Agelas

IV.1.1.1. Physical properties

Brominated pyrroles have been isolated on several occasions as major

constituents of marine sponges (Whitehead, 1999). Many of the simpler members of this group of compounds are structurally related. They comprise two heterocyclic rings linked by a linear chain (Whitehead, 1999) called pyrrole-imidazole alkaloids.

Interesting properties revealed from this group of compounds are their distinct UV spectra. These compounds share the same chromophore, a pyrrole-2-carbonyl ring which according to Jaffe and Orchin (1962), should exhibit an absorption maximum at around 270 nm. This characteristic band is observed in all of the metabolites isolated in this study with some minor to major modification (Fig.IV.1a-1d).
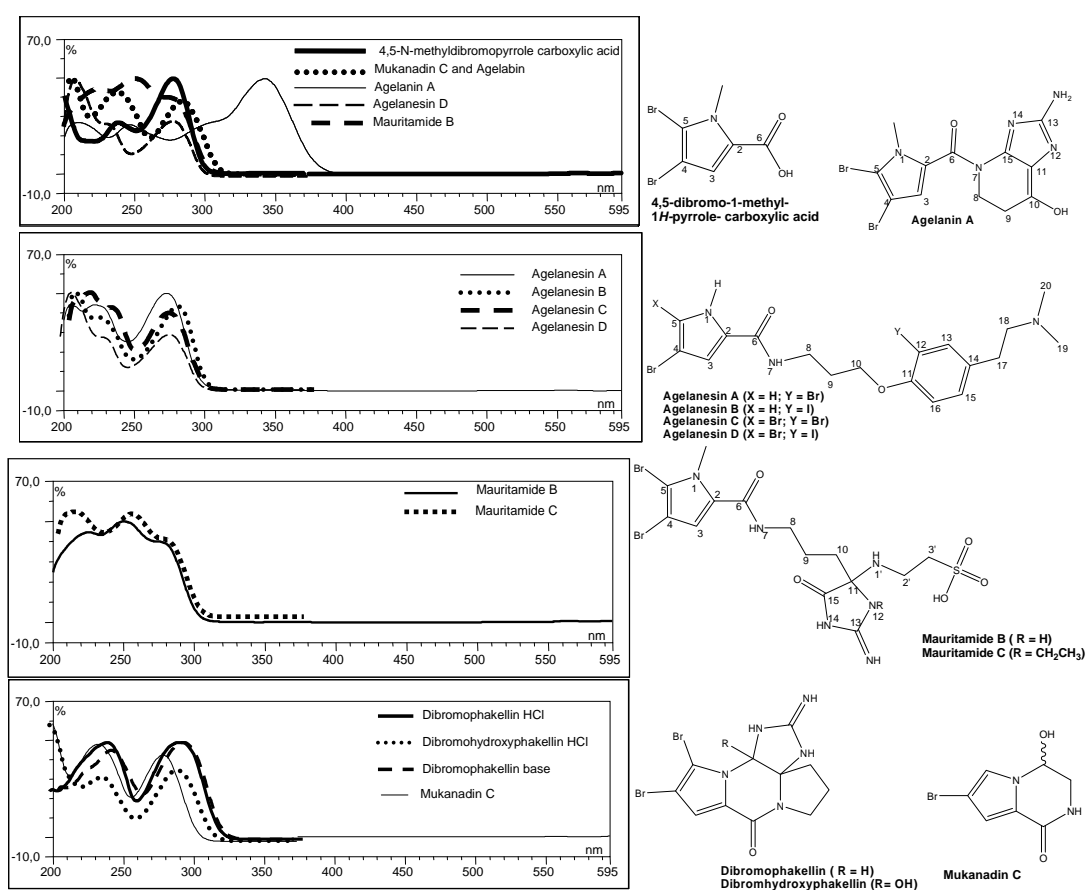
Fig.IV.1a-d. UV absorption pattern of several pyrrole imidazole alkaloids from *Agelas* sponges

UV absorption comparison of each group of compounds is shown on

Fig.IV.1a. Additional tyramine in the molecule as can be found in agelanesins (**4** – **7**) will reduce the intensity of the absorption band at around 270 nm and increase the absorption band at around 210 nm which represent the additional phenolic unit (Fig.IV.1b). A cyclization of the linear chain to form the pyrrolopyrazinone bicyclic system as can be observed in mukanadin C (**21**) and its new congener longamide C (**20**), as well as in the phakellins (**11a**, **11b**, **12**) will intensify the absorption band at around 230 nm (Fig.IV.2d). Interestingly, if the cyclization occurred between N-7 to the imidazole ring as in agelanin A (**2**), major modification is encountered. A pronounced bathocromic shift of the major band to λ 340 nm is observed (Fig.IV.1a). This kind of bathocromic shift can also be observed in hymenialdisins (Fig.IV.2). Stevensine which differs in the imidazoline ring part, loses the second band and only shows a major peak at around 240 nm, while in 2-bromoaldisin the second band is encountered at around 315 nm (Pedradab, 2005).
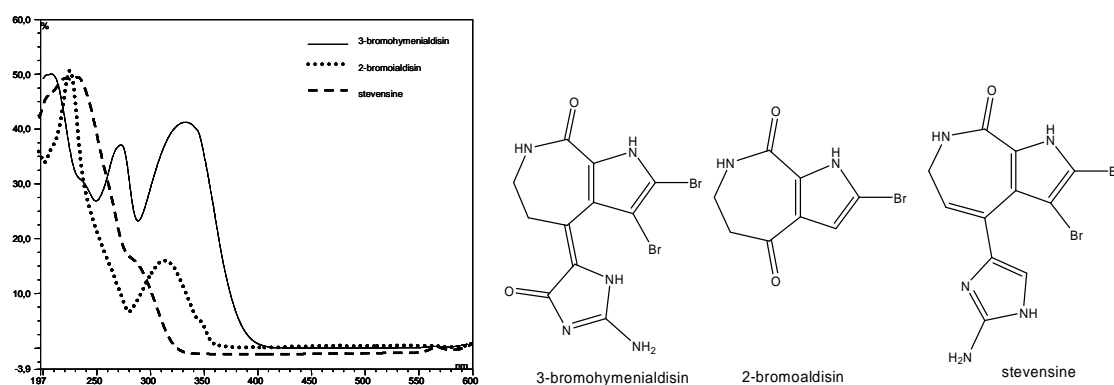
Fig.IV.2. UV absorption pattern of several pyrrole imidazole alkaloids (modified from Baker, 2004; Pedaradap, 2005)

Pyrrole-imidazole alkaloids are exclusively found in marine sponges, mainly of the families Agelasidae, Axinellidae, and Halichondridae. The underlying $C_{11}N_5$ building block consists of a pyrrolyl-2-carbonyl unit being connected via an amide

linkage to a 2-amino-5-(3-amino) propylimidazole partial structure (Lindel *et al*., 2000a). The pyrrole-2-carbonyl unit can be non-, mono-, or dibrominated in the 4- and 5- positions. Bromination of the pyrrole 3-position or of the imidazole part has not been observed (Hoffmann and Lindel, 2003). In some metabolites, the linear chain is cyclized to form an AB core of a pyrrolopyrazinone bicyclic system such as in dibromophakellin, agelastatin A, pala'uamine, longamide A, and cyclooroidin (Fig.IV.3) (Jacquot *et al*., 2004).
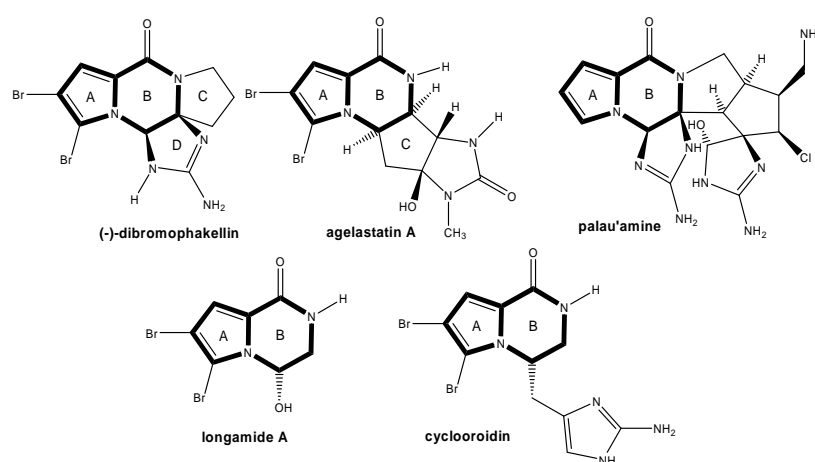
Fig.IV.3. Some pyrrole-imidazole compounds having a pyrrolopyrazinone bicyclic system (Jacquot *et al*., 2004)

Sixteen different brominated pyrrole derivatives (compounds **1** to **16**) are obtained from *Agelas* n.sp., whereas only five congeners are obtained from *Agelas nakamurai* (compound **20**-**24**). Twelve of the isolated compounds are new pyrrole-imidazole derivatives.

Interestingly, the *Agelas nakamurai* secondary metabolites are all derived from monobrominated pyrrole, while in most of *Agelas* n.sp. metabolites, the pyrrole rings are dibrominated with exception of agelanesin A (**4**), agelanesin B (**5**) and agelongine (**14**) which are monobrominated pyrroles. Another difference observed is

that all metabolites of *Agelas nakamurai* found in this study have a free NH pyrrole while in most of the *Agelas* n.sp. metabolites, the NH pyrrole is methylated. A clear example is provided by the presence of 4-bromo-1*H*-pyrrole-2-carboxylic acid (**23**) in *Agelas nakamurai*, and its dibrominated *N*-methyl pyrrole congener (**15**) in *Agelas* n.sp. Furthermore, an analogue of the new *Agelas* n.sp. metabolite, 4-(4,5-dibromo-1-methyl-1*H*-pyrrole-2-carboxamido) butanoic acid (**1**) was previously reported from *Agelas nakamurai* as 4-bromo-2-carboxamido-butanoic acid (Murti, 2006).
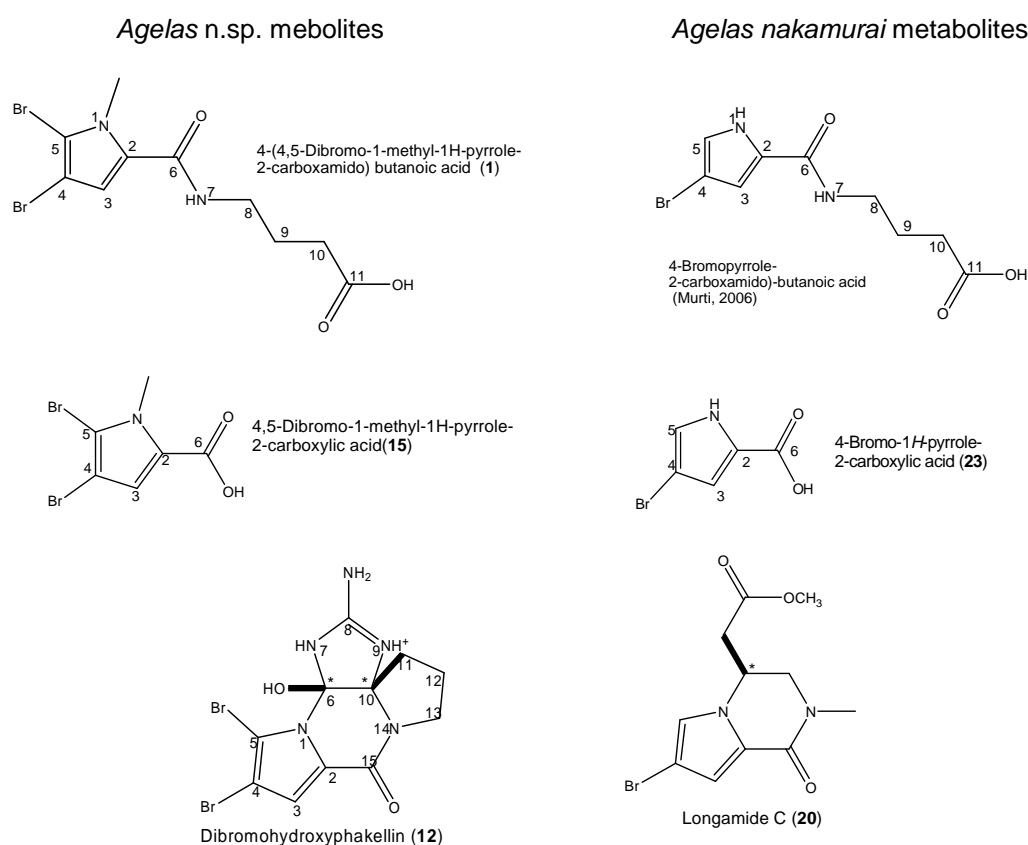
Fig.IV.4. Some pyrrole-imidazole compounds isolated from *Agelas* n.sp. and *Agelas nakamurai* showing the difference in the structure of related compound
* Only relative stereochemistry is shown

The pyrrole-imidazole compounds in *Agelas* n.sp. are highly diverse. Some new functionality is concurrently introduced. Agelanin B (**3**), a new midpacamide

related compound, displays a very unusual open ring system of 3-hydroxyl-4-oxo-pentanoic acid to replace the hydantoin ring. Moreover, a novel mode of intramolecular cyclization found in agelanin A (**2**) introduces a unique functionality as the propylamide chain is cylized to form a dihydroimidazopyridinol ring. Despite its very rare mode of cyclization, a related structure was previously reported as dibromoagelaspongin, a phakellin related compound isolated from Tanzanian sponge *Agelas* sp. (Fedoreyev *et al.*, 1989). The phakellins, as one of the unique members of pyrrole imidazole metabolites (**11a**, **11b** and **12**) exhibit a unique array of functionality including a cyclic guanidine, a pyrrole carboxylic acid, a pyrrolidine, and a congener with potentially delicate vicinal diaminal stereocenters (Poullennec *et al.*, 2002). From a structural perspective, oroidin is related to (-)-dibromophakellin by a complex cyclization of oroidin that formally connects the pyrrole nitrogen atom (N-1) to the unalkylated aminoimidazole carbon (C-6) and the amino nitrogen atom (N-14). Whereas in dibromohydroxyphakellin (**12**), dibromophakellin HCl (**11a**) and dibromophakellin base (**11b**) the linear chain is cyclized to form a pyrrolopyrazinone ring, in agelanesins, the imidazole ring is replaced with a halogenated tyramine (described separately in section IV.1.2). New taurine related compounds are also encountered in two mauritamide A congeners, mauritamide B (**8**) and C (**9**), along with a quite simple compound 2-(4,5-dibromo-1-methyl-1*H*-pyrrole-2-carboxamido) ethanesulfonic acid (**10**). Moreover, a co-occurrence of the known serotonergic agent, agelongine (**14**) with its pyridinium ring in the structure to replace the imidazole nucleus and an ester linkage to replace the amidic bond (Cafieri *et al.*, 1995) is also isolated from this *Agelas* n.sp. sponge.

IV.1.1.2.Biosynthesis

Although pyrrole-imidazole alkaloids are important for their pharmacological activities and for chemotaxonomic considerations (Braekman *et al.*, 1992), their biosynthesis remains in question (Travert and Al-Mourabit, 2004). Since the oroidin family of bromopyrole alkaloids is reported from an assortment of sponge genera together with large populations of heterotrophic bacteria found in Carribean sponge *Agelas conifera*, symbiotic microorganisms were suggested to play a role in the biosynthesis of these compounds. But cellular localization studies by differential centrifugation and Ficoll density gradients demonstrated that oroidin and sceptrin were associated with sponge spherulous cells which is found in abundance and not with the bacterial fraction (Richelle-Maurer *et al.*, 2003). This finding is in agreement with several studies showing that spherulous cells, when present, are producers of the bioactive metabolites (Marin *et al.*, 1998; Müller *et al.*, 1986; Salomon *et al.*, 2001; Thompson *et al.*, 1983; Turon *et al.*, 2000; Uriz *et al.*, 1996; Richelle-Maurer *et al.*, 2003). The production of an oroidin dimer, stevensine, from amino acid precursors through a sponge cell culture performed by Andrade *et al.* (1999) supports that these alkaloids are produced by sponge cell and not by microorganism symbiont (Richelle-Maurer *et al.*, 2003).

Since all pyrrole imidazole alkaloids are closely related, they may share the same biosynthetic pathway. It is fascinating that this large, structurally diverse family of compounds have a biogenetic relationship based on a common key metabolite, oroidin (Al Mourabit and Potier, 2001; Hoffmann and Lindel, 2003).
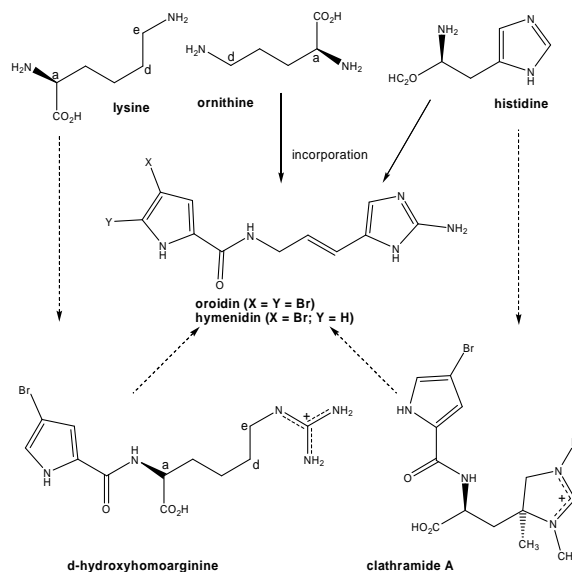
Fig.IV.5. Plausible biosynthetic pathways leading to the key pyrrole-imidazole alkaloid (according zo Hoffmann and Lindel, 2003)

Several alternatives have been discussed with regard to their biosynthesis. While the pyrrole part is generally expected to be derived from proline/ornithine, different proposals have been put forward for the 2-amino-5-(3-amino) propylimidazole part (Lindel *et al.*, 2000a). Considering that the metabolism of proline in some plants and microorganisms is known to be stress dependent (Hare and Cress, 1997; Ballantyne and Storey, 1983), even though the ecological role of proline in sponges is not known, one can suppose that its role under stress conditions is also crucial. Thus, if proline is involved in $C_{11}N_5$ formation under oxidative conditions, this would be in accordance with the ecological role of "oroidin-based" alkaloids used by sponges as a chemical arsenal for their defense (Travert and Al-Mourabit, 2004).

Braekman and collaborators (1992) proposed that proline, ornithine, and guanidine are probable precursors of both the bromopyrrole and 2-aminoimidazolinone moieties based on the following arguments:

(a)   proline and ornithine are two closely related amino acids of the glutamate group

254

and the oxidation of proline into pyrrole-2-carboxylic acid is a general catabolic pathway (Michal, 1972);

(b) analogous aminopropylimidazole moieties are found in saxitoxin, which some of the atoms forming this moiety arise from ornithine (Shimizu *et al.*, 1984);

(c) the isolation of girolline from "*Pseuodaxynissa" cantharella* (Ahond *et al.*, 1988) with co occurrence of linear or cyclized pyrrole derivatives, suggests that the biosynthetic pathway of these alkaloids proceeds by formation of an amide bond between a pyrrole-2-carboxylic acid precursor and an amino propylimidazole moiety (Braekman *et al.*, 1992).

Furthermore Hoffmann and Lindel (2003) suggested that ornithine would be incorporated into proline, which then could be oxidized to the pyrrole-2-carboxylic acid moiety of the pyrrole-imidazole alkaloids (Hoffmann and Lindel, 2003). This argument is supported by the result of a biosynthetic experiment performed by Kerr and co-workers (1999). The biosynthetic experiment conducted in cell cultures of the sponge which produce stevensine (odiline) showed that [^{14}C]-labeled proline, ornithine, and histidine were incorporated into stevensine. Natural compounds 3-amino-1-(2-aminoimidazolyl)-prop-1-ene and 4,5-dibromopyrrole carboxylic acid were proposed as intermediates (Andrade *et al.*, 1999).

Hoffman and Lindel (2003) proposed that if histidine is a biogenetic precursor, the natural product clathramide A could be a biogenetic intermediate in the oroidin source, *Agelas clathrodes* (Cafieri *et al.*, 1998a; Cafieri *et al.*, 1996). The missing carbon atom would be incorporated into the histidine-derived portion via methylation of the imidazole 5-portion, followed by conversion of clathramide A to a cyclopropane and subsequent ring opening (Fig.IV.5) (Hoffman and Lindel, 2003).

Travert and Al-Mourabit (2004) proposed another alternative biosynthetic pathway stating that a pseudo dipeptide pyrrole-proline-guanidine could be the precursor leading to the amide-connected $C_{11}N_5$ pyrrole and 2-aminoimidazolinone sections (Fig.IV.6). First specific step in pyrrole 2-aminoimidazole biosynthesis would involve proline-based peptide synthesis, followed by oxidation of the proline to pyrrole section and then by oxidation rearrangement of proline-guanidine moiety to the 2-aminoimidazolinone. Biomimetic spontaneous conversion study of proline to 2-aminoimidazolinone derivatives pointed to dispacamide A as the forerunner of oroidin. As a consequence of this proposed pathway, 4,5-dibromopyrrole-2-carboxylic acid and 2-amino-5-(3-amino)propylimidazole are probably hydrolysis products and not precursors (Travert and Al-Mourabit, 2004).
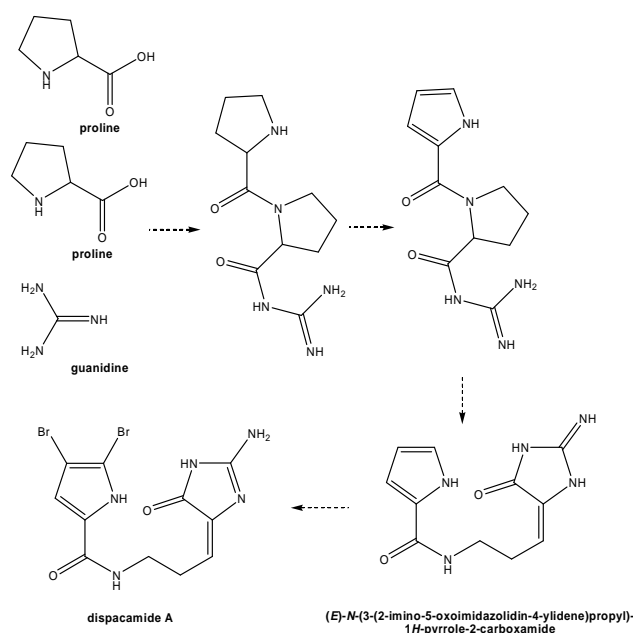
Fig.IV.6. Sequential pyrrole and 2-aminoimidazolinone sections formations (according to Travert and Al-Mourabit, 2004)

Actually, either oroidin or dispacamide A are good candidates as a key metabolite linking the amino acid precursors to the pyrrole 2-aminoimidazole family. Moreover, both compounds are frequently found in sponges together with their

closely related polycyclic derivatives (Travert and Al-Mourabit, 2004).

Isolation of homoarginine derivative by Köck *et al.* (1999) eventually opens the possibility of another alternative biosynthetic pathway. This new pyrrole-imidazole alkaloid derivate indicates the existence of a biosynthetic pathway via an open chain intermediate (Assman *et al.*, 1999). Hoffmann and Lindel (2003) proposed that hydroxylation of homoarginine at the δ-position, followed by oxidation and cyclization generates 2-aminohomohistidine which then undergoes oxidative decarboxylation and isomerization of the resulting double bond, eventually forms oroidin (Fig.IV.5) (Lindel *et al.*, 2000a). Similar co occurence of homoarginine and 2-amino-3-prop(en)ylimidazoles in the case of the aplysinamisines I and II from the sponge *Aplysina* sp. (Rodriquez and Piña, 1993) and the similar biogenesis pathway of enduracididine, an arginine-derived amino acid which has an imidazoline analogue of aminohistidine in its structure (Horii and Kameda, 1968; Hatano, *et al.*, 1984; Garcia *et al.*, 1996; Hemscheidt *et al.*, 1995) support the above hypothesis (Hoffman and Lindel, 2003).
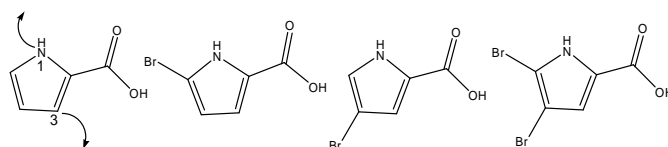
Fig.IV.7. Four building blocks and new nucleophilic positions (N-1 and C-3) (Al-Mourabit and Potier, 2001)

On the other hand, Al Mourabit and Potier (2001) proposed different intra molecular cyclization mechanisms of the oroidin/hymenidin which further lead to the structure diversity of pyrrole imidazole alkaloids. In the pyrrole-imidazole alkaloids, positions N-1 and C-3 of the pyrrole part usually participate in intramolecular cyclizations of the pyrrole-imidazole alkaloid key building block (Fig.IV.7) (Al Mourabit

and Potier, 2001). Position C-2, which is the most nucleophilic in free pyrrole has only rarely been quaternized (Hoffmann and Lindel, 2003). Among the simple heterocycles, free or *N*-methylated pyrrole exhibits a relatively strong nucleophicity at C-2 which even rivals with nucleophilic solvents (Richard *et al.*, 1998; Mayr *et al.*, 2003; Hoffmann and Lindel, 2003).

Tautomerism properties of 2-amino-imidazole building block (Fig.IV.8 and Fib.IV.9) as well as its ambivalent reactivity (Fig.IV.9 and Fig.IV.10) were described by Al-Mourabit and Potier to play an important role in the molecular diversity of pyrrole-imidazole alkaloids. The tautomerism which can exist simultaneously will give rise to polycyclic metabolites through various combinations with pyrrolic building blocks and diverse modes of cyclization dimerization. Each tautomer engaged in this process may act as an initiator of controlled chain reactions leading to various and complex compounds (Al-Mourabit and Potier, 2001).
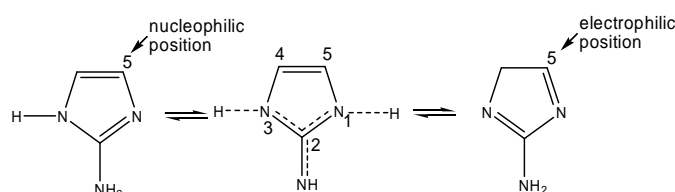
Fig.IV.8.The tautomerism and ambivalent reactivity of 2-amino-imidazole (Al-Mourabit and Potier, 2001)

Proton migration leading to selected tautomers **36-I**, **36-II**, **36-III** and **36-IV** (Fig.IV.9) seems to be the key step of this metabolic route. The protonation-deprotonation property of the 2-aminoimidazole ring is crucial for this proton mediating transfer. In the same time, the formation of tautomers **36-V, 36-VI, 36-VII and 36-VIII** of iminoimidazole ring are also possible (Fig.IV.10) (Al-Mourabit and Potier, 2001). The flexibility and versatility of this system should be controlled by the coexistence of all these tautomers in a pH-dependent equilibrium. Due to their simple

structures and reactivity, such a tautomeric equilibrium exists under prebiotic conditions at an early stage of their bioorganic synthesis (Al-Mourabit and Potier, 2001).
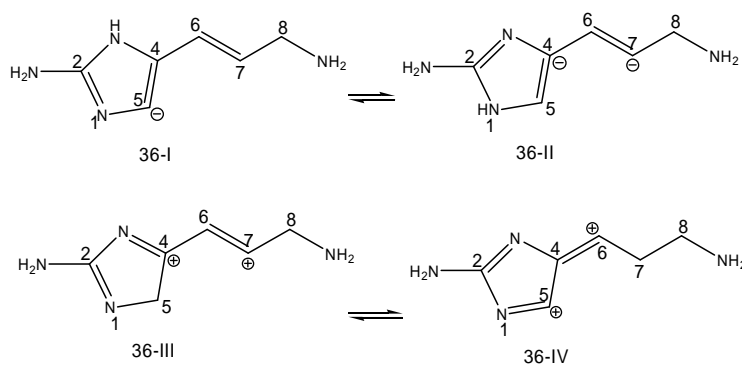
Fig.IV.9.The tautomerism and ambivalent reactivity of vinylogous 2-aminoimidazole which may participate in the biosynthesis of the pyrrole-midazole alkaloids, according to Al-Mourabit and Potier (2001)
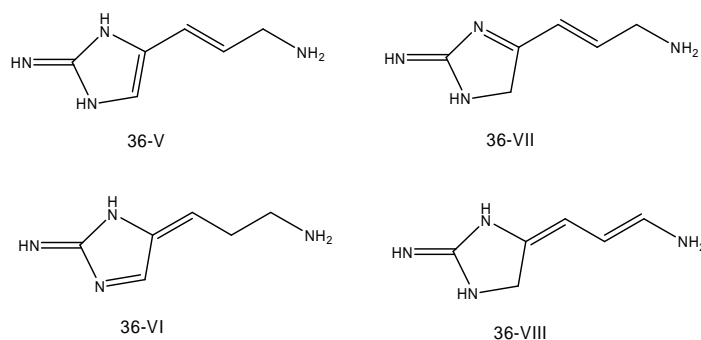
Fig.IV.10.Other possible tautomerism of 2-imino-imidazole (Al-Mourabit and Potier, 2001)

Based on the available theory about the pyrrole-imidazole alkaloids biosynthesis, it can be concluded that in the case of the Balinese *Agelas nakamurai*, where all of the afforded pyrrole imidazole compounds are monobrominated, it is more likely that hymenidin (**22**) is the key building block in their biosynthesis. Intermolecular cyclization involving the *N*-pyrrole and C-9 of this building block leads to compounds like mukanadin C (**21**) and its new derivative longamide C (**20**).

In the case of Seribu Islands sample, *Agelas* n.sp., beside its possession of more diverse pyrrole-imidazole alkaloids, there are no oroidin or dispacamide as well as homoarginine alkaloids present, whereas some metabolite functionalities can not

be explained by the available theory. Midpacamide (**13**) as the major metabolite together with the co-existence of mauritamides which exhibit relatively similar functional groups in the imidazole ring with a dehydro dispacamide A recommends a putative biosynthetic pathway as described in Fig.IV.11. This pathway may explain the relation of almost all *Agelas* n.sp. metabolites including, midpacamide, mauritamides, agelanin A as well as the phakellins.
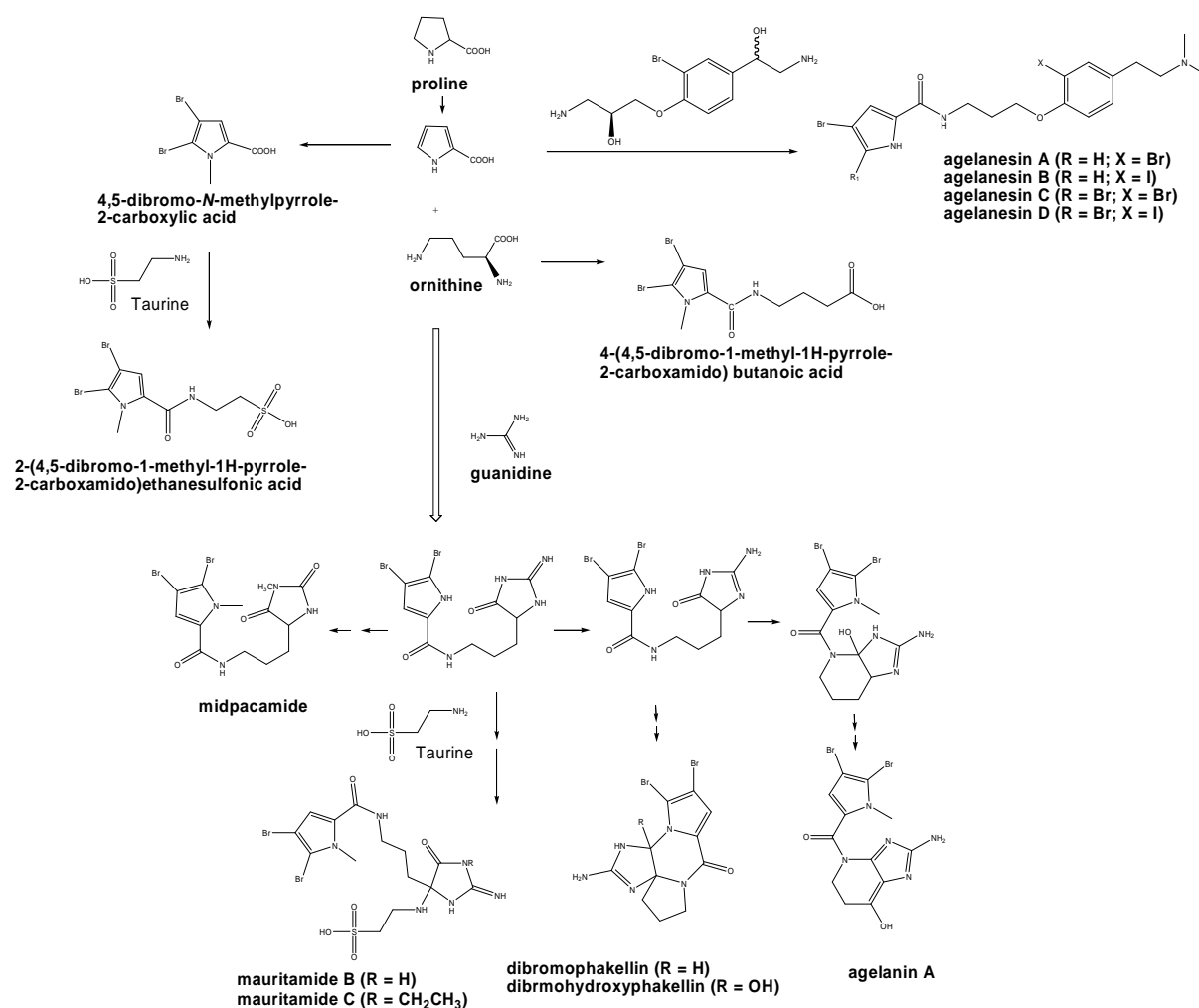
Fig.IV.11. Proposed chemical pathway leading to several *Agelas* n.sp. metabolites
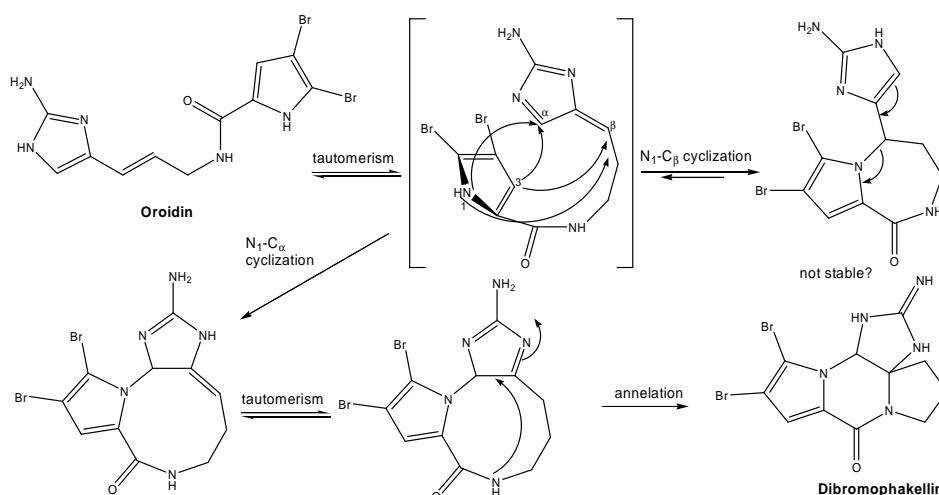
Fig.IV.12. Proposed chemical pathway leading to dibromophakellin according to Al Mourabit and Potier (2001)

Since the phakellins and dihydrooroidin appear to be biogenetically related (Faulkner and Andersen, 1974), Sharma and Magdoff-Fairchild (1977) proposed that the guanidine double bound should be located at the C-8, C-9 position. Once the tetracyclic skeleton has been formed, the migration of this double bond to the exocyclic position will involve a transition state which requires the imidazoline ring to be planar. Considering that this ring can not become planar, the guanidine double bond in phakellins and their derivatives is forever locked at the C-8, C-9 position (Sharma and Magdoff-Fairchild, 1977). Therefore another plausible biosynthetic pathway leading to phakellin proposed by Al-Mourabit and Potier (2001) may not be suitable (Fig.IV.12)

An involvement of other amino acids as precursors may be observed in the taurine containing compounds, mauritamides and *N*-methyl-4,5-dibromopyrrole taurocarboxamide biosynthesis. Meanwhile, tyrosine may play this role in the agelanesins biosynthesis through a brominated tyramine related intermediate (described further in Section IV.1.3).

Bioconversion pathway of several bromopyrrole alkaloids isolated in this study remains in question. Bizarre structure of agelanin B recommends an involvement of another alternative precursor. On the other hand, a co-existence of the agelongine alcoholic portion, pyridinebetaine A (Fig.IV.13) in *Agelas* longissima by Cafieri *et al.* (1998b) may be the answer to the agelongine unusual structure.
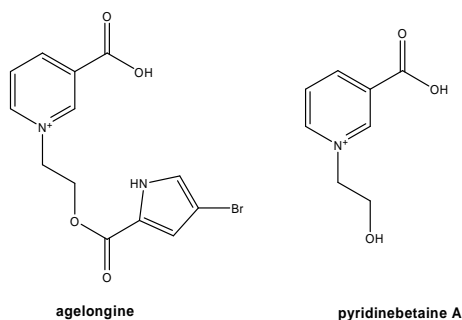
Fig.IV.13. Agelongine and pyridinebetaine A (Cafieri *et al.*, 1998b)

IV.1.1.3. Bioactivity and Ecology

Considering that biosynthesis of alkaloids consumes valuable amino acids, whereas efficiency is a decisive criterion in living organisms, it should be an evolutionary advantage to be able to generate a maximum degree of molecular diversity, and presumably function, on the basis of a common building block. It would be even better, if that building block would in itself be life saving. This is the case for oroidin, which secures the chemical defense of sponges of the genus *Agelas* against predation by reef fishes as well as its role as a key building block of pyrrole imidazole alkaloids. Meanwhile, the system of cyclized and dimerized pyrrole-imidazole alkaloids appears to be the answer to yet unknown questions of biological function (Hoffmann and Lindel, 2003).

The conservation of brominated pyrrole-imidazole alkaloids as natural products in the tissue of sponges within the genus *Agelas* suggests that these

compounds have been evolutionary elaborated and retained as chemical defenses (Lindel *et al.*, 2000b). From an ecological point of view, the anti-predatory role of oroidin-based alkaloids could be their most important biological function (Assmann *et al.*, 2000; Assmann *et al.*, 2001).

Lindel *et al.* (2000b) formulated the structure-activity relationship of several oroidin related compounds for feeding deterrent activity. They reported that even though the pyrrole ring is required for the activity, this alone is not sufficient. It is also important to note that methylation of the *N*-pyrrole did not alter the activity. In addition, dibrominated pyrrole exhibited higher activity in comparison to less brominated analogues. On the other hand, the imidazole moiety is not feeding deterrent on its own, but enhances the activity of the pyrrole ring. The oxidation state of the imidazole ring at the 4-position found to give no influence on activity as well as the functionalization of the imidazole 2-position. Removal of the imidazole moiety with retention of the chain resulted in loss of activity, except for the acid. Among the similar, active compounds, increasing polarity appeared to enhance feeding deterrence. This anti feeding assay also revealed an additive effect of the active compounds but no synergy is observed (Lindel *et al.*, 2000b).

Field assays performed by Richele-Maurer *et al.* (2003) showed that concentration of pyrrole imidazole alkaloids, oroidin and sceptrin in *A. conifera* were unaffected by prolonged protection from fish predators. This suggested that there is always a minimal production of these compounds, possibly at the limit of effectiveness. Meanwhile, wounding induced a three- to four-fold increase production of both compounds and higher amount of these bromopyrroles exuded into the surrounding seawater than normal. This action may prevent further predation as well

as protection against invading microorganisms and from fouling (Richele-Maurer *et al.*, 2003). This argument is in accordance with the activity of oroidin and several other bromopyrrole alkaloids against fouling and bacterial infection (Tsukamoto *et al.*, 1998). According to the optimal defence theory, the enhanced production of bioactive compounds in response to environmental changes would maximize individual fitness, since defences are costly and that energy is needed for other function such as growth and reproduction (Schupp *et al.*, 1999; Richele-Maurer *et al.*, 2003).

Based on the assumption that effect of calcium influx and calcium levels in neurons, secretory cells may be related to the feeding deterrence through smell and taste, Bickmeyer *et al.* (2004; 2005) performed an experiment to observe the effect of several bromopyrrole alkaloids on calcium levels in PC12 cells (rat phaeochromocytoma cell line). It was reported that unpalatable 4,5-dibromopyrrole-2-carboxylic acid against predatory reef fish is not (only) transduced by specific membrane receptors present on sensory nerve cells but (additionally) has a more general pharmacological effect on the cellular calcium homeostasis (Bickmeyer *et al.*, 2004).

Basically, chemo-receptive cells are exposed to the environment, and cellular signalling may be modulated by substances interacting with the basic physiology of the cell, but not necessarily by binding to specific taste receptors (Bickmeyer *et al.*, 2004, 2005). As the same mechanism may work in sensory cells of predatory fishes and other animals like snails the inhibition of Ca^{2+} influx into receptor cells may be one reason for chemoreceptive detection (Bickmeyer *et al.*, 2004, 2005). In harmony with the ecological point of view, blockade on calcium entry may be pharmacologically important since it can induce vasorelaxation as obseved in

many hypertension drugs (Bickmeyer *et al.*, 2004).

Midpacamide (**13**, 1.01% of sponge dried weight) is the major constituent of the *Agelas* n.sp. It is a dibrominated pyrrole having a *N*-methylated hydantoin ring connected through a propylamide chain. According to Lindel and collaborators (2000b), this compound is the most potent as feeding deterrent in comparison to the other six pyrrole imidazole alkaloids tested, 4,5-dibrompyrole carboxamide, 4,5-dibromopyrrole-2-carboxylic acid, oroidin, keramadine dispacamide and *racemic* longamide A. Based on this finding accompanied with its predominance in the sponge. It is likely to assume that midpacamide functions as the main chemical weapon of *Agelas* n.sp. against its predators.

Relatively high structure diversity and predominance of the pyrrole-imidazole alkaloids in *Agelas* n.sp. may be due to their function as chemical defense for the host sponge in order to provide broader spectrum of protection. Midpacamide, as a main feeding deterrent (Lindel *et al.*, 2000b) displays moderate cytotoxicity against mouse lymphoma cell L5178Y (46.7% inhibition in 10 μg/ml sample concentration) and only low antibacterial activity against *B. subtilis*. The role of cytotoxic activity as well as antimicrobial and antifouling activity is presumably taken by other metabolites, the agelanesins (discussed further in IV.1.2).

In contrary to *Agelas* n.sp., the major metabolites observed from *Agelas nakamurai* are not pyrrole-imidazole compounds, but diterpenes (section IV.2.1). Considering that these diterpenoids also play a role in sponge defense may be the answer to the less diverse production of pyrrole-imidazole alkaloids. Among the pyrrole-imidazole metabolites, 4-bromo-1*H*-pyrrole-2-carboxylic acid (**23**) and hymenidin (**22**) are discovered to be predominating. From their structure one can

predict that it also contributes in the anti feeding deterrent activity of the sponge producer, together with the other congener, 4-bromo-1*H*-pyrrole-2-carboxamide (**24**).

IV.1.2. Tyrosine derived brominated compounds from *Agelas* n.sp.

As already mentioned before (Section IV.1.1.1), four brominated pyrrole derivatives connected to a halogenated tyramine unit are obtained from *Agelas* n.sp. Interestingly, halogen-bearing tyrosine-derived metabolites are more likely to be found in Verongid sponges, although they were also reported from several other marine sponges (Constantino *et al.*, 1994; König and Wright, 1993). Up to now, agelorin A and B as well as 11-*epi*-fistularin-3 are the only known tyrosine-related representatives from the marine sponge genus *Agelas* (König and Wright, 1993). It is noteworthy that the presence of a halogenated tyramine moiety linked to a brominated pyrrole unit has never been reported before in natural products. Replacement of the brominated tyramine moiety in agelanesin A (**4**) and agelanesin C (**6**) with iodinated tyramine in agelanesin B (**5**) and agelanesin D (**7**) makes this group of compounds even more attractive.
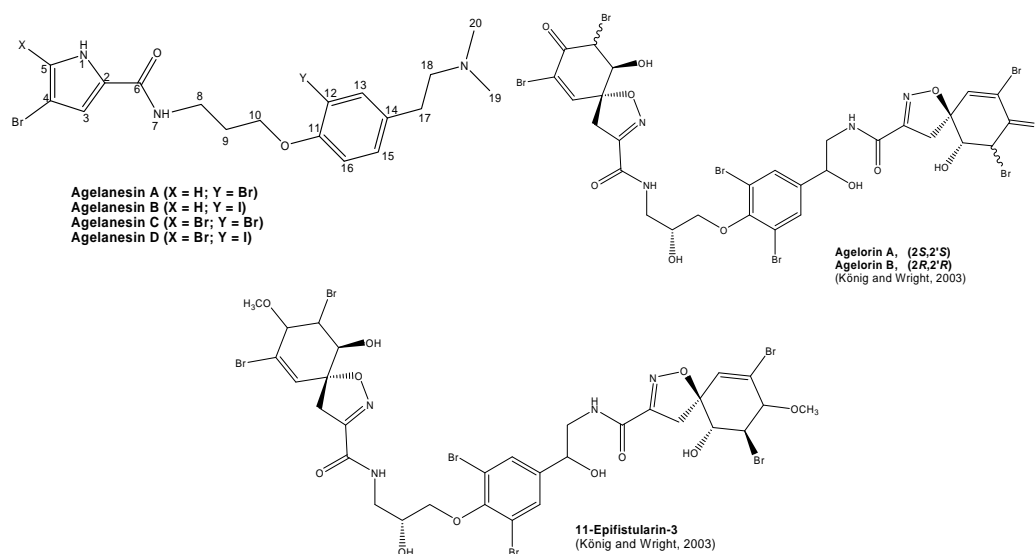
Fig.IV.14. Chemical structures of tyrosine-derived brominated compounds from *Agelas oroides* (König and Wright, 2003) and from *Agelas* n.sp. (agelanesin A-D)

It is very challenging to find out why this *Agelas* sponge incorporated iodine into the agelanesins to substitute bromine. Iodo-alkaloids are known to be very rare natural products which are until now only isolated from marine organisms, (Gribble, 1996a, 1996b, 1998, 2000; Faulkner, 1995) more specifically from very few algae and sponges (Niedleman and Geigert, 1986; Constantino *et al.*, 1994). It may be due to the iodide present in sea water which is far below other halogens such as bromide and chloride. Despite its low concentration, unlike chloride, all known haloperoxidases are effective in oxidizing iodide (Niedleman and Geigert, 1986). According to Constantino *et al.* (1994), biosynthesis of iodinated metabolites seems to be related to the capability of organisms to concentrate iodine from sea water, rather than to the presence of a specific peroxidase. This argument was based on the fact that most iodo-metabolites have been isolated from red algae, which are known to contain iodine concentrations as high as 0.5% of weight wt (Constantino *et al.*, 1994). Interestingly, one iodotyrosine alkaloids sponge producer, *Iotrochota birotulata* was reported to contain significant amounts of iodine (0.12 – 1.21%), together with comparable quantities of bromine (0.16-2.66%) (Kaestner, 1967). Hence this supports the relationship between the presence of iodo- metabolites and high concentration of iodine in the sponge tissue (Constantino *et al.*, 1994).

Another interesting question arising from the agelanesins unique structure is their biosynthesis. According to Richele-Maurer (2003), pyrrole imidazole family of compounds such as oroidin and sceptrin are predicted to be produced by sponge cells and not by the associated bacteria. Meanwhile Simmons and collaborators (2005) proposed that the brominated tyrosine metabolites may actually be derived from the biosynthetic pathway of microorganisms living in association with sponges.

This argument was based on the fact that these kinds of metabolites such as psammaplins have been isolated from a diversity of sponge "sources" and that brominated aromatic amino acid derivatives are common metabolites of marine bacteria (Simmons *et al.*, 2005). This finding suggests that in the case of agelanesins, the brominated pyrrole 2-carboxylic acids are produced by the sponge cell and further converted by associated bacteria to afford agelanesins.

In addition to its unique chemical structure, this group of compounds also shows interesting bioactivity. Agelanesin A - D are cytotoxic against the mouse lymphoma cell line (L1578Y) with IC_{50} value 4.5 μg/mL; 4.8 μg/mL; 9.2 μg/mL; and 7.8 μg/mL respectively (Fig.IV.15). In comparison to other brominated pyrroles obtained in this study, only this group of compounds shows pronounced activity. At the same time, aplysamine-2 (**27**) and aeroplysinin-1 (**28**), obtained from *Pseudoceratina purpurea* exhibits the same activity as well. Some other brominated tyrosine compounds have also been previously reported to be cytotoxic such as psammaplin A and bisaprasin (Arabshahi and Schmitz, 1987; Quiñoà and Crews, 1987; Rodriquez *et al.*, 1987). Hence it is suggestive that the halotyramine moiety of agelanesin A – D is important for the activity.
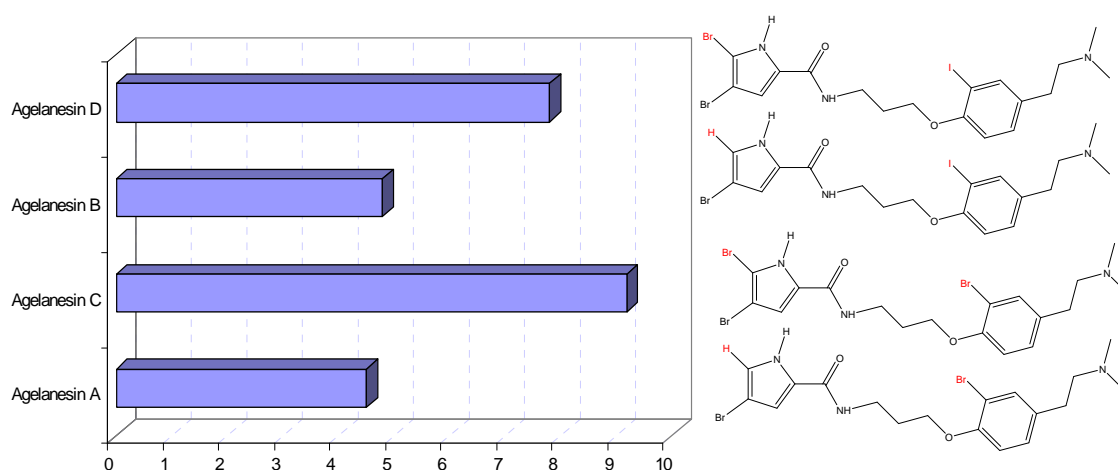
Fig.IV.15. IC$_{50}$ value of the agelanesins against L5178Y mouse lymphoma cell line

Based on the IC$_{50}$ values of the agelanesines against mouse lymphoma cell line (L5178Y), a possible structure activity relationship is suggested. Since the highest activity was shown by agelanesin A followed by agelanesin B, D and C, respectively, less bromination on the pyrrole ring seems to be important for the activity. This is somehow in contrast to the result of feeding deterrent activity reported by Lindel *et al.*, 2000b, since higher degree of the bromination in the pyrrole ring will increase the activity (Lindel *et al.*, 2000b). Meanwhile, different halogen atom attached to the tyramine unit (C-12) causes only slight difference on the cytotoxicity

IV.1.3. Tyrosine derived brominated compounds from *Pseudoceratina purpurea*

Sponges of the genus *Pseudoceratina* (order Verongida, family Aplysinellidae) have furnished a variety of brominated tyrosine or heterocyclic derivatives (Kijjoa *et al.*, 2005). These bromotyrosine-derived compounds have been observed to show a wide range of interesting biological activities including antiviral (Gunasekera and Cross, 1992; Kobayashi *et al.*, 1991); antibiotic (Capon and

MacLeod, 1987; Yagi *et al.*, 1993; Kazlauskas *et al.*, 1981; Kobayashi *et al.*, 1991; Andersen and Faulkner, 1973; Krejcarek *et al.*, 1975; Gao *et al.*, 1999), Na^+/K^+ ATPase inhibitor (Tsuda *et al.*, 1992; Longeon *et al.*, 1990; Nakamura *et al.*, 1985b; Wu et al., 1986; Okamoto et al., 2000), anti HIV (Ichiba and Scheuer, 1993; Ross *et al.*, 2000), antifouling (Tsukamoto *et al.*, 1986; Tsukamoto *et al.*, 1996a; Tsukamoto *et al.*, 1996b; Tsukamoto *et al.*, 1996c), and antihistamine-H_3 antagonist (Mierzwa *et al.*, 1994), as well as interesting anticancer activities (Copp and Ireland, 1992; Pordesimo and Schmitz, 1990; Hirano *et al.*, 2000; Kobayashi, 1991; Acosta and Rodriguez, 1992; Tabudravu and Jaspars, 2002; Kijjoa *et al.*, 2005).

Undamaged *Pseudoceratina purpurea* exhibits yellow colour underwater which turns slowly to dark colour when exposed to the air. This may be due to a possession of an unstable pigment. The similar phenomenon was shown by another Verongid sponge, *Verongia aerophoba* Schmidt (Cimino *et al.,* (1984). By transferring the sponge to the water surface, its yellow pigment, uranidine (3,5,8-trihydroxy-4-quinolon) will be slowly oxidized to an unstable blue quinone. Furthermore, this blue substance will be quickly polymerized to an insoluble black material (Cimino *et al.*, 1984). In this study, *Pseudoceratina purpurea* affords several brominated tyrosine derived metabolites i.e., aplysamine-2, aeroplysinin-1, bisoxazolidinone derivative, dienone dimethoxy ketal and dienone ethoxy-methoxy ketal.

Aplysamine-2 was reported for the first time by Xynas and Capon (1989) from the Australian sponge *Aplysina* sp. In 2005, Kijjoa and collaborators reported its presence in *Pseudoceratina purpurea* collected in the Gulf of Thailand. Aplysamine-2 has been reported to exhibit moderate dose dependent growth inhibitory effects against human tumour cell lines, MCF-7 (breast); NCI-H460 (lung) and SF-268 (CNS)

(Kijjoa *et al.*, 2005). Furthermore, antifouling assay on aplysamine-2 towards *Balanus improvisus* Darwin resulted in inhibition activity without cytotoxic effect encountered at 10 μM (Ortlepp, 2007). In addition, pronounced cytotoxicity activity against mouse lymphoma cell (L5178Y) was observed with IC_{50} 1.7 μg/ml.

Besides aplysamine-2, aeroplysinin-1 also shows pronounced cytotoxic activity against mouse lymphoma cell (L5178Y) with IC_{50} 0.57 μg/ml. This compound is already well known as a potential cytotoxic agent against HeLa tumour cell (Koulman *et al.*, 1996), human breast cancer cells and also inhibits the EGFR tyrosine kinase in an in vitro system (Kreuter *et al.*, 1990). Promising anticancer activity against L5178Y mouse lymphoma cells (ED_{50} 0.5 μM), Friend erythroleukemia cells (ED_{50} 0.7 μM), human mamma carcinoma cells (ED_{50} 0.3 microM) and human colon carcinoma cells (ED_{50} 3.0 μM) were reported in vitro by Kreuter and collaborators (1989). In addition, anti leukemic activity of aeroplysinin-1 in vivo using the L5178Y cell/NMRI mouse system was also reported (Kreuter *et al.*, 1989). Preliminary toxicology studies revealed an acute LD_{50} of 202 mg/kg and a sub-acute LD_{50} of 150 mg/kg. Assay on the umu/ *Salmonella typhimurium* test system showed that aeroplysinin-1 was neither a direct mutagen nor a premutagen (Kreuter *et al.*, 1989). Morerover, it also displays antimicrobial activity against gram positive and gram negative bacteria (Fulmor *et al.*, 1970; Teeyapant *et al.*, 1993) as well as antiangiogenic activity (Rodríguez-Nieto *et al.*, 2002).

The presence of aeroplysinin-1 (**28**) along with a bisoxazolidinone derivative (**29**) and dienone ketals (**30** and **31**) in *P. purpurea* sponge are somehow related to the previously reported chemical defense mechanism for Verongid sponges e.g., *Aplysina aerophoba*. This sponge, as well as other Verongid sponge produces

isoxazoline alkaloids, a group of compounds possessing antifeeding activity. The isoxazoline alkaloids such as aerophobin-2 and isofistularin-3 are precursors of smaller compounds, aeroplysinin-1 and dienone (Teeyapant *et al.*, 1993; Ebel *et al.*, 1997; Thoms *et al.*, 2004, 2006), whereas bisoxazolidinone derivative would be expected as a by product of the proposed cleavage of isofistularin-3 into aeroplysinin-1 (Fig.IV.16) (Thoms *et al.*, 2006).

Bioconversion of the isoxazoline alkaloids in *Aplysina s*ponges is paralleled to an increase of their antibiotic and cytotoxic activity (Teeyapant *et al.*, 1993; Weiss *et al.*, 1996). In contrast, feeding deterrent activity of the bioconversion products against the Mediterranean fish species *Blennius sphinx* is significantly weaker than observed for their isoxazoline precursors (Thoms *et al.*, 2004).

The biotransformation of these isoxazoline alkaloids is somehow related to the sponge activated chemical defense mechanism, i.e., rapid conversions of inactive precursor compounds into ecologically active products (reviewed in Havel, 1986; Adler and Harvell, 1990; Paul and Puglisi, 2004; Thoms *et al.*, 2006). These mechanisms are typically catalyzed by enzymes that are usually separated from their substrates (precursors) by compartmentalization. Upon tissue damage, these compartments are disrupted, allowing contact between substrates and enzymes, which in turn induces the bioconversion. In many cases, the compounds resulted from such reactions arise from cleavage of the precursors (Thoms *et al.*, 2006). Compartmentalization is also observed in the mesohyl tissue of *Aplysina* sponges, where the brominated isoxazoline alkaloids are mainly stored in spherulous cells (Thompson *et al.*, 1983; Turon *et al.*, 2000; Thoms *et al.*, 2006).
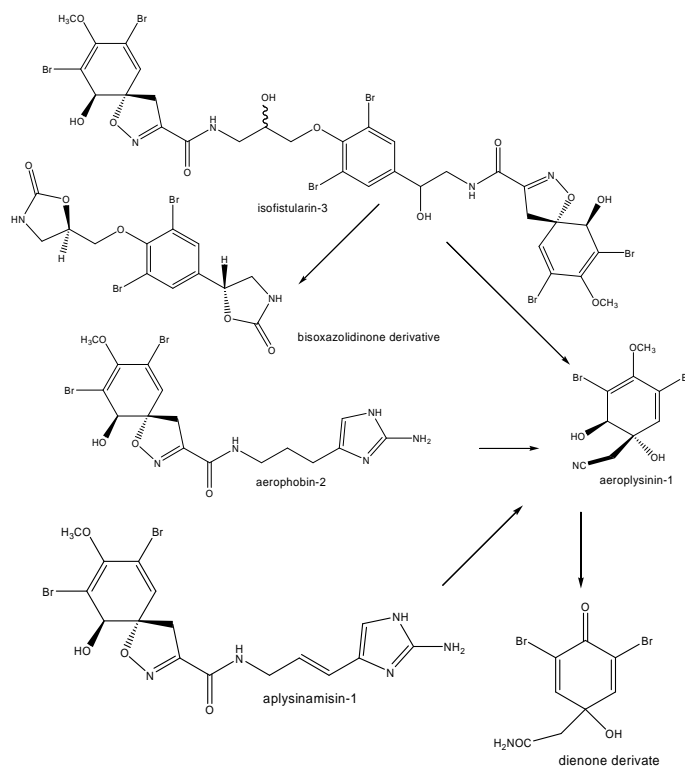
Fig.IV.16. Wound-induced bioconversion of the brominated isoxazoline alkaloids in tissue of *Aplysina aerophoba*. (Thoms *et al.*, 2006)

Agelas longissima which is not a Verongid sponge was reported to yield the isoxazoline derivatives i.e., agelorin A and B as well as 11-isofistularin-3 (König *et al.*, 1993). But interestingly, there was no bioconversion of these isoxazoline alkaloids observed. This finding is somehow in agreement with Thoms *et al.* (2006) who proposed that the bioconversion reactions of isoxazoline alkaloids are specific for Verongid sponges as other investigated marine invertebrates, the sponge *C. crambe* and the opistobranch *T. perversa*, were unable to convert isoxazoline alkaloids (Ebel *et al.*, 1999; Thoms *et al.*, 2003).

Co-occurrence of dienone dimethoxy ketal and dienone ethoxy methoxy ketal are suspected to be artefacts formed by adding water, methanol or ethanol during the extraction and or purification. The presence of dienone dimethoxy ketal as diastereoisomers is suggestive that the ketals are not natural products.   The mixed

ketal would not be expected to be formed from the dienone without simultaneous formation of the corresponding dimethoxyketal (Andersen and Faulkner, 1973).

Absence of the isoxazolines and on the contrary the presence of aeroplysinin-1 and the ketals in *P. purpurea* studied here may be due to the isolation procedure performed on this sponge. Regarding the biotransformation of the isoxazolines to aeroplysinin-1 and to the dienones happens so fast (45 second to 1 minute, Ebel *et al.*, 1997; Thoms *et al.*, 2006), no isoxazolines could be detected in the ethanol extract. But the existence of bisoxazolidinone derivative together with aeroplysinin-1 is suggestive for the presence of isofistularin-3 in the fresh sponge, since this precursor is bioconverted to its bisoxazolidinone derivative as by product (Thoms *et al.*, 2006). Meanwhile, absence of a dienone may be due to its conversion to ketals in the presence of methanol and water during the isolation procedure (Andersen and Faulkner, 1973). Aplysamine-2 is not an isoxazoline derivative. Therefore it experiences neither this biotransformation nor the solvent degradation and therefore could be isolated from the methanol extract.

Most brominated Verongid metabolites are derived from transformation of the precursor 3,5-dibromotyrosine (Rogers *et al.*, 2005). This hypothesis is supported by in situ ^{14}C labelling studies done on the sponge *Aplysina fistularis* (*Verongia aurea*) which showed the incorporation of [U]-^{14}C-Tyr, [U]-^{14}C-Phe (Tymiak and Rinehart, 1981), and [U-^{14}C]-3,5-dibromotyrosine (Carney and Rinehart, 1995) precursors into the of brominated natural products (Rogers *et al.*, 2005). Moreover, 3,5-dibromotyrosine has been isolated from Verongid sponges, both in its free form and as an amino acid residue in matrix protein (Ackermann and Müller, 1941; Low, 1951; Roche, 1952; Rogers *et al.*, 2005).

The fate of 3,5-dibromotyrosine in secondary metabolism of Verongid metabolites was proposed by Rogers *et al.* (2005) to follow several pathways parallel to the transformations of tyrosine in plant secondary metabolism. This pathway includes decarboxylation to 3,5-dibromotyramine, or oxidative transformation and conjugation, presumably through the putative intermediates (**IIa** and **IIb,** Fig.IV.17) (Rogers *et al.*, 2005). Fistularin-3 on the other hand, arise from oxidation of the aromatic α-amino group to form a ketoxime and oxidation of the aromatic ring in 3,5-dibromotyrosine, through the involvement of an arene epoxide (e.g., the hypotetical **Ia**), which undergoes intramolecular *endo*-trig ring opening by the ketoxime to give **Ib** (Aiello *et al.*, 1995; Rogers *et al.*, 2005).
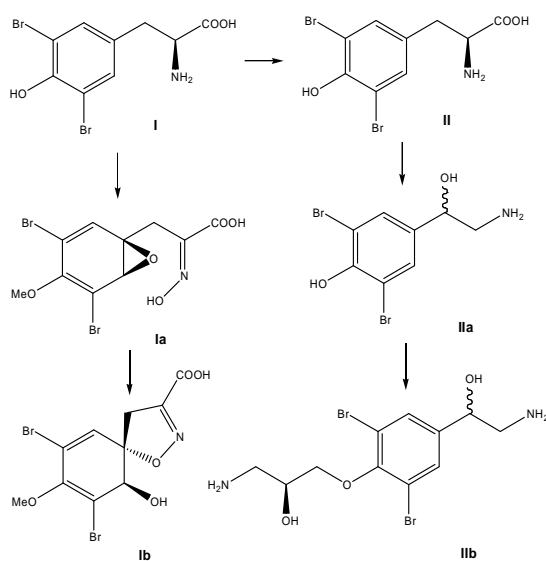
Fig.IV.17. Biosyntesis pathway of brominated Verongid metabolites (Rogers *et al.*, 2005)

IV.2.   Terpenoid compounds from marine sponges

IV.2.2.   Diterpenoids from *Agelas nakamurai*

Beside the oroidin family of compounds, *Agelas* sponges also produce unique terpenoids such as the adenine derivatives of diterpenes and the terpenoid derivatives of hypotaurocyamine (Braekman *et al.*, 1992). Unlike the oroidin

derivatives, these agelas terpenoids have not yet been reported from other group of sponges. But since they are not found in every *Agelas* sponge, they can not be used as a chemotaxomic marker (Braekman *et al*., 1992). The same phenomenon is also observed in the two *Agelas* sponges examined in this study. Together with the brominated pyrrole derivatives, *Agelas nakamurai* produces two new adenine derivatives diterpenoids and one diterpene bearing a hypotaurocyamine functionality.

It is already known that secondary metabolites, including terpenes, play an important role in competition for space and reproduction, maintenance of an unfouled surface and deterrence of predation (Coll, 1992; Fusetani, 2004). In several cases, however, chemical defense using terpenoids fails to prevent feeding by specific predators (Gross and König, 2006). This may be the answer to the existence of brominated pyrrole derivatives in *Agelas nakamurai* together with the diterpenoids, to provide a broader spectrum of protection or chemical defense for the host.

Diterpenoids (C-20) constitute a large group of compounds derived from 2*E*, 6*E*, 10*E*-geranylgeranyl pyrophosphate. The mode of cyclization of the bicyclic diterpenoids is initiated by protonation of the double bond of the starter isopropylidene unit and leads to the formation of bicyclic perhydronaphtalene derivatives (Chinou, 2005).

Agelasines are a group of mono- or bicyclic diterpenoids bearing a 9-methyladeninium moiety. There are up to now more than ten different metabolites reported from this group of compounds. (-)-Agelasine-D, is found to be the major metabolite from the studied *Agelas nakamurai* (1.95 g, 0.78% of sponge crude extract). Its possible antipode, (+)-agelasine D was previously reported by Nakamura and collaborators (1984) from the Okinawan *Agelas* sp. This compound was reported

to display powerful inhibitory effect on Na$^+$, K$^+$-ATPase as well as antimicrobial activity (Nakamura *et al.*, 1984). (+)-Agelasine D, has been successfully synthesized by Utenova and Gundersen (2004) and later by Vik and collaborators (2006) and its prominent cytotoxicity against several cancer cells as well as multidrug-resistant cell line was reported (Vik *et al.*, 2006). It also exhibited antibacterial activities on *M. tuberculosis* and both aerobes and anaerobes gram-positive and gram-negative bacteria were also reported (Vik *et al.*, 2006). In this study, (-)-agelasine D was isolated together with its likewise oxime congener, (-)-ageloxime D.

There were interesting findings in regards to the possible role of (-)-agelasine D and (-)-ageloxime D in the *Agelas nakamurai* chemical defense strategy against biofouling organisms. Considering that in biofouling mechanism, biofilm formation by bacteria is often a precursor to subsequent fouling by bigger colonizer such as the larvae or spores of barnacle, sea squirt, sea weed, etc. (Chambers *et al.*, 2006), compounds act as antimicrobial or biofilm inhibitor may play an important role to control epibiosis (Paul *et al.*, 2006). At the same time, against bigger colonizer such as the barnacles, possession of compound which is toxic to the larvae or inhibit the settlement will be of advantage (Fusetani, 2004; Paul *et al.*, 2006).

The term biofilm itself refers to a collection of adhered cells and their products on the surface (Characklis and Cooksey, 1983). It has been generally accepted that the first step in the formation of a biofilm on a clean surface is the adsorption of an organic layer onto the surface from the aqueous milieu (Cooksey and Wigglesworth-Cooksey, 1995). On the other hand, biofilm associated microbes have great significance for public health, since they will exhibit a dramatically decrease in susceptibility to antimicrobial agents (Donlan, 2001). The susceptibility of

biofilms to antimicrobials agents cannot be determined by means of standard microdilution assay, since these tests rely upon the response of planktonic (suspended) rather than biofilm (surface-associated) organisms. Instead, susceptibility must be determined directly against biofilm-associated organisms, preferably under conditions that simulate the conditions in vivo (Donlan, 2001).

In this study, the (-)-agelasine D shows prominent growth inhibition against several microorganism including *S. epidermidis* (MIC of < 0.31 µg/mL), but it is not active to inhibit the *S. epidermidis* biofilm formation. On the other way around, its oxime congener, (-)-ageloxime D is not active against the growth of *S. epidermidis* but inhibits the biofilm formation. Since the difference between these two compounds is only on the C-6'-substitution, it is strongly suggestive that an amine substituent will be responsibe for the antibacterial activity while the oxime is responsible for the antifouling activity against barnacles and biofilm forming bacteria. Additionally, another adenine related diterpenoid tested at the same time, agelasine I which differ to agelasine D in the diterpene part, shows neither growth inhibition of *S. epidermidis* nor the biofilm inhibition. Thus the diterpene part of agelasines should also be important for the activity.

In addition to the antibacterial activity and biofilm inhibition, (-)-agelasine D and (-)-ageloxime D were also tested against cyprids larvae of *Balanus improvisus*. The result shows that both compounds are rather toxic to the larvae than inhibit the settlement, since below toxic concentration both compound do not inhibit the settlement of the larvae in comparison to the control. Furthermore, (-)-ageloxime D is approximately 10 times more toxic to the larvae (4.39 µg/mL) in comparison to (-)-agelasine D (42.2 µg/mL).

Surprisingly, the opposite result is showed in the cytotoxicity assay against the mouse lymphoma L5178Y cell line. In this assay, (-)-agelasine D shows higher toxicity (IC_{50} of 1.7 µg/mL) in comparison to its congener, (-)-ageloxime D (IC_{50} of 5.5 µg/mL).
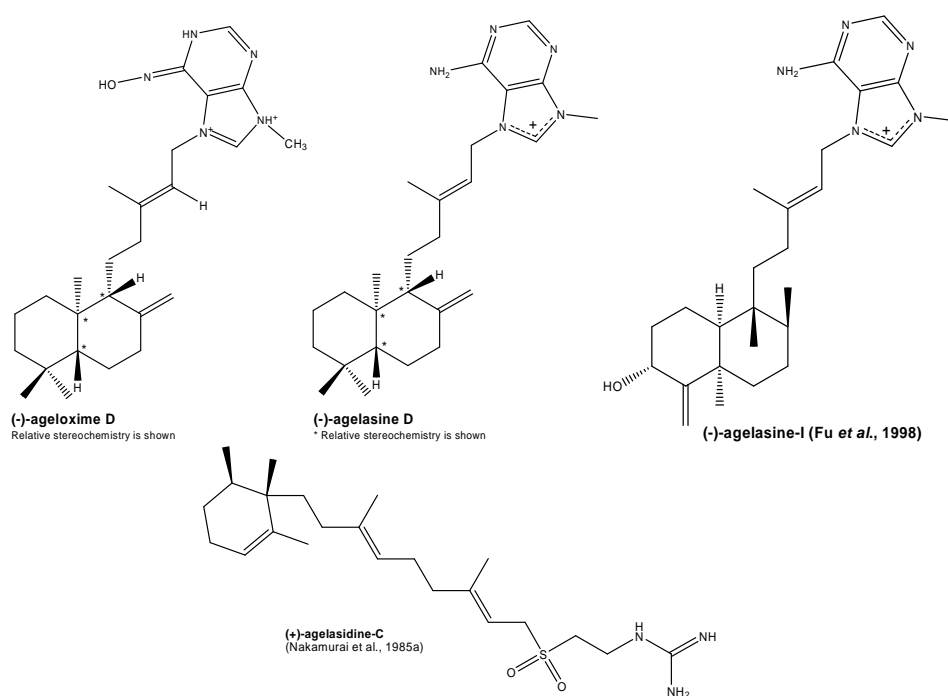
Fig.IV.18. Several diterpenoids found in *Agelas* sponges

It is worth to note that the presence of biofilm inhibitors such as ageloxime D and antibacterial agents such as agelasine-D which both are also toxic to the cyprids larvae of *Balanus improvisus* may take important role in sponge's chemical defense against biofouling. On the other hand, the brominated pyrroles of *Agelas nakamurai* such as hymenidin (**22**), which are not active neither against the barnacles nor the biofilm formation, have been previously reported as feeding-deterrents (Lindel *et al*., 2000b). This corroborates of the "job description" of each of the metabolites in the sponge.

Following the ecological role of (-)-agelasine D and (-)-ageloxime D as part

of *Agelas nakamurai* chemical defense, it can be suggested that a usage of these adenine related diterpene alkaloids in combination may serve as one promising strategy against biofilm associated bacteria such as *S. epidermidis*. While (-)-ageloxime D prevent bacteria from forming the biofilm, (-)-agelasine D can inhibit the growth of the non adherent bacteria. Other investigation to prove this suggestion is certainly required.

Besides the adenine related diterpenes, monocyclic diterpenoids bearing a hypotaurocymine functionality, (+)-agelasidine-C was also obtained from *Agelas nakamurai*. This compound shows moderate cytotoxic activity against mouse lymphoma cell (L5178Y) and antifungal activity against *C. cucumerinum* and *C. herbarium*, as well as prominent antibacterial activity against *S. epidermidis* (MIC of 2.5 μg/mL). Agelasidines was reported to inhibit growth of microorganisms such as *Staphylococcus aureus* (MIC 3.3 μg/mL) as well as antispasmodic activity (Nakamura *et al.*, 1984).

An experiment of Na^+, K^+ ATPases inhibition activity by agelasines A–F and their synthetic analogues as well as by agelasidine A–C was previously described by Kobayashi and collaborators (1987). They reported that agelasidine C and agelasidine B are the most potent congeners. It was formulated that the ionized moiety in agelasidine C and the long non polar side chains in agelasidine B play important roles in their inhibitory action (Kobayashi *et al.*, 1987). Since agelasines and agelasidines do not act as a detergent at low concentrations at which they exerted inhibitory effects on Na^+, K^+ ATPases, so it seems unlikely that the observed effects of agelasidines or agelasines were due to their ability to form micelles (Kobayashi, 1987).
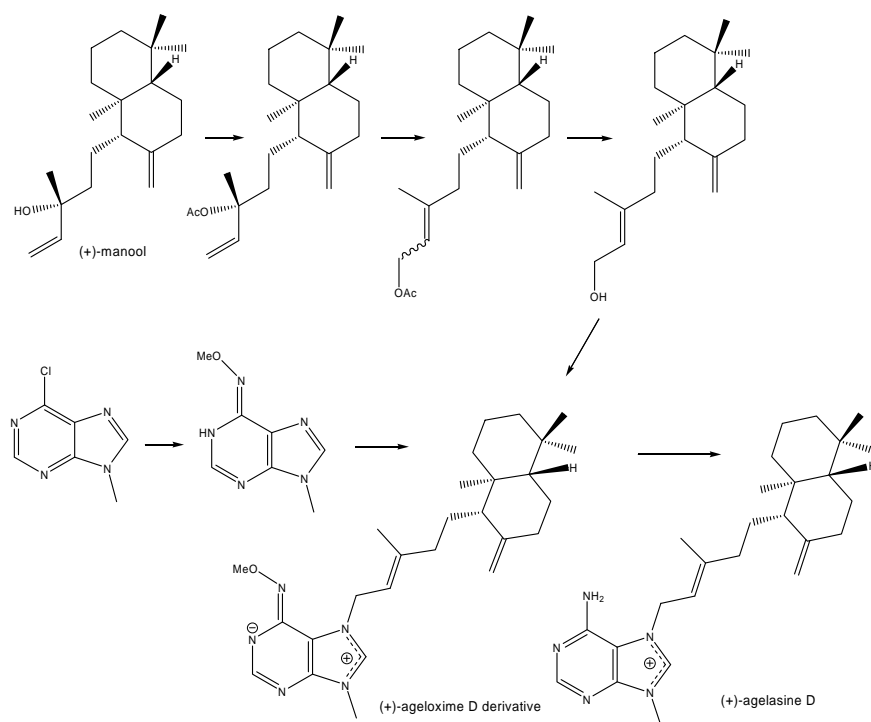
Fig.IV.19. Summary of synthesis pathway leads to (+)-agelasine D and ageloxime D related compound (modified from Vik *et al.*, 2006)

Presence of the 9-methyl-adeninium moiety in agelasine and ageloxime suggests an involvement of adenosine (**26**) and 9-methyl-adenine (**25**) in the agelasine-D and ageloxime biosynthesis. Labdane type diterpenoids were incorporated into a 9-methyl-adenine derivative to form agelasine D (Utenova and Gundersen, 2004; Vik *et al.*, 2006). With (+)-manool as starting precursor, the synthesis of (+)-agelasine D involved an (+)-ageloxime related compound as intermediate (Fig.IV.19) (Utenova and Gundersen, 2004; Vik *et al.*, 2006). A similar pathway may be involved in the (-)-agelasine-D and (-)-ageloxime-D biosynthesis which is probably started from a respective bicyclic diterpene alcohol. In another case, agelasidines may also be produced from the corresponding terpene alcohols through direct replacement by hypotaurocyamine or sigmatropic rearrangement of their hypotaurocyamine sulphonic acid esters (Nakamura *et al.*, 1985a).

IV.2.3. Sesquiterpene phenol from *Axynissa* sp.
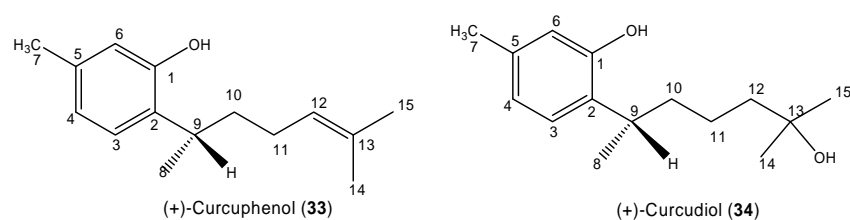
Fig.IV.20. Sesquiterpene phenols from *Axynissa* sp.

Another representative terpenoid compound originated from a marine sponge obtained in this study are the sesquiterpene alcohol derivatives, (+)-curcuphenol (**33**) and (+)-curcudiol (**34**). Unlike the previously described sponge metabolites, this group of compounds exhibits structural similarity with their terrestrial counterpart. The only difference observed is that all known sponge-derived bisabolenes possess a 9*S* configuration while the remaining marine and terrestrial metabolites exhibit a 9*R* configuration (Harrison and Crews, 1997).

(+)-Curcuphenol (**33**) and (+)-curcudiol (**34**) were previously isolated from several marine sponges and were described as ichtyotoxic and antifouling metabolites (Braekman *et al.*, 1989; Tsukamoto *et al.*, 1997). (+)-Curcuphenol also was reported to exhibit several antimicrobial activity, anti yeast activity towards *Candida albicans*, cytotoxicity against P388 murine leukaemia, A-549 lung, HCT-9 colon, MDAMB mammary cancer cell lines and the activity of gastric H, K-ATP-ase inhibition (Wright *et al.*, 1987; Duque *et al.*, 1988; Fusetani *et al.*, 1987), as well as strong antioxidant activity in the DPPH assay (Takamatsu, 2003). (+)-Curcuphenol inhibited the growth of several phytopathogenic and wood surface contaminant fungi as well as the human pathogenic fungus *Trichophyton mentagrophytes* (Gaspar *et al.*, 2004). Gaspar and collaborators (2004) suggested that the double bond in the

aliphatic chain of (+)-curcuphenol is required for antifungal activity since this compound showed a broader antifungal spectrum property of (+)-curcuphenol when compared to its congener (+)-curcudiol which only partially inhibited the growth of *Absidia ramose* (Gaspar *et al.*, 2004).

In this study, (+)-curcuphenol and (+)-curcudiol are discovered to inhibit different protein kinases. (+)-Curcuphenol inhibits SRC protein kinase with IC_{50} value of 7.8 µg/mL while (+)-curcudiol inibits FAK (focal adhesion kinase) with IC_{50} value of 9.2 µg/ml. FAK is an important component of the focal adhesion signalling complex (Zachary and Rozengurt, 1992; Hanks and Polte, 1997) and is implicated in several fundamental cellular biological functions including migration, adhesion, survival, embryonic development and cell-cycle control (Hanks and Polte, 1997; Ilic *et al.*, 1995; Richardson and Parson, 1996; Gilmore and Romer, 1996; Frisch *et al.*, 1996; Hungerford *et al.*, 1996; Zhao *et al.*, 1998; Abu Ghazaleh *et al.*, 2001). Cell attachment, spreading, and motility are complex processes requiring the integration of diverse signalling networks and structural assemblies (Jockusch *et al.*, 1995; Sastry and Burridge, 2000; Juliano, 2002). One of the earliest steps in transducing extracelluler cues through integrins to the cytoskeleton is the activation of the tyrosine kinases SRC and FAK (Schwartz *et al.*, 1995; Giancotti and Tarone, 2003; Brown *et al.*, 2005).

As reviewed by Cichewicy and collaborator (2005), (+)-curcuphenol has been encountered as a major constituent with a yield of >1% dry sponge weight) in four sponge genera which includes *Arenochalina* (Butler *et al.*, 1991), *Didiscus* (El Sayed *et al.*, 2002; Wright *et al.*, 1987), *Epipolasis* (Fusetani *et al.*, 1987; Rodriguez *et al.*, 2001), and *Myrmekioderma* (Peng *et al.*, 2002). In contrast, the marine

occurrences of the optical antipode (*R*)-(-)-curcuphenol, have been limited to several New World gorgonians from the genus *Pseudopterogorgia (*D'Armas *et al.*, 2000; Freyer *et al.*, 1997; McEnroe and Fenical, 1978). (+)-Curcupenol in this study is also obtained as the one of the major constituents of the *Axynissa* sp. crude extract (1% of sponge crude extract), together with its natural occurring hydration product, (+)-curcudiol (1.2% of sponge crude extract).

IV.3. Pyrrole carbaldehyde from *Mycale phylophilla*

Sponges of the genus *Mycale* (Mycalidae) are known to be a rich source of bioactive natural compounds with a high structural diversity (Venkatesham, 2000). Up to now there was no report on the chemical constituents of the marine sponge *Mycale phylophilla*. 5-Alkyl-pyrrole-2-carbaldehyde derivatives (**32a**) were isolated and elucidated in this study together with their congener (6'*E*)-5-(6'Pentadecenyl-1*H*-pyrrole-2-carbaldehyde (**32b**).

5-Pentadecyl)-1H-pyrrole-2-carbaldehyde (**32a**) (6'*E*)-5-(6'Pentadecenyl-1*H*-pyrrole-2-carbaldehyde (**32b**)
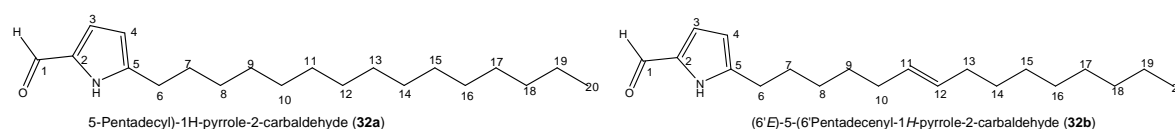
Fig.IV.19. Pyrrole carbaldehydes isolated from *Mycale phylophilla*

5-Alkyl-pyrrole-2-carbaldehyde derivatives were previously reported from other *Mycale* sponges (Ortega *et al.*, 2004, 1997; Reddy and Bhananjaya, 2000; Venkatesham *et al.*, 2000; Compagnone *et al.*, 1999); as well as from *Laxosuberites* sp. (Stierle and Faulkner, 1980); *Desmapsamma* sponge (Compagnone *et al.*, 1999) an an unidentified Great Barrier Reef Demospongia (Bowden *et al.*, 1984).

In this study, this mixture of 5-alkylpyrrole-2-caboxyldehyde shows profound cytotoxicity activity against mouse lymphoma cell (L5178Y) (MIC of 1.8 μg/mL). Their

congeners, the mycalazols, a 5-alkyl-2-hydroxymethylpyrroles derivatives, as well as mycalazals were previously reported by Ortega and collaborators (1997, 2004) to exhibit cytotoxicity activity against several cell line e.g., P388 and SCHABEL mice lymphoma, A 549 human lung carcinoma, HT29 human colon carcinoma, MEL28 human melanoma cell lines and LNcaP, while several pyrrole-2-carbaldehydes possessing hydrocarbon side chains of different length and/or number of unsaturations at C-5 was reported to exhibit anti diabetic activities (Reddy and Dhananjaya, 2000).

V. CONCLUSION AND SUMMARY

A total of 35 compounds comprising diverse structural groups of compounds including both alkaloids and terpenes were isolated; fourteen of which are new derivatives. The structures of the new compounds were unambiguously established on the basis of NMR spectroscopic (^{1}H, ^{13}C, COSY, ^{1}H-detected direct and long range ^{13}C-^{1}H correlations) and mass spectrometric (EI, and ESI) data. The identities of the known compounds were established by comparison with published data.

Sponge samples originated from several collection sites in Indonesia. A combination of a chemically-and biologically driven approach for drug discovery was employed. Extracts were screened for antibacterial, antifungal, and cytotoxic activities as well as protein kinase inhibition parallel to the usage of TLC, and HPLC coupled to UV and MS in the isolation of the chemically most interesting substances.

Enumerated below are the compounds which have been isolated and structurally elucidated and whose bioactivities have been further characterized.

V.1. *Agelas* n.sp. secondary metabolites

Extract of the unidentified *Agelas* sponge from Peniki East Island (Seribu Islands), Jakarta, yielded sixteen structurally related brominated pyrroles, including eleven new congeners. Diverse structures of the brominated pyrroles are elucidated wherein several new functionalities are shown to be introduced in the molecule such as in agelanin A (**2**), agelanin B (**3**), and agelanesins (**4** to **7**). Pronounced cytotoxicity against mouse lymphoma cell (L5178Y) was shown by all agelanesins. The tyramine moiety must be responsible for the cytotoxic activity since other

congeners without the tyramine unit displayed no cell-growth inhibition. Less degree of bromination on the pyrrole ring may also play a role in its cytotoxicity, considering that the monobrominated pyrrole-agelanesins, agelanesin A (**4**) and B (**5**) display lower IC_{50} in comparison to their dibrominated congeners, agelanesin C (**6**) and D (**7**). The iodine substituent presumably is not important for the cytotoxicity.

V.2.   *Agelas nakamurai* **secondary metabolites**

Extract of the sponge *Agelas nakamurai* collected in Menjangan Island, yielded five monobrominated pyrrole derivatives, one of which is found to be a new congener, longamide C (**20**). A hypotaurocyamine diterpenoid, (+)-agelasidine C (**19**) was isolated together along with adenine related compounds, adenosine and 9-methyladenine as well as the new diterpenoids derivatves, (-)-agelasine-D (**18**) and its congener (-)-ageloxime-D (**17**).

(-)-Agelasine D, (-)-ageloxime D and (+)-agelasidine-C exhibit prominent cytotoxicity towards the mouse lymphoma cell line L5178Y. Biofilm inhibition assay done on (-)-agelasine D, (-)-ageloxime D, (+)-agelasidine C as well as on (-)-agelasine I suggests that the diterpene part is important for the activity together with the adeninium part. Between the (-)-agelasine D and (-)-ageloxime D, the amine unit on C-6' is important for the antibacterial activity. A replacement of the amine unit with an oxime group as in the ageloxime D will displace the antibacterial activity but on the other hand will inhibit biofilm-formation of *S. epidermidis*. Both (-)-agelasine-D and (-)-ageloxime D were toxic to the cyprids larva of *Balanus improvisus* Darwin, where (-)-ageloxime D was approximately 10 times more toxic than (-)-agelasine D.

V.3.   *Pseudoceratina purpurea* secondary metabolites

Extract of the sponge *Pseudoceratina purpurea* collected in Watudodol, Banyuwangi, yielded five brominated tyrosine derivatives. The presence of the antifouling substance, aplysamine-2 (**27**) as well as isofistularin-3-bioconversion products, (**+**)-aeroplysinin-1 (**28**), bisoxazolidinone derivatives (**29**), together with the dienone ketal congeners **30** and **31** were identified.

V.4.   *Axynissa* sp. secondary metabolites

Search on bioactive compounds as protein kinase inhibitors has lead to the isolation of two bisabolene phenol derivatives, (**+**)-curcuphenol (**33**) and (**+**)-curcudiol (**34**) in the active fractions of *Axynissa* sp. collected from Ambon, Maluku.

V.5.   *Mycale phyllophyla* secondary metabolites

Study on the sponge extract *Mycale phyllophyla* collected from Menjangan Island, Bali, revealed the presence of 5-pentadecyl-1*H*-pyrrole-2-carbaldehyde derivatives (**32a**) together with (*E*)-5-pentadec-6-enyl-1*H*-pyrrole-2-carbaldehyde (**32b**) in a cytotoxic active fraction.
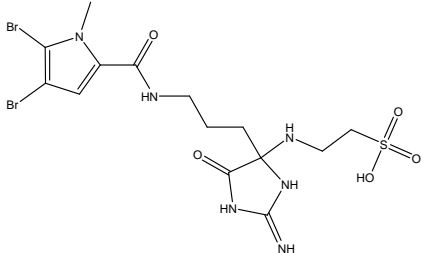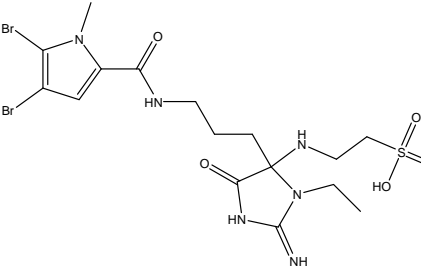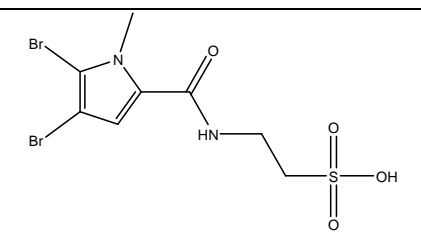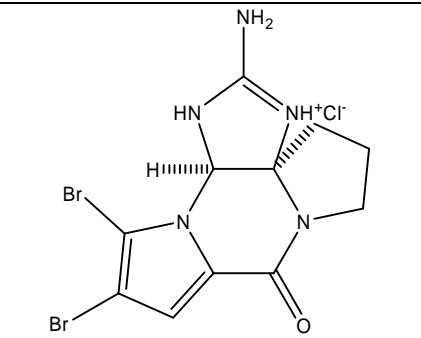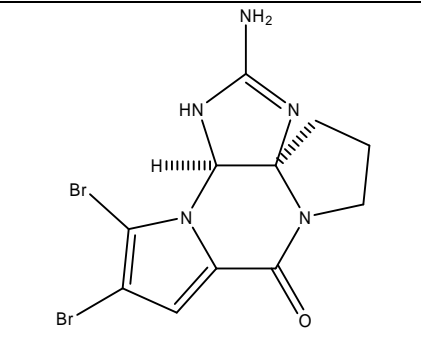
V.6.   *Rhabdastrella rowi* secondary metabolite

The quinolin-4-ol (**35**) was obtained from the Balinese marine sponge *Rhabdastrella rowi* extract in minute quantity. Up to now this compound has only been obtained synthetically and has never been reported from natural sources.
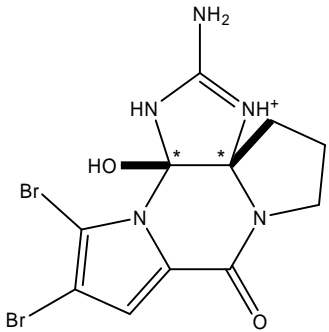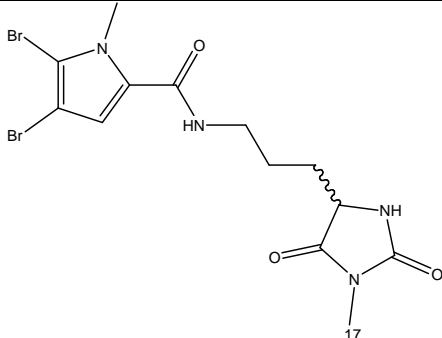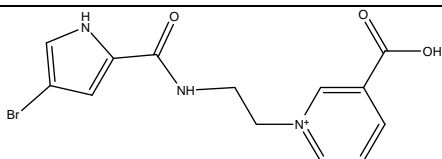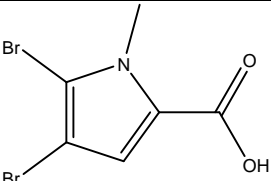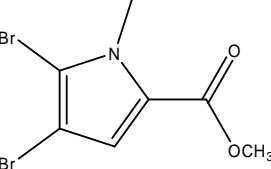
Summary of Isolated Compounds from Indonesian Marine Sponges
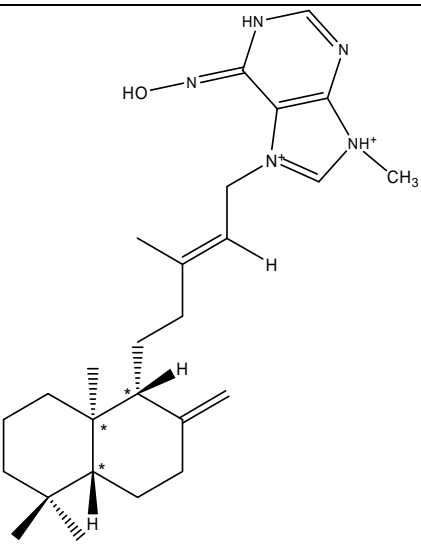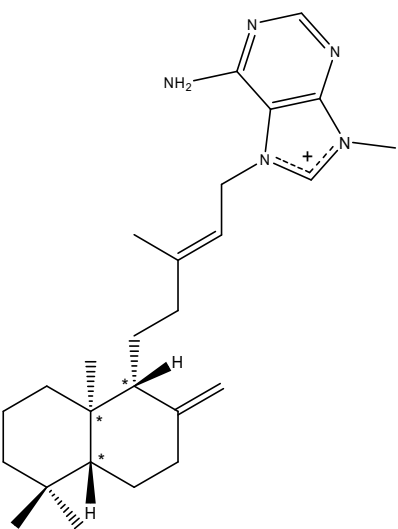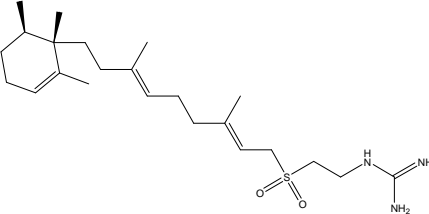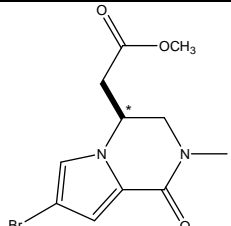
No.	Source	Trivial Name	Chemical Structure	MW (g/mol)	Amount (mg)	Note
1.	*Agelas* nsp.	**4-(4,5-Dibromo-1-methyl-1*H*-pyrrole-2-carboxamido) butanoic acid**		366/368/370 (1:2:1)	190.0	New
2.	*Agelas* nsp.	**Agelanin A**		415/417/419 (1:2:1)	8.0	New
3.	*Agelas* nsp.	**Agelanin B**		452/454/456 (1:2:1)	25.0	New
4.	*Agelas* nsp.	**Agelanesin A**		471/473/475 (1:2:1)	20.0	New
5.	*Agelas* nsp.	**Agelanesin B**		518/520 (1:1)	24.0	New
6.	*Agelas* nsp.	**Agelanesin C**		549/551/553 / 555 (1:2:2:19	6.0	New
7.	*Agelas* nsp.	**Agelanesin D**		597/599/601 (1:2:1)	7.0	New
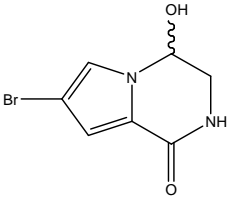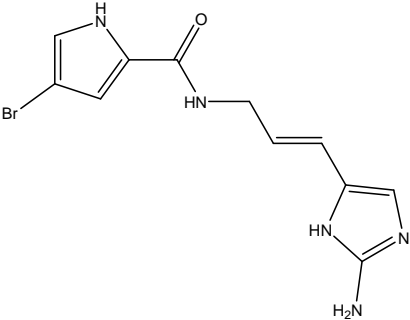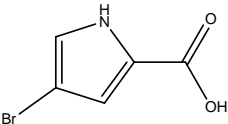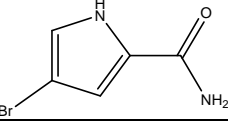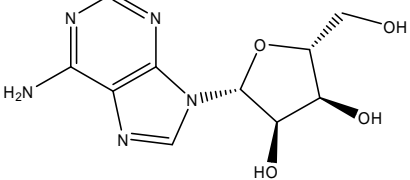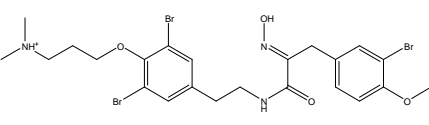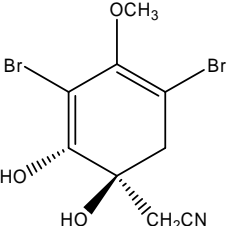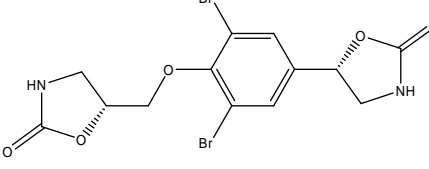
No.	Source	Name	Structure	m/z		Status
8.	*Agelas* nsp.	**Mauritamide B**		542/544/546 (1:2:1)	88.0	New
9.	*Agelas* nsp.	**Mauritamide C**		570/572/574 (1:2:1)	33.0	New
10.	*Agelas* nsp.	**2-(4,5-Dibromo-1-methyl-1*H*-pyrrole-2-carboxamido) ethanesulfonic acid**		388/390/392 (1:2:1)	6.0	New
11a.	*Agelas* nsp.	**Dibromophakellin HCl**		387/389/391 (1:2:1)	17.0	Known
11b.	*Agelas* nsp.	**Dibromophakellin (base)**		387/389/391 (1:2:1)	3.0	Known
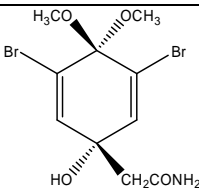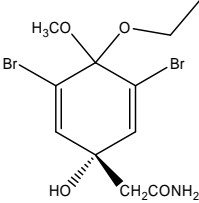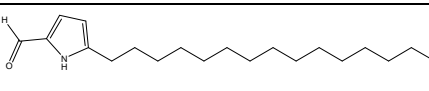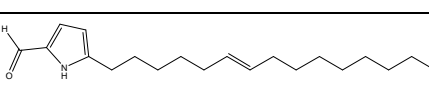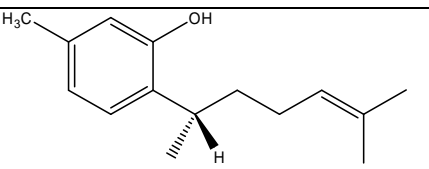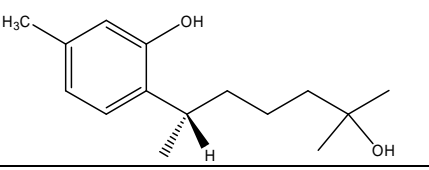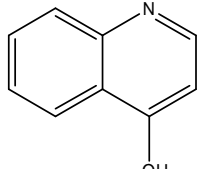
12.	*Agelas* nsp.	**Dibromophydroxy phakellin HCl**	* Relative stereochemistry is shown	403/405/407 (1:2:1)	47.0	New
13.	*Agelas* nsp.	**Midpacamide**		434/436/438 1:2:1)	2,000	Known
14.	*Agelas* nsp.	**Agelongine**		338:340 (1:1	20.0	Known
15.	*Agelas sp.*	**4,5-Dibromo-1-methyl-1*H*-pyrrole-2-carboxylic acid**		281/283/285 (1:2:1)	100.0	Known
16.	*Agelas* nsp.	**Methyl-4,5-dibromo-1-methyl-1*H*-pyrrole-2-carboxylate**		295/297/299 (1:2:1)	21.0	Known

17.	*Agelas nakamurai*	**(-)-Ageloxime-D**	 * Relative stereochemistry is shown	439	110.0	New
18.	*Agelas nakamurai*	**(-)-Agelasine-D**	 * Relative stereochemistry is shown	421	1,950	New
19.	*Agelas nakamurai*	**(+)-Agelasidine-C**		423	67.0	Known
20.	*Agelas nakamurai*	**Longamide C**	 * Relative stereochemistry is shown	300/302 (1:1)	1.13	New

21.	*Agelas nakamurai*	**Mukanadin-C**		230/232 (1:1)	12.0	Known
22.	*Agelas nakamurai*	**Hymenidin**		308/310 (1:1)	41.0	Known
23.	*Agelas nakamurai*	**4-Bromo-1*H*-pyrrole-2-carboxylic acid**		189/191 (1:1)	66.0	Known
24.	*Agelas nakamurai*	**4-Bromo-1*H*-pyrrole-2-carboxylic acid**		188/190 (1:1)	35.0	Known
25.	*Agelas nakamurai*	**Adenosine**		267	1.0	Known
27.	*Pseudoceratina purpurea*	**Aplysamine-2**		647/649/651 / 653 (1:2:2.1)	11.0	Known
28.	*Pseudoceratina purpurea*	**(+)-Aeroplysinin-1**		337/339/341 (1:2:1)	79.0	Known
29	*Pseudoceratina purpurea*	**5-(3,5-Dibromo-4-((2-oxooxazolidin-5yl)methoxy) phenyl)oxazolidin-2-one**		434/436/438 (1:2:1)	26.0	Known

30.	*Pseudoceratina purpurea*	**Dienone dimethoxyketal**		369/371/373 (1:2:1)	40.0	Known
31.	*Pseudoceratina purpurea*	**Dienone methoxy ethoxy ketal**		385/387/389 (1:2:1)	2.0	Known
32a.	*Mycale phylophylla*	**5-Pentadecyl)-1*H*-pyrrole-2-carbaldehyde**		305	28.0	Known
32b		**(*E*)-5-Pentadec-6-enyl)-1*H*-pyrrole-2-carbaldehyde**		303		Known
33.	*Axynissa sp*	**(+) Curcuphenol**		218	19.0	Known
34.	*Axynissa* sp.	**(+) Curcudiol**		236	24.0	Known
35.	*Rhabdastrella rowi*	**Quinolin-4-ol**		145	2.0	New as natural product

294

List of References

Abu-Ghazaleh, R., Kabir, J., Jia, H., Lobo, M., and Zachary, I., *Biochem. J.*, 2001, **360**, 255-64

Ackermann, D., and Müller, E., *Z. Physiol. Chem.*, 1941, **269**, 146-157

Acosta, A.L., and Rodriguez, A.D., *J. Nat. Prod.*, 1992, **55**, 1007-1012

Adler, F.R, and Harvell, C.D., *Trends Ecol. Evol.*, 1990, **5**, 407-410

Ahmed, K., and Thomas, B.S., *J. Biol. Chem.*, 1971, **246**, 103-109

Ahond, A., Zurita, M.B., Colin, M., Fizames, C., Laboute, F., Laurent, D., Poupat, C., Pusset, J., Thoison, M., and Potier, P., *C.R. Acad. Paris*, 1988, **307**, 145-148

Aiello, A., Fattorusso, E., Menna, M., and Pansini, M., *Biochem. Syst. Ecol.*, 1995, **23**, 377-381

Albizati, K.F., and Faulkner, D.J., *J. Org. Chem.*, 1985, **50**, 4163-4164

Al Mourabit, A., and Potier, P., *Eur. J. Org. Chem.*, 2001, 237 – 243

Amador, M.L., Jimeno, J., Paz-Ares, L., Cortes-Funes, H., and Hidalgo, M., *Ann. Oncol.*, 2003, **14**, 1607-1615

Amir, I., A comparison of sponge fauna of exposed and sheltered reef flats in eastern Indonesia, *Mar. Res. Indonesia*, 1992, **28,** 1-12, *cit* Calcinai, Barbara; Bavestrello, Giorgio; and Cerrano, Carlo, *Zoological Studies*, 2005, **44**(1): 5-18

Andrade, P., Willoughby, R., Pomponi, S.A., and Kerr, R.G., *Tetrahedron Lett.*, 1999, **40**, 4775-4778

Andersen, R.J., and Faulkner, D.J., *Tetrahedron Lett.*, 1973, **14**, 1175-1178

Arabshahi, L., and Schmitz, F.J., *J. Org. Chem.*, 1987, **52**, 3584-3586

Ardrey, R.E., *Liquid Chromatography mass Spectrometry: An Introduction (Analytical techniques in the sciences)*, 2003, John Wiley and Sons,

Assmann, M., Van Soest, R.W.M., and Köck, M., *J. Nat. Prod.*, 2001, **64**, 1345-1347

Assmann, M., Lichte, E., Pawlik, J.R., and Köck, M., *Mar. Ecol. Prog. Ser.*, 2000, **207**, 255 – 262

Assmann, M., Lichte, E., Van Soest, R.W.M., and Köck, M., *Organic Letters*, 1999, **1**(3), 455-457

Ayanoglu, E., Kornprobst, J. M., Aboud-Bichara, A., and Djerassi, C., *Tetrahedron Lett.*, 1983, **24**, 1111

Baker, Z., Isolation and Structure Elucidation of Bioactive Secondary Metabolites from Marine Sponges and Tunicates, *Dissertation*, 2004, Heinrich-Heine Universität, Düsseldorf

Ballantyne, J.S., and Storey, K.B., *Comp. Biochem. Physiol.*, 1983, **76B**, 133-138

Bauer, A.W., Kirby, W.M.M., Sherris, J.C., and Turck, M., *American Journal of Clinical Pathology*, 1996, **45**(4), 493-496

Benharref , A., Païs, M., and Debitus, C., *J. Nat. Prod.*, 1996, **59**, 177-180

Bergmann, W., and Feeney, R.J., *J.O.C.*, 1951, **16**, 981 – 987

Bergmann, W., and Feeney, R.J., *J. Am. Chem. Soc.*, 1950, **72**, 2809

Bergquist, P.R., and Cook, S.C., In: Hooper, J.N.A., and Van Soest, R.W.M. (Eds.), *Systema Porifera: A guide to the classification of sponges*, 2002, Kluwer Academic/Plenum, New York, 1081, 1086-1088

Berntsson, K.M., Jonsson, O.R., Lejhall, M., and Gatenholm, P., *Journal of Experimental Marine Biology and Ecology*, 2000, **251**, 59-83

Bevan, P., Ryder, H., and Shaw, I., *TIBTECH*, 1995, **13**, 115 – 121

Bickmeyer, U., Drechsler, C., Köck, M., and Assmann, M., *Toxicon*, 2004, **44**, 45 – 51

Bickmeyer, U., Assmann, M., Köck, M., and Schütt, C., *Environt. Toxicol. Pharmacol.*, 2005, **19**, 423 - 427

Blunt, J.W., Copp, B.R., Munro, M.H.G., Northcote, P.T., and Prinsep, M.R., *Nat. Prod. Rep.*, 2006, **23**, 26 – 78

Blunt, J.W., Copp, B.R., Munro, M.H.G., Northcote, P.T., and Prinsep, M.R., *Nat. Prod. Rep.*, 2005, **22**, 15 - 61

Blunt, J.W., Copp, B.R., Munro, M.H.G., Northcote, P.T., and Prinsep, M.R., *Nat. Prod. Rep.*, 2004, **21**, 1 - 49

Bourguet-Kondracki, M.L., Longeon, A., Debitus, C., and Guyot, M., *Tetrahedron Lett.*, 2000, **41**, 3087-3090

Bowden, B.F., Clezy, P.S., Coll, J.C., Ravi, B.N.; and Tapiolas, D.M., *Aust. J. Chem.*, 1984, **37**, 227 – 230

Borders, D.B., Morton, G.O., and Wetzel, E.R., *Tetrahedron Lett.*, 1974, **31**, 2709-2712

Braekman, J.C., Daloze, D., Stoller, C., and Van Soest, R.W.M., *Biochemical Systematics and Ecology*, 1992, **20** (5), 417–431

Braekman, J.C., Daloze, D., Moussiaux, B., Stoller, C., and Deneubourg, F., *Pure and Appl. Chem.*, 1989, **61**, 509-512

Bramley, A.M., Langlands, J.M., Jones, A.K., Burgoyne, D.L., Li Y.; Andersen, R.J., Salari, H., *Br. J. Pharmacol.*, 1995, **115**(8), 1433-1438

Bringmann, G., and Lang, G., *Full absolute stereostructures of natural products directly from crude extracts: the HPLC-MS/MS-NMR-CD 'triad'*, In: Müller, W.E.G. (Ed.), *Sponges (Porifera),* 2003, Marine Molecular Biotechnology, Springer, Berlin, 89 - 116

Brown, M.C., Cary, L.A., Jamieson, J.S., Cooper, J.A., and Turner, C.E., *Molecular Biology of the Cell*, 2005, **16**, 4316-438

Burgoyne, D.L., Andersen, R.J., and Allen T.M., *J. Org. Chem.*, 1992, **57**, 525-528

Butler, M.S., Capon, R.J., Nadeson, R., and Beveridge, A.A., *J. Nat. Prod.*, 1991, **54**, 619

Cafieri, F., Fattorusso, E., and Taglialatela-Scafati, O., *J. Nat. Prod.*, 1998a, **61**, 122

Cafieri, F., Fattorusso, E., and Taglialatela-Scafati, O., *J. Nat. Prod.*, 1998b, **61**, 1171-1173

Cafieri, F., Fattorusso, E., Mangoni, A., and Taglialatela-Scafati, O., *Tetrahedron*, 1996, **52**, 13713

Cafieri, F., Fattorusso, E., Mangoni, A., and Taglialatela-Scafati, O., *Bioorg. Med. Chem. Lett.*, 1995, **5**, 799-804

Calcinai, B., Bavestrello, G., and Cerrano, C., *Zoological Studies*, 2005, **44**(1): 5-18

Capon, R.J., *Eur. J. Org. Chem.*, 2001, Issue 4, 633-645

Capon, R.J., and Macleod, J.K., *Aust. J. Chem.*, 1987, **40**, 341-346

Carpenter, R.C., Partitioning herbivory and its effects on coral algal communities, *Ecol. Monogr.*, 1986, **56**, 345-365

Carte, B.K., *Curr. Opin. Biotechnol.*, 1993, **4**(3),275-279

Carney, J.R., and Rinehart, K.L., *J. Nat. Prod.*, 1995, **58**, 971-985

Carmichael, J., DeGraff, W.G., Gazdar, A.F., Minna, J.D., and Mitchell, J.B., *Cancer Res.*, 1987, **47**, 943-946

Chamber, L.D., Stokes, K.R., Walsh, F.C., and Wood, R.J.K., *Surface and Coatings Technology*, 2006, **201**, 3642-3652

Chanas, B., Pawlik, J.R., Lindel, T., and Fenical, W., *J. Exp. Mar. Biol. Ecol.* 1996, **208**, 185 – 196

Chang, C.W.J., *Prog. Chem. Org. Nat. Prod.*, 2000, **80**, 1

Chang, C.W.J., and Weinheimer, A.J., *Tetrahedron Lett.*, 1977, **46**, 4005-4008

Characklis, W.G., and Cooksey, K.E., Biofilms and microbial fouling. In: Laskin Al (Ed.), *Applied Microbiology*, **29**, Academic Press, New York, 93-138

Chenon, M.T., Pugmire, R.J., Grant, D.M.,Panzica, R.P., and Townsend, L.B., *J. Am. Chem. Soc.*, 1975, **97**(16), 4636-4642

Chevolot, L., Padua, S., Ravi, B.N., Blyth, P.C., and Scheuer, P.J., *Heterocycles*, 1977, **7**, Issue 2, 891-894

Chinou, I., *Current Medicinal Chemistry*, 2005, **12**, 1295-1317

Christian, M.C., Pluda, J.M., and Ho, P.T., *Semin. Oncol.*, 1997, **24**, 219-240

Cichewicz, R.H., Clifford, L.J., Lassen, P.R., Cao, X., Freedman, T.B., Nafie, L.A., Deschamps, J.D., Kenyon, V.A., Flanary, J.R., Holman, T.R., Crews, P., *Bioorganic, and Medicinal Chemistry*, 2005, **13**, 5600-5612

Cimino, G., de Rosa, S., de Stefano, S., Spinella, A., and Sodano, G., *Tetrahedron Lett.*, 1984, **25** (27), 2925 – 2928

Clare, A.S., Rittschof, D., Gerhart, D.J., Hooper, I.R.; and Bonaventura, J., *Mar. Biotechnol.*, 1999, **1**, 427 – 436

Cohen, P., *Nature Rev. Drug Discov.*, 2002, **1**, 309

Cooksey, K.E., and Wigglesworth-Cooksey, B., *Aquatic Microbial Ecology*, 1995, **9**, 87-96

Coll, J.C., *Chem. Rev.*, 1992, **90**, 613

Compagnone, R., Oliveri, M.C., Piña, I., Márquez, S., Rangel, H., Dagger, F. Suárez, A., Gomez, M., *Natural Products Letters*, 1999, **13**, 203-221

Compagnone, R.S., and Faulkner, D.J., *J. Nat. Prod.*, 1995, **58**(1), 145-148

Copp, B.R., and Ireland, C.M., *J. Nat. Prod.*, 1992, **55**, 822-823

Corriero, G., Madaio, A., Mayol, L., Piccialli, V., and Sica, D., *Tetrahedron*, 1989, **45**, 277-288

Costantino, V., Fattorusso, E., and Mangoni, A., *J. Nat. Prod.*, 1994, Vol. **57**, No.11, 1552 - 1556

Cosulich, D.B., and Lovell, F.M., *Chem. Comm.*, 1971, 397-399

Costerton, J.W., Stewart, P.S., Greenberg, E.P., *Science*, 1999, **284**, 1318-1322

Cragg, G.M., Newman, D.J., and Yang, S.S., *J. Nat. Prod.*, **69**, 2006, 488 - 498

Czesnik, D., Rössler, W., Kirchner, F., Gennerich, A., Schild, D., *Eur. J. Neurosci.*, 2003, **17**, 113-118

D'Ambrosio, M., Guerriero, A., Debitus, C., Ribes, O., Pusset, J., Leroy, S., and Pietra, F., *J. Chem. Soc., Chem. Commun.*, 1993, 1305 – 1306

D'Ambrosio, M.D., Guerriero, A., and Pietra, F., *Helv. Chim. Acta*, 1984, **67**, 1484-1492

D'Ambrosio, M., Guerriero, A., Traldi, P., and Pietra, F., *Tetrahedron Lett.*, 1982, **23**(42), 4403-4406

D'Armas, H.T., Mootoo, B.S., and Reynolds, W.F., *J. Nat. Prod.*, 2000, **63**, 1593

Debitus, C., Guella, G., Mancini, I., Walkedre, J., Guemas, J.G., Nicolas, J.L., and Pietra, F., *J. Mar. Biotechnol.*, 1998, **6**, 136-141

De Hoffmann, E., 1996, *J. Mass Spectrom.*, 1996, **31**, 129-137

De Nanteuil, G., Ahond, A., Guilhem, J., Poupat, C., and Tran Huu Dau, E., Potier, P., Pusset, M., Pusset, J., and Laboute, P., *Tetrahedron*, 1985, **41**, No. 24, 6019 – 6033

De Silva, E. Dilip, and Scheuer, Paul J., *Tetrahedron Lett.*, 1980, **21**, 1611-1614

Diop, M., Samb, A., Costantino, V., Fattorusso, E., and Mangoni A., *J. Nat. Prod.*, 1996, **59**, 271-272

Dodson, C.D., Dyer, L.A., Searcy J., Wright, Z., Letourneau, D.K., *Phytochemistry*, 2000, **53**(1), 51-54

Donlan, R.M., and Costerton, J.W., *Clin. Microbiol. Rev.*, 2002, **15**, 167-193

Donlan, R.M., *Clinical Infectious Disease*, 2001, **33**, 1387-1392

Dunne, W., Mason, E., and Kaplan, S.L., *Antimicrob. Agents Chemother.*, 1993, **37**, 2522-2526

Duque, C., Zea, S., De Silvestri, Calderon A., and Medina, A., *Rev. Colomb. Quim*, 1988, **17**, 39-46

Dreyfus, M., Dodin, G., Bensaude, O., and Dubois, J.E., *J. Am. Chem. Soc.*, 1975, **97**(9), 2369-2376

Ebel, R., Marin, A., and Proksch, P., *Biochem. Syst. Ecol.*, 1999, **27**, 769-777

Ebel, R., Brenzinger, M., Kunze, A., Gross, H.J., and Proksch, P., *J. Chem. Ecol.*, 1997, **23**, 1451-1462

Edrada R.A., Wray, V., Handayani, D., Schupp, P., Balbin-Oliveros, M., and Proksch, P., Structure-activity relationships of bioactive metabolites from some Indo-Pacific marine invertebrates. In: Atta-ur-Rahman (ed.) *Studies in natural products chemistry*, 2000, Vol 21. Elsevier, Amsterdam, 251-292

El Sayed, K.A., Yousaf, M., Hamman, M.T., Avery, M.A., Kelly, M., and Wipf, P., *J. Nat. Prod.*, 2002, **65**, 1547

Erpenbeck, D., and Van Soest, R.W.M., In: Hooper, J.N.A., and Van Soest, R.W.M. (Eds.), *Systema Porifera: A guide to the classification of sponges*, 2002, Kluwer Academic/Plenum, New York, 787-816

Fabbro, D., Ruetz, S., Buchdunger, E., Cowan-Jacob, S.W., Fendrich, G., Liebetanz, J., Mestan, J., O'Reilly, T., Traxler, P., Chandhuri, B., Fretz, H., Zimmermann, J., Meyer, T., Caravatti, G., Furet, P., and Manley, P.W., *Pharmacol. Ther.*, 2002, **93**(2-3), 79-98

Fattorusso, E., Minale, L., and Sodano, G., Chem. Communs., 1970, 751-752

Faulkner, D.J., *Nat. Prod. Rep.*, 2002, **19**, 1–48

Faulkner, D.J., *Nat. Prod. Rep.*, 2001, **18**, 1-49

Faulkner, D.J., *Nat. Prod. Rep.*, 2000, **17**, 7–55

Faulkner, D.J., *Nat. Prod. Rep.*, 1995, **12**, 223-269

Faulkner, D.J., *Nat. Prod. Rep.*, 1984, **1**, 551-598

Faulkner, D.J., and Andersen, R.J., *The Sea*, 1974, Vol. 5, Wiley, New York, London, Sydney, and Toronto, 679-714

Fathi-Afshar, R., and Allen, T.M., *Can. J. Chem.*, 1988, **66**, 45 – 50

Fedoreyev, S.A., Ilyin, S.G., Utkina, N.K., Maximov, O.B., and Reshetnyak, M.V., Antipin, M.Y., and Struchkov, Y.T., *Tetrahedron*, 1989, **45**(11), 3487-3492

Forenza, S., Minale, L.; Riccio, R., and Fattorusso, E., *J. Chem.* Soc., *Chem. Commun.*, 1971, 1129 – 1130

Fouad, M., Edrada, R.A., Ebel, R., Wray, V., Müller, W.E.G., Lin, W.H., and Proksch, P., *J. Nat. Prod.*, 2006, **69**, 211-218

Fouad, M.A., Isolation and Structure Elucidation of Bioactive Secondary Metabolites from Marine Sponges, *Dissertation*, 2004, Heinrich-Heine Universität, Düsseldorf

Freyer, A.J., Patil, A.D:, Killmer, L., Zuber, G., Myers, C., and Johnson, R.K., *J. Nat. Prod.*, 1997, **60**, 309

Frisch, S.M., Vuori, K., Ruosiahti, E., and Chan-Hui, P.Y., *J. Biol. Chem.*, 1996, **134**, 739-799

Fulmor, W., Van Lear, G.e, Morton, G.O., and Mills, R.D., *Tetrahedron Lett.*, 1970, **52**, 4551-4552

Fusetani, N., *Nat. Prod. Rep.*, 2004, **21**, 94-104

Fusetani, N., Hirota, H., Okino, T., Tomono, Y., and Yoshimura, E., *J. Nat. Toxins*, 1996, **5**, 249

Fusetani, N., Sugawara, T., Matsunaga, S., and Hirota, H., *J. Org. Chem.*, 1991, **56**, 4971-4974

Fusetani, N., Yasumuro, K., Matsunaga, S., and Hashimoto, K., *Tetrahedron Lett.*, 1989, **30**, 2809-2812

Fusetani, N., Sugano, M., Matsunaga, S., and Hashimoto, K., *Experientia,* 1987, **43**, 1234-1235

Gao, H., Kelly, M., and Hamman, M.T., *Tetrahedron*, 1999, **55**, 9717-9726

Gautschi, J.T., Whitman, S., Holman, T.R., and Crews, P., *J. Nat. Prod.*, 2004, **67**, 1256 – 1261

Garcia, A., Vazquez, M.J., Quiñoa, E., Riguera, R., and Debitus, C., *J. Nat. Prod.*, 1996, **59**, 782

Gaspar, H., Feio, S.S., Rodrigues, A.I., and Van Soest, R.W.M., *Mar. Drugs.*, 2004, 2, 8-13

Giancotti, F.G., and Tarone, G., *Annu. Rev. Cell. Dev. Biol.*, 2003, **19**, 173-206

Giordano, F., Mayol, L., Notaro, G., Piccialli, V., and Sica, D., *J. Chem. Soc. Chem. Commun.*, 1990, **22**, 1559-1561

Gilbert, P., Collier, P.J., and Brown M.R.W., *Antimicrob. Agents Chemoter.*, 1990, **34**, 1865-1868

Gilmore, A.P., and Romer, L.H., *Mol. Biol. Cell.*, 1996, **7**, 1209-1224

Glaser, K.B., de Carvalho, M.S.; Jacobs, R.S.; Kernan, M.R.; and Faulkner, D.J., *Mol. Pharmacol.*, 1989, **36**, 782

Glaser, K.B., and Jacobs, R.S., *Biochem. Pharmacol.*, 1987, **36**, 2079

Glaser, K.B., and Jacobs, R.S., *Biochem. Pharmacol.*, 1986, **35**, 449

Goldenstein, G., Fendert, T., Proksch, P., and Winterfeldt, E., *Tetrahedron*, 2000, **56**, 4173-4185

Gopichand, Y., and Schmitz, F.J., *Tetrahedron Lett.*, 1979, **41**, 3921-3924

Gordon, C.A., Hodges, N.A., and Marriott, C., *J. Antimicrob. Chemother.*, 1988, **22**, 667-674

Götz, F., *Molecular Microbiology*, 2002, **43**(6), 1367-1378

Gribble, G.W., *Natural organohalogens*, 2004, Eurochlor, Brussels, 11-13, 29

Gribble, G.W., The Natural production of organobromine compounds, *Environ. Sci. Pollut. Res.*, 2000, **7**, 37-49

Gribble, G.W., *Acc. Chem. Res.*, 1998, **31**, 141-152

Gribble, G.W., Naturally occurring organohalogen compounds - A comprehensive survey, *Prog. Chem. Org. Nat. Prod.*, 1996a, **68**, 1-498

Gribble, G.W., *Pure and Appl.* Chem., 1996b, **68**(9), 1699-1812

Grifo, F.; Newman, D., Fairfeld, A., Bhattacharya, B., and Grupenhoff, J.T., In: Grifo, F., Rosenthal, J. (Eds.), Biodiversity and Human Health, 1997, Island Press, Washington, DC, 131 – 163

Gross, H., and König, G.M., *Phytochemical Reviews*, 2006, **5**, 115-141

Gualtieri, M., Bastide, L., Villain-Guillot, P., Michaux-Charachon, S., Latouche, J., and Leonetti, J.L., *Journal of Antimicrobial Chemotherapy*, 2006, **58**, 778-783

Gunasekera, S.P. and Cross, S.S., *J. Nat. Prod.*, 1992, **5**(4), 509-512

Gudbjarnason, S., *Rit Fiskideildar*, 1999, **16**, 107-110

Hamann, M.T., and Scheuer, P.J., *J. Org. Chem.*, 1993, **56**, 6565 – 6569

Hanks, S.K., and Polte, T.R., *Bioassays*, 1997, **19**, 137-145

Hare, P.D., and Cress, P.D., *Plant Growth Regul.*, 1997, **21**, 79-102

Harrison, B., and Crews, P., *J. Org. Chem.*, 1997, **62**, 2646

Hart, S., *Business Briefing: Exploration and Production: The Oil and Gas Review*, 2005, Issue **2**, 1-2

Hassan, W., Isolation and Structure Elucidation of Bioactive Secondary Metabolites from Marine Sponges, Dissertation, 2004, Heinrich-Heine Universität, Düsseldorf

Hatano, K., Nogami, I., Higashide, E., and Kishi, T., *Agric. Biol. Chem.*, 1984, **48**, 1503

Hattori, T., Adachi, K., and Shizuri, Y., *J. Nat. Prod.*, 1998, **61**, 823-826

Havel, J., Predator-induced defenses: A review. In: Kerfoot, W.C., and Sih, A. (Eds.), *Predation: Direct and Indirect Effects on Aquatic Communities*, 1986, University Press of New England, Hanover, NH, 268-278

Hemscheidt, T., Burgoyne, D.L., Moore, R.E., *J. Chem. Soc. Chem. Commun.*, 1995, 205

Hirano, K., Kubota, T., Tsuda, M., Watanabe, K., Fromont, J., and Kobayashi, J., *Tetrahedron*, 2000, **56**, 8107-8110

Hirota, H., Tomono, Y., and Fusetani, N., *Tetrahedron*, **52**(7), 2359-2368

Hoffmann, H., and Lindel, T., *Synthesis*, 2003, **12**, 1753 – 1783

Holmes, N., *Marine Pollution Bulletin*, 1970, **1**, 105-106

Hong, T.W.; Jímenez, D.R., and Molinski, T.F., *J. Nat. Prod.*, 1998, **61**, 158-161

Hooper, J.N.A., Van Soest, R.W.M., and Debrenne, F. In: Hooper, J.N.A.; and Van Soest, R.W.M. (Eds.), *Systema porifera: A guide to the classification of sponges*, 2002, Kluwer Academic/ Plenum Publisher, New York, 9-14

Horii, S., and Kameda, Y., *J. Antibiot.*, 1968, **21**, 665

Houghton, D.R., *Ocean Manage*, **4**, 347-352

Hoyle, B.D:, Alcantara, J., Costerton, J.W., *Antimicrob. Agents Chemother.*, 1992, **36**, 2054-2056

Hungerford, J.E., Compton, M.T., Matter, M.L., Hoffstrom, B.G., and Otey, C.A., *J. Biol. Chem.*, 1996, **135**, 1383-1390

Hunter, T., *Cell*, 2000, **100**, 113-127

Ichiba, T., and Scheuer, P.J., *J. Org. Chem.*, 1993, **58**, 4149-4150

Illic, D., Furuta, Y., Kanazawa, S., Takeda, N., Sobue, K., Nakatsuji, N., Nomura, S., Fujimoto, J., Okada, M., Yamamoto, T., and Aizawa, S., *Nature* (London), 1995, **377**, 539-544

Ishibashi, M., Tsuda, M., Ohizumi, Y., Sasaki, T., and Kobayashi, J., *Experientia*, 1991, **47**, 299 – 300

Jacquot, D.E.N., Mayer, P., and Lindel, T., *Chem. Eur. J.*, 2004, **10**, 1141 – 1148

Jadulco, R.C., Isolation and Structure Elucidation of Bioactive Secondary Metabolites from Marine Sponges and Sponge-derived Fungi, *Dissertation*, 2002, Cuvillier Verlag, Göttingen

Jaffe, H.H., and Orchin, M., *Theory and Application of Ultra Violet Spectroscopy*, 1962, Willey, New York, 350 – 351

Jemal, A., Tiwar, R.C., Murray, T., Ghafoor, A., Samuels, A., Ward, E., Feuer, E.J.; and Thun, M.J., *CA Cancer J Clin*, 2004, **54**, 8-29

Jimènez; C., and Crews, P., *Tetrahedron Letters,* 1994, **35**, No. 9, 1375 – 1378

Jockusch, B.M., Bubeck, P., Giehl, K., Kroemker, M., Moshner, J., Rothkegel, M., Rudiger, M., Schluter, K., Stanke, G., and Winkler, J., *Annu. Rev. Cell. Dev. Biol.*, 1995, 379-416

Jones, R.A., and Bean, G.P., *The chemistry of pyrroles*, 1977, Academic Press, New York

Joseph-Nathan, P., Tovar-Miranda, R., Martínez, E., and Santillan, R.L., *J. Nat. Prod.*, 1988, **51**(6), 1116-1128

Juliano, R.L., *Annu. Rev. Pharmacol. Toxicol.*, 2002, **42**, 283-323

Kaandorp, J.A., and Kübler, J.E., *The algorithmic beauty of seaweeds, sponges and corals*, 2001, Springer, Berlin Heidelberg New York

Kaestner, A., *Invertebrate Zoology*, 1967, Interscience, New York, Vol. I, 24

Kato,Y., Fusetani, N., Matsunaga, S., and Hashimoto, K., *Tetrahedron Lett.*, 1985, **26**, 3483-3486

Katratnitsas, A., Castritsi-Catharios, J., and Persoone, G., *Mar. Pollut. Bull.*, 2003, **46**, 1491-1494

Kazlauskas, R., Lidgrad, R.O., Murphy, P.T., Wells, R.J., and Blount, J.F., *Aust. J. Chem.*, 1981, **34**, 765-786

Kernan, M.R., Faulkner, D. J., and Jacobs, R.S., *J. Org. Chem.*, 1987, **52**, 3081-3083

Keyzers, R.A., and Davies-Coleman, M.T., *Chem. Soc. Rev.*, 2005, **34**, 355-365

Kijjoa, A., Bessa, J., Wattanadilok, R., Sawangwong, P., Nascimento, M.S.J., Pedro, M., Silva, A.M.S., Eaton, G., Van Soest, R.W., and Herz, W., *Z. Naturforsch.*, 2005, **60b**, 904 – 908

Kim, D., Lee, I.S., Jung, J.H., Lee, C.O., and Choi, S.U., *Anticancer Res.*, 1999, **19**(5B), 4085-4090

Kinnel, R.B., Gehrken, H.P., Swali, R., Skoropowski, G., and Scheuer, Paul J., *J. Org. Chem.*, 1998, **63**, 3281-3286

Kitagawa, I., Kobayashi, M., Kitanaka, K., Kido, M., and Kyogoku, Y., *Chem. Pharm. Bull.*, 1983, **31**, 2321 -2328

Kobayashi, J., Inaba, K., and Tsuda, M., *Tetrahedron*, 1997, **53**, 16679 – 16682

Kobayashi, J., Tsuda, M., Shigemori, H., Ishibashi, M., Sasaki, T., and Mikami, Y., *Tetrahedron*, 1991, **47**(33), 6617-6622

Kobayashi, M., Nakamura, H., Wu, H., Kobayasji, J., and Ohizumi, Y., *Archives of Biochemistry and Biophysics*, 1987, **259**(1), 179-184

Kobayashi, J., 1986 Ohizumi, Y., Nakamura, H., and Hirata, Y., *Experientia*, 1986, **42**, 1176-1177

Kobayashi, M., Kajiwara, A., Takahashi, M., Ohizumi, Y., Shoji, J., and Takenoto, T., *J. Biol. Chem.*, 1984, **259**, 15007-15009

König, G., and Wright A.D., *Heterocycles*, 1993, **36**, No. 6, 1351 – 1358

Konstantinou, I.K., and Albanis, T.A., *Environment Int.*, 2004, 30, 235-248

Kossuga, M.H., MacMillan, J.B., Rogers, E.W., Molinski, T.F., Nascimento, G.G.F., Rocha, R.M., and Berlinck, R.G.S., *J. Nat. Prod.*, 2004, **67**, 1879-1881

Koulman, A., Proksch, P., Ebel., R., Beekman, A., van Uden, W., Konings, A.W.T., Pedersen, J.A., Pras, N., and Woerdenbag, H.J., *J. Nat. Prod.*, 1996, **59**, 591-594

Krejcarek, G.E., White, R.H., Hager, L.P., McClure, W.O., Johnson, R.D., Rinehart, J.K.R., Shaw, D.S., and Brusca, R.C., *Tetrahedron Lett.*, 1975, **8**, 507-510

Kreuter, M.H., Leake, R.E., Rinaldi, F., Müller-Klieser, W., Maidhof, A., Müller, W.E.G., Schröder, H.C., *Comp. Biochem. Physiol.*, 1990, **97B**, 151-158

Kreuter, M.H., Bernd, A., Holzmann, H., Müller.Klieser, W., Maidhof, A., Weissmann, N., Kljajic, E., Batel, R., Schröder, H.C., and Müller, W.E.G., *Z. Naturforsch.*, 1989, **44c**, 680-688

Kubanek, J., Whalen, K.E., Engel, S., Kelly, S.R., Henkel, T.P., Fenical, W., and Pawlik, J.R., *Oecologia*, 2002, **1**, 125-136

Levitzky, A., *Acc. Chem. Res.*, 2993, **36**, 462

Leys, S.P., Rohksar, D.S., and Degnan, B.M., *Current Biology*, 2005, **15**, No. 4, 114 - 115

Li, C.J., Schmitz, F.J., and Kelly, M., *J. Nat. Prod.*, 1999, **62**, 1330-1332

Lindel, T., Hochgürtel, M., Assmann, M., and Köck, M., *J. Nat. Prod.*, 2000a, **63**, 1566 -1569

Lindel, T., Hoffman, H., Hochgürtel, M., and Pawlik, J.R., *Journal of Chemical Ecology*, 2000b, **26** (6), 1477 -1496

Longeon, A., Guyot, M., and Vacelet, J., *Experientia*, 1990, **46**, 548-550

Low, E.M., *J. Mar. Res.*, 1951, **10**, 239-245

Lv, F., Deng, Z., Li, J., Fu, H., Van Soest, R.W.M., Proksch, P., and Lin, W., *J. Nat. Prod.,* 2004, **67**(12), 2033 -2036

Mack, D., Nedelmann, M., Krokotsch, A., Schwarzkopf, A., Heesemann, J.,and Laufs, R., *Infection and Immunity*, 1994, **62**(8), 3244-3253

McEnroe, F.J., and Fenical, W., 1978, *Tetrahedron*, **34**, 1661-1664

Makarieva, T.N., Stonik, V.A., Alcolado, P., and Elyakov, Y.B., *Comp. Biochem. Physiol.*, 1981, **68B**, 481-484

Mancini, I., Guella, G., Amade, P., Roussakis, C., and Pietra, F., *Tetrahedron Lett.*, **38**(35), 6271-6274

Mangel, A., Leitao, J.M., Batel., R., Zimmermann, H., Müller, W.E.G., Schröder, H.C., *Eur. J. Biochem.*, 1992, **210**, 499 – 507

Manning, G., Whyte, D.B., Martinez, R., Hunter, T., and Sudarsanam, S., *Science*, 2002, **298**(5600), 1912-1934

Marcus, A.H., Molinsky, T.F., Fahy, E., Faulkner, D.J., Xu, C., and Clardy, J., *J. Org. Chem.*, 1989, **54**, 5184-5186

Marin, A., López, M.D., Esteban, M.A., Meseguer, J., and Muñoz, J., Fontana, A., *Mar. Biol.*, 1998, **131**, 639-645

MarinLit database, 2006, Department of Chemistry, University of Canterbury Zealand: http://www.chem.canterbury.ac.nz/marinlit/marinlit.shtml

MarinLit database, 2004, Department of Chemistry, University of Canterbury, New Zealand: http://www.chem.canterbury.ac.nz/marinlit/marinlit.shtml

MarinLit database, 2002, Department of Chemistry, University of Canterbury Zealand: http://www.chem.canterbury.ac.nz/marinlit/marinlit.shtml

MarinLit database, 1999, Department of Chemistry, University of Canterbury Zealand: http://www.chem.canterbury.ac.nz/marinlit/marinlit.shtml

Mayer, A.M.S., and Gustafson, K.R., *Int. J. Cancer*, 2003, 105, 291-299

Mayr, H., Kempf, B., and Ofial, A.R., *Acc. Chem. Res.*, 2003, **36**, 66

McClintock, J.B., and Baker, B.J. (Eds.), *Marine Chemical Ecology*, 2001, CRC, Boca Raton, Florida

McConnel, O.J.; Longley, R.E., and Koehn, F.E., *Biotechnology*, 1994, **26**, 109 -174

McEnroe, F.J., and Fenical, W., *Tetrahedron*, 1978, **34**, 1661-1664

Mendola, D., In Fusetani, N., (Ed.), *Drugs from the Sea*, 2000, S. Karger, A.G., Basel, 120 – 133

Michal, G., *Biochemical Pathways*, 1972, Boehringer Mannheim

Michel, W.C., and Ache, B.W., *Chem. Senses*, 1994, **19**, 11-24

Minale, L., Cimino, G., DeStefano, S., and Sodano, G., *Fortschr. Chem. Org. Naturst.*, 1976, **33**, 1-72

Mierzwa, R.A.K., Conover, M.A., Tozzi, S., Puar, M.S., Patel, M., and Coval, S.J., *J. Nat. Prod.*, 1994, **57**, 175-177

Moody, K., Thomson, R.H., Fattorusso, E., Minale, L., and Sodano, G., *J. Chem. Soc., Perkin Trans.1*, 1972, 18-24

Morales, J.J., and Rodriquez, A.D., 1992, *J. Nat. Prod.*, **55**(2), 389-394

Müller, W.E.G., Diehl-Seifert, B., Sobel, C., Bechtold, A., Kljajic, Z, and Dom, A., *J. Histochem. Cytochem.*, 1986, **34**, 1687-1690

Murti, Y.B., Isolation and Structure Elucidation of Bioactive Secondary metabolites from sponges collected at Ujung pandang and in the Bali Sea, Indonesia, *Dissertation*, 2006, 61 - 64

Müller, W.E.G., Klemt, M., Thakur, N.L., Schröder, H.C., Aiello, A., D'Esposito, M., Menna, M., and Fattorusso, E., *Marine Biology*, 2004, **144**, 19 – 29

Müller, W.E.G.; Brümmer, F., Batel, R., Müller, I.M., and Schröder, H.C., *Naturwissenschaften*, 2003, **90**, 103 – 120

Müller, W.E.G., Zahn, R.K., Kurelec, B., Lucu, C., Muller, I., and Uhlenbruck, G., *J. Bacteriol.*, 1981, **145**, 548 - 558

Mutter, R., and Wills, M., Chemistry and clinical biology of the bryostatins, *Bioorg Med Chem,* 2000, **8**, 1841 – 1860

Nakamura, H., Wu, H., Kobayashi, J., Kobayashi, M., Ohizumi, Y., and Hirata, Y., *J. Org. Chem.*, 1985a, **50**, 2494-2497

Nakamura, H., Wu, H., and Kobayashi, J., *Tetrahedron Lett.*, 1985ba, **26**, 4517-4520

Nakamura, H., Ohizumi, Y., Kobayashi, J., and Hirata, Y., *Tetrahedron Lett.*, 1984a, **25**(23), 2475-2478

Nakamura, H., Wu, H., Ohizumi, Y., and Hirata, Y., *Tetrahedron Lett.*, 1984b, **25**(28), 2989-2992

Nakatsu, T., Faulkner, D.J., Matsumoto, G.K., and Clardy, J., *Tetrahedron Lett.*, 1984, **25**(9), 935-938

Neidleman, S.L., and Geigert, J., *Biohalogenation: Principles, Basic Roles, and Applications*, 1986, Ellis Horwood Ltd., Chichester, UK, 46 – 47

Newman, D.J., and Cragg, G.M., *J. Nat. Prod.*, 2004, **67**, 1216 – 1238

Newman, D.J.; Cragg, G.M.; and Snader, K.M., *J. Nat. Prod.*, 2003, **66,** 1022-1037

Nogata, Y., Yoshimura, E., Shinshima, K., Kitano, Y., and Sakaguchi, I., *Biofouling*, 2003, **19** (Suppl.), 193

Norte, M., Rodriguez, M.L., Fernández, J.J., Eguron, L., and estrada, D.M., *Tetrahedron*, 1988, **44**(15), 4973-4980

O'Gara and J.P., Humphreys, H., *J. Med. Microbiol.*, 2001, **50**, 582-587

Okamoto, Y., Ojika, M., Kato, S., and Sakagami, Y., *Tetrahedron*, 2000, **56**, 5813-5818

Okino, T., Yoshimura, E., Hirota, H., and Fusetani,N., *J. Nat. Prod.*, 1996a, **69**, 1081

Okino, T., Yoshimura, E., Hirota, H., and Fusetani, N., *Tetrahedron*, 1996b, **52**, 9447

Okino, T., Yoshimura, E., Hirot, H., and Fusetani, N., *Tetrahedron Lett.*, 1995, **36**, 8637

Ortega, Maria J.; Zubia, Eva; Sánchez, M. Carmen; Salvá, Javier; and Carballo, J. Luis, *Tetrahedron*, 2004, **60**, 2517 – 2524

Ortega, M.J., Zubia, E., Carballo, J.L., and Salvá, *Tetrahedron*, 1997, **53**, 331 – 340

Ortiz, A.R; Pisabarro, M.T.; and Gago, F.; *J. Med. Chem.*, 1993, **36**, 1866

Ortlepp, S., Dissertation, 2007, Heinrich-Heine Universität, Düsseldorf

Patel, J., Pelloux-Léon, N., Minassian, F., and Vallée, Y., *J. Org. Chem.*, 2005, **70**, 9081-9084

Paul, V.J., Puglisi, M.P.; and Ritson-Williams, R., *Nat. Prod. Rep.*, 2006, **23**, 153-180

Paul, V.J., and Puglisi, M.P., *Nat. Prod. Rep.*, 2004, **21**, 189-209

Pawlik, J.R.; Chanas, B.; Toones, R.J.; and Fenical, W., *Mar. Ecol. Prog. Ser.*, 1995, **127**, 183–194

Pearse, V., Pearse, J., Buchsbaum, M., and Buchsbaum R., *Living Invertebrates*, 1987, Blackwell Sci. Pub. and Boxwood Press, Palo Alto, California

Pechenik, J.A., *Biology of the invertebrates*, 2000, McGraw Hill, Boston

Pedradab, S., Isolation and Structure Elucidation of Secondary Metabolites from Marine Sponges and a Marine-derived Fungus, *Dissertation*, 2000, Heinrich-Heine Universität, Düsseldorf, 71-86

Peng, J., Franzblau, S.G., Zhang, F., and Hamman, M.T., *Tetrahedron Lett.*, 2002, **43**, 9699

Perry, N.B., Blunt, W.J., Munro, M.H.G., and Thompson, A.M., *J. Org. Chem.*, 1990, **55**, 223-227

Pettit, G.R.; Knight, J.C.; Collins, J.C.; Herald, D.L.; and Young, V.G., *J. Nat. Prod.*, 2000, **63**, 793–798

Pina, Ivette C.; Gautschi, Jeffrey T.; Wang, Gui-Yang-Sheng; Sanders, Miranda L.; Schmitz, Francis J.; France, Dennis; Cornell-Kennon, Susan; Sambucetti, Lidia C.; Remiszewski, Stacy W.; Perez, Larry B.; Bair, Kenneth W.; and Crews, Phillip, *J. Org. Chem.*, 2003, **68**, 3866-3873

Pordesimo, O.E., and Schmitz, F., *J. Org. Chem.*, 1990, **55**, 4704-4709

Potts, B.C.M.; Faulkner, D.J.; and Jacobs, R., *J. Nat. Prod.*, 1992, **55**, 1701

Potts, B.C.M.; Faulkner, D.J.; de Carvalho, M.S.; and Jacobs, R.S., *J. Am. Chem. Soc.*, 1992, **114**, 5093

Poullennec, K.G., Kelly, A.T., and Romo, D., *Organic Letters*, 2992, **4**(16), 2645-2648

Pratt, D.J., Endicott, J.A., and Noble, M.E., *Curr. Opin. Drug Discov. Dev.*, 2004, 7, 428-436

Proksch, P., Ebel, R., Edrada, R., Wray, V., and Steube, K., Bioactive natural products from marine invertebrates and associated fungi. In: Müller, W.E.G. (Ed.), *Sponges (Porifera),* 2003, 117-142

Proksch, P., Edrada, R., and Ebel, R., *App. Microbiol. Biotechnol*, 2002, **59,** 125-134

Proksch, P., Chemical defense in marine ecosystems. In: Wink, M. (Ed.) *Functions of plant secondary metabolites and their exploitation in biotechnology*, 1999, Academic, Sheffield, 134- 154

Proksch, P., and Ebel, R., Ecological significance of alkaloids from marine invertebrates. In: Roberts, M.F.; and Wink, M. (eds.), *Alkaloids, biochemistry, ecology and medicinal applications*, 1998, Plenum, New York, 379 – 394

Proksch, P., *Toxicon.*, 1994, **32**(6), 639 - 655

Pullman, B., Berthod, H., and Dreyfus, M., *Theoret. Chim. Acta (Berl.)*, 1969, **15**, 265-268

Quiñoà, E., and Crews, P., *Tetrahedron Lett.*, 1987, **28**(28), 3229-3232

Railkin, A.I., *Marine Biofouling: Colonization Processes and Defenses*, 2004, Boca Raton, CRC Press

Rao, Z., Deng, S., Wu, H., and Jiang, S., *J. Nat. Prod.*, 1997, **60**, 1163-1164

Rao, Z., Deng, S., Wu, H., and Jiang, S., *J. Nat. Prod.*, 1998, **19**, 406-407

Rao, R.N., *Current Opinion in Oncol.*, 1996, **8**,516-524

Reddy, G. Bala Show; and Dhananjaya, N., *Bioorg. Med. Chem.*, 2000, **8**, 27 – 36

Remiszewski, Stacy W., *Current Medicinal Chemistry*, 2003, **10**(22), 2393-2402

Richard, J.P., Szymanski, P., Williams, K.B., *J. Am. Chem. Soc.*, 1998, **120**, 10372

Richardson, A., and Parsons, J.T., *Nature* (London), 1996, **380**, 538-540

Richelle-Maurer, E.; Gomez, R.; Braekman, J.C.; Van de Vyver, G.; Van Soest, R.W.M.; Devijver, C., *J. Biotechnol.*, 2003, **100**, 169 - 176

Roberts, Callum M.; McClean, Colin, J.; Veron, John E.N.; Hawkins, Julie P.; Allen, Gerald R.; McAllister, Don E.; Mittermeier, Christina G., Schueler, Frederick, W.; Spalding, Mark; Wells, Fred; Vynne, Carly; and Werner, Timothy B., *Science*, 2002, **295**, 1280 – 1284

Roche, J., *Experientia*, 1952, **8**, 45-54

Rodríguez-Nieto, S., González-Iriarte, M., Carmona, R., Muñoz-Chápuli, R., Medina, M.A., and Quesada, A.R., *FASEB J.*, 2002, **16**, 261-263

Rodriquez, A.D., and Vera, B., *J. Org. Chem.*, 2001, **66**, 6364

Rodriguez, A.D., and Piña, I.C., *J. Nat. Prod.*, 1993, **56**(6), 907-914

Rodriquez, A.D., Akee, R., and Scheuer, P., *Tetrahedron Lett.*, 1987, **28**, 4989-4992

Rogers, E.W., de Oliveira, M.F., Berlinck, R.G.S., König, G.M., and Molinski, T.F., *J. Nat. Prod.*, 2005, **68**, 891-896

Roll, M.D., Chang, W.J.C., Scheuer, P.K., Gray, G.A., Shoolery, J.N., Matsumoto, G.K., Van, D.G.D., Clardy, J., *J. Am. Chem. Soc.*, 1985, **107**, 2916-2920

Ross, C.A., Weete, J.D., Schinazi, R.F., Wirtz, S.S., Tharnish, P., Scheuer, P.J., and Hamman, M.T., *J. Nat. Prod.*, 2000, **63**, 501-503

Sachs, L., *Angewandte Statistik*, 1984, Springer Verlag, Berlin

Salituro, G.M., and Dufresne, C. In: Cannell, R.J.P., *Natural products isolation*, 1998, Humana Press, Totowa, New Jersey, 111-140

Salomon, C.E., Deerinck, T., Ellisman, M.H., and Faulkner, D.J., *Mar. Biol.*, 2001, **139**, 313-319

Sastry, S.K., and Burridge, K., *Exp. Cell. Res.*, 2000, **261**, 25-36

Schoenfeld, R.C:, Conova, S., Rittschof, D.,and Ganem, B., *Bioorg. Med. Chem. Lett.*, 2002, **12**, 823

Schreier, P., Bernreuther, A., and Huffer, M., *Analysis of chiral organic molecules, methodology and applications*, 1995, Walter de Gruyter, Berlin, New York

Schröder, H.C.; Ushijima, H.; Krasko, A.; Gamulin, V.; Thakur, N.L.; Diehl-Seifert, B.; Müller, I.M.; and Müller, W.E.G., *J. Biol. Chem.*, 2003, **278** (35), 32810 - 32817

Schupp, P., Eder, C., Paul, V., and Proksch, P., *Mar. Biol.*, 1999, **135**, 573-580

Schwartz, M.A., Schaller, M.D., and Ginsberg, M.H., *Annu. Rev. Cell. Dev. Biol.*, 1995, **11**, 549-599

Sera, Y., Adachi, K., and Shizuri, Y., *J. Nat. Prod.*, 1999, **62**, 152-154

Sharma, G., and Burkholder, P.R., *J. Chem. Soc. Chem. Comm.*, 1971, 151-152

Sharma, G.; and Magdoff-Fairchild, B., *J. Org. Chem.*Vol., 1977, **42**, No. 25, 4118 – 4124

Sheppard, C.; and Wells, S.M., () *Coral reefs of the world*, Vol. 2: Indian Ocean, red Sea and Gulf, Nairobi, Kenya,1988, UNEP, and Cambridge, UK: IUCN, 389

Shimizu, Y., Norte, M., Hori, A., Genenah, A., and Kobayashi, M., *J. Am. Chem. Soc.*, 1984, **106**, 6433-6434

Simmons, T. Luke; Andrianasolo, Eric; McPhail, Kerry, Flatt, Patricia; and Gerwick, William, *Mol. Cancer Ther.*, 2005, **4**(2) 333-342

Shim, Joong Sup; Lee, Hyi-Seung; Shin, Jongheon; Kwon Ho Jeong, *Cancer Letters*, 2004, **203**, 163-169

Showalter, H.D., and Kraker, A.J., *Pharmacol. Ther.*, 1997, **76**(1-3), 55-71

Shu, Yue-Zhong, *J. Nat. Prod.*, 1998, **61**, 1053 - 1071

Simpson, T.L., The cell biology of sponges, 1984, Springer, Berlin Heidelberg, New York

Sipkema, Detmer; Osinga, Ronald; Schatton, Wolfgang; Mendola, Dominick; Tramper, Johannes; and Wijffels, Renè, H., *Biotechnology and Bioengineering*, 2005, **90** (2), 201 - 222

Sipkema, D.; Franssen M.C.R.; Osinga R.; Tramper, J.; and Wijffels R.H., *Marine Biotechnology*, 2005, **7**, 142-146

Smith, R.M., *Understanding mass spectra: a basic approach*, 2005, Wiley-Interscience, New Jersey

Stead, P. In: Cannell, R.J.P., *Natural products isolation*, 1998, Humana Press, Totowa, New Jersey, 165-208

Stierle, D.B., and Faulkner, D.J., *J. Org. Chem.*, 1980, **45**, 4980-4982

Tabudravu, J.N.; and Jaspars M., *J. Nat. Prod.*, 2002 **65**, 1798 – 1801

Takamatsu, S., Hodges, T.W., Rajbhandari, I., Gerwick, W.H., Hamann, M.T., and Nagle, D.G., *J. Nat. Prod.*, 2003, **66**, 605-608

Takei, Masao; Burgoyne, David L.; and Andersen, Raymond J., *Journal of Pharmaceutical Sciences*, 1994, Vol. **83**, Issue 9, 1234 - 1235

Tasdemir, D., Bugni, T.S., Mangalindan, G.C., Concepción, G.P., Harper, M.K., Ireland, C.M., *Turk. J. Che*m., 2003, **27**, 273-279

Tasdemir, D., Mangalindan, G.C., Concepción, G.P., Verbitski, S.M., Rabindran, M.M., Greenstein, M., Hooper, J.N.A., Harper, M.K., and Ireland, C.M., *J. Nat. Prod.*, 2002, **65**, 210-214

Teeyapant, R., Woerdenbag, H.J., Kreis, P., Hacker, J., Wray, V., Witte, L., and Proksch, P., *Z. Naturforsch.*, 1993, **48c**, 939-945

Thakur, Narsinh L.; and Müller Werner E. G., *Current Science*, 2004, **86** (11), 1506 – 1512

Thakur, N.L., Hentschel, U., Krasko, A., Anil, A.C., and Müller, W.E.G., *Aquatic Microbiol. Ecol.*, 2003, **31**, 77 – 83

Thompson, J.E., *Marine Biology*, 1985, **88**, 23 – 26

Thompson, J.E., Barrow, K.D., and Faulkner, D.J., *Acta Zool.*, 1983, **64**, 199-210

Thoms, C., Ebel, R., and Proksch, P., *J. Chem. Ecol.*, 2006, **32**(1), 97-123

Thoms, C., Wolff, M., Padmakumar, K., Ebel., R., and Proksch, P., *Z. Naturforsch.*, 2004, **59c**, 113-122

Thoms, C., Ebel, R., Hentschel, U., and Proksch, P., *Z. Naturforsch.*, 2003, **58c**, 426-432

Travert, N., and Al-Mourabit, A., *J. Am. Chem. Soc.*, 2004, **126**, 10252 – 10253

Tsuda, M., Shigemori, H., Ishibashi, M., and Kobayashi, J., *Tetrahedron Lett.,* 1992, **33**, 2597-2598

Tsukamoto, S., Kato, H., Hirota, H., and Fusetani, N. In: Watanabe, Y., Fusetani, N. (Eds.), *Sponge Sciences*, 1998, Springer Verlag, 399-412

Tsukamoto, S., Kato, H., Hirota, H., Fusetani, N., *Biofouling*, 1997, **11**, 283-291

Tsukamoto, S., Kato, H., Hirota, H., and Fusetani, N., *Tetrahedron*, 1996a, **52**, 8181-8186

Tsukamoto, S., Kato, H., Hirota, H., and Fusetani, N., *Tetrahedron Lett.*, 1996b, **37**, 1439-1440

Tsukamoto, S., Kato, H., Hirota, H., and Fusetani, N., *J. Nat. Prod.*, 1996c, **59**, 501-503

Tsukamoto, S., Kato, H., Hirota, H., Fusetani, N., *Tetrahedron*, 1986, **52**, 8181-8186

Turon, X., Becerro, M.A., and Uriz, M.J., *Cell Tissue Res.*, 2000, **301**, 311-322

Tymiak, A.A., and Rinehart, Jr., K.L., *J. Am., Chem., Soc.*, 1981, **103**, 6763-6765

Umeyama, A., Ito, S., Yuasa, E., Arihara, S., and Yamada, T., *J. Nat. Prod.*, 1998, **61**, 1433-1434

Unson, M.D.; Holland, N.D.; and Faulkner, D.J., *Marine Biology*, 1994, **119**, 1 - 11

Uriz, M.J. In: Hooper, J.N.A., and Van Soest, R.W.M. (Eds.), *Systema porifera: A guide to the classification of sponge*s, 2002, Kluwer Academic/ Plenum Publisher, New York, 108-126

Uriz, M.J., Becerro, M.A., Tur, J.M., and Turon, X., *Mar. Biol.*, 1996, **124**, 583-590

Utenova, B.T., and Gundersen, L.L., *Tetrahedron Letters*, 2004, **45**, 4233-4235

Utkina, N.K.; Fedoreyev, S.A., and Maksimov, O.B., *Chem. Nat. Compd.* (Engl. Transl.), 1985, **21**, 547-548

Van Bramer, S.E., *An introduction to Mass Spectrometry*, 1998, http://science.widener.edu/~svanbram

Van Pee, K.H., *Arch. Microbiol.*, 2001, **175**, 250

Van Soest, R.W.M., and Hajdu, E. In: Hooper, J.N.A., and Van Soest, R.W.M. (Eds.), *Systema porifera: A guide to the classification of sponge*s, 2002, Kluwer Academic/ Plenum Publisher, New York, 819-823

Van Soest, R.W.M. In: Hooper, J.N.A., and Van Soest, R.W.M. (Eds.), *Systema porifera: A guide to the classification of sponge*s, 2002, Kluwer Academic/ Plenum Publisher, New York, 669-690

Van Soest, R.W.M., *Netherlands Journal of Sea Research*, 1989, **23**(2), 223 – 230

Venkatesham, U., Rao, M.R., Venkateswarlu, Y., *J. Nat. Prod.*, 2000, **63**, 1318-1320

Venkateswarlu, Y., Venkatesham, U., and Rao, M.R., *J. Nat. Prod.*, 1999, **62**, 893-894

Vik, A., Hedner, E., Charnock, C., Samuelson, O., Larsson, R., Gundersen, L.L. and Bohlin, L., *J. Nat. Prod.*, 2006, **69**, 381-386

Vogler, C., and Schild, D., *J. Exp. Biol.*, 1999, **202**, 997-1003

Von Eiff, C.,Peters, G., and Heilmann, C., *Lancet Infect. Dis.*, 2002, **2**, 677-685

Walters, K.D.; and Pawlik, J.R., *Integr. Comp. Biol.*, 2005, **45**, 352 – 358

Weiss, B., Ebel, R., Elbrächter, M., Kirchner, M., and Proksch, P., *Biochem. Syst. Ecol.*, 1996, **24**, 1-12

Whitehead, Roger, *Annu. Rep. Prog. Chem.*, *Sec B*, 1999, **95**, 183 – 205

Wiens, M.; Luckas, B.; Brümmer, F.; Ammar, M.S.A, Steffen, R, Batel, R.; Diehl-Seifert, B.; Schröder, H.C.; and Müller, W.E.G., *Mar. Biol*, 2003, **142**, 213 - 223

Williams, David H.; and Faulkner, D. John, *Tetrahedron*, 1996, **52**(15), 5381-5390

Wu, H., Nakamura, H., Kobayashi, J., Ohizumi, Y., and Hirata, Y., *Experientia*, 1986, **42**, 855-856

Wolfenden, R.V., *J. Mol. Biol.*, 1969, **40**, 307

Wright, A.E., Pomponi, S.A., McConnell., O.J., Kohmoto, S., and McCarthy, P.J., *J. Nat. Prod.*, 1987, **50**(5), 976-978

Xynas, R., and Capon, R., *Aust. J. Chem.*, 1989, **42**, 1427-1433

Yagi, H., Matsunaga, S., and Fusetani, N., *Tetrahedron*, 1993, **49**, 3749-3754

Yang, Lu; and Andersen, Raymond J., *J. Nat. Prod.*, 2002, **65**, 1924-1926

Yunker, M.B.; and Scheuer, P.J., *Tetrahedron Lett.*, 1978, **47**, 4651 – 4652

Zachary, I., and Rozengurt, E., *Cell,* 1992, **71**, 891-894

Zhao, J.H., Reiske, H., and Guan, J.L., *J. Cell Biol.*, 1998, **143**, 1997-2008

Curriculum Vitae

Name	: Triana Hertiani
Date of Birth and Place	: Jakarta, Indonesia, 9th of June 1973
Civil Status	: Married
Number of child	: 1 (one)
Address	: Himmelgeister Strasse 83 App. 95 Düsseldorf 40225
Home address	: J. Ki Ageng Pemanahan 43 Sorosutan Jogjakarta, 55162 Indonesia
E mail	: hadna3ana@yahoo.com
Home Office	: Department of Pharmaceutical Biology, Faculty of Pharmacy, Gadjah Mada University Sekip Utara, Jogjakarta, Indonesia 55281

Educations :

2004 – 2007	: PhD., Institut für Pharmazeutische Biologie und Biotechnologie, Heinrich-Heine Universität Düsseldorf, Germany Supervisor: Prof. Dr. Peter Proksch
1997 – 2000	: Master of Science, Faculty of Pharmacy, Gadjah Mada University (GMU), Indonesia Thesis: Isolation and identification of antioxidant flavonoid substances from *Plantago major* L. leaves Supervisor: Prof. Dr. Suwijiyo Pramono, Apt.
1996 – 1997	: Pharmacist, Faculty of Pharmacy, GMU
1991 – 1996	: Undergraduate, Faculty of Pharmacy, GMU Thesis: Effect of several ratio of combination of ethambutol HCl and rifampin against *Mycobacterium tuberculosis* H37Rv in vitro Advisor: Dr. Ahmad Purnomo, Apt.

1989 – 1991	: Senior High School
1986 – 1989	: Junior High School
1979 – 1986	: Elementary School

Occupations:

1998 – present	: Educative Staff in Department of Pharmaceutical Biology, Faculty of Pharmacy, Gadjah Mada University, Indonesia